



**QUEEN'S
UNIVERSITY
BELFAST**

Meta-Analysis of Genome-Wide Association Studies for Abdominal Aortic Aneurysm Identifies Four New Disease-Specific Risk Loci

Jones, G. T., Tromp, G., Kuivaniemi, H., Gretarsdottir, S., Baas, A. F., Giusti, B., Strauss, E., van 't Hof, F. N., Webb, T., Erdman, R., Ritchie, M. D., Elmore, J. R., Verma, A., Pendergrass, S., Kullo, I. J., Ye, Z., Peissig, P. L., Gottesman, O., Verma, S. S., ... Bown, M. J. (2016). Meta-Analysis of Genome-Wide Association Studies for Abdominal Aortic Aneurysm Identifies Four New Disease-Specific Risk Loci. *Circulation Research*.
<https://doi.org/10.1161/CIRCRESAHA.116.308765>

Published in:
Circulation Research

Document Version:
Publisher's PDF, also known as Version of record

Queen's University Belfast - Research Portal:
[Link to publication record in Queen's University Belfast Research Portal](#)

Publisher rights

© 2016 The Authors. *Circulation Research* is published on behalf of the American Heart Association, Inc., by Wolters Kluwer Health, Inc. This is an open access article under the terms of the Creative Commons Attribution License, which permits use, distribution, and reproduction in any medium, provided that the original work is properly cited.

General rights

Copyright for the publications made accessible via the Queen's University Belfast Research Portal is retained by the author(s) and / or other copyright owners and it is a condition of accessing these publications that users recognise and abide by the legal requirements associated with these rights.

Take down policy

The Research Portal is Queen's institutional repository that provides access to Queen's research output. Every effort has been made to ensure that content in the Research Portal does not infringe any person's rights, or applicable UK laws. If you discover content in the Research Portal that you believe breaches copyright or violates any law, please contact openaccess@qub.ac.uk.

Open Access

This research has been made openly available by Queen's academics and its Open Research team. We would love to hear how access to this research benefits you. – Share your feedback with us: <http://go.qub.ac.uk/oa-feedback>

OPEN

Meta-Analysis of Genome-Wide Association Studies for Abdominal Aortic Aneurysm Identifies Four New Disease-Specific Risk Loci

Gregory T. Jones, Gerard Tromp, Helena Kuivaniemi, Solveig Gretarsdottir, Annette F. Baas, Betti Giusti, Ewa Strauss, Femke N.G. van't Hof, Thomas R. Webb, Robert Erdman, Marylyn D. Ritchie, James R. Elmore, Anurag Verma, Sarah Pendergrass, Iftikhar J. Kullo, Zi Ye, Peggy L. Peissig, Omri Gottesman, Shefali S. Verma, Jennifer Malinowski, Laura J. Rasmussen-Torvik, Kenneth M. Borthwick, Diane T. Smelser, David R. Crosslin, Mariza de Andrade, Evan J. Ryer, Catherine A. McCarty, Erwin P. Böttlinger, Jennifer A. Pacheco, Dana C. Crawford, David S. Carrell, Glenn S. Gerhard, David P. Franklin, David J. Carey, Victoria L. Phillips, Michael J.A. Williams, Wenhua Wei, Ross Blair, Andrew A. Hill, Thodor M. Vasudevan, David R. Lewis, Ian A. Thomson, Jo Krysa, Geraldine B. Hill, Justin Roake, Tony R. Merriman, Grzegorz Oszkini, Silvia Galora, Claudia Saracini, Rosanna Abbate, Raffaele Pulli, Carlo Pratesi, The Cardiogenics Consortium, The International Consortium for Blood Pressure, Athanasios Saratzis, Ana R. Verissimo, Suzannah Bumpstead, Stephen A. Badger, Rachel E. Clough, Gillian Cockerill, Hany Hafez, D. Julian A. Scott, T. Simon Futers, Simon P.R. Romaine, Katherine Bridge, Kathryn J. Griffin, Marc A. Bailey, Alberto Smith, Matthew M. Thompson, Frank M. van Bockxmeer, Stefan E. Matthiasson, Gudmar Thorleifsson, Unnur Thorsteinsdottir, Jan D. Blankensteijn, Joep A.W. Teijink, Cisca Wijmenga, Jacqueline de Graaf, Lambertus A. Kiemeny, Jes S. Lindholt, Anne Hughes, Declan T. Bradley, Kathleen Stirrups, Jonathan Golledge, Paul E. Norman, Janet T. Powell, Steve E. Humphries, Stephen E. Hamby, Alison H. Goodall, Christopher P. Nelson, Natzli Sakalihasan, Audrey Courtois, Robert E. Ferrell, Per Eriksson, Lasse Folkersen, Anders Franco-Cereceda, John D. Eicher, Andrew D. Johnson, Christer Betsholtz, Arno Ruusalepp, Oscar Franzén, Eric E. Schadt, Johan L.M. Björkegren, Leonard Lipovich, Anne M. Drolet, Eric L. Verhoeven, Clark J. Zebregs, Robert H. Geelkerken, Marc R. van Sambeek, Steven M. van Sterkenburg, Jean-Paul de Vries, Kari Stefansson, John R. Thompson, Paul I.W. de Bakker, Panos Deloukas, Robert D. Sayers, Seamus C. Harrison, Andre M. van Rij, Nilesh J. Samani, Matthew J. Bown

Rationale: Abdominal aortic aneurysm (AAA) is a complex disease with both genetic and environmental risk factors. Together, 6 previously identified risk loci only explain a small proportion of the heritability of AAA.

Objective: To identify additional AAA risk loci using data from all available genome-wide association studies.

Methods and Results: Through a meta-analysis of 6 genome-wide association study data sets and a validation study totaling 10 204 cases and 107 766 controls, we identified 4 new AAA risk loci: 1q32.3 (*SMYD2*), 13q12.11 (*LINC00540*), 20q13.12 (near *PCIF1/MMP9/ZNF335*), and 21q22.2 (*ERG*). In various database searches, we observed no new associations between the lead AAA single nucleotide polymorphisms and coronary artery disease, blood pressure, lipids, or diabetes mellitus. Network analyses identified *ERG*, *IL6R*, and *LDLR* as modifiers of *MMP9*, with a direct interaction between *ERG* and *MMP9*.

Conclusions: The 4 new risk loci for AAA seem to be specific for AAA compared with other cardiovascular diseases and related traits suggesting that traditional cardiovascular risk factor management may only have limited value in preventing the progression of aneurysmal disease.

(*Circ Res.* 2017;120:341-353. DOI: 10.1161/CIRCRESAHA.116.308765.)

Key Words: aortic aneurysm, abdominal ■ computational biology ■ genetics ■ genome-wide association study ■ matrix metalloproteinases ■ meta-analysis

Original received March 23, 2016; revision received October 28, 2016; accepted November 21, 2016. In October 2016, the average time from submission to first decision for all original research papers submitted to *Circulation Research* was 15.7 days.

For the author affiliations, please see the Appendix.

The online-only Data Supplement is available with this article at <http://circres.ahajournals.org/lookup/suppl/doi:10.1161/CIRCRESAHA.116.308765/-/DC1>.

Correspondence to Matthew J. Bown, MBBCh, MD, Cardiovascular Sciences, University of Leicester Robert Kilpatrick Bldg, Leicester, LE2 7LX, United Kingdom. E-mail m.bown@le.ac.uk; or Gregory T. Jones, PhD, Surgery Department, University of Otago, Dunedin 9054, New Zealand. E-mail greg.jones@otago.ac.nz

© 2016 The Authors. *Circulation Research* is published on behalf of the American Heart Association, Inc., by Wolters Kluwer Health, Inc. This is an open access article under the terms of the [Creative Commons Attribution](https://creativecommons.org/licenses/by/4.0/) License, which permits use, distribution, and reproduction in any medium, provided that the original work is properly cited.

Circulation Research is available at <http://circres.ahajournals.org>

DOI: 10.1161/CIRCRESAHA.116.308765

Novelty and Significance

What Is Known?

- Abdominal aortic aneurysm (AAA) has a prevalence of $\approx 1.5\%$ in men aged >65 years.
- Positive family history of AAA is a strong risk factor for AAA; however, only 6 robust and independently validated AAA genetic loci have been identified to date.

What New Information Does This Article Contribute?

- Four novel genetic loci associated with AAA were identified.
- Pathway analysis highlighted the potential importance of lipoprotein metabolism, inflammation, and matrix metalloproteinases in AAA pathobiology.
- Potentially novel mechanisms, involving genes such as *ERG*, *PLTP*, and *FGF9*, were implicated.

AAA is a significant health burden, particularly among elderly males. It has a strong heritable component; however, previously

identified risk loci explain only a small proportion of this effect. No current effective medical therapies that slow AAA growth exist, highlighting the need to better understand factors influencing pathogenesis and disease progression. This study is the first meta-analysis of genome-wide association studies for AAA (10204 cases). Four novel loci were identified and 5 of the 6 previous AAA genetic associations were confirmed. The new loci showed no significant associations with other arterial disease phenotypes, potentially suggesting associations more specific to AAA than known loci (such as *CDKN2BAS1*, *SORT1*, and *LDLR*). Associations were consistent with known AAA pathobiology, implicating lipoprotein metabolism, inflammation, and matrix metalloproteinases but also identified potentially novel mechanisms relating to genes such as *ERG* and *FGF9*. This study has identified novel, potentially disease-specific, genetic associations with AAA. Further functional studies, investigating the translational potential of these observations, will be required.

Nonstandard Abbreviations and Acronyms

AAA	abdominal aortic aneurysm
CAD	coronary artery disease
eQTL	expression quantitative trait locus
GWAS	genome-wide association study
IL	interleukin
IPA	ingenuity pathway analysis
LDLR	low-density lipoprotein receptor
LRP1	low-density lipoprotein receptor related protein 1
SMYD2	SET and MYND domain containing 2 (SET domain-containing proteins, such as catalyze lysine methylation)
SNP	single nucleotide polymorphism
TNF	tumor necrosis factor

Abdominal aortic aneurysms (AAAs; MIM100070) are a significant cause of mortality and morbidity in the Western world. Although much less common than ischemic heart disease or stroke, AAA is responsible for ≈ 11000 deaths/y in the United States, with no clinical treatment other than expensive, high-risk surgery.¹ The US Preventative Services taskforce recommends AAA screening by ultrasound for all men aged 65 to 75 years who have ever smoked.² The UK NHS AAA Screening Program screens all men at the age of 65 years irrespective of smoking history yielding a prevalence of AAA (>29 mm) of 1.2% .³

Editorial, see p 259

AAA is an enigmatic complex disease. Although sharing risk factors for, and often coexisting with atherosclerosis, AAA can be considered to be a distinct entity from atherosclerosis. Smoking, a positive family history of AAA, and male sex have been consistently identified as the strongest risk factors for AAA. There is uncertainty over the influence of other traditional cardiovascular risk markers such as hypertension

and hyperlipidemia. Furthermore, diabetes mellitus has been found to be negatively associated with AAA and is strongly protective against disease progression (AAA growth).¹

Heritability of AAA is >0.7 ,⁴ and individuals with a first-degree relative with AAA have a 2-fold higher risk of developing an AAA.⁵ Genome-wide association studies (GWAS) have identified 3 AAA risk loci on chromosomes 9 (*DAB2IP*⁶ [DAB2 interacting protein]), 12 (*LRP1*⁷ [low-density lipoprotein receptor related protein 1]), and 19 (*LDLR*⁸ [low-density lipoprotein receptor]). Further AAA risk loci on chromosomes 1 (*SORT1*⁹ [sortilin 1] and *IL6R*¹⁰ [interleukin 6 receptor]) and 9 (*CDKN2BAS1/ANRIL*¹¹ [also known as CDKN2B-AS1, CDKN2B antisense RNA 1]) were identified by candidate gene/locus approaches. Together, these explain only a small proportion of the heritability of AAA.

Overall, the high heritability estimates for AAA and the small number of loci identified suggest that there are further risk loci yet to be found. In the current study, we performed a meta-analysis of 6 available GWAS data sets for AAA on 4972 cases and 99858 controls and confirmed the findings within validation data sets of 5232 cases and 7908 controls. This resulted in identification of 4 novel validated loci for AAA. We followed up positive results with extensive bioinformatics analyses and used data available from various databases to elucidate the potential biological significance of our findings to the pathobiology of AAA.

Methods

Detailed Methods are available in the Online [Data Supplement](#).

Expanded Aneurysm Consortium

All known studies with AAA genome-wide genotyping (Online Methods; Online Table I) were invited to join the International Aneurysm Consortium. Additional samples (Online Methods; Online Table II) were used for the validation study. All AAA cases had an infrarenal aortic diameter of >30 mm. AAAs secondary to connective tissue diseases were excluded. The use of the samples in each study cohort was approved by local Ethics Committees or Institutional Review Boards.

Meta-Analysis

The discovery phase of the meta-GWAS was conducted using the METAL (a tool for meta-analysis of genome-wide association scans) software package¹² on the 6 cohorts detailed in Online Table I, comprising 4972 AAA cases and 99 858 controls. An effective sample number (N_{eff}) weighted analysis¹² was conducted because of case/control asymmetry within some of the contributing cohorts. Quality control included assessments for population stratification in each data set and adjustment was performed if necessary. The analysis of each contributing GWAS had been performed independently, and there was therefore no uniform analysis plan across all data sets. The individual GWAS data sets from Iceland and the Netherlands were adjusted for genomic inflation before inclusion in the meta-analysis. The overall meta-analysis was then adjusted for genomic inflation (λ ; Online Table I; Online Figure I). An initial (λ -adjusted) discovery threshold of $P < 5 \times 10^{-6}$ was used to identify single nucleotide polymorphisms (SNPs) for subsequent validation genotyping. SNPs with high heterogeneity ($P_{\text{het}} < 0.005$ or $P > 70\%$) were not taken forward for validation.

The lead SNPs [or their proxies in high linkage disequilibrium], identified in the discovery analyses, were then genotyped in a further 8 independent cohorts with 5,232 cases and 7,908 controls (Online Table II). Allele association analysis of each individual validation study cohort was carried out using the SHeSis (software platform for analyses of linkage disequilibrium, haplotype construction, and genetic association at polymorphism loci) web-based software package.¹³ A combined (discovery-validation) fixed effect meta-analysis was performed using a Maentel-Haenzel method with the genome-wide P -value significance threshold being set at 5×10^{-8} . Random-effects (Han-Eskin method¹⁴) meta-analysis was also performed to determine whether any results were sensitive to between-study heterogeneity.

SNP Lookup in GWAS for Other Traits Associated With AAA

GWAS data sets for other traits were searched for associations with the AAA-associated SNPs to determine whether the associations were unique to AAA or related to generalized cardiovascular disease. Results were obtained from meta-analyses of multiple primary GWAS data sets for each trait. Summary data for each AAA associated SNP (P value and effect size) were extracted. P values $< 5 \times 10^{-8}$ were considered to be significant. Results were available for type 2 diabetes mellitus¹⁵ (DIAGRAM [a consortium called DIABetes Genetics Replication And Meta-analysis] consortium; <http://www.diagram-consortium.org/index.html>), coronary artery disease (CAD; CARDIOGRAM consortium (a consortium called Coronary Artery Disease Genome wide Replication and Meta-analysis)¹⁶; www.CARDIOGRAMPLUSC4D.ORG), lipids (the Global Lipids Genetics Consortium¹⁷; <http://csg.sph.umich.edu/abecasis/public/lipids2013>), and blood pressure (the International Consortium for Blood Pressure¹⁸; http://www.ncbi.nlm.nih.gov/projects/gap/cgi-bin/study.cgi?study_id=phs000585.v1.p1).

Search for Other Associated Traits and Diseases Using GWAS Databases

The Phenotype-Genotype Integrator¹⁹ (<http://www.ncbi.nlm.nih.gov/gap/phegeni#GenomeView>), the GWAS catalog (<http://www.gwascentral.org/index>), and the NHLBI GRASP (The Genome-wide Repository of Associations between SNPs and Phenotypes) catalog (GRASP v2.0; <http://grasp.nhlbi.nih.gov/Overview.aspx>)²⁰ were searched for diseases and traits associated with the lead SNPs at the AAA loci.

Phenome-Wide Association Study Analysis

We performed a phenome-wide association study (PheWAS)^{21,22} exploring associations between the 9 AAA-associated SNPs and an extensive group of diagnoses to identify novel associations and uncover potential pleiotropy. For the PheWAS, we used data from the eMERGE (electronic Medical Records and Genomics) Network²³ with a total of 27 077 unrelated patients of European ancestry aged

>19 years. We divided these samples into 2 data sets by proportional sampling based on eMERGE site, sex, and genotyping platform (13 559 and 13 518 individuals in sets 1 and 2, respectively). We calculated associations between the 9 AAA-associated SNPs and case or control status based on the extensive set of 9th edition of the *International Statistical Classification of Diseases and Related Health Problems* diagnoses (2408 and 2385 in sets 1 and 2, respectively) where for a specific diagnosis, individuals with the diagnosis are considered cases. Associations were adjusted for sex, site, genotyping platform, and the first 3 principal components to account for global ancestry.

Annotation of AAA Associated SNPs Using the University of California Santa Cruz Genome Browser, Pupasuite, and GWAS3D

Confirmed AAA-associated loci were manually annotated using the University of California Santa Cruz Genome Browser (<http://genome.ucsc.edu/cgi-bin/hgGateway>) on the hg19 human genome assembly. For the Pupasuite analyses SNPs in linkage disequilibrium ($r^2 > 0.5$) and with lead SNPs at the novel AAA risk loci identified were extracted from the 1000 Genomes data and then entered into Pupasuite v3.1.²⁴ In addition, all known (novel and previously identified) AAA-associated SNPs were entered into the GWAS3D (bioinformatics tool detecting human regulatory variants by integrative analysis of genome-wide associations, chromosome interactions, and histone modifications)²⁵ web-portal (<http://jjwanglab.org/gwas3d>) to identify functional SNPs.

Bioinformatic Identification of Candidate AAA Genes and Pathways Using DEPICT (Data-Driven Expression-Prioritized Integration for Complex Traits)

An integrated gene function analysis was performed using the DEPICT tool (version 1.1).²⁶ Two separate runs were performed using either all independent SNPs with discovery meta-GWAS $P < 5 \times 10^{-6}$ or just those 9 SNPs that reached $P < 5 \times 10^{-8}$ in the combined analysis. Both nominal P values and false discovery rates were calculated.

Experimental Evidence for Functional Variants at AAA Loci

SNPs at loci confirmed to be associated with AAA were examined for functional effects using multiple methods (Online Methods). (1) To search for evidence of functional effects of SNPs at AAA associated loci 2 expression quantitative trait locus (eQTL) data sets based on publically available data, and a broad range of tissues with relatively large sample sizes were examined. First, index and proxy SNPs were queried in a collected database of published expressed SNP results. The collected expressed SNP results met criteria for statistical thresholds for association with gene transcript levels as described in the original publications. Second, additional eQTL data were integrated from online sources including ScanDB (SNP and CNV Annotation Database), the Broad Institute The Genotype-Tissue Expression browser, and the Pritchard Laboratory (eql.uchicago.edu). (2) To search for vascular tissue-specific effects, eQTL data were also obtained from the ASAP (Advanced Study of Aortic Pathology) data set²⁷ and RNA-seq (whole-genome RNA-sequence generated by high-throughput methods) data were from the Stockholm-Tartu Atherosclerosis Reverse Network Engineering Task (STARNET) database²⁸ (<http://www.mountsinai.org/profiles/johan-bjorkegren>). (3) Because some genes at AAA loci were associated with monocyte function and AAA is known to be an inflammatory disease,²⁹ data from an eQTL analysis of peripheral blood monocytes were obtained from the Cardiogenics Consortium (<http://www.cardiogramplusc4d.org/>). (4) Finally to search for effects in AAA tissue specifically, mRNA expression profiles of all the GWAS3D predicted distal targets, as well as SNP proximity implicated genes, were examined using a previously published genome-wide expression data set on human aorta (GSE57691),³⁰

from which 49 AAA samples were compared with 10 organ donor control aortic samples. Transcription factor (TF) binding data were also obtained from a previous study,³¹ which described chromatin-immunoprecipitation (ChIP)-chip for TFs ELF1, ETS2, RUNX1, and STAT5 using human aortic tissue in AAAs and healthy control aorta.

Network Analysis

We investigated whether most of the loci could be connected into a single network through intermediate nodes and interactions. A network integrating most of the loci would suggest mechanisms by which the loci could act in concert, whether synergistically or antagonistically, to affect the phenotype. The network(s) would also provide hypotheses for future investigation. Using the genes harboring AAA-associated SNPs as a starting set, we analyzed potential interactions between the proteins and known intermediates (proteins, noncoding RNA, and metabolites) using 2 independent analysis tools, Ingenuity Pathway Analysis (IPA) tool version 9.0 (Qiagen's Ingenuity Systems, Redwood City, CA; www.ingenuity.com) and Consensus PathDB (<http://cpdb.molgen.mpg.de/CPDB>).^{32,33} The analyzed gene set had 14 genes because 2 of the 9 AAA loci included clusters of 3 genes and tumor necrosis factor (TNF) was added because of the recent literature demonstrating the strong effect of SMYD2 (SET and MYND domain containing 2 [SET domain-containing proteins, such as catalyze lysine methylation]) on interleukin-6 (IL6) and TNF production^{34,35} (see Online Table XIV for SNP annotations and Online Methods).

Results

Meta-Analysis of 6 GWAS Data sets for AAA Followed by a Validation Study Reveals 4 New AAA Susceptibility Loci

The meta-analysis of 6 GWAS data sets (4972 AAA cases; 99 858 controls; Online Table I) revealed 19 loci of interest

($P < 1 \times 10^{-6}$, Online Tables III and IV; Figure 1). Lead SNPs from these loci, including the 6 AAA risk loci reported previously, were analyzed in a validation study of 5232 AAA cases and 7908 controls (Online Tables II, V, VI, and VII). Four new loci were independently significant ($P < 0.05$) in the validation cohort, had a direction of effect consistent with the discovery cohort and when combined with the discovery cohort had a P value that surpassed a genome-wide significance (5×10^{-8}): 1q32.3 (*SMYD2*), 13q12.11 (*LINC00540* [long intergenic nonprotein coding RNA 540]), 20q13.12 (near *PCIF1* [C-terminal inhibiting factor 1 of a protein called pancreatic and duodenal homeobox 1]/*MMP9* [matrix metalloproteinase 9]/*ZNF335* [zinc finger protein 335]), and 21q22.2 (*ERG* [v-ets avian erythroblastosis virus E26 oncogene homolog]; Table 1; Online Tables V, VI, and VII; Figure 2). All previously reported associations with AAA were confirmed at genome-wide significance (Table 1; Online Table VII; Online Figure II) with the exception of 12q13.3 (*LRP1*), where the lead SNP identified in this meta-analysis and tested in our validation study only demonstrated a borderline association with AAA in the combined analysis ($P = 6.4 \times 10^{-7}$). There was evidence of significant heterogeneity in the results observed for rs1795061 (near *SMYD2*) and rs2836411 (*ERG*) (Online Table VII). A random-effects model sensitivity analysis (Hanskin¹⁴ method) demonstrated minimal effect on the results for these 2 loci (Online Table VIII). The lead SNPs at 2 loci that were both below the threshold for genome-wide significance under the fixed-effects model (rs6516091, 20p12.3, near *FERMT1* and rs5954362, Xq27.2, *SPANXA1*) were significant

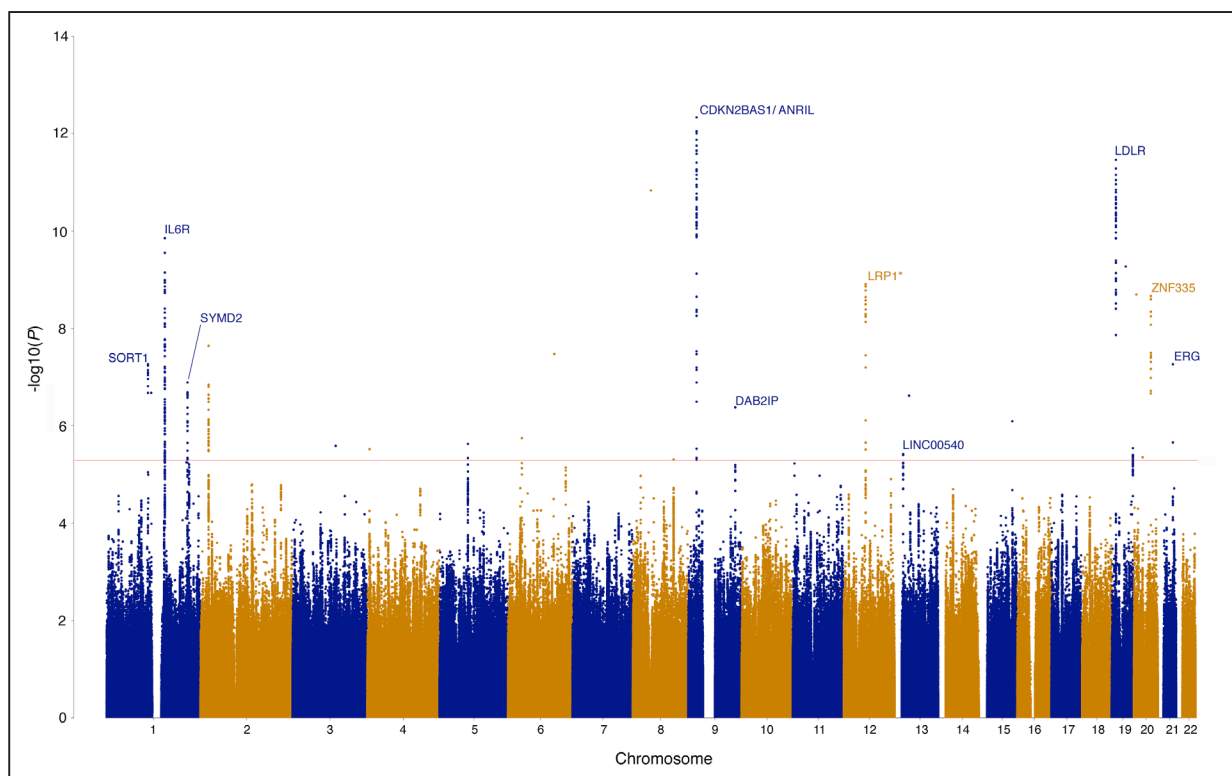


Figure 1. Whole-genome association plot for the primary meta-analysis of genome-wide association studies of abdominal aortic aneurysm (AAA). Data represent a meta-analysis of 4972 AAA cases and 99 858 controls. The horizontal line indicates the P value threshold of 5×10^{-6} used to select loci for validation studies. The 9 subsequently validated AAA loci are indicated along with the previously identified *LRP1* locus, which fell to $P = 6.4 \times 10^{-7}$ in the combined discovery/ validation analysis (Online Tables III and IV).

Table 1. List of AAA Associated Loci Surpassing a Genome-Wide Significance Threshold After Combining GWAS data (4972 cases and 99 858 controls) and Validation Data (5232 cases and 7908 controls)

SNP	Chr	Position	Nearest Gene(s)	Min_All*	Maj_All*	MAF	Discovery Phase			Validation Phase			Combined			
							OR	PValue	<i>P</i>	OR	PValue	<i>P</i>	OR	95% CI	PValue	<i>P</i>
Previously reported AAA risk loci																
rs602633	1	109821511	<i>PSRC1-CELSR2-SORT1</i>	T	G*	0.199	0.845	3.12×10 ⁻⁰⁸	29.4	0.920	9.83×10 ⁻³	55.7	0.879	0.842–0.918	6.58×10 ⁻⁹	54.5
rs4129267	1	154426264	<i>IL6R</i>	T	C*	0.370	0.854	1.74×10 ⁻¹⁰	0	0.904	1.81×10 ⁻⁴	17.2	0.876	0.846–0.908	4.76×10 ⁻¹³	0.0
rs10757274	9	22096055	<i>CDKN2BAS1/ANRIL</i>	A	G*	0.462	0.832	2.71×10 ⁻¹³	10.0	0.774	1.02×10 ⁻²¹	64.2	0.806	0.778–0.834	1.54×10 ⁻³³	55.6
rs10985349	9	124425243	<i>DAB2IP</i>	T*	C	0.195	1.185	2.01×10 ⁻⁷	18.1	1.155	2.30×10 ⁻⁵	3.9	1.171	1.118–1.226	2.40×10 ⁻¹¹	9.2
rs6511720	19	11202306	<i>LDLR</i>	T	G*	0.096	0.743	8.60×10 ⁻¹³	0	0.868	6.02×10 ⁻⁴	68.2	0.804	0.759–0.851	7.90×10 ⁻¹⁴	61.0
Novel AAA risk loci																
rs1795061	1	214409280	<i>SMYD2</i>	T*	C	0.337	1.154	3.26×10 ⁻⁸	47.9	1.105	3.49×10 ⁻⁴	70.3	1.131	1.090–1.174	8.80×10 ⁻¹¹	61.9
rs9316871	13	22861921	<i>LINC00540</i>	A	G*	0.201	0.864	1.23×10 ⁻⁶	33.2	0.883	8.28×10 ⁻⁵	0.0	0.873	0.837–0.911	4.75×10 ⁻¹⁰	0.0
rs3827066	20	44586023	<i>PCIF1-ZNF335-MMP9</i>	T*	C	0.179	1.232	1.88×10 ⁻¹⁰	0	1.213	2.00×10 ⁻⁸	16.5	1.223	1.168–1.281	2.13×10 ⁻¹⁷	0.0
rs2836411	21	39819830	<i>ERG</i>	T*	C	0.369	1.149	2.51×10 ⁻⁸	30.1	1.072	1.13×10 ⁻²	28.3	1.113	1.074–1.154	5.80×10 ⁻⁹	42.2

For all loci shown the direction of effect was consistent across all studies in the discovery phase. Full details are shown in Online Tables III, IV, V, VI, and VII. Results shown for the discovery, validation and combined analyses are all Maentel–Haenzel fixed effect meta-analysis method. AAA indicates abdominal aortic aneurysm; CI, confidence interval; MAF, minor allele frequency; and OR, odds ratio.

*Effect allele.

in the random-effects model. However, because both demonstrated extreme heterogeneity ($I^2 \geq 0.7$), we did not consider these to be newly identified loci for AAA and these were excluded from further analysis.

New AAA Loci Seem to be Specific for AAA

To assess whether the loci identified in our meta-analysis were specific to AAA or were also associated with diseases or risk factors known to be associated with AAA, we looked up results from GWAS of CAD,⁶ hypertension,¹⁸ and lipid traits.¹⁷ We also obtained results for diabetes mellitus¹⁵ to determine whether there was a reverse effect at these loci because diabetes mellitus is a negative risk factor for AAA and negatively influences AAA growth.¹ Other than the known associations at 1p13.3 (*SORT1*), 9p21 (*CDKN2BAS1/ANRIL*) with CAD, 1p13.3 (*SORT1*) with high-density lipoprotein/LDL, and 19p13.2 (*LDLR*) with LDL, we observed no new associations between the lead SNPs at any of the AAA risk loci we had identified and these traits (Figure 3; Online Table IX). In particular, no association was observed between diabetes mellitus and these SNPs. Literature searching revealed an association between rs4845625 at 1q21.3 (*IL6R*) and CAD, but this was not in high linkage disequilibrium with the lead SNP genotyped in our study at this locus ($R^2=0.54$).³⁶

We also searched GWAS Central (database providing integrative visualization of and access to GWAS data) and Phenotype-Genotype Integrator and performed a GRASP³⁷ analysis for any associations of the lead AAA SNPs with traits other than those listed above. We identified additional genome-wide significant associations between 1q21.3/*IL6R* (rs4129267) and C-reactive protein/asthma, and nominal associations between 1p13.3/*SORT1* (rs602633), 21q22.2/*ERG* (rs2836411), and 19p13.2/*LDLR* (rs6511720) and height (Online Tables X, XI, and XII), a potential risk factor for AAA.³⁸

We also performed a PheWAS^{21,22} in the eMERGE data sets exploring the association between the 9 AAA-associated SNPs and an extensive group of diagnoses to identify novel associations and uncover potential pleiotropy. We considered identification of previously known associations, such as rs602633 associated with hyperglyceridemia and rs10757274 associated with CAD, to be indications that the PheWAS approach was robust. The PheWAS results demonstrated the known associations with CAD and lipid levels but did not identify any novel disease associations (Online Table XIII).

Annotation of SNPs at AAA Loci

Annotation did not identify any nonsynonymous variants in high linkage disequilibrium ($R^2>0.5$) with the lead SNPs at the AAA risk loci (Online Tables XIV and XV). Based on GWAS3D analysis, all 9 lead SNPs were associated with TF-binding site affinity variants (Online Tables XVI and XVII). Eight SNPs had potential long-range interactions with distal genomic regions (Figure 4). GWAS3D analysis also provided potential mechanistic insight for intergenic AAA variants such as rs9316871 (13q12.11) that had significant predicted regulatory variant interaction with *FGF9* (fibroblast growth factor 9; 13q12.11). In addition, although the AAA association with rs599839 (1p13.3) showed strong long-range chromatin interaction with *SORT1* (as previously reported specifically in AAA⁹), it also had predicted distal interactions with other genes including *BCAR3* (breast cancer antiestrogen resistance 3; 1p22.1) and *NOTCH2* (notch 2 member of type 1 transmembrane protein family; 1p12-p11).

DEPICT Gene Pathway Prediction

DEPICT identified 633 and 482 gene enrichment sets with nominal $P<0.05$ using the discovery meta-GWAS SNP set

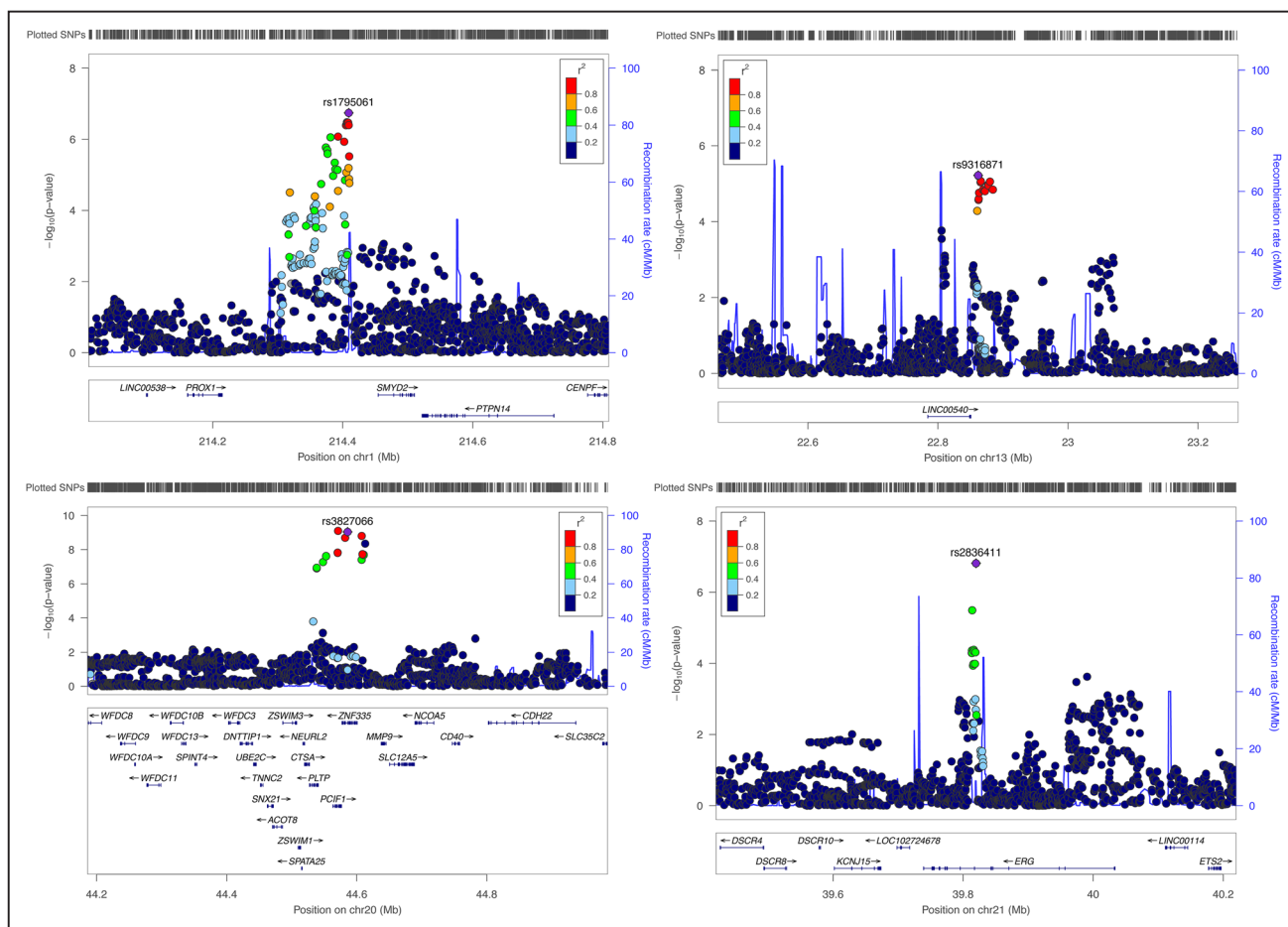


Figure 2. Regional association plots for 4 new abdominal aortic aneurysm (AAA) genome-wide significant loci at 1q32.3, 13q12.11, 20q13.12, and 21q22.2. New AAA genome-wide significant loci at 1q32.3 (near *SMYD2*), 13q12.11 (*LINC00540*), 20q13.12 (near *MMP9/ZNF335*), and 21q22.2 (*ERG*). $-\log_{10}(P_{\text{fixed}})$ values for single nucleotide polymorphisms (SNPs) from the AAA discovery meta-analysis of 4972 cases and 99 858 controls were plotted against their genomic positions using LocusZoom (1000Genomes, EUR, November 2014). The peak SNP in each region is labeled (purple diamond), whereas the color indicates LD (r^2) with the peak.

($P < 5 \times 10^{-6}$) and top 9 SNPs from the combined analysis, respectively. Only one of the gene sets (decreased long bone epiphyseal plate size) had a false discovery rate of < 0.2 . Gene set descriptions included multiple functional classes relevant to vascular biology, ie, transforming growth factor- β regulation, lipoprotein metabolism, inflammation-induced extracellular matrix remodeling (regulatory factor X1), vascular smooth muscle cell function, vascular injury including hemorrhage, immune cell function (particularly T and B cells), acute phase response including IL6 secretion, apoptosis, hyperglycemia and the phosphatidylinositol-4,5-bisphosphate 3-kinase catalytic subunit alpha, c-Jun N-terminal kinase, and mitogen-activated kinase-like protein cascades. In addition, there were multiple gene sets associated with long bone size and epiphyseal plate formation (Table 2; Online Table XVIII and Online Data File).

Functional Effects of SNPs at AAA Loci

The lookup of SNPs at AAA loci in studies of functional effects included multitissue eQTL studies, vascular/monocyte-specific eQTL, and AAA-specific studies (mRNA expression and chromatin-immunoprecipitation-chip). These analyses revealed several potential functional associations (Online Tables XI,

XX, XXI, and XXII; Online Figure III).^{27,39} Of most relevance to AAA, eQTLs were observed for rs3827066 (20q13.3) and *PLTP* (phospholipid transfer protein) expression in aortic tissue and for rs4129267 (1q21.3) and *IL6R* expression in mammary artery. RNA-Seq data also demonstrated independent eQTLs in mammary artery for 2 of the novel AAA associations we have identified: rs2836411 and *ERG* expression and rs9316871 and *FGF9* expression. All eQTLs, with the exception of rs9316871 and *FGF9* were also seen in tissues other than arterial samples.

Several GWAS3D-predicted distal interacting genes had significantly different mRNA expression between AAA and control samples (Table 3; Online Table XXIII and Figure IV).³⁰ For example, *BCAR3* had decreased mRNA expression in AAA tissue (as did *SORT1* itself). In addition, although the closest gene to rs9316871, a long intergenic noncoding RNA (*LINC00540*), was not part of the mRNA data set, the predicted distal target *FGF9* had significantly increased mRNA expression in AAA tissue (Online Table XXIII).

Chromatin-immunoprecipitation-chip data from human AAA tissue³¹ revealed TF-binding sites in 5 genes (*SMYD2*, *SORT1*, *CDKN2BAS1/ANRIL*, *ERG*, and *DAB2IP*), which harbor AAA risk loci, but none of these binding sites included

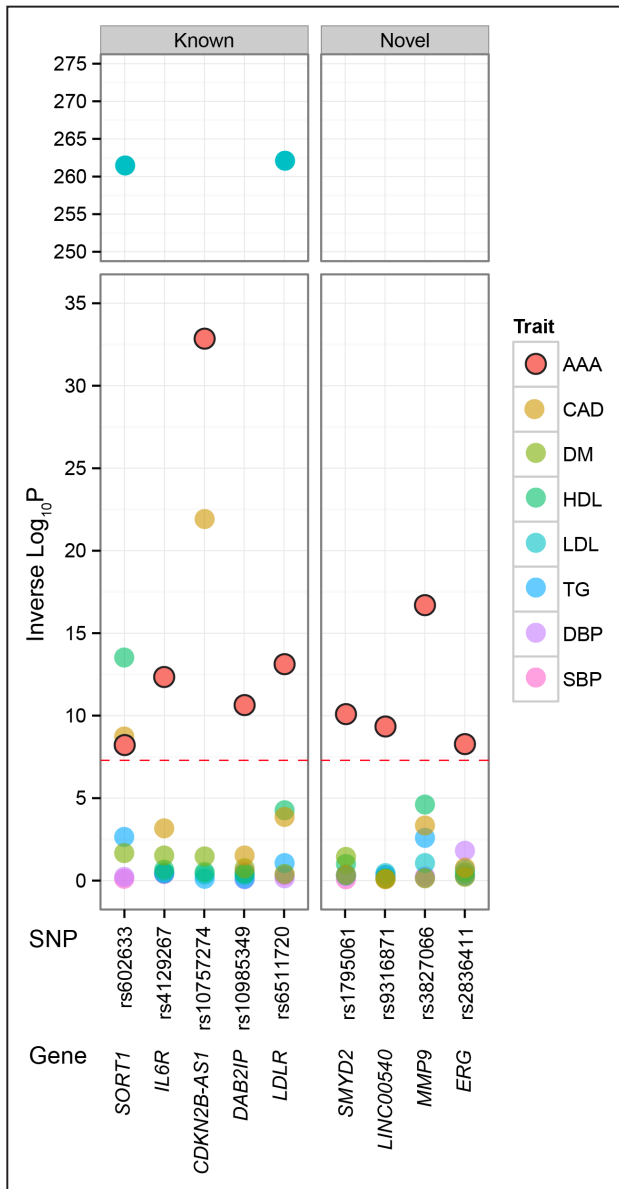


Figure 3. Association between the lead single nucleotide polymorphisms (SNP) at the abdominal aortic aneurysm risk loci and association P values for other cardiovascular risk factors/traits (Online Table IX). CAD indicates coronary artery disease; DBP, diastolic blood pressure; DM, diabetes mellitus; HDL, high-density lipoprotein; LDL, low-density lipoprotein; SBP, systolic blood pressure; and TG, triglyceride.

the lead SNP tested for association with AAA (Online Table XXIV).

Network Analysis Reveals a Central Role for Matrix Metalloproteinase 9

Network analysis using both IPA and Consensus PathDB demonstrated similar results (Online Figures V and VI). Both analyses revealed a central role for MMP9 in AAA, with IPA identifying direct interactions (physical contact between 2 molecules such as binding or phosphorylation) between ERG, IL6R and LDLR, and MMP9, and Consensus PathDB identifying a direct interaction between ERG and MMP9 with secondary interactions (interactions without physical contact,

such as signaling events) between both SMYD2 and LDLR, and MMP9. On removing TNF from the analysis (which had been added based on the strong effect of SMYD2 on IL6 and TNF production^{34,35}), the genes at AAA loci each remained in independent subnetworks. Inclusion of transforming growth factor-B1, implicated in thoracic aneurysms and Marfan syndrome, instead of TNF failed to coalesce the subnetworks. The long noncoding RNA ANRIL (*CDKN2BAS1*), our strongest hit in the genome (Figure 1), has been reported in numerous studies as a GWAS hotspot and a candidate gene for CAD, intracranial aneurysms, and diverse cardiometabolic disorders⁴⁰; however, this was not represented in either the IPA or Consensus PathDB networks.

Discussion

The present study is the largest genetic association study of AAA performed to date, utilizing 6 GWAS data sets for AAA with a total of 4972 cases and 99 858 controls. Furthermore, we used an independent validation set of 5232 AAA cases and 7908 controls and then performed a pooled analysis of all 10204 cases and 107 766 controls. We confirmed the association of 5 previously reported loci and identified 4 new loci associated with AAA at genome-wide levels of significance. In contrast to previously identified loci, lead SNPs at the newly identified loci did not demonstrate evidence of cross-phenotype association with other cardiometabolic phenotypes. In summary, the genetic evidence to date mirrors that seen in the epidemiological literature where it is clear that AAA and other forms of cardiovascular diseases are seen as distinct but overlapping phenotypes.

Previous genetic discoveries in AAA have pointed to inflammation and immune function (*IL6R* and *CDKN2BAS1/ANRIL*) and low-density lipoprotein metabolism (*SORT1* and *LDLR*) as important mediators of AAA development. The genes at the novel AAA loci identified here are relevant to aneurysm biology, but their precise roles require further investigation. *MMP9* is within the 20q13.12 locus and matrix degradation via MMP9 is known to play a key role in the development of AAA, evidenced by the observation of high levels of MMP9 in end-stage disease specimens.⁴¹ This is also an important finding given the development of novel pharmacotherapies that target inflammation and matrix degradation pathways such as tofacitinib (a novel Janus kinase inhibitor). Although it is tempting to assume that MMP9 is the causal association at this locus, there are, however, other candidate genes at this locus. Examination of the region and the association pattern with AAA (Figure 2) shows that the strongest signals are seen upstream of *MMP9* and are separated from *MMP9* by a recombination hotspot. Closer to the strongest association signal are *ZNF335* and *PCIF1*. There is no literature evidence for any potential link for *ZNF335* to AAA and the only identified genetic association of *ZNF335* is with celiac disease.⁴² Although rs181914932 is upstream and more proximal to *PCIF1*, it has been associated with the activity of *PLTP*,⁴³ an adjacent gene in the same locus. Our eQTL analyses demonstrated an association between the lead SNP we assessed at this locus (rs3827066) and *PLTP* expression in aortic tissue (Online Tables XX and XXI). We have also shown that *PLTP* expression is significantly higher in aneurysmal aortic

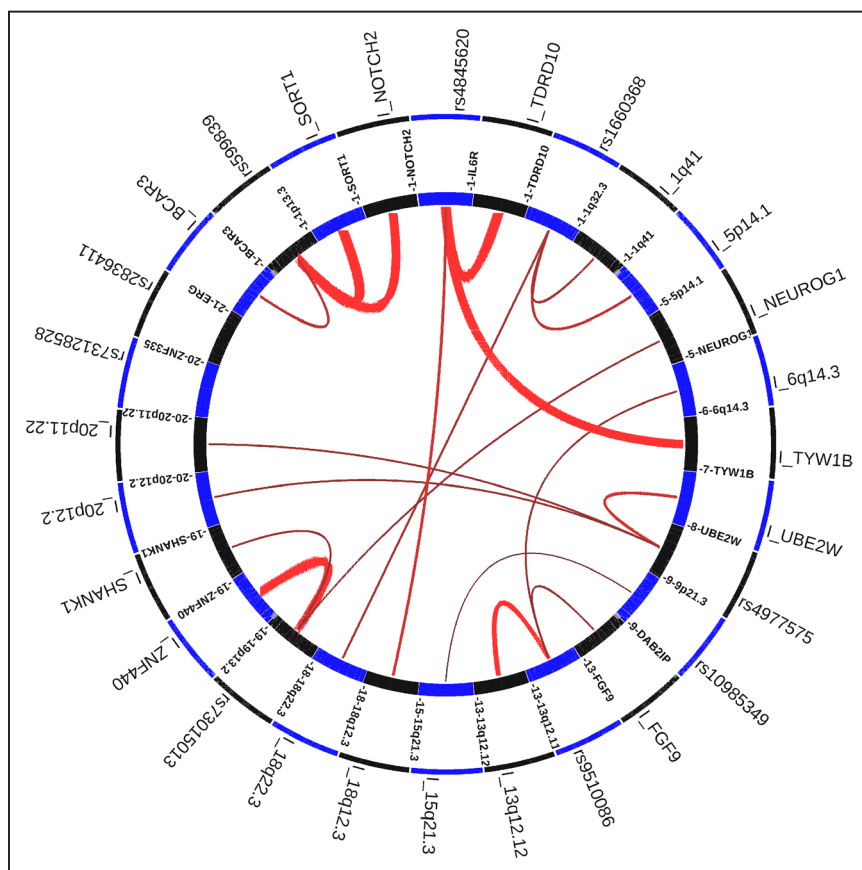


Figure 4. Circle plot showing the lead single nucleotide polymorphism (SNP) distal interaction regions based on the 9 replicated abdominal aortic aneurysm genome-wide association study SNPs. Top variants with highest regulatory signals and distal interaction regions are shown on the outer circle (significant regulatory variants are labeled with I). The inner circle shows genes and genomic loci, whereas the distal interactive signals are shown with red lines (width corresponds to intensity of interaction). Note the long-range interactions, such as that between variants associated with *IL6R* (rs4845620, 1q21.3) and *TYW1B* (7q11.23).

tissue than in control aorta (Online Table XXIII and Figure IV). *PLTP* plays a role in cholesterol transport. These data strengthen the evidence, particularly when taken together with the *SORT1* and *LDLR* associations confirmed here, that aberrations of lipid metabolism play a key role in the development of AAA.

The other novel AAA loci identified here contain *LINC00540*, *ERG*, and *SMYD2*. *LINC00540* is a long noncoding RNA with no currently known function; however, both our GWAS3D and eQTL analyses independently suggested an association with *FGF9*, which was also differentially expressed within AAA tissue. *ERG* encodes a TF that is normally present in hematopoietic and endothelial cells. *ERG* has a role in vascular endothelial growth factor/mitogen-activated kinase-like protein-mediated vascular development,⁴⁴ as well as regulating angiogenesis, which is known to play a role in the development of AAA.^{45,46} *ERG* also plays a role in the embryonic development of the aorta,⁴⁴ and it has been hypothesized that in utero aortic development has a role in the later development of an AAA.⁴⁷ In prostate cancer, *ERG* has been shown to regulate the expression of *MMP9*.⁴⁸ Taken together this limited evidence points to several potential roles by which *ERG* may influence the development of AAA and, along with our significant eQTL observations, strongly suggest that further work in this area is warranted.

The role of *SMYD2* in AAA is less clear. *SMYD2* regulates *HSP90* (heat shock protein 90) methylation,⁴⁹ and the inhibition of heat shock protein 90 has been shown to reduce AAA formation in murine models,⁵⁰ suggesting this as a possible link between *SMYD2* and AAA. *SMYD2* also plays a

role in the differentiation of embryonic stem cells,⁵¹ again suggesting a possible role for aberrations of in utero aortic development influencing the risk of aortic disease later in life.

The integrated gene function analysis tool DEPICT identified numerous pathways that are potentially relevant to aneurysm pathogenesis (Table 2). In particular, we note with interest that the strongest predicted set was associated with long bone epiphyseal plate formation, which is possibly consistent with previous studies reporting tall stature as a risk factor for AAA⁵² and conversely short stature with occlusive CAD.^{53,54}

Our network analyses using 2 different bioinformatics tools also revealed a central role for *MMP9* in AAA, with IPA identifying direct interactions between *ERG*, *IL6R* and *LDLR*, and *MMP9*, and Consensus PathDB identifying a direct interaction between *ERG* and *MMP9* with secondary interactions between both *SMYD2* and *LDLR* and *MMP9*. These results suggest that the novel loci could act in concert, either synergistically or antagonistically, to affect the AAA phenotype, and provide hypotheses for future investigation using animal and cell culture models.

In this study, we did not replicate the association previously identified between *LRP1* and AAA.⁷ The samples from the original study that identified this association were included in this analysis, suggesting that this may have been a false-positive association. However, there is evidence supporting *LRP1* as a biologically plausible candidate pathway for AAA.^{55,56} Variants at, or close to, *LRP1* are also associated with other vascular/related phenotypes (aortic dissection,⁵⁷ migraine,⁵⁸ and lipid traits¹⁷). Because we observed a degree

Table 2. DEPICT Gene Enrichment Sets Based on the Top 10 Validated Loci

Original Gene Set ID	Original Gene Set Description	DEPICT Nominal P Value
MP:0006396*	Decreased long bone epiphyseal plate size	1.14×10 ⁻⁹
GO:0034381	Plasma lipoprotein particle clearance	5.22×10 ⁻⁷
ENSG00000132005	RFX1 PPI subnetwork	2.28×10 ⁻⁶
MP:0005595	Abnormal vascular smooth muscle physiology	1.55×10 ⁻³
ENSG00000122641	INHBA PPI subnetwork	1.79×10 ⁻³
MP:0002764	Short tibia	1.79×10 ⁻³
ENSG00000169047	IRS1 PPI subnetwork	2.21×10 ⁻³
GO:0050431	Transforming growth factor beta binding	2.47×10 ⁻³
MP:0005590	Increased vasodilation	3.45×10 ⁻³
GO:0071813	Lipoprotein particle binding	3.51×10 ⁻³
GO:0005178	Integrin binding	4.08×10 ⁻³
ENSG00000133056	PIK3C2B PPI subnetwork	4.40×10 ⁻³
MP:0005095	Decreased T cell proliferation	4.84×10 ⁻³
ENSG00000149257	SERPINH1 PPI subnetwork	5.79×10 ⁻³
ENSG00000034152	MAP2K3 PPI subnetwork	6.58×10 ⁻³
ENSG00000017427	IGF1 PPI subnetwork	7.51×10 ⁻³
GO:0043406	Positive regulation of MAP kinase activity	7.65×10 ⁻³
MP:0000180	Abnormal circulating cholesterol level	7.71×10 ⁻³
MP:0001915	Intracranial hemorrhage	8.00×10 ⁻³
MP:0004883	Abnormal vascular wound healing	8.15×10 ⁻³
ENSG00000106992	AK1 PPI subnetwork	8.69×10 ⁻³
MP:0003419	Delayed endochondral bone ossification	8.98×10 ⁻³
MP:0000716	Abnormal immune system cell morphology	9.63×10 ⁻³
ENSG00000170581	STAT2 PPI subnetwork	9.79×10 ⁻³
GO:0043277	Apoptotic cell clearance	9.98×10 ⁻³
MP:0001828	Abnormal T—ell activation	0.01
ENSG00000141506	PIK3R5 PPI subnetwork	0.01

(Continued)

Table 2. Continued

Original Gene Set ID	Original Gene Set Description	DEPICT Nominal P Value
GO:0000989	Transcription factor binding/transcription factor activity	0.01
GO:0007254	JNK cascade	0.01
GO:0014910	Regulation of smooth muscle cell migration	0.02
MP:0001552	Increased circulating triglyceride level	0.02
MP:0001559	Hyperglycemia	0.02
ENSG00000105851	PIK3CG PPI subnetwork	0.02
GO:0050900	Leukocyte migration	0.03
MP:0003957	Abnormal nitric oxide homeostasis	0.03
GO:0006953	Acute-phase response	0.03
ENSG00000206240	HLA-DRB1 PPI subnetwork	0.03
GO:0043123	Positive regulation of I-kappaB kinase/NF-kappaB cascade	0.03
ENSG00000145431	PDGFC PPI subnetwork	0.04
MP:0008706	Decreased interleukin-6 secretion	0.04
MP:0008688	Decreased interleukin-2 secretion	0.04

This table is a truncated version of the full list available in the Online Table XVIII. DEPICT indicates Data-Driven Expression-Prioritized Integration for Complex Traits.

*The gene sets that had a false discovery rate of <0.2.

of heterogeneity at this locus in our analysis (Online Table VII), we consider that further investigation of this locus remains warranted despite our findings.

Our GWAS3D genome analysis predicted potential novel biological pathways in AAA pathogenesis. For example, *FGF9* was shown to have a possible distal interaction with the intergenic SNP rs9316871. *FGF9*, although not previously considered a strong candidate in AAA pathogenesis, was nevertheless at least partially validated by its increased mRNA expression in AAA tissue (Table 3). In AAA, both the medial and adventitial layers of the vessel wall are significantly more vascularized compared with nonaneurysmal tissue,⁵⁹ and it is therefore interesting to note that *FGF9* has been shown to enhance angiogenesis and neovascularization within mouse models of myocardial infarction.⁶⁰

The main strength of this study is the inclusion of all currently available worldwide GWAS data sets for AAA and formation of an expanded International Aneurysm Consortium. We acknowledge several limitations in our work. The overall numbers of samples included in our analysis are lower than for more common traits such as diabetes mellitus¹⁵ and CAD.¹⁶ We also did not have an adequate number of females in our sample set to perform sex-specific analyses that may

Table 3. Genes Predicted by GWAS3D Analysis to Be Associated With Putative AAA Loci Identified in the Discovery Study Demonstrating Significantly Different mRNA Expression in Aneurysmal Aortic Wall Samples From 49 Patients With AAA Compared With 10 Organ Donor Control Aortic Samples

GWAS3D Gene Selection Criteria	Gene	Locus	mRNA <i>P</i> Value	AAA mRNA expression
Predicted distal interaction (SORT1)	BCAR3	1p22.1	1.8×10 ⁻⁴	Decreased
SNP in proximity with lead SNP at AAA locus	SORT1	1p13.3	1.1×10 ⁻⁴	Decreased
Predicted distal interaction (SORT1)	NOTCH2	1p12	4.6×10 ⁻⁷	Increased
Predicted distal interaction (IL6R)	TDRD10	1q21.3	0.006	Increased
Predicted distal interaction (CDKN2BAS1/ANRIL)	UBE2W	8q21.11	0.030	Increased
SNP in proximity with lead SNP at AAA locus	CDKN2BAS1/ANRIL	9p21.3	0.003	Increased
SNP in proximity with lead SNP at AAA locus	LRP1	12q13.3	0.008	Decreased
SNP in proximity with lead SNP at AAA locus	NAB2	12q13.3	1.1×10 ⁻⁵	Decreased
Predicted distal interaction (LINC0540)	FGF9	13q11	0.002	Increased
SNP in proximity with lead SNP at AAA locus	PLTP	20q13.12	0.011	Increased

Nonsignificant results (30 genes) are shown in Online Table XXIII, and box and whiskers plots on mRNA expression levels are presented in Online Figure IV. See Figure 4 for results from the GWAS3D analysis. AAA indicates abdominal aortic aneurysm; GWAS, genome-wide association studies; and SNP, single nucleotide polymorphism.

have been informative given the strong sexual dimorphism exhibited by AAA.⁶¹ We recognize this limitation, but the current focus of AAA screening programs on men alone^{2,3} and the much reduced prevalence of AAA in women means that collecting adequate samples for such analyses is likely to be challenging. Some of the contributing GWAS studies such as the Aneurysm Consortium GWAS were derived from multicenter sample collections that led to intercohort heterogeneity in clinical phenotyping of the case groups. Together with the limited covariate data available for the control groups in the GWAS studies that used population control samples, this led to an inability to reliably adjust for clinical covariates in our overall analysis. Given these limitations, and in particular about the numbers of samples available for analysis in AAA, alternative approaches for investigating the genetic cause of AAA need to be considered. The natural history of AAA with a long latent period (if detected early), during which patients are monitored by serial imaging studies, offers the opportunity to study disease progression as a continuous trait, leveraging additional power over discrete trait approaches for the limited sample sizes available.³⁷

In conclusion, our meta-GWAS and the bioinformatics analyses, applying multiple techniques, has highlighted

several potentially novel mechanisms of AAA pathobiology. These will require direct investigation in future studies to confirm their role in the development and progression of AAA.

Acknowledgments

The Abdominal Aortic Aneurysm Consortium made use of the Wellcome Trust Case Control Consortium data. The full list of investigators is available at www.wtccc.org.uk. Data on coronary artery disease/myocardial infarction were contributed by CARDIoGRAMplusC4D (Coronary ARtery DIsease Genome wide Replication and Meta-analysis) investigators and were downloaded from www.CARDIOGRAMPLUSC4D.ORG. Data on Blood Pressure were contributed by the International Consortium for Blood Pressure. Contributing members of all consortia are listed in the Online Supplement.

Sources of Funding

The Wellcome Trust Case Control Consortium project was funded by the Wellcome Trust (awards 076113 and 085475). The New Zealand project was funded by the Health Research Council of New Zealand (08–75, 14–155). Recruitment of abdominal aortic aneurysm patients and controls in Belgium, Canada, and Pittsburgh, USA, was funded in part by the National Heart, Lung, and Blood Institute, National Institutes of Health (HL064310 and HL044682). The Geisinger sample collection was funded in part by the Pennsylvania Commonwealth Universal Research Enhancement program, the Geisinger Clinical Research Fund, the American Heart Association, and the Ben Franklin Technology Development Fund of Pennsylvania. The Barts and the Leicester Cardiovascular Biomedical Research Units are funded by the National Institute for Health Research. The eMERGE (electronic Medical Records and Genomics) Network is funded by the National Human Genome Research Institute, with additional funding from the National Institute of General Medical Sciences through the following grants: U01HG004438 to Johns Hopkins University; U01HG004424 to The Broad Institute; U01HG004438 to CIDR; U01HG004610 and U01HG006375 to Group Health Cooperative; U01HG004608 to Marshfield Clinic; U01HG006389 to Essentia Institute of Rural Health; U01HG04599 and U01HG006379 to Mayo Clinic; U01HG004609 and U01HG006388 to Northwestern University; U01HG04603 and U01HG006378 to Vanderbilt University; U01HG006385 to the Coordinating Center; U01HG006382 to Geisinger Health System; U01HG006380 to Icahn School of Medicine Mount Sinai. The generation and management of genome-wide association study (GWAS) data for the Rotterdam Study (control samples for the Dutch GWAS) is supported by the Netherlands Organization of Scientific Research (NWO) Investments (175.010.2005.011, 911-03-012). This study is funded by the Research Institute for Diseases in the Elderly (014-93-015; RIDE2), the Netherlands Genomics Initiative/NWO project nr. 050-060-810. The Italian sample collection were funded by grants from Ente Cassa di Risparmio di Firenze to Fiorgen Foundation, Florence, Italy, and from the Italian Ministry of Health. Sample collections from Poland were funded in part by the National Science Centre in Poland (6P05A03921, NN403250440). The Mayo Vascular Disease Biorepository was funded by a Marriot Award for Individualized Medicine and an Award from the Mayo Center of Individualized Medicine. The Vanderbilt data set(s) were obtained from Vanderbilt University Medical Center's BioVU supported by institutional funding and by the National Center for Research Resources (UL1 RR024975-01, which is now at the National Center for Advancing Translational Sciences, UL1 TR000445-06). The ASAP study (Advanced Study of Aortic Pathology) was supported by the Swedish Research Council, the Swedish Heart-Lung Foundation, the Leducq Foundation (MIBAVA), and a donation by Fredrik Lundberg. S.E. Humphries holds a Chair funded by the British Heart Foundation, and is supported by the British Heart Foundation (BHF; PG08/008) and by the National Institute for Health Research University College London Hospitals Biomedical Research Centre. The Cardiogenics project was supported by the European Union 6th

Framework Programme (LSHM-CT-2006-037593). S.C. Harrison was funded by a BHF clinical training fellowship (FS/11/16/28696). The Stockholm-Tartu Atherosclerosis Reverse Network Engineering Task biobank and the generation of the RNASeq data set was funded by Astra-Zeneca Translational Science Centre-Karolinska Institutet, the University of Tartu (SPIGVARENG), the Estonian Research Council (ETF 8853), the Torsten and Ragnar Söderberg Foundation, the Knut and Alice Wallenberg Foundation, the American Heart Association (A14SFRN20840000) and by the National Institute of Health (R01HL71207).

Appendix

From the Surgery Department (G.T.J., V.L.P., W.W., I.A.T., J.K., G.B.H., A.M.v.R.), Medicine Department (M.J.A.W.), and Biochemistry Department (T.R.M.), University of Otago, Dunedin, New Zealand; The Sigfried and Janet Weis Center for Research (G.T., H.K., R.E., K.M.B., D.T.S., D.J.C.) and Biomedical and Translational Informatics (M.D.R., S.P.), Geisinger Health System, Danville, PA; Division of Molecular Biology and Human Genetics, Department of Biomedical Sciences, Faculty of Medicine and Health Sciences, Stellenbosch University, Tygerberg, South Africa (G.T., H.K.); deCODE/Amgen, Reykjavik, Iceland (S.G., G.T., U.T., A.R., K.S.); Department of Medical Genetics (A.F.B., P.I.W.d.B.), and Department of Epidemiology, Julius Center for Health Sciences and Primary Care (P.I.W.d.B.), University Medical Center Utrecht, The Netherlands; Atherothrombotic Disease Center, Department of Experimental and Clinical Medicine (B.G., S.G., C.S., R.A., A.C.) and Vascular Surgery Unit, Department of Experimental and Clinical Medicine (R.P., C.P.), University of Florence, Careggi Hospital, Florence, Italy; Institute of Human Genetics, Polish Academy of Sciences, Faculty of Nucleic Acid Function, Poznan, Poland (E.S.); Department of General and Vascular Surgery, Poznan University of Medical Sciences, Poland (E.S., G.O.); Department of Cardiovascular Sciences (T.R.W., A.S., A.R.V., S.P.R.R., S.E.H., A.H.G., C.P.N., R.D.S., S.C.H., N.J.S., M.J.B.) and Department of Health Sciences (J.R.T.), University of Leicester, United Kingdom; NIHR Leicester Cardiovascular Biomedical Research Unit, Glenfield General Hospital, Leicester, United Kingdom (T.R.W., A.S., A.R.V., S.E.H., A.H.G., C.P.N., N.J.S., M.J.B.); The Pennsylvania State University, University Park, PA (M.D.R., A.V., S.P., S.S.V.); The Department of Vascular Surgery at Geisinger Medical Center, Danville, PA (J.R.E., E.J.R.); Mayo Clinic Rochester, MN (I.J.K., Z.Y., M.d.A.); Marshfield Clinic Research Foundation, WI (P.L.P.); Icahn School of Medicine at Mount Sinai (O.G., E.P.B.) and Department of Genetics and Genomic Sciences, Institute of Genomics and Multiscale Biology (O.F., E.E.S., J.L.M.B.), Icahn School of Medicine at Mount Sinai, New York, NY; Vanderbilt University Nashville, TN (J.M.); Northwestern University Feinberg School of Medicine, Chicago, IL (L.J.R.-T., J.A.P.); Department of Biomedical Informatics and Medical Education, University of Washington, Seattle (D.R.C.); Research Division, Essentia Institute of Rural Health, Duluth, MN (C.A.M.); Case Western Reserve University, Cleveland, OH (D.C.C.); Group Health Research Institute, Seattle, WA (D.S.C.); Department of Medical Genetics and Molecular Biochemistry, Temple University School of Medicine, PA (G.S.G.); Mission Clinic, Mission Health System, Asheville, NC (D.P.F.); Waikato Hospital, Hamilton, New Zealand (R.B., T.M.V.); Auckland City Hospital, New Zealand (A.A.H.); Surgery Department, University of Otago, Christchurch, New Zealand (D.R.L., J.R.); Genetics of Complex Traits in Humans Group, Wellcome Trust Sanger Institute, Cambridge, United Kingdom (S.B.), School of Medicine (S.A.B.) and Centre for Public Health (D.T.B.), Queens University Belfast, United Kingdom; Department of Vascular Surgery (R.E.C.) and Department of Vascular Surgery, Cardiovascular Division/British Heart Foundation Centre of Research Excellence (A.S.), King's College London, United Kingdom; Department of Vascular Surgery, St George's University of London, United Kingdom (G.C., M.M.T.); King Faisal Specialist Hospital and Research Centre, Jeddah, Saudi Arabia (H.H.); The Leeds Institute of Cardiovascular and Metabolic Medicine, University of Leeds, United Kingdom (D.J.A.S., T.S.F., S.P.R.R.,

K.B., K.J.G., M.A.B.); Department of Surgery, University of Western Australia, Crawley, Australia (F.M.v.B., P.E.N.); Laekning Medical Clinics, Reykjavik, Iceland (S.E.M.); University of Iceland, Faculty of Medicine, Reykjavik (U.T., K.S.); Department of Vascular Surgery, VU Medical Center, Amsterdam, The Netherlands (J.D.B.); CAPHRI Research School, University Maastricht, Eindhoven, The Netherlands (J.A.W.T.); Department of Vascular Surgery, Catharina Ziekenhuis, Eindhoven, The Netherlands (J.A.W.T., M.R.v.S.); Department of Genetics, UMC Groningen, The Netherlands (C.W.); Radboud University Medical Centre, Radboud Institute for Health Sciences, Nijmegen, The Netherlands (J.d.G., L.A.K.); Elitry Research Centre of Individualized Medicine in Arterial Disease (CIMA), Department of Cardiothoracic and Vascular Surgery, Odense University Hospital, Denmark (J.S.L.); Belfast, United Kingdom (A.H.); William Harvey Research Institute, Barts and The London School of Medicine and Dentistry, Queen Mary University of London, United Kingdom (K.S., P.D.); Department of Haematology, University of Cambridge, United Kingdom (K.S.); Vascular Biology Unit, Queensland Research Centre for Peripheral Vascular Disease and the Department of Vascular and Endovascular Surgery, James Cook University and Townsville Hospital, Australia (J.G.); Department of Surgery and Cancer, Imperial College London, United Kingdom (J.T.P.); Cardiovascular Genetics, Institute of Cardiovascular Science, University College London, United Kingdom (S.E.H.); Surgical Research Center GIGA-Cardiovascular Science Unit, University of Liège, Belgium (N.S.); Department of Human Genetics, University of Pittsburgh School of Public Health, PA (R.E.F.); Atherosclerosis Research Unit, Center for Molecular Medicine, Department of Medicine (P.E., L.F.), Cardiothoracic Surgery Unit, Department of Molecular Medicine and Surgery (A.F.-C.), Department of Medical Biochemistry and Biophysics, Vascular Biology Unit (C.B.), Department of Medical Biochemistry and Biophysics (J.L.M.B.), Karolinska Institutet, Stockholm, Sweden; Center for Biological Sequence Analysis, Technical University of Denmark, Copenhagen, Denmark (L.F.); Center for Population Studies, National Heart, Lung, and Blood Institute, The Framingham Heart Study, MA (J.D.E., A.D.J.); Department of Immunology, Genetics and Pathology, Rudbeck Laboratory, Uppsala University, Sweden (C.B.); Department of Physiology, Institute of Biomedicine and Translation Medicine, University of Tartu, Estonia (J.L.M.B.); Department of Cardiac Surgery, Tartu University Hospital, Estonia (A.R.); Clinical Gene Networks AB, Stockholm, Sweden (A.R., O.F., J.L.M.B.); Department of Neurology (L.L.) and Center for Molecular Medicine and Genetics (A.M.D.), Wayne State University, Detroit, MI; Department of Vascular and Endovascular Surgery, Paracelsus Medical University Nuremberg, Germany (E.L.V.); Department of Surgery (Division of Vascular Surgery), University Medical Center Groningen, University of Groningen, The Netherlands (C.J.Z.); Chirurgiecoöperatie Oost Nederland, Enschede, The Netherlands (R.H.G.); Department of Surgery, TweeSteden Hospital, Tilburg, The Netherlands (S.M.v.S.); Department of Vascular Surgery, Rijnstate Ziekenhuis, Arnhem, The Netherlands (S.M.v.S.); Department of Vascular Surgery, St. Antonius Hospital, Nieuwegein, The Netherlands (J.P.d.V.); and The Princess Al-Jawhara Al-Brahim Centre of Excellence in Research of Hereditary Disorders (PACER-HD), King Abdulaziz University, Jeddah, Saudi Arabia (P.D.).

Disclosures

Johan L.M. Björkegren is founder and major shareholder in Clinical Gene Networks AB (CGN) together with Arno Ruusalepp. Björkegren, Ruusalepp, and Eric E Schadt are members of the board of directors. Clinical Gene Networks AB has an invested interest in the Stockholm-Tartu Atherosclerosis Reverse Network Engineering Task biobank and data set.

References

1. Lederle FA. In the clinic. Abdominal aortic aneurysm. *Ann Intern Med.* 2009;150:ITC5-ITC1. doi: 10.7326/0003-4819-150-9-200905050-01005.
2. Guirguis-Blake JM, Beil TL, Senger CA, Whitlock EP. Ultrasonography screening for abdominal aortic aneurysms: a systematic evidence

- review for the U.S. Preventive Services Task Force. *Ann Intern Med*. 2014;160:321–329. doi: 10.7326/M13-1844.
- Abdominal aortic aneurysm screening: 2014 to 2015 data. The NHS AAA Screening Programme. <https://www.gov.uk/government/publications/abdominal-aortic-aneurysm-screening-2014-to-2015-data>. Accessed July 12, 2016.
 - Wahlgren CM, Larsson E, Magnusson PK, Hultgren R, Swedenborg J. Genetic and environmental contributions to abdominal aortic aneurysm development in a twin population. *J Vasc Surg*. 2010;51:3–7; discussion 7. doi: 10.1016/j.jvs.2009.08.036.
 - Larsson E, Granath F, Swedenborg J, Hultgren R. A population-based case-control study of the familial risk of abdominal aortic aneurysm. *J Vasc Surg*. 2009;49:47–50; discussion 51. doi: 10.1016/j.jvs.2008.08.012.
 - Gretarsdottir S, Baas AF, Thorleifsson G, et al. Genome-wide association study identifies a sequence variant within the DAB2IP gene conferring susceptibility to abdominal aortic aneurysm. *Nat Genet*. 2010;42:692–697. doi: 10.1038/ng.622.
 - Bown MJ, Jones GT, Harrison SC, et al; CARDIoGRAM Consortium; Global BPgen Consortium; DIAGRAM Consortium; VRCNZ Consortium. Abdominal aortic aneurysm is associated with a variant in low-density lipoprotein receptor-related protein 1. *Am J Hum Genet*. 2011;89:619–627. doi: 10.1016/j.ajhg.2011.10.002.
 - Bradley DT, Hughes AE, Badger SA, et al. A variant in LDLR is associated with abdominal aortic aneurysm. *Circ Cardiovasc Genet*. 2013;6:498–504. doi: 10.1161/CIRCGENETICS.113.000165.
 - Jones GT, Bown MJ, Gretarsdottir S, et al. A sequence variant associated with sortilin-1 (SORT1) on 1p13.3 is independently associated with abdominal aortic aneurysm. *Hum Mol Genet*. 2013;22:2941–2947. doi: 10.1093/hmg/ddt141.
 - Harrison SC, Smith AJ, Jones GT, et al; Aneurysm Consortium. Interleukin-6 receptor pathways in abdominal aortic aneurysm. *Eur Heart J*. 2013;34:3707–3716. doi: 10.1093/eurheartj/ehs354.
 - Helgadottir A, Thorleifsson G, Magnusson KP, et al. The same sequence variant on 9p21 associates with myocardial infarction, abdominal aortic aneurysm and intracranial aneurysm. *Nat Genet*. 2008;40:217–224. doi: 10.1038/ng.72.
 - Willer CJ, Li Y, Abecasis GR. METAL: fast and efficient meta-analysis of genome-wide association scans. *Bioinformatics*. 2010;26:2190–2191. doi: 10.1093/bioinformatics/btq340.
 - Shi YY, He L. SHEsis, a powerful software platform for analyses of linkage disequilibrium, haplotype construction, and genetic association at polymorphism loci. *Cell Res*. 2005;15:97–98. doi: 10.1038/sj.cr.7290272.
 - Han B, Eskin E. Random-effects model aimed at discovering associations in meta-analysis of genome-wide association studies. *Am J Hum Genet*. 2011;88:586–598. doi: 10.1016/j.ajhg.2011.04.014.
 - Morris AP, Voight BF, Teslovich TM, et al; Wellcome Trust Case Control Consortium; Meta-Analyses of Glucose and Insulin-related traits Consortium (MAGIC) Investigators; Genetic Investigation of ANthropometric Traits (GIANT) Consortium; Asian Genetic Epidemiology Network–Type 2 Diabetes (AGEN-T2D) Consortium; South Asian Type 2 Diabetes (SAT2D) Consortium; DIAbetes Genetics Replication And Meta-analysis (DIAGRAM) Consortium. Large-scale association analysis provides insights into the genetic architecture and pathophysiology of type 2 diabetes. *Nat Genet*. 2012;44:981–990. doi: 10.1038/ng.2383.
 - Schunkert H, König IR, Kathiresan S, et al; Cardiogenics; CARDIoGRAM Consortium. Large-scale association analysis identifies 13 new susceptibility loci for coronary artery disease. *Nat Genet*. 2011;43:333–338. doi: 10.1038/ng.784.
 - Willer CJ, Schmidt EM, Sengupta S, et al. Discovery and refinement of loci associated with lipid levels. *Nat Genet*. 2013;45:1274–1283.
 - Wain LV, Verwoert GC, O'Reilly PF, et al; LifeLines Cohort Study; EchoGen consortium; AortaGen Consortium; CHARGE Consortium Heart Failure Working Group; KidneyGen consortium; CKDGen consortium; Cardiogenics consortium; CardioGram. Genome-wide association study identifies six new loci influencing pulse pressure and mean arterial pressure. *Nat Genet*. 2011;43:1005–1011. doi: 10.1038/ng.922.
 - Ramos EM, Hoffman D, Junkins HA, Maglott D, Phan L, Sherry ST, Feolo M, Hindorf LA. Phenotype-Genotype Integrator (PheGenI): synthesizing genome-wide association study (GWAS) data with existing genomic resources. *Eur J Hum Genet*. 2014;22:144–147. doi: 10.1038/ejhg.2013.96.
 - Leslie R, O'Donnell CJ, Johnson AD. GRASP: analysis of genotype-phenotype results from 1390 genome-wide association studies and corresponding open access database. *Bioinformatics*. 2014;30:i185–i194. doi: 10.1093/bioinformatics/btu273.
 - Denny JC, Ritchie MD, Basford MA, Pulley JM, Bastarache L, Brown-Gentry K, Wang D, Masys DR, Roden DM, Crawford DC. TheWAS: demonstrating the feasibility of a phenome-wide scan to discover gene-disease associations. *Bioinformatics*. 2010;26:1205–1210. doi: 10.1093/bioinformatics/btq126.
 - Pendergrass SA, Brown-Gentry K, Dudek S, et al. Phenome-wide association study (PheWAS) for detection of pleiotropy within the Population Architecture using Genomics and Epidemiology (PAGE) Network. *PLoS Genet*. 2013;9:e1003087. doi: 10.1371/journal.pgen.1003087.
 - Gottesman O, Kuivaniemi H, Tromp G, et al; eMERGE Network. The Electronic Medical Records and Genomics (eMERGE) Network: past, present, and future. *Genet Med*. 2013;15:761–771. doi: 10.1038/gim.2013.72.
 - Reumers J, Conde L, Medina I, Maurer-Stroh S, Van Durme J, Dopazo J, Rousseau F, Schymkowitz J. Joint annotation of coding and non-coding single nucleotide polymorphisms and mutations in the SNPeff and PupaSuite databases. *Nucleic Acids Res*. 2008;36:D825–D829. doi: 10.1093/nar/gkm979.
 - Li MJ, Wang LY, Xia Z, Sham PC, Wang J. GWAS3D: Detecting human regulatory variants by integrative analysis of genome-wide associations, chromosome interactions and histone modifications. *Nucleic Acids Res*. 2013;41:W150–W158. doi: 10.1093/nar/gkt456.
 - Pers TH, Karjalainen JM, Chan Y, et al; Genetic Investigation of ANthropometric Traits (GIANT) Consortium. Biological interpretation of genome-wide association studies using predicted gene functions. *Nat Commun*. 2015;6:5890. doi: 10.1038/ncomms6890.
 - Folkersen L, van't Hooft F, Chernogubova E, Agardh HE, Hansson GK, Hedin U, Liska J, Syvänen AC, Paulsson-Berne G, Paulsson-Berne G, Franco-Cereceda A, Hamsten A, Gabrielsen A, Eriksson P; BiKE and ASAP Study Groups. Association of genetic risk variants with expression of proximal genes identifies novel susceptibility genes for cardiovascular disease. *Circ Cardiovasc Genet*. 2010;3:365–373. doi: 10.1161/CIRCGENETICS.110.948935.
 - Björkregren JL, Kovacic JC, Dudley JT, Schadt EE. Genome-wide significant loci: how important are they? Systems genetics to understand heritability of coronary artery disease and other common complex disorders. *J Am Coll Cardiol*. 2015;65:830–845. doi: 10.1016/j.jacc.2014.12.033.
 - Kuivaniemi H, Platsoucas CD, Tilson MD 3rd. Aortic aneurysms: an immune disease with a strong genetic component. *Circulation*. 2008;117:242–252. doi: 10.1161/CIRCULATIONAHA.107.690982.
 - Biros E, Gabel G, Moran CS, Schreurs C, Lindeman JH, Walker PJ, Nataatmadja M, West M, Holdt LM, Hinterseher I, Pilarsky C, Golledge J. Differential gene expression in human abdominal aortic aneurysm and aortic occlusive disease. *Oncotarget*. 2015;6:12984–12996. doi: 10.18632/oncotarget.3848.
 - Pahl MC, Erdman R, Kuivaniemi H, Lillvis JH, Elmore JR, Tromp G. Transcriptional (ChIP-Chip) analysis of ELF1, ETS2, RUNX1 and STAT5 in human abdominal aortic aneurysm. *Int J Mol Sci*. 2015;16:11229–11258. doi: 10.3390/ijms160511229.
 - Kamburov A, Stelzl U, Lehrach H, Herwig R. The ConsensusPathDB interaction database: 2013 update. *Nucleic Acids Res*. 2013;41:D793–D800. doi: 10.1093/nar/gks1055.
 - Pentchev K, Ono K, Herwig R, Ideker T, Kamburov A. Evidence mining and novelty assessment of protein-protein interactions with the ConsensusPathDB plugin for Cytoscape. *Bioinformatics*. 2010;26:2796–2797. doi: 10.1093/bioinformatics/btq522.
 - Nguyen H, Allali-Hassani A, Antonyamy S, et al. LLY-507, a cell-active, potent, and selective inhibitor of protein-lysine methyltransferase SMYD2. *J Biol Chem*. 2015;290:13641–13653. doi: 10.1074/jbc.M114.626861.
 - Xu G, Liu G, Xiong S, Liu H, Chen X, Zheng B. The histone methyltransferase Smyd2 is a negative regulator of macrophage activation by suppressing interleukin 6 (IL-6) and tumor necrosis factor α (TNF- α) production. *J Biol Chem*. 2015;290:5414–5423. doi: 10.1074/jbc.M114.610345.
 - Deloukas P, Kanoni S, Willenborg C, et al. Large-scale association analysis identifies new risk loci for coronary artery disease. *Nat Genet*. 2013;45:25–33.
 - Eicher JD, Landowski C, Stackhouse B, Sloan A, Chen W, Jensen N, Lien JP, Leslie R, Johnson AD. GRASP v2.0: an update on the Genome-Wide Repository of Associations between SNPs and phenotypes. *Nucleic Acids Res*. 2015;43:D799–D804. doi: 10.1093/nar/gku1202.
 - Smelser DT, Tromp G, Elmore JR, Kuivaniemi H, Franklin DP, Kirchner HL, Carey DJ. Population risk factor estimates for abdominal aortic aneurysm from electronic medical records: a case control study. *BMC Cardiovasc Disord*. 2014;14:174. doi: 10.1186/1471-2261-14-174.

39. Zhang X, Gierman HJ, Levy D, Plump A, Dobrin R, Goring HH, Curran JE, Johnson MP, Blangero J, Kim SK, O'Donnell CJ, Emilsson V, Johnson AD. Synthesis of 53 tissue and cell line expression QTL datasets reveals master eQTLs. *BMC Genomics*. 2014;15:532. doi: 10.1186/1471-2164-15-532.
40. Hannou SA, Wouters K, Paumelle R, Staels B. Functional genomics of the CDKN2A/B locus in cardiovascular and metabolic disease: what have we learned from GWASs? *Trends Endocrinol Metab*. 2015;26:176–184. doi: 10.1016/j.tem.2015.01.008.
41. Pearce WH, Shively VP. Abdominal aortic aneurysm as a complex multifactorial disease: interactions of polymorphisms of inflammatory genes, features of autoimmunity, and current status of MMPs. *Ann NY Acad Sci*. 2006;1085:117–132. doi: 10.1196/annals.1383.025.
42. Coleman C, Quinn EM, Ryan AW, et al. Common polygenic variation in coeliac disease and confirmation of ZNF335 and NIFA as disease susceptibility loci. *Eur J Hum Genet*. 2016;24:291–297. doi: 10.1038/ejhg.2015.87.
43. Kim DS, Burt AA, Ranchalis JE, Vuletic S, Vaisar T, Li WF, Rosenthal EA, Dong W, Eintracht JF, Motulsky AG, Brunzell JD, Albers JJ, Furlong CE, Jarvik GP. PLTP activity inversely correlates with CAAD: effects of PON1 enzyme activity and genetic variants on PLTP activity. *J Lipid Res*. 2015;56:1351–1362. doi: 10.1194/jlr.P058032.
44. Wythe JD, Dang LT, Devine WP, Boudreau E, Artap ST, He D, Schachterle W, Stainier DY, Oettgen P, Black BL, Bruneau BG, Fish JE. ETS factors regulate Vegf-dependent arterial specification. *Dev Cell*. 2013;26:45–58. doi: 10.1016/j.devcel.2013.06.007.
45. Choke E, Cockerill GW, Dawson J, Wilson RW, Jones A, Loftus IM, Thompson MM. Increased angiogenesis at the site of abdominal aortic aneurysm rupture. *Ann NY Acad Sci*. 2006;1085:315–319. doi: 10.1196/annals.1383.007.
46. Choke E, Thompson MM, Dawson J, Wilson WR, Sayed S, Loftus IM, Cockerill GW. Abdominal aortic aneurysm rupture is associated with increased medial neovascularization and overexpression of proangiogenic cytokines. *Arterioscler Thromb Vasc Biol*. 2006;26:2077–2082. doi: 10.1161/01.ATV.0000234944.22509.f9.
47. Norman PE, Powell JT. Site specificity of aneurysmal disease. *Circulation*. 2010;121:560–568. doi: 10.1161/CIRCULATIONAHA.109.880724.
48. Tian TV, Tomavo N, Huot L, Flourens A, Bonnelye E, Flajollet S, Hot D, Leroy X, de Launoit Y, Duterque-Coquillaud M. Identification of novel TMPRSS2:ERG mechanisms in prostate cancer metastasis: involvement of MMP9 and PLXNA2. *Oncogene*. 2014;33:2204–2214. doi: 10.1038/onc.2013.176.
49. Du SJ, Tan X, Zhang J. SMYD proteins: key regulators in skeletal and cardiac muscle development and function. *Anat Rec (Hoboken)*. 2014;297:1650–1662. doi: 10.1002/ar.22972.
50. Qi J, Yang P, Yi B, Huo Y, Chen M, Zhang J, Sun J. Heat shock protein 90 inhibition by 17-DMAG attenuates abdominal aortic aneurysm formation in mice. *Am J Physiol Heart Circ Physiol*. 2015;308:H841–H852. doi: 10.1152/ajpheart.00470.2014.
51. Sesé B, Barrero MJ, Fabregat MC, Sander V, Izpisua Belmonte JC. SMYD2 is induced during cell differentiation and participates in early development. *Int J Dev Biol*. 2013;57:357–364. doi: 10.1387/ijdb.130051ji.
52. Reed D, Reed C, Stemmermann G, Hayashi T. Are aortic aneurysms caused by atherosclerosis? *Circulation*. 1992;85:205–211.
53. Pajajanen TA, Oksala NK, Kuukasjärvi P, Karhunen PJ. Short stature is associated with coronary heart disease: a systematic review of the literature and a meta-analysis. *Eur Heart J*. 2010;31:1802–1809. doi: 10.1093/eurheartj/ehq155.
54. Nelson CP, Hamby SE, Saleheen D, et al; CARDIoGRAM+C4D Consortium. Genetically determined height and coronary artery disease. *N Engl J Med*. 2015;372:1608–1618. doi: 10.1056/NEJMoa1404881.
55. Chan CY, Chan YC, Cheuk BL, Cheng SW. A pilot study on low-density lipoprotein receptor-related protein-1 in Chinese patients with abdominal aortic aneurysm. *Eur J Vasc Endovasc Surg*. 2013;46:549–556. doi: 10.1016/j.ejvs.2013.08.006.
56. Muratoglu SC, Belgrave S, Hampton B, Migliorini M, Coksaygan T, Chen L, Mikhailenko I, Strickland DK. LRP1 protects the vasculature by regulating levels of connective tissue growth factor and HtrA1. *Arterioscler Thromb Vasc Biol*. 2013;33:2137–2146. doi: 10.1161/ATVBAHA.113.301893.
57. Guo DC, Grove ML, Prakash SK, et al; GenTAC Investigators; BAVCon Investigators. Genetic variants in LRP1 and ULK4 are associated with acute aortic dissections. *Am J Hum Genet*. 2016;99:762–769. doi: 10.1016/j.ajhg.2016.06.034.
58. Chasman DI, Schürks M, Anttila V, et al. Genome-wide association study reveals three susceptibility loci for common migraine in the general population. *Nat Genet*. 2011;43:695–698. doi: 10.1038/ng.856.
59. Jones GT. The pathohistology of abdominal aortic aneurysm. In: Grundmann R (Ed.), *Diagnosis, Screening and Treatment of Abdominal, Thoracoabdominal and Thoracic Aortic Aneurysms*. Rijeka: InTech; 2011. Last accessed December 20, 2016. doi: 10.5772/7746.
60. Singla D, Wang J. Fibroblast growth factor-9 activates c-Kit progenitor cells and enhances angiogenesis in the infarcted diabetic heart. *Oxid Med Cell Longev*. 2016;2016:5810908. doi: 10.1155/2016/5810908.
61. Bloomer LD, Bown MJ, Tomaszewski M. Sexual dimorphism of abdominal aortic aneurysms: a striking example of “male disadvantage” in cardiovascular disease. *Atherosclerosis*. 2012;225:22–28. doi: 10.1016/j.atherosclerosis.2012.06.057.

Meta-Analysis of Genome-Wide Association Studies for Abdominal Aortic Aneurysm Identifies Four New Disease-Specific Risk Loci

Gregory T. Jones, Gerard Tromp, Helena Kuivaniemi, Solveig Gretarsdottir, Annette F. Baas, Betti Giusti, Ewa Strauss, Femke N.G. van't Hof, Thomas R. Webb, Robert Erdman, Marylyn D. Ritchie, James R. Elmore, Anurag Verma, Sarah Pendergrass, Iftikhar J. Kullo, Zi Ye, Peggy L. Peissig, Omri Gottesman, Shefali S. Verma, Jennifer Malinowski, Laura J.

Rasmussen-Torvik, Kenneth M. Borthwick, Diane T. Smelser, David R. Crosslin, Mariza de Andrade, Evan J. Ryer, Catherine A. McCarty, Erwin P. Böttiger, Jennifer A. Pacheco, Dana C. Crawford, David S. Carrell, Glenn S. Gerhard, David P. Franklin, David J. Carey, Victoria L.

Phillips, Michael J.A. Williams, Wenhua Wei, Ross Blair, Andrew A. Hill, Thodor M. Vasudevan, David R. Lewis, Ian A. Thomson, Jo Krysa, Geraldine B. Hill, Justin Roake, Tony R. Merriman, Grzegorz Oszkinis, Silvia Galora, Claudia Saracini, Rosanna Abbate, Raffaele Pulli, Carlo Pratesi, Athanasios Saratzis, Ana R. Verissimo, Suzannah Bumpstead, Stephen A. Badger, Rachel E. Clough, Gillian Cockerill, Hany Hafez, D. Julian A. Scott, T. Simon Futers, Simon P.R. Romaine, Katherine Bridge, Kathryn J. Griffin, Marc A. Bailey, Alberto Smith,

Matthew M. Thompson, Frank M. van Bockxmeer, Stefan E. Matthiasson, Gudmar Thorleifsson, Unnur Thorsteinsdottir, Jan D. Blankensteijn, Joep A.W. Teijink, Cisca Wijmenga, Jacqueline de Graaf, Lambertus A. Kiemeny, Jes S. Lindholt, Anne Hughes, Declan T. Bradley, Kathleen Stirrups, Jonathan Golledge, Paul E. Norman, Janet T. Powell, Steve E. Humphries, Stephen E. Hamby, Alison H. Goodall, Christopher P. Nelson, Natzi Sakalihan, Audrey Courtois, Robert E. Ferrell, Per Eriksson, Lasse Folkersen, Anders Franco-Cereceda, John D. Eicher, Andrew D. Johnson, Christer Betsholtz, Arno Ruusalepp, Oscar Franzén, Eric E. Schadt, Johan L.M. Björkegren, Leonard Lipovich, Anne M. Drolet, Eric L. Verhoeven, Clark J. Zebregs, Robert H. Geelkerken, Marc R. van Sambeek, Steven M. van Sterkenburg, Jean-Paul de Vries, Kari Stefansson, John R. Thompson, Paul I.W. de Bakker, Panos Deloukas, Robert D. Sayers, Seamus C. Harrison, Andre M. van Rij, Nilesh J. Samani and Matthew J.

Bown

Permissions: Requests for permissions to reproduce figures, tables, or portions of articles originally published in *Circulation Research* can be obtained via RightsLink, a service of the Copyright Clearance Center, not the Editorial Office. Once the online version of the published article for which permission is being requested is located, click Request Permissions in the middle column of the Web page under Services. Further information about this process is available in the [Permissions and Rights Question and Answer](#) document.

Reprints: Information about reprints can be found online at:
<http://www.lww.com/reprints>

Subscriptions: Information about subscribing to *Circulation Research* is online at:
<http://circres.ahajournals.org/subscriptions/>

Circ Res. 2017;120:341-353; originally published online November 29, 2016;
doi: 10.1161/CIRCRESAHA.116.308765
Circulation Research is published by the American Heart Association, 7272 Greenville Avenue, Dallas, TX 75231
Copyright © 2016 American Heart Association, Inc. All rights reserved.
Print ISSN: 0009-7330. Online ISSN: 1524-4571

The online version of this article, along with updated information and services, is located on the
World Wide Web at:
<http://circres.ahajournals.org/content/120/2/341>
Free via Open Access

Data Supplement (unedited) at:
<http://circres.ahajournals.org/content/suppl/2016/11/29/CIRCRESAHA.116.308765.DC1>

Permissions: Requests for permissions to reproduce figures, tables, or portions of articles originally published in *Circulation Research* can be obtained via RightsLink, a service of the Copyright Clearance Center, not the Editorial Office. Once the online version of the published article for which permission is being requested is located, click Request Permissions in the middle column of the Web page under Services. Further information about this process is available in the [Permissions and Rights Question and Answer](#) document.

Reprints: Information about reprints can be found online at:
<http://www.lww.com/reprints>

Subscriptions: Information about subscribing to *Circulation Research* is online at:
<http://circres.ahajournals.org/subscriptions/>

Original gene set ID

MP:0006396
GO:0034381
ENSG000000205250
ENSG000000132005
MP:0000708
ENSG000000167553
ENSG000000170421
MP:0003645
ENSG000000166866
REACTOME_APOPTOTIC_EXECUTION__PHASE
MP:0008182
GO:0008375
ENSG000000131941
ENSG000000169710
REACTOME_APOPTOTIC_CLEAVAGE_OF_CELLULAR_PROTEINS
ENSG00000013297
ENSG000000070159
ENSG000000091409
ENSG000000178209
REACTOME_P75_NTR_RECEPTOR:MEDIATED_SIGNALLING
GO:0001890
ENSG000000164344
MP:0002136
MP:0002655
ENSG000000143375
MP:0005595
ENSG000000122641
MP:0002764
MP:0003662
ENSG000000169047
ENSG000000125503
MP:0001179
GO:0043256
ENSG000000116809
GO:0050431
ENSG000000039560
ENSG000000164733
ENSG000000139567
MP:0005590
GO:0071813
GO:0071814
MP:0002082
GO:0071902
ENSG000000130147
GO:0005178
ENSG000000133056
ENSG000000172725
ENSG000000136286
ENSG000000078142

Original gene set description

decreased long bone epiphyseal plate size
plasma lipoprotein particle clearance
E2F4 PPI subnetwork
RFX1 PPI subnetwork
thymus hyperplasia
TUBA1C PPI subnetwork
KRT8 PPI subnetwork
increased pancreatic beta cell number
MYO1A PPI subnetwork
REACTOME_APOPTOTIC_EXECUTION__PHASE
decreased marginal zone B cell number
acetylglucosaminyltransferase activity
RHPN2 PPI subnetwork
FASN PPI subnetwork
REACTOME_APOPTOTIC_CLEAVAGE_OF_CELLULAR_PROTEINS
CLDN11 PPI subnetwork
PTPN3 PPI subnetwork
ITGA6 PPI subnetwork
PLEC PPI subnetwork
REACTOME_P75_NTR_RECEPTOR:MEDIATED_SIGNALLING
placenta development
KLKB1 PPI subnetwork
abnormal kidney physiology
abnormal keratinocyte morphology
CGN PPI subnetwork
abnormal vascular smooth muscle physiology
INHBA PPI subnetwork
short tibia
abnormal long bone epiphyseal plate proliferative zone
IRS1 PPI subnetwork
PPP1R12C PPI subnetwork
thick pulmonary interalveolar septum
laminin complex
ZBTB17 PPI subnetwork
transforming growth factor beta binding
RAI14 PPI subnetwork
CTSB PPI subnetwork
ACVRL1 PPI subnetwork
increased vasodilation
lipoprotein particle binding
protein-lipid complex binding
postnatal lethality
positive regulation of protein serine/threonine kinase activity
SH3BP4 PPI subnetwork
integrin binding
PIK3C2B PPI subnetwork
CORO1B PPI subnetwork
MYO1G PPI subnetwork
PIK3C3 PPI subnetwork

Nominal P value

1.14E-09
5.22E-07
1.27E-06
2.28E-06
6.32E-06
3.18E-05
9.59E-05
1.12E-04
2.32E-04
2.92E-04
3.06E-04
3.62E-04
3.75E-04
4.55E-04
5.46E-04
6.28E-04
6.56E-04
7.26E-04
8.57E-04
1.07E-03
1.08E-03
1.09E-03
1.17E-03
1.45E-03
1.48E-03
1.55E-03
1.79E-03
1.79E-03
2.01E-03
2.21E-03
2.23E-03
2.30E-03
2.33E-03
2.46E-03
2.47E-03
2.60E-03
2.64E-03
2.75E-03
3.45E-03
3.51E-03
3.51E-03
3.53E-03
3.87E-03
3.91E-03
4.08E-03
4.40E-03
4.45E-03
4.65E-03
4.72E-03

Original gene set ID

MP:0005095
 ENSG00000145715
 ENSG00000104725
 KEGG_PATHWAYS_IN_CANCER
 GO:0008194
 ENSG00000078747
 ENSG00000149257
 ENSG00000114062
 ENSG00000139144
 ENSG00000143393
 ENSG00000148498
 ENSG00000196455
 ENSG00000148660
 ENSG00000034152
 ENSG00000123124
 MP:0008813
 ENSG00000204175
 GO:0001772
 REACTOME_CASPASE:MEDIATED_CLEAVAGE_OF_CYTOSKELETAL_PROTEINS
 ENSG00000017427
 MP:0001954
 GO:0016051
 GO:0043406
 REACTOME_CELL_DEATH_SIGNALLING_VIA_NRAGE_NRIF_AND_NADE
 MP:0000180
 ENSG00000170759
 ENSG00000180530
 ENSG00000138771
 ENSG00000065882
 ENSG00000138592
 MP:0001915
 ENSG00000131746
 MP:0004883
 ENSG00000091073
 ENSG00000081189
 ENSG00000154415
 ENSG00000188313
 MP:0004933
 ENSG00000147065
 ENSG00000165409
 ENSG00000106992
 GO:0007292
 ENSG00000144061
 MP:0003419
 ENSG00000110880
 ENSG00000197879
 ENSG00000176476
 ENSG00000176108
 REACTOME_INTEGRIN_CELL_SURFACE_INTERACTIONS

Original gene set description

decreased T cell proliferation
 RASA1 PPI subnetwork
 ENSG00000104725 PPI subnetwork
 KEGG_PATHWAYS_IN_CANCER
 UDP-glycosyltransferase activity
 ITCH PPI subnetwork
 SERPINH1 PPI subnetwork
 UBE3A PPI subnetwork
 PIK3C2G PPI subnetwork
 PI4KB PPI subnetwork
 PARD3 PPI subnetwork
 PIK3R4 PPI subnetwork
 CAMK2G PPI subnetwork
 MAP2K3 PPI subnetwork
 WWP1 PPI subnetwork
 decreased common myeloid progenitor cell number
 GPRIN2 PPI subnetwork
 immunological synapse
 REACTOME_CASPASE:MEDIATED_CLEAVAGE_OF_CYTOSKELETAL_PROTEINS
 IGF1 PPI subnetwork
 respiratory distress
 carbohydrate biosynthetic process
 positive regulation of MAP kinase activity
 REACTOME_CELL_DEATH_SIGNALLING_VIA_NRAGE_NRIF_AND_NADE
 abnormal circulating cholesterol level
 KIF5B PPI subnetwork
 NRIP1 PPI subnetwork
 SHROOM3 PPI subnetwork
 TBC1D1 PPI subnetwork
 USP8 PPI subnetwork
 intracranial hemorrhage
 TNS4 PPI subnetwork
 abnormal vascular wound healing
 ENSG00000091073 PPI subnetwork
 MEF2C PPI subnetwork
 PPP1R3A PPI subnetwork
 PLSCR1 PPI subnetwork
 abnormal epididymis epithelium morphology
 MSN PPI subnetwork
 TSHR PPI subnetwork
 AK1 PPI subnetwork
 female gamete generation
 NPHP1 PPI subnetwork
 delayed endochondral bone ossification
 CORO1C PPI subnetwork
 MYO1C PPI subnetwork
 CCDC101 PPI subnetwork
 CHMP6 PPI subnetwork
 REACTOME_INTEGRIN_CELL_SURFACE_INTERACTIONS

Nominal P value

4.84E-03
 4.96E-03
 5.08E-03
 5.17E-03
 5.46E-03
 5.48E-03
 5.79E-03
 5.85E-03
 5.85E-03
 5.87E-03
 6.00E-03
 6.19E-03
 6.48E-03
 6.58E-03
 6.95E-03
 7.37E-03
 7.39E-03
 7.40E-03
 7.46E-03
 7.51E-03
 7.56E-03
 7.65E-03
 7.65E-03
 7.67E-03
 7.71E-03
 7.79E-03
 7.86E-03
 7.89E-03
 7.97E-03
 7.99E-03
 8.00E-03
 8.01E-03
 8.15E-03
 8.22E-03
 8.24E-03
 8.33E-03
 8.55E-03
 8.61E-03
 8.64E-03
 8.64E-03
 8.69E-03
 8.93E-03
 8.95E-03
 8.98E-03
 9.04E-03
 9.22E-03
 9.31E-03
 9.44E-03
 9.47E-03

Original gene set ID	Original gene set description	Nominal P value
GO:0030247	polysaccharide binding	0.02
ENSG00000126934	MAP2K2 PPI subnetwork	0.02
ENSG00000110395	CBL PPI subnetwork	0.02
ENSG00000179151	EDC3 PPI subnetwork	0.02
ENSG00000154162	CDH12 PPI subnetwork	0.02
ENSG00000184363	PKP3 PPI subnetwork	0.02
ENSG00000020577	SAMD4A PPI subnetwork	0.02
MP:0004139	abnormal gastric parietal cell morphology	0.02
ENSG00000168476	REEP4 PPI subnetwork	0.02
ENSG00000110651	CD81 PPI subnetwork	0.02
ENSG00000134184	GSTM1 PPI subnetwork	0.02
ENSG00000105376	ICAM5 PPI subnetwork	0.02
ENSG00000196954	CASP4 PPI subnetwork	0.02
MP:0003704	abnormal hair follicle development	0.02
ENSG00000050820	BCAR1 PPI subnetwork	0.02
ENSG00000151748	SAV1 PPI subnetwork	0.02
GO:0003714	transcription corepressor activity	0.02
ENSG00000115904	SOS1 PPI subnetwork	0.02
ENSG00000175793	SFN PPI subnetwork	0.02
ENSG00000100345	MYH9 PPI subnetwork	0.02
GO:0035091	phosphatidylinositol binding	0.02
ENSG00000149930	TAOK2 PPI subnetwork	0.02
GO:0042054	histone methyltransferase activity	0.02
MP:0000689	abnormal spleen morphology	0.02
GO:0001892	embryonic placenta development	0.02
ENSG00000130294	KIF1A PPI subnetwork	0.02
ENSG00000148965	SAA4 PPI subnetwork	0.02
GO:0034774	secretory granule lumen	0.02
ENSG00000166483	WEE1 PPI subnetwork	0.02
ENSG00000110237	ARHGEF17 PPI subnetwork	0.02
GO:0032608	interferon-beta production	0.02
ENSG00000152518	ZFP36L2 PPI subnetwork	0.02
MP:0010792	abnormal stomach mucosa morphology	0.02
ENSG00000189319	FAM53B PPI subnetwork	0.02
ENSG00000117461	PIK3R3 PPI subnetwork	0.02
GO:0034362	low-density lipoprotein particle	0.02
ENSG00000134072	CAMK1 PPI subnetwork	0.02
ENSG00000163362	C1orf106 PPI subnetwork	0.02
MP:0002816	colitis	0.02
GO:0050900	leukocyte migration	0.03
GO:0044304	main axon	0.03
ENSG00000071909	MYO3B PPI subnetwork	0.03
ENSG00000100714	MTHFD1 PPI subnetwork	0.03
ENSG00000198836	OPA1 PPI subnetwork	0.03
ENSG00000197442	MAP3K5 PPI subnetwork	0.03
ENSG00000206306	HLA-DRB1 PPI subnetwork	0.03
ENSG00000206240	HLA-DRB1 PPI subnetwork	0.03
GO:0031983	vesicle lumen	0.03
KEGG_REGULATION_OF_ACTIN_CYTOSKELETON	KEGG_REGULATION_OF_ACTIN_CYTOSKELETON	0.03

Original gene set ID	Original gene set description	Nominal P value
GO:0004713	protein tyrosine kinase activity	0.03
GO:0006953	acute-phase response	0.03
GO:0003712	transcription cofactor activity	0.03
MP:0000295	trabecula carnea hypoplasia	0.03
ENSG00000105647	PIK3R2 PPI subnetwork	0.03
GO:0060205	cytoplasmic membrane-bounded vesicle lumen	0.03
ENSG00000107566	ERLIN1 PPI subnetwork	0.03
ENSG00000114270	COL7A1 PPI subnetwork	0.03
ENSG00000135930	EIF4E2 PPI subnetwork	0.03
MP:0006413	increased T cell apoptosis	0.03
ENSG00000211949	ENSG00000211949 PPI subnetwork	0.03
ENSG00000125731	SH2D3A PPI subnetwork	0.03
MP:0000414	alopecia	0.03
ENSG00000160691	SHC1 PPI subnetwork	0.03
MP:0001282	short vibrissae	0.03
MP:0003996	clonic seizures	0.03
ENSG00000019991	HGF PPI subnetwork	0.03
MP:0010025	decreased total body fat amount	0.03
GO:0007568	aging	0.03
GO:0042809	vitamin D receptor binding	0.03
MP:0005331	insulin resistance	0.03
GO:0045682	regulation of epidermis development	0.03
MP:0001923	reduced female fertility	0.03
MP:0001219	thick epidermis	0.03
ENSG00000068615	REEP1 PPI subnetwork	0.03
ENSG00000171219	CDC42BPG PPI subnetwork	0.03
MP:0009583	increased keratinocyte proliferation	0.03
ENSG00000105810	CDK6 PPI subnetwork	0.03
ENSG00000105662	CRTC1 PPI subnetwork	0.03
MP:0003957	abnormal nitric oxide homeostasis	0.03
KEGG_SMALL_CELL_LUNG_CANCER	KEGG_SMALL_CELL_LUNG_CANCER	0.03
GO:0030669	clathrin-coated endocytic vesicle membrane	0.03
ENSG00000100030	MAPK1 PPI subnetwork	0.03
GO:0046328	regulation of JNK cascade	0.03
GO:0014070	response to organic cyclic compound	0.03
GO:0033500	carbohydrate homeostasis	0.03
GO:0042593	glucose homeostasis	0.03
REACTOME_PTM_GAMMA_CARBOXYLATION_HYPUSINE_FORMATION_AND_AF	REACTOME_PTM_GAMMA_CARBOXYLATION_HYPUSINE_FORMATION_AND_ARYLS	0.03
REACTOME_REGULATION_OF_SIGNALING_BY_CBL	REACTOME_REGULATION_OF_SIGNALING_BY_CBL	0.03
MP:0002418	increased susceptibility to viral infectior	0.03
MP:0003721	increased tumor growth/size	0.03
GO:0071845	cellular component disassembly at cellular leve	0.03
GO:0030518	intracellular steroid hormone receptor signaling pathway	0.03
ENSG00000116824	CD2 PPI subnetwork	0.03
MP:0003566	abnormal cell adhesion	0.03
GO:0034061	DNA polymerase activity	0.03
ENSG00000141968	VAV1 PPI subnetwork	0.03
GO:0001701	in utero embryonic development	0.03
MP:0000166	abnormal chondrocyte morphology	0.03

Original gene set ID	Original gene set description	Nominal P value
MP:0003400	kinked neural tube	0.03
GO:0000790	nuclear chromatin	0.03
ENSG000000197102	DYNC1H1 PPI subnetwork	0.03
GO:0043566	structure-specific DNA binding	0.03
ENSG000000075413	MARK3 PPI subnetwork	0.03
GO:0000271	polysaccharide biosynthetic process	0.03
REACTOME_CELL:CELL_COMMUNICATION	REACTOME_CELL:CELL_COMMUNICATION	0.03
MP:0000410	waved hair	0.03
ENSG000000154556	SORBS2 PPI subnetwork	0.03
ENSG000000104368	PLAT PPI subnetwork	0.03
GO:0043123	positive regulation of I-kappaB kinase/NF-kappaB cascade	0.03
ENSG000000156127	BATF PPI subnetwork	0.03
ENSG000000132470	ITGB4 PPI subnetwork	0.03
GO:0038024	cargo receptor activity	0.03
ENSG000000100014	SPECC1L PPI subnetwork	0.03
ENSG000000163083	INHBB PPI subnetwork	0.03
ENSG000000110931	CAMKK2 PPI subnetwork	0.03
MP:0002088	abnormal embryonic growth/weight/body size	0.03
GO:0016571	histone methylation	0.03
GO:0033559	unsaturated fatty acid metabolic process	0.03
MP:0005350	increased susceptibility to autoimmune disorder	0.03
ENSG000000136111	TBC1D4 PPI subnetwork	0.03
REACTOME_NEPHRIN_INTERACTIONS	REACTOME_NEPHRIN_INTERACTIONS	0.03
ENSG000000182195	LDOC1 PPI subnetwork	0.03
ENSG000000123685	BATF3 PPI subnetwork	0.03
ENSG000000215699	ENSG000000215699 PPI subnetwork	0.03
GO:0005720	nuclear heterochromatin	0.03
ENSG000000092969	TGFB2 PPI subnetwork	0.03
KEGG_ECM_RECEPTOR_INTERACTION	KEGG_ECM_RECEPTOR_INTERACTION	0.03
MP:0001201	translucent skin	0.03
GO:0016278	lysine N-methyltransferase activity	0.03
GO:0016279	protein-lysine N-methyltransferase activity	0.03
ENSG000000196586	MYO6 PPI subnetwork	0.03
GO:0004702	receptor signaling protein serine/threonine kinase activity	0.03
ENSG000000072518	MARK2 PPI subnetwork	0.03
ENSG000000165025	SYK PPI subnetwork	0.03
MP:0002109	abnormal limb morphology	0.03
ENSG000000157764	BRAF PPI subnetwork	0.03
ENSG000000152256	PDK1 PPI subnetwork	0.03
ENSG000000065618	COL17A1 PPI subnetwork	0.04
ENSG000000169220	RGS14 PPI subnetwork	0.04
ENSG000000100311	PDGFB PPI subnetwork	0.04
ENSG000000134202	GSTM3 PPI subnetwork	0.04
ENSG000000142515	KLK3 PPI subnetwork	0.04
MP:0002619	abnormal lymphocyte morphology	0.04
ENSG000000161395	PGAP3 PPI subnetwork	0.04
ENSG000000145431	PDGFC PPI subnetwork	0.04
ENSG000000170962	PDGFD PPI subnetwork	0.04
ENSG000000153879	CEBPG PPI subnetwork	0.04

Original gene set ID	Original gene set description	Nominal P value
ENSG00000077380	DYNC1I2 PPI subnetwork	0.04
ENSG000000197122	SRC PPI subnetwork	0.04
MP:0004399	abnormal cochlear outer hair cell morphology	0.04
ENSG000000174996	KLC2 PPI subnetwork	0.04
MP:0002376	abnormal dendritic cell physiology	0.04
MP:0000709	enlarged thymus	0.04
MP:0008706	decreased interleukin-6 secretion	0.04
MP:0004686	decreased length of long bones	0.04
GO:0050810	regulation of steroid biosynthetic process	0.04
ENSG000000138396	ENSG000000138396 PPI subnetwork	0.04
ENSG000000148400	NOTCH1 PPI subnetwork	0.04
ENSG000000137171	KLC4 PPI subnetwork	0.04
ENSG000000196396	PTPN1 PPI subnetwork	0.04
ENSG000000148672	GLUD1 PPI subnetwork	0.04
GO:0000975	regulatory region DNA binding	0.04
GO:0001067	regulatory region nucleic acid binding	0.04
GO:0022411	cellular component disassembly	0.04
ENSG00000026025	VIM PPI subnetwork	0.04
ENSG000000061273	HDAC7 PPI subnetwork	0.04
ENSG000000104067	TJP1 PPI subnetwork	0.04
MP:0004813	absent linear vestibular evoked potentia	0.04
ENSG000000091136	LAMB1 PPI subnetwork	0.04
KEGG_RENAL_CELL_CARCINOMA	KEGG_RENAL_CELL_CARCINOMA	0.04
KEGG_FOCAL_ADHESION	KEGG_FOCAL_ADHESION	0.04
GO:0031581	hemidesmosome assembly	0.04
ENSG000000141068	KSR1 PPI subnetwork	0.04
MP:0004214	abnormal long bone diaphysis morphology	0.04
ENSG000000123836	PFKFB2 PPI subnetwork	0.04
ENSG000000168090	COPS6 PPI subnetwork	0.04
ENSG000000132356	PRKAA1 PPI subnetwork	0.04
GO:0031093	platelet alpha granule lumen	0.04
GO:0048545	response to steroid hormone stimulus	0.04
MP:0003109	short femur	0.04
ENSG000000113758	DBN1 PPI subnetwork	0.04
GO:0008276	protein methyltransferase activity	0.04
MP:0003383	abnormal gluconeogenesis	0.04
ENSG000000162614	NEXN PPI subnetwork	0.04
ENSG000000162614	NEXN PPI subnetwork	0.04
ENSG000000169641	LUZP1 PPI subnetwork	0.04
MP:0002152	abnormal brain morphology	0.04
ENSG000000204257	HLA-DMA PPI subnetwork	0.04
ENSG000000206229	ENSG000000206229 PPI subnetwork	0.04
ENSG000000206293	ENSG000000206293 PPI subnetwork	0.04
ENSG000000138439	FAM117B PPI subnetwork	0.04
GO:0006636	unsaturated fatty acid biosynthetic process	0.04
ENSG000000176444	CLK2 PPI subnetwork	0.04
MP:0000703	abnormal thymus morphology	0.04
REACTOME_ZINC_TRANSPORTERS	REACTOME_ZINC_TRANSPORTERS	0.04
ENSG000000125952	MAX PPI subnetwork	0.04

Original gene set ID	Original gene set description	Nominal P value
GO:0046456	icosanoid biosynthetic process	0.04
ENSG00000132964	CDK8 PPI subnetwork	0.04
MP:0008688	decreased interleukin-2 secretion	0.04
ENSG00000196218	RYR1 PPI subnetwork	0.04
MP:0004770	abnormal synaptic vesicle recycling	0.04
ENSG00000121879	PIK3CA PPI subnetwork	0.04
ENSG00000196735	HLA-DQA1 PPI subnetwork	0.04
MP:0009355	increased liver triglyceride level	0.04
MP:0009399	increased skeletal muscle fiber size	0.04
ENSG00000160678	S100A1 PPI subnetwork	0.04
ENSG00000064999	ANKS1A PPI subnetwork	0.04
ENSG00000173327	MAP3K11 PPI subnetwork	0.04
GO:0051183	vitamin transporter activity	0.04
GO:0006690	icosanoid metabolic process	0.04
ENSG00000134363	FST PPI subnetwork	0.04
GO:0060053	neurofilament cytoskeleton	0.04
ENSG00000151914	DST PPI subnetwork	0.04
ENSG00000189079	ARID2 PPI subnetwork	0.04
ENSG00000065559	MAP2K4 PPI subnetwork	0.05
ENSG00000120709	FAM53C PPI subnetwork	0.05
MP:0002110	abnormal digit morphology	0.05
GO:0005976	polysaccharide metabolic process	0.05
ENSG00000054523	KIF1B PPI subnetwork	0.05
ENSG00000100906	NFKBIA PPI subnetwork	0.05
ENSG00000136518	ACTL6A PPI subnetwork	0.05
GO:0004709	MAP kinase kinase kinase activity	0.05
GO:0060711	labyrinthine layer development	0.05
KEGG_CIRCADIAN_RHYTHM_MAMMAL	KEGG_CIRCADIAN_RHYTHM_MAMMAL	0.05
REACTOME_CLASSICAL_ANTIBODY:MEDIATED_COMPLEMENT_ACTIVATION	REACTOME_CLASSICAL_ANTIBODY:MEDIATED_COMPLEMENT_ACTIVATION	0.05
ENSG00000211979	ENSG00000211979 PPI subnetwork	0.05
ENSG00000211973	ENSG00000211973 PPI subnetwork	0.05
ENSG00000172534	HCFC1 PPI subnetwork	0.05
ENSG00000136270	TBRG4 PPI subnetwork	0.05
GO:0032648	regulation of interferon-beta production	0.05
GO:0034375	high-density lipoprotein particle remodeling	0.05
ENSG00000185811	IKZF1 PPI subnetwork	0.05
ENSG00000198802	ENSG00000198802 PPI subnetwork	0.05
MP:0006262	testis tumor	0.05
ENSG00000171992	SYNPO PPI subnetwork	0.05
ENSG00000213341	CHUK PPI subnetwork	0.05
ENSG00000175197	DDIT3 PPI subnetwork	0.05
MP:0005150	cachexia	0.05
GO:0043122	regulation of I-kappaB kinase/NF-kappaB cascade	0.05
GO:0097006	regulation of plasma lipoprotein particle levels	0.05
ENSG00000162772	ATF3 PPI subnetwork	0.05
GO:0000122	negative regulation of transcription from RNA polymerase II promoter	0.05
GO:0005858	axonemal dynein complex	0.05
ENSG00000051382	PIK3CB PPI subnetwork	0.05
GO:0043405	regulation of MAP kinase activity	0.05

Original gene set ID	Original gene set description	Nominal P value
MP:0008722	abnormal chemokine secretion	0.05
KEGG_CHRONIC_MYELOID_LEUKEMIA	KEGG_CHRONIC_MYELOID_LEUKEMIA	0.05
REACTOME_REGULATED_PROTEOLYSIS_OF_P75NTR	REACTOME_REGULATED_PROTEOLYSIS_OF_P75NTR	0.05
GO:0043588	skin development	0.05
GO:0010627	regulation of intracellular protein kinase cascade	0.05
GO:0044212	transcription regulatory region DNA binding	0.05
GO:0030027	lamellipodium	0.05
ENSG00000105976	MET PPI subnetwork	0.05
MP:0002792	abnormal retinal vasculature morphology	0.05
MP:0000069	kyphoscoliosis	0.05
GO:0034339	regulation of transcription from RNA polymerase II promoter by nuclear hormone receptor	0.05
ENSG00000141551	CSNK1D PPI subnetwork	0.05
MP:0005108	abnormal ulna morphology	0.05
MP:0002419	abnormal innate immunity	0.05
GO:0016757	transferase activity, transferring glycosyl groups	0.05
ENSG00000161800	RACGAP1 PPI subnetwork	0.05
MP:0006387	abnormal T cell number	0.05
GO:0005089	Rho guanyl-nucleotide exchange factor activity	0.05
ENSG00000117984	CTSD PPI subnetwork	0.05
ENSG00000105971	CAV2 PPI subnetwork	0.05
ENSG00000115085	ZAP70 PPI subnetwork	0.05
MP:0004609	vertebral fusion	0.05
ENSG00000135862	LAMC1 PPI subnetwork	0.05
MP:0003449	abnormal intestinal goblet cell morphology	0.05
MP:0002687	oligozoospermia	0.05
MP:0000714	increased thymocyte number	0.05
ENSG00000133030	MPRIP PPI subnetwork	0.05
ENSG00000079841	RIMS1 PPI subnetwork	0.05
ENSG00000130638	ATXN10 PPI subnetwork	0.05
MP:0002656	abnormal keratinocyte differentiation	0.05
ENSG00000129691	ASH2L PPI subnetwork	0.05
MP:0002650	abnormal ameloblast morphology	0.05
ENSG00000135503	ACVR1B PPI subnetwork	0.05
GO:0004715	non-membrane spanning protein tyrosine kinase activity	0.05
ENSG00000001497	LAS1L PPI subnetwork	0.05
GO:0018024	histone-lysine N-methyltransferase activity	0.05
GO:0000792	heterochromatin	0.05
ENSG00000111961	SASH1 PPI subnetwork	0.05
MP:0008840	abnormal spike wave discharge	0.05
ENSG00000139514	SLC7A1 PPI subnetwork	0.05
GO:0007249	I-kappaB kinase/NF-kappaB cascade	0.05
MP:0009886	failure of palatal shelf elevation	0.06
ENSG00000144668	ITGA9 PPI subnetwork	0.06
MP:0001798	impaired macrophage phagocytosis	0.06
MP:0004148	increased compact bone thickness	0.06
GO:0034637	cellular carbohydrate biosynthetic process	0.06
REACTOME_PLATELET_SENSITIZATION_BY_LDL	REACTOME_PLATELET_SENSITIZATION_BY_LDL	0.06
GO:0008170	N-methyltransferase activity	0.06
GO:0046890	regulation of lipid biosynthetic process	0.06

Original gene set ID	Original gene set description	Nominal P value
MP:0004047	abnormal milk composition	0.06
MP:0005670	abnormal white adipose tissue physiology	0.06
ENSG000000132906	CASP9 PPI subnetwork	0.06
ENSG000000167601	AXL PPI subnetwork	0.06
ENSG000000136731	UGGT1 PPI subnetwork	0.06
GO:0015926	glucosidase activity	0.06
ENSG000000107560	RAB11FIP2 PPI subnetwork	0.06
ENSG000000179344	HLA-DQB1 PPI subnetwork	0.06
MP:0008973	decreased erythroid progenitor cell number	0.06
GO:0060350	endochondral bone morphogenesis	0.06
ENSG000000136160	EDNRB PPI subnetwork	0.06
ENSG000000070882	OSBPL3 PPI subnetwork	0.06
GO:0046942	carboxylic acid transport	0.06
ENSG000000106991	ENG PPI subnetwork	0.06
ENSG000000204673	AKT1S1 PPI subnetwork	0.06
ENSG000000145349	CAMK2D PPI subnetwork	0.06
MP:0000552	abnormal radius morphology	0.06
GO:0033692	cellular polysaccharide biosynthetic process	0.06
ENSG000000164078	MST1R PPI subnetwork	0.06
ENSG000000160271	RALGDS PPI subnetwork	0.06
GO:0031663	lipopolysaccharide-mediated signaling pathway	0.06
MP:0002444	abnormal T cell physiology	0.06
ENSG000000169714	CNBP PPI subnetwork	0.06
GO:0048185	activin binding	0.06
ENSG000000197694	SPTAN1 PPI subnetwork	0.06
MP:0004255	abnormal spongiotrophoblast layer morphology	0.06
GO:0004712	protein serine/threonine/tyrosine kinase activity	0.06
ENSG000000171094	ALK PPI subnetwork	0.06
GO:0003706	ligand-regulated transcription factor activity	0.06
ENSG000000104892	KLC3 PPI subnetwork	0.07
REACTOME_APOPTOTIC_CLEAVAGE_OF_CELL_ADHESION__PROTEINS	REACTOME_APOPTOTIC_CLEAVAGE_OF_CELL_ADHESION__PROTEINS	0.07
ENSG000000077514	POLD3 PPI subnetwork	0.07
ENSG000000116455	WDR77 PPI subnetwork	0.07
GO:0030183	B cell differentiation	0.07
MP:0000609	abnormal liver physiology	0.07
MP:0004792	abnormal synaptic vesicle number	0.07
GO:0042303	molting cycle	0.07
GO:0042633	hair cycle	0.07
MP:0000558	abnormal tibia morphology	0.07
REACTOME_ACTIVATION_OF_CHAPERONES_BY_IRE1ALPHA	REACTOME_ACTIVATION_OF_CHAPERONES_BY_IRE1ALPHA	0.07
ENSG000000185122	HSF1 PPI subnetwork	0.07
ENSG000000125686	MED1 PPI subnetwork	0.07
ENSG000000115415	STAT1 PPI subnetwork	0.07
ENSG000000158195	WASF2 PPI subnetwork	0.07
MP:0000559	abnormal femur morphology	0.07
ENSG000000136153	LMO7 PPI subnetwork	0.07
ENSG000000132780	NASP PPI subnetwork	0.07
ENSG000000174744	BRMS1 PPI subnetwork	0.07
ENSG000000198793	MTOR PPI subnetwork	0.07

Original gene set ID**Original gene set description****Nominal P value**

MP:0001846	increased inflammatory response	0.07
MP:0005178	increased circulating cholesterol leve	0.07
ENSG000000165219	GAPVD1 PPI subnetwork	0.07
ENSG000000104695	PPP2CB PPI subnetwork	0.07
MP:0001539	decreased caudal vertebrae number	0.07
REACTOME_BMAL1CLOCKNPAS2_ACTIVATES_GENE_EXPRESSION	REACTOME_BMAL1CLOCKNPAS2_ACTIVATES_GENE_EXPRESSION	0.07
ENSG000000164597	COG5 PPI subnetwork	0.07
ENSG000000122679	RAMP3 PPI subnetwork	0.07
MP:0008563	decreased interferon-alpha secretion	0.07
ENSG000000203747	FCGR3A PPI subnetwork	0.07
ENSG000000129250	KIF1C PPI subnetwork	0.07
MP:0005018	decreased T cell number	0.07
REACTOME_TRAF6_MEDIATED_NF:KB_ACTIVATION	REACTOME_TRAF6_MEDIATED_NF:KB_ACTIVATION	0.07
ENSG000000144021	CIAO1 PPI subnetwork	0.07
ENSG000000184967	NOC4L PPI subnetwork	0.07
ENSG000000105245	NUMBL PPI subnetwork	0.07
MP:0002401	abnormal lymphopoiesis	0.07
REACTOME_SIGNALLING_BY_NGF	REACTOME_SIGNALLING_BY_NGF	0.07
MP:0001973	increased thermal nociceptive threshold	0.07
GO:0033077	T cell differentiation in thymus	0.07
MP:0003723	abnormal long bone morphology	0.07
ENSG000000133997	MED6 PPI subnetwork	0.07
ENSG000000007968	E2F2 PPI subnetwork	0.07
GO:0030286	dynein complex	0.07
GO:0002526	acute inflammatory response	0.07
ENSG000000182901	RGS7 PPI subnetwork	0.07
ENSG000000214485	ENSG000000214485 PPI subnetwork	0.07
GO:0035097	histone methyltransferase complex	0.07
GO:0034708	methyltransferase complex	0.07
ENSG000000171608	PIK3CD PPI subnetwork	0.07
ENSG000000149923	PPP4C PPI subnetwork	0.07
MP:0001922	reduced male fertility	0.07
GO:0005416	cation:amino acid symporter activity	0.07
MP:0001129	impaired ovarian folliculogenesis	0.07
MP:0003231	abnormal placenta vasculature	0.07
ENSG000000055332	EIF2AK2 PPI subnetwork	0.07
GO:0015849	organic acid transport	0.07
GO:0048011	nerve growth factor receptor signaling pathway	0.07
GO:0005605	basal lamina	0.07
MP:0001858	intestinal inflammation	0.07
GO:0003690	double-stranded DNA binding	0.07
ENSG000000180879	SSR4 PPI subnetwork	0.07
REACTOME_OTHER_SEMAPHORIN_INTERACTIONS	REACTOME_OTHER_SEMAPHORIN_INTERACTIONS	0.07
GO:0043408	regulation of MAPK cascade	0.07
MP:0008479	decreased spleen white pulp amount	0.07
ENSG000000185963	BICD2 PPI subnetwork	0.07
GO:0046969	NAD-dependent histone deacetylase activity (H3-K9 specific)	0.07
GO:0032129	histone deacetylase activity (H3-K9 specific)	0.07
ENSG000000105723	GSK3A PPI subnetwork	0.07

Original gene set ID	Original gene set description	Nominal P value
MP:0005439	decreased glycogen level	0.08
MP:0000493	rectal prolapse	0.08
REACTOME_CIRCADIAN_CLOCK	REACTOME_CIRCADIAN_CLOCK	0.08
ENSG00000182511	FES PPI subnetwork	0.08
ENSG00000065054	SLC9A3R2 PPI subnetwork	0.08
REACTOME_TRANSCRIPTIONAL_REGULATION_OF_WHITE_ADIPOCYTE_DIFFERENTIATION	REACTOME_TRANSCRIPTIONAL_REGULATION_OF_WHITE_ADIPOCYTE_DIFFERENTIATION	0.08
KEGG_DORSO_VENTRAL_AXIS_FORMATION	KEGG_DORSO_VENTRAL_AXIS_FORMATION	0.08
ENSG00000158402	CDC25C PPI subnetwork	0.08
ENSG00000107186	MPDZ PPI subnetwork	0.08
ENSG00000117395	EBNA1BP2 PPI subnetwork	0.08
GO:0032606	type I interferon production	0.08
ENSG00000101057	MYBL2 PPI subnetwork	0.08
ENSG00000163629	PTPN13 PPI subnetwork	0.08
REACTOME_METABOLISM_OF_WATER:SOLUBLE_VITAMINS_AND_COFACTORS	REACTOME_METABOLISM_OF_WATER:SOLUBLE_VITAMINS_AND_COFACTORS	0.08
REACTOME_METABOLISM_OF_VITAMINS_AND_COFACTORS	REACTOME_METABOLISM_OF_VITAMINS_AND_COFACTORS	0.08
ENSG00000133895	MEN1 PPI subnetwork	0.08
ENSG00000197451	HNRNPAB PPI subnetwork	0.08
GO:0043029	T cell homeostasis	0.08
GO:0031252	cell leading edge	0.08
GO:0009101	glycoprotein biosynthetic process	0.08
MP:0004616	lumbar vertebral transformation	0.08
MP:0003892	abnormal gastric gland morphology	0.08
MP:0002740	heart hypoplasia	0.08
MP:0000133	abnormal long bone metaphysis morphology	0.08
ENSG00000140009	ESR2 PPI subnetwork	0.08
KEGG_PANCREATIC_CANCER	KEGG_PANCREATIC_CANCER	0.08
MP:0001209	spontaneous skin ulceration	0.08
MP:0005017	decreased B cell number	0.08
ENSG00000107262	BAG1 PPI subnetwork	0.08
ENSG00000118260	CREB1 PPI subnetwork	0.08
ENSG00000169967	MAP3K2 PPI subnetwork	0.08
GO:0050840	extracellular matrix binding	0.08
ENSG00000198286	CARD11 PPI subnetwork	0.08
GO:0005085	guanyl-nucleotide exchange factor activity	0.08
ENSG00000126001	CEP250 PPI subnetwork	0.08
ENSG00000203879	GDI1 PPI subnetwork	0.08
GO:0046970	NAD-dependent histone deacetylase activity (H4-K16 specific)	0.08
GO:0034739	histone deacetylase activity (H4-K16 specific)	0.08
GO:0031078	histone deacetylase activity (H3-K14 specific)	0.08
GO:0032041	NAD-dependent histone deacetylase activity (H3-K14 specific)	0.08
REACTOME_INTERFERON_ALPHABETA_SIGNALING	REACTOME_INTERFERON_ALPHABETA_SIGNALING	0.08
MP:0000951	sporadic seizures	0.08
ENSG00000119401	TRIM32 PPI subnetwork	0.08
ENSG00000080815	PSEN1 PPI subnetwork	0.08
GO:0033674	positive regulation of kinase activity	0.08
ENSG00000102898	NUTF2 PPI subnetwork	0.08
GO:0008378	galactosyltransferase activity	0.08
MP:0000751	myopathy	0.08
ENSG00000119630	PGF PPI subnetwork	0.08

Original gene set ID	Original gene set description	Nominal P value
REACTOME_N:GLYCAN_TRIMMING_IN_THE_ER_AND_CALNEXINCALRETICULIN_CYC	REACTOME_N:GLYCAN_TRIMMING_IN_THE_ER_AND_CALNEXINCALRETICULIN_CYC	0.08
GO:0030728	ovulation	0.08
GO:0002577	regulation of antigen processing and presentation	0.08
GO:0031100	organ regeneration	0.08
ENSG00000063046	EIF4B PPI subnetwork	0.08
REACTOME_IMMUNOREGULATORY_INTERACTIONS_BETWEEN_A_LYMPHOID_AND_A_T_CELL	REACTOME_IMMUNOREGULATORY_INTERACTIONS_BETWEEN_A_LYMPHOID_AND_A_T_CELL	0.08
MP:0001745	increased circulating corticosterone level	0.08
MP:0003087	absent allantoin	0.08
ENSG00000198959	TGM2 PPI subnetwork	0.08
ENSG00000154380	ENAH PPI subnetwork	0.08
GO:0051347	positive regulation of transferase activity	0.08
ENSG00000099308	MAST3 PPI subnetwork	0.08
GO:0035250	UDP-galactosyltransferase activity	0.08
ENSG00000129682	FGF13 PPI subnetwork	0.08
MP:0008577	increased circulating interferon-gamma level	0.08
ENSG00000170579	DLGAP1 PPI subnetwork	0.08
GO:0005539	glycosaminoglycan binding	0.08
MP:0005090	increased double-negative T cell number	0.08
REACTOME_PEPTIDE_HORMONE_BIOSYNTHESIS	REACTOME_PEPTIDE_HORMONE_BIOSYNTHESIS	0.08
GO:0071900	regulation of protein serine/threonine kinase activity	0.09
GO:0045723	positive regulation of fatty acid biosynthetic process	0.09
GO:0016298	lipase activity	0.09
GO:0035770	ribonucleoprotein granule	0.09
ENSG00000085721	RRN3 PPI subnetwork	0.09
ENSG00000136250	AOAH PPI subnetwork	0.09
ENSG00000081237	PTPRC PPI subnetwork	0.09
ENSG00000143621	ILF2 PPI subnetwork	0.09
GO:0031098	stress-activated protein kinase signaling cascade	0.09
KEGG_STEROID_BIOSYNTHESIS	KEGG_STEROID_BIOSYNTHESIS	0.09
GO:0015936	coenzyme A metabolic process	0.09
ENSG00000212981	ENSG00000212981 PPI subnetwork	0.09
MP:0008750	abnormal interferon level	0.09
ENSG00000206297	TAP1 PPI subnetwork	0.09
ENSG00000206233	ENSG00000206233 PPI subnetwork	0.09
ENSG00000168394	TAP1 PPI subnetwork	0.09
GO:0031929	TOR signaling cascade	0.09
ENSG00000068305	MEF2A PPI subnetwork	0.09
ENSG00000090339	ICAM1 PPI subnetwork	0.09
ENSG00000049618	ARID1B PPI subnetwork	0.09
MP:0002665	decreased circulating corticosterone level	0.09
GO:0005796	Golgi lumen	0.09
REACTOME_INITIAL_TRIGGERING_OF_COMPLEMENT	REACTOME_INITIAL_TRIGGERING_OF_COMPLEMENT	0.09
GO:0006305	DNA alkylation	0.09
GO:0006306	DNA methylation	0.09
GO:0045061	thymic T cell selection	0.09
ENSG00000198734	F5 PPI subnetwork	0.09
ENSG00000130762	ARHGEF16 PPI subnetwork	0.09
ENSG00000166913	YWHAB PPI subnetwork	0.09
ENSG00000099917	MED15 PPI subnetwork	0.09

Original gene set ID	Original gene set description	Nominal P value
GO:0042755	eating behavior	0.09
GO:0045334	clathrin-coated endocytic vesicle	0.09
ENSG000000133104	SPG20 PPI subnetwork	0.09
GO:0008213	protein alkylation	0.09
GO:0006479	protein methylation	0.09
GO:0010740	positive regulation of intracellular protein kinase cascade	0.09
GO:0008584	male gonad development	0.09
MP:0002722	abnormal immune system organ morphology	0.09
ENSG000000120509	PDZD11 PPI subnetwork	0.09
ENSG000000204361	FAM55B PPI subnetwork	0.09
MP:0001655	multifocal hepatic necrosis	0.09
MP:0004374	bowed radius	0.09
MP:0000764	abnormal tongue epithelium morphology	0.09
ENSG000000185634	SHC4 PPI subnetwork	0.09
ENSG000000140368	PSTPIP1 PPI subnetwork	0.09
GO:0008610	lipid biosynthetic process	0.09
ENSG000000109471	IL2 PPI subnetwork	0.09
GO:0005637	nuclear inner membrane	0.09
ENSG000000169131	ZNF354A PPI subnetwork	0.09
GO:0046943	carboxylic acid transmembrane transporter activity	0.09
MP:0002086	abnormal extraembryonic tissue morphology	0.09
MP:0005325	abnormal renal glomerulus morphology	0.09
GO:0042110	T cell activation	0.09
ENSG000000107338	SHB PPI subnetwork	0.09
GO:0045860	positive regulation of protein kinase activity	0.09
GO:0002920	regulation of humoral immune response	0.09
ENSG000000106052	TAX1BP1 PPI subnetwork	0.09
ENSG000000118690	ARMC2 PPI subnetwork	0.09
ENSG000000142273	CBLC PPI subnetwork	0.09
MP:0001236	abnormal epidermis stratum spinosum morphology	0.09
GO:0009100	glycoprotein metabolic process	0.09
ENSG000000056972	TRAF3IP2 PPI subnetwork	0.09
MP:0004852	decreased testis weight	0.09
GO:0044272	sulfur compound biosynthetic process	0.09
GO:0042605	peptide antigen binding	0.09
GO:0000187	activation of MAPK activity	0.09
GO:0006029	proteoglycan metabolic process	0.09
GO:0002080	acrosomal membrane	0.09
GO:0031293	membrane protein intracellular domain proteolysis	0.09
ENSG000000110092	CCND1 PPI subnetwork	0.09
MP:0000473	abnormal stomach glandular epithelium morphology	0.09
GO:0031258	lamellipodium membrane	0.09
GO:0006694	steroid biosynthetic process	0.09
MP:0000592	short tail	0.09
GO:0010608	posttranscriptional regulation of gene expressior	0.09
ENSG000000198911	SREBF2 PPI subnetwork	0.09
GO:0045446	endothelial cell differentiation	0.09
GO:0005035	death receptor activity	0.09
GO:0051346	negative regulation of hydrolase activity	0.09

Original gene set ID	Original gene set description	Nominal P value
ENSG00000136169	SETDB2 PPI subnetwork	0.09
GO:0002260	lymphocyte homeostasis	0.09
MP:0003339	decreased pancreatic beta cell number	0.09
REACTOME_COMPLEMENT_CASCADE	REACTOME_COMPLEMENT_CASCADE	0.09
MP:0001792	impaired wound healing	0.09
GO:0008406	gonad development	0.09
ENSG00000171720	HDAC3 PPI subnetwork	0.09
GO:0004620	phospholipase activity	0.09
ENSG00000101266	CSNK2A1 PPI subnetwork	0.09
ENSG00000067191	CACNB1 PPI subnetwork	0.09
KEGG_FC_GAMMA_R_MEDIATED_PHAGOCYTOSIS	KEGG_FC_GAMMA_R_MEDIATED_PHAGOCYTOSIS	0.09
REACTOME_CHYLOMICRON:MEDIATED_LIPID_TRANSPORT	REACTOME_CHYLOMICRON:MEDIATED_LIPID_TRANSPORT	0.09
MP:0002780	decreased circulating testosterone leve	0.09
MP:0001216	abnormal epidermal layer morphology	0.09
GO:0045058	T cell selection	0.09
ENSG00000215440	NPEPL1 PPI subnetwork	0.09
GO:0007565	female pregnancy	0.09
GO:0010638	positive regulation of organelle organization	0.09
MP:0001147	small testis	0.1
ENSG00000101210	EEF1A2 PPI subnetwork	0.1
MP:0005294	abnormal heart ventricle morphology	0.1
GO:0030323	respiratory tube development	0.1
GO:0005542	folic acid binding	0.1
ENSG00000141646	SMAD4 PPI subnetwork	0.1
ENSG00000100888	CHD8 PPI subnetwork	0.1
ENSG00000072062	PRKACA PPI subnetwork	0.1
ENSG00000134853	PDGFRA PPI subnetwork	0.1
ENSG00000135069	PSAT1 PPI subnetwork	0.1
GO:0000118	histone deacetylase complex	0.1
GO:0071887	leukocyte apoptotic process	0.1
MP:0008271	abnormal bone ossification	0.1
GO:0008201	heparin binding	0.1
ENSG00000124222	STX16 PPI subnetwork	0.1
GO:0030299	intestinal cholesterol absorption	0.1
ENSG00000122194	PLG PPI subnetwork	0.1
MP:0001951	abnormal breathing pattern	0.1
ENSG00000105369	CD79A PPI subnetwork	0.1
ENSG00000170889	RPS9 PPI subnetwork	0.1
ENSG00000136149	ENSG00000136149 PPI subnetwork	0.1
GO:0043410	positive regulation of MAPK cascade	0.1
MP:0000642	enlarged adrenal glands	0.1
MP:0003795	abnormal bone structure	0.1
MP:0003648	abnormal radial glial cell morphology	0.1
MP:0004151	decreased circulating iron level	0.1
REACTOME_TRANSPORT_OF_INORGANIC_CATIONSANIONS_AND_AMINO_ACIDS	REACTOME_TRANSPORT_OF_INORGANIC_CATIONSANIONS_AND_AMINO_ACIDS	0.1
ENSG00000154727	GABPA PPI subnetwork	0.1
MP:0003427	parakeratosis	0.1
GO:0031300	intrinsic to organelle membrane	0.1
MP:0002098	abnormal vibrissa morphology	0.1

Original gene set ID	Original gene set description	Nominal P value
MP:0000702	enlarged lymph nodes	0.1
ENSG00000142675	CNKSRI PPI subnetwork	0.1
GO:0000217	DNA secondary structure binding	0.1
MP:0003453	abnormal keratinocyte physiology	0.1
GO:0006730	one-carbon metabolic process	0.1
ENSG00000099204	ABLIM1 PPI subnetwork	0.1
ENSG00000179335	CLK3 PPI subnetwork	0.1
GO:0034358	plasma lipoprotein particle	0.1
GO:0032994	protein-lipid complex	0.1
GO:0005938	cell cortex	0.1
GO:0003158	endothelium development	0.1
MP:0004974	decreased regulatory T cell number	0.1
MP:0005278	abnormal cholesterol homeostasis	0.1
GO:0030132	clathrin coat of coated pit	0.1
MP:0005167	abnormal blood-brain barrier function	0.1
ENSG00000118971	CCND2 PPI subnetwork	0.1
GO:0005024	transforming growth factor beta-activated receptor activity	0.1
MP:0000445	short snout	0.1
REACTOME_P130CAS_LINKAGE_TO_MAPK_SIGNALING_FOR_INTEGRINS	REACTOME_P130CAS_LINKAGE_TO_MAPK_SIGNALING_FOR_INTEGRINS	0.1
GO:0022405	hair cycle process	0.1
GO:0001942	hair follicle development	0.1
GO:0022404	molting cycle process	0.1
REACTOME_P75NTR_SIGNALS_VIA_NF:KB	REACTOME_P75NTR_SIGNALS_VIA_NF:KB	0.1
ENSG00000163932	PRKCD PPI subnetwork	0.1
GO:0043691	reverse cholesterol transport	0.1
ENSG00000007866	TEAD3 PPI subnetwork	0.1
GO:0070613	regulation of protein processing	0.1
ENSG00000107643	MAPK8 PPI subnetwork	0.1
MP:0001196	shiny skin	0.1
ENSG00000009954	BAZ1B PPI subnetwork	0.1
ENSG00000182953	ENSG00000182953 PPI subnetwork	0.1
REACTOME_SLC:MEDIATED_TRANSMEMBRANE_TRANSPORT	REACTOME_SLC:MEDIATED_TRANSMEMBRANE_TRANSPORT	0.1
MP:0003050	abnormal sacral vertebrae morphology	0.1
ENSG00000151617	EDNRA PPI subnetwork	0.1
GO:0009595	detection of biotic stimulus	0.1
MP:0005458	increased percent body fat	0.1
MP:0008751	abnormal interleukin level	0.1
REACTOME_INTEGRIN_ALPHAIIIB_BETA3_SIGNALING	REACTOME_INTEGRIN_ALPHAIIIB_BETA3_SIGNALING	0.1
ENSG00000119699	TGFB3 PPI subnetwork	0.1
ENSG00000147383	NSDHL PPI subnetwork	0.1
MP:0009674	decreased birth weight	0.1
GO:0000165	MAPK cascade	0.1
ENSG00000096060	FKBP5 PPI subnetwork	0.1
GO:0006790	sulfur compound metabolic process	0.1
ENSG00000134215	VAV3 PPI subnetwork	0.1
REACTOME_INTERLEUKIN:6_SIGNALING	REACTOME_INTERLEUKIN:6_SIGNALING	0.1
MP:0001786	skin edema	0.1
ENSG00000134333	LDHA PPI subnetwork	0.1
GO:0044264	cellular polysaccharide metabolic process	0.1

Original gene set ID	Original gene set description	Nominal P value
GO:0032607	interferon-alpha production	0.1
GO:0032647	regulation of interferon-alpha production	0.1
MP:0004358	bowed tibia	0.1
GO:0008544	epidermis development	0.1
ENSG00000101224	CDC25B PPI subnetwork	0.1
ENSG00000106144	CASP2 PPI subnetwork	0.1
MP:0001208	blistering	0.1
REACTOME_INTERLEUKIN:7_SIGNALING	REACTOME_INTERLEUKIN:7_SIGNALING	0.1
REACTOME_GAMMA:CARBOXYLATION_TRANSPORT_AND_AMINO:TERMINAL_C	REACTOME_GAMMA:CARBOXYLATION_TRANSPORT_AND_AMINO:TERMINAL_CLEA	0.1
ENSG00000107562	CXCL12 PPI subnetwork	0.1
GO:0005342	organic acid transmembrane transporter activity	0.1
GO:0005385	zinc ion transmembrane transporter activity	0.1
MP:0008883	abnormal enterocyte proliferation	0.1
GO:0048020	CCR chemokine receptor binding	0.1
ENSG00000172936	MYD88 PPI subnetwork	0.1
MP:0002375	abnormal thymus medulla morphology	0.1
GO:0003774	motor activity	0.1
GO:0071356	cellular response to tumor necrosis factor	0.11
MP:0003954	abnormal Reichert's membrane morphology	0.11
MP:0004592	small mandible	0.11
MP:0008111	abnormal granulocyte differentiation	0.11
GO:0030055	cell-substrate junction	0.11
MP:0000628	abnormal mammary gland development	0.11
ENSG00000158560	DYNC111 PPI subnetwork	0.11
GO:0019955	cytokine binding	0.11
GO:0034385	triglyceride-rich lipoprotein particle	0.11
GO:0034361	very-low-density lipoprotein particle	0.11
MP:0002759	abnormal caudal vertebrae morphology	0.11
GO:0055038	recycling endosome membrane	0.11
ENSG00000119139	TJP2 PPI subnetwork	0.11
REACTOME_PLATELET_DEGRANULATION	REACTOME_PLATELET_DEGRANULATION	0.11
GO:0007159	leukocyte cell-cell adhesion	0.11
ENSG00000096968	JAK2 PPI subnetwork	0.11
MP:0008050	decreased memory T cell number	0.11
GO:0006413	translational initiation	0.11
MP:0001393	ataxia	0.11
ENSG00000089009	RPL6 PPI subnetwork	0.11
REACTOME_NF:KB_IS_ACTIVATED_AND_SIGNALS_SURVIVAL	REACTOME_NF:KB_IS_ACTIVATED_AND_SIGNALS_SURVIVAL	0.11
ENSG00000089737	DDX24 PPI subnetwork	0.11
ENSG00000091831	ESR1 PPI subnetwork	0.11
GO:0034340	response to type I interferon	0.11
ENSG00000147507	ENSG00000147507 PPI subnetwork	0.11
MP:0004521	abnormal cochlear hair cell stereociliary bundle morphology	0.11
GO:0032354	response to follicle-stimulating hormone stimulus	0.11
ENSG00000108953	YWHAE PPI subnetwork	0.11
ENSG00000213923	CSNK1E PPI subnetwork	0.11
ENSG00000170017	ALCAM PPI subnetwork	0.11
GO:0016863	intramolecular oxidoreductase activity, transposing C=C bonds	0.11
ENSG00000146729	GBAS PPI subnetwork	0.11

Original gene set ID	Original gene set description	Nominal P value
MP:0002730	head shaking	0.11
GO:0008203	cholesterol metabolic process	0.11
ENSG000000171148	TADA3 PPI subnetwork	0.11
MP:0001157	small seminal vesicle	0.11
GO:0060349	bone morphogenesis	0.11
KEGG_ABC_TRANSPORTERS	KEGG_ABC_TRANSPORTERS	0.11
GO:0032479	regulation of type I interferon production	0.11
MP:0002111	abnormal tail morphology	0.11
ENSG000000197043	ANXA6 PPI subnetwork	0.11
ENSG000000172809	RPL38 PPI subnetwork	0.11
ENSG000000140575	IQGAP1 PPI subnetwork	0.11
GO:0043046	DNA methylation involved in gamete generation	0.11
ENSG000000084073	ZMPSTE24 PPI subnetwork	0.11
ENSG000000143801	PSEN2 PPI subnetwork	0.11
ENSG000000187672	ERC2 PPI subnetwork	0.11
GO:0051093	negative regulation of developmental process	0.11
ENSG000000165699	TSC1 PPI subnetwork	0.11
ENSG000000170847	ENSG000000170847 PPI subnetwork	0.11
ENSG000000173534	ENSG000000173534 PPI subnetwork	0.11
ENSG000000146950	SHROOM2 PPI subnetwork	0.11
ENSG000000157456	CCNB2 PPI subnetwork	0.11
REACTOME_REGULATION_OF_GENE_EXPRESSION_IN_BETA_CELLS	REACTOME_REGULATION_OF_GENE_EXPRESSION_IN_BETA_CELLS	0.11
GO:0071357	cellular response to type I interferon	0.11
GO:0060337	type I interferon-mediated signaling pathway	0.11
ENSG000000167657	DAPK3 PPI subnetwork	0.11
ENSG000000132693	CRP PPI subnetwork	0.11
ENSG000000005339	CREBBP PPI subnetwork	0.11
ENSG000000075945	KIFAP3 PPI subnetwork	0.11
ENSG000000120833	SOCS2 PPI subnetwork	0.11
GO:0003713	transcription coactivator activity	0.11
MP:0000218	increased leukocyte cell number	0.11
MP:0001222	epidermal hyperplasia	0.11
ENSG000000105221	AKT2 PPI subnetwork	0.11
ENSG000000167526	RPL13 PPI subnetwork	0.11
GO:0015718	monocarboxylic acid transport	0.11
ENSG000000164403	SHROOM1 PPI subnetwork	0.11
ENSG000000102804	TSC22D1 PPI subnetwork	0.11
ENSG000000074181	NOTCH3 PPI subnetwork	0.11
GO:0022626	cytosolic ribosome	0.11
ENSG000000010810	FYN PPI subnetwork	0.11
ENSG000000204592	HLA-E PPI subnetwork	0.11
REACTOME_A_THIRD_PROTEOLYTIC_CLEAVAGE_RELEASES_NICD	REACTOME_A_THIRD_PROTEOLYTIC_CLEAVAGE_RELEASES_NICD	0.11
ENSG000000143815	LBR PPI subnetwork	0.11
MP:0002497	increased IgE level	0.11
GO:0005905	coated pit	0.11
GO:0002579	positive regulation of antigen processing and presentati or	0.11
ENSG000000150867	PIP4K2A PPI subnetwork	0.11
ENSG000000075426	FOSL2 PPI subnetwork	0.11
MP:0002408	abnormal double-positive T cell morphology	0.11

Original gene set ID	Original gene set description	Nominal P value
ENSG00000181827	RFX7 PPI subnetwork	0.11
ENSG00000116285	ERRF1 PPI subnetwork	0.11
ENSG00000105193	RPS16 PPI subnetwork	0.11
ENSG00000093167	LRRFIP2 PPI subnetwork	0.11
KEGG_N_GLYCAN_BIOSYNTHESIS	KEGG_N_GLYCAN_BIOSYNTHESIS	0.11
ENSG00000113580	NR3C1 PPI subnetwork	0.11
ENSG00000058335	RASGRF1 PPI subnetwork	0.11
ENSG00000100815	TRIP11 PPI subnetwork	0.11
ENSG00000001630	CYP51A1 PPI subnetwork	0.11
ENSG00000166986	MARS PPI subnetwork	0.11
GO:0044403	symbiosis, encompassing mutualism through parasitism	0.11
MP:0008246	abnormal leukocyte morphology	0.12
MP:0003884	decreased macrophage cell number	0.12
REACTOME_DSCAM_INTERACTIONS	REACTOME_DSCAM_INTERACTIONS	0.12
ENSG00000126749	ENSG00000126749 PPI subnetwork	0.12
ENSG00000106665	CLIP2 PPI subnetwork	0.12
ENSG00000179776	CDH5 PPI subnetwork	0.12
ENSG00000142534	RPS11 PPI subnetwork	0.12
ENSG00000170677	SOCS6 PPI subnetwork	0.12
GO:0005272	sodium channel activity	0.12
MP:0008074	increased CD4-positive T cell number	0.12
ENSG00000077943	ITGA8 PPI subnetwork	0.12
GO:0016125	sterol metabolic process	0.12
GO:0071345	cellular response to cytokine stimulus	0.12
GO:0004004	ATP-dependent RNA helicase activity	0.12
MP:0005179	decreased circulating cholesterol leve	0.12
GO:0031301	integral to organelle membrane	0.12
ENSG00000010610	CD4 PPI subnetwork	0.12
ENSG00000056345	ENSG00000056345 PPI subnetwork	0.12
ENSG00000100181	ENSG00000100181 PPI subnetwork	0.12
GO:0001078	RNA polymerase II core promoter proximal region sequence-specific DNA binding tr	0.12
ENSG00000130402	ACTN4 PPI subnetwork	0.12
ENSG00000084207	GSTP1 PPI subnetwork	0.12
ENSG00000183305	MAGEA2B PPI subnetwork	0.12
ENSG00000034971	MYOC PPI subnetwork	0.12
MP:0004471	short nasal bone	0.12
MP:0003304	large intestinal inflammation	0.12
ENSG00000112078	KCTD20 PPI subnetwork	0.12
MP:0000565	oligodactyly	0.12
GO:0044419	interspecies interaction between organisms	0.12
MP:0001177	atelectasis	0.12
GO:0017136	NAD-dependent histone deacetylase activity	0.12
GO:0034979	NAD-dependent protein deacetylase activity	0.12
GO:0008585	female gonad development	0.12
ENSG00000105173	CCNE1 PPI subnetwork	0.12
ENSG00000105974	CAV1 PPI subnetwork	0.12
MP:0005296	abnormal humerus morphology	0.12
REACTOME_CHOLESTEROL_BIOSYNTHESIS	REACTOME_CHOLESTEROL_BIOSYNTHESIS	0.12
KEGG_GLYCOSPHINGOLIPID_BIOSYNTHESIS_LACTO_AND_NEOLACTO_SERIES	KEGG_GLYCOSPHINGOLIPID_BIOSYNTHESIS_LACTO_AND_NEOLACTO_SERIES	0.12

Original gene set ID	Original gene set description	Nominal P value
ENSG00000126218	F10 PPI subnetwork	0.12
MP:0005425	increased macrophage cell number	0.12
ENSG00000182010	RTKN2 PPI subnetwork	0.12
MP:0002191	abnormal artery morphology	0.12
GO:0051180	vitamin transport	0.12
MP:0000116	abnormal tooth development	0.12
GO:0002275	myeloid cell activation involved in immune response	0.12
MP:0011109	partial lethality throughout fetal growth and development	0.12
MP:0000383	abnormal hair follicle orientation	0.12
GO:0006094	gluconeogenesis	0.12
ENSG00000058404	CAMK2B PPI subnetwork	0.12
MP:0001967	deafness	0.12
MP:0008735	increased susceptibility to endotoxin shock	0.12
GO:0006957	complement activation, alternative pathway	0.12
GO:0080008	CUL4 RING ubiquitin ligase complex	0.12
GO:0019212	phosphatase inhibitor activity	0.12
ENSG00000182754	ENSG00000182754 PPI subnetwork	0.12
ENSG00000163682	RPL9 PPI subnetwork	0.12
MP:0001192	scaly skin	0.12
MP:0003809	abnormal hair shaft morphology	0.12
ENSG00000105568	PPP2R1A PPI subnetwork	0.12
GO:0006702	androgen biosynthetic process	0.12
ENSG00000177606	JUN PPI subnetwork	0.12
ENSG00000213380	COG8 PPI subnetwork	0.12
GO:0070003	threonine-type peptidase activity	0.12
GO:0004298	threonine-type endopeptidase activity	0.12
GO:0032933	SREBP-mediated signaling pathway	0.12
ENSG00000123612	ACVR1C PPI subnetwork	0.12
ENSG00000112049	ENSG00000112049 PPI subnetwork	0.12
GO:0005925	focal adhesion	0.12
ENSG00000004975	DVL2 PPI subnetwork	0.12
GO:0051017	actin filament bundle assembly	0.12
ENSG00000078043	PIAS2 PPI subnetwork	0.12
MP:0005306	abnormal phalanx morphology	0.12
ENSG00000176105	YES1 PPI subnetwork	0.12
GO:0001666	response to hypoxia	0.12
GO:0019221	cytokine-mediated signaling pathway	0.12
GO:0004553	hydrolase activity, hydrolyzing O-glycosyl compounds	0.12
ENSG00000164305	CASP3 PPI subnetwork	0.12
GO:0045022	early endosome to late endosome transport	0.12
MP:0005547	abnormal Muller cell morphology	0.12
MP:0008561	decreased tumor necrosis factor secretior	0.12
ENSG00000112033	PPARD PPI subnetwork	0.12
ENSG00000198909	MAP3K3 PPI subnetwork	0.12
MP:0008670	decreased interleukin-12b secretion	0.12
REACTOME_STEROID_HORMONES	REACTOME_STEROID_HORMONES	0.12
MP:0004810	decreased hematopoietic stem cell number	0.12
ENSG00000132382	MYBBP1A PPI subnetwork	0.12
ENSG00000134909	ARHGAP32 PPI subnetwork	0.12

Original gene set ID	Original gene set description	Nominal P value
GO:0035194	posttranscriptional gene silencing by RNA	0.13
GO:0016441	posttranscriptional gene silencing	0.13
ENSG000000120899	PTK2B PPI subnetwork	0.13
ENSG000000106683	LIMK1 PPI subnetwork	0.13
MP:0000427	abnormal hair cycle	0.13
GO:0015399	primary active transmembrane transporter activity	0.13
GO:0015405	P-P-bond-hydrolysis-driven transmembrane transporter activity	0.13
ENSG000000136999	NOV PPI subnetwork	0.13
GO:0034623	cellular macromolecular complex disassembly	0.13
GO:0006304	DNA modification	0.13
ENSG000000112658	SRF PPI subnetwork	0.13
GO:0043414	macromolecule methylation	0.13
ENSG000000114126	TFDP2 PPI subnetwork	0.13
GO:0045103	intermediate filament-based process	0.13
KEGG_MELANOMA	KEGG_MELANOMA	0.13
MP:0005076	abnormal cell differentiation	0.13
ENSG000000168487	BMP1 PPI subnetwork	0.13
MP:0001676	abnormal apical ectodermal ridge morphology	0.13
GO:0034698	response to gonadotropin stimulus	0.13
GO:0003777	microtubule motor activity	0.13
GO:0048365	Rac GTPase binding	0.13
ENSG000000138069	RAB1A PPI subnetwork	0.13
MP:0001240	abnormal epidermis stratum corneum morphology	0.13
MP:0002060	abnormal skin morphology	0.14
ENSG000000141434	MEP1B PPI subnetwork	0.14
MP:0011099	complete lethality throughout fetal growth and development	0.14
ENSG000000198755	RPL10A PPI subnetwork	0.14
ENSG000000135424	ITGA7 PPI subnetwork	0.14
ENSG000000197303	ENSG000000197303 PPI subnetwork	0.14
GO:0050764	regulation of phagocytosis	0.14
MP:0001847	brain inflammation	0.14
ENSG000000080839	RBL1 PPI subnetwork	0.14
MP:0002404	increased intestinal adenoma incidence	0.14
MP:0008470	abnormal spleen B cell follicle morphology	0.14
GO:0019218	regulation of steroid metabolic process	0.14
GO:0003724	RNA helicase activity	0.14
MP:0003436	decreased susceptibility to induced arthritis	0.14
MP:0009009	absent estrous cycle	0.14
ENSG000000135144	DTX1 PPI subnetwork	0.14
ENSG000000185432	METTL7A PPI subnetwork	0.14
GO:0015278	calcium-release channel activity	0.14
GO:0005604	basement membrane	0.14
ENSG000000117242	ENSG000000117242 PPI subnetwork	0.14
ENSG000000099399	MAGEB2 PPI subnetwork	0.14
GO:0014909	smooth muscle cell migration	0.14
ENSG000000185386	MAPK11 PPI subnetwork	0.14
ENSG000000150527	CTAGE5 PPI subnetwork	0.14
GO:0043624	cellular protein complex disassembly	0.14
GO:0051607	defense response to virus	0.14

Original gene set ID	Original gene set description	Nominal P value
GO:0007276	gamete generation	0.14
ENSG00000163519	TRAT1 PPI subnetwork	0.14
ENSG00000174748	RPL15 PPI subnetwork	0.14
MP:0006317	decreased urine sodium level	0.14
GO:0045104	intermediate filament cytoskeleton organizati	0.14
MP:0001284	absent vibrissae	0.14
ENSG00000185499	MUC1 PPI subnetwork	0.14
MP:0008127	decreased dendritic cell number	0.14
ENSG00000134242	PTPN22 PPI subnetwork	0.14
GO:0005044	scavenger receptor activity	0.14
ENSG00000087245	MMP2 PPI subnetwork	0.14
MP:0002727	decreased circulating insulin level	0.14
GO:0015012	heparan sulfate proteoglycan biosynthetic process	0.14
GO:0031965	nuclear membrane	0.14
GO:0005792	microsome	0.14
ENSG00000161835	GRASP PPI subnetwork	0.14
MP:0005089	decreased double-negative T cell number	0.14
REACTOME_CD28_DEPENDENT_PI3KAKT_SIGNALING	REACTOME_CD28_DEPENDENT_PI3KAKT_SIGNALING	0.14
GO:0051604	protein maturation	0.14
GO:0050691	regulation of defense response to virus by host	0.14
MP:0010465	aberrant origin of the right subclavian artery	0.14
REACTOME_REGULATION_OF_LIPID_METABOLISM_BY_PEROXISOME_PROLIFERATION	REACTOME_REGULATION_OF_LIPID_METABOLISM_BY_PEROXISOME_PROLIFERATION	0.14
REACTOME_P75NTR_RECRUITS_SIGNALLING_COMPLEXES	REACTOME_P75NTR_RECRUITS_SIGNALLING_COMPLEXES	0.14
REACTOME_NUCLEAR_RECEPTOR_TRANSCRIPTION_PATHWAY	REACTOME_NUCLEAR_RECEPTOR_TRANSCRIPTION_PATHWAY	0.14
ENSG00000139318	DUSP6 PPI subnetwork	0.14
MP:0003396	abnormal embryonic hematopoiesis	0.14
GO:0007346	regulation of mitotic cell cycle	0.14
GO:0045596	negative regulation of cell differentiation	0.14
GO:0007584	response to nutrient	0.14
GO:0048194	Golgi vesicle budding	0.14
REACTOME_METABOLISM_OF_PROTEINS	REACTOME_METABOLISM_OF_PROTEINS	0.14
MP:0003156	abnormal leukocyte migration	0.14
GO:0050654	chondroitin sulfate proteoglycan metabolic process	0.14
ENSG00000177731	FLII PPI subnetwork	0.14
GO:0071339	MLL1 complex	0.14
MP:0000598	abnormal liver morphology	0.14
GO:0002673	regulation of acute inflammatory response	0.14
ENSG00000130956	HABP4 PPI subnetwork	0.14
ENSG00000171490	RSL1D1 PPI subnetwork	0.14
ENSG00000169896	ITGAM PPI subnetwork	0.14
REACTOME_RESPONSE_TO_ELEVATED_PLATELET_CYTOSOLIC_CA2	REACTOME_RESPONSE_TO_ELEVATED_PLATELET_CYTOSOLIC_CA2	0.14
GO:0014911	positive regulation of smooth muscle cell migration	0.14
MP:0001953	respiratory failure	0.14
ENSG00000169398	PTK2 PPI subnetwork	0.14
ENSG00000182636	NDN PPI subnetwork	0.14
MP:0008209	decreased pre-B cell number	0.14
REACTOME_POST:TRANSLATIONAL_PROTEIN_MODIFICATION	REACTOME_POST:TRANSLATIONAL_PROTEIN_MODIFICATION	0.14
MP:0002113	abnormal skeleton development	0.14
ENSG00000171862	PTEN PPI subnetwork	0.14

Original gene set ID	Original gene set description	Nominal P value
GO:0008158	hedgehog receptor activity	0.14
GO:0006414	translational elongation	0.14
GO:0042598	vesicular fraction	0.14
ENSG00000213949	ITGA1 PPI subnetwork	0.14
GO:0042446	hormone biosynthetic process	0.14
GO:0008186	RNA-dependent ATPase activity	0.14
ENSG00000155506	LARP1 PPI subnetwork	0.14
ENSG00000127947	PTPN12 PPI subnetwork	0.14
ENSG00000166333	ILK PPI subnetwork	0.14
REACTOME_FACILITATIVE_NA:INDEPENDENT_GLUCCOSE_TRANSPORTERS	REACTOME_FACILITATIVE_NA:INDEPENDENT_GLUCCOSE_TRANSPORTERS	0.14
GO:0002831	regulation of response to biotic stimulus	0.14
GO:0009103	lipopolysaccharide biosynthetic process	0.14
ENSG00000158092	NCK1 PPI subnetwork	0.14
GO:0030324	lung development	0.14
GO:0070001	aspartic-type peptidase activity	0.14
GO:0004190	aspartic-type endopeptidase activity	0.14
REACTOME_METABOLISM_OF_LIPIDS_AND_LIPOPROTEINS	REACTOME_METABOLISM_OF_LIPIDS_AND_LIPOPROTEINS	0.14
ENSG00000143537	ADAM15 PPI subnetwork	0.15
ENSG00000052802	MSMO1 PPI subnetwork	0.15
GO:0002437	inflammatory response to antigenic stimulus	0.15
ENSG00000143398	PIP5K1A PPI subnetwork	0.15
GO:0019902	phosphatase binding	0.15
ENSG00000105329	TGFB1 PPI subnetwork	0.15
GO:0006909	phagocytosis	0.15
ENSG00000184557	SOCS3 PPI subnetwork	0.15
ENSG00000073614	KDMA5 PPI subnetwork	0.15
ENSG00000212664	ENSG00000212664 PPI subnetwork	0.15
MP:0002216	abnormal seminiferous tubule morphology	0.15
ENSG00000120235	IFNA6 PPI subnetwork	0.15
ENSG00000134318	ROCK2 PPI subnetwork	0.15
GO:0001816	cytokine production	0.15
ENSG00000083642	PDS5B PPI subnetwork	0.15
MP:0008037	abnormal T cell morphology	0.15
ENSG00000102189	EEA1 PPI subnetwork	0.15
ENSG00000175189	INHBC PPI subnetwork	0.15
ENSG00000139239	ENSG00000139239 PPI subnetwork	0.15
GO:0015179	L-amino acid transmembrane transporter activity	0.15
GO:0003730	mRNA 3'-UTR binding	0.15
ENSG00000118046	STK11 PPI subnetwork	0.15
GO:0003707	steroid hormone receptor activity	0.15
GO:0001958	endochondral ossification	0.15
GO:0006090	pyruvate metabolic process	0.15
REACTOME_REGULATION_OF_BETA:CELL_DEVELOPMENT	REACTOME_REGULATION_OF_BETA:CELL_DEVELOPMENT	0.15
ENSG00000138794	CASP6 PPI subnetwork	0.15
ENSG00000104973	MED25 PPI subnetwork	0.15
ENSG00000180008	SOCS4 PPI subnetwork	0.15
ENSG00000087303	NID2 PPI subnetwork	0.15
MP:0003911	increased drinking behavior	0.15
MP:0000240	extramedullary hematopoiesis	0.15

Original gene set ID	Original gene set description	Nominal P value
ENSG00000206088	ENSG00000206088 PPI subnetwork	0.15
MP:0008215	decreased immature B cell number	0.15
ENSG00000154262	ABCA6 PPI subnetwork	0.15
GO:0070161	anchoring junction	0.15
GO:0030203	glycosaminoglycan metabolic process	0.15
ENSG00000029725	RABEP1 PPI subnetwork	0.15
GO:0016458	gene silencing	0.15
ENSG00000134987	WDR36 PPI subnetwork	0.15
ENSG00000118058	MLL PPI subnetwork	0.15
MP:0000812	abnormal dentate gyrus morphology	0.15
GO:0000922	spindle pole	0.15
ENSG00000147604	RPL7 PPI subnetwork	0.15
MP:0002864	abnormal ocular fundus morphology	0.15
ENSG00000136488	CSH1 PPI subnetwork	0.15
ENSG00000082805	ERC1 PPI subnetwork	0.15
GO:0050868	negative regulation of T cell activation	0.15
GO:0019900	kinase binding	0.15
ENSG00000180182	MED14 PPI subnetwork	0.15
ENSG00000115053	NCL PPI subnetwork	0.15
ENSG00000137500	CCDC90B PPI subnetwork	0.15
ENSG00000141510	TP53 PPI subnetwork	0.15
ENSG00000172766	NAA16 PPI subnetwork	0.15
ENSG00000111676	ATN1 PPI subnetwork	0.15
REACTOME_ABC:FAMILY_PROTEINS_MEDIATED_TRANSPORT	REACTOME_ABC:FAMILY_PROTEINS_MEDIATED_TRANSPORT	0.15
ENSG00000047936	ROS1 PPI subnetwork	0.15
GO:0032984	macromolecular complex disassembly	0.15
GO:0006085	acetyl-CoA biosynthetic process	0.15
GO:0003682	chromatin binding	0.15
ENSG00000196363	WDR5 PPI subnetwork	0.15
ENSG00000173402	DAG1 PPI subnetwork	0.15
MP:0000160	kyphosis	0.15
GO:0019838	growth factor binding	0.15
MP:0008475	intermingled spleen red and white pulp	0.15
MP:0003887	increased hepatocyte apoptosis	0.15
ENSG00000136244	IL6 PPI subnetwork	0.15
GO:0042826	histone deacetylase binding	0.15
ENSG00000211592	ENSG00000211592 PPI subnetwork	0.15
GO:0033157	regulation of intracellular protein transport	0.15
ENSG00000171208	NETO2 PPI subnetwork	0.15
ENSG00000115232	ITGA4 PPI subnetwork	0.15
ENSG00000163346	PBXIP1 PPI subnetwork	0.15
ENSG00000104549	SQLE PPI subnetwork	0.15
ENSG00000117222	RBBP5 PPI subnetwork	0.15
MP:0009238	coiled sperm flagellum	0.15
GO:0006024	glycosaminoglycan biosynthetic process	0.15
ENSG00000137757	CASP5 PPI subnetwork	0.15
ENSG00000185591	SP1 PPI subnetwork	0.15
ENSG00000108504	ENSG00000108504 PPI subnetwork	0.15
MP:0003055	abnormal long bone epiphyseal plate morphology	0.15

Original gene set ID	Original gene set description	Nominal P value
GO:0003705	RNA polymerase II distal enhancer sequence-specific DNA binding transcription factor	0.15
GO:0001570	vasculogenesis	0.15
MP:0002731	megacolon	0.15
ENSG00000147403	RPL10 PPI subnetwork	0.15
ENSG00000175592	FOSL1 PPI subnetwork	0.15
ENSG00000174697	LEP PPI subnetwork	0.15
MP:0001919	abnormal reproductive system physiology	0.15
ENSG00000136574	GATA4 PPI subnetwork	0.15
ENSG00000162891	IL20 PPI subnetwork	0.15
MP:0000321	increased bone marrow cell number	0.15
GO:0046966	thyroid hormone receptor binding	0.15
GO:0019319	hexose biosynthetic process	0.15
GO:0032580	Golgi cisterna membrane	0.15
MP:0003638	abnormal response/metabolism to endogenous compounds	0.15
GO:0030947	regulation of vascular endothelial growth factor receptor signaling pathway	0.15
ENSG00000120948	TARDBP PPI subnetwork	0.15
ENSG00000166285	ENSG00000166285 PPI subnetwork	0.15
ENSG00000204359	CFB PPI subnetwork	0.15
GO:0008653	lipopolysaccharide metabolic process	0.15
GO:0042803	protein homodimerization activity	0.15
ENSG00000037241	RPL26L1 PPI subnetwork	0.15
GO:0048514	blood vessel morphogenesis	0.15
MP:0000416	sparse hair	0.15
ENSG00000128487	SPECC1 PPI subnetwork	0.15
REACTOME_GTP_HYDROLYSIS_AND_JOINING_OF_THE_60S_RIBOSOMAL_SUBUNIT	REACTOME_GTP_HYDROLYSIS_AND_JOINING_OF_THE_60S_RIBOSOMAL_SUBUNIT	0.15
ENSG00000189403	HMGB1 PPI subnetwork	0.15
ENSG00000148297	MED22 PPI subnetwork	0.15
GO:0006916	anti-apoptosis	0.15
ENSG00000117408	IPO13 PPI subnetwork	0.15
ENSG00000156273	BACH1 PPI subnetwork	0.16
MP:0000454	abnormal jaw morphology	0.16
ENSG00000213625	LEPROT PPI subnetwork	0.16
GO:0005313	L-glutamate transmembrane transporter activity	0.16
GO:0050650	chondroitin sulfate proteoglycan biosynthetic process	0.16
GO:0005179	hormone activity	0.16
MP:0002493	increased IgG level	0.16
GO:0004806	triglyceride lipase activity	0.16
GO:0015103	inorganic anion transmembrane transporter activity	0.16
GO:0070482	response to oxygen levels	0.16
ENSG00000196700	ZNF512B PPI subnetwork	0.16
ENSG00000134588	USP26 PPI subnetwork	0.16
GO:0001568	blood vessel development	0.16
GO:0016585	chromatin remodeling complex	0.16
REACTOME_RHO_GTPASE_CYCLE	REACTOME_RHO_GTPASE_CYCLE	0.16
REACTOME_SIGNALING_BY_RHO_GTPASES	REACTOME_SIGNALING_BY_RHO_GTPASES	0.16
GO:0043449	cellular alkene metabolic process	0.16
GO:0006691	leukotriene metabolic process	0.16
GO:0030098	lymphocyte differentiation	0.16
ENSG00000072195	SPEG PPI subnetwork	0.16

Original gene set ID

GO:0016814
ENSG00000104365
MP:0004905
GO:0005790
GO:0008028
ENSG00000170871
ENSG00000206340
ENSG00000172172
MP:0002932
GO:0015909
GO:0060537
MP:0008075
ENSG00000147955
GO:0006023
GO:0034405
MP:0001874
ENSG00000206413
ENSG00000206493
MP:0011320
MP:0001156
GO:0019198
GO:0005001
GO:0001726
GO:0031047
MP:0005232
ENSG00000071537
ENSG00000189037
GO:0033209
GO:0030658
ENSG00000065989
ENSG00000175333
ENSG00000177283
GO:0035725
MP:0001732
GO:0018195
GO:0001893
REACTOME_PPARG_ACTIVATES_GENE_EXPRESSION
ENSG00000127329
MP:0011143
ENSG00000121989
MP:0005015
GO:0001501
ENSG00000111241
ENSG00000107831
ENSG00000158815
ENSG00000162344
ENSG00000156427
ENSG00000070388
ENSG00000183337

Original gene set description

hydrolase activity, acting on carbon-nitrogen (but not peptide) bonds, in cyclic amid 0.16
IKKBK PPI subnetwork 0.16
decreased uterus weight 0.16
smooth endoplasmic reticulum 0.16
monocarboxylic acid transmembrane transporter activity 0.16
KIAA0232 PPI subnetwork 0.16
C4A PPI subnetwork 0.16
MRPL13 PPI subnetwork 0.16
abnormal joint morphology 0.16
long-chain fatty acid transport 0.16
muscle tissue development 0.16
decreased CD4-positive T cell number 0.16
SIGMAR1 PPI subnetwork 0.16
aminoglycan biosynthetic process 0.16
response to fluid shear stress 0.16
acanthosis 0.16
ENSG00000206413 PPI subnetwork 0.16
HLA-E PPI subnetwork 0.16
abnormal glomerular capillary morphology 0.16
abnormal spermatogenesis 0.16
transmembrane receptor protein phosphatase activity 0.16
transmembrane receptor protein tyrosine phosphatase activity 0.16
ruffle 0.16
gene silencing by RNA 0.16
abnormal mesenteric lymph node morphology 0.16
SEL1L PPI subnetwork 0.16
DUSP21 PPI subnetwork 0.16
tumor necrosis factor-mediated signaling pathway 0.16
transport vesicle membrane 0.16
PDE4A PPI subnetwork 0.16
ENSG00000175333 PPI subnetwork 0.16
FZD8 PPI subnetwork 0.16
sodium ion transmembrane transport 0.16
postnatal growth retardation 0.16
peptidyl-arginine modification 0.16
maternal placenta development 0.16
REACTOME_PPARG_ACTIVATES_GENE_EXPRESSION 0.16
PTPRB PPI subnetwork 0.16
thick lung-associated mesenchyme 0.16
ACVR2A PPI subnetwork 0.16
increased T cell number 0.16
skeletal system development 0.16
FGF6 PPI subnetwork 0.16
FGF8 PPI subnetwork 0.16
FGF17 PPI subnetwork 0.16
FGF19 PPI subnetwork 0.16
FGF18 PPI subnetwork 0.16
FGF22 PPI subnetwork 0.16
BCOR PPI subnetwork 0.17

Nominal P value

Original gene set ID	Original gene set description	Nominal P value
GO:0043900	regulation of multi-organism process	0.17
GO:0033865	nucleoside bisphosphate metabolic process	0.17
ENSG00000007816	ENSG00000007816 PPI subnetwork	0.17
GO:0043500	muscle adaptation	0.17
ENSG00000086598	TMED2 PPI subnetwork	0.17
GO:0044241	lipid digestion	0.17
ENSG00000137285	TUBB2B PPI subnetwork	0.17
MP:0001191	abnormal skin condition	0.17
MP:0000367	abnormal coat/ hair morphology	0.17
ENSG00000120156	TEK PPI subnetwork	0.17
GO:0016529	sarcoplasmic reticulum	0.17
GO:0046661	male sex differentiation	0.17
GO:0046527	glucosyltransferase activity	0.17
MP:0008873	increased physiological sensitivity to xenobiotic	0.17
ENSG0000005884	ITGA3 PPI subnetwork	0.17
GO:0033273	response to vitamin	0.17
ENSG00000197045	GMFB PPI subnetwork	0.17
ENSG00000071539	TRIP13 PPI subnetwork	0.17
GO:0032012	regulation of ARF protein signal transduction	0.17
REACTOME_GLYCOPHINGOLIPID_METABOLISM	REACTOME_GLYCOPHINGOLIPID_METABOLISM	0.17
MP:0006354	abnormal fourth branchial arch artery morphology	0.17
KEGG_GALACTOSE_METABOLISM	KEGG_GALACTOSE_METABOLISM	0.17
ENSG00000087269	NOP14 PPI subnetwork	0.17
ENSG00000123416	TUBA1B PPI subnetwork	0.17
GO:0071706	tumor necrosis factor superfamily cytokine productior	0.17
GO:0005903	brush border	0.17
GO:0006641	triglyceride metabolic process	0.17
MP:0008208	decreased pro-B cell number	0.17
ENSG00000166598	HSP90B1 PPI subnetwork	0.17
ENSG00000118705	RPN2 PPI subnetwork	0.17
ENSG00000129214	SHBG PPI subnetwork	0.17
GO:0046889	positive regulation of lipid biosynthetic process	0.17
GO:0019888	protein phosphatase regulator activity	0.17
ENSG00000108264	TADA2A PPI subnetwork	0.17
ENSG00000132196	HSD17B7 PPI subnetwork	0.17
MP:0008280	male germ cell apoptosis	0.17
GO:0051250	negative regulation of lymphocyte activation	0.17
GO:0008299	isoprenoid biosynthetic process	0.17
ENSG00000055957	ITIH1 PPI subnetwork	0.17
GO:0046128	purine ribonucleoside metabolic process	0.17
ENSG00000002330	BAD PPI subnetwork	0.17
GO:0016570	histone modification	0.17
ENSG00000141522	ARHGDI1 PPI subnetwork	0.17
MP:0000358	abnormal cell morphology	0.17
ENSG00000107242	PIP5K1B PPI subnetwork	0.17
GO:0019748	secondary metabolic process	0.17
ENSG00000167244	IGF2 PPI subnetwork	0.17
GO:0000139	Golgi membrane	0.17
ENSG00000138675	FGF5 PPI subnetwork	0.17

Original gene set ID	Original gene set description	Nominal P value
REACTOME_REGULATION_OF_PYRUVATE_DEHYDROGENASE_PDH_COMPLEX	REACTOME_REGULATION_OF_PYRUVATE_DEHYDROGENASE_PDH_COMPLEX	0.17
ENSG00000169136	ATF5 PPI subnetwork	0.17
MP:0006397	disorganized long bone epiphyseal plate	0.17
GO:0046546	development of primary male sexual characteristics	0.17
ENSG00000127318	IL22 PPI subnetwork	0.17
MP:0003998	decreased thermal nociceptive threshold	0.17
MP:0008782	increased B cell apoptosis	0.17
ENSG00000033327	GAB2 PPI subnetwork	0.17
GO:0015172	acidic amino acid transmembrane transporter activity	0.17
ENSG00000110492	MDK PPI subnetwork	0.17
GO:0010741	negative regulation of intracellular protein kinase cascade	0.17
GO:0005251	delayed rectifier potassium channel activity	0.17
GO:0042158	lipoprotein biosynthetic process	0.17
MP:0003140	dilated heart atrium	0.17
ENSG00000012660	ELOVL5 PPI subnetwork	0.17
REACTOME_HEMOSTASIS	REACTOME_HEMOSTASIS	0.17
ENSG00000127511	SIN3B PPI subnetwork	0.17
ENSG00000150281	CTF1 PPI subnetwork	0.17
ENSG00000125998	FAM83C PPI subnetwork	0.17
MP:0001190	reddish skin	0.17
GO:0043687	post-translational protein modification	0.17
GO:0006415	translational termination	0.18
GO:0032312	regulation of ARF GTPase activity	0.18
GO:0030198	extracellular matrix organization	0.18
GO:0043062	extracellular structure organization	0.18
GO:0046777	protein autophosphorylation	0.18
ENSG00000175221	MED16 PPI subnetwork	0.18
ENSG00000167721	TSR1 PPI subnetwork	0.18
GO:0019210	kinase inhibitor activity	0.18
GO:0022625	cytosolic large ribosomal subunit	0.18
MP:0001925	male infertility	0.18
ENSG00000129219	PLD2 PPI subnetwork	0.18
ENSG00000058729	RIOK2 PPI subnetwork	0.18
GO:0015450	P-P-bond-hydrolysis-driven protein transmembrane transporter activity	0.18
ENSG00000103742	IGDCC4 PPI subnetwork	0.18
MP:0002447	abnormal erythrocyte morphology	0.18
REACTOME_CELL_JUNCTION_ORGANIZATION	REACTOME_CELL_JUNCTION_ORGANIZATION	0.18
ENSG00000161970	RPL26 PPI subnetwork	0.18
ENSG00000147873	IFNA5 PPI subnetwork	0.18
ENSG00000186803	IFNA10 PPI subnetwork	0.18
ENSG00000120247	ENSG00000120247 PPI subnetwork	0.18
ENSG00000147877	ENSG00000147877 PPI subnetwork	0.18
ENSG00000188379	IFNA2 PPI subnetwork	0.18
ENSG00000186809	ENSG00000186809 PPI subnetwork	0.18
ENSG00000147885	IFNA16 PPI subnetwork	0.18
ENSG00000137080	IFNA21 PPI subnetwork	0.18
ENSG00000120242	IFNA8 PPI subnetwork	0.18
GO:0043967	histone H4 acetylation	0.18
MP:0002904	increased circulating parathyroid hormone leve	0.18

Original gene set ID	Original gene set description	Nominal P value
GO:0046697	decidualization	0.18
MP:0008115	abnormal dendritic cell differentiation	0.18
ENSG000000086189	DIMT1 PPI subnetwork	0.18
ENSG00000113889	KNG1 PPI subnetwork	0.18
MP:0005146	decreased circulating VLDL cholesterol level	0.18
MP:0005136	decreased growth hormone level	0.18
ENSG00000188130	MAPK12 PPI subnetwork	0.18
GO:0016779	nucleotidyltransferase activity	0.18
GO:0010907	positive regulation of glucose metabolic process	0.18
ENSG00000100842	EFS PPI subnetwork	0.18
REACTOME_METAL_ION_SLC_TRANSPORTERS	REACTOME_METAL_ION_SLC_TRANSPORTERS	0.18
GO:0006829	zinc ion transport	0.18
GO:0090263	positive regulation of canonical Wnt receptor signaling pathway	0.18
KEGG_TERPENOID_BACKBONE_BIOSYNTHESIS	KEGG_TERPENOID_BACKBONE_BIOSYNTHESIS	0.18
MP:0000187	abnormal triglyceride level	0.18
GO:0030246	carbohydrate binding	0.18
GO:0017048	Rho GTPase binding	0.18
MP:0000259	abnormal vascular development	0.18
MP:0008844	decreased subcutaneous adipose tissue amount	0.18
KEGG_BASAL_CELL_CARCINOMA	KEGG_BASAL_CELL_CARCINOMA	0.18
GO:0050839	cell adhesion molecule binding	0.18
GO:0015145	monosaccharide transmembrane transporter activity	0.18
GO:0004181	metallocarboxypeptidase activity	0.18
ENSG00000155957	TMBIM4 PPI subnetwork	0.18
GO:0006412	translation	0.18
REACTOME_GPVI:MEDIATED_ACTIVATION_CASCADE	REACTOME_GPVI:MEDIATED_ACTIVATION_CASCADE	0.18
MP:0008658	decreased interleukin-1 beta secretion	0.18
ENSG00000163956	LRPAP1 PPI subnetwork	0.18
GO:0016528	sarcoplasm	0.18
ENSG00000082781	ITGB5 PPI subnetwork	0.18
GO:0045069	regulation of viral genome replication	0.18
MP:0005048	thrombosis	0.18
ENSG00000206308	HLA-DRA PPI subnetwork	0.18
GO:0005635	nuclear envelope	0.18
GO:0044420	extracellular matrix part	0.18
REACTOME_INTERFERON_SIGNALING	REACTOME_INTERFERON_SIGNALING	0.18
MP:0000706	small thymus	0.18
GO:0051569	regulation of histone H3-K4 methylation	0.18
ENSG00000204983	PRSS1 PPI subnetwork	0.18
MP:0004841	abnormal small intestine crypts of Lieberkuhn morphology	0.18
ENSG00000115866	DARS PPI subnetwork	0.18
GO:0001825	blastocyst formation	0.18
MP:0009414	skeletal muscle fiber necrosis	0.18
ENSG00000173039	RELA PPI subnetwork	0.18
KEGG_ENDOCYTOSIS	KEGG_ENDOCYTOSIS	0.18
ENSG00000171223	JUNB PPI subnetwork	0.18
ENSG00000136110	LECT1 PPI subnetwork	0.18
GO:0005537	mannose binding	0.18
ENSG00000138326	RPS24 PPI subnetwork	0.18

Original gene set ID	Original gene set description	Nominal P value
ENSG00000183311	TUBB PPI subnetwork	0.18
ENSG00000196230	TUBB PPI subnetwork	0.18
ENSG00000137379	ENSG00000137379 PPI subnetwork	0.18
GO:0004659	prenyltransferase activity	0.18
MP:0004229	abnormal embryonic erythropoiesis	0.18
MP:0000554	abnormal carpal bone morphology	0.18
ENSG00000133511	ENSG00000133511 PPI subnetwork	0.18
REACTOME_PLATELET_ACTIVATION_SIGNALING_AND_AGGREGATION	REACTOME_PLATELET_ACTIVATION_SIGNALING_AND_AGGREGATION	0.18
GO:0070085	glycosylation	0.18
ENSG00000133935	C14orf1 PPI subnetwork	0.18
REACTOME_NF:KB_ACTIVATION_THROUGH_FADDRIP:1_PATHWAY_MEDIATED_BY	REACTOME_NF:KB_ACTIVATION_THROUGH_FADDRIP:1_PATHWAY_MEDIATED_BY	0.18
MP:0002724	enhanced wound healing	0.18
ENSG00000110169	HPX PPI subnetwork	0.18
REACTOME_PLATELET_AGGREGATION_PLUG_FORMATION	REACTOME_PLATELET_AGGREGATION_PLUG_FORMATION	0.18
MP:0009743	preaxial polydactyly	0.18
ENSG00000188223	LIN37 PPI subnetwork	0.18
ENSG00000182774	RPS17L PPI subnetwork	0.18
ENSG00000184779	RPS17 PPI subnetwork	0.18
GO:0004675	transmembrane receptor protein serine/threonine kinase activity	0.18
MP:0009940	abnormal hippocampus pyramidal cell morphology	0.18
MP:0000928	incomplete cephalic closure	0.18
MP:0002666	increased circulating aldosterone level	0.18
REACTOME_TERMINATION_OF_O:GLYCAN_BIOSYNTHESIS	REACTOME_TERMINATION_OF_O:GLYCAN_BIOSYNTHESIS	0.18
GO:0015924	mannosyl-oligosaccharide mannosidase activity	0.18
ENSG00000133805	AMPD3 PPI subnetwork	0.18
ENSG00000106125	FAM188B PPI subnetwork	0.18
ENSG00000157168	NRG1 PPI subnetwork	0.18
MP:0005025	abnormal response to infection	0.18
ENSG00000183405	ENSG00000183405 PPI subnetwork	0.18
ENSG00000182446	NPLOC4 PPI subnetwork	0.18
MP:0001819	abnormal immune cell physiology	0.18
MP:0003408	increased width of hypertrophic chondrocyte zone	0.18
MP:0009142	decreased prepulse inhibition	0.18
REACTOME_CYTOKINE_SIGNALING_IN_IMMUNE_SYSTEM	REACTOME_CYTOKINE_SIGNALING_IN_IMMUNE_SYSTEM	0.18
GO:0032680	regulation of tumor necrosis factor production	0.18
GO:0032640	tumor necrosis factor production	0.18
MP:0004808	abnormal hematopoietic stem cell morphology	0.18
GO:0043330	response to exogenous dsRNA	0.18
GO:0002922	positive regulation of humoral immune response	0.18
MP:0002432	abnormal CD4-positive T cell morphology	0.18
ENSG00000188529	SRSF10 PPI subnetwork	0.18
ENSG00000160213	CSTB PPI subnetwork	0.18
MP:0010067	increased red blood cell distribution width	0.18
ENSG00000111845	PAK1IP1 PPI subnetwork	0.18
ENSG00000198467	TPM2 PPI subnetwork	0.18
ENSG00000163513	TGFBR2 PPI subnetwork	0.18
ENSG00000075539	FRYL PPI subnetwork	0.18
MP:0006059	decreased susceptibility to ischemic brain injury	0.18
ENSG00000186468	RPS23 PPI subnetwork	0.18

Original gene set ID	Original gene set description	Nominal P value
GO:0003697	single-stranded DNA binding	0.18
ENSG00000155926	SLA PPI subnetwork	0.18
ENSG00000136891	TEX10 PPI subnetwork	0.18
MP:0011108	partial embryonic lethality during organogenesis	0.18
GO:0032008	positive regulation of TOR signaling cascade	0.18
ENSG00000198265	HELZ PPI subnetwork	0.18
ENSG00000106617	PRKAG2 PPI subnetwork	0.18
GO:0051129	negative regulation of cellular component organization	0.18
ENSG00000121653	MAPK8IP1 PPI subnetwork	0.18
GO:0072659	protein localization in plasma membrane	0.18
ENSG00000176273	SLC35G1 PPI subnetwork	0.19
GO:0043413	macromolecule glycosylation	0.19
GO:0006486	protein glycosylation	0.19
MP:0003799	impaired macrophage chemotaxis	0.19
MP:0002644	decreased circulating triglyceride level	0.19
ENSG00000205813	ENSG00000205813 PPI subnetwork	0.19
ENSG00000109272	PF4V1 PPI subnetwork	0.19
GO:0002456	T cell mediated immunity	0.19
ENSG00000161202	DVL3 PPI subnetwork	0.19
GO:0015144	carbohydrate transmembrane transporter activity	0.19
ENSG00000197561	ELANE PPI subnetwork	0.19
MP:0001879	abnormal lymphatic vessel morphology	0.19
GO:0046982	protein heterodimerization activity	0.19
ENSG00000168214	RBPJ PPI subnetwork	0.19
MP:0001698	decreased embryo size	0.19
GO:0045834	positive regulation of lipid metabolic process	0.19
ENSG00000103510	KAT8 PPI subnetwork	0.19
REACTOME_REGULATION_OF_IFNA_SIGNALING	REACTOME_REGULATION_OF_IFNA_SIGNALING	0.19
ENSG00000122406	RPL5 PPI subnetwork	0.19
ENSG00000111615	KRR1 PPI subnetwork	0.19
ENSG00000185479	KRT6B PPI subnetwork	0.19
ENSG00000137807	KIF23 PPI subnetwork	0.19
MP:0000440	domed cranium	0.19
REACTOME_ETHANOL_OXIDATION	REACTOME_ETHANOL_OXIDATION	0.19
GO:0010830	regulation of myotube differentiation	0.19
MP:0004351	short humerus	0.19
ENSG00000158417	EIF5B PPI subnetwork	0.19
GO:0030695	GTPase regulator activity	0.19
GO:0004198	calcium-dependent cysteine-type endopeptidase activity	0.19
GO:0060541	respiratory system development	0.19
MP:0008083	decreased single-positive T cell number	0.19
MP:0002461	increased immunoglobulin level	0.19
GO:0017119	Golgi transport complex	0.19
GO:0005875	microtubule associated complex	0.19
MP:0000060	delayed bone ossification	0.19
REACTOME_SIGNALING_BY_INTERLEUKINS	REACTOME_SIGNALING_BY_INTERLEUKINS	0.19
GO:0008209	androgen metabolic process	0.19
REACTOME_ASPARAGINE_N:LINKED_GLYCOSYLATION	REACTOME_ASPARAGINE_N:LINKED_GLYCOSYLATION	0.19
GO:0045987	positive regulation of smooth muscle contraction	0.19

Original gene set ID	Original gene set description	Nominal P value
GO:0031985	Golgi cisterna	0.19
ENSG00000118402	ELOVL4 PPI subnetwork	0.19
ENSG00000104969	SGTA PPI subnetwork	0.19
MP:0003984	embryonic growth retardation	0.19
KEGG_CELL_CYCLE	KEGG_CELL_CYCLE	0.19
ENSG00000145781	COMMD10 PPI subnetwork	0.19
GO:0043492	ATPase activity, coupled to movement of substances	0.19
ENSG00000169083	AR PPI subnetwork	0.19
ENSG00000115718	PROC PPI subnetwork	0.19
ENSG00000083845	RPS5 PPI subnetwork	0.19
ENSG00000197959	DNM3 PPI subnetwork	0.19
GO:0043401	steroid hormone mediated signaling pathway	0.19
MP:0003216	absence seizures	0.19
MP:0001289	persistence of hyaloid vascular system	0.19
ENSG00000064012	CASP8 PPI subnetwork	0.19
ENSG00000119408	NEK6 PPI subnetwork	0.19
MP:0001622	abnormal vasculogenesis	0.19
ENSG00000113520	IL4 PPI subnetwork	0.19
ENSG00000196656	ENSG00000196656 PPI subnetwork	0.19
ENSG00000197728	RPS26 PPI subnetwork	0.19
ENSG00000117410	ATP6V0B PPI subnetwork	0.19
REACTOME_METABOLISM_OF_STEROID_HORMONES_AND_VITAMINS_A_AND_D	REACTOME_METABOLISM_OF_STEROID_HORMONES_AND_VITAMINS_A_AND_D	0.19
ENSG00000164022	AIMP1 PPI subnetwork	0.19
MP:0001127	small ovary	0.19
MP:0000291	enlarged pericardium	0.19
ENSG00000163347	CLDN1 PPI subnetwork	0.19
ENSG00000112118	MCM3 PPI subnetwork	0.19
ENSG00000163050	ADCK3 PPI subnetwork	0.19
GO:0032480	negative regulation of type I interferon productior	0.19
GO:0090179	planar cell polarity pathway involved in neural tube closure	0.19
GO:0090178	regulation of establishment of planar polarity involved in neural tube closure	0.19
MP:0001601	abnormal myelopoiesis	0.19
ENSG00000106462	EZH2 PPI subnetwork	0.19
REACTOME_RNA_POLYMERASE_III_ABORTIVE_AND_RETRACTIVE_INITIATION	REACTOME_RNA_POLYMERASE_III_ABORTIVE_AND_RETRACTIVE_INITIATION	0.19
REACTOME_RNA_POLYMERASE_III_TRANSCRIPTION	REACTOME_RNA_POLYMERASE_III_TRANSCRIPTION	0.19
ENSG00000196365	LONP1 PPI subnetwork	0.19
MP:0002078	abnormal glucose homeostasis	0.19
ENSG00000006062	MAP3K14 PPI subnetwork	0.19
ENSG00000077150	NFKB2 PPI subnetwork	0.19
ENSG00000166197	NOLC1 PPI subnetwork	0.19
ENSG00000133101	CCNA1 PPI subnetwork	0.19
GO:0014706	striated muscle tissue development	0.19
MP:0010300	increased skin tumor incidence	0.19
GO:0009749	response to glucose stimulus	0.19
ENSG00000013441	CLK1 PPI subnetwork	0.19
ENSG00000120800	UTP20 PPI subnetwork	0.19
ENSG00000175387	SMAD2 PPI subnetwork	0.19
ENSG00000124006	OBSL1 PPI subnetwork	0.19
GO:0032494	response to peptidoglycan	0.19

Original gene set ID	Original gene set description	Nominal P value
REACTOME_GLUCOSE_METABOLISM	REACTOME_GLUCOSE_METABOLISM	0.19
ENSG00000198517	MAFK PPI subnetwork	0.19
MP:0005185	decreased circulating progesterone level	0.19
GO:0055017	cardiac muscle tissue growth	0.19
MP:0002543	brachyphalangia	0.19
GO:0007266	Rho protein signal transduction	0.19
MP:0001802	arrested B cell differentiation	0.19
ENSG00000182393	IL29 PPI subnetwork	0.19
ENSG00000111536	IL26 PPI subnetwork	0.19
ENSG00000142224	IL19 PPI subnetwork	0.19
ENSG00000145839	IL9 PPI subnetwork	0.19
ENSG00000183709	IL28A PPI subnetwork	0.19
ENSG00000162892	IL24 PPI subnetwork	0.19
ENSG00000104432	IL7 PPI subnetwork	0.19
ENSG00000177047	IFNW1 PPI subnetwork	0.19
ENSG00000164136	IL15 PPI subnetwork	0.19
ENSG00000147896	IFNK PPI subnetwork	0.19
ENSG00000138684	IL21 PPI subnetwork	0.19
ENSG00000128342	LIF PPI subnetwork	0.19
ENSG00000184995	IFNE PPI subnetwork	0.19
ENSG00000197110	IL28B PPI subnetwork	0.19
GO:0003779	actin binding	0.19
ENSG00000104938	CLEC4M PPI subnetwork	0.19
GO:0000803	sex chromosome	0.19
GO:0017153	sodium:dicarboxylate symporter activity	0.19
ENSG00000110944	IL23A PPI subnetwork	0.19
GO:0007530	sex determination	0.19
ENSG00000188994	ZNF292 PPI subnetwork	0.19
MP:0011506	glomerular crescent	0.19
MP:0000572	abnormal autopod morphology	0.19
KEGG_COLORECTAL_CANCER	KEGG_COLORECTAL_CANCER	0.19
MP:0008102	lymph node hyperplasia	0.19
GO:0007548	sex differentiation	0.19
ENSG00000213764	ENSG00000213764 PPI subnetwork	0.2
ENSG00000196459	TRAPPC2 PPI subnetwork	0.2
ENSG00000105202	FBL PPI subnetwork	0.2
GO:0030159	receptor signaling complex scaffold activity	0.2
ENSG00000010278	CD9 PPI subnetwork	0.2
GO:0002690	positive regulation of leukocyte chemotaxis	0.2
ENSG00000107282	APBA1 PPI subnetwork	0.2
KEGG_NOTCH_SIGNALING_PATHWAY	KEGG_NOTCH_SIGNALING_PATHWAY	0.2
ENSG00000198646	NCOA6 PPI subnetwork	0.2
ENSG00000131051	RBM39 PPI subnetwork	0.2
ENSG00000154134	ROBO3 PPI subnetwork	0.2
MP:0008347	decreased gamma-delta T cell number	0.2
ENSG00000130396	MLLT4 PPI subnetwork	0.2
ENSG00000145192	AHSG PPI subnetwork	0.2
ENSG00000170027	YWHAG PPI subnetwork	0.2
ENSG00000132603	NIP7 PPI subnetwork	0.2

Original gene set ID	Original gene set description	Nominal P value
GO:0071383	cellular response to steroid hormone stimulus	0.2
ENSG00000113407	TARS PPI subnetwork	0.2
ENSG00000124228	DDX27 PPI subnetwork	0.2
MP:0003227	abnormal vascular branching morphogenesis	0.2
GO:0045351	type I interferon biosynthetic process	0.2
GO:2000106	regulation of leukocyte apoptotic process	0.2
REACTOME_GLYCOLYSIS	REACTOME_GLYCOLYSIS	0.2
ENSG00000102391	ENSG00000102391 PPI subnetwork	0.2
ENSG00000035403	VCL PPI subnetwork	0.2
ENSG00000164134	NAA15 PPI subnetwork	0.2
ENSG00000164399	IL3 PPI subnetwork	0.2
GO:0043901	negative regulation of multi-organism process	0.2
MP:0000825	dilated lateral ventricles	0.2
ENSG00000119285	HEATR1 PPI subnetwork	0.2
ENSG0000011243	AKAP8L PPI subnetwork	0.2
GO:0016485	protein processing	0.2
ENSG00000160285	LSS PPI subnetwork	0.2
ENSG00000127022	CANX PPI subnetwork	0.2
MP:0000462	abnormal digestive system morphology	0.2
ENSG00000005961	ITGA2B PPI subnetwork	0.2
GO:0061097	regulation of protein tyrosine kinase activity	0.2
GO:0048770	pigment granule	0.2
GO:0042470	melanosome	0.2
ENSG00000144713	RPL32 PPI subnetwork	0.2
REACTOME_3_:_UTR:MEDIATED_TRANSLATIONAL_REGULATION	REACTOME_3_:_UTR:MEDIATED_TRANSLATIONAL_REGULATION	0.2
REACTOME_L13A:MEDIATED_TRANSLATIONAL_SILENCING_OF_CERULOPLASMI	REACTOME_L13A:MEDIATED_TRANSLATIONAL_SILENCING_OF_CERULOPLASMIN_E	0.2
ENSG00000114391	RPL24 PPI subnetwork	0.2
GO:0042278	purine nucleoside metabolic process	0.2
KEGG_MTOR_SIGNALING_PATHWAY	KEGG_MTOR_SIGNALING_PATHWAY	0.2
ENSG00000215412	ENSG00000215412 PPI subnetwork	0.2
ENSG00000198563	DDX39B PPI subnetwork	0.2
ENSG00000215425	DDX39B PPI subnetwork	0.2
GO:0050921	positive regulation of chemotaxis	0.2
ENSG00000123159	GIPC1 PPI subnetwork	0.2
ENSG00000169194	IL13 PPI subnetwork	0.2
ENSG00000038002	AGA PPI subnetwork	0.2
MP:0005091	increased double-positive T cell number	0.2
MP:0003720	abnormal neural tube closure	0.2
MP:0001260	increased body weight	0.2
GO:0006342	chromatin silencing	0.2
GO:0006006	glucose metabolic process	0.2
GO:0055102	lipase inhibitor activity	0.2
REACTOME_TRAF3:DEPENDENT_IRF_ACTIVATION_PATHWAY	REACTOME_TRAF3:DEPENDENT_IRF_ACTIVATION_PATHWAY	0.2
MP:0008511	thin retinal inner nuclear layer	0.2
MP:0000715	decreased thymocyte number	0.2
GO:0008289	lipid binding	0.2
ENSG00000131069	ACSS2 PPI subnetwork	0.2
ENSG00000205246	RPSAP58 PPI subnetwork	0.2
GO:0008593	regulation of Notch signaling pathway	0.2

Original gene set ID	Original gene set description	Nominal P value
MP:0000694	spleen hypoplasia	0.21
ENSG00000177200	CHD9 PPI subnetwork	0.21
ENSG00000136718	IMP4 PPI subnetwork	0.21
ENSG00000164163	ABCE1 PPI subnetwork	0.22
MP:0006144	increased systemic arterial systolic blood pressure	0.22
ENSG00000164220	F2RL2 PPI subnetwork	0.22
MP:0005602	decreased angiogenesis	0.22
MP:0000465	gastrointestinal hemorrhage	0.22
GO:0002709	regulation of T cell mediated immunity	0.22
MP:0003659	abnormal lymph circulation	0.22
ENSG00000164751	PEX2 PPI subnetwork	0.22
GO:0010951	negative regulation of endopeptidase activity	0.22
MP:0005169	abnormal male meiosis	0.22
MP:0002467	impaired neutrophil phagocytosis	0.22
ENSG00000188846	RPL14 PPI subnetwork	0.22
ENSG00000108256	NUFIP2 PPI subnetwork	0.22
KEGG_MATURITY_ONSET_DIABETES_OF_THE_YOUNG	KEGG_MATURITY_ONSET_DIABETES_OF_THE_YOUNG	0.22
ENSG00000115414	FN1 PPI subnetwork	0.22
ENSG00000136869	TLR4 PPI subnetwork	0.22
ENSG00000108270	AATF PPI subnetwork	0.22
GO:0018200	peptidyl-glutamic acid modification	0.22
GO:0002230	positive regulation of defense response to virus by host	0.22
KEGG_RIBOSOME	KEGG_RIBOSOME	0.22
ENSG00000142541	RPL13A PPI subnetwork	0.22
GO:0008757	S-adenosylmethionine-dependent methyltransferase activity	0.22
GO:0008217	regulation of blood pressure	0.22
GO:0006417	regulation of translation	0.22
ENSG00000075391	RASAL2 PPI subnetwork	0.22
ENSG00000138442	WDR12 PPI subnetwork	0.22
ENSG00000099797	TECR PPI subnetwork	0.22
GO:0003727	single-stranded RNA binding	0.22
MP:0000601	small liver	0.22
MP:0002784	abnormal Sertoli cell morphology	0.22
GO:0008060	ARF GTPase activator activity	0.22
MP:0005244	hemopericardium	0.22
MP:0005559	increased circulating glucose level	0.22
GO:0019865	immunoglobulin binding	0.22
ENSG00000186141	POLR3C PPI subnetwork	0.22
GO:0032095	regulation of response to food	0.22
GO:0007018	microtubule-based movement	0.22
ENSG00000075643	MOCOS PPI subnetwork	0.22
MP:0002836	abnormal chorion morphology	0.22
ENSG00000185010	F8 PPI subnetwork	0.22
ENSG00000179958	DCTPP1 PPI subnetwork	0.22
GO:0015631	tubulin binding	0.22
ENSG00000149480	MTA2 PPI subnetwork	0.22
GO:0042771	DNA damage response, signal transduction by p53 class mediator resulting in induction of	0.22
GO:0032760	positive regulation of tumor necrosis factor production	0.22
GO:0044319	wound healing, spreading of cells	0.22

Original gene set ID	Original gene set description	Nominal P value
ENSG00000166313	APBB1 PPI subnetwork	0.22
GO:0022415	viral reproductive process	0.22
ENSG00000135090	TAKO3 PPI subnetwork	0.22
MP:0004014	abnormal uterine environment	0.22
MP:0002001	blindness	0.22
MP:0002689	abnormal molar morphology	0.22
GO:0004683	calmodulin-dependent protein kinase activity	0.22
ENSG00000145833	DDX46 PPI subnetwork	0.22
ENSG00000118513	MYB PPI subnetwork	0.22
GO:0016569	covalent chromatin modification	0.22
ENSG00000097007	ABL1 PPI subnetwork	0.22
MP:0001577	anemia	0.22
MP:0002551	abnormal blood coagulation	0.22
ENSG00000179222	MAGED1 PPI subnetwork	0.22
ENSG00000138398	PPIG PPI subnetwork	0.22
GO:0002252	immune effector process	0.22
MP:0001242	hyperkeratosis	0.22
GO:0050688	regulation of defense response to virus	0.22
MP:0001722	pale yolk sac	0.22
GO:0042476	odontogenesis	0.22
MP:0001274	curly vibrissae	0.22
GO:0060338	regulation of type I interferon-mediated signaling pathway	0.22
ENSG00000117266	CDK18 PPI subnetwork	0.22
GO:0072509	divalent inorganic cation transmembrane transporter activity	0.22
MP:0004362	cochlear hair cell degeneration	0.22
GO:0048730	epidermis morphogenesis	0.22
GO:0048732	gland development	0.22
GO:0016884	carbon-nitrogen ligase activity, with glutamine as amido-N-donor	0.23
GO:0005520	insulin-like growth factor binding	0.23
MP:0004989	decreased osteoblast cell number	0.23
ENSG00000180340	FZD2 PPI subnetwork	0.23
ENSG00000049759	NEDD4L PPI subnetwork	0.23
REACTOME_FORMATION_OF_A_POOL_OF_FREE_40S_SUBUNITS	REACTOME_FORMATION_OF_A_POOL_OF_FREE_40S_SUBUNITS	0.23
GO:0045823	positive regulation of heart contraction	0.23
GO:0007566	embryo implantation	0.23
MP:0008211	decreased mature B cell number	0.23
REACTOME_ANTIVIRAL_MECHANISM_BY_IFN:STIMULATED_GENES	REACTOME_ANTIVIRAL_MECHANISM_BY_IFN:STIMULATED_GENES	0.23
REACTOME_ISG15_ANTIVIRAL_MECHANISM	REACTOME_ISG15_ANTIVIRAL_MECHANISM	0.23
GO:0030662	coated vesicle membrane	0.23
ENSG00000034053	APBA2 PPI subnetwork	0.23
GO:0032481	positive regulation of type I interferon production	0.23
ENSG00000160293	VAV2 PPI subnetwork	0.23
MP:0008603	decreased circulating interleukin-4 level	0.23
ENSG00000013364	MVP PPI subnetwork	0.23
ENSG00000197766	CFD PPI subnetwork	0.23
ENSG00000140986	RPL3L PPI subnetwork	0.23
ENSG00000187498	COL4A1 PPI subnetwork	0.23
ENSG00000012983	MAP4K5 PPI subnetwork	0.23
MP:0002272	abnormal nervous system electrophysiology	0.23

Original gene set ID	Original gene set description	Nominal P value
GO:0004252	serine-type endopeptidase activity	0.23
REACTOME_ABCA_TRANSPORTERS_IN_LIPID_HOMEOSTASIS	REACTOME_ABCA_TRANSPORTERS_IN_LIPID_HOMEOSTASIS	0.23
ENSG000000124587	PEX6 PPI subnetwork	0.23
GO:0015171	amino acid transmembrane transporter activity	0.23
GO:0001569	patterning of blood vessels	0.23
MP:0006398	increased long bone epiphyseal plate size	0.23
ENSG000000186350	RXRA PPI subnetwork	0.23
ENSG000000140988	RPS2 PPI subnetwork	0.23
GO:0045746	negative regulation of Notch signaling pathway	0.23
MP:0000223	decreased monocyte cell number	0.23
GO:0071219	cellular response to molecule of bacterial origin	0.23
GO:0002448	mast cell mediated immunity	0.23
ENSG000000011422	PLAUR PPI subnetwork	0.23
GO:0042439	ethanolamine-containing compound metabolic process	0.23
GO:0019901	protein kinase binding	0.23
ENSG000000141837	CACNA1A PPI subnetwork	0.23
MP:0001891	hydroencephaly	0.23
ENSG000000175505	CLCF1 PPI subnetwork	0.23
GO:0060589	nucleoside-triphosphatase regulator activity	0.23
ENSG000000198641	ENSG000000198641 PPI subnetwork	0.23
ENSG000000134070	IRAK2 PPI subnetwork	0.23
GO:0072657	protein localization in membrane	0.23
GO:0035272	exocrine system development	0.23
GO:0010510	regulation of acetyl-CoA biosynthetic process from pyruvate	0.23
GO:0006086	acetyl-CoA biosynthetic process from pyruvate	0.23
ENSG000000101361	NOP56 PPI subnetwork	0.23
GO:0031667	response to nutrient levels	0.23
ENSG000000100448	CTSG PPI subnetwork	0.23
ENSG000000174469	CNTNAP2 PPI subnetwork	0.23
ENSG000000172531	PPP1CA PPI subnetwork	0.23
GO:0009086	methionine biosynthetic process	0.23
GO:0030176	integral to endoplasmic reticulum membrane	0.23
GO:0051650	establishment of vesicle localization	0.23
ENSG000000143851	PTPN7 PPI subnetwork	0.23
ENSG000000119812	FAM98A PPI subnetwork	0.23
ENSG000000116711	PLA2G4A PPI subnetwork	0.23
ENSG000000170145	SIK2 PPI subnetwork	0.23
ENSG000000164934	DCAF13 PPI subnetwork	0.23
ENSG000000150337	FCGR1A PPI subnetwork	0.23
ENSG000000171863	RPS7 PPI subnetwork	0.23
MP:0001004	abnormal retinal photoreceptor morphology	0.23
ENSG000000033800	PIAS1 PPI subnetwork	0.23
ENSG000000112715	VEGFA PPI subnetwork	0.23
ENSG000000064703	DDX20 PPI subnetwork	0.23
GO:0035019	somatic stem cell maintenance	0.23
GO:0033673	negative regulation of kinase activity	0.23
GO:0031227	intrinsic to endoplasmic reticulum membrane	0.23
ENSG000000076248	UNG PPI subnetwork	0.23
GO:0009792	embryo development ending in birth or egg hatching	0.23

Original gene set ID	Original gene set description	Nominal P value
GO:0004602	glutathione peroxidase activity	0.23
GO:0005765	lysosomal membrane	0.23
GO:0031018	endocrine pancreas development	0.23
ENSG00000163879	DNALI1 PPI subnetwork	0.23
GO:0002467	germinal center formation	0.23
ENSG00000111276	CDKN1B PPI subnetwork	0.23
ENSG00000088035	ALG6 PPI subnetwork	0.23
GO:0071222	cellular response to lipopolysaccharide	0.23
REACTOME_TAK1_ACTIVATES_NFKB_BY_PHOSPHORYLATION_AND_ACTIVATIO	REACTOME_TAK1_ACTIVATES_NFKB_BY_PHOSPHORYLATION_AND_ACTIVATION_O	0.23
GO:0019953	sexual reproduction	0.23
ENSG00000155868	MED7 PPI subnetwork	0.23
ENSG00000160307	S100B PPI subnetwork	0.23
ENSG00000070193	FGF10 PPI subnetwork	0.23
MP:0001106	abnormal Schwann cell morphology	0.23
MP:0001125	abnormal oocyte morphology	0.23
GO:0032870	cellular response to hormone stimulus	0.23
GO:0015711	organic anion transport	0.23
MP:0001829	increased activated T cell number	0.23
ENSG00000213023	SYT3 PPI subnetwork	0.23
GO:0005868	cytoplasmic dynein complex	0.23
GO:0070371	ERK1 and ERK2 cascade	0.23
GO:0035265	organ growth	0.23
MP:0004804	decreased susceptibility to autoimmune diabetes	0.23
MP:0008723	impaired eosinophil recruitment	0.23
ENSG00000111707	SUDS3 PPI subnetwork	0.23
GO:0060041	retina development in camera-type eye	0.23
MP:0003402	decreased liver weight	0.24
GO:0005811	lipid particle	0.24
REACTOME_FATTY_ACYL:COA_BIOSYNTHESIS	REACTOME_FATTY_ACYL:COA_BIOSYNTHESIS	0.24
ENSG00000108298	RPL19 PPI subnetwork	0.24
GO:0043009	chordate embryonic development	0.24
GO:0050866	negative regulation of cell activation	0.24
GO:0031114	regulation of microtubule depolymerization	0.24
ENSG00000101680	LAMA1 PPI subnetwork	0.24
KEGG_NITROGEN_METABOLISM	KEGG_NITROGEN_METABOLISM	0.24
MP:0003009	abnormal cytokine secretion	0.24
MP:0003755	abnormal palate morphology	0.24
REACTOME_INHIBITION_OF_REPLICATION_INITIATION_OF_DAMAGED_DNA_BY	REACTOME_INHIBITION_OF_REPLICATION_INITIATION_OF_DAMAGED_DNA_BY_RE	0.24
GO:0032259	methylation	0.24
ENSG00000186081	KRT5 PPI subnetwork	0.24
ENSG00000211614	ENSG00000211614 PPI subnetwork	0.24
ENSG00000141736	ERBB2 PPI subnetwork	0.24
ENSG00000165458	INPPL1 PPI subnetwork	0.24
MP:0008721	abnormal chemokine level	0.24
MP:0003071	decreased vascular permeability	0.24
MP:0005087	decreased acute inflammation	0.24
ENSG00000100294	MCAT PPI subnetwork	0.24
MP:0009789	decreased susceptibility to bacterial infection induced morbidity/mortality	0.24
MP:0008080	abnormal CD8-positive T cell differentiation	0.24

Original gene set ID	Original gene set description	Nominal P value
GO:0019203	carbohydrate phosphatase activity	0.24
GO:0030217	T cell differentiation	0.24
REACTOME_RIG:IMDA5_MEDIATED_INDUCION_OF_IFN:ALPHABETA_PATHWA	REACTOME_RIG:IMDA5_MEDIATED_INDUCION_OF_IFN:ALPHABETA_PATHWAYS	0.24
MP:0000162	lordosis	0.24
GO:0046649	lymphocyte activation	0.24
ENSG00000170248	PDCD61P PPI subnetwork	0.24
ENSG000000089597	GANAB PPI subnetwork	0.24
ENSG00000185630	PBX1 PPI subnetwork	0.24
GO:0002886	regulation of myeloid leukocyte mediated immunity	0.24
ENSG00000044524	EPHA3 PPI subnetwork	0.24
GO:0006497	protein lipidation	0.24
GO:0033017	sarcoplasmic reticulum membrane	0.24
REACTOME_TRAF6_MEDIATED_IRF7_ACTIVATION	REACTOME_TRAF6_MEDIATED_IRF7_ACTIVATION	0.24
ENSG00000164362	TERT PPI subnetwork	0.24
ENSG00000148082	SHC3 PPI subnetwork	0.24
GO:0044452	nucleolar part	0.24
GO:0005200	structural constituent of cytoskeleton	0.24
MP:0000784	forebrain hypoplasia	0.24
REACTOME_TRANSPORT_OF_VITAMINS_NUCLEOSIDES_AND_RELATED_MOLEC	REACTOME_TRANSPORT_OF_VITAMINS_NUCLEOSIDES_AND_RELATED_MOLECULE:	0.24
GO:0008138	protein tyrosine/serine/threonine phosphatase activity	0.24
ENSG00000173406	DAB1 PPI subnetwork	0.24
GO:0042056	chemoattractant activity	0.24
MP:0010825	abnormal lung saccule morphology	0.24
ENSG000000075388	FGF4 PPI subnetwork	0.24
ENSG00000008988	RPS20 PPI subnetwork	0.24
GO:0006270	DNA-dependent DNA replication initiation	0.24
ENSG00000122484	RPAP2 PPI subnetwork	0.24
GO:0048608	reproductive structure development	0.24
ENSG00000152556	PFKM PPI subnetwork	0.24
ENSG00000104267	CA2 PPI subnetwork	0.24
ENSG00000168028	RPSA PPI subnetwork	0.24
MP:0005508	abnormal skeleton morphology	0.24
GO:0003229	ventricular cardiac muscle tissue development	0.24
ENSG00000133703	KRAS PPI subnetwork	0.24
MP:0001304	cataracts	0.24
MP:0002765	short fibula	0.24
ENSG00000005844	ITGAL PPI subnetwork	0.24
MP:0003641	small lung	0.24
ENSG00000160741	CRTC2 PPI subnetwork	0.24
GO:0046474	glycerophospholipid biosynthetic process	0.24
GO:0006633	fatty acid biosynthetic process	0.24
ENSG00000169067	ACTBL2 PPI subnetwork	0.24
MP:0002416	abnormal proerythroblast morphology	0.24
ENSG00000158874	APOA2 PPI subnetwork	0.24
ENSG00000204843	DCTN1 PPI subnetwork	0.24
ENSG00000064601	CTSA PPI subnetwork	0.24
MP:0008135	small Peyer's patches	0.24
MP:0009655	abnormal secondary palate development	0.24
ENSG00000164251	F2RL1 PPI subnetwork	0.25

Original gene set ID	Original gene set description	Nominal P value
ENSG00000082146	STRADB PPI subnetwork	0.26
ENSG00000137713	PPP2R1B PPI subnetwork	0.26
ENSG00000117133	RPF1 PPI subnetwork	0.26
GO:0016581	NuRD complex	0.26
GO:0048705	skeletal system morphogenesis	0.26
REACTOME_SIGNALING_BY_NOTCH	REACTOME_SIGNALING_BY_NOTCH	0.26
ENSG00000116473	RAP1A PPI subnetwork	0.26
ENSG00000174791	RIN1 PPI subnetwork	0.26
GO:0045940	positive regulation of steroid metabolic process	0.26
MP:0002026	leukemia	0.26
GO:0048200	Golgi transport vesicle coating	0.26
GO:0035964	COPI-coated vesicle budding	0.26
GO:0048205	COPI coating of Golgi vesicle	0.26
MP:0008537	increased susceptibility to induced colitis	0.26
GO:0042157	lipoprotein metabolic process	0.26
MP:0000596	abnormal liver development	0.26
REACTOME_MITOCHONDRIAL_TRNA_AMINOACYLATION	REACTOME_MITOCHONDRIAL_TRNA_AMINOACYLATION	0.26
REACTOME_FATTY_ACID_TRIACYLGLYCEROL_AND_KETONE_BODY_METABOLISM	REACTOME_FATTY_ACID_TRIACYLGLYCEROL_AND_KETONE_BODY_METABOLISM	0.26
ENSG00000136383	ALPK3 PPI subnetwork	0.26
ENSG00000121274	PAPD5 PPI subnetwork	0.26
ENSG00000115170	ACVR1 PPI subnetwork	0.26
ENSG00000128731	HERC2 PPI subnetwork	0.26
MP:0011086	partial postnatal lethality	0.26
GO:0004725	protein tyrosine phosphatase activity	0.26
MP:0000091	short premaxilla	0.26
ENSG00000069399	BCL3 PPI subnetwork	0.26
MP:0002980	abnormal postural reflex	0.26
ENSG00000164404	GDF9 PPI subnetwork	0.26
GO:0008376	acetylgalactosaminyltransferase activity	0.26
GO:0005247	voltage-gated chloride channel activity	0.26
ENSG00000166025	AMOTL1 PPI subnetwork	0.26
ENSG00000108821	COL1A1 PPI subnetwork	0.26
ENSG00000078304	PPP2R5C PPI subnetwork	0.26
ENSG00000103502	CDIPT PPI subnetwork	0.26
GO:0045321	leukocyte activation	0.26
GO:0005614	interstitial matrix	0.26
ENSG00000196549	MME PPI subnetwork	0.26
ENSG00000124788	ATXN1 PPI subnetwork	0.26
ENSG00000166603	MC4R PPI subnetwork	0.26
REACTOME_ADAPTIVE_IMMUNE_SYSTEM	REACTOME_ADAPTIVE_IMMUNE_SYSTEM	0.26
ENSG00000120690	ELF1 PPI subnetwork	0.26
MP:0005036	diarrhea	0.26
ENSG00000198785	GRIN3A PPI subnetwork	0.26
ENSG00000162736	NCSTN PPI subnetwork	0.26
GO:0030173	integral to Golgi membrane	0.26
MP:0010402	ventricular septal defect	0.26
GO:0007229	integrin-mediated signaling pathway	0.26
GO:0006700	C21-steroid hormone biosynthetic process	0.26
ENSG00000106366	SERPINE1 PPI subnetwork	0.26

Original gene set ID	Original gene set description	Nominal P value
MP:0009230	abnormal sperm head morphology	0.26
ENSG00000091127	PUS7 PPI subnetwork	0.26
ENSG000000065427	KARS PPI subnetwork	0.26
GO:0005057	receptor signaling protein activity	0.26
ENSG00000128050	PAICS PPI subnetwork	0.26
ENSG00000198242	RPL23A PPI subnetwork	0.26
ENSG00000075886	TUBA3D PPI subnetwork	0.26
ENSG00000198033	TUBA3C PPI subnetwork	0.26
GO:0006473	protein acetylation	0.26
ENSG00000186832	KRT16 PPI subnetwork	0.26
KEGG_JAK_STAT_SIGNALING_PATHWAY	KEGG_JAK_STAT_SIGNALING_PATHWAY	0.26
ENSG00000108312	UBTF PPI subnetwork	0.26
MP:0002874	decreased hemoglobin content	0.26
MP:0000467	abnormal esophagus morphology	0.26
ENSG00000108510	MED13 PPI subnetwork	0.26
MP:0008476	increased spleen red pulp amount	0.26
MP:0008525	decreased cranium height	0.26
ENSG00000101421	CHMP4B PPI subnetwork	0.26
MP:0004794	increased anti-nuclear antigen antibody leve	0.26
ENSG00000166233	ARIH1 PPI subnetwork	0.26
ENSG00000116044	NFE2L2 PPI subnetwork	0.26
GO:0004859	phospholipase inhibitor activity	0.26
ENSG00000103089	FA2H PPI subnetwork	0.26
MP:0003717	pallor	0.26
GO:0015149	hexose transmembrane transporter activity	0.26
ENSG00000205609	EIF3CL PPI subnetwork	0.26
GO:0034062	RNA polymerase activity	0.26
GO:0003899	DNA-directed RNA polymerase activity	0.26
MP:0008499	increased IgG1 level	0.26
ENSG00000105141	CASP14 PPI subnetwork	0.26
ENSG00000100934	SEC23A PPI subnetwork	0.26
ENSG00000054267	ARID4B PPI subnetwork	0.26
GO:0034367	macromolecular complex remodeling	0.26
GO:0034368	protein-lipid complex remodeling	0.26
GO:0034369	plasma lipoprotein particle remodeling	0.26
ENSG00000099985	OSM PPI subnetwork	0.26
GO:0033764	steroid dehydrogenase activity, acting on the CH-OH group of donors, NAD or NADP	0.26
ENSG00000186831	ENSG00000186831 PPI subnetwork	0.26
ENSG00000188763	FZD9 PPI subnetwork	0.26
REACTOME_INNATE_IMMUNE_SYSTEM	REACTOME_INNATE_IMMUNE_SYSTEM	0.26
ENSG00000128245	YWHAH PPI subnetwork	0.26
REACTOME_NUCLEAR_EVENTS_KINASE_AND_TRANSCRIPTION_FACTOR_ACTIVATION	REACTOME_NUCLEAR_EVENTS_KINASE_AND_TRANSCRIPTION_FACTOR_ACTIVATION	0.26
MP:0002344	abnormal lymph node B cell domain morphology	0.26
ENSG00000111652	COPS7A PPI subnetwork	0.26
ENSG00000155760	FZD7 PPI subnetwork	0.26
GO:0002218	activation of innate immune response	0.26
MP:0000550	abnormal forelimb morphology	0.26
MP:0001272	increased metastatic potential	0.26
ENSG00000186716	BCR PPI subnetwork	0.26

Original gene set ID	Original gene set description	Nominal P value
MP:0001152	Leydig cell hyperplasia	0.27
ENSG00000113712	CSNK1A1 PPI subnetwork	0.27
ENSG00000125508	SRMS PPI subnetwork	0.27
ENSG00000060140	STYK1 PPI subnetwork	0.27
GO:0007596	blood coagulation	0.27
GO:0045638	negative regulation of myeloid cell differentiation	0.27
ENSG00000106355	LSM5 PPI subnetwork	0.27
GO:0045089	positive regulation of innate immune response	0.27
ENSG00000132155	RAF1 PPI subnetwork	0.27
GO:0048635	negative regulation of muscle organ development	0.27
ENSG00000119689	DLST PPI subnetwork	0.27
GO:0016493	C-C chemokine receptor activity	0.27
ENSG00000105993	DNAJB6 PPI subnetwork	0.27
GO:0005112	Notch binding	0.27
MP:0003135	increased erythroid progenitor cell number	0.27
REACTOME_RECYCLING_PATHWAY_OF_L1	REACTOME_RECYCLING_PATHWAY_OF_L1	0.27
GO:0071565	nBAF complex	0.27
ENSG00000186111	PIP5K1C PPI subnetwork	0.27
ENSG00000106344	RBM28 PPI subnetwork	0.27
GO:0009168	purine ribonucleoside monophosphate biosynthetic process	0.27
GO:0009127	purine nucleoside monophosphate biosynthetic process	0.27
GO:0050817	coagulation	0.27
GO:0042310	vasoconstriction	0.27
MP:0000854	abnormal cerebellum development	0.27
ENSG00000111731	KIAA0528 PPI subnetwork	0.27
ENSG00000132589	FLOT2 PPI subnetwork	0.27
ENSG00000130669	PAK4 PPI subnetwork	0.27
MP:0008770	decreased survivor rate	0.27
MP:0002796	impaired skin barrier function	0.27
GO:0045445	myoblast differentiation	0.27
GO:0006446	regulation of translational initiation	0.27
GO:0005355	glucose transmembrane transporter activity	0.27
ENSG00000101040	ZMYND8 PPI subnetwork	0.27
GO:0046470	phosphatidylcholine metabolic process	0.27
GO:0045619	regulation of lymphocyte differentiation	0.27
MP:0005309	increased circulating ammonia level	0.27
GO:0070325	lipoprotein particle receptor binding	0.27
GO:0071577	zinc ion transmembrane transport	0.27
ENSG00000105438	KDELRL1 PPI subnetwork	0.27
ENSG00000197756	RPL37A PPI subnetwork	0.27
MP:0000026	abnormal inner ear morphology	0.27
GO:0016805	dipeptidase activity	0.27
ENSG00000023191	RNH1 PPI subnetwork	0.27
ENSG00000169682	SPNS1 PPI subnetwork	0.27
ENSG00000165280	VCP PPI subnetwork	0.27
GO:0019199	transmembrane receptor protein kinase activity	0.27
GO:0002683	negative regulation of immune system process	0.27
GO:0007599	hemostasis	0.27
ENSG00000100393	EP300 PPI subnetwork	0.27

Original gene set ID	Original gene set description	Nominal P value
ENSG00000104517	UBR5 PPI subnetwork	0.27
GO:0022829	wide pore channel activity	0.27
ENSG00000092208	GEMIN2 PPI subnetwork	0.27
MP:0008597	decreased circulating interleukin-6 level	0.27
MP:0008395	abnormal osteoblast differentiation	0.27
ENSG00000140319	SRP14 PPI subnetwork	0.27
ENSG00000137818	RPLP1 PPI subnetwork	0.27
ENSG00000198034	RPS4X PPI subnetwork	0.27
REACTOME_NONSENSE_MEDIATED_DECAY_INDEPENDENT_OF_THE_EXON_JUNCTION	REACTOME_NONSENSE_MEDIATED_DECAY_INDEPENDENT_OF_THE_EXON_JUNCTION	0.27
MP:0004952	increased spleen weight	0.27
GO:0009161	ribonucleoside monophosphate metabolic process	0.27
GO:0006367	transcription initiation from RNA polymerase II promoter	0.27
REACTOME_TRAF6_MEDIATED_INDUCTION_OF_NFKB_AND_MAP_KINASES_UPON_ACTIVATION_OF_TOLL_LIKE_RECEPTOR_78_TLR78_CASCADE	REACTOME_TRAF6_MEDIATED_INDUCTION_OF_NFKB_AND_MAP_KINASES_UPON_ACTIVATION_OF_TOLL_LIKE_RECEPTOR_78_TLR78_CASCADE	0.27
REACTOME_MYD88_DEPENDENT_CASCADE_INITIATED_ON_ENDOSOME	REACTOME_MYD88_DEPENDENT_CASCADE_INITIATED_ON_ENDOSOME	0.27
GO:0019208	phosphatase regulator activity	0.27
MP:0003077	abnormal cell cycle	0.27
ENSG00000139626	ITGB7 PPI subnetwork	0.27
ENSG00000184787	UBE2G2 PPI subnetwork	0.27
GO:0030949	positive regulation of vascular endothelial growth factor receptor signaling pathway	0.27
MP:0001533	abnormal skeleton physiology	0.27
MP:0002075	abnormal coat/hair pigmentation	0.27
ENSG00000145912	NHP2 PPI subnetwork	0.27
GO:0055010	ventricular cardiac muscle tissue morphogenesis	0.27
GO:0006814	sodium ion transport	0.27
ENSG00000131368	MRPS25 PPI subnetwork	0.27
GO:0045120	pronucleus	0.27
MP:0005092	decreased double-positive T cell number	0.27
ENSG00000078808	SDF4 PPI subnetwork	0.27
ENSG00000198873	GRK5 PPI subnetwork	0.27
ENSG00000160584	SIK3 PPI subnetwork	0.27
KEGG_PYRUVATE_METABOLISM	KEGG_PYRUVATE_METABOLISM	0.27
MP:0003068	enlarged kidney	0.27
GO:0051591	response to cAMP	0.27
ENSG00000116030	SUMO1 PPI subnetwork	0.27
GO:0031012	extracellular matrix	0.27
ENSG00000150990	DHX37 PPI subnetwork	0.27
ENSG00000075618	FSCN1 PPI subnetwork	0.27
GO:0045814	negative regulation of gene expression, epigenetic	0.27
GO:0015893	drug transport	0.27
ENSG00000115705	TPO PPI subnetwork	0.27
ENSG00000185920	PTCH1 PPI subnetwork	0.27
ENSG00000115221	ITGB6 PPI subnetwork	0.28
GO:0007422	peripheral nervous system development	0.28
ENSG00000031698	SARS PPI subnetwork	0.28
MP:0003270	intestinal obstruction	0.28
GO:0048534	hemopoietic or lymphoid organ development	0.28
ENSG00000150760	DOCK1 PPI subnetwork	0.28
GO:0016741	transferase activity, transferring one-carbon groups	0.28

Original gene set ID	Original gene set description	Nominal P value
GO:0042974	retinoic acid receptor binding	0.28
MP:0001259	abnormal body weight	0.28
MP:0004993	decreased bone resorption	0.28
GO:0000228	nuclear chromosome	0.28
MP:0008481	increased spleen germinal center number	0.28
GO:0007431	salivary gland development	0.28
ENSG00000198554	WDHD1 PPI subnetwork	0.28
ENSG00000100324	TAB1 PPI subnetwork	0.28
ENSG00000160469	BRSK1 PPI subnetwork	0.28
GO:0045668	negative regulation of osteoblast differentiation	0.28
MP:0008174	decreased follicular B cell number	0.28
ENSG00000043462	LCP2 PPI subnetwork	0.28
ENSG00000188153	COL4A5 PPI subnetwork	0.28
ENSG00000067057	PFKP PPI subnetwork	0.28
GO:0005518	collagen binding	0.28
ENSG00000092847	EIF2C1 PPI subnetwork	0.28
ENSG00000180210	F2 PPI subnetwork	0.28
ENSG00000163251	FZD5 PPI subnetwork	0.28
ENSG00000078295	ADCY2 PPI subnetwork	0.28
ENSG00000149806	FAU PPI subnetwork	0.28
ENSG00000129460	NGDN PPI subnetwork	0.28
GO:0019083	viral transcription	0.28
GO:0019080	viral genome expression	0.28
ENSG00000118579	MED28 PPI subnetwork	0.28
ENSG00000101412	E2F1 PPI subnetwork	0.28
GO:2000116	regulation of cysteine-type endopeptidase activity	0.28
MP:0006325	impaired hearing	0.28
GO:0070328	triglyceride homeostasis	0.28
GO:0007250	activation of NF-kappaB-inducing kinase activity	0.28
REACTOME_FGFR3_LIGAND_BINDING_AND_ACTIVATION	REACTOME_FGFR3_LIGAND_BINDING_AND_ACTIVATION	0.28
REACTOME_FGFR3C_LIGAND_BINDING_AND_ACTIVATION	REACTOME_FGFR3C_LIGAND_BINDING_AND_ACTIVATION	0.28
ENSG00000007047	MARK4 PPI subnetwork	0.28
ENSG00000112304	ACOT13 PPI subnetwork	0.28
ENSG00000125691	RPL23 PPI subnetwork	0.28
MP:0004800	decreased susceptibility to experimental autoimmune encephalomyelitis	0.28
GO:0052547	regulation of peptidase activity	0.28
ENSG00000107625	DDX50 PPI subnetwork	0.28
MP:0000711	thymus cortex hypoplasia	0.28
GO:0015295	solute:hydrogen symporter activity	0.28
ENSG00000164104	HMGB2 PPI subnetwork	0.28
ENSG00000163902	RPN1 PPI subnetwork	0.28
GO:0008329	pattern recognition receptor activity	0.28
MP:0011098	complete embryonic lethality during organogenesis	0.28
MP:0002389	abnormal Peyer's patch follicle morphology	0.28
MP:0001399	hyperactivity	0.28
KEGG_ADHERENS_JUNCTION	KEGG_ADHERENS_JUNCTION	0.28
MP:0004259	small placenta	0.28
GO:0022618	ribonucleoprotein complex assembly	0.28
MP:0002578	impaired ability to fire action potentials	0.28

Original gene set ID	Original gene set description	Nominal P value
REACTOME_POST:TRANSLATIONAL_MODIFICATION_SYNTHESIS_OF_GPI:ANCHOR	REACTOME_POST:TRANSLATIONAL_MODIFICATION_SYNTHESIS_OF_GPI:ANCHOR	0.28
MP:0000267	abnormal heart development	0.28
ENSG000000205659	LINS2 PPI subnetwork	0.28
ENSG000000136352	NKX2-1 PPI subnetwork	0.28
ENSG000000108848	LUC7L3 PPI subnetwork	0.28
ENSG000000079335	CDC14A PPI subnetwork	0.28
MP:0003628	abnormal leukocyte adhesion	0.28
GO:0061008	hepaticobiliary system development	0.28
GO:0090287	regulation of cellular response to growth factor stimulus	0.28
MP:0006042	increased apoptosis	0.28
MP:0002144	abnormal B cell differentiation	0.28
ENSG000000107863	ARHGAP21 PPI subnetwork	0.28
ENSG000000196924	FLNA PPI subnetwork	0.28
ENSG000000160999	SH2B2 PPI subnetwork	0.28
GO:0051091	positive regulation of sequence-specific DNA binding transcription factor activity	0.28
ENSG000000132424	PNISR PPI subnetwork	0.28
GO:0017171	serine hydrolase activity	0.28
ENSG000000029534	ANK1 PPI subnetwork	0.28
REACTOME_SEMA4D_IN_SEMAPHORIN_SIGNALING	REACTOME_SEMA4D_IN_SEMAPHORIN_SIGNALING	0.28
ENSG000000160633	SAFB PPI subnetwork	0.28
GO:0050870	positive regulation of T cell activation	0.28
ENSG000000196498	NCOR2 PPI subnetwork	0.28
ENSG000000113460	BRX1 PPI subnetwork	0.28
GO:0002703	regulation of leukocyte mediated immunity	0.28
ENSG000000198625	MDM4 PPI subnetwork	0.28
ENSG000000178585	CTNNBIP1 PPI subnetwork	0.28
GO:0004435	phosphatidylinositol phospholipase C activity	0.28
KEGG_MAPK_SIGNALING_PATHWAY	KEGG_MAPK_SIGNALING_PATHWAY	0.28
GO:0002685	regulation of leukocyte migration	0.28
GO:0052548	regulation of endopeptidase activity	0.28
MP:0004200	decreased fetal size	0.28
GO:0045923	positive regulation of fatty acid metabolic process	0.28
MP:0004830	short incisors	0.28
MP:0002566	abnormal sexual interaction	0.28
GO:0015114	phosphate ion transmembrane transporter activity	0.28
GO:0050777	negative regulation of immune response	0.28
GO:0031589	cell-substrate adhesion	0.28
ENSG000000187778	MCRS1 PPI subnetwork	0.28
ENSG000000065154	OAT PPI subnetwork	0.28
ENSG000000182255	KCNA4 PPI subnetwork	0.28
GO:0005801	cis-Golgi network	0.28
ENSG000000109606	DHX15 PPI subnetwork	0.28
MP:0004773	abnormal bile composition	0.28
MP:0002417	abnormal megakaryocyte morphology	0.28
GO:0007129	synapsis	0.28
GO:0006544	glycine metabolic process	0.28
GO:0000785	chromatin	0.28
ENSG000000145907	G3BP1 PPI subnetwork	0.28
REACTOME_NEGATIVE_REGULATORS_OF_RIG:IMDA5_SIGNALING	REACTOME_NEGATIVE_REGULATORS_OF_RIG:IMDA5_SIGNALING	0.28

Original gene set ID	Original gene set description	Nominal P value
MP:0002411	decreased susceptibility to bacterial infection	0.28
ENSG00000145414	NAF1 PPI subnetwork	0.28
GO:0014902	myotube differentiation	0.28
ENSG00000115207	GTF3C2 PPI subnetwork	0.28
ENSG00000138768	USO1 PPI subnetwork	0.28
ENSG00000162434	JAK1 PPI subnetwork	0.28
MP:0001672	abnormal embryogenesis/ development	0.28
ENSG00000113525	IL5 PPI subnetwork	0.28
GO:0048010	vascular endothelial growth factor receptor signaling pathway	0.28
ENSG00000125810	CD93 PPI subnetwork	0.28
GO:0017038	protein import	0.28
GO:0006638	neutral lipid metabolic process	0.28
ENSG00000101365	IDH3B PPI subnetwork	0.29
MP:0005441	increased urine calcium level	0.29
ENSG00000164985	PSIP1 PPI subnetwork	0.29
MP:0005423	abnormal somatic nervous system physiology	0.29
MP:0009435	abnormal miniature inhibitory postsynaptic currents	0.29
ENSG00000173545	ZNF622 PPI subnetwork	0.29
ENSG00000139921	TMX1 PPI subnetwork	0.29
GO:0042113	B cell activation	0.29
GO:0010675	regulation of cellular carbohydrate metabolic process	0.29
ENSG00000064547	LPAR2 PPI subnetwork	0.29
GO:0018393	internal peptidyl-lysine acetylation	0.29
GO:0033202	DNA helicase complex	0.29
GO:0031011	Ino80 complex	0.29
ENSG00000167004	PDIA3 PPI subnetwork	0.29
GO:0005097	Rab GTPase activator activity	0.29
REACTOME_TRANSPORT_TO_THE_GOLGI_AND_SUBSEQUENT_MODIFICATION	REACTOME_TRANSPORT_TO_THE_GOLGI_AND_SUBSEQUENT_MODIFICATION	0.29
MP:0004803	increased susceptibility to autoimmune diabetes	0.29
ENSG00000170365	SMAD1 PPI subnetwork	0.29
GO:0008239	dipeptidyl-peptidase activity	0.29
GO:0043574	peroxisomal transport	0.29
GO:0042035	regulation of cytokine biosynthetic process	0.29
GO:0044144	modulation of growth of symbiont involved in interaction with host	0.29
GO:0044126	regulation of growth of symbiont in host	0.29
GO:0044116	growth of symbiont involved in interaction with host	0.29
GO:0044117	growth of symbiont in host	0.29
GO:0044146	negative regulation of growth of symbiont involved in interaction with host	0.29
GO:0044130	negative regulation of growth of symbiont in host	0.29
GO:0044110	growth involved in symbiotic interaction	0.29
ENSG00000163399	ATP1A1 PPI subnetwork	0.29
ENSG00000186868	MAPT PPI subnetwork	0.29
ENSG00000198001	IRAK4 PPI subnetwork	0.29
GO:0070374	positive regulation of ERK1 and ERK2 cascade	0.29
KEGG_TYPE_II_DIABETES_MELLITUS	KEGG_TYPE_II_DIABETES_MELLITUS	0.29
MP:0008554	decreased circulating tumor necrosis factor level	0.29
GO:0005881	cytoplasmic microtubule	0.29
GO:0006954	inflammatory response	0.29
ENSG00000125740	FOSB PPI subnetwork	0.29

Original gene set ID	Original gene set description	Nominal P value
GO:0033280	response to vitamin D	0.29
REACTOME_RAP1_SIGNALLING	REACTOME_RAP1_SIGNALLING	0.29
GO:0005246	calcium channel regulator activity	0.29
MP:0004423	abnormal squamosal bone morphology	0.29
GO:0006399	tRNA metabolic process	0.29
GO:0019216	regulation of lipid metabolic process	0.29
REACTOME_NUCLEOTIDE:BINDING_DOMAIN_LEUCINE_RICH_REPEAT_CONTAINING	REACTOME_NUCLEOTIDE:BINDING_DOMAIN_LEUCINE_RICH_REPEAT_CONTAINING	0.29
ENSG000000131023	LATS1 PPI subnetwork	0.29
REACTOME_EFFECTS_OF_PIP2_HYDROLYSIS	REACTOME_EFFECTS_OF_PIP2_HYDROLYSIS	0.29
ENSG000000148606	POLR3A PPI subnetwork	0.29
MP:0001314	corneal opacity	0.29
GO:0035914	skeletal muscle cell differentiation	0.29
ENSG000000124383	MPHOSPH10 PPI subnetwork	0.29
GO:0045907	positive regulation of vasoconstriction	0.29
REACTOME_TRIGLYCERIDE_BIOSYNTHESIS	REACTOME_TRIGLYCERIDE_BIOSYNTHESIS	0.29
ENSG000000107882	SUFU PPI subnetwork	0.29
ENSG000000136982	DSCC1 PPI subnetwork	0.29
GO:0043966	histone H3 acetylation	0.29
ENSG000000082397	EPB41L3 PPI subnetwork	0.29
MP:0005013	increased lymphocyte cell number	0.29
GO:0051272	positive regulation of cellular component movement	0.29
GO:0015238	drug transmembrane transporter activity	0.29
ENSG000000206412	GNL1 PPI subnetwork	0.29
ENSG000000204590	GNL1 PPI subnetwork	0.29
ENSG000000206492	GNL1 PPI subnetwork	0.29
REACTOME_VITAMIN_B5_PANTOTHENATE_METABOLISM	REACTOME_VITAMIN_B5_PANTOTHENATE_METABOLISM	0.29
ENSG000000184922	FMNL1 PPI subnetwork	0.29
GO:0005070	SH3/SH2 adaptor activity	0.29
ENSG000000164930	FZD6 PPI subnetwork	0.29
ENSG000000111432	FZD10 PPI subnetwork	0.29
ENSG000000057593	F7 PPI subnetwork	0.29
ENSG000000155966	AFF2 PPI subnetwork	0.29
GO:0016820	hydrolase activity, acting on acid anhydrides, catalyzing transmembrane movement	0.29
GO:0006400	tRNA modification	0.29
GO:0001755	neural crest cell migration	0.29
ENSG000000113263	ITK PPI subnetwork	0.29
GO:0009746	response to hexose stimulus	0.29
GO:0000977	RNA polymerase II regulatory region sequence-specific DNA binding	0.29
GO:0000932	cytoplasmic mRNA processing body	0.29
ENSG000000120705	ETF1 PPI subnetwork	0.29
ENSG000000188536	HBA2 PPI subnetwork	0.29
ENSG000000206172	HBA1 PPI subnetwork	0.29
MP:0001806	decreased IgM level	0.29
MP:0001501	abnormal sleep pattern	0.29
GO:0045087	innate immune response	0.29
MP:0001325	abnormal retina morphology	0.29
ENSG000000145425	RPS3A PPI subnetwork	0.29
ENSG000000138018	EPT1 PPI subnetwork	0.29
ENSG000000166794	PPIB PPI subnetwork	0.29

Original gene set ID	Original gene set description	Nominal P value
ENSG00000134248	HBXIP PPI subnetwork	0.29
ENSG00000130985	UBA1 PPI subnetwork	0.29
ENSG00000117480	FAAH PPI subnetwork	0.29
MP:0002657	chondrodystrophy	0.29
GO:0016791	phosphatase activity	0.29
ENSG00000112964	GHR PPI subnetwork	0.29
ENSG00000107937	GTPBP4 PPI subnetwork	0.29
MP:0000808	abnormal hippocampus development	0.29
MP:0011087	complete neonatal lethality	0.29
MP:0009657	failure of chorioallantoic fusion	0.29
GO:0032102	negative regulation of response to external stimulus	0.29
GO:0048872	homeostasis of number of cells	0.29
GO:0001818	negative regulation of cytokine production	0.29
GO:0016568	chromatin modification	0.29
GO:0006906	vesicle fusion	0.29
GO:0042641	actomyosin	0.29
ENSG00000111641	NOP2 PPI subnetwork	0.29
ENSG00000130810	PPAN PPI subnetwork	0.29
GO:0051648	vesicle localization	0.29
ENSG00000149269	PAK1 PPI subnetwork	0.29
ENSG00000088205	DDX18 PPI subnetwork	0.29
MP:0000875	abnormal cerebellar Purkinje cell layer	0.29
MP:0005597	decreased susceptibility to type I hypersensitivity reactor	0.29
GO:0000979	RNA polymerase II core promoter sequence-specific DNA binding	0.29
ENSG00000141141	DDX52 PPI subnetwork	0.29
REACTOME_TRANSLATION	REACTOME_TRANSLATION	0.29
GO:0043281	regulation of cysteine-type endopeptidase activity involved in apoptotic proces:	0.29
GO:2000241	regulation of reproductive process	0.29
ENSG000000005022	SLC25A5 PPI subnetwork	0.29
ENSG00000132153	DHX30 PPI subnetwork	0.29
ENSG00000064393	HIPK2 PPI subnetwork	0.29
GO:0043903	regulation of symbiosis, encompassing mutualism through parasitism	0.29
GO:0050892	intestinal absorption	0.29
GO:0006555	methionine metabolic process	0.29
GO:0051656	establishment of organelle localization	0.29
MP:0002652	thin myocardium	0.29
GO:0010718	positive regulation of epithelial to mesenchymal transitior	0.29
ENSG00000188404	SELL PPI subnetwork	0.29
MP:0000872	abnormal cerebellum external granule cell layer morphology	0.29
ENSG00000074054	CLASP1 PPI subnetwork	0.29
GO:0017187	peptidyl-glutamic acid carboxylation	0.29
GO:0018214	protein carboxylation	0.29
ENSG00000118523	CTGF PPI subnetwork	0.3
MP:0002207	abnormal long term potentiation	0.3
GO:0005795	Golgi stack	0.3
ENSG00000068793	CYFIP1 PPI subnetwork	0.3
ENSG00000102158	MAGT1 PPI subnetwork	0.3
GO:0030133	transport vesicle	0.3
ENSG00000116544	DLGAP3 PPI subnetwork	0.3

Original gene set ID

ENSG00000074201
ENSG00000112242
REACTOME_MYD88_CASCADE_INITIATED_ON_PLASMA_MEMBRANE
REACTOME_TOLL_LIKE_RECEPTOR_10_TLR10_CASCADE
REACTOME_TOLL_LIKE_RECEPTOR_5_TLR5_CASCADE
GO:0004143
GO:0050852
GO:0051270
ENSG00000166908
MP:0002460
GO:0007507
GO:0007265
ENSG00000187391
ENSG00000178913
REACTOME_TRNA_AMINOACYLATION
MP:0005292
REACTOME_TOLL_LIKE_RECEPTOR_4_TLR4_CASCADE
GO:0045773
GO:0045637
ENSG00000132507
GO:0004521
MP:0008040
MP:0002463
GO:0032432
ENSG00000136936
REACTOME_TOLL_RECEPTOR_CASCADES
ENSG00000182718
KEGG_GLYCOSAMINOGLYCAN_BIOSYNTHESIS_HEPARAN_SULFATE
GO:0008320
GO:0022884
ENSG00000152147
GO:0055024
GO:0008637
ENSG00000108296
GO:0070227
GO:0002675
GO:0001104
ENSG00000196781
ENSG00000177105
GO:0006109
ENSG00000120071
ENSG00000106804
GO:0008373
ENSG00000187109
GO:0090329
ENSG00000198742
GO:0045646
GO:0032655
ENSG00000204319

Original gene set description

CLNS1A PPI subnetwork 0.3
E2F3 PPI subnetwork 0.3
REACTOME_MYD88_CASCADE_INITIATED_ON_PLASMA_MEMBRANE 0.3
REACTOME_TOLL_LIKE_RECEPTOR_10_TLR10_CASCADE 0.3
REACTOME_TOLL_LIKE_RECEPTOR_5_TLR5_CASCADE 0.3
diacylglycerol kinase activity 0.3
T cell receptor signaling pathway 0.3
regulation of cellular component movement 0.3
PIP4K2C PPI subnetwork 0.3
decreased immunoglobulin level 0.3
heart development 0.3
Ras protein signal transduction 0.3
MAGI2 PPI subnetwork 0.3
TAF7 PPI subnetwork 0.3
REACTOME_TRNA_AMINOACYLATION 0.3
improved glucose tolerance 0.3
REACTOME_TOLL_LIKE_RECEPTOR_4_TLR4_CASCADE 0.3
positive regulation of axon extension 0.3
regulation of myeloid cell differentiation 0.3
EIF5A PPI subnetwork 0.3
endoribonuclease activity 0.3
decreased NK T cell number 0.3
abnormal neutrophil physiology 0.3
actin filament bundle 0.3
XPA PPI subnetwork 0.3
REACTOME_TOLL_RECEPTOR_CASCADES 0.3
ANXA2 PPI subnetwork 0.3
KEGG_GLYCOSAMINOGLYCAN_BIOSYNTHESIS_HEPARAN_SULFATE 0.3
protein transmembrane transporter activity 0.3
macromolecule transmembrane transporter activity 0.3
GEMIN6 PPI subnetwork 0.3
regulation of cardiac muscle tissue development 0.3
apoptotic mitochondrial changes 0.3
CWC25 PPI subnetwork 0.3
lymphocyte apoptotic process 0.3
positive regulation of acute inflammatory response 0.3
RNA polymerase II transcription cofactor activity 0.3
TLE1 PPI subnetwork 0.3
RHOG PPI subnetwork 0.3
regulation of carbohydrate metabolic process 0.3
KIAA1267 PPI subnetwork 0.3
C5 PPI subnetwork 0.3
sialyltransferase activity 0.3
NAP1L1 PPI subnetwork 0.3
regulation of DNA-dependent DNA replication 0.3
SMURF1 PPI subnetwork 0.3
regulation of erythrocyte differentiatior 0.3
regulation of interleukin-12 production 0.3
ENSG00000204319 PPI subnetwork 0.3

Nominal P value

Original gene set ID	Original gene set description	Nominal P value
MP:0002945	abnormal inhibitory postsynaptic currents	0.3
ENSG00000161939	C17orf49 PPI subnetwork	0.3
MP:0009403	increased variability of skeletal muscle fiber size	0.3
GO:0005372	water transmembrane transporter activity	0.3
GO:0031099	regeneration	0.3
ENSG00000196405	EVL PPI subnetwork	0.3
ENSG00000105216	ENSG00000105216 PPI subnetwork	0.3
GO:0072332	signal transduction by p53 class mediator resulting in induction of apoptosis	0.3
ENSG00000086205	FOLH1 PPI subnetwork	0.3
REACTOME_SHC:MEDIATED_CASCADE	REACTOME_SHC:MEDIATED_CASCADE	0.31
GO:0033267	axon part	0.31
GO:0000123	histone acetyltransferase complex	0.31
GO:0031016	pancreas development	0.31
REACTOME_N:GLYCAN_ANTENNAE_ELONGATION_IN_THE_MEDIALTRANS:GOLGI	REACTOME_N:GLYCAN_ANTENNAE_ELONGATION_IN_THE_MEDIALTRANS:GOLGI	0.31
ENSG00000148296	SURF6 PPI subnetwork	0.31
GO:0051495	positive regulation of cytoskeleton organization	0.31
ENSG00000138448	ITGAV PPI subnetwork	0.31
ENSG00000137497	NUMA1 PPI subnetwork	0.31
GO:0004721	phosphoprotein phosphatase activity	0.31
MP:0002743	glomerulonephritis	0.31
MP:0010024	increased total body fat amount	0.31
ENSG00000135903	PAX3 PPI subnetwork	0.31
MP:0002625	heart left ventricle hypertrophy	0.31
MP:0003089	decreased skin tensile strength	0.31
ENSG00000196591	HDAC2 PPI subnetwork	0.31
GO:0043086	negative regulation of catalytic activity	0.31
ENSG00000127564	PKMYT1 PPI subnetwork	0.31
GO:0032313	regulation of Rab GTPase activity	0.31
GO:0032483	regulation of Rab protein signal transduction	0.31
GO:0016775	phosphotransferase activity, nitrogenous group as acceptor	0.31
ENSG00000138594	TMOD3 PPI subnetwork	0.31
ENSG00000132170	PPARG PPI subnetwork	0.31
MP:0002092	abnormal eye morphology	0.31
GO:0045060	negative thymic T cell selection	0.31
ENSG00000124641	MED20 PPI subnetwork	0.31
GO:0043038	amino acid activation	0.31
GO:0043039	tRNA aminoacylation	0.31
ENSG00000137275	RIPK1 PPI subnetwork	0.31
ENSG00000171681	ATF7IP PPI subnetwork	0.31
ENSG00000136238	RAC1 PPI subnetwork	0.31
GO:0017124	SH3 domain binding	0.31
GO:0003073	regulation of systemic arterial blood pressure	0.31
MP:0004157	interrupted aortic arch	0.31
ENSG00000181856	SLC2A4 PPI subnetwork	0.31
ENSG00000162702	ZNF281 PPI subnetwork	0.31
GO:0005732	small nucleolar ribonucleoprotein complex	0.31
MP:0005215	abnormal pancreatic islet morphology	0.31
ENSG00000063177	RPL18 PPI subnetwork	0.31
ENSG00000011260	UTP18 PPI subnetwork	0.31

Original gene set ID	Original gene set description	Nominal P value
ENSG00000108559	NUP88 PPI subnetwork	0.34
GO:0006084	acetyl-CoA metabolic process	0.34
GO:0050920	regulation of chemotaxis	0.34
MP:0000333	decreased bone marrow cell number	0.34
GO:0003725	double-stranded RNA binding	0.34
MP:0010403	atrial septal defect	0.34
GO:0005921	gap junction	0.34
GO:0003013	circulatory system process	0.34
ENSG00000102871	TRADD PPI subnetwork	0.34
GO:0046134	pyrimidine nucleoside biosynthetic process	0.34
GO:0032103	positive regulation of response to external stimulus	0.34
GO:0045055	regulated secretory pathway	0.34
GO:0043189	H4/H2A histone acetyltransferase complex	0.34
ENSG00000156697	UTP14A PPI subnetwork	0.34
GO:0045182	translation regulator activity	0.34
ENSG00000080824	HSP90AA1 PPI subnetwork	0.34
GO:0002753	cytoplasmic pattern recognition receptor signaling pathway	0.34
GO:0070423	nucleotide-binding oligomerization domain containing signaling pathway	0.34
GO:0035872	nucleotide-binding domain, leucine rich repeat containing receptor signaling pathway	0.34
MP:0011093	complete embryonic lethality at implantation	0.34
GO:0015934	large ribosomal subunit	0.34
ENSG00000134376	CRB1 PPI subnetwork	0.34
ENSG00000131269	ABCB7 PPI subnetwork	0.34
ENSG00000155438	MKI67IP PPI subnetwork	0.34
MP:0000217	abnormal leukocyte cell number	0.34
REACTOME_NOTCH:HLH_TRANSCRIPTION_PATHWAY	REACTOME_NOTCH:HLH_TRANSCRIPTION_PATHWAY	0.34
REACTOME_NICD_TRAFFICS_TO_NUCLEUS	REACTOME_NICD_TRAFFICS_TO_NUCLEUS	0.34
ENSG00000198918	RPL39 PPI subnetwork	0.34
MP:0000141	abnormal vertebral body morphology	0.34
GO:0050768	negative regulation of neurogenesis	0.34
GO:0046545	development of primary female sexual characteristics	0.34
GO:0007589	body fluid secretion	0.34
ENSG00000131462	TUBG1 PPI subnetwork	0.34
ENSG00000026508	CD44 PPI subnetwork	0.34
ENSG00000066926	FECH PPI subnetwork	0.34
MP:0000063	decreased bone mineral density	0.34
GO:0002684	positive regulation of immune system process	0.34
MP:0003052	omphalocele	0.34
GO:0009395	phospholipid catabolic process	0.34
ENSG00000064300	NGFR PPI subnetwork	0.34
ENSG00000185745	IFIT1 PPI subnetwork	0.34
ENSG00000171314	PGAM1 PPI subnetwork	0.34
GO:0045576	mast cell activation	0.34
GO:0015296	anion:cation symporter activity	0.34
ENSG00000125485	DDX31 PPI subnetwork	0.34
ENSG00000114978	MOB1A PPI subnetwork	0.34
ENSG00000197063	MAFG PPI subnetwork	0.35
ENSG00000076003	MCM6 PPI subnetwork	0.35
REACTOME_GLYCOGEN_BREAKDOWN_GLYCOGENOLYSIS	REACTOME_GLYCOGEN_BREAKDOWN_GLYCOGENOLYSIS	0.35

Original gene set ID	Original gene set description	Nominal P value
GO:0045672	positive regulation of osteoclast differentiation	0.36
GO:0005625	soluble fraction	0.36
GO:0006487	protein N-linked glycosylation	0.36
MP:0008582	short photoreceptor inner segment	0.36
ENSG00000147649	MTDH PPI subnetwork	0.36
GO:0046486	glycerolipid metabolic process	0.36
KEGG_GLYCOSPHINGOLIPID_BIOSYNTHESIS_GLOBO_SERIES	KEGG_GLYCOSPHINGOLIPID_BIOSYNTHESIS_GLOBO_SERIES	0.36
ENSG00000174175	SELP PPI subnetwork	0.36
GO:0005922	connexon complex	0.36
GO:0006493	protein O-linked glycosylation	0.36
ENSG00000162613	FUBP1 PPI subnetwork	0.36
ENSG00000162924	REL PPI subnetwork	0.36
GO:0090257	regulation of muscle system process	0.36
MP:0009937	abnormal neuron differentiation	0.36
MP:0000164	abnormal cartilage development	0.36
MP:0004982	abnormal osteoclast morphology	0.36
REACTOME_NFKB_AND_MAP_KINASES_ACTIVATION_MEDIATED_BY_TLR4_SIGI	REACTOME_NFKB_AND_MAP_KINASES_ACTIVATION_MEDIATED_BY_TLR4_SIGNALI	0.36
GO:0008656	cysteine-type endopeptidase activator activity involved in apoptotic proces:	0.36
GO:0018298	protein-chromophore linkage	0.36
ENSG00000112282	MED23 PPI subnetwork	0.36
ENSG00000114209	PDCD10 PPI subnetwork	0.36
GO:0061035	regulation of cartilage development	0.36
MP:0008641	increased circulating interleukin-1 beta leve	0.36
KEGG_GLYCEROPHOSPHOLIPID_METABOLISM	KEGG_GLYCEROPHOSPHOLIPID_METABOLISM	0.36
GO:0050931	pigment cell differentiation	0.36
GO:0009408	response to heat	0.36
REACTOME_ENDOGENOUS_STEROLS	REACTOME_ENDOGENOUS_STEROLS	0.36
GO:0001916	positive regulation of T cell mediated cytotoxicity	0.36
GO:0046949	fatty-acyl-CoA biosynthetic process	0.36
GO:0035337	fatty-acyl-CoA metabolic process	0.36
REACTOME_CONVERSION_FROM_APCCDC20_TO_APCCCDH1_IN_LATE_ANAPI	REACTOME_CONVERSION_FROM_APCCDC20_TO_APCCCDH1_IN_LATE_ANAPHASI	0.36
GO:0007141	male meiosis I	0.36
ENSG00000153395	LPCAT1 PPI subnetwork	0.36
MP:0008540	abnormal cerebrum morphology	0.36
REACTOME_MYD88:INDEPENDENT_CASCADE_INITIATED_ON_PLASMA_MEMBR	REACTOME_MYD88:INDEPENDENT_CASCADE_INITIATED_ON_PLASMA_MEMBRANI	0.37
GO:0070936	protein K48-linked ubiquitination	0.37
REACTOME_REGULATION_OF_INSULIN:LIKE_GROWTH_FACTOR_IGF_ACTIVITY_	REACTOME_REGULATION_OF_INSULIN:LIKE_GROWTH_FACTOR_IGF_ACTIVITY_BY_	0.37
MP:0003651	abnormal axon outgrowth	0.37
GO:0005923	tight junction	0.37
GO:0070160	occluding junction	0.37
GO:0008037	cell recognition	0.37
GO:0070193	synaptonemal complex organization	0.37
ENSG00000165630	PRPF18 PPI subnetwork	0.37
ENSG00000184110	EIF3C PPI subnetwork	0.37
ENSG00000149187	CEL1 PPI subnetwork	0.37
ENSG00000066336	SPI1 PPI subnetwork	0.37
GO:0005516	calmodulin binding	0.37
GO:0003016	respiratory system process	0.37
ENSG00000185236	RAB11B PPI subnetwork	0.37

Original gene set ID	Original gene set description	Nominal P value
GO:0048589	developmental growth	0.38
ENSG00000100347	SAMM50 PPI subnetwork	0.38
MP:0004751	increased length of allograft survival	0.38
GO:0042562	hormone binding	0.38
MP:0004618	thoracic vertebral transformation	0.38
MP:0005070	impaired NK cell cytotoxicity	0.38
ENSG00000169783	LINGO1 PPI subnetwork	0.38
ENSG00000171530	TBCA PPI subnetwork	0.38
ENSG00000164053	ATRIP PPI subnetwork	0.38
ENSG00000139083	ETV6 PPI subnetwork	0.38
REACTOME_SEMA4D_INDUCED_CELL_MIGRATION_AND_GROWTH: CONE_COLLAPSE	REACTOME_SEMA4D_INDUCED_CELL_MIGRATION_AND_GROWTH: CONE_COLLAPSE	0.38
GO:0042493	response to drug	0.38
ENSG00000101084	C20orf24 PPI subnetwork	0.38
REACTOME_INSULIN_RECEPTOR_SIGNALING_CASCADE	REACTOME_INSULIN_RECEPTOR_SIGNALING_CASCADE	0.38
GO:0043560	insulin receptor substrate binding	0.38
GO:0007339	binding of sperm to zona pellucida	0.38
MP:0008168	decreased B-1a cell number	0.38
ENSG00000137841	PLCB2 PPI subnetwork	0.38
ENSG00000150995	ITPR1 PPI subnetwork	0.38
GO:0050851	antigen receptor-mediated signaling pathway	0.38
REACTOME_CHAPERONIN:MEDIATED_PROTEIN_FOLDING	REACTOME_CHAPERONIN:MEDIATED_PROTEIN_FOLDING	0.38
GO:0034433	steroid esterification	0.38
GO:0034435	cholesterol esterification	0.38
GO:0034434	sterol esterification	0.38
GO:0009108	coenzyme biosynthetic process	0.38
MP:0005616	decreased susceptibility to type IV hypersensitivity reaction	0.38
GO:0031527	filopodium membrane	0.38
MP:0004007	abnormal lung vasculature morphology	0.38
ENSG00000205022	PABPN1L PPI subnetwork	0.38
ENSG00000138696	BMPR1B PPI subnetwork	0.38
ENSG00000142657	PGD PPI subnetwork	0.38
MP:0002451	abnormal macrophage physiology	0.38
GO:0042445	hormone metabolic process	0.38
MP:0008261	arrest of male meiosis	0.38
GO:0000146	microfilament motor activity	0.38
MP:0000564	syndactyly	0.38
MP:0002339	abnormal lymph node morphology	0.38
MP:0004919	abnormal positive T cell selection	0.38
ENSG00000196083	IL1RAP PPI subnetwork	0.38
ENSG00000142871	CYR61 PPI subnetwork	0.38
GO:0009988	cell-cell recognition	0.38
ENSG00000143466	IKBKE PPI subnetwork	0.38
ENSG00000148175	STOM PPI subnetwork	0.38
GO:0048864	stem cell development	0.38
ENSG00000143768	LEFTY2 PPI subnetwork	0.38
GO:0010564	regulation of cell cycle process	0.38
REACTOME_GLUCOSE_TRANSPORT	REACTOME_GLUCOSE_TRANSPORT	0.38
GO:0002279	mast cell activation involved in immune response	0.38
GO:0001667	ameboidal cell migration	0.38

Original gene set ID	Original gene set description	Nominal P value
REACTOME_GRB2SOS_PROVIDES_LINKAGE_TO_MAPK_SIGNALING_FOR_INTERGRIN	REACTOME_GRB2SOS_PROVIDES_LINKAGE_TO_MAPK_SIGNALING_FOR_INTERGRIN	0.39
GO:0007608	sensory perception of smell	0.39
MP:0000220	increased monocyte cell number	0.39
GO:0022604	regulation of cell morphogenesis	0.39
MP:0002407	abnormal double-negative T cell morphology	0.39
GO:0030834	regulation of actin filament depolymerization	0.39
GO:0033522	histone H2A ubiquitination	0.39
MP:0000039	abnormal otic capsule morphology	0.39
ENSG00000116213	WRAP73 PPI subnetwork	0.39
MP:0003123	paternal imprinting	0.39
MP:0006355	abnormal sixth branchial arch artery morphology	0.39
MP:0011104	partial embryonic lethality before implantation	0.39
GO:0032868	response to insulin stimulus	0.39
GO:0051303	establishment of chromosome localization	0.39
GO:0050000	chromosome localization	0.39
GO:0051875	pigment granule localization	0.39
GO:0007031	peroxisome organization	0.39
ENSG00000010803	SCMH1 PPI subnetwork	0.39
GO:0001750	photoreceptor outer segment	0.39
GO:0030674	protein binding, bridging	0.39
GO:0016628	oxidoreductase activity, acting on the CH-CH group of donors, NAD or NADP as acceptor	0.39
MP:0008584	photoreceptor outer segment degeneration	0.39
ENSG00000063322	MED29 PPI subnetwork	0.39
MP:0000495	abnormal colon morphology	0.39
ENSG00000015475	BID PPI subnetwork	0.39
MP:0000556	abnormal hindlimb morphology	0.39
ENSG000000174804	FZD4 PPI subnetwork	0.39
ENSG000000170653	ATF7 PPI subnetwork	0.39
REACTOME_INTRINSIC_PATHWAY_FOR_APOPTOSIS	REACTOME_INTRINSIC_PATHWAY_FOR_APOPTOSIS	0.39
GO:0045580	regulation of T cell differentiation	0.39
GO:0017046	peptide hormone binding	0.39
KEGG_STARCH_AND_SUCROSE_METABOLISM	KEGG_STARCH_AND_SUCROSE_METABOLISM	0.39
GO:0006501	C-terminal protein lipidation	0.39
ENSG000000162105	SHANK2 PPI subnetwork	0.39
ENSG000000084623	EIF3I PPI subnetwork	0.39
KEGG_MELANOGENESIS	KEGG_MELANOGENESIS	0.39
ENSG000000115947	ORC4 PPI subnetwork	0.39
ENSG000000110107	PRPF19 PPI subnetwork	0.39
MP:0002358	abnormal spleen periaerterial lymphoid sheath morphology	0.39
ENSG000000105404	RABAC1 PPI subnetwork	0.39
GO:0016922	ligand-dependent nuclear receptor binding	0.39
ENSG000000131043	C20orf4 PPI subnetwork	0.39
MP:0002455	abnormal dendritic cell antigen presentation	0.39
GO:0002708	positive regulation of lymphocyte mediated immunity	0.39
GO:0002705	positive regulation of leukocyte mediated immunity	0.39
ENSG000000123349	PFDN5 PPI subnetwork	0.39
MP:0005657	abnormal neural plate morphology	0.39
GO:0030672	synaptic vesicle membrane	0.39
GO:0046822	regulation of nucleocytoplasmic transport	0.39

Original gene set ID	Original gene set description	Nominal P value
ENSG00000108797	CNTNAP1 PPI subnetwork	0.39
MP:0000743	muscle spasm	0.39
ENSG00000175216	CKAP5 PPI subnetwork	0.39
GO:0040017	positive regulation of locomotion	0.39
ENSG00000183943	PRKX PPI subnetwork	0.39
GO:0045880	positive regulation of smoothened signaling pathway	0.39
MP:0004567	decreased myocardial fiber number	0.39
MP:0002599	increased mean platelet volume	0.4
GO:0008305	integrin complex	0.4
ENSG00000174125	TLR1 PPI subnetwork	0.4
MP:0008596	increased circulating interleukin-6 level	0.4
MP:0002258	abnormal cricoid cartilage morphology	0.4
GO:0043304	regulation of mast cell degranulation	0.4
ENSG00000172795	DCP2 PPI subnetwork	0.4
ENSG00000105649	RAB3A PPI subnetwork	0.4
REACTOME_CENTROSOME_MATURATION	REACTOME_CENTROSOME_MATURATION	0.4
REACTOME_RECRUITMENT_OF_MITOTIC_CENTROSOME_PROTEINS_AND_COM	REACTOME_RECRUITMENT_OF_MITOTIC_CENTROSOME_PROTEINS_AND_COMPLE	0.4
GO:0030218	erythrocyte differentiation	0.4
MP:0000717	abnormal lymphocyte cell number	0.4
GO:0034138	toll-like receptor 3 signaling pathway	0.4
REACTOME_G2M_TRANSITION	REACTOME_G2M_TRANSITION	0.4
GO:0045787	positive regulation of cell cycle	0.4
GO:0030010	establishment of cell polarity	0.4
KEGG_VEGF_SIGNALING_PATHWAY	KEGG_VEGF_SIGNALING_PATHWAY	0.4
MP:0001385	pup cannibalization	0.4
GO:0033002	muscle cell proliferation	0.4
GO:0061061	muscle structure development	0.4
ENSG00000112306	RPS12 PPI subnetwork	0.4
GO:0007423	sensory organ development	0.4
GO:0009067	aspartate family amino acid biosynthetic process	0.4
GO:0005730	nucleolus	0.4
REACTOME_INFLUENZA_INFECTION	REACTOME_INFLUENZA_INFECTION	0.4
KEGG_BLADDER_CANCER	KEGG_BLADDER_CANCER	0.4
ENSG00000156508	EEF1A1 PPI subnetwork	0.4
ENSG00000004897	CDC27 PPI subnetwork	0.4
ENSG00000077080	ACTL6B PPI subnetwork	0.4
KEGG_METABOLISM_OF_XENOBIOTICS_BY_CYTOCHROME_P450	KEGG_METABOLISM_OF_XENOBIOTICS_BY_CYTOCHROME_P450	0.4
GO:0032587	ruffle membrane	0.4
ENSG00000115310	RTN4 PPI subnetwork	0.4
GO:0003208	cardiac ventricle morphogenesis	0.4
GO:0002697	regulation of immune effector process	0.4
ENSG00000141456	ENSG00000141456 PPI subnetwork	0.4
ENSG00000003400	CASP10 PPI subnetwork	0.4
GO:0048041	focal adhesion assembly	0.4
ENSG00000158373	HIST1H2BD PPI subnetwork	0.4
ENSG00000101246	ARFRP1 PPI subnetwork	0.4
MP:0008277	abnormal sternum ossification	0.4
ENSG00000136504	KAT7 PPI subnetwork	0.4
ENSG00000100767	PAPLN PPI subnetwork	0.4

Original gene set ID	Original gene set description	Nominal P value
ENSG00000117020	AKT3 PPI subnetwork	0.42
GO:0033344	cholesterol efflux	0.42
ENSG00000153006	SREK1IP1 PPI subnetwork	0.42
GO:0005774	vacuolar membrane	0.42
MP:0008617	increased circulating interleukin-12 level	0.42
ENSG00000156711	MAPK13 PPI subnetwork	0.42
MP:0003871	abnormal myelin sheath morphology	0.42
ENSG00000118965	WDR35 PPI subnetwork	0.42
GO:0005104	fibroblast growth factor receptor binding	0.42
MP:0001940	testis hypoplasia	0.42
ENSG00000138468	SENP7 PPI subnetwork	0.42
ENSG00000118640	VAMP8 PPI subnetwork	0.42
ENSG00000105663	ENSG00000105663 PPI subnetwork	0.42
MP:0000292	distended pericardium	0.42
MP:0001790	abnormal immune system physiology	0.42
MP:0001554	increased circulating free fatty acid leve	0.42
GO:0030099	myeloid cell differentiation	0.42
MP:0003633	abnormal nervous system physiology	0.42
GO:0016053	organic acid biosynthetic process	0.42
GO:0046394	carboxylic acid biosynthetic process	0.42
MP:0004696	abnormal thyroid follicle morphology	0.42
ENSG00000100353	EIF3D PPI subnetwork	0.42
GO:0051153	regulation of striated muscle cell differentiator	0.42
ENSG00000196611	MMP1 PPI subnetwork	0.42
ENSG00000213024	NUP62 PPI subnetwork	0.42
ENSG00000118007	STAG1 PPI subnetwork	0.42
ENSG00000106554	CHCHD3 PPI subnetwork	0.42
ENSG00000080608	KIAA0020 PPI subnetwork	0.42
GO:0031110	regulation of microtubule polymerization or depolymerizati	0.42
GO:0035384	thioester biosynthetic process	0.42
GO:0071616	acyl-CoA biosynthetic process	0.42
REACTOME_IRS:RELATED_EVENTS	REACTOME_IRS:RELATED_EVENTS	0.42
REACTOME_IRS:MEDIATED_SIGNALLING	REACTOME_IRS:MEDIATED_SIGNALLING	0.42
GO:0042559	pteridine-containing compound biosynthetic process	0.42
REACTOME_METABOLISM_OF_RNA	REACTOME_METABOLISM_OF_RNA	0.42
GO:0005529	GO:0005529	0.42
ENSG00000089902	RCOR1 PPI subnetwork	0.42
MP:0009404	centrally nucleated skeletal muscle fibers	0.42
REACTOME_ASSOCIATION_OF_TRICCT_WITH_TARGET_PROTEINS_DURING_BI	REACTOME_ASSOCIATION_OF_TRICCT_WITH_TARGET_PROTEINS_DURING_BIOSY	0.42
ENSG00000146587	RBAK PPI subnetwork	0.42
ENSG00000081248	CACNA1S PPI subnetwork	0.42
ENSG00000007402	CACNA2D2 PPI subnetwork	0.42
MP:0000822	abnormal brain ventricle morphology	0.42
GO:0045776	negative regulation of blood pressure	0.42
GO:0009266	response to temperature stimulus	0.42
GO:0006940	regulation of smooth muscle contraction	0.42
GO:0031111	negative regulation of microtubule polymerization or depolymerizati	0.42
MP:0002118	abnormal lipid homeostasis	0.42
ENSG00000177565	TBL1XR1 PPI subnetwork	0.42

Original gene set ID	Original gene set description	Nominal P value
GO:0070412	R-SMAD binding	0.45
ENSG00000188739	RBM34 PPI subnetwork	0.45
GO:0035176	social behavior	0.45
ENSG00000144597	EAF1 PPI subnetwork	0.45
GO:0042987	amyloid precursor protein catabolic process	0.45
ENSG00000196226	HIST1H2BB PPI subnetwork	0.45
ENSG00000150907	FOXO1 PPI subnetwork	0.45
ENSG00000147536	GIN54 PPI subnetwork	0.45
REACTOME_ANTIGEN_PRESENTATION_FOLDING_ASSEMBLY_AND_PEPTIDE_LO	REACTOME_ANTIGEN_PRESENTATION_FOLDING_ASSEMBLY_AND_PEPTIDE_LOADII	0.45
ENSG00000117335	CD46 PPI subnetwork	0.45
ENSG00000135018	UBQLN1 PPI subnetwork	0.45
GO:0032956	regulation of actin cytoskeleton organization	0.45
MP:0001634	internal hemorrhage	0.45
ENSG00000124813	RUNX2 PPI subnetwork	0.45
GO:0043025	neuronal cell body	0.45
ENSG00000104332	SFRP1 PPI subnetwork	0.45
ENSG00000120057	SFRP5 PPI subnetwork	0.45
ENSG00000106483	SFRP4 PPI subnetwork	0.45
REACTOME_PHOSPHOLIPASE_C:MEDIATED_CASCADE	REACTOME_PHOSPHOLIPASE_C:MEDIATED_CASCADE	0.45
MP:0003360	abnormal depression-related behavior	0.45
GO:0060363	cranial suture morphogenesis	0.45
GO:0097094	craniofacial suture morphogenesis	0.45
GO:0043367	CD4-positive, alpha-beta T cell differentiation	0.45
GO:0000982	RNA polymerase II core promoter proximal region sequence-specific DNA binding tr	0.45
MP:0001719	absent vitelline blood vessels	0.45
GO:0016725	oxidoreductase activity, acting on CH or CH2 groups	0.45
ENSG00000145555	MYO10 PPI subnetwork	0.45
KEGG_ONE_CARBON_POOL_BY_FOLATE	KEGG_ONE_CARBON_POOL_BY_FOLATE	0.45
MP:0005410	abnormal fertilization	0.45
GO:0016746	transferase activity, transferring acyl groups	0.45
ENSG00000178982	EIF3K PPI subnetwork	0.45
GO:0016311	dephosphorylation	0.45
GO:0046112	nucleobase biosynthetic process	0.45
ENSG00000153187	HNRNPU PPI subnetwork	0.45
ENSG00000014138	POLA2 PPI subnetwork	0.45
ENSG00000112739	PRPF4B PPI subnetwork	0.45
ENSG00000132849	INADL PPI subnetwork	0.45
MP:0008560	increased tumor necrosis factor secretion	0.45
ENSG00000068976	PYGM PPI subnetwork	0.45
MP:0002928	abnormal bile duct morphology	0.45
GO:0031253	cell projection membrane	0.45
GO:0007163	establishment or maintenance of cell polarity	0.45
ENSG00000117528	ABCD3 PPI subnetwork	0.45
MP:0000603	pale liver	0.45
MP:0003944	abnormal T cell subpopulation ratio	0.45
MP:0002458	abnormal B cell number	0.45
ENSG00000214026	MRPL23 PPI subnetwork	0.45
ENSG00000156603	MED19 PPI subnetwork	0.45
GO:0007605	sensory perception of sound	0.45

Original gene set ID	Original gene set description	Nominal P value
ENSG00000178105	DDX10 PPI subnetwork	0.45
ENSG00000156931	VPS8 PPI subnetwork	0.45
ENSG00000141985	SH3GL1 PPI subnetwork	0.45
ENSG00000108819	ENSG00000108819 PPI subnetwork	0.45
GO:0070306	lens fiber cell differentiation	0.45
ENSG00000102144	PGK1 PPI subnetwork	0.45
GO:0006958	complement activation, classical pathway	0.45
REACTOME_LOSS_OF_PROTEINS_REQUIRED_FOR_INTERPHASE_MICROTUBULE	REACTOME_LOSS_OF_PROTEINS_REQUIRED_FOR_INTERPHASE_MICROTUBULE_OR	0.45
REACTOME_LOSS_OF_NLP_FROM_MITOTIC_CENTROSOMES	REACTOME_LOSS_OF_NLP_FROM_MITOTIC_CENTROSOMES	0.45
GO:0032663	regulation of interleukin-2 production	0.45
GO:0035258	steroid hormone receptor binding	0.45
GO:0030178	negative regulation of Wnt receptor signaling pathway	0.45
ENSG00000166710	B2M PPI subnetwork	0.45
GO:0042058	regulation of epidermal growth factor receptor signaling pathway	0.45
GO:0031968	organelle outer membrane	0.45
ENSG00000071051	NCK2 PPI subnetwork	0.45
ENSG00000163516	ANKZF1 PPI subnetwork	0.45
REACTOME_GAP_JUNCTION_TRAFFICKING	REACTOME_GAP_JUNCTION_TRAFFICKING	0.45
ENSG00000136044	APPL2 PPI subnetwork	0.45
ENSG00000125868	DSTN PPI subnetwork	0.45
ENSG00000095564	BTAF1 PPI subnetwork	0.45
ENSG00000196890	HIST3H2BB PPI subnetwork	0.45
GO:0000793	condensed chromosome	0.45
ENSG00000101442	ACTR5 PPI subnetwork	0.45
MP:0000753	paralysis	0.45
MP:0006020	decreased tympanic ring size	0.45
GO:0006760	folic acid-containing compound metabolic process	0.45
ENSG00000165632	TAF3 PPI subnetwork	0.45
GO:0048844	artery morphogenesis	0.45
ENSG00000128739	SNRPN PPI subnetwork	0.45
GO:0006664	glycolipid metabolic process	0.45
GO:0043209	myelin sheath	0.45
ENSG00000087191	PSMC5 PPI subnetwork	0.45
ENSG00000175536	LIPT2 PPI subnetwork	0.45
GO:0014704	intercalated disc	0.45
ENSG00000106682	EIF4H PPI subnetwork	0.45
GO:0002889	regulation of immunoglobulin mediated immune response	0.45
GO:0042104	positive regulation of activated T cell proliferator	0.45
ENSG00000148377	ID12 PPI subnetwork	0.45
GO:0043094	cellular metabolic compound salvage	0.45
ENSG00000196220	SRGAP3 PPI subnetwork	0.45
MP:0008518	retinal outer nuclear layer degeneration	0.45
ENSG00000116957	TBCE PPI subnetwork	0.45
MP:0000163	abnormal cartilage morphology	0.45
ENSG00000184009	ACTG1 PPI subnetwork	0.45
ENSG00000169032	MAP2K1 PPI subnetwork	0.45
GO:0008156	negative regulation of DNA replication	0.45
GO:0044433	cytoplasmic vesicle part	0.45
MP:0006058	decreased cerebral infarction size	0.45

Original gene set ID	Original gene set description	Nominal P value
GO:0051092	positive regulation of NF-kappaB transcription factor activity	0.46
GO:0015697	quaternary ammonium group transport	0.46
REACTOME_TETRAHYDROBIOPTERIN_BH4_SYNTHESIS_RECYCLING_SALVAGE_A	REACTOME_TETRAHYDROBIOPTERIN_BH4_SYNTHESIS_RECYCLING_SALVAGE_AND_	0.46
MP:0000065	abnormal bone marrow cavity morphology	0.46
GO:0002286	T cell activation involved in immune response	0.46
MP:0002672	abnormal branchial arch artery morphology	0.46
MP:0003990	decreased neurotransmitter release	0.46
GO:0019637	organophosphate metabolic process	0.46
REACTOME_NEUROTRANSMITTER_RELEASE_CYCLE	REACTOME_NEUROTRANSMITTER_RELEASE_CYCLE	0.46
GO:0008047	enzyme activator activity	0.46
REACTOME_FGFR2C_LIGAND_BINDING_AND_ACTIVATION	REACTOME_FGFR2C_LIGAND_BINDING_AND_ACTIVATION	0.46
GO:0003206	cardiac chamber morphogenesis	0.46
MP:0002275	abnormal type II pneumocyte morphology	0.46
ENSG00000196419	XRCC6 PPI subnetwork	0.46
MP:0008217	abnormal B cell activation	0.46
GO:0006096	glycolysis	0.46
GO:0005916	fascia adherens	0.46
GO:0005248	voltage-gated sodium channel activity	0.46
KEGG_LONG_TERM_DEPRESSION	KEGG_LONG_TERM_DEPRESSION	0.46
MP:0004418	small parietal bone	0.46
ENSG00000187079	TEAD1 PPI subnetwork	0.46
ENSG00000165156	ZHX1 PPI subnetwork	0.46
ENSG00000131788	PIAS3 PPI subnetwork	0.46
ENSG00000155229	MMS19 PPI subnetwork	0.46
GO:0060411	cardiac septum morphogenesis	0.46
GO:0000819	sister chromatid segregation	0.46
GO:0060412	ventricular septum morphogenesis	0.46
GO:0050909	sensory perception of taste	0.46
GO:0043584	nose development	0.46
GO:0006026	aminoglycan catabolic process	0.46
ENSG00000145692	BHMT PPI subnetwork	0.46
GO:0048665	neuron fate specification	0.46
GO:0031519	PcG protein complex	0.46
ENSG00000125249	RAP2A PPI subnetwork	0.46
GO:0048610	cellular process involved in reproduction	0.46
ENSG00000039319	ZFYVE16 PPI subnetwork	0.46
ENSG00000124207	CSE1L PPI subnetwork	0.46
ENSG00000147010	SH3KBP1 PPI subnetwork	0.46
ENSG00000143867	OSR1 PPI subnetwork	0.46
ENSG00000141447	OSBPL1A PPI subnetwork	0.46
ENSG00000154310	TNIK PPI subnetwork	0.46
GO:0060444	branching involved in mammary gland duct morphogenesis	0.46
ENSG00000180855	ZNF443 PPI subnetwork	0.46
ENSG00000077549	CAPZB PPI subnetwork	0.46
GO:0015108	chloride transmembrane transporter activity	0.46
MP:0011088	partial neonatal lethality	0.46
MP:0002702	decreased circulating free fatty acid leve	0.46
ENSG00000174307	PHLDA3 PPI subnetwork	0.47
ENSG00000130758	MAP3K10 PPI subnetwork	0.47

Original gene set ID	Original gene set description	Nominal P value
ENSG00000110799	VWF PPI subnetwork	0.47
REACTOME_PURINE_METABOLISM	REACTOME_PURINE_METABOLISM	0.47
ENSG00000126458	RRAS PPI subnetwork	0.47
MP:0001529	abnormal vocalization	0.47
MP:0000599	enlarged liver	0.47
MP:0003560	osteoarthritis	0.47
ENSG00000145817	YIPF5 PPI subnetwork	0.47
GO:0001502	cartilage condensation	0.47
ENSG00000164708	PGAM2 PPI subnetwork	0.47
ENSG00000089154	GCN1L1 PPI subnetwork	0.47
GO:0042059	negative regulation of epidermal growth factor receptor signaling pathway	0.47
ENSG00000105447	GRWD1 PPI subnetwork	0.47
MP:0001364	decreased anxiety-related response	0.47
REACTOME_RNA_POLYMERASE_III_TRANSCRIPTION_INITIATION_FROM_TYPE_1_P	REACTOME_RNA_POLYMERASE_III_TRANSCRIPTION_INITIATION_FROM_TYPE_1_P	0.47
ENSG00000183520	UTP11L PPI subnetwork	0.47
REACTOME_FGFR4_LIGAND_BINDING_AND_ACTIVATION	REACTOME_FGFR4_LIGAND_BINDING_AND_ACTIVATION	0.47
ENSG00000130561	SAG PPI subnetwork	0.47
ENSG00000173011	TADA2B PPI subnetwork	0.47
ENSG00000197892	KIF13B PPI subnetwork	0.47
ENSG00000198851	CD3E PPI subnetwork	0.47
ENSG00000135547	HEY2 PPI subnetwork	0.47
MP:0008212	absent mature B cells	0.47
GO:0015837	amine transport	0.47
GO:0006749	glutathione metabolic process	0.47
ENSG00000150455	TIRAP PPI subnetwork	0.47
ENSG00000183117	CSMD1 PPI subnetwork	0.47
ENSG00000069275	NUCKS1 PPI subnetwork	0.47
ENSG00000108515	ENO3 PPI subnetwork	0.47
GO:0060840	artery development	0.47
ENSG00000178028	DMAP1 PPI subnetwork	0.47
ENSG00000163602	RYBP PPI subnetwork	0.47
ENSG00000125991	ERGIC3 PPI subnetwork	0.47
ENSG00000144029	MRP5 PPI subnetwork	0.47
REACTOME_FRS2:MEDIATED_ACTIVATION	REACTOME_FRS2:MEDIATED_ACTIVATION	0.47
MP:0000067	osteopetrosis	0.47
ENSG00000040199	PHLPP2 PPI subnetwork	0.47
ENSG00000135338	LCA5 PPI subnetwork	0.47
ENSG00000144566	RAB5A PPI subnetwork	0.47
KEGG_PATHOGENIC_ESCHERICHIA_COLI_INFECTION	KEGG_PATHOGENIC_ESCHERICHIA_COLI_INFECTION	0.47
ENSG00000072210	ALDH3A2 PPI subnetwork	0.47
GO:0032365	intracellular lipid transport	0.47
MP:0004024	aneuploidy	0.47
REACTOME_HORMONE:SENSITIVE_LIPASE_HSL:MEDIATED_TRIACYLGLYCEROL_HYD	REACTOME_HORMONE:SENSITIVE_LIPASE_HSL:MEDIATED_TRIACYLGLYCEROL_HYD	0.47
KEGG_SPHINGOLIPID_METABOLISM	KEGG_SPHINGOLIPID_METABOLISM	0.47
ENSG00000214265	SNURF PPI subnetwork	0.47
GO:0032269	negative regulation of cellular protein metabolic process	0.47
ENSG00000007237	GAS7 PPI subnetwork	0.47
MP:0002643	poikilocytosis	0.47
GO:0001783	B cell apoptotic process	0.47

Original gene set ID	Original gene set description	Nominal P value
GO:0031670	cellular response to nutrient	0.5
MP:0004726	abnormal nasal capsule morphology	0.5
ENSG000000055208	TAB2 PPI subnetwork	0.5
GO:0002573	myeloid leukocyte differentiation	0.5
ENSG00000196497	IPO4 PPI subnetwork	0.5
GO:0015081	sodium ion transmembrane transporter activity	0.5
ENSG00000130803	ZNF317 PPI subnetwork	0.5
MP:0005145	increased circulating VLDL cholesterol leve	0.5
ENSG00000148943	LIN7C PPI subnetwork	0.5
MP:0005630	increased lung weight	0.5
GO:0006754	ATP biosynthetic process	0.5
ENSG000000082014	SMARCD3 PPI subnetwork	0.5
MP:0002397	abnormal bone marrow morphology	0.5
ENSG000000090054	SPTLC1 PPI subnetwork	0.5
ENSG00000158186	MRAS PPI subnetwork	0.5
MP:0005659	decreased susceptibility to diet-induced obesity	0.5
GO:0030897	HOPS complex	0.5
GO:0042074	cell migration involved in gastrulation	0.5
GO:0010639	negative regulation of organelle organization	0.5
GO:0050880	regulation of blood vessel size	0.5
ENSG00000153107	ANAPC1 PPI subnetwork	0.5
ENSG00000166147	FBN1 PPI subnetwork	0.5
ENSG00000174233	ADCY6 PPI subnetwork	0.5
REACTOME_RAS_ACTIVATION_UOPN_CA2_INFUX_THROUGH_NMDA_RECEPTO	REACTOME_RAS_ACTIVATION_UOPN_CA2_INFUX_THROUGH_NMDA_RECEPTOR	0.5
GO:0035036	sperm-egg recognition	0.5
ENSG00000117500	TMED5 PPI subnetwork	0.5
ENSG00000127914	AKAP9 PPI subnetwork	0.51
GO:0050798	activated T cell proliferation	0.51
ENSG00000117360	PRPF3 PPI subnetwork	0.51
ENSG00000173372	C1QA PPI subnetwork	0.51
ENSG00000204301	NOTCH4 PPI subnetwork	0.51
REACTOME_MAP_KINASE_ACTIVATION_IN_TLR_CASCADE	REACTOME_MAP_KINASE_ACTIVATION_IN_TLR_CASCADE	0.51
GO:0043186	P granule	0.51
GO:0045495	pole plasm	0.51
GO:0060293	germ plasm	0.51
GO:0048016	inositol phosphate-mediated signaling	0.51
MP:0002024	T cell derived lymphoma	0.51
GO:0055037	recycling endosome	0.51
MP:0005172	reduced eye pigmentation	0.51
GO:0004866	endopeptidase inhibitor activity	0.51
MP:0003194	abnormal frequency of paradoxical sleep	0.51
MP:0005543	corneal thinning	0.51
ENSG00000071127	WDR1 PPI subnetwork	0.51
ENSG00000117322	CR2 PPI subnetwork	0.51
ENSG000000065675	PRKCQ PPI subnetwork	0.51
MP:0002747	abnormal aortic valve morphology	0.51
GO:0001948	glycoprotein binding	0.51
GO:0043473	pigmentation	0.51
GO:0050867	positive regulation of cell activation	0.51

Original gene set ID	Original gene set description	Nominal P value
GO:0006631	fatty acid metabolic process	0.51
GO:0048546	digestive tract morphogenesis	0.51
GO:0045444	fat cell differentiation	0.51
REACTOME_GLUTATHIONE_SYNTHESIS_AND_RECYCLING	REACTOME_GLUTATHIONE_SYNTHESIS_AND_RECYCLING	0.51
ENSG00000169375	SIN3A PPI subnetwork	0.51
ENSG00000147854	UHRF2 PPI subnetwork	0.51
ENSG00000173876	TUBB8 PPI subnetwork	0.51
MP:0000049	abnormal middle ear morphology	0.51
GO:0051222	positive regulation of protein transport	0.51
ENSG00000119917	IFIT3 PPI subnetwork	0.51
GO:0060113	inner ear receptor cell differentiation	0.51
GO:0060219	camera-type eye photoreceptor cell differentiator	0.51
GO:0035051	cardiac cell differentiation	0.51
ENSG00000115750	TAF1B PPI subnetwork	0.51
MP:0001516	abnormal motor coordination/ balance	0.51
GO:0019835	cytolysis	0.51
MP:0002273	abnormal pulmonary alveolus epithelial cell morphology	0.51
GO:0050864	regulation of B cell activation	0.51
MP:0003132	increased pre-B cell number	0.51
GO:0060828	regulation of canonical Wnt receptor signaling pathway	0.51
REACTOME_SEROTONIN_NEUROTRANSMITTER_RELEASE_CYCLE	REACTOME_SEROTONIN_NEUROTRANSMITTER_RELEASE_CYCLE	0.51
REACTOME_DOPAMINE_NEUROTRANSMITTER_RELEASE_CYCLE	REACTOME_DOPAMINE_NEUROTRANSMITTER_RELEASE_CYCLE	0.51
GO:0008629	induction of apoptosis by intracellular signals	0.51
ENSG00000167513	CDT1 PPI subnetwork	0.51
GO:0051251	positive regulation of lymphocyte activation	0.51
MP:0001092	abnormal trigeminal ganglion morphology	0.51
GO:0051147	regulation of muscle cell differentiation	0.51
REACTOME_RNA_POLYMERASE_III_TRANSCRIPTION_INITIATION_FROM_TYPE_2_Pf	REACTOME_RNA_POLYMERASE_III_TRANSCRIPTION_INITIATION_FROM_TYPE_2_Pf	0.51
ENSG00000131459	GFPT2 PPI subnetwork	0.51
ENSG00000008294	SPAG9 PPI subnetwork	0.51
GO:0040014	regulation of multicellular organism growth	0.51
KEGG_GLYCOPHINGOLIPID_BIOSYNTHESIS_GANGLIO_SERIES	KEGG_GLYCOPHINGOLIPID_BIOSYNTHESIS_GANGLIO_SERIES	0.51
GO:0030194	positive regulation of blood coagulation	0.51
MP:0006298	abnormal platelet activation	0.51
ENSG00000156313	RPGR PPI subnetwork	0.51
ENSG00000078399	HOXA9 PPI subnetwork	0.51
GO:0030837	negative regulation of actin filament polymerization	0.51
REACTOME_INTERACTIONS_OF_VPR_WITH_HOST_CELLULAR_PROTEINS	REACTOME_INTERACTIONS_OF_VPR_WITH_HOST_CELLULAR_PROTEINS	0.51
GO:0060021	palate development	0.51
GO:0008180	signalosome	0.51
REACTOME_CREB_PHOSPHORYLATION_THROUGH_THE_ACTIVATION_OF_RAS	REACTOME_CREB_PHOSPHORYLATION_THROUGH_THE_ACTIVATION_OF_RAS	0.51
ENSG00000153914	SREK1 PPI subnetwork	0.51
MP:0004098	abnormal cerebellar granule cell morphology	0.51
GO:0014031	mesenchymal cell development	0.52
GO:2000514	regulation of CD4-positive, alpha-beta T cell activation	0.52
ENSG00000139372	TDG PPI subnetwork	0.52
MP:0005362	abnormal Langerhans cell physiology	0.52
REACTOME_RNA_POLYMERASE_III_CHAIN_ELONGATION	REACTOME_RNA_POLYMERASE_III_CHAIN_ELONGATION	0.52
GO:0070201	regulation of establishment of protein localizator	0.52

Original gene set ID	Original gene set description	Nominal P value
GO:0005657	replication fork	0.52
ENSG00000081479	LRP2 PPI subnetwork	0.52
ENSG00000071243	ING3 PPI subnetwork	0.52
GO:0007043	cell-cell junction assembly	0.52
MP:0003938	abnormal ear development	0.52
ENSG00000100722	ZC3H14 PPI subnetwork	0.52
ENSG00000135679	MDM2 PPI subnetwork	0.52
ENSG00000116106	EPHA4 PPI subnetwork	0.52
REACTOME_HIGHLY_CALCIUM_PERMEABLE_POSTSYNAPTIC_NICOTINIC_ACETY	REACTOME_HIGHLY_CALCIUM_PERMEABLE_POSTSYNAPTIC_NICOTINIC_ACETYLCHI	0.52
GO:0006937	regulation of muscle contraction	0.52
ENSG00000165732	DDX21 PPI subnetwork	0.52
GO:0019438	aromatic compound biosynthetic process	0.52
ENSG00000175073	VCPIP1 PPI subnetwork	0.52
GO:0009113	purine base biosynthetic process	0.52
GO:0072655	establishment of protein localization in mitochondrion	0.52
GO:0044269	glycerol ether catabolic process	0.52
GO:0046464	acylglycerol catabolic process	0.52
GO:0046461	neutral lipid catabolic process	0.52
MP:0003627	abnormal leukocyte tethering or rolling	0.52
KEGG_TGF_BETA_SIGNALING_PATHWAY	KEGG_TGF_BETA_SIGNALING_PATHWAY	0.52
GO:0046148	pigment biosynthetic process	0.52
ENSG00000215754	ENSG00000215754 PPI subnetwork	0.52
ENSG00000156802	ATAD2 PPI subnetwork	0.52
REACTOME_SYNTHESIS_OF_GLYCOSYLPHOSPHATIDYLINOSITOL_GPI	REACTOME_SYNTHESIS_OF_GLYCOSYLPHOSPHATIDYLINOSITOL_GPI	0.52
ENSG00000185024	BRF1 PPI subnetwork	0.52
ENSG00000149970	CNKS2 PPI subnetwork	0.52
GO:0016579	protein deubiquitination	0.52
GO:0043021	ribonucleoprotein complex binding	0.52
MP:0006082	CNS inflammation	0.52
GO:0006362	transcription elongation from RNA polymerase I promoter	0.52
ENSG00000197238	HIST1H4J PPI subnetwork	0.52
ENSG00000183941	HIST2H4A PPI subnetwork	0.52
ENSG00000197914	HIST1H4K PPI subnetwork	0.52
ENSG00000198518	HIST1H4E PPI subnetwork	0.52
ENSG00000197837	HIST4H4 PPI subnetwork	0.52
ENSG00000182217	HIST2H4B PPI subnetwork	0.52
ENSG00000158406	HIST1H4H PPI subnetwork	0.52
ENSG00000198558	HIST1H4L PPI subnetwork	0.52
ENSG00000124529	HIST1H4B PPI subnetwork	0.52
ENSG00000197061	HIST1H4C PPI subnetwork	0.52
ENSG00000188987	HIST1H4D PPI subnetwork	0.52
ENSG00000198339	HIST1H4I PPI subnetwork	0.52
ENSG00000198327	HIST1H4F PPI subnetwork	0.52
ENSG00000196176	HIST1H4A PPI subnetwork	0.52
ENSG00000104738	MCM4 PPI subnetwork	0.52
GO:0005930	axoneme	0.52
ENSG00000168374	ARF4 PPI subnetwork	0.52
GO:0002696	positive regulation of leukocyte activation	0.52
MP:0006138	congestive heart failure	0.52

Original gene set ID	Original gene set description	Nominal P value
GO:0051324	prophase	0.53
GO:0031498	chromatin disassembly	0.53
GO:0032986	protein-DNA complex disassembly	0.53
GO:0006337	nucleosome disassembly	0.53
MP:0001394	circling	0.53
MP:0004542	impaired acrosome reaction	0.53
ENSG00000077782	FGFR1 PPI subnetwork	0.53
ENSG00000006125	AP2B1 PPI subnetwork	0.53
MP:0002413	abnormal megakaryocyte progenitor cell morphology	0.53
MP:0001006	abnormal retinal cone cell morphology	0.53
ENSG00000015479	MATR3 PPI subnetwork	0.53
ENSG000000198130	HIBCH PPI subnetwork	0.53
GO:0031058	positive regulation of histone modification	0.53
GO:0016050	vesicle organization	0.53
MP:0000692	small spleen	0.53
ENSG000000144158	ENSG000000144158 PPI subnetwork	0.53
GO:0030529	ribonucleoprotein complex	0.53
ENSG00000069956	MAPK6 PPI subnetwork	0.53
REACTOME_PREFOLDIN_MEDIATED_TRANSFER_OF_SUBSTRATE_TO_CCTTRIC	REACTOME_PREFOLDIN_MEDIATED_TRANSFER_OF_SUBSTRATE_TO_CCTTRIC	0.53
REACTOME_COOPERATION_OF_PREFOLDIN_AND_TRICCT_IN_ACTIN_AND_TUBU	REACTOME_COOPERATION_OF_PREFOLDIN_AND_TRICCT_IN_ACTIN_AND_TUBU	0.53
ENSG000000169592	INO80E PPI subnetwork	0.53
ENSG000000162552	WNT4 PPI subnetwork	0.53
ENSG000000133027	PEMT PPI subnetwork	0.53
ENSG000000185627	PSMD13 PPI subnetwork	0.53
GO:0030424	axon	0.53
KEGG_FC_EPSILON_RI_SIGNALING_PATHWAY	KEGG_FC_EPSILON_RI_SIGNALING_PATHWAY	0.53
GO:0002755	MyD88-dependent toll-like receptor signaling pathway	0.53
ENSG00000081052	COL4A4 PPI subnetwork	0.53
ENSG000000067596	DHX8 PPI subnetwork	0.53
MP:0000248	macrocytosis	0.53
REACTOME_GABA_SYNTHESIS_RELEASE_REUPTAKE_AND_DEGRADATION	REACTOME_GABA_SYNTHESIS_RELEASE_REUPTAKE_AND_DEGRADATION	0.53
ENSG000000160712	IL6R PPI subnetwork	0.53
GO:0005852	eukaryotic translation initiation factor 3 complex	0.53
GO:0048598	embryonic morphogenesis	0.53
ENSG000000001626	CFTR PPI subnetwork	0.53
ENSG000000005175	RPAP3 PPI subnetwork	0.53
GO:0042461	photoreceptor cell development	0.53
GO:0007128	meiotic prophase I	0.53
GO:0031063	regulation of histone deacetylation	0.53
GO:0001085	RNA polymerase II transcription factor binding	0.53
ENSG000000149557	FEZ1 PPI subnetwork	0.53
ENSG000000049540	ELN PPI subnetwork	0.53
ENSG000000206279	DAXX PPI subnetwork	0.53
ENSG000000206206	DAXX PPI subnetwork	0.53
ENSG000000204209	DAXX PPI subnetwork	0.53
GO:0090175	regulation of establishment of planar polarity	0.53
GO:0060071	Wnt receptor signaling pathway, planar cell polarity pathway	0.53
GO:0001843	neural tube closure	0.53
ENSG000000163877	SNIP1 PPI subnetwork	0.53

Original gene set ID	Original gene set description	Nominal P value
ENSG00000139618	BRCA2 PPI subnetwork	0.54
ENSG00000100239	PPP6R2 PPI subnetwork	0.54
ENSG00000112159	MDN1 PPI subnetwork	0.54
ENSG00000100109	TFIP11 PPI subnetwork	0.54
ENSG00000187990	HIST1H2BG PPI subnetwork	0.54
ENSG00000168242	HIST1H2BI PPI subnetwork	0.54
ENSG00000180596	HIST1H2BC PPI subnetwork	0.54
ENSG00000197846	HIST1H2BF PPI subnetwork	0.54
ENSG00000126261	UBA2 PPI subnetwork	0.54
ENSG0000011485	PPP5C PPI subnetwork	0.54
ENSG00000101146	RAE1 PPI subnetwork	0.54
ENSG00000163810	TGM4 PPI subnetwork	0.54
ENSG00000142208	AKT1 PPI subnetwork	0.54
ENSG00000170312	CDK1 PPI subnetwork	0.54
KEGG_PORPHYRIN_AND_CHLOROPHYLL_METABOLISM	KEGG_PORPHYRIN_AND_CHLOROPHYLL_METABOLISM	0.54
GO:0010948	negative regulation of cell cycle process	0.54
GO:0070555	response to interleukin-1	0.54
GO:0009982	pseudouridine synthase activity	0.54
GO:0030934	anchoring collagen	0.54
GO:0005253	anion channel activity	0.54
GO:0019841	retinol binding	0.54
GO:0006885	regulation of pH	0.54
MP:0002887	decreased susceptibility to pharmacologically induced seizures	0.54
ENSG00000163069	SGCB PPI subnetwork	0.54
MP:0008807	increased liver iron level	0.54
GO:0043202	lysosomal lumen	0.54
ENSG00000197903	HIST1H2BK PPI subnetwork	0.54
ENSG00000164086	DUSP7 PPI subnetwork	0.54
GO:0008287	protein serine/threonine phosphatase complex	0.54
ENSG00000174989	FBXW8 PPI subnetwork	0.54
GO:0034483	heparan sulfate sulfotransferase activity	0.54
ENSG00000177879	AP3S1 PPI subnetwork	0.54
GO:0021549	cerebellum development	0.54
GO:0008175	tRNA methyltransferase activity	0.54
KEGG_GRAFT_VERSUS_HOST_DISEASE	KEGG_GRAFT_VERSUS_HOST_DISEASE	0.54
GO:0031577	spindle checkpoint	0.54
GO:0008366	axon ensheathment	0.54
GO:0007272	ensheathment of neurons	0.54
GO:0016339	calcium-dependent cell-cell adhesion	0.54
ENSG00000129993	CBFA2T3 PPI subnetwork	0.54
MP:0001363	increased anxiety-related response	0.54
ENSG00000126067	PSMB2 PPI subnetwork	0.54
ENSG00000066933	MYO9A PPI subnetwork	0.54
GO:0071855	neuropeptide receptor binding	0.54
REACTOME_SIGNAL_AMPLIFICATION	REACTOME_SIGNAL_AMPLIFICATION	0.54
ENSG00000006468	ETV1 PPI subnetwork	0.54
GO:0071295	cellular response to vitamin	0.54
ENSG00000111348	ARHGDI3 PPI subnetwork	0.54
ENSG00000143437	ARNT PPI subnetwork	0.54

Original gene set ID

Original gene set description

Nominal P value

ENSG00000104419	NDRG1 PPI subnetwork	0.55
MP:0000245	abnormal erythropoiesis	0.55
ENSG00000117601	SERPINC1 PPI subnetwork	0.55
GO:0060485	mesenchyme development	0.55
GO:0042575	DNA polymerase complex	0.55
MP:0001120	abnormal uterus morphology	0.55
ENSG00000108055	SMC3 PPI subnetwork	0.55
ENSG00000102974	CTCF PPI subnetwork	0.55
MP:0004939	abnormal B cell morphology	0.55
GO:0005100	Rho GTPase activator activity	0.55
MP:0008528	polycystic kidney	0.55
MP:0009862	abnormal aorta elastic tissue morphology	0.55
MP:0004876	decreased mean systemic arterial blood pressure	0.55
GO:0007017	microtubule-based process	0.55
GO:0003007	heart morphogenesis	0.55
ENSG00000111262	KCNA1 PPI subnetwork	0.56
MP:0005159	azoospermia	0.56
ENSG00000180628	PCGF5 PPI subnetwork	0.56
ENSG00000177469	PTRF PPI subnetwork	0.56
ENSG00000122965	RBM19 PPI subnetwork	0.56
GO:0046658	anchored to plasma membrane	0.56
GO:0042625	ATPase activity, coupled to transmembrane movement of ions	0.56
ENSG00000162946	DISC1 PPI subnetwork	0.56
ENSG00000085231	TAF9 PPI subnetwork	0.56
ENSG00000069431	ABCC9 PPI subnetwork	0.56
GO:0006182	cGMP biosynthetic process	0.56
ENSG00000123374	CDK2 PPI subnetwork	0.56
REACTOME_CYTOSOLIC_TRNA_AMINOACYLATION	REACTOME_CYTOSOLIC_TRNA_AMINOACYLATION	0.56
REACTOME_SCFSKP2:MEDIATED_DEGRADATION_OF_P27P21	REACTOME_SCFSKP2:MEDIATED_DEGRADATION_OF_P27P21	0.56
MP:0011100	complete preweaning lethality	0.56
MP:0002176	increased brain weight	0.56
REACTOME_CGMP_EFFECTS	REACTOME_CGMP_EFFECTS	0.56
ENSG00000092203	TOX4 PPI subnetwork	0.56
ENSG00000165527	ARF6 PPI subnetwork	0.56
ENSG00000067704	IARS2 PPI subnetwork	0.56
GO:0090312	positive regulation of protein deacetylation	0.56
GO:2000027	regulation of organ morphogenesis	0.56
GO:0045177	apical part of cell	0.56
MP:0004779	abnormal production of surfactant	0.56
ENSG00000106976	DNM1 PPI subnetwork	0.56
ENSG00000106348	IMPDH1 PPI subnetwork	0.56
ENSG00000174446	SNAPC5 PPI subnetwork	0.56
ENSG00000167751	KLK2 PPI subnetwork	0.56
ENSG00000102572	STK24 PPI subnetwork	0.56
GO:0003950	NAD+ ADP-ribosyltransferase activity	0.56
ENSG00000159840	ZYX PPI subnetwork	0.56
ENSG00000105664	COMP PPI subnetwork	0.56
ENSG00000165684	SNAPC4 PPI subnetwork	0.56
GO:0061387	regulation of extent of cell growth	0.56

Original gene set ID	Original gene set description	Nominal P value
REACTOME_MITOTIC_SPINDLE_CHECKPOINT	REACTOME_MITOTIC_SPINDLE_CHECKPOINT	0.56
REACTOME_UNBLOCKING_OF_NMDA_RECEPTOR_Glutamate_Binding_And	REACTOME_UNBLOCKING_OF_NMDA_RECEPTOR_Glutamate_Binding_And_AC	0.56
MP:0002621	delayed neural tube closure	0.56
ENSG00000101558	VAPA PPI subnetwork	0.56
GO:0007040	lysosome organization	0.56
ENSG00000097046	CDC7 PPI subnetwork	0.56
MP:0008703	decreased interleukin-5 secretion	0.56
MP:0004486	decreased response of heart to induced stress	0.56
ENSG00000101189	C20orf20 PPI subnetwork	0.56
REACTOME_G1S:SPECIFIC_TRANSCRIPTION	REACTOME_G1S:SPECIFIC_TRANSCRIPTION	0.56
ENSG00000099341	PSMD8 PPI subnetwork	0.56
GO:0043534	blood vessel endothelial cell migration	0.56
ENSG00000106211	HSPB1 PPI subnetwork	0.56
ENSG00000198380	GFPT1 PPI subnetwork	0.56
GO:0005254	chloride channel activity	0.56
ENSG00000171867	PRNP PPI subnetwork	0.56
GO:0032368	regulation of lipid transport	0.56
ENSG00000206232	ENSG00000206232 PPI subnetwork	0.56
ENSG00000204261	ENSG00000204261 PPI subnetwork	0.56
ENSG00000206296	ENSG00000206296 PPI subnetwork	0.56
GO:0016776	phosphotransferase activity, phosphate group as acceptor	0.56
ENSG00000129559	NEDD8 PPI subnetwork	0.56
ENSG00000152661	GJA1 PPI subnetwork	0.56
GO:0016709	oxidoreductase activity, acting on paired donors, with incorporation or reduction of	0.56
GO:0035050	embryonic heart tube development	0.56
ENSG00000175084	DES PPI subnetwork	0.56
GO:0007588	excretion	0.56
GO:0050770	regulation of axonogenesis	0.56
ENSG00000114251	WNT5A PPI subnetwork	0.56
MP:0000111	cleft palate	0.56
ENSG00000155561	NUP205 PPI subnetwork	0.56
ENSG00000198018	ENTPD7 PPI subnetwork	0.56
REACTOME_P2Y_RECEPTORS	REACTOME_P2Y_RECEPTORS	0.56
GO:0043498	cell surface binding	0.56
MP:0008189	increased transitional stage B cell number	0.56
GO:0007059	chromosome segregation	0.56
GO:0008023	transcription elongation factor complex	0.56
MP:0005324	ascites	0.56
KEGG_FRUCTOSE_AND_MANNANOSE_METABOLISM	KEGG_FRUCTOSE_AND_MANNANOSE_METABOLISM	0.56
ENSG00000167930	ITFG3 PPI subnetwork	0.56
GO:0016514	SWI/SNF complex	0.56
GO:0016055	Wnt receptor signaling pathway	0.56
MP:0005334	abnormal fat pad morphology	0.56
ENSG00000108379	WNT3 PPI subnetwork	0.56
MP:0005464	abnormal platelet physiology	0.56
GO:0016064	immunoglobulin mediated immune response	0.56
GO:0032609	interferon-gamma production	0.56
GO:0035162	embryonic hemopoiesis	0.56
ENSG00000103168	TAF1C PPI subnetwork	0.56

Original gene set ID	Original gene set description	Nominal P value
ENSG00000122884	P4HA1 PPI subnetwork	0.57
GO:0003143	embryonic heart tube morphogenesis	0.57
ENSG00000153234	NR4A2 PPI subnetwork	0.57
ENSG00000135363	LMO2 PPI subnetwork	0.57
GO:0019894	kinesin binding	0.57
GO:0042440	pigment metabolic process	0.57
GO:0060538	skeletal muscle organ development	0.57
GO:0006275	regulation of DNA replication	0.57
ENSG00000100079	LGALS2 PPI subnetwork	0.57
REACTOME_ACTIVATION_OF_CHAPERONES_BY_ATF6:ALPHA	REACTOME_ACTIVATION_OF_CHAPERONES_BY_ATF6:ALPHA	0.57
GO:0016604	nuclear body	0.57
MP:0002199	abnormal brain commissure morphology	0.57
ENSG00000165996	PTPLA PPI subnetwork	0.57
GO:0004115	3',5'-cyclic-AMP phosphodiesterase activity	0.57
ENSG00000175792	RUVBL1 PPI subnetwork	0.57
ENSG00000111752	PHC1 PPI subnetwork	0.57
MP:0002085	abnormal embryonic tissue morphology	0.57
ENSG00000114982	KANSL3 PPI subnetwork	0.57
GO:0010745	negative regulation of macrophage derived foam cell differentiation	0.57
GO:0007094	mitotic cell cycle spindle assembly checkpoint	0.57
ENSG00000108823	SGCA PPI subnetwork	0.57
GO:0008395	steroid hydroxylase activity	0.57
GO:0001754	eye photoreceptor cell differentiation	0.57
GO:0032393	MHC class I receptor activity	0.57
REACTOME_CELL_CYCLE_MITOTIC	REACTOME_CELL_CYCLE_MITOTIC	0.57
GO:0030193	regulation of blood coagulation	0.57
GO:0019239	deaminase activity	0.57
MP:0005341	decreased susceptibility to atherosclerosis	0.57
ENSG00000102054	RBBP7 PPI subnetwork	0.57
MP:0001182	lung hemorrhage	0.57
GO:0021904	dorsal/ventral neural tube patterning	0.57
ENSG00000166478	ZNF143 PPI subnetwork	0.57
KEGG_BASAL_TRANSCRIPTION_FACTORS	KEGG_BASAL_TRANSCRIPTION_FACTORS	0.57
GO:0048566	embryonic digestive tract development	0.57
MP:0000788	abnormal cerebral cortex morphology	0.57
ENSG00000144285	SCN1A PPI subnetwork	0.57
MP:0000562	polydactyly	0.57
REACTOME_ION_TRANSPORT_BY_P:TYPE_ATPASES	REACTOME_ION_TRANSPORT_BY_P:TYPE_ATPASES	0.57
ENSG00000105287	PRKD2 PPI subnetwork	0.57
ENSG00000181610	MRPS23 PPI subnetwork	0.57
ENSG00000116478	HDAC1 PPI subnetwork	0.57
GO:0030901	midbrain development	0.57
ENSG00000158517	NCF1 PPI subnetwork	0.57
ENSG00000152818	UTRN PPI subnetwork	0.57
MP:0008076	abnormal CD4-positive T cell differentiation	0.57
KEGG_LYSINE_DEGRADATION	KEGG_LYSINE_DEGRADATION	0.57
MP:0011346	renal tubule atrophy	0.57
ENSG00000142599	RERE PPI subnetwork	0.57
REACTOME_METABOLISM_OF_NON:CODING_RNA	REACTOME_METABOLISM_OF_NON:CODING_RNA	0.57

Original gene set ID	Original gene set description	Nominal P value
REACTOME_SNRNP_ASSEMBLY	REACTOME_SNRNP_ASSEMBLY	0.57
ENSG00000159199	ATP5G1 PPI subnetwork	0.57
KEGG_CALCIIUM_SIGNALING_PATHWAY	KEGG_CALCIIUM_SIGNALING_PATHWAY	0.57
GO:0002039	p53 binding	0.57
ENSG00000148798	INA PPI subnetwork	0.57
GO:0030551	cyclic nucleotide binding	0.57
ENSG00000150347	ARID5B PPI subnetwork	0.57
GO:0032147	activation of protein kinase activity	0.57
ENSG00000188064	WNT7B PPI subnetwork	0.57
MP:0005307	head tossing	0.58
GO:0060047	heart contraction	0.58
ENSG00000163288	GABRB1 PPI subnetwork	0.58
GO:0051048	negative regulation of secretion	0.58
ENSG00000012223	LTF PPI subnetwork	0.58
GO:0045765	regulation of angiogenesis	0.58
ENSG00000089094	KDM2B PPI subnetwork	0.58
GO:0002504	antigen processing and presentation of peptide or polysaccharide antigen via MHC class II	0.58
ENSG00000186676	ENSG00000186676 PPI subnetwork	0.58
MP:0001876	decreased inflammatory response	0.58
GO:0046632	alpha-beta T cell differentiation	0.58
ENSG00000109339	MAPK10 PPI subnetwork	0.58
ENSG00000171564	FGB PPI subnetwork	0.58
GO:0010165	response to X-ray	0.58
ENSG00000135365	PHF21A PPI subnetwork	0.58
MP:0000633	abnormal pituitary gland morphology	0.58
MP:0000334	decreased granulocyte number	0.58
GO:0004984	olfactory receptor activity	0.58
GO:0034446	substrate adhesion-dependent cell spreading	0.58
ENSG00000136930	PSMB7 PPI subnetwork	0.58
ENSG00000139190	VAMP1 PPI subnetwork	0.58
ENSG00000075884	ARHGAP15 PPI subnetwork	0.58
REACTOME_BIOLOGICAL_OXIDATIONS	REACTOME_BIOLOGICAL_OXIDATIONS	0.58
ENSG00000115641	FHL2 PPI subnetwork	0.58
GO:0016409	palmitoyltransferase activity	0.58
MP:0002230	abnormal primitive streak formation	0.58
GO:0048306	calcium-dependent protein binding	0.58
GO:0001934	positive regulation of protein phosphorylation	0.58
ENSG00000115361	ACADL PPI subnetwork	0.58
REACTOME_VPR:MEDIATED_NUCLEAR_IMPORT_OF_PICS	REACTOME_VPR:MEDIATED_NUCLEAR_IMPORT_OF_PICS	0.58
GO:0030593	neutrophil chemotaxis	0.58
MP:0002651	abnormal sciatic nerve morphology	0.58
MP:0002233	abnormal nose morphology	0.58
ENSG00000075089	ACTR6 PPI subnetwork	0.58
ENSG00000107581	EIF3A PPI subnetwork	0.58
REACTOME_INTERACTIONS_OF_REV_WITH_HOST_CELLULAR_PROTEINS	REACTOME_INTERACTIONS_OF_REV_WITH_HOST_CELLULAR_PROTEINS	0.58
GO:0015116	sulfate transmembrane transporter activity	0.58
ENSG00000095794	CREM PPI subnetwork	0.58
GO:0010769	regulation of cell morphogenesis involved in differentiation	0.58
GO:0071363	cellular response to growth factor stimulus	0.58

Original gene set ID	Original gene set description	Nominal P value
MP:0004405	absent cochlear hair cells	0.58
GO:0043583	ear development	0.58
MP:0004261	abnormal embryonic neuroepithelium morphology	0.58
REACTOME_ANTIGEN_PROCESSING_UBIQUITINATION__PROTEASOME_DEGRAI	REACTOME_ANTIGEN_PROCESSING_UBIQUITINATION__PROTEASOME_DEGRADATI	0.58
GO:0031514	motile cilium	0.58
GO:0046415	urate metabolic process	0.58
ENSG00000114867	EIF4G1 PPI subnetwork	0.58
ENSG00000198677	TTC37 PPI subnetwork	0.58
ENSG00000116717	GADD45A PPI subnetwork	0.58
REACTOME_CLASS_I_MHC_MEDIATED_ANTIGEN_PROCESSING__PRESENTATIOI	REACTOME_CLASS_I_MHC_MEDIATED_ANTIGEN_PROCESSING__PRESENTATION	0.58
GO:0033119	negative regulation of RNA splicing	0.58
MP:0000914	exencephaly	0.58
GO:0048659	smooth muscle cell proliferation	0.58
GO:0060271	cilium morphogenesis	0.58
MP:0004774	abnormal bile salt level	0.58
MP:0001695	abnormal gastrulation	0.58
ENSG00000131504	DIAPH1 PPI subnetwork	0.58
GO:0048762	mesenchymal cell differentiation	0.58
REACTOME_ACTIVATION_OF_BH3:ONLY_PROTEINS	REACTOME_ACTIVATION_OF_BH3:ONLY_PROTEINS	0.58
ENSG00000073969	NSF PPI subnetwork	0.58
GO:0005548	phospholipid transporter activity	0.58
ENSG00000215120	ENSG00000215120 PPI subnetwork	0.58
ENSG00000134086	VHL PPI subnetwork	0.58
ENSG00000134058	CDK7 PPI subnetwork	0.58
MP:0004924	abnormal behavior	0.58
ENSG00000163531	NFASC PPI subnetwork	0.58
REACTOME_CYTOCHROME_P450_:ARRANGED_BY_SUBSTRATE_TYPE	REACTOME_CYTOCHROME_P450_:ARRANGED_BY_SUBSTRATE_TYPE	0.58
ENSG00000103051	COG4 PPI subnetwork	0.58
ENSG00000137345	MOG PPI subnetwork	0.58
ENSG00000206456	ENSG00000206456 PPI subnetwork	0.58
ENSG00000204655	MOG PPI subnetwork	0.58
GO:0019915	lipid storage	0.58
MP:0001654	hepatic necrosis	0.58
MP:0001328	disorganized retinal layers	0.58
GO:0000726	non-recombinational repair	0.58
ENSG00000185787	MORF4L1 PPI subnetwork	0.58
MP:0006011	abnormal endolymphatic duct morphology	0.58
REACTOME_ER:PHAGOSOME_PATHWAY	REACTOME_ER:PHAGOSOME_PATHWAY	0.58
ENSG00000123080	CDKN2C PPI subnetwork	0.58
REACTOME_SYNTHESIS_OF_DNA	REACTOME_SYNTHESIS_OF_DNA	0.58
GO:0035145	exon-exon junction complex	0.58
GO:0015079	potassium ion transmembrane transporter activity	0.58
GO:0050730	regulation of peptidyl-tyrosine phosphorylation	0.58
MP:0008388	hypochromic microcytic anemia	0.58
GO:0055008	cardiac muscle tissue morphogenesis	0.58
GO:0045664	regulation of neuron differentiation	0.58
ENSG00000168685	IL7R PPI subnetwork	0.58
KEGG_UBIQUITIN_MEDIATED_PROTEOLYSIS	KEGG_UBIQUITIN_MEDIATED_PROTEOLYSIS	0.58
ENSG00000044115	CTNNA1 PPI subnetwork	0.58

Original gene set ID	Original gene set description	Nominal P value
ENSG00000123338	NCKAP1L PPI subnetwork	0.58
GO:0042611	MHC protein complex	0.58
ENSG000000065613	SLK PPI subnetwork	0.58
ENSG00000133318	RTN3 PPI subnetwork	0.58
GO:0030818	negative regulation of cAMP biosynthetic process	0.58
GO:0030815	negative regulation of cAMP metabolic process	0.58
GO:0003015	heart process	0.58
GO:0032321	positive regulation of Rho GTPase activity	0.58
ENSG00000182533	CAV3 PPI subnetwork	0.58
ENSG00000143632	ACTA1 PPI subnetwork	0.58
ENSG00000008277	ADAM22 PPI subnetwork	0.58
REACTOME_EXPORT_OF_VIRAL_RIBONUCLEOPROTEINS_FROM_NUCLEUS	REACTOME_EXPORT_OF_VIRAL_RIBONUCLEOPROTEINS_FROM_NUCLEUS	0.58
GO:0045807	positive regulation of endocytosis	0.58
GO:0018212	peptidyl-tyrosine modification	0.58
GO:0034374	low-density lipoprotein particle remodeling	0.58
GO:0070851	growth factor receptor binding	0.58
GO:0006607	NLS-bearing substrate import into nucleus	0.59
ENSG00000131711	MAP1B PPI subnetwork	0.59
GO:0070585	protein localization in mitochondrion	0.59
REACTOME_MTOR_SIGNALLING	REACTOME_MTOR_SIGNALLING	0.59
MP:0010763	abnormal hematopoietic stem cell physiology	0.59
ENSG00000198087	CD2AP PPI subnetwork	0.59
REACTOME_MITOTIC_G1:G1S_PHASES	REACTOME_MITOTIC_G1:G1S_PHASES	0.59
GO:0031346	positive regulation of cell projection organization	0.59
ENSG00000023608	SNAPC1 PPI subnetwork	0.59
ENSG00000183735	TBK1 PPI subnetwork	0.59
ENSG00000112312	GMNN PPI subnetwork	0.59
GO:0016049	cell growth	0.59
GO:0001558	regulation of cell growth	0.59
GO:0046875	ephrin receptor binding	0.59
ENSG00000077238	IL4R PPI subnetwork	0.59
ENSG00000196305	IARS PPI subnetwork	0.59
ENSG00000136738	STAM PPI subnetwork	0.59
GO:0032649	regulation of interferon-gamma production	0.59
GO:0002294	CD4-positive, alpha-beta T cell differentiation involved in immune response	0.59
GO:0042093	T-helper cell differentiation	0.59
ENSG00000185359	HGS PPI subnetwork	0.59
GO:0030111	regulation of Wnt receptor signaling pathway	0.59
KEGG_INOSITOL_PHOSPHATE_METABOLISM	KEGG_INOSITOL_PHOSPHATE_METABOLISM	0.59
GO:0048538	thymus development	0.59
ENSG00000171566	PLRG1 PPI subnetwork	0.59
GO:0030120	vesicle coat	0.59
ENSG00000197459	HIST1H2BH PPI subnetwork	0.59
ENSG00000167645	YIF1B PPI subnetwork	0.59
MP:0002693	abnormal pancreas physiology	0.59
GO:0051259	protein oligomerization	0.59
GO:0000302	response to reactive oxygen species	0.59
ENSG00000170142	UBE2E1 PPI subnetwork	0.59
ENSG00000185619	PCGF3 PPI subnetwork	0.59

Original gene set ID	Original gene set description	Nominal P value
ENSG00000160007	ARHGAP35 PPI subnetwork	0.59
KEGG_PPAR_SIGNALING_PATHWAY	KEGG_PPAR_SIGNALING_PATHWAY	0.59
ENSG00000175602	CCDC85B PPI subnetwork	0.59
MP:0000233	abnormal blood flow velocity	0.59
MP:0006113	abnormal heart septum morphology	0.59
KEGG_PROPANOATE_METABOLISM	KEGG_PROPANOATE_METABOLISM	0.59
GO:0009743	response to carbohydrate stimulus	0.59
MP:0001263	weight loss	0.59
GO:0048660	regulation of smooth muscle cell proliferation	0.59
GO:0070830	tight junction assembly	0.59
GO:0018108	peptidyl-tyrosine phosphorylation	0.59
MP:0003733	abnormal retinal inner nuclear layer morphology	0.59
GO:0050818	regulation of coagulation	0.59
GO:0048934	peripheral nervous system neuron differentiation	0.59
GO:0048935	peripheral nervous system neuron development	0.59
ENSG00000086619	ERO1LB PPI subnetwork	0.59
ENSG00000198700	IPO9 PPI subnetwork	0.59
ENSG00000130208	APOC1 PPI subnetwork	0.59
ENSG00000067606	PRKCZ PPI subnetwork	0.59
GO:0003179	heart valve morphogenesis	0.59
REACTOME_CYCLIN_ACDK2:ASSOCIATED_EVENTS_AT_S_PHASE_ENTRY	REACTOME_CYCLIN_ACDK2:ASSOCIATED_EVENTS_AT_S_PHASE_ENTRY	0.59
GO:0005761	mitochondrial ribosome	0.59
GO:0000313	organellar ribosome	0.59
GO:0043198	dendritic shaft	0.59
ENSG00000151164	RAD9B PPI subnetwork	0.59
ENSG00000117594	HSD11B1 PPI subnetwork	0.59
ENSG00000157087	ATP2B2 PPI subnetwork	0.59
MP:0000848	abnormal pons morphology	0.59
GO:0042327	positive regulation of phosphorylation	0.59
ENSG00000113575	PPP2CA PPI subnetwork	0.59
MP:0005566	decreased blood urea nitrogen level	0.59
ENSG00000077522	ACTN2 PPI subnetwork	0.59
REACTOME_INHIBITION_OF_THE_PROTEOLYTIC_ACTIVITY_OF_APCC_REQUIRED	REACTOME_INHIBITION_OF_THE_PROTEOLYTIC_ACTIVITY_OF_APCC_REQUIRED_FC	0.59
REACTOME_INACTIVATION_OF_APCC_VIA_DIRECT_INHIBITION_OF_THE_APCC	REACTOME_INACTIVATION_OF_APCC_VIA_DIRECT_INHIBITION_OF_THE_APCC_COI	0.59
ENSG00000088833	NSFL1C PPI subnetwork	0.59
KEGG_AUTOIMMUNE_THYROID_DISEASE	KEGG_AUTOIMMUNE_THYROID_DISEASE	0.59
ENSG00000106829	TLE4 PPI subnetwork	0.59
GO:0019884	antigen processing and presentation of exogenous antigen	0.59
GO:0030135	coated vesicle	0.59
MP:0003644	thymus atrophy	0.59
ENSG00000173566	NUDT18 PPI subnetwork	0.59
GO:0015645	fatty acid ligase activity	0.59
ENSG00000099960	SLC7A4 PPI subnetwork	0.59
ENSG00000013293	SLC7A14 PPI subnetwork	0.59
ENSG00000173786	CNP PPI subnetwork	0.59
GO:0050679	positive regulation of epithelial cell proliferation	0.59
GO:0046427	positive regulation of JAK-STAT cascade	0.59
ENSG00000162692	VCAM1 PPI subnetwork	0.59
GO:0007350	blastoderm segmentation	0.59

Original gene set ID**Original gene set description****Nominal P value**

KEGG_PROTEASOME	KEGG_PROTEASOME	0.59
ENSG00000197860	SGTB PPI subnetwork	0.59
REACTOME_LIGAND:GATED_ION_CHANNEL_TRANSPORT	REACTOME_LIGAND:GATED_ION_CHANNEL_TRANSPORT	0.59
REACTOME_RNA_POLYMERASE_I_TRANSCRIPTION_INITIATION	REACTOME_RNA_POLYMERASE_I_TRANSCRIPTION_INITIATION	0.59
GO:0015276	ligand-gated ion channel activity	0.59
GO:0022834	ligand-gated channel activity	0.59
ENSG00000172780	RAB43 PPI subnetwork	0.59
ENSG00000174547	MRPL11 PPI subnetwork	0.59
GO:0008652	cellular amino acid biosynthetic process	0.59
KEGG_PHENYLALANINE_METABOLISM	KEGG_PHENYLALANINE_METABOLISM	0.59
GO:0030863	cortical cytoskeleton	0.59
GO:0019842	vitamin binding	0.59
ENSG00000160867	FGFR4 PPI subnetwork	0.59
ENSG00000135597	REPS1 PPI subnetwork	0.59
MP:0003722	absent ureter	0.59
GO:0009411	response to UV	0.59
ENSG00000113240	CLK4 PPI subnetwork	0.59
ENSG00000168118	RAB4A PPI subnetwork	0.59
ENSG00000137462	TLR2 PPI subnetwork	0.59
ENSG00000134352	IL6ST PPI subnetwork	0.59
ENSG00000151532	VT1A PPI subnetwork	0.59
GO:0048333	mesodermal cell differentiation	0.59
ENSG00000197956	S100A6 PPI subnetwork	0.59
GO:0032733	positive regulation of interleukin-10 production	0.59
ENSG00000125835	SNRNP PPI subnetwork	0.59
MP:0002572	abnormal emotion/affect behavior	0.59
ENSG00000198056	PRIM1 PPI subnetwork	0.59
ENSG00000151148	UBE3B PPI subnetwork	0.59
ENSG00000054118	THRAP3 PPI subnetwork	0.59
ENSG00000120438	TCP1 PPI subnetwork	0.59
MP:0002335	decreased airway responsiveness	0.59
ENSG00000141027	NCOR1 PPI subnetwork	0.59
ENSG00000072952	MRVI1 PPI subnetwork	0.59
REACTOME_PI3KAKT_ACTIVATION	REACTOME_PI3KAKT_ACTIVATION	0.59
ENSG00000109846	CRYAB PPI subnetwork	0.59
REACTOME_REPAIR_SYNTHESIS_OF_PATCH_27:30_BASES_LONG_BY_DNA_PO	REACTOME_REPAIR_SYNTHESIS_OF_PATCH_27:30_BASES_LONG_BY_DNA_POLYM	0.59
REACTOME_REPAIR_SYNTHESIS_FOR_GAP:FILLING_BY_DNA_POLYMERASE_IN_	REACTOME_REPAIR_SYNTHESIS_FOR_GAP:FILLING_BY_DNA_POLYMERASE_IN_TC:N	0.59
REACTOME_SHC1_EVENTS_IN_ERBB4_SIGNALING	REACTOME_SHC1_EVENTS_IN_ERBB4_SIGNALING	0.59
GO:0030326	embryonic limb morphogenesis	0.59
GO:0035113	embryonic appendage morphogenesis	0.59
MP:0002628	hepatic steatosis	0.59
GO:0004653	polypeptide N-acetylgalactosaminyltransferase activity	0.6
GO:0072331	signal transduction by p53 class mediator	0.6
MP:0006069	abnormal retinal neuronal layer morphology	0.6
MP:0008699	increased interleukin-4 secretion	0.6
GO:0019724	B cell mediated immunity	0.6
KEGG_NON_HOMOLOGOUS_END_JOINING	KEGG_NON_HOMOLOGOUS_END_JOINING	0.6
REACTOME_PHASE_II_CONJUGATION	REACTOME_PHASE_II_CONJUGATION	0.6
ENSG00000120063	GNA13 PPI subnetwork	0.6

Original gene set ID	Original gene set description	Nominal P value
KEGG_PENTOSE_PHOSPHATE_PATHWAY	KEGG_PENTOSE_PHOSPHATE_PATHWAY	0.6
ENSG00000177426	TGIF1 PPI subnetwork	0.6
ENSG00000015153	YAF2 PPI subnetwork	0.6
REACTOME_XENOBIOTICS	REACTOME_XENOBIOTICS	0.6
ENSG00000137673	MMP7 PPI subnetwork	0.6
REACTOME_CDK:MEDIATED_PHOSPHORYLATION_AND_REMOVAL_OF_CDC6	REACTOME_CDK:MEDIATED_PHOSPHORYLATION_AND_REMOVAL_OF_CDC6	0.6
GO:0007631	feeding behavior	0.6
ENSG00000134287	ARF3 PPI subnetwork	0.6
GO:0043297	apical junction assembly	0.6
ENSG00000206274	ENSG00000206274 PPI subnetwork	0.6
ENSG00000206383	HSPA1L PPI subnetwork	0.6
ENSG00000124299	PEPD PPI subnetwork	0.6
ENSG00000162191	UBXN1 PPI subnetwork	0.6
ENSG00000139180	NDUFA9 PPI subnetwork	0.6
ENSG00000183049	CAMK1D PPI subnetwork	0.6
ENSG00000139549	DHH PPI subnetwork	0.6
GO:0042579	microbody	0.6
GO:0005777	peroxisome	0.6
REACTOME_SIGNALING_BY_INSULIN_RECEPTOR	REACTOME_SIGNALING_BY_INSULIN_RECEPTOR	0.6
ENSG00000155657	TTN PPI subnetwork	0.6
REACTOME_UBIQUITIN:DEPENDENT_DEGRADATION_OF_CYCLIN_D	REACTOME_UBIQUITIN:DEPENDENT_DEGRADATION_OF_CYCLIN_D	0.6
REACTOME_UBIQUITIN:DEPENDENT_DEGRADATION_OF_CYCLIN_D1	REACTOME_UBIQUITIN:DEPENDENT_DEGRADATION_OF_CYCLIN_D1	0.6
ENSG00000134759	ELP2 PPI subnetwork	0.6
GO:0030031	cell projection assembly	0.6
ENSG00000100867	DHRS2 PPI subnetwork	0.6
GO:0030433	ER-associated protein catabolic process	0.6
MP:0001491	unresponsive to tactile stimuli	0.6
ENSG00000106245	BUD31 PPI subnetwork	0.6
KEGG_SELENOAMINO_ACID_METABOLISM	KEGG_SELENOAMINO_ACID_METABOLISM	0.6
GO:0043535	regulation of blood vessel endothelial cell migration	0.6
GO:0015300	solute:solute antiporter activity	0.6
GO:0046364	monosaccharide biosynthetic process	0.6
GO:0050907	detection of chemical stimulus involved in sensory perceptior	0.6
KEGG_PURINE_METABOLISM	KEGG_PURINE_METABOLISM	0.6
MP:0001417	decreased exploration in new environment	0.6
ENSG00000114698	PLSCR4 PPI subnetwork	0.6
ENSG00000153922	CHD1 PPI subnetwork	0.6
MP:0000188	abnormal circulating glucose level	0.6
GO:0001763	morphogenesis of a branching structure	0.6
REACTOME_NEPNS2_INTERACTS_WITH_THE_CELLULAR_EXPORT_MACHINERY	REACTOME_NEPNS2_INTERACTS_WITH_THE_CELLULAR_EXPORT_MACHINERY	0.6
ENSG00000091428	RAPGEF4 PPI subnetwork	0.6
ENSG00000087460	GNAS PPI subnetwork	0.6
GO:0045214	sarcomere organization	0.6
MP:0001431	abnormal eating behavior	0.6
GO:0071174	mitotic cell cycle spindle checkpoint	0.6
ENSG00000196235	SUPT5H PPI subnetwork	0.6
GO:0031669	cellular response to nutrient levels	0.6
ENSG00000101856	PGRMC1 PPI subnetwork	0.6
ENSG00000173692	PSMD1 PPI subnetwork	0.6

Original gene set ID	Original gene set description	Nominal P value
MP:0000097	short maxilla	0.6
MP:0002064	seizures	0.6
MP:0000807	abnormal hippocampus morphology	0.6
GO:0018149	peptide cross-linking	0.6
ENSG00000120616	EPC1 PPI subnetwork	0.6
GO:0006303	double-strand break repair via nonhomologous end joining	0.6
GO:0030855	epithelial cell differentiation	0.6
GO:0005249	voltage-gated potassium channel activity	0.6
ENSG00000135100	HNF1A PPI subnetwork	0.6
ENSG00000163435	ELF3 PPI subnetwork	0.6
MP:0000880	decreased Purkinje cell number	0.6
ENSG00000082074	FYB PPI subnetwork	0.6
MP:0005221	abnormal rostral-caudal axis patterning	0.6
KEGG_NON_SMALL_CELL_LUNG_CANCER	KEGG_NON_SMALL_CELL_LUNG_CANCER	0.6
ENSG00000108443	RPS6KB1 PPI subnetwork	0.6
REACTOME_SIGNAL_TRANSDUCTION_BY_L1	REACTOME_SIGNAL_TRANSDUCTION_BY_L1	0.6
ENSG00000150991	UBC PPI subnetwork	0.6
REACTOME_REGULATION_OF_DNA_REPLICATION	REACTOME_REGULATION_OF_DNA_REPLICATION	0.6
ENSG00000133710	SPINK5 PPI subnetwork	0.6
GO:0033059	cellular pigmentation	0.6
MP:0008539	decreased susceptibility to induced colitis	0.6
ENSG00000166407	LMO1 PPI subnetwork	0.6
GO:0047485	protein N-terminus binding	0.6
KEGG_AXON_GUIDANCE	KEGG_AXON_GUIDANCE	0.6
ENSG00000086758	HUWE1 PPI subnetwork	0.6
ENSG00000092470	WDR76 PPI subnetwork	0.6
GO:0060606	tube closure	0.6
ENSG00000137561	TTPA PPI subnetwork	0.6
GO:0005496	steroid binding	0.6
GO:0071230	cellular response to amino acid stimulus	0.6
GO:0033365	protein localization to organelle	0.6
GO:0005798	Golgi-associated vesicle	0.6
REACTOME_NOREPINEPHRINE_NEUROTRANSMITTER_RELEASE_CYCLE	REACTOME_NOREPINEPHRINE_NEUROTRANSMITTER_RELEASE_CYCLE	0.6
GO:0004601	peroxidase activity	0.6
GO:0016684	oxidoreductase activity, acting on peroxide as acceptor	0.6
GO:0042274	ribosomal small subunit biogenesis	0.6
ENSG00000154473	BUB3 PPI subnetwork	0.6
GO:2000045	regulation of G1/S transition of mitotic cell cycle	0.6
GO:0008064	regulation of actin polymerization or depolymerization	0.6
GO:0048588	developmental cell growth	0.6
MP:0005668	decreased circulating leptin level	0.6
ENSG00000086827	ZW10 PPI subnetwork	0.6
GO:0002009	morphogenesis of an epithelium	0.6
GO:0020037	heme binding	0.6
MP:0001475	reduced long term depression	0.6
GO:0006164	purine nucleotide biosynthetic process	0.6
ENSG00000065978	YBX1 PPI subnetwork	0.6
ENSG00000130816	DNMT1 PPI subnetwork	0.6
ENSG00000168078	PBK PPI subnetwork	0.6

Original gene set ID	Original gene set description	Nominal P value
ENSG00000171824	EXOSC10 PPI subnetwork	0.6
GO:0009312	oligosaccharide biosynthetic process	0.6
MP:0002398	abnormal bone marrow cell morphology/development	0.61
GO:0006325	chromatin organization	0.61
GO:0006361	transcription initiation from RNA polymerase I promoter	0.61
GO:0006112	energy reserve metabolic process	0.61
KEGG_BUTANOATE_METABOLISM	KEGG_BUTANOATE_METABOLISM	0.61
REACTOME_ION_CHANNEL_TRANSPORT	REACTOME_ION_CHANNEL_TRANSPORT	0.61
GO:0021915	neural tube development	0.61
ENSG00000213658	LAT PPI subnetwork	0.61
KEGG_Cysteine_and_Methionine_Metabolism	KEGG_Cysteine_and_Methionine_Metabolism	0.61
ENSG000000099783	HNRNPM PPI subnetwork	0.61
MP:0003690	abnormal glial cell physiology	0.61
ENSG00000196331	HIST1H2BO PPI subnetwork	0.61
GO:0007498	mesoderm development	0.61
ENSG00000172680	MOS PPI subnetwork	0.61
ENSG00000110367	DDX6 PPI subnetwork	0.61
ENSG00000173175	ADCY5 PPI subnetwork	0.61
MP:0003209	abnormal pulmonary elastic fiber morphology	0.61
MP:0011427	mesangial cell hyperplasia	0.61
GO:0005262	calcium channel activity	0.61
MP:0008332	decreased lactotroph cell number	0.61
MP:0010103	small thoracic cage	0.61
ENSG000000095319	NUP188 PPI subnetwork	0.61
GO:0051289	protein homotetramerization	0.61
ENSG00000198722	UNC13B PPI subnetwork	0.61
GO:0048048	embryonic eye morphogenesis	0.61
ENSG00000113368	LMNB1 PPI subnetwork	0.61
MP:0008173	increased follicular B cell number	0.61
ENSG00000100346	CACNA1I PPI subnetwork	0.61
ENSG00000171311	EXOSC1 PPI subnetwork	0.61
ENSG000000095139	ARCN1 PPI subnetwork	0.61
ENSG00000101367	MAPRE1 PPI subnetwork	0.61
GO:0022600	digestive system process	0.61
ENSG00000008018	PSMB1 PPI subnetwork	0.61
GO:0032816	positive regulation of natural killer cell activator	0.61
ENSG00000156076	WIF1 PPI subnetwork	0.61
GO:0001959	regulation of cytokine-mediated signaling pathway	0.61
REACTOME_ADP_SIGNALING_THROUGH_P2Y_PURINOCEPTOR_1	REACTOME_ADP_SIGNALING_THROUGH_P2Y_PURINOCEPTOR_1	0.61
GO:0050434	positive regulation of viral transcription	0.61
ENSG00000100926	TM9SF1 PPI subnetwork	0.61
ENSG00000006634	DBF4 PPI subnetwork	0.61
GO:0042102	positive regulation of T cell proliferation	0.61
ENSG00000089048	ESF1 PPI subnetwork	0.61
ENSG00000110244	APOA4 PPI subnetwork	0.61
ENSG00000128908	INO80 PPI subnetwork	0.61
ENSG00000182872	RBM10 PPI subnetwork	0.61
MP:0009643	abnormal urine homeostasis	0.61
ENSG00000154342	WNT3A PPI subnetwork	0.61

Original gene set ID	Original gene set description	Nominal P value
ENSG00000163002	NUP35 PPI subnetwork	0.61
ENSG00000187266	EPOR PPI subnetwork	0.61
REACTOME_HOMOLOGOUS_RECOMBINATION_REPAIR	REACTOME_HOMOLOGOUS_RECOMBINATION_REPAIR	0.61
REACTOME_HOMOLOGOUS_RECOMBINATION_REPAIR_OF_REPLICATION:INDEP	REACTOME_HOMOLOGOUS_RECOMBINATION_REPAIR_OF_REPLICATION:INDEPEN	0.61
GO:0019200	carbohydrate kinase activity	0.61
ENSG00000085276	MECOM PPI subnetwork	0.61
ENSG00000187239	FNBP1 PPI subnetwork	0.61
GO:0006352	transcription initiation, DNA-dependent	0.61
ENSG00000109917	ZNF259 PPI subnetwork	0.61
MP:0002913	abnormal PNS synaptic transmission	0.61
ENSG00000113594	LIFR PPI subnetwork	0.61
MP:0000781	decreased corpus callosum size	0.61
GO:0006833	water transport	0.61
ENSG00000100285	NEFH PPI subnetwork	0.61
GO:0003746	translation elongation factor activity	0.61
ENSG00000125482	TTF1 PPI subnetwork	0.61
MP:0004799	increased susceptibility to experimental autoimmune encephalomyeliti	0.61
ENSG00000148468	FAM171A1 PPI subnetwork	0.61
ENSG00000112992	NNT PPI subnetwork	0.61
REACTOME_OLFACTORY_SIGNALING_PATHWAY	REACTOME_OLFACTORY_SIGNALING_PATHWAY	0.61
GO:0006821	chloride transport	0.61
MP:0003703	abnormal vestibulocochlear ganglion morphology	0.61
GO:0045076	regulation of interleukin-2 biosynthetic process	0.61
GO:0009069	serine family amino acid metabolic process	0.61
REACTOME_ORC1_REMOVAL_FROM_CHROMATIN	REACTOME_ORC1_REMOVAL_FROM_CHROMATIN	0.61
REACTOME_SWITCHING_OF_ORIGINS_TO_A_POST:REPLICATIVE_STATE	REACTOME_SWITCHING_OF_ORIGINS_TO_A_POST:REPLICATIVE_STATE	0.61
ENSG00000164742	ADCY1 PPI subnetwork	0.61
ENSG00000178409	BEND3 PPI subnetwork	0.61
REACTOME_CELL_CYCLE	REACTOME_CELL_CYCLE	0.61
ENSG00000198900	TOP1 PPI subnetwork	0.61
GO:2000146	negative regulation of cell motility	0.61
GO:0090066	regulation of anatomical structure size	0.61
ENSG00000170315	UBB PPI subnetwork	0.61
GO:0001673	male germ cell nucleus	0.61
REACTOME_REGULATION_OF_APOPTOSIS	REACTOME_REGULATION_OF_APOPTOSIS	0.61
MP:0001407	short stride length	0.61
ENSG00000119392	GLE1 PPI subnetwork	0.61
ENSG00000016402	IL20RA PPI subnetwork	0.61
MP:0011186	abnormal visceral endoderm morphology	0.61
MP:0000890	thin cerebellar molecular layer	0.61
GO:0000930	gamma-tubulin complex	0.61
ENSG00000110324	IL10RA PPI subnetwork	0.61
MP:0001340	abnormal eyelid morphology	0.61
ENSG00000173020	ADRBK1 PPI subnetwork	0.61
REACTOME_GAB1_SIGNALOSOME	REACTOME_GAB1_SIGNALOSOME	0.61
REACTOME_CYCLIN_AB1_ASSOCIATED_EVENTS_DURING_G2M_TRANSITION	REACTOME_CYCLIN_AB1_ASSOCIATED_EVENTS_DURING_G2M_TRANSITION	0.61
GO:0048008	platelet-derived growth factor receptor signaling pathway	0.61
ENSG00000167088	SNRPD1 PPI subnetwork	0.61
GO:0055013	cardiac muscle cell development	0.61

Original gene set ID	Original gene set description	Nominal P value
MP:0008705	increased interleukin-6 secretion	0.62
MP:0009434	paraparesis	0.62
ENSG00000076555	ACACB PPI subnetwork	0.62
KEGG_OLFACTORY_TRANSDUCTION	KEGG_OLFACTORY_TRANSDUCTION	0.62
ENSG00000112983	BRD8 PPI subnetwork	0.62
GO:0010883	regulation of lipid storage	0.62
ENSG00000175334	BANF1 PPI subnetwork	0.62
ENSG00000171560	FGA PPI subnetwork	0.62
MP:0002989	small kidney	0.62
ENSG00000138757	G3BP2 PPI subnetwork	0.62
MP:0008024	absent lymph nodes	0.62
MP:0002446	abnormal macrophage morphology	0.62
ENSG00000130725	UBE2M PPI subnetwork	0.62
REACTOME_NUCLEAR_IMPORT_OF_REV_PROTEIN	REACTOME_NUCLEAR_IMPORT_OF_REV_PROTEIN	0.62
MP:0001386	abnormal maternal nurturing	0.62
ENSG00000162594	IL23R PPI subnetwork	0.62
GO:0032272	negative regulation of protein polymerization	0.62
ENSG00000206281	TAPBP PPI subnetwork	0.62
ENSG00000112493	TAPBP PPI subnetwork	0.62
ENSG00000206208	TAPBP PPI subnetwork	0.62
ENSG00000186298	PPP1CC PPI subnetwork	0.62
MP:0000968	abnormal sensory neuron innervation pattern	0.62
REACTOME_AXON_GUIDANCE	REACTOME_AXON_GUIDANCE	0.62
GO:0048407	platelet-derived growth factor binding	0.62
REACTOME_PROLACTIN_RECEPTOR_SIGNALING	REACTOME_PROLACTIN_RECEPTOR_SIGNALING	0.62
MP:0004190	abnormal direction of embryo turning	0.62
ENSG00000023734	STRAP PPI subnetwork	0.62
GO:0031225	anchored to membrane	0.62
GO:0046906	tetrapyrrole binding	0.62
GO:0031272	regulation of pseudopodium assembly	0.62
MP:0001680	abnormal mesoderm development	0.62
MP:0000522	kidney cortex cysts	0.62
REACTOME_SPHINGOLIPID_DE_NOVO_BIOSYNTHESIS	REACTOME_SPHINGOLIPID_DE_NOVO_BIOSYNTHESIS	0.62
GO:0035567	non-canonical Wnt receptor signaling pathway	0.62
GO:0031513	nonmotile primary cilium	0.62
GO:0070603	SWI/SNF-type complex	0.62
ENSG00000140307	GTF2A2 PPI subnetwork	0.62
GO:0042462	eye photoreceptor cell development	0.62
REACTOME_POST_NMDA_RECEPTOR_ACTIVATION_EVENTS	REACTOME_POST_NMDA_RECEPTOR_ACTIVATION_EVENTS	0.62
GO:0000018	regulation of DNA recombination	0.62
GO:0072507	divalent inorganic cation homeostasis	0.62
MP:0000832	abnormal thalamus morphology	0.62
GO:0046782	regulation of viral transcription	0.62
MP:0008058	abnormal DNA repair	0.62
ENSG00000167414	GNG8 PPI subnetwork	0.62
ENSG00000092841	MYL6 PPI subnetwork	0.62
GO:0030425	dendrite	0.62
GO:0002063	chondrocyte development	0.62
GO:0048741	skeletal muscle fiber development	0.62

Original gene set ID	Original gene set description	Nominal P value
REACTOME_TRANSPORT_OF_GLUCCOSE_AND_OTHER_SUGARS_BILE_SALTS_ANI MP:0008533	REACTOME_TRANSPORT_OF_GLUCCOSE_AND_OTHER_SUGARS_BILE_SALTS_AND_O abnormal anterior visceral endoderm morphology	0.62
ENSG000000177542 MP:0003111	SLC25A22 PPI subnetwork abnormal cell nucleus morphology	0.62
MP:0004672	short ribs	0.62
ENSG000000116830 MP:0005545	TTF2 PPI subnetwork abnormal lens development	0.62
GO:0045622	regulation of T-helper cell differentiator	0.62
MP:0000031	abnormal cochlea morphology	0.62
GO:0032814	regulation of natural killer cell activation	0.62
MP:0004620	cervical vertebral fusion	0.62
GO:0044448	cell cortex part	0.62
GO:0030513	positive regulation of BMP signaling pathway	0.62
ENSG000000171453	POLR1C PPI subnetwork	0.62
REACTOME_RNA_POLYMERASE_III_TRANSCRIPTION_INITIATION_FROM_TYPE_3_Pf MP:0009814	REACTOME_RNA_POLYMERASE_III_TRANSCRIPTION_INITIATION_FROM_TYPE_3_Pf increased prostaglandin level	0.62
GO:0000084	S phase of mitotic cell cycle	0.62
GO:0047555	3',5'-cyclic-GMP phosphodiesterase activity	0.62
REACTOME_FACTORS_INVOLVED_IN_MEGAKARYOCYTE_DEVELOPMENT_AND_PLA GO:0002027	REACTOME_FACTORS_INVOLVED_IN_MEGAKARYOCYTE_DEVELOPMENT_AND_PLA regulation of heart rate	0.62
MP:0000430	absent maxillary shelf	0.62
GO:0006809	nitric oxide biosynthetic process	0.62
ENSG000000144908	ALDH1L1 PPI subnetwork	0.62
GO:0035136	forelimb morphogenesis	0.62
ENSG000000159023	EPB41 PPI subnetwork	0.62
ENSG000000169062	UPF3A PPI subnetwork	0.62
REACTOME_AUTODEGRADATION_OF_THE_E3_UBIQUITIN_LIGASE_COP1 ENSG000000083093	REACTOME_AUTODEGRADATION_OF_THE_E3_UBIQUITIN_LIGASE_COP1 PALB2 PPI subnetwork	0.63
ENSG000000120500	ARR3 PPI subnetwork	0.63
ENSG000000134001	EIF2S1 PPI subnetwork	0.63
REACTOME_DESTABILIZATION_OF_MRNA_BY_AUF1_HNRNP_D0 GO:0014032	REACTOME_DESTABILIZATION_OF_MRNA_BY_AUF1_HNRNP_D0 neural crest cell development	0.63
GO:0016591	DNA-directed RNA polymerase II, holoenzyme	0.63
GO:0071346	cellular response to interferon-gamma	0.63
GO:0014033	neural crest cell differentiation	0.63
MP:0004814	reduced linear vestibular evoked potentia	0.63
GO:0032722	positive regulation of chemokine production	0.63
ENSG000000139719	VPS33A PPI subnetwork	0.63
ENSG000000124334	IL9R PPI subnetwork	0.63
GO:0030330	DNA damage response, signal transduction by p53 class mediator	0.63
ENSG000000103152	MPG PPI subnetwork	0.63
ENSG000000126785	RHOJ PPI subnetwork	0.63
ENSG000000107263	RAPGEF1 PPI subnetwork	0.63
GO:0007091	mitotic metaphase/anaphase transition	0.63
GO:0003203	endocardial cushion morphogenesis	0.63
ENSG000000166900	STX3 PPI subnetwork	0.63
ENSG000000123562	MORF4L2 PPI subnetwork	0.63
MP:0001963	abnormal hearing physiology	0.63
MP:0004100	abnormal spinal cord interneuron morphology	0.63

Original gene set ID	Original gene set description	Nominal P value
ENSG00000158169	FANCC PPI subnetwork	0.63
MP:0004189	abnormal alveolar process morphology	0.63
KEGG_PENTOSE_AND_GLUCURONATE_INTERCONVERSIONS	KEGG_PENTOSE_AND_GLUCURONATE_INTERCONVERSIONS	0.63
ENSG00000005249	PRKAR2B PPI subnetwork	0.63
ENSG00000078369	GNB1 PPI subnetwork	0.63
ENSG00000088305	DNMT3B PPI subnetwork	0.63
ENSG00000176884	GRIN1 PPI subnetwork	0.63
GO:0006893	Golgi to plasma membrane transport	0.63
ENSG00000122966	CIT PPI subnetwork	0.63
ENSG00000137486	ARRB1 PPI subnetwork	0.63
REACTOME_REGULATION_OF_ACTIVATED_PAK:2P34_BY_PROTEASOME_MEDIATED	REACTOME_REGULATION_OF_ACTIVATED_PAK:2P34_BY_PROTEASOME_MEDIATED	0.63
GO:0031069	hair follicle morphogenesis	0.63
ENSG00000204390	HSPA1L PPI subnetwork	0.63
ENSG00000034713	GABARAPL2 PPI subnetwork	0.63
ENSG00000126351	THRA PPI subnetwork	0.63
GO:0051320	S phase	0.63
GO:0046849	bone remodeling	0.63
GO:0006376	mRNA splice site selection	0.63
GO:0016840	carbon-nitrogen lyase activity	0.63
ENSG00000106400	ZNHIT1 PPI subnetwork	0.63
ENSG00000167880	EVPL PPI subnetwork	0.63
GO:0015669	gas transport	0.63
GO:0044306	neuron projection terminus	0.63
GO:0060330	regulation of response to interferon-gamma	0.63
GO:0060334	regulation of interferon-gamma-mediated signaling pathway	0.63
GO:0070838	divalent metal ion transport	0.63
GO:0006302	double-strand break repair	0.63
ENSG00000113812	ACTR8 PPI subnetwork	0.63
REACTOME_REGULATION_OF_APCC_ACTIVATORS_BETWEEN_G1S_AND_EARLY	REACTOME_REGULATION_OF_APCC_ACTIVATORS_BETWEEN_G1S_AND_EARLY	0.63
MP:0008965	increased basal metabolism	0.63
MP:0001663	abnormal digestive system physiology	0.63
GO:0001539	ciliary or flagellar motility	0.63
ENSG00000025293	PHF20 PPI subnetwork	0.63
ENSG00000067900	ROCK1 PPI subnetwork	0.63
REACTOME_APC:CDC20_MEDIATED_DEGRADATION_OF_NEK2A	REACTOME_APC:CDC20_MEDIATED_DEGRADATION_OF_NEK2A	0.63
ENSG00000142684	ZNF593 PPI subnetwork	0.63
GO:0030336	negative regulation of cell migration	0.63
GO:0001947	heart looping	0.63
GO:0061371	determination of heart left/right asymmetry	0.63
MP:0002906	increased susceptibility to pharmacologically induced seizure	0.63
GO:0070979	protein K11-linked ubiquitination	0.63
ENSG00000103043	VAC14 PPI subnetwork	0.63
ENSG00000132002	DNAJB1 PPI subnetwork	0.63
GO:0048814	regulation of dendrite morphogenesis	0.63
ENSG00000172020	GAP43 PPI subnetwork	0.63
GO:0016209	antioxidant activity	0.63
ENSG00000113194	FAF2 PPI subnetwork	0.63
GO:0090103	cochlea morphogenesis	0.63
GO:0030101	natural killer cell activation	0.63

Original gene set ID	Original gene set description	Nominal P value
ENSG00000070501	POLB PPI subnetwork	0.64
ENSG00000129675	ARHGEF6 PPI subnetwork	0.64
MP:0009642	abnormal blood homeostasis	0.64
ENSG00000073756	PTGS2 PPI subnetwork	0.64
ENSG00000117650	NEK2 PPI subnetwork	0.64
ENSG00000131153	GINS2 PPI subnetwork	0.64
GO:0001727	lipid kinase activity	0.64
MP:0000159	abnormal xiphoid process morphology	0.64
ENSG00000135390	ATP5G2 PPI subnetwork	0.64
ENSG00000198626	RYR2 PPI subnetwork	0.64
GO:0015932	nucleobase-containing compound transmembrane transporter activity	0.64
GO:0071013	catalytic step 2 spliceosome	0.64
ENSG00000125166	GOT2 PPI subnetwork	0.64
GO:0045429	positive regulation of nitric oxide biosynthetic process	0.64
GO:0042472	inner ear morphogenesis	0.64
GO:0042491	auditory receptor cell differentiation	0.64
GO:0045995	regulation of embryonic development	0.64
GO:0051085	chaperone mediated protein folding requiring cofactor	0.64
GO:0007015	actin filament organization	0.64
ENSG00000139269	INHBE PPI subnetwork	0.64
ENSG00000181222	POLR2A PPI subnetwork	0.64
ENSG00000126583	PRKCG PPI subnetwork	0.64
ENSG00000185721	DRG1 PPI subnetwork	0.64
ENSG00000211456	SACM1L PPI subnetwork	0.64
ENSG00000168490	PHYHIP PPI subnetwork	0.64
GO:0050729	positive regulation of inflammatory response	0.64
GO:0030032	lamellipodium assembly	0.64
GO:0034702	ion channel complex	0.64
ENSG00000135624	CCT7 PPI subnetwork	0.64
GO:0001619	lysosphingolipid and lysophosphatidic acid receptor activity	0.64
GO:0004402	histone acetyltransferase activity	0.64
MP:0002423	abnormal mast cell physiology	0.64
ENSG00000089289	IGBP1 PPI subnetwork	0.64
ENSG00000182578	CSF1R PPI subnetwork	0.64
MP:0004395	increased cochlear inner hair cell number	0.64
MP:0005565	increased blood urea nitrogen level	0.64
GO:0045841	negative regulation of mitotic metaphase/anaphase transition	0.64
ENSG00000134597	RBMX2 PPI subnetwork	0.64
ENSG00000206466	GABBR1 PPI subnetwork	0.64
ENSG00000204681	GABBR1 PPI subnetwork	0.64
ENSG00000206511	GABBR1 PPI subnetwork	0.64
GO:0048592	eye morphogenesis	0.64
ENSG00000134470	IL15RA PPI subnetwork	0.64
ENSG00000125630	POLR1B PPI subnetwork	0.64
MP:0009750	impaired behavioral response to addictive substance	0.64
GO:0048384	retinoic acid receptor signaling pathway	0.64
GO:0043240	Fanconi anaemia nuclear complex	0.64
MP:0003451	absent olfactory bulb	0.64
ENSG00000133216	EPHB2 PPI subnetwork	0.64

Original gene set ID**Original gene set description****Nominal P value**

GO:0016712	oxidoreductase activity, acting on paired donors, with incorporation or reduction of	0.64
ENSG00000214528	ENSG00000214528 PPI subnetwork	0.64
GO:0005758	mitochondrial intermembrane space	0.64
GO:0006900	membrane budding	0.64
GO:0010878	cholesterol storage	0.64
ENSG00000109103	UNC119 PPI subnetwork	0.64
GO:0019933	cAMP-mediated signaling	0.64
GO:0004889	acetylcholine-activated cation-selective channel activity	0.64
MP:0000371	diluted coat color	0.64
REACTOME_INTEGRATION_OF_ENERGY_METABOLISM	REACTOME_INTEGRATION_OF_ENERGY_METABOLISM	0.64
ENSG00000145623	OSMR PPI subnetwork	0.64
ENSG00000137070	IL11RA PPI subnetwork	0.64
GO:0016874	ligase activity	0.64
MP:0002102	abnormal ear morphology	0.64
GO:0090092	regulation of transmembrane receptor protein serine/threonine kinase signaling pat	0.64
KEGG_CHEMOKINE_SIGNALING_PATHWAY	KEGG_CHEMOKINE_SIGNALING_PATHWAY	0.64
GO:0042094	interleukin-2 biosynthetic process	0.64
GO:0009164	nucleoside catabolic process	0.64
GO:0021795	cerebral cortex cell migration	0.64
GO:0000780	condensed nuclear chromosome, centromeric region	0.64
GO:0045666	positive regulation of neuron differentiation	0.64
ENSG00000092853	CLSPN PPI subnetwork	0.64
ENSG00000129354	AP1M2 PPI subnetwork	0.64
ENSG00000141380	SS18 PPI subnetwork	0.64
GO:0002089	lens morphogenesis in camera-type eye	0.64
REACTOME_RNA_POLYMERASE_I_PROMOTER_ESCAPE	REACTOME_RNA_POLYMERASE_I_PROMOTER_ESCAPE	0.64
REACTOME_REGULATORY_RNA_PATHWAYS	REACTOME_REGULATORY_RNA_PATHWAYS	0.64
REACTOME_MICRORNA_MIRNA_BIOGENESIS	REACTOME_MICRORNA_MIRNA_BIOGENESIS	0.64
MP:0004765	decreased brainstem auditory evoked potentia	0.64
REACTOME_FORMATION_OF_TUBULIN_FOLDING_INTERMEDIATES_BY_CCTTRIC	REACTOME_FORMATION_OF_TUBULIN_FOLDING_INTERMEDIATES_BY_CCTTRIC	0.64
GO:0022890	inorganic cation transmembrane transporter activity	0.64
MP:0001297	microphthalmia	0.65
MP:0001183	overexpanded pulmonary alveoli	0.65
MP:0004046	abnormal mitosis	0.65
GO:0043204	perikaryon	0.65
ENSG00000143093	FAM40A PPI subnetwork	0.65
GO:0045667	regulation of osteoblast differentiation	0.65
GO:0001708	cell fate specification	0.65
GO:0007616	long-term memory	0.65
ENSG00000129465	RIPK3 PPI subnetwork	0.65
MP:0005558	decreased creatinine clearance	0.65
GO:0007501	mesodermal cell fate specification	0.65
ENSG00000007171	NOS2 PPI subnetwork	0.65
KEGG_VASCULAR_SMOOTH_MUSCLE_CONTRACTION	KEGG_VASCULAR_SMOOTH_MUSCLE_CONTRACTION	0.65
MP:0004324	vestibular hair cell degeneration	0.65
KEGG_ALLOGRAFT_REJECTION	KEGG_ALLOGRAFT_REJECTION	0.65
MP:0002023	B cell derived lymphoma	0.65
ENSG00000166592	RRAD PPI subnetwork	0.65
MP:0001783	decreased white adipose tissue amount	0.65

Original gene set ID	Original gene set description	Nominal P value
MP:0002746	abnormal semilunar valve morphology	0.65
GO:0048332	mesoderm morphogenesis	0.65
REACTOME_G_BETAGAMMA_SIGNALLING_THROUGH_PI3KGAMMA	REACTOME_G_BETAGAMMA_SIGNALLING_THROUGH_PI3KGAMMA	0.65
MP:0005551	abnormal eye electrophysiology	0.65
GO:0046459	short-chain fatty acid metabolic process	0.65
MP:0005407	hyperalgesia	0.65
MP:0004077	abnormal striatum morphology	0.65
ENSG00000002822	MAD1L1 PPI subnetwork	0.65
ENSG00000105486	LIG1 PPI subnetwork	0.65
ENSG00000125885	MCM8 PPI subnetwork	0.65
ENSG00000120659	TNFSF11 PPI subnetwork	0.65
ENSG00000115289	PCGF1 PPI subnetwork	0.65
ENSG00000164091	WDR82 PPI subnetwork	0.65
ENSG00000164077	MON1A PPI subnetwork	0.65
GO:0006944	cellular membrane fusion	0.65
ENSG00000073910	FRY PPI subnetwork	0.65
GO:0051223	regulation of protein transport	0.65
ENSG00000023445	BIRC3 PPI subnetwork	0.65
ENSG00000197958	RPL12 PPI subnetwork	0.65
GO:0008207	C21-steroid hormone metabolic process	0.65
REACTOME_APCCDC20_MEDIATED_DEGRADATION_OF_CYCLIN_B	REACTOME_APCCDC20_MEDIATED_DEGRADATION_OF_CYCLIN_B	0.65
ENSG00000163283	ALPP PPI subnetwork	0.65
GO:2001056	positive regulation of cysteine-type endopeptidase activity	0.65
GO:0043280	positive regulation of cysteine-type endopeptidase activity involved in apoptotic proc	0.65
MP:0008456	abnormal retinal rod cell outer segment morphology	0.65
KEGG_RNA_POLYMERASE	KEGG_RNA_POLYMERASE	0.65
GO:0001077	RNA polymerase II core promoter proximal region sequence-specific DNA binding tr	0.65
ENSG00000111907	TPD52L1 PPI subnetwork	0.65
ENSG00000175575	PAAF1 PPI subnetwork	0.65
ENSG00000100138	NHP2L1 PPI subnetwork	0.65
ENSG00000100395	L3MBTL2 PPI subnetwork	0.65
MP:0005619	increased urine potassium level	0.65
GO:0070661	leukocyte proliferation	0.65
ENSG00000176386	CDC26 PPI subnetwork	0.65
ENSG00000020426	MNAT1 PPI subnetwork	0.65
ENSG00000135829	DHX9 PPI subnetwork	0.65
ENSG00000181072	CHRM2 PPI subnetwork	0.65
ENSG00000104812	GYS1 PPI subnetwork	0.65
GO:0000779	condensed chromosome, centromeric region	0.65
ENSG00000135775	COG2 PPI subnetwork	0.65
GO:0030139	endocytic vesicle	0.65
ENSG00000120805	ARL1 PPI subnetwork	0.65
GO:0042100	B cell proliferation	0.65
MP:0001406	abnormal gait	0.65
MP:0001689	incomplete somite formation	0.65
MP:0004985	decreased osteoclast cell number	0.65
ENSG00000100462	PRMT5 PPI subnetwork	0.65
REACTOME_S_PHASE	REACTOME_S_PHASE	0.65
ENSG00000115884	SDC1 PPI subnetwork	0.65

Original gene set ID	Original gene set description	Nominal P value
ENSG00000182492	BGN PPI subnetwork	0.65
GO:0019843	rRNA binding	0.65
GO:0000301	retrograde transport, vesicle recycling within Golg	0.65
GO:0060395	SMAD protein signal transduction	0.65
GO:0071804	cellular potassium ion transport	0.65
GO:0071805	potassium ion transmembrane transport	0.65
GO:0048562	embryonic organ morphogenesis	0.65
GO:0048661	positive regulation of smooth muscle cell proliferati	0.65
MP:0002971	abnormal brown adipose tissue morphology	0.65
GO:0061025	membrane fusion	0.65
ENSG00000119772	DNMT3A PPI subnetwork	0.65
ENSG00000130255	RPL36 PPI subnetwork	0.65
REACTOME_REMOVAL_OF_LICENSING_FACTORS_FROM_ORIGINS	REACTOME_REMOVAL_OF_LICENSING_FACTORS_FROM_ORIGINS	0.65
MP:0002810	microcytic anemia	0.65
GO:0019866	organelle inner membrane	0.65
ENSG00000092010	PSME1 PPI subnetwork	0.65
GO:0045786	negative regulation of cell cycle	0.65
ENSG00000008952	SEC62 PPI subnetwork	0.65
ENSG00000185436	IL28RA PPI subnetwork	0.65
GO:0043028	cysteine-type endopeptidase regulator activity involved in apoptotic proces:	0.65
GO:0004114	3',5'-cyclic-nucleotide phosphodiesterase activity	0.65
GO:0008083	growth factor activity	0.65
ENSG00000116678	LEPR PPI subnetwork	0.65
ENSG00000100813	ACIN1 PPI subnetwork	0.65
GO:0015026	coreceptor activity	0.65
KEGG_ARACHIDONIC_ACID_METABOLISM	KEGG_ARACHIDONIC_ACID_METABOLISM	0.65
MP:0003503	decreased activity of thyroid	0.65
ENSG00000110321	EIF4G2 PPI subnetwork	0.65
ENSG00000133818	RRAS2 PPI subnetwork	0.65
ENSG00000143995	MEIS1 PPI subnetwork	0.65
MP:0008497	decreased IgG2b level	0.65
GO:0000315	organellar large ribosomal subunit	0.65
GO:0005762	mitochondrial large ribosomal subunit	0.65
GO:0060389	pathway-restricted SMAD protein phosphorylation	0.65
GO:0002011	morphogenesis of an epithelial sheet	0.65
ENSG00000169282	KCNAB1 PPI subnetwork	0.65
GO:0034341	response to interferon-gamma	0.65
ENSG00000132467	UTP3 PPI subnetwork	0.65
ENSG00000100941	PNN PPI subnetwork	0.65
GO:0048593	camera-type eye morphogenesis	0.65
ENSG00000174371	EXO1 PPI subnetwork	0.65
GO:0010885	regulation of cholesterol storage	0.65
ENSG00000093217	XYLB PPI subnetwork	0.65
ENSG00000163904	SEN2 PPI subnetwork	0.65
ENSG00000100568	VT1B PPI subnetwork	0.65
GO:0009267	cellular response to starvation	0.65
GO:0035587	purinergic receptor signaling pathway	0.65
MP:0008587	short photoreceptor outer segment	0.65
ENSG00000171549	ENSG00000171549 PPI subnetwork	0.65

Original gene set ID	Original gene set description	Nominal P value
ENSG00000182520	ENSG00000182520 PPI subnetwork	0.65
MP:0000967	abnormal sensory neuron projections	0.66
GO:0051186	cofactor metabolic process	0.66
ENSG00000058668	ATP2B4 PPI subnetwork	0.66
ENSG00000161547	SRSF2 PPI subnetwork	0.66
MP:0004784	abnormal anterior cardinal vein morphology	0.66
ENSG00000096401	CDC5L PPI subnetwork	0.66
GO:0042026	protein refolding	0.66
ENSG00000163191	S100A11 PPI subnetwork	0.66
ENSG00000159113	ENSG00000159113 PPI subnetwork	0.66
REACTOME_APCCCDH1_MEDIATED_DEGRADATION_OF_CDC20_AND_OTHER_A	REACTOME_APCCCDH1_MEDIATED_DEGRADATION_OF_CDC20_AND_OTHER_APCC	0.66
ENSG00000139343	SNRPF PPI subnetwork	0.66
GO:0090102	cochlea development	0.66
GO:0008565	protein transporter activity	0.66
GO:0001664	G-protein coupled receptor binding	0.66
ENSG00000183691	NOG PPI subnetwork	0.66
GO:0019005	SCF ubiquitin ligase complex	0.66
GO:0042474	middle ear morphogenesis	0.66
ENSG000000004700	RECQL PPI subnetwork	0.66
REACTOME_PYRIMIDINE_METABOLISM	REACTOME_PYRIMIDINE_METABOLISM	0.66
MP:0003084	abnormal skeletal muscle fiber morphology	0.66
GO:0009952	anterior/posterior pattern specification	0.66
GO:0016072	rRNA metabolic process	0.66
GO:0031331	positive regulation of cellular catabolic process	0.66
ENSG00000127314	RAP1B PPI subnetwork	0.66
GO:0048839	inner ear development	0.66
GO:0050767	regulation of neurogenesis	0.66
ENSG00000125730	C3 PPI subnetwork	0.66
GO:0010035	response to inorganic substance	0.66
GO:0009615	response to virus	0.66
ENSG00000108883	EFTUD2 PPI subnetwork	0.66
GO:0018345	protein palmitoylation	0.66
MP:0002664	decreased circulating adrenocorticotropin level	0.66
ENSG00000112186	CAP2 PPI subnetwork	0.66
ENSG00000159459	UBR1 PPI subnetwork	0.66
ENSG00000131652	THOC6 PPI subnetwork	0.66
ENSG00000065548	ZC3H15 PPI subnetwork	0.66
GO:0009798	axis specification	0.66
ENSG00000027697	IFNGR1 PPI subnetwork	0.66
GO:0009314	response to radiation	0.66
GO:0000777	condensed chromosome kinetochore	0.66
MP:0002835	abnormal cranial suture morphology	0.66
MP:0005205	abnormal eye anterior chamber morphology	0.66
ENSG00000179950	PUF60 PPI subnetwork	0.66
GO:0071779	G1/S transition checkpoint	0.66
GO:0043087	regulation of GTPase activity	0.66
GO:0072372	primary cilium	0.66
GO:0001841	neural tube formation	0.66
ENSG00000169306	IL1RAPL1 PPI subnetwork	0.66

Original gene set ID	Original gene set description	Nominal P value
GO:0031072	heat shock protein binding	0.66
MP:0009456	impaired cued conditioning behavior	0.66
REACTOME_CRMP5_IN_SEMA3A_SIGNALING	REACTOME_CRMP5_IN_SEMA3A_SIGNALING	0.66
MP:0000154	rib fusion	0.66
GO:0007389	pattern specification process	0.66
MP:0008500	increased IgG2a level	0.66
ENSG00000165731	RET PPI subnetwork	0.66
GO:0010952	positive regulation of peptidase activity	0.66
GO:0021515	cell differentiation in spinal cord	0.66
GO:0002440	production of molecular mediator of immune response	0.66
ENSG00000136631	VPS45 PPI subnetwork	0.66
GO:0050873	brown fat cell differentiation	0.66
ENSG00000138190	EXOC6 PPI subnetwork	0.66
ENSG00000173744	AGFG1 PPI subnetwork	0.66
GO:0043073	germ cell nucleus	0.66
GO:0042552	myelination	0.66
ENSG00000069345	DNAJA2 PPI subnetwork	0.66
REACTOME_G_ALPHA_S_SIGNALLING_EVENTS	REACTOME_G_ALPHA_S_SIGNALLING_EVENTS	0.66
ENSG00000003436	TFPI PPI subnetwork	0.66
GO:0042044	fluid transport	0.66
ENSG00000138430	OLA1 PPI subnetwork	0.66
MP:0000194	hypercalcemia	0.66
GO:0000062	fatty-acyl-CoA binding	0.66
ENSG00000205220	PSMB10 PPI subnetwork	0.66
GO:0000038	very long-chain fatty acid metabolic process	0.66
GO:0018208	peptidyl-proline modification	0.66
GO:0032981	mitochondrial respiratory chain complex I assembly	0.66
GO:0097031	mitochondrial respiratory chain complex I biogenesis	0.66
GO:0010257	NADH dehydrogenase complex assembly	0.66
ENSG00000115561	CHMP3 PPI subnetwork	0.66
MP:0004022	abnormal cone electrophysiology	0.66
ENSG00000092199	HNRNPC PPI subnetwork	0.66
ENSG00000106070	GRB10 PPI subnetwork	0.66
GO:0007093	mitotic cell cycle checkpoint	0.66
ENSG00000072958	AP1M1 PPI subnetwork	0.66
ENSG00000142677	IL22RA1 PPI subnetwork	0.66
ENSG00000132361	KIAA0664 PPI subnetwork	0.66
MP:0011501	increased glomerular capsule space	0.66
ENSG00000103342	GSPT1 PPI subnetwork	0.66
GO:0030983	mismatched DNA binding	0.66
REACTOME_CELL:CELL_JUNCTION_ORGANIZATION	REACTOME_CELL:CELL_JUNCTION_ORGANIZATION	0.66
GO:0010171	body morphogenesis	0.66
MP:0006358	absent pinna reflex	0.66
ENSG00000088247	KHSRP PPI subnetwork	0.66
ENSG00000134871	COL4A2 PPI subnetwork	0.66
MP:0001463	abnormal spatial learning	0.66
GO:0031432	titin binding	0.66
GO:0008021	synaptic vesicle	0.66
GO:0015464	acetylcholine receptor activity	0.66

Original gene set ID	Original gene set description	Nominal P value
MP:0002703	abnormal renal tubule morphology	0.66
GO:0002062	chondrocyte differentiation	0.67
ENSG000000100644	HIF1A PPI subnetwork	0.67
GO:0051258	protein polymerization	0.67
ENSG000000114745	GORASP1 PPI subnetwork	0.67
ENSG000000144381	HSPD1 PPI subnetwork	0.67
GO:0009124	nucleoside monophosphate biosynthetic process	0.67
ENSG000000159128	IFNGR2 PPI subnetwork	0.67
GO:0000216	M/G1 transition of mitotic cell cycle	0.67
ENSG000000154277	UCHL1 PPI subnetwork	0.67
ENSG000000170624	SGCD PPI subnetwork	0.67
GO:0033151	V(D)J recombination	0.67
GO:0016254	preassembly of GPI anchor in ER membrane	0.67
ENSG000000151693	ASAP2 PPI subnetwork	0.67
GO:0030216	keratinocyte differentiation	0.67
MP:0002823	abnormal rib development	0.67
ENSG000000095261	PSMD5 PPI subnetwork	0.67
GO:0030041	actin filament polymerization	0.67
GO:0021903	rostrocaudal neural tube patterning	0.67
ENSG000000070831	CDC42 PPI subnetwork	0.67
ENSG000000165912	PACSL1 PPI subnetwork	0.67
ENSG000000187741	FANCA PPI subnetwork	0.67
GO:0006766	vitamin metabolic process	0.67
GO:0070167	regulation of biomineral tissue development	0.67
GO:0051597	response to methylmercury	0.67
KEGG_TASTE_TRANSDUCTION	KEGG_TASTE_TRANSDUCTION	0.67
ENSG000000175582	RAB6A PPI subnetwork	0.67
KEGG_TYROSINE_METABOLISM	KEGG_TYROSINE_METABOLISM	0.67
GO:0048736	appendage development	0.67
GO:0060173	limb development	0.67
ENSG000000100380	ST13 PPI subnetwork	0.67
GO:0030663	COPI coated vesicle membrane	0.67
REACTOME_CDC20PHOSPHO:APCC_MEDIATED_DEGRADATION_OF_CYCLIN_A	REACTOME_CDC20PHOSPHO:APCC_MEDIATED_DEGRADATION_OF_CYCLIN_A	0.67
GO:0055074	calcium ion homeostasis	0.67
GO:0042471	ear morphogenesis	0.67
GO:0007067	mitosis	0.67
GO:0000280	nuclear division	0.67
ENSG000000186051	TAL2 PPI subnetwork	0.67
GO:0009066	aspartate family amino acid metabolic process	0.67
GO:0009950	dorsal/ventral axis specification	0.67
ENSG000000074800	ENO1 PPI subnetwork	0.67
GO:0016811	hydrolase activity, acting on carbon-nitrogen (but not peptide) bonds, in linear amid	0.67
MP:0000733	abnormal muscle development	0.67
GO:0007595	lactation	0.67
KEGG_AMINO_SUGAR_AND_NUCLEOTIDE_SUGAR_METABOLISM	KEGG_AMINO_SUGAR_AND_NUCLEOTIDE_SUGAR_METABOLISM	0.67
ENSG000000074211	PPP2R2C PPI subnetwork	0.67
ENSG000000147889	CDKN2A PPI subnetwork	0.67
MP:0001944	abnormal pancreas morphology	0.67
ENSG000000147684	NDUFB9 PPI subnetwork	0.67

Original gene set ID	Original gene set description	Nominal P value
ENSG00000068654	POLR1A PPI subnetwork	0.67
REACTOME_METABOLISM_OF_POLYAMINES	REACTOME_METABOLISM_OF_POLYAMINES	0.67
GO:0000087	M phase of mitotic cell cycle	0.67
GO:0007158	neuron cell-cell adhesion	0.67
GO:0032452	histone demethylase activity	0.67
GO:0046519	sphingoid metabolic process	0.67
MP:0002591	decreased mean corpuscular volume	0.67
ENSG00000120149	MSX2 PPI subnetwork	0.67
MP:0004772	abnormal bile secretion	0.67
GO:0032844	regulation of homeostatic process	0.67
MP:0002916	increased synaptic depression	0.67
MP:0004321	short sternum	0.67
ENSG00000172137	CALB2 PPI subnetwork	0.67
ENSG00000101400	SNTA1 PPI subnetwork	0.67
GO:0016597	amino acid binding	0.67
ENSG00000069248	NUP133 PPI subnetwork	0.67
REACTOME_G:PROTEIN_BETAGAMMA_SIGNALLING	REACTOME_G:PROTEIN_BETAGAMMA_SIGNALLING	0.67
GO:0005778	peroxisomal membrane	0.67
GO:0031903	microbody membrane	0.67
GO:0004950	chemokine receptor activity	0.67
GO:0001637	G-protein coupled chemoattractant receptor activity	0.67
ENSG00000137936	BCAR3 PPI subnetwork	0.67
GO:0051890	regulation of cardioblast differentiation	0.67
ENSG00000057608	GDI2 PPI subnetwork	0.67
GO:0035326	enhancer binding	0.67
GO:0060627	regulation of vesicle-mediated transport	0.67
MP:0003604	single kidney	0.67
REACTOME_SIGNALING_BY_EGFR_IN_CANCER	REACTOME_SIGNALING_BY_EGFR_IN_CANCER	0.67
GO:0001659	temperature homeostasis	0.67
ENSG00000076924	XAB2 PPI subnetwork	0.67
MP:0005344	increased circulating bilirubin level	0.67
ENSG00000082458	DLG3 PPI subnetwork	0.67
ENSG00000169016	E2F6 PPI subnetwork	0.67
GO:0005164	tumor necrosis factor receptor binding	0.67
GO:0000407	pre-autophagosomal structure	0.67
MP:0001176	abnormal lung development	0.67
GO:0000041	transition metal ion transport	0.67
GO:0007194	negative regulation of adenylate cyclase activity	0.67
GO:0031280	negative regulation of cyclase activity	0.67
ENSG00000055163	CYFIP2 PPI subnetwork	0.67
GO:0001707	mesoderm formation	0.67
GO:0030832	regulation of actin filament length	0.67
ENSG00000114942	EEF1B2 PPI subnetwork	0.67
ENSG00000094914	AAAS PPI subnetwork	0.67
GO:0002717	positive regulation of natural killer cell mediated immunity	0.67
GO:0045954	positive regulation of natural killer cell mediated cytotoxicity	0.67
ENSG00000123496	IL13RA2 PPI subnetwork	0.67
ENSG00000164485	IL22RA2 PPI subnetwork	0.67
ENSG00000103522	IL21R PPI subnetwork	0.67

Original gene set ID	Original gene set description	Nominal P value
ENSG00000076944	STXBP2 PPI subnetwork	0.67
MP:0008392	decreased primordial germ cell number	0.67
MP:0003921	abnormal heart left ventricle morphology	0.67
MP:0003446	renal hypoplasia	0.67
ENSG00000136603	SKIL PPI subnetwork	0.67
ENSG00000147162	OGT PPI subnetwork	0.67
GO:0048286	lung alveolus development	0.67
GO:0033003	regulation of mast cell activation	0.67
GO:0055007	cardiac muscle cell differentiation	0.67
REACTOME_STABILIZATION_OF_P53	REACTOME_STABILIZATION_OF_P53	0.67
MP:0003797	abnormal compact bone morphology	0.67
ENSG00000105204	DYRK1B PPI subnetwork	0.67
GO:0071214	cellular response to abiotic stimulus	0.67
REACTOME_NITRIC_OXIDE_STIMULATES_GUANYLATE_CYCLASE	REACTOME_NITRIC_OXIDE_STIMULATES_GUANYLATE_CYCLASE	0.67
REACTOME_POSTSYNAPTIC_NICOTINIC_ACETYLCHOLINE_RECEPTORS	REACTOME_POSTSYNAPTIC_NICOTINIC_ACETYLCHOLINE_RECEPTORS	0.67
REACTOME_ACETYLCHOLINE_BINDING_AND_DOWNSTREAM_EVENTS	REACTOME_ACETYLCHOLINE_BINDING_AND_DOWNSTREAM_EVENTS	0.67
REACTOME_ACTIVATION_OF_NICOTINIC_ACETYLCHOLINE_RECEPTORS	REACTOME_ACTIVATION_OF_NICOTINIC_ACETYLCHOLINE_RECEPTORS	0.67
GO:0003170	heart valve development	0.67
GO:0010817	regulation of hormone levels	0.67
REACTOME_REGULATION_OF_MRNA_STABILITY_BY_PROTEINS_THAT_BIND_AU	REACTOME_REGULATION_OF_MRNA_STABILITY_BY_PROTEINS_THAT_BIND_AU:RIK	0.67
ENSG00000104325	DECR1 PPI subnetwork	0.67
GO:0033124	regulation of GTP catabolic process	0.67
GO:0051350	negative regulation of lyase activity	0.67
KEGG_RENIN_ANGIOTENSIN_SYSTEM	KEGG_RENIN_ANGIOTENSIN_SYSTEM	0.67
GO:0010038	response to metal ion	0.67
ENSG00000163631	ALB PPI subnetwork	0.67
ENSG00000104897	SF3A2 PPI subnetwork	0.67
ENSG00000163806	SPDYA PPI subnetwork	0.67
MP:0004404	cochlear outer hair cell degeneration	0.67
REACTOME_PLATELET_ADHESION_TO_EXPOSED_COLLAGEN	REACTOME_PLATELET_ADHESION_TO_EXPOSED_COLLAGEN	0.67
GO:0030530	heterogeneous nuclear ribonucleoprotein complex	0.67
ENSG00000066117	SMARCD1 PPI subnetwork	0.67
GO:0008094	DNA-dependent ATPase activity	0.67
GO:0006013	mannose metabolic process	0.67
GO:0043200	response to amino acid stimulus	0.67
MP:0005553	increased circulating creatinine level	0.67
ENSG00000011052	NME2 PPI subnetwork	0.67
ENSG00000179051	RCC2 PPI subnetwork	0.68
MP:0001077	abnormal spinal nerve morphology	0.68
GO:0035107	appendage morphogenesis	0.68
GO:0035108	limb morphogenesis	0.68
GO:0005942	phosphatidylinositol 3-kinase complex	0.68
GO:0072384	organelle transport along microtubule	0.68
GO:0006520	cellular amino acid metabolic process	0.68
GO:0090068	positive regulation of cell cycle process	0.68
MP:0008498	decreased IgG3 level	0.68
ENSG00000182979	MTA1 PPI subnetwork	0.68
GO:0048285	organelle fission	0.68
ENSG00000101161	PRPF6 PPI subnetwork	0.68

Original gene set ID

REACTOME_PLATELET_HOMEOSTASIS

MP:0000752

GO:0045165

ENSG00000184486

GO:0008514

GO:0015672

GO:0045766

MP:0006359

ENSG00000150672

ENSG00000137076

ENSG00000153147

GO:0015804

ENSG00000173867

MP:0003059

GO:0007006

GO:0002763

ENSG00000072849

ENSG00000179036

GO:0016830

ENSG00000053900

GO:0072522

ENSG00000101199

ENSG00000171533

MP:0009766

ENSG00000136045

GO:0055001

ENSG00000143761

GO:0017144

MP:0000043

REACTOME_APCCDC20_MEDIATED_DEGRADATION_OF_SECURIN

ENSG00000197822

ENSG00000134852

GO:0001573

ENSG00000039537

ENSG00000213585

ENSG00000025770

ENSG00000146007

GO:0005741

GO:0006874

MP:0008410

MP:0002642

GO:0021543

REACTOME_EARLY_PHASE_OF_HIV_LIFE_CYCLE

REACTOME_CYCLIN_E_ASSOCIATED_EVENTS_DURING_G1S_TRANSITION

GO:0019320

REACTOME_LAGGING_STRAND_SYNTHESIS

REACTOME_DESTABILIZATION_OF_MRNA_BY_TRISTETRAPROLIN_TTP

ENSG00000167815

MP:0008535

Original gene set description

REACTOME_PLATELET_HOMEOSTASIS

dystrophic muscle

cell fate commitment

POU3F2 PPI subnetwork

organic anion transmembrane transporter activity

monovalent inorganic cation transport

positive regulation of angiogenesis

absent startle reflex

DLG2 PPI subnetwork

TLN1 PPI subnetwork

SMARCA5 PPI subnetwork

neutral amino acid transport

ENSG00000173867 PPI subnetwork

decreased insulin secretion

mitochondrial membrane organization

positive regulation of myeloid leukocyte differentiator

DERL2 PPI subnetwork

ENSG00000179036 PPI subnetwork

carbon-carbon lyase activity

ANAPC4 PPI subnetwork

purine-containing compound biosynthetic process

ARFGAP1 PPI subnetwork

MAP6 PPI subnetwork

increased sensitivity to xenobiotic induced morbidity/mortality

PWP1 PPI subnetwork

muscle cell development

ARF1 PPI subnetwork

drug metabolic process

organ of Corti degeneration

REACTOME_APCCDC20_MEDIATED_DEGRADATION_OF_SECURIN

OCLN PPI subnetwork

CLOCK PPI subnetwork

ganglioside metabolic process

C6 PPI subnetwork

VDAC1 PPI subnetwork

NCAPH2 PPI subnetwork

ZMAT2 PPI subnetwork

mitochondrial outer membrane

cellular calcium ion homeostasis

increased cellular sensitivity to ultraviolet irradiation

anisocytosis

pallium development

REACTOME_EARLY_PHASE_OF_HIV_LIFE_CYCLE

REACTOME_CYCLIN_E_ASSOCIATED_EVENTS_DURING_G1S_TRANSITION

hexose catabolic process

REACTOME_LAGGING_STRAND_SYNTHESIS

REACTOME_DESTABILIZATION_OF_MRNA_BY_TRISTETRAPROLIN_TTP

PRDX2 PPI subnetwork

enlarged lateral ventricles

Nominal P value

0.68

0.68

0.68

0.68

0.68

0.68

0.68

0.68

0.68

0.68

0.68

0.68

0.68

0.68

0.68

0.68

0.68

0.68

0.68

0.68

0.68

0.68

0.68

0.68

0.68

0.68

0.68

0.68

0.68

0.68

0.68

0.68

0.68

0.68

0.68

0.68

0.68

0.68

0.68

0.68

0.68

0.68

0.68

0.68

0.68

0.68

0.68

0.68

0.68

Original gene set ID	Original gene set description	Nominal P value
GO:0043648	dicarboxylic acid metabolic process	0.68
ENSG00000140795	MYLK3 PPI subnetwork	0.68
GO:0030512	negative regulation of transforming growth factor beta receptor signaling pathway	0.68
ENSG00000133243	BTBD2 PPI subnetwork	0.68
GO:0015077	monovalent inorganic cation transmembrane transporter activity	0.68
GO:0003151	outflow tract morphogenesis	0.68
ENSG000000085840	ORC1 PPI subnetwork	0.68
GO:0009123	nucleoside monophosphate metabolic process	0.68
ENSG00000130204	TOMM40 PPI subnetwork	0.68
ENSG00000120708	TGFBI PPI subnetwork	0.68
ENSG00000165392	WRN PPI subnetwork	0.68
ENSG00000081985	IL12RB2 PPI subnetwork	0.68
ENSG00000175029	CTBP2 PPI subnetwork	0.68
MP:0002813	microcytosis	0.68
GO:0019898	extrinsic to membrane	0.68
ENSG00000206267	ENSG00000206267 PPI subnetwork	0.68
ENSG00000204351	SKIV2L PPI subnetwork	0.68
ENSG00000076242	MLH1 PPI subnetwork	0.68
ENSG00000076554	TPD52 PPI subnetwork	0.68
ENSG00000006451	RALA PPI subnetwork	0.68
GO:0007076	mitotic chromosome condensation	0.68
GO:0033762	response to glucagon stimulus	0.68
ENSG00000173805	HAP1 PPI subnetwork	0.68
ENSG00000206495	TRIM39 PPI subnetwork	0.68
ENSG00000206419	ENSG00000206419 PPI subnetwork	0.68
ENSG00000204599	TRIM39 PPI subnetwork	0.68
GO:0019905	syntaxin binding	0.68
GO:0061351	neural precursor cell proliferation	0.68
ENSG00000079950	STX7 PPI subnetwork	0.68
MP:0000242	impaired fertilization	0.68
REACTOME_GABA_RECEPTOR_ACTIVATION	REACTOME_GABA_RECEPTOR_ACTIVATION	0.68
ENSG00000206407	ENSG00000206407 PPI subnetwork	0.68
ENSG00000204569	PPP1R10 PPI subnetwork	0.68
ENSG00000206489	PPP1R10 PPI subnetwork	0.68
GO:0006266	DNA ligation	0.68
GO:2000179	positive regulation of neural precursor cell proliferation	0.68
GO:0044439	peroxisomal part	0.69
GO:0044438	microbody part	0.69
MP:0002626	increased heart rate	0.69
ENSG00000007392	LUC7L PPI subnetwork	0.69
GO:0060562	epithelial tube morphogenesis	0.69
ENSG00000101811	CSTF2 PPI subnetwork	0.69
ENSG00000121741	ZMYM2 PPI subnetwork	0.69
GO:0009896	positive regulation of catabolic process	0.69
GO:0031341	regulation of cell killing	0.69
GO:0005759	mitochondrial matrix	0.69
GO:0030659	cytoplasmic vesicle membrane	0.69
ENSG00000131724	IL13RA1 PPI subnetwork	0.69
KEGG_GLUTATHIONE_METABOLISM	KEGG_GLUTATHIONE_METABOLISM	0.69

Original gene set ID	Original gene set description	Nominal P value
MP:0008663	increased interleukin-12 secretion	0.69
ENSG00000173418	NAA20 PPI subnetwork	0.69
GO:0010573	vascular endothelial growth factor production	0.69
GO:0010574	regulation of vascular endothelial growth factor productior	0.69
ENSG00000206353	SKIV2L PPI subnetwork	0.69
ENSG00000138814	PPP3CA PPI subnetwork	0.69
MP:0004096	abnormal midbrain-hindbrain boundary development	0.69
GO:0009880	embryonic pattern specification	0.69
ENSG00000127616	SMARCA4 PPI subnetwork	0.69
ENSG00000153046	CDYL PPI subnetwork	0.69
MP:0006036	abnormal mitochondrial physiology	0.69
GO:0007214	gamma-aminobutyric acid signaling pathway	0.69
GO:0021987	cerebral cortex development	0.69
MP:0005608	cardiac interstitial fibrosis	0.69
MP:0004532	abnormal inner hair cell stereociliary bundle morphology	0.69
ENSG00000079102	RUNX1T1 PPI subnetwork	0.69
GO:0042490	mechanoreceptor differentiation	0.69
GO:0016045	detection of bacterium	0.69
GO:0015985	energy coupled proton transport, down electrochemical gradient	0.69
GO:0015986	ATP synthesis coupled proton transport	0.69
MP:0002797	increased thigmotaxis	0.69
GO:0055003	cardiac myofibril assembly	0.69
KEGG_O_GLYCAN_BIOSYNTHESIS	KEGG_O_GLYCAN_BIOSYNTHESIS	0.69
ENSG00000011304	PTBP1 PPI subnetwork	0.69
ENSG00000130177	CDC16 PPI subnetwork	0.69
GO:0051247	positive regulation of protein metabolic proces	0.69
GO:0048596	embryonic camera-type eye morphogenesis	0.69
MP:0005318	decreased triglyceride level	0.69
ENSG000000091129	NRCAM PPI subnetwork	0.69
ENSG00000112062	MAPK14 PPI subnetwork	0.69
ENSG00000156374	PCGF6 PPI subnetwork	0.69
ENSG00000142192	APP PPI subnetwork	0.69
ENSG00000116754	SRSF11 PPI subnetwork	0.69
ENSG00000173598	NUDT4 PPI subnetwork	0.69
GO:0030833	regulation of actin filament polymerization	0.69
GO:0060560	developmental growth involved in morphogenesis	0.69
ENSG000000005156	LIG3 PPI subnetwork	0.69
ENSG00000124422	USP22 PPI subnetwork	0.69
MP:0005403	abnormal nerve conduction	0.69
ENSG00000178896	EXOSC4 PPI subnetwork	0.69
ENSG00000132535	DLG4 PPI subnetwork	0.69
GO:0045649	regulation of macrophage differentiation	0.69
GO:0090307	spindle assembly involved in mitosis	0.69
GO:0043279	response to alkaloid	0.69
MP:0000432	abnormal head morphology	0.69
REACTOME_AUTODEGRADATION_OF_CDH1_BY_CDH1APCC	REACTOME_AUTODEGRADATION_OF_CDH1_BY_CDH1APCC	0.69
ENSG00000172943	PHF8 PPI subnetwork	0.69
GO:0031674	I band	0.69
ENSG00000139436	GIT2 PPI subnetwork	0.69

Original gene set ID	Original gene set description	Nominal P value
ENSG00000029363	BCLAF1 PPI subnetwork	0.69
GO:0010575	positive regulation vascular endothelial growth factor productior	0.69
ENSG000000130382	MLLT1 PPI subnetwork	0.69
ENSG000000177733	HNRNPA0 PPI subnetwork	0.69
ENSG000000111802	TDP2 PPI subnetwork	0.69
ENSG000000157601	MX1 PPI subnetwork	0.69
ENSG000000141959	PFKL PPI subnetwork	0.69
GO:0030018	Z disc	0.69
MP:0006264	decreased systemic arterial systolic blood pressure	0.69
GO:0021885	forebrain cell migration	0.69
ENSG000000139842	CUL4A PPI subnetwork	0.69
GO:0006898	receptor-mediated endocytosis	0.69
MP:0005026	decreased susceptibility to parasitic infectior	0.69
ENSG000000164418	GRIK2 PPI subnetwork	0.69
ENSG000000094631	HDAC6 PPI subnetwork	0.69
GO:0005892	acetylcholine-gated channel complex	0.69
GO:0044440	endosomal part	0.69
ENSG000000117748	RPA2 PPI subnetwork	0.69
ENSG000000164611	PTTG1 PPI subnetwork	0.69
GO:0035064	methylated histone residue binding	0.69
MP:0002914	abnormal endplate potential	0.69
ENSG000000138795	LEF1 PPI subnetwork	0.69
GO:0010810	regulation of cell-substrate adhesion	0.69
MP:0000748	progressive muscle weakness	0.69
MP:0002929	abnormal bile duct development	0.69
GO:0048485	sympathetic nervous system development	0.69
GO:0034703	cation channel complex	0.69
ENSG000000067225	PKM2 PPI subnetwork	0.69
ENSG000000142453	CARM1 PPI subnetwork	0.69
REACTOME_PIP3_ACTIVATES_AKT_SIGNALING	REACTOME_PIP3_ACTIVATES_AKT_SIGNALING	0.69
GO:0045921	positive regulation of exocytosis	0.69
GO:0016747	transferase activity, transferring acyl groups other than amino-acyl group:	0.69
MP:0000279	ventricular hypoplasia	0.69
MP:0005298	abnormal clavicle morphology	0.69
ENSG000000108344	PSMD3 PPI subnetwork	0.69
GO:0061041	regulation of wound healing	0.69
MP:0004355	short radius	0.69
MP:0005166	decreased susceptibility to injury	0.69
GO:0046320	regulation of fatty acid oxidation	0.69
MP:0008687	increased interleukin-2 secretion	0.69
MP:0003632	abnormal nervous system morphology	0.69
GO:0051480	cytosolic calcium ion homeostasis	0.69
KEGG_MISMATCH_REPAIR	KEGG_MISMATCH_REPAIR	0.69
ENSG000000185345	PARK2 PPI subnetwork	0.69
GO:0045686	negative regulation of glial cell differentiator	0.69
REACTOME_TRANSPORT_OF_RIBONUCLEOPROTEINS_INTO_THE_HOST_NUCLEI	REACTOME_TRANSPORT_OF_RIBONUCLEOPROTEINS_INTO_THE_HOST_NUCLEUS	0.69
ENSG000000117318	ID3 PPI subnetwork	0.69
GO:0046651	lymphocyte proliferation	0.69
ENSG000000166206	GABRB3 PPI subnetwork	0.7

Original gene set ID	Original gene set description	Nominal P value
GO:0006919	activation of cysteine-type endopeptidase activity involved in apoptotic proces:	0.7
GO:0002052	positive regulation of neuroblast proliferati	0.7
GO:0046635	positive regulation of alpha-beta T cell activation	0.7
GO:0030278	regulation of ossification	0.7
ENSG00000080503	SMARCA2 PPI subnetwork	0.7
ENSG00000175203	DCTN2 PPI subnetwork	0.7
ENSG00000118495	PLAGL1 PPI subnetwork	0.7
GO:0050830	defense response to Gram-positive bacterium	0.7
GO:0032570	response to progesterone stimulus	0.7
GO:0042451	purine nucleoside biosynthetic process	0.7
GO:0042455	ribonucleoside biosynthetic process	0.7
GO:0046129	purine ribonucleoside biosynthetic process	0.7
ENSG00000173465	SSSCA1 PPI subnetwork	0.7
GO:0022836	gated channel activity	0.7
ENSG00000168005	C11orf84 PPI subnetwork	0.7
GO:0015459	potassium channel regulator activity	0.7
ENSG00000039068	CDH1 PPI subnetwork	0.7
GO:0002495	antigen processing and presentation of peptide antigen via MHC class I	0.7
REACTOME_DAG_AND_IP3_SIGNALING	REACTOME_DAG_AND_IP3_SIGNALING	0.7
ENSG00000136026	CKAP4 PPI subnetwork	0.7
ENSG00000112640	PPP2R5D PPI subnetwork	0.7
ENSG00000145332	KLHL8 PPI subnetwork	0.7
GO:0051146	striated muscle cell differentiation	0.7
ENSG00000142945	KIF2C PPI subnetwork	0.7
ENSG00000148180	GSN PPI subnetwork	0.7
ENSG00000107295	SH3GL2 PPI subnetwork	0.7
ENSG00000059378	PARP12 PPI subnetwork	0.7
GO:0048488	synaptic vesicle endocytosis	0.7
ENSG00000163440	PDCL2 PPI subnetwork	0.7
MP:0005542	corneal vascularization	0.7
ENSG00000173702	MUC13 PPI subnetwork	0.7
ENSG00000186879	ENSG00000186879 PPI subnetwork	0.7
GO:0050829	defense response to Gram-negative bacterium	0.7
GO:2000736	regulation of stem cell differentiation	0.7
GO:0030516	regulation of axon extension	0.7
GO:0051301	cell division	0.7
GO:0006942	regulation of striated muscle contraction	0.7
GO:0004112	cyclic-nucleotide phosphodiesterase activity	0.7
MP:0005333	decreased heart rate	0.7
GO:0022029	telencephalon cell migration	0.7
MP:0001924	infertility	0.7
MP:0011228	abnormal vitamin D level	0.7
ENSG00000147130	ZMYM3 PPI subnetwork	0.7
ENSG00000082258	CCNT2 PPI subnetwork	0.7
GO:0009416	response to light stimulus	0.7
REACTOME_AQUAPORIN:MEDIATED_TRANSPORT	REACTOME_AQUAPORIN:MEDIATED_TRANSPORT	0.7
MP:0004113	abnormal aortic arch morphology	0.7
MP:0004398	cochlear inner hair cell degeneration	0.7
MP:0004505	decreased renal glomerulus number	0.7

Original gene set ID	Original gene set description	Nominal P value
GO:0007187	G-protein coupled receptor signaling pathway, coupled to cyclic nucleotide second r	0.7
GO:0032039	integrator complex	0.7
ENSG000000128340	RAC2 PPI subnetwork	0.7
GO:0003001	generation of a signal involved in cell-cell signaling	0.7
GO:0023061	signal release	0.7
MP:0008502	increased IgG3 level	0.7
GO:0000421	autophagic vacuole membrane	0.7
GO:0014014	negative regulation of gliogenesis	0.7
MP:0002492	decreased IgE level	0.7
ENSG000000132182	NUP210 PPI subnetwork	0.7
MP:0002663	failure to form blastocele	0.7
GO:0031575	mitotic cell cycle G1/S transition checkpoint	0.7
GO:0046488	phosphatidylinositol metabolic process	0.7
ENSG000000196911	KPNA5 PPI subnetwork	0.7
MP:0001426	polydipsia	0.7
ENSG000000148229	POLE3 PPI subnetwork	0.7
ENSG000000183684	ALYREF PPI subnetwork	0.7
KEGG_BASE_EXCISION_REPAIR	KEGG_BASE_EXCISION_REPAIR	0.7
GO:0051960	regulation of nervous system development	0.7
REACTOME_ASSOCIATION_OF_LICENSING_FACTORS_WITH_THE_PRE:REPLICAT	REACTOME_ASSOCIATION_OF_LICENSING_FACTORS_WITH_THE_PRE:REPLICATIVE_	0.7
MP:0006030	abnormal otic vesicle development	0.7
ENSG000000166971	AKTIP PPI subnetwork	0.7
REACTOME_SIGNALING_BY_PDGF	REACTOME_SIGNALING_BY_PDGF	0.7
MP:0008181	increased marginal zone B cell number	0.7
GO:0010874	regulation of cholesterol efflux	0.7
ENSG000000085063	CD59 PPI subnetwork	0.7
GO:0008076	voltage-gated potassium channel complex	0.7
GO:0034705	potassium channel complex	0.7
GO:0035137	hindlimb morphogenesis	0.7
GO:0014048	regulation of glutamate secretion	0.7
ENSG000000163875	MEAF6 PPI subnetwork	0.7
ENSG000000156299	TIAM1 PPI subnetwork	0.7
ENSG000000188229	TUBB4B PPI subnetwork	0.7
GO:0060415	muscle tissue morphogenesis	0.7
ENSG000000100368	CSF2RB PPI subnetwork	0.7
ENSG000000134717	BTF3L4 PPI subnetwork	0.7
KEGG_DILATED_CARDIOMYOPATHY	KEGG_DILATED_CARDIOMYOPATHY	0.7
GO:0008234	cysteine-type peptidase activity	0.7
GO:0045216	cell-cell junction organization	0.7
MP:0008734	decreased susceptibility to endotoxin shock	0.7
ENSG000000103343	ZNF174 PPI subnetwork	0.7
ENSG000000120875	DUSP4 PPI subnetwork	0.7
MP:0002941	increased circulating alanine transaminase leve	0.7
GO:0009791	post-embryonic development	0.7
GO:0050804	regulation of synaptic transmission	0.7
GO:0030136	clathrin-coated vesicle	0.7
GO:0050994	regulation of lipid catabolic process	0.7
ENSG000000013561	RNF14 PPI subnetwork	0.7
GO:0030808	regulation of nucleotide biosynthetic process	0.7

Original gene set ID	Original gene set description	Nominal P value
GO:0030802	regulation of cyclic nucleotide biosynthetic process	0.7
MP:0000480	increased rib number	0.7
ENSG000000127588	GNG13 PPI subnetwork	0.7
GO:0033116	endoplasmic reticulum-Golgi intermediate compartment membrane	0.7
ENSG000000126226	PCID2 PPI subnetwork	0.7
GO:0032642	regulation of chemokine production	0.7
REACTOME_SIGNALING_BY_EGFR	REACTOME_SIGNALING_BY_EGFR	0.7
GO:0032943	mononuclear cell proliferation	0.7
GO:0030162	regulation of proteolysis	0.7
GO:0008154	actin polymerization or depolymerization	0.7
REACTOME_DCC_MEDIATED_ATTRACTIVE_SIGNALING	REACTOME_DCC_MEDIATED_ATTRACTIVE_SIGNALING	0.71
REACTOME_RNA_POLYMERASE_I_TRANSCRIPTION	REACTOME_RNA_POLYMERASE_I_TRANSCRIPTION	0.71
MP:0000520	absent kidney	0.71
REACTOME_POTASSIUM_CHANNELS	REACTOME_POTASSIUM_CHANNELS	0.71
GO:0048486	parasympathetic nervous system development	0.71
GO:0005884	actin filament	0.71
ENSG000000173120	KDM2A PPI subnetwork	0.71
REACTOME_G1S_TRANSITION	REACTOME_G1S_TRANSITION	0.71
GO:0006007	glucose catabolic process	0.71
MP:0002608	increased hematocrit	0.71
GO:0010720	positive regulation of cell development	0.71
GO:0030521	androgen receptor signaling pathway	0.71
GO:0072531	pyrimidine-containing compound transmembrane transport	0.71
KEGG_B_CELL_RECEPTOR_SIGNALING_PATHWAY	KEGG_B_CELL_RECEPTOR_SIGNALING_PATHWAY	0.71
MP:0000823	abnormal lateral ventricle morphology	0.71
MP:0002910	abnormal excitatory postsynaptic currents	0.71
REACTOME_GAP:FILLING_DNA_REPAIR_SYNTHESIS_AND_LIGATION_IN_TC:NER	REACTOME_GAP:FILLING_DNA_REPAIR_SYNTHESIS_AND_LIGATION_IN_TC:NER	0.71
REACTOME_GAP:FILLING_DNA_REPAIR_SYNTHESIS_AND_LIGATION_IN_GG:NEF	REACTOME_GAP:FILLING_DNA_REPAIR_SYNTHESIS_AND_LIGATION_IN_GG:NER	0.71
ENSG000000104164	PLDN PPI subnetwork	0.71
ENSG000000102312	PORCN PPI subnetwork	0.71
MP:0005176	eyelids fail to open	0.71
ENSG000000122585	NPY PPI subnetwork	0.71
REACTOME_TAT:MEDIATED_HIV:1_ELONGATION_ARREST_AND_RECOVERY	REACTOME_TAT:MEDIATED_HIV:1_ELONGATION_ARREST_AND_RECOVERY	0.71
REACTOME_PAUSING_AND_RECOVERY_OF_TAT:MEDIATED_HIV:1_ELONGATIO	REACTOME_PAUSING_AND_RECOVERY_OF_TAT:MEDIATED_HIV:1_ELONGATION	0.71
GO:0000776	kinetochore	0.71
ENSG000000111664	GNB3 PPI subnetwork	0.71
MP:0008034	enhanced lipolysis	0.71
GO:0002237	response to molecule of bacterial origin	0.71
GO:0004536	deoxyribonuclease activity	0.71
ENSG000000163017	ACTG2 PPI subnetwork	0.71
GO:0060048	cardiac muscle contraction	0.71
GO:0009410	response to xenobiotic stimulus	0.71
GO:0071466	cellular response to xenobiotic stimulus	0.71
ENSG000000164105	SAP30 PPI subnetwork	0.71
GO:0016042	lipid catabolic process	0.71
GO:0032496	response to lipopolysaccharide	0.71
GO:0012506	vesicle membrane	0.71
ENSG000000152413	HOMER1 PPI subnetwork	0.71
REACTOME_G_ALPHA_Q_SIGNALLING_EVENTS	REACTOME_G_ALPHA_Q_SIGNALLING_EVENTS	0.71

Original gene set ID	Original gene set description	Nominal P value
GO:0048489	synaptic vesicle transport	0.71
MP:0005617	increased susceptibility to type IV hypersensitivity reactor	0.71
MP:0005459	decreased percent body fat	0.71
ENSG00000168439	STIP1 PPI subnetwork	0.71
GO:0002793	positive regulation of peptide secretion	0.71
GO:0006378	mRNA polyadenylation	0.71
MP:0000298	absent atrioventricular cushions	0.71
GO:0010008	endosome membrane	0.71
MP:0004204	absent stapes	0.71
ENSG00000185008	ROBO2 PPI subnetwork	0.71
GO:0044427	chromosomal part	0.71
REACTOME_HIV:1_ELONGATION_ARREST_AND_RECOVERY	REACTOME_HIV:1_ELONGATION_ARREST_AND_RECOVERY	0.71
REACTOME_PAUSING_AND_RECOVERY_OF_HIV:1_ELONGATION	REACTOME_PAUSING_AND_RECOVERY_OF_HIV:1_ELONGATION	0.71
REACTOME_PAUSING_AND_RECOVERY_OF_ELONGATION	REACTOME_PAUSING_AND_RECOVERY_OF_ELONGATION	0.71
REACTOME_ELONGATION_ARREST_AND_RECOVERY	REACTOME_ELONGATION_ARREST_AND_RECOVERY	0.71
MP:0010551	abnormal coronary vessel morphology	0.71
GO:0070330	aromatase activity	0.71
ENSG00000138709	LARP1B PPI subnetwork	0.71
ENSG00000033122	LRRC7 PPI subnetwork	0.71
MP:0008536	enlarged third ventricle	0.71
GO:0002562	somatic diversification of immune receptors via germline recombination within a sir	0.71
GO:0016444	somatic cell DNA recombination	0.71
MP:0011353	expanded mesangial matrix	0.71
ENSG00000158769	F11R PPI subnetwork	0.71
GO:0046058	cAMP metabolic process	0.71
ENSG00000017797	RALBP1 PPI subnetwork	0.71
GO:0006354	transcription elongation, DNA-dependent	0.71
REACTOME_GABA_B_RECEPTOR_ACTIVATION	REACTOME_GABA_B_RECEPTOR_ACTIVATION	0.71
REACTOME_ACTIVATION_OF_GABAB_RECEPTORS	REACTOME_ACTIVATION_OF_GABAB_RECEPTORS	0.71
GO:0035116	embryonic hindlimb morphogenesis	0.71
GO:0000784	nuclear chromosome, telomeric region	0.71
ENSG00000129562	DAD1 PPI subnetwork	0.71
MP:0000536	hydroureter	0.71
ENSG00000122756	CNTFR PPI subnetwork	0.72
ENSG00000124642	ENSG00000124642 PPI subnetwork	0.72
ENSG00000184825	HIST1H2AH PPI subnetwork	0.72
GO:0005487	nucleocytoplasmic transporter activity	0.72
ENSG00000162231	NXF1 PPI subnetwork	0.72
GO:0051241	negative regulation of multicellular organismal process	0.72
ENSG00000133119	RFC3 PPI subnetwork	0.72
MP:0003728	abnormal retinal photoreceptor layer morphology	0.72
GO:0031683	G-protein beta/gamma-subunit complex binding	0.72
ENSG00000180573	HIST1H2AC PPI subnetwork	0.72
GO:0051262	protein tetramerization	0.72
GO:0010927	cellular component assembly involved in morphogenesis	0.72
ENSG00000118515	SGK1 PPI subnetwork	0.72
ENSG00000101306	MYLK2 PPI subnetwork	0.72
ENSG00000174720	LARP7 PPI subnetwork	0.72
GO:0019935	cyclic-nucleotide-mediated signaling	0.72

Original gene set ID	Original gene set description	Nominal P value
GO:0045777	positive regulation of blood pressure	0.72
REACTOME_PRESYNAPTIC_NICOTINIC_ACETYLCHOLINE_RECEPTORS	REACTOME_PRESYNAPTIC_NICOTINIC_ACETYLCHOLINE_RECEPTORS	0.72
ENSG00000137403	HLA-F PPI subnetwork	0.72
ENSG00000213066	FGFR1OP PPI subnetwork	0.72
ENSG00000157766	ACAN PPI subnetwork	0.72
GO:0032451	demethylase activity	0.72
REACTOME_CROSS_PRESENTATION_OF_SOLUBLE_EXOGENOUS_ANTIGENS_ENDOSOMAL_PATHWAY	REACTOME_CROSS_PRESENTATION_OF_SOLUBLE_EXOGENOUS_ANTIGENS_ENDOSOMAL_PATHWAY	0.72
ENSG00000120837	NFYB PPI subnetwork	0.72
GO:0000226	microtubule cytoskeleton organization	0.72
GO:0051145	smooth muscle cell differentiation	0.72
ENSG00000111052	LIN7A PPI subnetwork	0.72
ENSG00000151247	EIF4E PPI subnetwork	0.72
ENSG00000130640	TUBGCP2 PPI subnetwork	0.72
GO:0010001	glial cell differentiation	0.72
MP:0005587	abnormal Meckel's cartilage morphology	0.72
GO:0015074	DNA integration	0.72
GO:0048715	negative regulation of oligodendrocyte differentiation	0.72
ENSG00000164975	SNAPC3 PPI subnetwork	0.72
ENSG00000158290	CUL4B PPI subnetwork	0.72
ENSG00000125743	SNRPD2 PPI subnetwork	0.72
ENSG00000138685	FGF2 PPI subnetwork	0.72
GO:0006364	rRNA processing	0.72
GO:0042092	type 2 immune response	0.72
REACTOME_RNA_POLYMERASE_I_PROMOTER_OPENING	REACTOME_RNA_POLYMERASE_I_PROMOTER_OPENING	0.72
GO:0033180	proton-transporting V-type ATPase, V1 domain	0.72
GO:0030509	BMP signaling pathway	0.72
GO:0035115	embryonic forelimb morphogenesis	0.72
ENSG00000115594	IL1R1 PPI subnetwork	0.72
GO:0048747	muscle fiber development	0.72
GO:0010744	positive regulation of macrophage derived foam cell differentiation	0.72
MP:0002196	absent corpus callosum	0.72
REACTOME_SYNTHESIS_SECRETION_AND_INACTIVATION_OF_GLUCAGON-LIKE_PEPTIDES	REACTOME_SYNTHESIS_SECRETION_AND_INACTIVATION_OF_GLUCAGON-LIKE_PEPTIDES	0.72
REACTOME_INCRETIN_SYNTHESIS_SECRETION_AND_INACTIVATION	REACTOME_INCRETIN_SYNTHESIS_SECRETION_AND_INACTIVATION	0.72
GO:0006643	membrane lipid metabolic process	0.72
MP:0001921	reduced fertility	0.72
GO:0010463	mesenchymal cell proliferation	0.72
MP:0001685	abnormal endoderm development	0.72
ENSG00000104388	RAB2A PPI subnetwork	0.72
MP:0001065	abnormal trigeminal nerve morphology	0.72
ENSG00000104320	NBN PPI subnetwork	0.72
MP:0005656	decreased aggression	0.72
ENSG00000215902	ENSG00000215902 PPI subnetwork	0.72
REACTOME_G:PROTEIN_MEDIATED_EVENTS	REACTOME_G:PROTEIN_MEDIATED_EVENTS	0.72
ENSG00000137672	TRPC6 PPI subnetwork	0.72
GO:0009190	cyclic nucleotide biosynthetic process	0.72
GO:0010833	telomere maintenance via telomere lengthening	0.72
MP:0001701	incomplete embryo turning	0.72
GO:0046365	monosaccharide catabolic process	0.72
ENSG00000149782	PLCB3 PPI subnetwork	0.72

Original gene set ID	Original gene set description	Nominal P value
GO:0008080	N-acetyltransferase activity	0.72
MP:0003354	astrocytosis	0.72
GO:0007041	lysosomal transport	0.72
ENSG00000082898	XPO1 PPI subnetwork	0.72
GO:0030119	AP-type membrane coat adaptor complex	0.72
GO:0090277	positive regulation of peptide hormone secretior	0.72
ENSG00000106399	RPA3 PPI subnetwork	0.72
ENSG00000164867	NOS3 PPI subnetwork	0.72
ENSG00000177700	POLR2L PPI subnetwork	0.72
ENSG00000079805	DNM2 PPI subnetwork	0.72
ENSG00000113196	HAND1 PPI subnetwork	0.72
ENSG00000104879	CKM PPI subnetwork	0.72
GO:0007492	endoderm development	0.72
ENSG00000110148	CCKBR PPI subnetwork	0.72
ENSG00000033050	ABCF2 PPI subnetwork	0.72
GO:0072132	mesenchyme morphogenesis	0.72
MP:0002020	increased tumor incidence	0.72
REACTOME_PROCESSIVE_SYNTHESIS_ON_THE_C:STRAND_OF_THE_TELOMERE	REACTOME_PROCESSIVE_SYNTHESIS_ON_THE_C:STRAND_OF_THE_TELOMERE	0.72
GO:0031406	carboxylic acid binding	0.72
GO:0031901	early endosome membrane	0.72
ENSG00000153767	GTF2E1 PPI subnetwork	0.72
ENSG00000118491	C6orf94 PPI subnetwork	0.72
ENSG00000181789	COPG PPI subnetwork	0.72
GO:0004549	tRNA-specific ribonuclease activity	0.72
ENSG00000024048	UBR2 PPI subnetwork	0.72
GO:0021532	neural tube patterning	0.72
MP:0003070	increased vascular permeability	0.72
GO:0008589	regulation of smoothened signaling pathway	0.72
ENSG00000100836	PABPN1 PPI subnetwork	0.72
GO:0030199	collagen fibril organization	0.72
REACTOME_RNA_POLYMERASE_I_PROMOTER_CLEARANCE	REACTOME_RNA_POLYMERASE_I_PROMOTER_CLEARANCE	0.72
GO:0032602	chemokine production	0.72
MP:0005165	increased susceptibility to injury	0.72
ENSG00000104626	ERI1 PPI subnetwork	0.72
MP:0001566	hyperphosphatemia	0.73
GO:0043679	axon terminus	0.73
GO:2000677	regulation of transcription regulatory region DNA binding	0.73
GO:0032319	regulation of Rho GTPase activity	0.73
ENSG00000204086	RPA4 PPI subnetwork	0.73
ENSG00000113318	MSH3 PPI subnetwork	0.73
ENSG00000103994	ZFP106 PPI subnetwork	0.73
GO:0006805	xenobiotic metabolic process	0.73
MP:0010769	abnormal survival	0.73
ENSG00000215727	ENSG00000215727 PPI subnetwork	0.73
ENSG00000065518	NDUFB4 PPI subnetwork	0.73
MP:0004543	abnormal sperm physiology	0.73
GO:0004693	cyclin-dependent protein kinase activity	0.73
ENSG00000186184	POLR1D PPI subnetwork	0.73
REACTOME_ACTIVATION_OF_NMDA_RECEPTOR_UPON_Glutamate_BINDING	REACTOME_ACTIVATION_OF_NMDA_RECEPTOR_UPON_Glutamate_BINDING_AN	0.73

Original gene set ID	Original gene set description	Nominal P value
GO:0048291	isotype switching to IgG isotypes	0.73
ENSG00000088367	EPB41L1 PPI subnetwork	0.73
GO:0030917	midbrain-hindbrain boundary development	0.73
GO:2001252	positive regulation of chromosome organization	0.73
REACTOME_TRANSCRIPTION	REACTOME_TRANSCRIPTION	0.73
GO:0006541	glutamine metabolic process	0.73
GO:0051051	negative regulation of transport	0.73
GO:0060429	epithelium development	0.73
MP:0002757	decreased vertical activity	0.73
ENSG00000153774	CFDP1 PPI subnetwork	0.73
GO:0010464	regulation of mesenchymal cell proliferation	0.73
ENSG00000023318	ERP44 PPI subnetwork	0.73
GO:0060322	head development	0.73
GO:0031954	positive regulation of protein autophosphorylation	0.73
MP:0004965	inner cell mass degeneration	0.73
GO:0044460	flagellum part	0.73
GO:0044442	microtubule-based flagellum part	0.73
ENSG00000167986	DDB1 PPI subnetwork	0.73
GO:0007193	adenylate cyclase-inhibiting G-protein coupled receptor signaling pathway	0.73
GO:0048302	regulation of isotype switching to IgG isotypes	0.73
KEGG_SYSTEMIC_LUPUS_ERYTHEMATOSUS	KEGG_SYSTEMIC_LUPUS_ERYTHEMATOSUS	0.73
GO:0004930	G-protein coupled receptor activity	0.73
ENSG00000168539	CHRM1 PPI subnetwork	0.73
ENSG00000125977	EIF2S2 PPI subnetwork	0.73
GO:0072511	divalent inorganic cation transport	0.73
ENSG00000104637	ENSG00000104637 PPI subnetwork	0.73
GO:0048663	neuron fate commitment	0.73
GO:0042165	neurotransmitter binding	0.73
ENSG00000154917	RAB6B PPI subnetwork	0.73
ENSG00000154016	GRAP PPI subnetwork	0.73
ENSG00000185518	SV2B PPI subnetwork	0.73
REACTOME_HOST_INTERACTIONS_OF_HIV_FACTORS	REACTOME_HOST_INTERACTIONS_OF_HIV_FACTORS	0.73
ENSG00000214133	ENSG00000214133 PPI subnetwork	0.73
ENSG00000158623	COPG2 PPI subnetwork	0.73
MP:0003656	abnormal erythrocyte physiology	0.73
ENSG00000152234	ATP5A1 PPI subnetwork	0.73
GO:0048675	axon extension	0.73
ENSG00000163539	CLASP2 PPI subnetwork	0.73
ENSG00000111653	ING4 PPI subnetwork	0.73
ENSG00000084463	WBP11 PPI subnetwork	0.73
GO:0048551	metalloenzyme inhibitor activity	0.73
GO:0008191	metalloendopeptidase inhibitor activity	0.73
MP:0001008	abnormal sympathetic ganglion morphology	0.73
MP:0003047	abnormal thoracic vertebrae morphology	0.73
MP:0005153	abnormal B cell proliferation	0.73
MP:0005225	abnormal vertebrae development	0.73
ENSG00000147202	DIAPH2 PPI subnetwork	0.73
ENSG00000049541	RFC2 PPI subnetwork	0.73
ENSG00000101608	MYL12A PPI subnetwork	0.73

Original gene set ID	Original gene set description	Nominal P value
MP:0001807	decreased IgA level	0.74
GO:0009145	purine nucleoside triphosphate biosynthetic process	0.74
ENSG000000134480	CCNH PPI subnetwork	0.74
REACTOME_DNA_REPLICATION	REACTOME_DNA_REPLICATION	0.74
ENSG000000151067	CACNA1C PPI subnetwork	0.74
ENSG000000169429	IL8 PPI subnetwork	0.74
GO:0007286	spermatid development	0.74
MP:0001402	hypoactivity	0.74
GO:0050808	synapse organization	0.74
ENSG000000166930	MS4A5 PPI subnetwork	0.74
ENSG000000077312	SNRPA PPI subnetwork	0.75
GO:0019002	GMP binding	0.75
ENSG000000065526	SPEN PPI subnetwork	0.75
ENSG000000184672	RALYL PPI subnetwork	0.75
ENSG000000136560	TANK PPI subnetwork	0.75
MP:0004947	skin inflammation	0.75
GO:0004690	cyclic nucleotide-dependent protein kinase activity	0.75
ENSG000000198569	SLC34A3 PPI subnetwork	0.75
ENSG000000123268	ATF1 PPI subnetwork	0.75
GO:0006184	GTP catabolic process	0.75
GO:0051385	response to mineralocorticoid stimulus	0.75
ENSG000000106628	POLD2 PPI subnetwork	0.75
GO:0055065	metal ion homeostasis	0.75
MP:0000538	abnormal urinary bladder morphology	0.75
REACTOME_BIOSYNTHESIS_OF_THE_N:GLYCAN_PRECURSOR_DOLICHOL_LIPID	REACTOME_BIOSYNTHESIS_OF_THE_N:GLYCAN_PRECURSOR_DOLICHOL_LIPID:LINK	0.75
GO:0050714	positive regulation of protein secretion	0.75
ENSG000000215320	ENSG000000215320 PPI subnetwork	0.75
ENSG000000143977	SNRPG PPI subnetwork	0.75
MP:0004986	abnormal osteoblast morphology	0.75
ENSG000000163453	IGFBP7 PPI subnetwork	0.75
MP:0011290	decreased nephron number	0.75
ENSG000000141552	ANAPC11 PPI subnetwork	0.75
GO:0006672	ceramide metabolic process	0.75
GO:0004386	helicase activity	0.75
ENSG00000014641	MDH1 PPI subnetwork	0.75
MP:0000150	abnormal rib morphology	0.75
ENSG000000102001	CACNA1F PPI subnetwork	0.75
ENSG000000162290	ENSG000000162290 PPI subnetwork	0.75
GO:0043547	positive regulation of GTPase activity	0.75
MP:0002972	abnormal cardiac muscle contractility	0.75
GO:0006040	amino sugar metabolic process	0.75
ENSG000000116062	MSH6 PPI subnetwork	0.75
ENSG000000126821	SGPP1 PPI subnetwork	0.75
MP:0000230	abnormal systemic arterial blood pressure	0.75
ENSG000000048052	HDAC9 PPI subnetwork	0.75
GO:0051588	regulation of neurotransmitter transport	0.75
GO:0001676	long-chain fatty acid metabolic process	0.75
ENSG000000187514	PTMA PPI subnetwork	0.75
ENSG00000030066	NUP160 PPI subnetwork	0.75

Original gene set ID	Original gene set description	Nominal P value
GO:0040013	negative regulation of locomotion	0.75
ENSG00000099800	TIMM13 PPI subnetwork	0.75
ENSG00000155897	ADCY8 PPI subnetwork	0.75
ENSG00000111716	LDHB PPI subnetwork	0.75
GO:0046883	regulation of hormone secretion	0.75
ENSG00000106305	AIMP2 PPI subnetwork	0.75
ENSG00000108518	PFN1 PPI subnetwork	0.75
ENSG00000087586	AURKA PPI subnetwork	0.75
GO:0040036	regulation of fibroblast growth factor receptor signaling pathway	0.75
MP:0000005	increased brown adipose tissue amount	0.75
GO:0030072	peptide hormone secretion	0.75
ENSG00000178999	AURKB PPI subnetwork	0.75
GO:0042176	regulation of protein catabolic process	0.75
GO:0003230	cardiac atrium development	0.75
MP:0003235	abnormal alisphenoid bone morphology	0.75
ENSG00000172613	RAD9A PPI subnetwork	0.75
ENSG00000165629	ATP5C1 PPI subnetwork	0.75
MP:0000455	abnormal maxilla morphology	0.75
MP:0005297	spina bifida occulta	0.75
MP:0001410	head bobbing	0.75
ENSG00000160789	LMNA PPI subnetwork	0.75
ENSG00000126602	TRAP1 PPI subnetwork	0.75
GO:0019439	aromatic compound catabolic process	0.75
GO:0002312	B cell activation involved in immune response	0.75
ENSG00000079819	EPB41L2 PPI subnetwork	0.75
GO:0007050	cell cycle arrest	0.75
GO:0044349	DNA excision	0.75
GO:0000718	nucleotide-excision repair, DNA damage removal	0.75
ENSG00000141404	GNAL PPI subnetwork	0.75
GO:0030799	regulation of cyclic nucleotide metabolic process	0.75
GO:0010742	macrophage derived foam cell differentiation	0.75
GO:0090077	foam cell differentiation	0.75
ENSG00000100142	POLR2F PPI subnetwork	0.75
GO:0008237	metallopeptidase activity	0.75
ENSG00000127337	YEATS4 PPI subnetwork	0.75
GO:0032543	mitochondrial translation	0.75
GO:0016624	oxidoreductase activity, acting on the aldehyde or oxo group of donors, disulfide as	0.75
MP:0002878	abnormal corticospinal tract morphology	0.75
ENSG00000145649	GZMA PPI subnetwork	0.75
GO:0033293	monocarboxylic acid binding	0.75
ENSG00000125970	RALY PPI subnetwork	0.75
ENSG00000168412	MTNR1A PPI subnetwork	0.75
ENSG00000070061	IKBKAP PPI subnetwork	0.75
MP:0005461	abnormal dendritic cell morphology	0.75
GO:0046209	nitric oxide metabolic process	0.75
MP:0002639	micrognathia	0.75
GO:0071496	cellular response to external stimulus	0.75
ENSG00000169031	COL4A3 PPI subnetwork	0.75
GO:0006283	transcription-coupled nucleotide-excision repair	0.75

Original gene set ID	Original gene set description	Nominal P value
ENSG00000171403	KRT9 PPI subnetwork	0.75
GO:0055002	striated muscle cell development	0.75
GO:0001158	enhancer sequence-specific DNA binding	0.75
ENSG00000128266	GNAZ PPI subnetwork	0.75
GO:0006725	cellular aromatic compound metabolic process	0.75
REACTOME_PLCG1_EVENTS_IN_ERBB2_SIGNALING	REACTOME_PLCG1_EVENTS_IN_ERBB2_SIGNALING	0.75
REACTOME_THROMBOXANE_SIGNALING_THROUGH_TP_RECEPTOR	REACTOME_THROMBOXANE_SIGNALING_THROUGH_TP_RECEPTOR	0.75
ENSG00000101150	TPD52L2 PPI subnetwork	0.75
KEGG_HYPERTROPHIC_CARDIOMYOPATHY_HCM	KEGG_HYPERTROPHIC_CARDIOMYOPATHY_HCM	0.75
ENSG00000147669	POLR2K PPI subnetwork	0.75
MP:0008023	abnormal styloid process morphology	0.75
GO:0014069	postsynaptic density	0.75
GO:0044327	dendritic spine head	0.75
GO:0006310	DNA recombination	0.75
REACTOME_P53:INDEPENDENT_G1S_DNA_DAMAGE_CHECKPOINT	REACTOME_P53:INDEPENDENT_G1S_DNA_DAMAGE_CHECKPOINT	0.75
REACTOME_P53:INDEPENDENT_DNA_DAMAGE_RESPONSE	REACTOME_P53:INDEPENDENT_DNA_DAMAGE_RESPONSE	0.75
REACTOME_UBIQUITIN_MEDIATED_DEGRADATION_OF_PHOSPHORYLATED_CD	REACTOME_UBIQUITIN_MEDIATED_DEGRADATION_OF_PHOSPHORYLATED_CDC25	0.75
ENSG00000149016	TUT1 PPI subnetwork	0.75
ENSG00000126767	ELK1 PPI subnetwork	0.75
ENSG00000108854	SMURF2 PPI subnetwork	0.75
ENSG00000126267	COX6B1 PPI subnetwork	0.75
ENSG00000092054	MYH7 PPI subnetwork	0.75
MP:0004131	abnormal embryonic cilium morphology	0.75
GO:0030071	regulation of mitotic metaphase/anaphase transition	0.75
GO:0004437	inositol or phosphatidylinositol phosphatase activity	0.75
MP:0003345	decreased rib number	0.75
GO:0051340	regulation of ligase activity	0.75
ENSG00000146535	GNA12 PPI subnetwork	0.75
ENSG00000105373	GLTSCR2 PPI subnetwork	0.75
REACTOME_EICOSANOID_LIGAND:BINDING_RECEPTORS	REACTOME_EICOSANOID_LIGAND:BINDING_RECEPTORS	0.76
ENSG00000170348	TMED10 PPI subnetwork	0.76
ENSG00000187953	ENSG00000187953 PPI subnetwork	0.76
ENSG00000122512	PMS2 PPI subnetwork	0.76
ENSG00000169249	ZRSR2 PPI subnetwork	0.76
ENSG00000136824	SMC2 PPI subnetwork	0.76
GO:0043567	regulation of insulin-like growth factor receptor signaling pathway	0.76
ENSG00000145736	GTF2H2 PPI subnetwork	0.76
GO:0032271	regulation of protein polymerization	0.76
ENSG00000116584	ARHGEF2 PPI subnetwork	0.76
ENSG00000168438	CDC40 PPI subnetwork	0.76
ENSG00000130024	PHF10 PPI subnetwork	0.76
GO:0060393	regulation of pathway-restricted SMAD protein phosphorylation	0.76
GO:0016866	intramolecular transferase activity	0.76
GO:0003002	regionalization	0.76
ENSG00000100028	SNRPD3 PPI subnetwork	0.76
ENSG00000169057	MECP2 PPI subnetwork	0.76
ENSG00000119335	SET PPI subnetwork	0.76
MP:0001052	abnormal muscle innervation	0.76
MP:0002206	abnormal CNS synaptic transmission	0.76

Original gene set ID	Original gene set description	Nominal P value
ENSG00000041357	PSMA4 PPI subnetwork	0.76
ENSG00000198910	L1CAM PPI subnetwork	0.76
GO:0015833	peptide transport	0.76
ENSG00000103671	TRIP4 PPI subnetwork	0.76
KEGG_NOD_LIKE_RECEPTOR_SIGNALING_PATHWAY	KEGG_NOD_LIKE_RECEPTOR_SIGNALING_PATHWAY	0.76
GO:0051384	response to glucocorticoid stimulus	0.76
ENSG00000153044	CENPH PPI subnetwork	0.76
ENSG00000160916	ENSG00000160916 PPI subnetwork	0.76
GO:0005743	mitochondrial inner membrane	0.76
GO:0005770	late endosome	0.76
GO:0051428	peptide hormone receptor binding	0.76
GO:0002790	peptide secretion	0.76
GO:0043161	proteasomal ubiquitin-dependent protein catabolic process	0.76
ENSG00000072682	P4HA2 PPI subnetwork	0.76
GO:0030279	negative regulation of ossification	0.76
GO:0002792	negative regulation of peptide secretion	0.76
ENSG00000110436	SLC1A2 PPI subnetwork	0.76
MP:0005517	decreased liver regeneration	0.76
ENSG00000121931	LRIF1 PPI subnetwork	0.76
ENSG00000198576	ARC PPI subnetwork	0.76
ENSG00000174231	PRPF8 PPI subnetwork	0.76
MP:0010404	ostium primum atrial septal defect	0.76
GO:0007204	elevation of cytosolic calcium ion concentration	0.76
ENSG00000128708	HAT1 PPI subnetwork	0.76
MP:0002135	abnormal kidney morphology	0.76
GO:0010576	metalloenzyme regulator activity	0.76
GO:0001510	RNA methylation	0.76
ENSG00000076053	RBM7 PPI subnetwork	0.76
GO:0031329	regulation of cellular catabolic process	0.76
ENSG00000106541	AGR2 PPI subnetwork	0.76
ENSG00000136875	PRPF4 PPI subnetwork	0.76
GO:0021782	glial cell development	0.76
GO:0051047	positive regulation of secretion	0.76
GO:0008144	drug binding	0.76
GO:0008227	G-protein coupled amine receptor activity	0.76
GO:0043392	negative regulation of DNA binding	0.76
GO:0021602	cranial nerve morphogenesis	0.76
GO:0090090	negative regulation of canonical Wnt receptor signaling pathway	0.77
GO:0006298	mismatch repair	0.77
ENSG00000133083	DCLK1 PPI subnetwork	0.77
GO:0010332	response to gamma radiation	0.77
GO:0009142	nucleoside triphosphate biosynthetic process	0.77
ENSG00000135486	HNRNPA1 PPI subnetwork	0.77
GO:0007369	gastrulation	0.77
REACTOME_M_PHASE	REACTOME_M_PHASE	0.77
ENSG00000174021	GNG5 PPI subnetwork	0.77
ENSG00000063244	U2AF2 PPI subnetwork	0.77
ENSG00000103194	USP10 PPI subnetwork	0.77
GO:0032412	regulation of ion transmembrane transporter activity	0.77

Original gene set ID	Original gene set description	Nominal P value
MP:0003702	abnormal chromosome morphology	0.77
REACTOME_CLASS_A1_RHODOPSIN:LIKE_RECEPTORS	REACTOME_CLASS_A1_RHODOPSIN:LIKE_RECEPTORS	0.77
ENSG000000116459	ATP5F1 PPI subnetwork	0.77
GO:0001533	cornified envelope	0.77
MP:0002998	abnormal bone remodeling	0.77
MP:0002682	decreased mature ovarian follicle number	0.77
ENSG00000205937	RNPS1 PPI subnetwork	0.77
ENSG000000101444	AHCY PPI subnetwork	0.77
GO:0030017	sarcomere	0.77
ENSG00000164109	MAD2L1 PPI subnetwork	0.77
GO:0010389	regulation of G2/M transition of mitotic cell cycle	0.77
ENSG00000108528	SLC25A11 PPI subnetwork	0.77
ENSG00000196284	SUPT3H PPI subnetwork	0.77
REACTOME_TANDEM_PORE_DOMAIN_POTASSIUM_CHANNELS	REACTOME_TANDEM_PORE_DOMAIN_POTASSIUM_CHANNELS	0.77
GO:0017091	AU-rich element binding	0.77
ENSG000000127928	GNGT1 PPI subnetwork	0.77
ENSG00000011007	TCEB3 PPI subnetwork	0.77
ENSG00000128609	NDUFA5 PPI subnetwork	0.77
ENSG00000182180	MRPS16 PPI subnetwork	0.77
GO:0006699	bile acid biosynthetic process	0.77
GO:0009954	proximal/distal pattern formation	0.77
REACTOME_PI3K_EVENTS_IN_ERBB2_SIGNALING	REACTOME_PI3K_EVENTS_IN_ERBB2_SIGNALING	0.77
ENSG00000136273	HUS1 PPI subnetwork	0.77
ENSG00000042832	TG PPI subnetwork	0.77
REACTOME_POLYMERASE_SWITCHING_ON_THE_C:STRAND_OF_THE_TELOMERE	REACTOME_POLYMERASE_SWITCHING_ON_THE_C:STRAND_OF_THE_TELOMERE	0.77
REACTOME_LEADING_STRAND_SYNTHESIS	REACTOME_LEADING_STRAND_SYNTHESIS	0.77
REACTOME_POLYMERASE_SWITCHING	REACTOME_POLYMERASE_SWITCHING	0.77
MP:0010856	dilated respiratory conducting tubes	0.77
KEGG_EPITHELIAL_CELL_SIGNALING_IN_HELICOBACTER_PYLORI_INFECTION	KEGG_EPITHELIAL_CELL_SIGNALING_IN_HELICOBACTER_PYLORI_INFECTION	0.77
GO:0008278	cohesin complex	0.77
ENSG00000213611	ENSG00000213611 PPI subnetwork	0.77
ENSG00000177889	UBE2N PPI subnetwork	0.77
REACTOME_PLC_BETA_MEDIATED_EVENTS	REACTOME_PLC_BETA_MEDIATED_EVENTS	0.77
MP:0002016	ovary cysts	0.77
ENSG00000147869	CER1 PPI subnetwork	0.77
ENSG00000108294	PSMB3 PPI subnetwork	0.77
GO:0042742	defense response to bacterium	0.77
GO:0008093	cytoskeletal adaptor activity	0.77
REACTOME_DUAL_INCISION_REACTION_IN_GG:NER	REACTOME_DUAL_INCISION_REACTION_IN_GG:NER	0.77
REACTOME_FORMATION_OF_INCISION_COMPLEX_IN_GG:NER	REACTOME_FORMATION_OF_INCISION_COMPLEX_IN_GG:NER	0.77
MP:0000757	herniated abdominal wall	0.77
ENSG000000164270	HTR4 PPI subnetwork	0.77
GO:0002293	alpha-beta T cell differentiation involved in immune response	0.77
GO:0002287	alpha-beta T cell activation involved in immune response	0.77
ENSG000000170558	CDH2 PPI subnetwork	0.77
ENSG00000117592	PRDX6 PPI subnetwork	0.77
ENSG000000197818	SLC9A8 PPI subnetwork	0.77
MP:0001636	irregular heartbeat	0.78
ENSG00000163082	SGPP2 PPI subnetwork	0.78

Original gene set ID**Original gene set description****Nominal P value**

MP:0001071	abnormal facial nerve morphology	0.78
ENSG00000002016	RAD52 PPI subnetwork	0.78
ENSG00000120253	NUP43 PPI subnetwork	0.78
GO:0051899	membrane depolarization	0.78
GO:0021766	hippocampus development	0.78
GO:0006836	neurotransmitter transport	0.78
GO:0042384	cilium assembly	0.78
ENSG00000179915	NRXN1 PPI subnetwork	0.78
GO:0010743	regulation of macrophage derived foam cell differentiatior	0.78
MP:0005431	decreased oocyte number	0.78
ENSG00000115233	PSMD14 PPI subnetwork	0.78
ENSG00000108272	DHRS11 PPI subnetwork	0.78
MP:0003896	prolonged PR interval	0.78
ENSG00000104852	SNRNP70 PPI subnetwork	0.78
ENSG00000067334	DNTTIP2 PPI subnetwork	0.78
MP:0000534	abnormal ureter morphology	0.78
MP:0008146	asymmetric rib-sternum attachment	0.78
MP:0000729	abnormal myogenesis	0.78
GO:0048167	regulation of synaptic plasticity	0.78
ENSG00000183023	SLC8A1 PPI subnetwork	0.78
ENSG00000153162	BMP6 PPI subnetwork	0.78
GO:0046039	GTP metabolic process	0.78
GO:0005504	fatty acid binding	0.78
ENSG00000156970	BUB1B PPI subnetwork	0.78
GO:0031966	mitochondrial membrane	0.78
ENSG00000111358	GTF2H3 PPI subnetwork	0.78
GO:0003207	cardiac chamber formation	0.78
GO:0000077	DNA damage checkpoint	0.78
ENSG00000114026	OGG1 PPI subnetwork	0.78
REACTOME_INHIBITION_OF_VOLTAGE_GATED_CA2_CHANNELS_VIA_GBETAG	REACTOME_INHIBITION_OF_VOLTAGE_GATED_CA2_CHANNELS_VIA_GBETAGAM	0.78
REACTOME_ACTIVATION_OF_G_PROTEIN_GATED_POTASSIUM_CHANNELS	REACTOME_ACTIVATION_OF_G_PROTEIN_GATED_POTASSIUM_CHANNELS	0.78
REACTOME_G_PROTEIN_GATED_POTASSIUM_CHANNELS	REACTOME_G_PROTEIN_GATED_POTASSIUM_CHANNELS	0.78
ENSG00000186852	ENSG00000186852 PPI subnetwork	0.78
GO:0007409	axonogenesis	0.78
GO:0019003	GDP binding	0.78
REACTOME_SEROTONIN_RECEPTORS	REACTOME_SEROTONIN_RECEPTORS	0.78
MP:0001093	small trigeminal ganglion	0.78
ENSG00000131876	SNRPA1 PPI subnetwork	0.78
MP:0008267	abnormal hippocampus CA3 region morphology	0.78
GO:0006595	polyamine metabolic process	0.78
GO:0007173	epidermal growth factor receptor signaling pathway	0.78
ENSG00000112559	MDF1 PPI subnetwork	0.78
MP:0003657	abnormal erythrocyte osmotic lysis	0.78
GO:0090278	negative regulation of peptide hormone secretior	0.78
ENSG00000067369	TP53BP1 PPI subnetwork	0.78
MP:0002286	cryptorchism	0.78
ENSG00000181218	HIST3H2A PPI subnetwork	0.78
ENSG00000212868	ENSG00000212868 PPI subnetwork	0.78
ENSG00000198727	MT-CYB PPI subnetwork	0.78

Original gene set ID	Original gene set description	Nominal P value
ENSG00000166508	MCM7 PPI subnetwork	0.78
ENSG00000100412	ACO2 PPI subnetwork	0.78
GO:0045202	synapse	0.78
REACTOME_JNK_C:JUN_KINASES_PHOSPHORYLATION_AND_ACTIVATION_MEDIATED_BY_JNK	REACTOME_JNK_C:JUN_KINASES_PHOSPHORYLATION_AND_ACTIVATION_MEDIATED_BY_JNK	0.78
KEGG_NICOTINATE_AND_NICOTINAMIDE_METABOLISM	KEGG_NICOTINATE_AND_NICOTINAMIDE_METABOLISM	0.78
ENSG00000075651	PLD1 PPI subnetwork	0.78
ENSG00000171848	RRM2 PPI subnetwork	0.78
GO:0030501	positive regulation of bone mineralization	0.78
MP:0006301	abnormal mesenchyme morphology	0.78
GO:0006684	sphingomyelin metabolic process	0.78
ENSG00000135823	STX6 PPI subnetwork	0.78
GO:0022898	regulation of transmembrane transporter activity	0.78
GO:0006397	mRNA processing	0.78
MP:0001096	abnormal glossopharyngeal ganglion morphology	0.78
ENSG00000168243	GNG4 PPI subnetwork	0.78
REACTOME_G2M_CHECKPOINTS	REACTOME_G2M_CHECKPOINTS	0.78
MP:0005637	abnormal iron homeostasis	0.78
ENSG00000141446	ESCO1 PPI subnetwork	0.78
ENSG00000183454	GRIN2A PPI subnetwork	0.78
GO:0019228	regulation of action potential in neuron	0.78
ENSG00000059769	DNAJC25 PPI subnetwork	0.78
ENSG00000162419	GMEB1 PPI subnetwork	0.78
GO:0009295	nucleoid	0.78
MP:0002229	neurodegeneration	0.78
ENSG00000132872	SYT4 PPI subnetwork	0.78
MP:0001525	impaired balance	0.78
REACTOME_PROTEOLYTIC_CLEAVAGE_OF_SNARE_COMPLEX_PROTEINS	REACTOME_PROTEOLYTIC_CLEAVAGE_OF_SNARE_COMPLEX_PROTEINS	0.78
REACTOME_REGULATION_OF_INSULIN_SECRETION_BY_ACETYLCHOLINE	REACTOME_REGULATION_OF_INSULIN_SECRETION_BY_ACETYLCHOLINE	0.78
REACTOME_SIGNALING_BY_ERBB2	REACTOME_SIGNALING_BY_ERBB2	0.78
ENSG00000213639	PPP1CB PPI subnetwork	0.78
ENSG00000117399	CDC20 PPI subnetwork	0.78
ENSG00000047315	POLR2B PPI subnetwork	0.78
KEGG_TYPE_I_DIABETES_MELLITUS	KEGG_TYPE_I_DIABETES_MELLITUS	0.78
ENSG00000005194	CIAPIN1 PPI subnetwork	0.78
MP:0004158	right aortic arch	0.78
MP:0003635	abnormal synaptic transmission	0.78
ENSG00000198788	MUC2 PPI subnetwork	0.78
ENSG00000198932	GPRASP1 PPI subnetwork	0.78
GO:0002292	T cell differentiation involved in immune response	0.78
ENSG00000125845	BMP2 PPI subnetwork	0.78
ENSG00000136807	CDK9 PPI subnetwork	0.78
MP:0006074	abnormal retinal rod bipolar cell morphology	0.78
REACTOME_ORGANIC_CATIONANIONZITTERION_TRANSPORT	REACTOME_ORGANIC_CATIONANIONZITTERION_TRANSPORT	0.78
GO:0005326	neurotransmitter transporter activity	0.78
GO:0010092	specification of organ identity	0.79
ENSG00000152822	GRM1 PPI subnetwork	0.79
ENSG00000071894	CPSF1 PPI subnetwork	0.79
MP:0000269	abnormal heart looping	0.79
REACTOME_BETA_DEFENSINS	REACTOME_BETA_DEFENSINS	0.79

Original gene set ID	Original gene set description	Nominal P value
GO:0070301	cellular response to hydrogen peroxide	0.79
ENSG00000213465	ARL2 PPI subnetwork	0.79
ENSG00000212874	ENSG00000212874 PPI subnetwork	0.79
ENSG00000198712	MT-CO2 PPI subnetwork	0.79
MP:0005329	abnormal myocardium layer morphology	0.79
ENSG00000196092	PAX5 PPI subnetwork	0.79
MP:0003232	abnormal forebrain development	0.79
GO:0019321	pentose metabolic process	0.79
MP:0001596	hypotension	0.79
ENSG00000182621	PLCB1 PPI subnetwork	0.79
GO:0030195	negative regulation of blood coagulation	0.79
ENSG00000173575	CHD2 PPI subnetwork	0.79
ENSG00000162704	ARPC5 PPI subnetwork	0.79
MP:0008788	abnormal fetal cardiomyocyte morphology	0.79
GO:0055080	cation homeostasis	0.79
ENSG00000164330	EBF1 PPI subnetwork	0.79
ENSG00000058272	PPP1R12A PPI subnetwork	0.79
ENSG00000142655	PEX14 PPI subnetwork	0.79
GO:0031576	G2/M transition checkpoint	0.79
GO:0008173	RNA methyltransferase activity	0.79
GO:0016849	phosphorus-oxygen lyase activity	0.79
GO:0016831	carboxy-lyase activity	0.79
ENSG00000100911	PSME2 PPI subnetwork	0.79
ENSG00000167863	ATP5H PPI subnetwork	0.79
MP:0001522	impaired swimming	0.79
GO:0001653	peptide receptor activity	0.79
MP:0000955	abnormal spinal cord morphology	0.79
GO:0031163	metallo-sulfur cluster assembly	0.79
GO:0016226	iron-sulfur cluster assembly	0.79
MP:0004252	abnormal direction of heart looping	0.79
ENSG00000181090	EHMT1 PPI subnetwork	0.79
REACTOME_ASSEMBLY_OF_THE_PRE:REPLICATIVE_COMPLEX	REACTOME_ASSEMBLY_OF_THE_PRE:REPLICATIVE_COMPLEX	0.79
REACTOME_APCCDC20_MEDIATED_DEGRADATION_OF_MITOTIC_PROTEINS	REACTOME_APCCDC20_MEDIATED_DEGRADATION_OF_MITOTIC_PROTEINS	0.79
GO:0016769	transferase activity, transferring nitrogenous groups	0.79
GO:0001935	endothelial cell proliferation	0.79
MP:0002988	decreased urine osmolality	0.79
ENSG00000100764	PSMC1 PPI subnetwork	0.79
ENSG00000165525	NEMF PPI subnetwork	0.79
MP:0005584	abnormal enzyme/coenzyme activity	0.79
MP:0001958	emphysema	0.79
GO:0009060	aerobic respiration	0.79
GO:0051707	response to other organism	0.79
GO:0051969	regulation of transmission of nerve impulse	0.79
ENSG00000177189	RPS6KA3 PPI subnetwork	0.79
MP:0003222	increased cardiomyocyte apoptosis	0.79
GO:0004518	nuclease activity	0.79
ENSG00000100567	PSMA3 PPI subnetwork	0.79
GO:0046164	alcohol catabolic process	0.79
REACTOME_DEPOLARIZATION_OF_THE_PRESYNAPTIC_TERMINAL_TRIGGERS_T	REACTOME_DEPOLARIZATION_OF_THE_PRESYNAPTIC_TERMINAL_TRIGGERS_THE_I	0.79

Original gene set ID	Original gene set description	Nominal P value
ENSG00000069329	VPS35 PPI subnetwork	0.79
MP:0000937	abnormal motor neuron morphology	0.79
REACTOME_ACTIVATED_AMPK_STIMULATES_FATTY:ACID_OXIDATION_IN_MUSCLE	REACTOME_ACTIVATED_AMPK_STIMULATES_FATTY:ACID_OXIDATION_IN_MUSCLE	0.79
ENSG00000124535	WRNIP1 PPI subnetwork	0.79
ENSG00000134371	CDC73 PPI subnetwork	0.79
ENSG00000085872	CHERP PPI subnetwork	0.79
GO:0046580	negative regulation of Ras protein signal transduction	0.79
MP:0001380	reduced male mating frequency	0.79
ENSG00000124333	VAMP7 PPI subnetwork	0.79
MP:0003313	abnormal locomotor activation	0.79
MP:0002183	gliosis	0.79
ENSG00000168522	FNTA PPI subnetwork	0.79
GO:0045669	positive regulation of osteoblast differentiation	0.79
GO:0010498	proteasomal protein catabolic process	0.79
KEGG_FATTY_ACID_METABOLISM	KEGG_FATTY_ACID_METABOLISM	0.79
REACTOME_LYSOSOME_VESICLE_BIOGENESIS	REACTOME_LYSOSOME_VESICLE_BIOGENESIS	0.79
GO:0009084	glutamine family amino acid biosynthetic process	0.79
ENSG00000117758	STX12 PPI subnetwork	0.79
GO:0021510	spinal cord development	0.79
ENSG00000178950	GAK PPI subnetwork	0.79
ENSG00000104835	FBXO17 PPI subnetwork	0.79
GO:0004745	retinol dehydrogenase activity	0.79
GO:0051537	2 iron, 2 sulfur cluster binding	0.79
ENSG00000125450	NUP85 PPI subnetwork	0.79
GO:0009201	ribonucleoside triphosphate biosynthetic process	0.79
ENSG00000104884	ERCC2 PPI subnetwork	0.79
ENSG00000003756	RBM5 PPI subnetwork	0.79
ENSG00000127922	SHFM1 PPI subnetwork	0.79
ENSG00000134899	ERCC5 PPI subnetwork	0.79
MP:0000297	abnormal atrioventricular cushion morphology	0.79
GO:0016607	nuclear speck	0.79
MP:0008221	abnormal hippocampal commissure morphology	0.79
ENSG00000173163	COMMD1 PPI subnetwork	0.79
ENSG00000139970	RTN1 PPI subnetwork	0.79
ENSG00000189283	FHIT PPI subnetwork	0.79
GO:0010578	regulation of adenylate cyclase activity involved in G-protein coupled receptor signaling pathway	0.79
GO:0007189	adenylate cyclase-activating G-protein coupled receptor signaling pathway	0.79
GO:0010579	positive regulation of adenylate cyclase activity involved in G-protein coupled receptor signaling pathway	0.79
GO:0007156	homophilic cell adhesion	0.79
ENSG00000101158	TH1L PPI subnetwork	0.79
GO:0030003	cellular cation homeostasis	0.79
ENSG00000143870	PDIAG PPI subnetwork	0.79
REACTOME_SIGNALING_BY_BMP	REACTOME_SIGNALING_BY_BMP	0.79
GO:0090087	regulation of peptide transport	0.79
GO:0002791	regulation of peptide secretion	0.79
ENSG00000035862	TIMP2 PPI subnetwork	0.79
GO:0007224	smoothed signaling pathway	0.79
GO:0042133	neurotransmitter metabolic process	0.79
GO:0000460	maturation of 5.8S rRNA	0.79

Original gene set ID	Original gene set description	Nominal P value
ENSG00000183207	RUVBL2 PPI subnetwork	0.79
MP:0005404	abnormal axon morphology	0.79
ENSG00000068323	TFE3 PPI subnetwork	0.79
GO:0051438	regulation of ubiquitin-protein ligase activity	0.79
ENSG00000117533	VAMP4 PPI subnetwork	0.79
GO:0005681	spliceosomal complex	0.79
ENSG00000140829	DHX38 PPI subnetwork	0.79
GO:0051052	regulation of DNA metabolic process	0.8
GO:0008277	regulation of G-protein coupled receptor protein signaling pathway	0.8
MP:0004966	abnormal inner cell mass proliferation	0.8
MP:0003008	enhanced long term potentiation	0.8
ENSG00000175054	ATR PPI subnetwork	0.8
ENSG00000114107	CEP70 PPI subnetwork	0.8
GO:0008430	selenium binding	0.8
ENSG00000113522	RAD50 PPI subnetwork	0.8
ENSG00000168061	SAC3D1 PPI subnetwork	0.8
ENSG00000128534	NAA38 PPI subnetwork	0.8
ENSG00000168067	MAP4K2 PPI subnetwork	0.8
GO:0031649	heat generation	0.8
ENSG00000075188	NUP37 PPI subnetwork	0.8
GO:0005865	striated muscle thin filament	0.8
ENSG00000111788	ENSG00000111788 PPI subnetwork	0.8
ENSG00000214826	ENSG00000214826 PPI subnetwork	0.8
ENSG00000137834	SMAD6 PPI subnetwork	0.8
ENSG00000172175	MALT1 PPI subnetwork	0.8
MP:0002675	asthenozoospermia	0.8
REACTOME_MITOTIC_M:MG1_PHASES	REACTOME_MITOTIC_M:MG1_PHASES	0.8
REACTOME_ACTIVATION_OF_APCC_AND_APCCDC20_MEDIATED_DEGRADATION_OF_CELL_SURFACE_RECEPTOR_TYROSINE_KINASE	REACTOME_ACTIVATION_OF_APCC_AND_APCCDC20_MEDIATED_DEGRADATION_OF_CELL_SURFACE_RECEPTOR_TYROSINE_KINASE	0.8
ENSG00000159720	ATP6V0D1 PPI subnetwork	0.8
REACTOME_NEF:MEDIATES_DOWN_MODULATION_OF_CELL_SURFACE_RECEPTOR_TYROSINE_KINASE	REACTOME_NEF:MEDIATES_DOWN_MODULATION_OF_CELL_SURFACE_RECEPTOR_TYROSINE_KINASE	0.8
GO:0000956	nuclear-transcribed mRNA catabolic process	0.8
MP:0006316	increased urine sodium level	0.8
ENSG00000140262	TCF12 PPI subnetwork	0.8
GO:0004691	cAMP-dependent protein kinase activity	0.8
GO:0031396	regulation of protein ubiquitination	0.8
ENSG00000189091	SF3B3 PPI subnetwork	0.8
REACTOME_GRB2_EVENTS_IN_ERBB2_SIGNALING	REACTOME_GRB2_EVENTS_IN_ERBB2_SIGNALING	0.8
MP:0000029	abnormal malleus morphology	0.8
GO:0044106	cellular amine metabolic process	0.8
ENSG00000151461	UPF2 PPI subnetwork	0.8
GO:0032561	guanyl ribonucleotide binding	0.8
GO:0019001	guanyl nucleotide binding	0.8
GO:0006977	DNA damage response, signal transduction by p53 class mediator resulting in cell cycle arrest	0.8
GO:0072401	signal transduction involved in DNA integrity checkpoint	0.8
GO:0072431	signal transduction involved in mitotic cell cycle G1/S transition DNA damage checkpoint	0.8
GO:0072413	signal transduction involved in mitotic cell cycle checkpoint	0.8
GO:0072422	signal transduction involved in DNA damage checkpoint	0.8
GO:0072474	signal transduction involved in mitotic cell cycle G1/S checkpoint	0.8
ENSG00000183558	HIST2H2AA3 PPI subnetwork	0.8

Original gene set ID	Original gene set description	Nominal P value
GO:0046633	alpha-beta T cell proliferation	0.8
GO:0008556	potassium-transporting ATPase activity	0.8
GO:0070663	regulation of leukocyte proliferation	0.8
ENSG00000152208	GRID2 PPI subnetwork	0.8
GO:0002053	positive regulation of mesenchymal cell proliferation	0.8
ENSG00000065609	SNAP91 PPI subnetwork	0.8
GO:0046676	negative regulation of insulin secretion	0.8
ENSG00000143228	NUF2 PPI subnetwork	0.8
ENSG00000170606	HSPA4 PPI subnetwork	0.8
ENSG00000108175	ZMIZ1 PPI subnetwork	0.8
ENSG00000172201	ID4 PPI subnetwork	0.8
GO:0051953	negative regulation of amine transport	0.8
GO:0042147	retrograde transport, endosome to Golgi	0.81
ENSG00000172572	PDE3A PPI subnetwork	0.81
ENSG00000198478	SH3BGRL2 PPI subnetwork	0.81
GO:0050819	negative regulation of coagulation	0.81
MP:0003862	decreased aggression towards males	0.81
ENSG00000102981	PARD6A PPI subnetwork	0.81
MP:0010264	increased hepatoma incidence	0.81
GO:0003211	cardiac ventricle formation	0.81
ENSG00000095002	MSH2 PPI subnetwork	0.81
REACTOME_TRANSMISSION_ACROSS_CHEMICAL_SYNAPSES	REACTOME_TRANSMISSION_ACROSS_CHEMICAL_SYNAPSES	0.81
ENSG00000170296	GABARAP PPI subnetwork	0.81
GO:0008528	G-protein coupled peptide receptor activity	0.81
GO:0006913	nucleocytoplasmic transport	0.81
GO:0031644	regulation of neurological system process	0.81
ENSG00000174243	DDX23 PPI subnetwork	0.81
GO:0032467	positive regulation of cytokinesis	0.81
ENSG00000169621	APLF PPI subnetwork	0.81
GO:0030816	positive regulation of cAMP metabolic process	0.81
GO:0030819	positive regulation of cAMP biosynthetic process	0.81
ENSG00000166579	NDEL1 PPI subnetwork	0.81
REACTOME_NCAM1_INTERACTIONS	REACTOME_NCAM1_INTERACTIONS	0.81
GO:0051046	regulation of secretion	0.81
ENSG00000106299	WASL PPI subnetwork	0.81
ENSG00000206505	HLA-A PPI subnetwork	0.81
GO:0097061	dendritic spine organization	0.81
GO:0060997	dendritic spine morphogenesis	0.81
ENSG00000129514	FOXA1 PPI subnetwork	0.81
ENSG00000211895	ENSG00000211895 PPI subnetwork	0.81
ENSG00000180353	HCLS1 PPI subnetwork	0.81
ENSG00000144231	POLR2D PPI subnetwork	0.81
MP:0001433	polyphagia	0.81
MP:0002106	abnormal muscle physiology	0.81
GO:0070717	poly-purine tract binding	0.81
ENSG00000099995	SF3A1 PPI subnetwork	0.81
ENSG00000163132	MSX1 PPI subnetwork	0.81
ENSG00000060069	CTDP1 PPI subnetwork	0.81
GO:0044243	multicellular organismal catabolic process	0.81

Original gene set ID	Original gene set description	Nominal P value
MP:0001544	abnormal cardiovascular system physiology	0.81
ENSG00000163041	H3F3A PPI subnetwork	0.81
ENSG00000132475	H3F3B PPI subnetwork	0.81
ENSG00000196285	ENSG00000196285 PPI subnetwork	0.81
ENSG00000079739	PGM1 PPI subnetwork	0.81
GO:0018209	peptidyl-serine modification	0.81
MP:0005642	decreased mean corpuscular hemoglobin concentration	0.81
MP:0001473	reduced long term potentiation	0.81
ENSG00000154582	TCEB1 PPI subnetwork	0.81
ENSG00000186318	BACE1 PPI subnetwork	0.81
GO:0009309	amine biosynthetic process	0.81
REACTOME_GABA_A_RECEPTOR_ACTIVATION	REACTOME_GABA_A_RECEPTOR_ACTIVATION	0.81
ENSG00000108840	HDAC5 PPI subnetwork	0.81
GO:0060968	regulation of gene silencing	0.81
GO:0051351	positive regulation of ligase activity	0.81
GO:0046640	regulation of alpha-beta T cell proliferation	0.81
ENSG00000064995	TAF11 PPI subnetwork	0.81
ENSG00000185049	WHSC2 PPI subnetwork	0.81
GO:0003012	muscle system process	0.81
GO:0005776	autophagic vacuole	0.81
GO:0070507	regulation of microtubule cytoskeleton organization	0.81
MP:0003130	anal atresia	0.81
ENSG00000070950	RAD18 PPI subnetwork	0.81
GO:0050662	coenzyme binding	0.81
GO:0030514	negative regulation of BMP signaling pathway	0.81
ENSG00000175166	PSMD2 PPI subnetwork	0.81
GO:0072207	metanephric epithelium development	0.81
GO:0045494	photoreceptor cell maintenance	0.81
ENSG00000105894	PTN PPI subnetwork	0.81
MP:0000690	absent spleen	0.81
ENSG00000141570	CBX8 PPI subnetwork	0.81
GO:0051606	detection of stimulus	0.81
GO:0050769	positive regulation of neurogenesis	0.81
GO:0019825	oxygen binding	0.81
ENSG00000130713	EXOSC2 PPI subnetwork	0.81
ENSG00000072501	SMC1A PPI subnetwork	0.81
REACTOME_CA:DEPENDENT_EVENTS	REACTOME_CA:DEPENDENT_EVENTS	0.81
MP:0004145	abnormal muscle electrophysiology	0.81
ENSG00000174622	ENSG00000174622 PPI subnetwork	0.81
GO:0043954	cellular component maintenance	0.81
GO:0009065	glutamine family amino acid catabolic process	0.81
ENSG00000100084	HIRA PPI subnetwork	0.81
ENSG00000153201	RANBP2 PPI subnetwork	0.81
MP:0008484	decreased spleen germinal center size	0.81
GO:0060740	prostate gland epithelium morphogenesis	0.81
ENSG00000134640	MTNR1B PPI subnetwork	0.81
MP:0005264	glomerulosclerosis	0.81
GO:0090276	regulation of peptide hormone secretion	0.81
GO:0005876	spindle microtubule	0.81

Original gene set ID	Original gene set description	Nominal P value
ENSG00000075856	SART3 PPI subnetwork	0.81
MP:0000953	abnormal oligodendrocyte morphology	0.81
MP:0003920	abnormal heart right ventricle morphology	0.81
ENSG00000166501	PRKCB PPI subnetwork	0.82
GO:0030670	phagocytic vesicle membrane	0.82
ENSG00000162923	WDR26 PPI subnetwork	0.82
ENSG00000138293	NCOA4 PPI subnetwork	0.82
KEGG_GLYCINE_SERINE_AND_THREONINE_METABOLISM	KEGG_GLYCINE_SERINE_AND_THREONINE_METABOLISM	0.82
GO:0006826	iron ion transport	0.82
GO:0022010	central nervous system myelination	0.82
GO:0032291	axon ensheathment in central nervous system	0.82
MP:0005620	abnormal muscle contractility	0.82
GO:0002042	cell migration involved in sprouting angiogenesis	0.82
GO:0005048	signal sequence binding	0.82
GO:0071248	cellular response to metal ion	0.82
ENSG00000078668	VDAC3 PPI subnetwork	0.82
ENSG00000108691	CCL2 PPI subnetwork	0.82
ENSG00000104177	MYEF2 PPI subnetwork	0.82
ENSG00000186810	CXCR3 PPI subnetwork	0.82
MP:0000153	rib bifurcation	0.82
ENSG00000155959	VBP1 PPI subnetwork	0.82
ENSG00000102683	SGCG PPI subnetwork	0.82
ENSG00000121552	CSTA PPI subnetwork	0.82
ENSG00000126215	XRCC3 PPI subnetwork	0.82
ENSG00000145494	NDUFS6 PPI subnetwork	0.82
MP:0006032	abnormal ureteric bud morphology	0.82
ENSG00000104915	STX10 PPI subnetwork	0.82
MP:0005599	increased cardiac muscle contractility	0.82
ENSG00000206328	ENSG00000206328 PPI subnetwork	0.82
ENSG00000204490	TNF PPI subnetwork	0.82
ENSG00000206439	TNF PPI subnetwork	0.82
GO:0007610	behavior	0.82
REACTOME_RNA_POLYMERASE_II_PRE:TRANSCRIPTION_EVENTS	REACTOME_RNA_POLYMERASE_II_PRE:TRANSCRIPTION_EVENTS	0.82
REACTOME_MITOTIC_PROMETAPHASE	REACTOME_MITOTIC_PROMETAPHASE	0.82
MP:0003161	absent lateral semicircular canal	0.82
GO:0032391	photoreceptor connecting cilium	0.82
ENSG00000137815	RTF1 PPI subnetwork	0.82
ENSG00000154174	TOMM70A PPI subnetwork	0.82
ENSG00000170260	ZNF212 PPI subnetwork	0.82
GO:0006406	mRNA export from nucleus	0.82
GO:0015802	basic amino acid transport	0.82
GO:0045761	regulation of adenylate cyclase activity	0.82
GO:0060198	clathrin sculpted vesicle	0.82
GO:0050755	chemokine metabolic process	0.82
ENSG00000115685	PPP1R7 PPI subnetwork	0.82
ENSG00000083312	TNPO1 PPI subnetwork	0.82
GO:0032964	collagen biosynthetic process	0.82
GO:0033205	cell cycle cytokinesis	0.82
GO:0009914	hormone transport	0.82

Original gene set ID	Original gene set description	Nominal P value
ENSG00000129170	CSRP3 PPI subnetwork	0.82
GO:0042776	mitochondrial ATP synthesis coupled proton transport	0.82
MP:0001968	abnormal touch/ nociception	0.82
KEGG_GAP_JUNCTION	KEGG_GAP_JUNCTION	0.82
REACTOME_FORMATION_OF_RNA_POL_II_ELONGATION_COMPLEX	REACTOME_FORMATION_OF_RNA_POL_II_ELONGATION_COMPLEX	0.82
REACTOME_RNA_POLYMERASE_II_TRANSCRIPTION_ELONGATION	REACTOME_RNA_POLYMERASE_II_TRANSCRIPTION_ELONGATION	0.82
REACTOME_FORMATION_OF_HIV:1_ELONGATION_COMPLEX_IN_THE_ABSENC	REACTOME_FORMATION_OF_HIV:1_ELONGATION_COMPLEX_IN_THE_ABSENCE_O	0.82
MP:0008661	decreased interleukin-10 secretion	0.82
ENSG00000143702	CEP170 PPI subnetwork	0.82
GO:0046961	proton-transporting ATPase activity, rotational mechanism	0.82
MP:0005449	abnormal food intake	0.82
ENSG00000090273	NUDC PPI subnetwork	0.82
GO:0045259	proton-transporting ATP synthase complex	0.82
GO:0021511	spinal cord patterning	0.82
ENSG00000111361	EIF2B1 PPI subnetwork	0.82
GO:0051932	synaptic transmission, GABAergic	0.82
GO:0009306	protein secretion	0.82
GO:0042744	hydrogen peroxide catabolic process	0.82
ENSG00000136152	COG3 PPI subnetwork	0.82
ENSG00000196961	AP2A1 PPI subnetwork	0.82
ENSG00000102096	PIM2 PPI subnetwork	0.82
ENSG00000169439	SDC2 PPI subnetwork	0.82
GO:0048645	organ formation	0.82
ENSG00000185624	P4HB PPI subnetwork	0.82
ENSG00000080986	NDC80 PPI subnetwork	0.82
GO:0097060	synaptic membrane	0.82
GO:0007632	visual behavior	0.82
MP:0004462	small basisphenoid bone	0.82
GO:0003785	actin monomer binding	0.82
REACTOME_GLUCAGON_SIGNALING_IN_METABOLIC_REGULATION	REACTOME_GLUCAGON_SIGNALING_IN_METABOLIC_REGULATION	0.82
GO:0050432	catecholamine secretion	0.82
GO:0031267	small GTPase binding	0.82
MP:0005352	small cranium	0.82
MP:0009712	impaired conditioned place preference behavior	0.82
ENSG00000175115	PACS1 PPI subnetwork	0.82
ENSG00000091651	ORC6 PPI subnetwork	0.82
GO:0005525	GTP binding	0.82
ENSG00000089280	FUS PPI subnetwork	0.82
GO:0034704	calcium channel complex	0.82
ENSG00000214122	ENSG00000214122 PPI subnetwork	0.82
ENSG00000145241	CENPC1 PPI subnetwork	0.82
ENSG00000117713	ARID1A PPI subnetwork	0.82
ENSG00000139546	TARBP2 PPI subnetwork	0.82
ENSG00000213672	NCKIPSD PPI subnetwork	0.82
ENSG00000170927	PKHD1 PPI subnetwork	0.82
ENSG00000080345	RIF1 PPI subnetwork	0.82
GO:0001660	fever generation	0.82
ENSG00000131795	RBM8A PPI subnetwork	0.82
ENSG00000015285	WAS PPI subnetwork	0.82

Original gene set ID	Original gene set description	Nominal P value
GO:0006103	2-oxoglutarate metabolic process	0.82
ENSG00000116350	SRSF4 PPI subnetwork	0.83
GO:0030073	insulin secretion	0.83
GO:0007602	phototransduction	0.83
GO:0032281	alpha-amino-3-hydroxy-5-methyl-4-isoxazolepropionic acid selective glutamate rece	0.83
GO:0032153	cell division site	0.83
GO:0032155	cell division site part	0.83
MP:0005027	increased susceptibility to parasitic infectior	0.83
ENSG00000125651	GTF2F1 PPI subnetwork	0.83
REACTOME_TAT:MEDIATED_ELONGATION_OF_THE_HIV:1_TRANSCRIPT	REACTOME_TAT:MEDIATED_ELONGATION_OF_THE_HIV:1_TRANSCRIPT	0.83
REACTOME_HIV:1_TRANSCRIPTION_ELONGATION	REACTOME_HIV:1_TRANSCRIPTION_ELONGATION	0.83
REACTOME_FORMATION_OF_HIV:1_ELONGATION_COMPLEX_CONTAINING_HI	REACTOME_FORMATION_OF_HIV:1_ELONGATION_COMPLEX_CONTAINING_HIV:1_	0.83
ENSG00000163541	SUCLG1 PPI subnetwork	0.83
MP:0010053	decreased grip strength	0.83
ENSG00000077420	APBB1P PPI subnetwork	0.83
GO:0051168	nuclear export	0.83
GO:0006997	nucleus organization	0.83
ENSG00000167110	GOLGA2 PPI subnetwork	0.83
GO:0009581	detection of external stimulus	0.83
ENSG00000159131	GART PPI subnetwork	0.83
ENSG00000168148	HIST3H3 PPI subnetwork	0.83
ENSG00000165916	PSMC3 PPI subnetwork	0.83
ENSG00000073792	IGF2BP2 PPI subnetwork	0.83
ENSG00000072315	TRPC5 PPI subnetwork	0.83
GO:0030574	collagen catabolic process	0.83
ENSG00000158869	FCER1G PPI subnetwork	0.83
MP:0003861	abnormal nervous system development	0.83
ENSG00000013573	DDX11 PPI subnetwork	0.83
GO:0001508	regulation of action potential	0.83
MP:0003924	herniated diaphragm	0.83
GO:0031076	embryonic camera-type eye development	0.83
ENSG00000122126	OCRL PPI subnetwork	0.83
ENSG00000168291	PDHB PPI subnetwork	0.83
ENSG00000183395	PMCH PPI subnetwork	0.83
ENSG00000182054	IDH2 PPI subnetwork	0.83
REACTOME_GLOBAL_GENOMIC_NER_GG:NER	REACTOME_GLOBAL_GENOMIC_NER_GG:NER	0.83
MP:0005107	abnormal stapes morphology	0.83
GO:0005484	SNAP receptor activity	0.83
MP:0003992	increased mortality induced by ionizing radiatior	0.83
GO:0019829	cation-transporting ATPase activity	0.83
ENSG00000167283	ATP5L PPI subnetwork	0.83
GO:0042730	fibrinolysis	0.83
GO:0034654	nucleobase-containing compound biosynthetic process	0.83
REACTOME_HIV:1_TRANSCRIPTION_INITIATION	REACTOME_HIV:1_TRANSCRIPTION_INITIATION	0.83
REACTOME_RNA_POLYMERASE_II_TRANSCRIPTION_PRE:INITIATION_AND_PRO	REACTOME_RNA_POLYMERASE_II_TRANSCRIPTION_PRE:INITIATION_AND_PROMO	0.83
REACTOME_RNA_POLYMERASE_II_TRANSCRIPTION_INITIATION	REACTOME_RNA_POLYMERASE_II_TRANSCRIPTION_INITIATION	0.83
REACTOME_RNA_POLYMERASE_II_HIV:1_PROMOTER_ESCAPE	REACTOME_RNA_POLYMERASE_II_HIV:1_PROMOTER_ESCAPE	0.83
REACTOME_RNA_POLYMERASE_II_TRANSCRIPTION_INITIATION_AND_PROMOT	REACTOME_RNA_POLYMERASE_II_TRANSCRIPTION_INITIATION_AND_PROMOTER_	0.83
REACTOME_RNA_POLYMERASE_II_PROMOTER_ESCAPE	REACTOME_RNA_POLYMERASE_II_PROMOTER_ESCAPE	0.83

Original gene set ID	Original gene set description	Nominal P value
GO:0051437	positive regulation of ubiquitin-protein ligase activity involved in mitotic cell cycle	0.83
ENSG00000185532	PRKG1 PPI subnetwork	0.83
ENSG00000089169	RPH3A PPI subnetwork	0.83
GO:0015980	energy derivation by oxidation of organic compounds	0.83
ENSG00000160062	ZBTB8A PPI subnetwork	0.83
MP:0000933	abnormal rhombomere morphology	0.83
ENSG00000178952	TUFM PPI subnetwork	0.83
GO:0033044	regulation of chromosome organization	0.83
GO:0016701	oxidoreductase activity, acting on single donors with incorporation of molecular oxy	0.83
ENSG00000160803	UBQLN4 PPI subnetwork	0.83
ENSG00000100519	PSMC6 PPI subnetwork	0.83
ENSG00000073050	XRCC1 PPI subnetwork	0.83
GO:0018130	heterocycle biosynthetic process	0.83
ENSG00000078140	UBE2K PPI subnetwork	0.83
ENSG00000171475	WIPF2 PPI subnetwork	0.83
MP:0001666	abnormal intestinal absorption	0.83
ENSG00000146047	HIST1H2BA PPI subnetwork	0.83
GO:0016445	somatic diversification of immunoglobulins	0.83
ENSG00000150753	CCT5 PPI subnetwork	0.83
GO:0009074	aromatic amino acid family catabolic process	0.83
ENSG00000171195	MUC7 PPI subnetwork	0.83
GO:0006901	vesicle coating	0.83
KEGG_RETINOL_METABOLISM	KEGG_RETINOL_METABOLISM	0.83
GO:0007271	synaptic transmission, cholinergic	0.83
GO:0006278	RNA-dependent DNA replication	0.83
MP:0004756	abnormal proximal convoluted tubule morphology	0.83
REACTOME_THE_ROLE_OF_NEF_IN_HIV:1_REPLICATION_AND_DISEASE_PATHC	REACTOME_THE_ROLE_OF_NEF_IN_HIV:1_REPLICATION_AND_DISEASE_PATHOGEN	0.83
ENSG00000129152	MYOD1 PPI subnetwork	0.83
MP:0001693	failure of primitive streak formation	0.83
GO:0000209	protein polyubiquitination	0.83
ENSG00000198211	TUBB3 PPI subnetwork	0.83
ENSG00000176788	BASP1 PPI subnetwork	0.83
ENSG00000094804	CDC6 PPI subnetwork	0.83
ENSG00000068796	KIF2A PPI subnetwork	0.83
MP:0010868	increased bone trabecula number	0.83
GO:0016675	oxidoreductase activity, acting on a heme group of donors	0.83
GO:0051339	regulation of lyase activity	0.83
ENSG00000176248	ANAPC2 PPI subnetwork	0.83
ENSG00000156467	UQCRB PPI subnetwork	0.83
GO:0005813	centrosome	0.83
ENSG00000135213	POM121C PPI subnetwork	0.83
ENSG00000119383	PPP2R4 PPI subnetwork	0.83
ENSG00000184381	PLA2G6 PPI subnetwork	0.83
ENSG00000138778	CENPE PPI subnetwork	0.83
ENSG00000167549	CORO6 PPI subnetwork	0.83
GO:0005126	cytokine receptor binding	0.83
ENSG00000188170	ENSG00000188170 PPI subnetwork	0.83
REACTOME_FORMATION_OF_ATP_BY_CHEMIOSMOTIC_COUPLING	REACTOME_FORMATION_OF_ATP_BY_CHEMIOSMOTIC_COUPLING	0.83
REACTOME_EGFR_DOWNREGULATION	REACTOME_EGFR_DOWNREGULATION	0.83

Original gene set ID	Original gene set description	Nominal P value
ENSG00000130340	SNX9 PPI subnetwork	0.83
GO:0005849	mRNA cleavage factor complex	0.83
GO:0048305	immunoglobulin secretion	0.83
REACTOME_PKA_ACTIVATION	REACTOME_PKA_ACTIVATION	0.83
REACTOME_PROCESSING_OF_CAPPED_INTRON:CONTAINING_PRE:MRNA	REACTOME_PROCESSING_OF_CAPPED_INTRON:CONTAINING_PRE:MRNA	0.83
ENSG00000177084	POLE PPI subnetwork	0.83
ENSG00000163161	ERCC3 PPI subnetwork	0.83
ENSG00000133116	KL PPI subnetwork	0.83
ENSG00000141034	C17orf39 PPI subnetwork	0.83
ENSG00000110801	PSMD9 PPI subnetwork	0.83
ENSG00000150086	GRIN2B PPI subnetwork	0.83
ENSG00000159164	SV2A PPI subnetwork	0.83
GO:0050670	regulation of lymphocyte proliferation	0.83
GO:0051169	nuclear transport	0.84
ENSG00000091181	IL5RA PPI subnetwork	0.84
GO:0009070	serine family amino acid biosynthetic process	0.84
MP:0003311	aminoaciduria	0.84
REACTOME_MRNA_SPLICING_:MINOR_PATHWAY	REACTOME_MRNA_SPLICING_:MINOR_PATHWAY	0.84
ENSG00000112379	KIAA1244 PPI subnetwork	0.84
MP:0001415	increased exploration in new environment	0.84
GO:0006260	DNA replication	0.84
GO:0009584	detection of visible light	0.84
ENSG00000100292	HMOX1 PPI subnetwork	0.84
ENSG00000178741	COX5A PPI subnetwork	0.84
GO:0090101	negative regulation of transmembrane receptor protein serine/threonine kinase signaling	0.84
GO:0031279	regulation of cyclase activity	0.84
MP:0006108	abnormal hindbrain development	0.84
GO:0031401	positive regulation of protein modification processes	0.84
MP:0002753	dilated heart left ventricle	0.84
GO:0008188	neuropeptide receptor activity	0.84
ENSG00000132464	ENAM PPI subnetwork	0.84
ENSG00000075785	RAB7A PPI subnetwork	0.84
GO:0006206	pyrimidine base metabolic process	0.84
GO:0016879	ligase activity, forming carbon-nitrogen bonds	0.84
ENSG00000133226	SRRM1 PPI subnetwork	0.84
GO:0016918	retinal binding	0.84
ENSG00000111786	SRSF9 PPI subnetwork	0.84
GO:0004222	metalloendopeptidase activity	0.84
GO:0048037	cofactor binding	0.84
REACTOME_DEADENYLATION:DEPENDENT_MRNA_DECAY	REACTOME_DEADENYLATION:DEPENDENT_MRNA_DECAY	0.84
GO:0006091	generation of precursor metabolites and energy	0.84
GO:0009607	response to biotic stimulus	0.84
ENSG00000204356	RDBP PPI subnetwork	0.84
ENSG00000206268	RDBP PPI subnetwork	0.84
ENSG00000206357	RDBP PPI subnetwork	0.84
ENSG00000183625	CCR3 PPI subnetwork	0.84
ENSG00000160201	U2AF1 PPI subnetwork	0.84
ENSG00000100650	SRSF5 PPI subnetwork	0.84
ENSG00000156261	CCT8 PPI subnetwork	0.84

Original gene set ID	Original gene set description	Nominal P value
ENSG00000169750	RAC3 PPI subnetwork	0.84
GO:0008333	endosome to lysosome transport	0.84
GO:0016180	snRNA processing	0.84
GO:0032270	positive regulation of cellular protein metabolic process	0.84
MP:0004777	abnormal phospholipid level	0.84
GO:0006816	calcium ion transport	0.84
ENSG000000085415	SEH1L PPI subnetwork	0.84
MP:0003484	abnormal channel response	0.84
GO:0005501	retinoid binding	0.84
GO:0005689	U12-type spliceosomal complex	0.84
GO:0030804	positive regulation of cyclic nucleotide biosynthetic process	0.84
GO:0030810	positive regulation of nucleotide biosynthetic process	0.84
ENSG00000137337	MDC1 PPI subnetwork	0.84
ENSG00000206385	ENSG00000206385 PPI subnetwork	0.84
GO:0035148	tube formation	0.84
REACTOME_CHEMOKINE_RECEPTORS_BIND_CHEMOKINES	REACTOME_CHEMOKINE_RECEPTORS_BIND_CHEMOKINES	0.84
ENSG00000117560	FASLG PPI subnetwork	0.84
ENSG00000120910	PPP3CC PPI subnetwork	0.84
ENSG00000103740	ACSBG1 PPI subnetwork	0.84
ENSG00000149295	DRD2 PPI subnetwork	0.84
REACTOME_LATE_PHASE_OF_HIV_LIFE_CYCLE	REACTOME_LATE_PHASE_OF_HIV_LIFE_CYCLE	0.84
ENSG00000141367	CLTC PPI subnetwork	0.84
ENSG00000152700	SAR1B PPI subnetwork	0.84
GO:2000177	regulation of neural precursor cell proliferation	0.84
REACTOME_DEFENSINS	REACTOME_DEFENSINS	0.84
ENSG00000215305	VPS16 PPI subnetwork	0.84
ENSG00000105926	MPP6 PPI subnetwork	0.84
GO:0007416	synapse assembly	0.84
GO:0031902	late endosome membrane	0.84
GO:0032673	regulation of interleukin-4 production	0.84
MP:0002893	ketoaciduria	0.84
ENSG00000168530	MYL1 PPI subnetwork	0.84
GO:0021537	telencephalon development	0.84
GO:0031397	negative regulation of protein ubiquitination	0.84
ENSG00000143727	ACP1 PPI subnetwork	0.84
REACTOME PRESYNAPTIC_FUNCTION_OF_KAINATE_RECEPTORS	REACTOME PRESYNAPTIC_FUNCTION_OF_KAINATE_RECEPTORS	0.84
GO:0009617	response to bacterium	0.84
GO:0030903	notochord development	0.84
GO:0006979	response to oxidative stress	0.84
ENSG00000158864	NDUFS2 PPI subnetwork	0.84
GO:0004033	aldo-keto reductase (NADP) activity	0.84
ENSG00000176986	SEC24C PPI subnetwork	0.84
GO:0006368	transcription elongation from RNA polymerase II promoter	0.84
REACTOME_HIV_LIFE_CYCLE	REACTOME_HIV_LIFE_CYCLE	0.84
GO:0048484	enteric nervous system development	0.84
MP:0010810	increased type II pneumocyte number	0.84
GO:0072079	nephron tubule formation	0.84
MP:0002084	abnormal developmental patterning	0.84
ENSG00000160551	TAOK1 PPI subnetwork	0.84

Original gene set ID	Original gene set description	Nominal P value
ENSG00000122180	MYOG PPI subnetwork	0.84
ENSG00000144642	RBMS3 PPI subnetwork	0.84
GO:0005125	cytokine activity	0.84
ENSG00000180190	C8orf42 PPI subnetwork	0.84
ENSG00000151224	MAT1A PPI subnetwork	0.84
GO:0032633	interleukin-4 production	0.84
ENSG00000164815	ORC5 PPI subnetwork	0.84
ENSG00000101413	RPRD1B PPI subnetwork	0.84
ENSG00000156049	GNA14 PPI subnetwork	0.84
ENSG00000125351	UPF3B PPI subnetwork	0.84
GO:0051054	positive regulation of DNA metabolic process	0.84
MP:0000877	abnormal Purkinje cell morphology	0.84
MP:0003730	abnormal photoreceptor inner segment morphology	0.84
GO:0032784	regulation of transcription elongation, DNA-dependent	0.84
GO:0002474	antigen processing and presentation of peptide antigen via MHC class	0.84
ENSG00000149311	ATM PPI subnetwork	0.84
GO:0060512	prostate gland morphogenesis	0.84
MP:0000929	open neural tube	0.84
GO:0042613	MHC class II protein complex	0.84
GO:0000375	RNA splicing, via transesterification reactions	0.84
REACTOME_E2F_MEDIATED_REGULATION_OF_DNA_REPLICATION	REACTOME_E2F_MEDIATED_REGULATION_OF_DNA_REPLICATION	0.84
ENSG00000134602	ENSG00000134602 PPI subnetwork	0.84
ENSG00000085662	AKR1B1 PPI subnetwork	0.84
GO:0009635	response to herbicide	0.84
GO:0008353	RNA polymerase II carboxy-terminal domain kinase activity	0.84
REACTOME_MUSCLE_CONTRACTION	REACTOME_MUSCLE_CONTRACTION	0.84
GO:0006220	pyrimidine nucleotide metabolic process	0.84
GO:0043395	heparan sulfate proteoglycan binding	0.84
GO:0007033	vacuole organization	0.84
MP:0004073	caudal body truncation	0.84
REACTOME_PROCESSING_OF_INTRONLESS_PRE:MRNAS	REACTOME_PROCESSING_OF_INTRONLESS_PRE:MRNAS	0.84
REACTOME_MRNA_PROCESSING	REACTOME_MRNA_PROCESSING	0.84
GO:0006511	ubiquitin-dependent protein catabolic process	0.84
GO:0000152	nuclear ubiquitin ligase complex	0.85
GO:0004993	serotonin receptor activity	0.85
ENSG00000138385	SSB PPI subnetwork	0.85
ENSG00000172409	CLP1 PPI subnetwork	0.85
GO:0009165	nucleotide biosynthetic process	0.85
ENSG00000163737	PF4 PPI subnetwork	0.85
REACTOME_DNA_REPAIR	REACTOME_DNA_REPAIR	0.85
ENSG00000169020	ATP5I PPI subnetwork	0.85
GO:0006813	potassium ion transport	0.85
REACTOME_TRANSCRIPTION_OF_THE_HIV_GENOME	REACTOME_TRANSCRIPTION_OF_THE_HIV_GENOME	0.85
GO:0030312	external encapsulating structure	0.85
GO:0006140	regulation of nucleotide metabolic process	0.85
ENSG00000100804	PSMB5 PPI subnetwork	0.85
MP:0005650	abnormal limb bud morphology	0.85
MP:0002718	abnormal inner cell mass morphology	0.85
REACTOME_MYOGENESIS	REACTOME_MYOGENESIS	0.85

Original gene set ID	Original gene set description	Nominal P value
REACTOME_CDO_IN_MYOGENESIS	REACTOME_CDO_IN_MYOGENESIS	0.85
GO:0048813	dendrite morphogenesis	0.85
MP:0009336	increased splenocyte proliferation	0.85
ENSG00000060339	CCAR1 PPI subnetwork	0.85
GO:0030838	positive regulation of actin filament polymerization	0.85
GO:0050807	regulation of synapse organization	0.85
MP:0003290	intestinal hypoperistalsis	0.85
REACTOME_TRANSPORT_OF_MATURE_MRNA_DERIVED_FROM_AN_INTRONLESS_TRANSCRIPT	REACTOME_TRANSPORT_OF_MATURE_MRNA_DERIVED_FROM_AN_INTRONLESS_TRANSCRIPT	0.85
GO:0009799	specification of symmetry	0.85
ENSG00000115145	STAM2 PPI subnetwork	0.85
GO:0032944	regulation of mononuclear cell proliferation	0.85
MP:0000272	abnormal aorta morphology	0.85
GO:0015812	gamma-aminobutyric acid transport	0.85
ENSG00000115875	SRSF7 PPI subnetwork	0.85
GO:0042220	response to cocaine	0.85
GO:0014073	response to tropane	0.85
ENSG00000171724	VAT1L PPI subnetwork	0.85
MP:0002575	increased circulating ketone body level	0.85
GO:0004842	ubiquitin-protein ligase activity	0.85
ENSG00000109111	SUPT6H PPI subnetwork	0.85
ENSG00000144028	SNRNP200 PPI subnetwork	0.85
MP:0000266	abnormal heart morphology	0.85
ENSG00000142039	CCDC97 PPI subnetwork	0.85
GO:0005815	microtubule organizing center	0.85
GO:0048701	embryonic cranial skeleton morphogenesis	0.85
ENSG00000198523	PLN PPI subnetwork	0.85
GO:0051443	positive regulation of ubiquitin-protein ligase activity	0.85
ENSG00000136450	SRSF1 PPI subnetwork	0.85
GO:0042743	hydrogen peroxide metabolic process	0.85
REACTOME_SIGNALLING_TO_P38_VIA_RIT_AND_RIN	REACTOME_SIGNALLING_TO_P38_VIA_RIT_AND_RIN	0.85
ENSG00000205531	NAP1L4 PPI subnetwork	0.85
ENSG00000088256	GNA11 PPI subnetwork	0.85
ENSG00000157020	SEC13 PPI subnetwork	0.85
REACTOME_PKA_ACTIVATION_IN_GLUCAGON_SIGNALLING	REACTOME_PKA_ACTIVATION_IN_GLUCAGON_SIGNALLING	0.85
REACTOME_CALCITONIN-LIKE_LIGAND_RECEPTORS	REACTOME_CALCITONIN-LIKE_LIGAND_RECEPTORS	0.85
ENSG00000110717	NDUFS8 PPI subnetwork	0.85
ENSG00000102387	TAF7L PPI subnetwork	0.85
ENSG00000129084	PSMA1 PPI subnetwork	0.85
ENSG00000100280	AP1B1 PPI subnetwork	0.85
GO:0006360	transcription from RNA polymerase I promoter	0.85
GO:0051536	iron-sulfur cluster binding	0.85
GO:0051540	metal cluster binding	0.85
ENSG00000134444	KIAA1468 PPI subnetwork	0.85
GO:0016032	viral reproduction	0.85
ENSG00000141232	TOB1 PPI subnetwork	0.85
GO:0030239	myofibril assembly	0.85
MP:0006089	abnormal vestibular sacculle morphology	0.85
ENSG00000105705	SUGP1 PPI subnetwork	0.85
MP:0003149	abnormal tectorial membrane morphology	0.85

Original gene set ID	Original gene set description	Nominal P value
GO:0003382	epithelial cell morphogenesis	0.86
GO:0008608	attachment of spindle microtubules to kinetochore	0.86
GO:0042354	L-fucose metabolic process	0.86
ENSG00000133812	SBF2 PPI subnetwork	0.86
ENSG00000124507	PACSIN1 PPI subnetwork	0.86
MP:0004738	abnormal brainstem auditory evoked potentia	0.86
REACTOME_PROSTACYCLIN_SIGNALLING_THROUGH_PROSTACYCLIN_RECEPTOR	REACTOME_PROSTACYCLIN_SIGNALLING_THROUGH_PROSTACYCLIN_RECEPTOR	0.86
ENSG00000143079	CTTNBP2NL PPI subnetwork	0.86
GO:0006887	exocytosis	0.86
ENSG00000152056	AP1S3 PPI subnetwork	0.86
REACTOME_CAM_PATHWAY	REACTOME_CAM_PATHWAY	0.86
REACTOME_CALMODULIN_INDUCED_EVENTS	REACTOME_CALMODULIN_INDUCED_EVENTS	0.86
GO:0000781	chromosome, telomeric region	0.86
REACTOME_AMINE_LIGAND_BINDING_RECEPTORS	REACTOME_AMINE_LIGAND_BINDING_RECEPTORS	0.86
ENSG00000107371	EXOSC3 PPI subnetwork	0.86
REACTOME_SIGNALING_BY_ROBO_RECEPTOR	REACTOME_SIGNALING_BY_ROBO_RECEPTOR	0.86
ENSG00000188986	COBRA1 PPI subnetwork	0.86
REACTOME_ADHERENS_JUNCTIONS_INTERACTIONS	REACTOME_ADHERENS_JUNCTIONS_INTERACTIONS	0.86
ENSG00000122566	HNRNPA2B1 PPI subnetwork	0.86
MP:0000359	abnormal mast cell morphology	0.86
MP:0004722	abnormal platelet dense granule number	0.86
ENSG00000188342	GTF2F2 PPI subnetwork	0.86
GO:0001774	microglial cell activation	0.86
ENSG00000127920	GNG11 PPI subnetwork	0.86
ENSG00000112079	STK38 PPI subnetwork	0.86
GO:0009953	dorsal/ventral pattern formation	0.86
GO:0031032	actomyosin structure organization	0.86
GO:0050912	detection of chemical stimulus involved in sensory perception of taste	0.86
ENSG00000132383	RPA1 PPI subnetwork	0.86
ENSG00000086102	NFX1 PPI subnetwork	0.86
ENSG00000182185	RAD51B PPI subnetwork	0.86
ENSG00000183856	IQGAP3 PPI subnetwork	0.86
GO:0048483	autonomic nervous system development	0.86
GO:0023021	termination of signal transduction	0.86
ENSG00000169813	HNRNPF PPI subnetwork	0.86
ENSG00000100503	NIN PPI subnetwork	0.86
ENSG00000159377	PSMB4 PPI subnetwork	0.86
GO:0016702	oxidoreductase activity, acting on single donors with incorporation of molecular oxy	0.86
GO:0009582	detection of abiotic stimulus	0.86
MP:0009760	abnormal mitotic spindle morphology	0.86
MP:0004568	fusion of glossopharyngeal and vagus nerve	0.86
MP:0008148	abnormal rib-sternum attachment	0.86
ENSG00000160199	PKNOX1 PPI subnetwork	0.86
MP:0004970	kidney atrophy	0.86
ENSG00000077063	CTTNBP2 PPI subnetwork	0.86
ENSG00000124193	SRSF6 PPI subnetwork	0.86
MP:0004163	abnormal adenohypophysis morphology	0.86
GO:0034622	cellular macromolecular complex assembly	0.86
ENSG00000145321	GC PPI subnetwork	0.86

Original gene set ID	Original gene set description	Nominal P value
REACTOME_G_ALPHA_I_SIGNALLING_EVENTS	REACTOME_G_ALPHA_I_SIGNALLING_EVENTS	0.86
ENSG00000175550	DRAP1 PPI subnetwork	0.86
MP:0002115	abnormal limb bone morphology	0.86
GO:0044242	cellular lipid catabolic process	0.86
ENSG00000176102	CSTF3 PPI subnetwork	0.86
GO:0016073	snRNA metabolic process	0.86
GO:0004065	arylsulfatase activity	0.86
REACTOME_MRNA_SPLICING	REACTOME_MRNA_SPLICING	0.86
REACTOME_MRNA_SPLICING_: _MAJOR_PATHWAY	REACTOME_MRNA_SPLICING_: _MAJOR_PATHWAY	0.86
ENSG00000185291	IL3RA PPI subnetwork	0.86
GO:0050908	detection of light stimulus involved in visual perceptior	0.86
GO:0050962	detection of light stimulus involved in sensory perceptior	0.86
GO:0006200	ATP catabolic process	0.86
MP:0001906	increased dopamine level	0.86
GO:0032228	regulation of synaptic transmission, GABAergic	0.86
ENSG00000156304	SCAF4 PPI subnetwork	0.86
ENSG00000114554	PLXNA1 PPI subnetwork	0.86
ENSG00000132561	MATN2 PPI subnetwork	0.86
ENSG00000100632	ERH PPI subnetwork	0.86
GO:0050660	flavin adenine dinucleotide binding	0.86
GO:0009855	determination of bilateral symmetry	0.86
GO:0045211	postsynaptic membrane	0.86
GO:0019941	modification-dependent protein catabolic process	0.86
ENSG00000137767	SQRDL PPI subnetwork	0.86
GO:0048706	embryonic skeletal system development	0.86
GO:0031201	SNARE complex	0.86
GO:0030258	lipid modification	0.86
GO:0030170	pyridoxal phosphate binding	0.86
GO:0070279	vitamin B6 binding	0.86
ENSG00000139433	GLTP PPI subnetwork	0.86
ENSG00000063601	MTMR1 PPI subnetwork	0.86
ENSG00000148773	MKI67 PPI subnetwork	0.86
REACTOME_SYNTHESIS_OF_BILE_ACIDS_AND_BILE_SALTS_VIA_7ALPHA:HYDRO	REACTOME_SYNTHESIS_OF_BILE_ACIDS_AND_BILE_SALTS_VIA_7ALPHA:HYDROXYC	0.86
MP:0001883	mammary adenocarcinoma	0.86
ENSG00000135744	AGT PPI subnetwork	0.86
MP:0004936	impaired branching involved in ureteric bud morphogenesis	0.86
ENSG00000162385	MAGOH PPI subnetwork	0.86
MP:0004835	abnormal miniature endplate potential	0.86
GO:0031398	positive regulation of protein ubiquitinatio	0.86
ENSG00000127527	EPS15L1 PPI subnetwork	0.86
ENSG00000103507	BCKDK PPI subnetwork	0.86
GO:0006071	glycerol metabolic process	0.86
KEGG_LONG_TERM_POTENTIATION	KEGG_LONG_TERM_POTENTIATION	0.86
MP:0001970	abnormal pain threshold	0.86
GO:0007420	brain development	0.86
ENSG00000116852	KIF21B PPI subnetwork	0.86
GO:0017016	Ras GTPase binding	0.87
GO:0042594	response to starvation	0.87
ENSG00000071794	HLTF PPI subnetwork	0.87

Original gene set ID	Original gene set description	Nominal P value
MP:0002920	decreased paired-pulse facilitation	0.87
MP:0008272	abnormal endochondral bone ossification	0.87
MP:0002066	abnormal motor capabilities/coordination/movement	0.87
MP:0009133	decreased white fat cell size	0.87
ENSG00000120254	MTHFD1L PPI subnetwork	0.87
GO:0005328	neurotransmitter:sodium symporter activity	0.87
GO:0033108	mitochondrial respiratory chain complex assembly	0.87
ENSG00000206503	HLA-A PPI subnetwork	0.87
ENSG00000013583	HEBP1 PPI subnetwork	0.87
MP:0005171	absent coat pigmentation	0.87
ENSG00000170310	STX8 PPI subnetwork	0.87
REACTOME_CLATHRIN_DERIVED_VESICLE_BUDDING	REACTOME_CLATHRIN_DERIVED_VESICLE_BUDDING	0.87
REACTOME_TRANS:GOLGI_NETWORK_VESICLE_BUDDING	REACTOME_TRANS:GOLGI_NETWORK_VESICLE_BUDDING	0.87
GO:0016790	thiolester hydrolase activity	0.87
ENSG00000151923	TIAL1 PPI subnetwork	0.87
MP:0005193	abnormal anterior eye segment morphology	0.87
ENSG00000137259	HIST1H2AB PPI subnetwork	0.87
ENSG00000168274	HIST1H2AE PPI subnetwork	0.87
REACTOME_NEUROTRANSMITTER_RECEPTOR_BINDING_AND_DOWNSTREAM_TRANSDUCTION	REACTOME_NEUROTRANSMITTER_RECEPTOR_BINDING_AND_DOWNSTREAM_TRANSDUCTION	0.87
GO:0050803	regulation of synapse structure and activity	0.87
ENSG00000163159	VPS72 PPI subnetwork	0.87
ENSG00000111245	MYL2 PPI subnetwork	0.87
ENSG00000155130	MARCKS PPI subnetwork	0.87
GO:0021953	central nervous system neuron differentiation	0.87
GO:0006213	pyrimidine nucleoside metabolic process	0.87
ENSG00000125354	SEPT6 PPI subnetwork	0.87
GO:0043632	modification-dependent macromolecule catabolic process	0.87
ENSG00000090060	PAPOLA PPI subnetwork	0.87
REACTOME_ADP_SIGNALLING_THROUGH_P2Y_PURINOCEPTOR_12	REACTOME_ADP_SIGNALLING_THROUGH_P2Y_PURINOCEPTOR_12	0.87
MP:0002633	persistent truncus arteriosus	0.87
ENSG00000134690	CDCA8 PPI subnetwork	0.87
ENSG00000116329	OPRD1 PPI subnetwork	0.87
GO:0051028	mRNA transport	0.87
MP:0002332	abnormal exercise endurance	0.87
GO:0019787	small conjugating protein ligase activity	0.87
GO:0051966	regulation of synaptic transmission, glutamatergic	0.87
ENSG00000167977	KCTD5 PPI subnetwork	0.87
ENSG00000168298	HIST1H1E PPI subnetwork	0.87
ENSG00000173636	ENSG00000173636 PPI subnetwork	0.87
ENSG00000166477	LEO1 PPI subnetwork	0.87
ENSG00000069424	KCNAB2 PPI subnetwork	0.87
ENSG00000085365	ENSG00000085365 PPI subnetwork	0.87
MP:0010107	abnormal renal reabsorption	0.87
ENSG00000089053	ANAPC5 PPI subnetwork	0.87
MP:0005445	abnormal neurotransmitter secretion	0.87
GO:0019363	pyridine nucleotide biosynthetic process	0.87
GO:0072525	pyridine-containing compound biosynthetic process	0.87
GO:0009064	glutamine family amino acid metabolic process	0.87
GO:0007190	activation of adenylate cyclase activity	0.87

Original gene set ID	Original gene set description	Nominal P value
ENSG00000165494	PCF11 PPI subnetwork	0.87
ENSG00000083857	FAT1 PPI subnetwork	0.87
ENSG00000070961	ATP2B1 PPI subnetwork	0.87
ENSG00000138668	HNRNPD PPI subnetwork	0.87
ENSG00000068878	PSME4 PPI subnetwork	0.87
MP:0003864	abnormal midbrain development	0.87
MP:0005191	head tilt	0.87
MP:0000189	hypoglycemia	0.87
ENSG00000171497	PPID PPI subnetwork	0.87
ENSG00000125266	EFNB2 PPI subnetwork	0.87
GO:0070403	NAD+ binding	0.87
ENSG00000149532	CPSF7 PPI subnetwork	0.87
GO:0021527	spinal cord association neuron differentiator	0.87
GO:0032813	tumor necrosis factor receptor superfamily binding	0.88
ENSG00000174851	YIF1A PPI subnetwork	0.88
GO:0060487	lung epithelial cell differentiation	0.88
ENSG00000141503	MINK1 PPI subnetwork	0.88
ENSG00000080603	SRCAP PPI subnetwork	0.88
ENSG00000099622	CIRBP PPI subnetwork	0.88
GO:0051213	dioxygenase activity	0.88
REACTOME_REGULATION_OF_INSULIN_SECRETION_BY_GLU	REACTOME_REGULATION_OF_INSULIN_SECRETION_BY_GLU	0.88
ENSG00000105011	ASF1B PPI subnetwork	0.88
MP:0004819	decreased skeletal muscle mass	0.88
REACTOME_AMYLOIDS	REACTOME_AMYLOIDS	0.88
MP:0005075	abnormal melanosome morphology	0.88
KEGG_TRYPTOPHAN_METABOLISM	KEGG_TRYPTOPHAN_METABOLISM	0.88
ENSG00000031691	CENPQ PPI subnetwork	0.88
GO:2000516	positive regulation of CD4-positive, alpha-beta T cell activator	0.88
GO:0043372	positive regulation of CD4-positive, alpha-beta T cell differentiator	0.88
ENSG00000120334	CENPL PPI subnetwork	0.88
ENSG00000116095	PLEKHA3 PPI subnetwork	0.88
GO:0045762	positive regulation of adenylate cyclase activity	0.88
GO:0031281	positive regulation of cyclase activity	0.88
ENSG00000089685	BIRC5 PPI subnetwork	0.88
GO:0021781	glial cell fate commitment	0.88
ENSG00000120699	EXOSC8 PPI subnetwork	0.88
ENSG00000103363	TCEB2 PPI subnetwork	0.88
MP:0010984	abnormal metanephric mesenchyme morphology	0.88
ENSG00000169213	RAB3B PPI subnetwork	0.88
ENSG00000179899	ENSG00000179899 PPI subnetwork	0.88
ENSG00000196531	NACA PPI subnetwork	0.88
GO:0072080	nephron tubule development	0.88
MP:0004066	abnormal primitive node morphology	0.88
GO:0051439	regulation of ubiquitin-protein ligase activity involved in mitotic cell cycle	0.88
ENSG00000148835	TAF5 PPI subnetwork	0.88
ENSG00000095585	BLNK PPI subnetwork	0.88
GO:0001838	embryonic epithelial tube formation	0.88
ENSG00000184408	KCND2 PPI subnetwork	0.88
ENSG00000171793	CTPS PPI subnetwork	0.88

Original gene set ID**Original gene set description****Nominal P value**

ENSG00000197905	TEAD4 PPI subnetwork	0.88
ENSG00000140379	BCL2A1 PPI subnetwork	0.88
MP:0002058	neonatal lethality	0.88
GO:0032934	sterol binding	0.88
MP:0005157	holoprosencephaly	0.88
GO:0048002	antigen processing and presentation of peptide antigen	0.88
GO:0051058	negative regulation of small GTPase mediated signal transduction	0.88
MP:0004599	abnormal vertebral arch morphology	0.88
GO:0051349	positive regulation of lyase activity	0.88
GO:0031145	anaphase-promoting complex-dependent proteasomal ubiquitin-dependent protein	0.88
GO:0007223	Wnt receptor signaling pathway, calcium modulating pathway	0.88
GO:0007218	neuropeptide signaling pathway	0.88
GO:0032835	glomerulus development	0.88
GO:0000236	mitotic prometaphase	0.88
REACTOME_AMINO_ACID_SYNTHESIS_AND_INTERCONVERSION_TRANSAMINATION	REACTOME_AMINO_ACID_SYNTHESIS_AND_INTERCONVERSION_TRANSAMINATION	0.88
GO:0035249	synaptic transmission, glutamatergic	0.88
GO:0005753	mitochondrial proton-transporting ATP synthase complex	0.88
ENSG00000184575	XPOT PPI subnetwork	0.88
ENSG00000137947	GTF2B PPI subnetwork	0.88
GO:0010972	negative regulation of G2/M transition of mitotic cell cycle	0.88
ENSG00000110768	GTF2H1 PPI subnetwork	0.88
ENSG00000117153	KLHL12 PPI subnetwork	0.88
ENSG00000168002	POLR2G PPI subnetwork	0.88
ENSG00000138663	COPS4 PPI subnetwork	0.88
MP:0003120	abnormal tracheal cartilage morphology	0.88
ENSG00000172660	TAF15 PPI subnetwork	0.88
ENSG00000119203	CPSF3 PPI subnetwork	0.88
ENSG00000164076	CAMKV PPI subnetwork	0.88
MP:0000783	abnormal forebrain morphology	0.88
ENSG00000132334	PTPRE PPI subnetwork	0.88
MP:0002841	impaired skeletal muscle contractility	0.88
ENSG00000132692	BCAN PPI subnetwork	0.88
ENSG00000095380	NANS PPI subnetwork	0.88
MP:0000270	abnormal heart tube morphology	0.88
GO:0003009	skeletal muscle contraction	0.88
GO:0034614	cellular response to reactive oxygen species	0.88
GO:0060590	ATPase regulator activity	0.88
REACTOME_MEMBRANE_TRAFFICKING	REACTOME_MEMBRANE_TRAFFICKING	0.88
ENSG00000102384	CENPI PPI subnetwork	0.88
GO:0032465	regulation of cytokinesis	0.88
GO:0006284	base-excision repair	0.88
ENSG00000137642	SORL1 PPI subnetwork	0.88
ENSG00000106100	NOD1 PPI subnetwork	0.88
GO:0045981	positive regulation of nucleotide metabolic process	0.88
ENSG00000197111	PCBP2 PPI subnetwork	0.88
ENSG00000177302	TOP3A PPI subnetwork	0.88
ENSG00000165934	CPSF2 PPI subnetwork	0.88
GO:0042088	T-helper 1 type immune response	0.88
GO:0047496	vesicle transport along microtubule	0.88

Original gene set ID	Original gene set description	Nominal P value
ENSG00000196747	HIST1H2AI PPI subnetwork	0.89
ENSG00000196787	HIST1H2AG PPI subnetwork	0.89
ENSG00000196866	HIST1H2AD PPI subnetwork	0.89
ENSG00000184348	HIST1H2AK PPI subnetwork	0.89
ENSG00000198374	HIST1H2AL PPI subnetwork	0.89
ENSG00000198728	LDB1 PPI subnetwork	0.89
GO:0000910	cytokinesis	0.89
ENSG00000103496	STX4 PPI subnetwork	0.89
REACTOME_PLATELET_CALCIIUM_HOMEOSTASIS	REACTOME_PLATELET_CALCIIUM_HOMEOSTASIS	0.89
MP:0005478	decreased circulating thyroxine level	0.89
MP:0003172	abnormal lysosome physiology	0.89
GO:0016620	oxidoreductase activity, acting on the aldehyde or oxo group of donors, NAD or NAC	0.89
ENSG00000184886	PIGW PPI subnetwork	0.89
ENSG00000159251	ACTC1 PPI subnetwork	0.89
ENSG00000169564	PCBP1 PPI subnetwork	0.89
REACTOME_TRANSPORT_OF_MATURE_MRNA_DERIVED_FROM_AN_INTRON:CONT	REACTOME_TRANSPORT_OF_MATURE_MRNA_DERIVED_FROM_AN_INTRON:CONT	0.89
GO:0050671	positive regulation of lymphocyte proliferation	0.89
ENSG00000100162	CENPM PPI subnetwork	0.89
ENSG00000198938	MT-CO3 PPI subnetwork	0.89
GO:0008374	O-acyltransferase activity	0.89
MP:0000940	abnormal motor neuron innervation	0.89
GO:0046605	regulation of centrosome cycle	0.89
MP:0001422	abnormal drinking behavior	0.89
GO:0021889	olfactory bulb interneuron differentiator	0.89
REACTOME_FORMATION_OF_THE_HIV:1_EARLY_ELONGATION_COMPLEX	REACTOME_FORMATION_OF_THE_HIV:1_EARLY_ELONGATION_COMPLEX	0.89
REACTOME_FORMATION_OF_THE_EARLY_ELONGATION_COMPLEX	REACTOME_FORMATION_OF_THE_EARLY_ELONGATION_COMPLEX	0.89
ENSG00000156052	GNAQ PPI subnetwork	0.89
GO:0030016	myofibril	0.89
ENSG00000152253	SPC25 PPI subnetwork	0.89
GO:0003156	regulation of organ formation	0.89
ENSG00000087250	MT3 PPI subnetwork	0.89
ENSG00000188312	CENPP PPI subnetwork	0.89
GO:0060428	lung epithelium development	0.89
MP:0002231	abnormal primitive streak morphology	0.89
ENSG00000165119	HNRNPK PPI subnetwork	0.89
REACTOME_ENDOSOMAL_SORTING_COMPLEX_REQUIRED_FOR_TRANSPORT_ESCR	REACTOME_ENDOSOMAL_SORTING_COMPLEX_REQUIRED_FOR_TRANSPORT_ESCR	0.89
GO:0008542	visual learning	0.89
ENSG00000114503	NCBP2 PPI subnetwork	0.89
ENSG00000115163	CENPA PPI subnetwork	0.89
MP:0003324	increased liver adenoma incidence	0.89
GO:0000149	SNARE binding	0.89
REACTOME_CDC6_ASSOCIATION_WITH_THE_ORCORIGIN_COMPLEX	REACTOME_CDC6_ASSOCIATION_WITH_THE_ORCORIGIN_COMPLEX	0.89
ENSG00000110955	ATP5B PPI subnetwork	0.89
GO:0005891	voltage-gated calcium channel complex	0.89
ENSG00000105669	COPE PPI subnetwork	0.89
GO:0001936	regulation of endothelial cell proliferati	0.89
KEGG_PEROXISOME	KEGG_PEROXISOME	0.89
ENSG00000013455	ENSG00000013455 PPI subnetwork	0.89
GO:0050997	quaternary ammonium group binding	0.89

Original gene set ID	Original gene set description	Nominal P value
MP:0004084	abnormal cardiac muscle relaxation	0.89
ENSG00000155974	GRIP1 PPI subnetwork	0.89
GO:0016331	morphogenesis of embryonic epithelium	0.89
ENSG00000115953	ENSG00000115953 PPI subnetwork	0.89
MP:0005192	increased motor neuron number	0.89
MP:0001286	abnormal eye development	0.89
MP:0005106	abnormal incus morphology	0.89
ENSG00000115252	PDE1A PPI subnetwork	0.89
GO:0005834	heterotrimeric G-protein complex	0.89
GO:0006000	fructose metabolic process	0.89
MP:0003271	abnormal duodenum morphology	0.89
GO:0045333	cellular respiration	0.89
ENSG00000136709	WDR33 PPI subnetwork	0.89
KEGG_SNARE_INTERACTIONS_IN_VESICULAR_TRANSPORT	KEGG_SNARE_INTERACTIONS_IN_VESICULAR_TRANSPORT	0.89
GO:0006873	cellular ion homeostasis	0.89
GO:0002208	somatic diversification of immunoglobulins involved in immune response	0.89
GO:0045190	isotype switching	0.89
GO:0002204	somatic recombination of immunoglobulin genes involved in immune response	0.89
GO:0021513	spinal cord dorsal/ventral patterning	0.89
REACTOME_TRANSPORT_OF_MATURE_MRNAS_DERIVED_FROM_INTRONLESS	REACTOME_TRANSPORT_OF_MATURE_MRNAS_DERIVED_FROM_INTRONLESS_TRA	0.89
REACTOME_THROMBIN_SIGNALLING_THROUGH_PROTEINASE_ACTIVATED_RECE	REACTOME_THROMBIN_SIGNALLING_THROUGH_PROTEINASE_ACTIVATED_RECE	0.89
KEGG_ARGININE_AND_PROLINE_METABOLISM	KEGG_ARGININE_AND_PROLINE_METABOLISM	0.9
ENSG00000108828	VAT1 PPI subnetwork	0.9
GO:0051082	unfolded protein binding	0.9
GO:0007215	glutamate receptor signaling pathway	0.9
MP:0002766	situs inversus	0.9
GO:0050806	positive regulation of synaptic transmission	0.9
GO:0042288	MHC class I protein binding	0.9
ENSG00000138674	SEC31A PPI subnetwork	0.9
ENSG00000105379	ETFB PPI subnetwork	0.9
ENSG00000187735	TCEA1 PPI subnetwork	0.9
MP:0002696	decreased circulating glucagon level	0.9
MP:0004566	myocardial fiber degeneration	0.9
GO:0007200	phospholipase C-activating G-protein coupled receptor signaling pathway	0.9
MP:0002279	abnormal diaphragm morphology	0.9
GO:0032880	regulation of protein localization	0.9
ENSG00000130066	SAT1 PPI subnetwork	0.9
MP:0005317	increased triglyceride level	0.9
GO:0022904	respiratory electron transport chain	0.9
GO:0006308	DNA catabolic process	0.9
ENSG00000112526	ENSG00000112526 PPI subnetwork	0.9
ENSG00000204256	BRD2 PPI subnetwork	0.9
ENSG00000215077	BRD2 PPI subnetwork	0.9
ENSG00000126698	DNAJC8 PPI subnetwork	0.9
ENSG00000002834	LASP1 PPI subnetwork	0.9
GO:0045063	T-helper 1 cell differentiation	0.9
ENSG00000169371	SNUPN PPI subnetwork	0.9
GO:0048710	regulation of astrocyte differentiation	0.9
GO:0060191	regulation of lipase activity	0.9

Original gene set ID	Original gene set description	Nominal P value
GO:0010243	response to organic nitrogen	0.9
GO:0017085	response to insecticide	0.9
ENSG000000134109	EDEM1 PPI subnetwork	0.9
GO:0046467	membrane lipid biosynthetic process	0.9
ENSG000000114573	ATP6V1A PPI subnetwork	0.9
GO:0072593	reactive oxygen species metabolic process	0.9
KEGG_SULFUR_METABOLISM	KEGG_SULFUR_METABOLISM	0.9
GO:0050881	musculoskeletal movement	0.9
GO:0050879	multicellular organismal movement	0.9
GO:0050953	sensory perception of light stimulus	0.9
ENSG000000169045	HNRNPH1 PPI subnetwork	0.9
ENSG000000096717	SIRT1 PPI subnetwork	0.9
GO:0007601	visual perception	0.9
GO:0005814	centriole	0.9
ENSG000000090989	EXOC1 PPI subnetwork	0.9
GO:0030163	protein catabolic process	0.9
ENSG000000181029	TRAPPC5 PPI subnetwork	0.9
GO:0032993	protein-DNA complex	0.9
ENSG000000184983	NDUFA6 PPI subnetwork	0.9
ENSG000000185658	BRWD1 PPI subnetwork	0.9
REACTOME_TRANSCRIPTION:COUPLED_NER_TC:NER	REACTOME_TRANSCRIPTION:COUPLED_NER_TC:NER	0.9
KEGG_CITRATE_CYCLE_TCA_CYCLE	KEGG_CITRATE_CYCLE_TCA_CYCLE	0.9
ENSG000000057468	MSH4 PPI subnetwork	0.9
ENSG000000147443	DOK2 PPI subnetwork	0.9
GO:0050690	regulation of defense response to virus by virus	0.9
ENSG000000105656	ELL PPI subnetwork	0.9
GO:0051983	regulation of chromosome segregation	0.9
GO:0034440	lipid oxidation	0.9
ENSG000000157344	ENSG000000157344 PPI subnetwork	0.9
ENSG000000105289	TJP3 PPI subnetwork	0.9
ENSG000000198648	STK39 PPI subnetwork	0.9
ENSG000000028137	TNFRSF1B PPI subnetwork	0.9
GO:0015949	nucleobase-containing small molecule interconversion	0.9
REACTOME_G:PROTEIN_ACTIVATION	REACTOME_G:PROTEIN_ACTIVATION	0.9
ENSG000000165023	DIRAS2 PPI subnetwork	0.9
ENSG000000092201	SUPT16H PPI subnetwork	0.9
GO:0051018	protein kinase A binding	0.9
MP:0003463	abnormal single cell response	0.9
ENSG000000128524	ATP6V1F PPI subnetwork	0.9
MP:0000841	abnormal hindbrain morphology	0.9
GO:0033013	tetrapyrrole metabolic process	0.9
GO:0006778	porphyrin-containing compound metabolic process	0.9
KEGG_NUCLEOTIDE_EXCISION_REPAIR	KEGG_NUCLEOTIDE_EXCISION_REPAIR	0.9
ENSG000000213619	NDUFS3 PPI subnetwork	0.91
KEGG_GLYCOSAMINOGLYCAN_BIOSYNTHESIS_KERATAN_SULFATE	KEGG_GLYCOSAMINOGLYCAN_BIOSYNTHESIS_KERATAN_SULFATE	0.91
GO:0048713	regulation of oligodendrocyte differentiation	0.91
GO:0060425	lung morphogenesis	0.91
GO:0015030	Cajal body	0.91
ENSG000000138092	CENPO PPI subnetwork	0.91

Original gene set ID	Original gene set description	Nominal P value
MP:0010392	prolonged QRS complex duration	0.91
ENSG00000008869	HEATR5B PPI subnetwork	0.91
ENSG00000171759	PAH PPI subnetwork	0.91
ENSG00000151834	GABRA2 PPI subnetwork	0.91
GO:0043292	contractile fiber	0.91
GO:0001823	mesonephros development	0.91
GO:0042311	vasodilation	0.91
ENSG00000205339	IPO7 PPI subnetwork	0.91
MP:0003817	abnormal pituitary diverticulum morphology	0.91
MP:0005332	abnormal amino acid level	0.91
GO:0030667	secretory granule membrane	0.91
MP:0000087	absent mandible	0.91
ENSG00000177455	CD19 PPI subnetwork	0.91
GO:0016447	somatic recombination of immunoglobulin gene segments	0.91
GO:0008484	sulfuric ester hydrolase activity	0.91
ENSG00000149503	INCENP PPI subnetwork	0.91
GO:0032886	regulation of microtubule-based process	0.91
ENSG00000113282	CLINT1 PPI subnetwork	0.91
MP:0005402	abnormal action potential	0.91
REACTOME_OPIOID_SIGNALLING	REACTOME_OPIOID_SIGNALLING	0.91
GO:0050708	regulation of protein secretion	0.91
ENSG00000145335	SNCA PPI subnetwork	0.91
MP:0006254	thin cerebral cortex	0.91
ENSG00000115091	ACTR3 PPI subnetwork	0.91
MP:0001292	abnormal lens vesicle development	0.91
GO:0008408	3'-5' exonuclease activity	0.91
GO:0045073	regulation of chemokine biosynthetic process	0.91
GO:0051233	spindle midzone	0.91
REACTOME_NUCLEOTIDE_EXCISION_REPAIR	REACTOME_NUCLEOTIDE_EXCISION_REPAIR	0.91
GO:0002381	immunoglobulin production involved in immunoglobulin mediated immune respons	0.91
REACTOME_GOLGI_ASSOCIATED_VESICLE_BIOGENESIS	REACTOME_GOLGI_ASSOCIATED_VESICLE_BIOGENESIS	0.91
ENSG00000143799	PARP1 PPI subnetwork	0.91
ENSG00000174442	ZWILCH PPI subnetwork	0.91
MP:0008874	decreased physiological sensitivity to xenobiotic	0.91
MP:0004754	abnormal kidney collecting duct morphology	0.91
ENSG00000100401	RANGAP1 PPI subnetwork	0.91
ENSG00000189060	H1FO PPI subnetwork	0.91
REACTOME_RESOLUTION_OF_ABASIC_SITES_AP_SITES	REACTOME_RESOLUTION_OF_ABASIC_SITES_AP_SITES	0.92
REACTOME_BASE_EXCISION_REPAIR	REACTOME_BASE_EXCISION_REPAIR	0.92
ENSG00000117697	NSL1 PPI subnetwork	0.92
GO:0072243	metanephric nephron epithelium development	0.92
GO:0072234	metanephric nephron tubule development	0.92
GO:0000175	3'-5'-exoribonuclease activity	0.92
REACTOME_REGULATION_OF_ORNITHINE_DECARBOXYLASE_ODC	REACTOME_REGULATION_OF_ORNITHINE_DECARBOXYLASE_ODC	0.92
MP:0001684	abnormal axial mesoderm	0.92
GO:0030880	RNA polymerase complex	0.92
GO:0042402	cellular biogenic amine catabolic process	0.92
ENSG00000159082	SYNJ1 PPI subnetwork	0.92
REACTOME_BILE_ACID_AND_BILE_SALT_METABOLISM	REACTOME_BILE_ACID_AND_BILE_SALT_METABOLISM	0.92

Original gene set ID	Original gene set description	Nominal P value
GO:0006613	cotranslational protein targeting to membrane	0.92
ENSG00000126945	HNRNPH2 PPI subnetwork	0.92
ENSG00000171747	LGALS4 PPI subnetwork	0.92
GO:0002828	regulation of type 2 immune response	0.92
ENSG00000004487	KDM1A PPI subnetwork	0.92
ENSG00000158022	TRIM63 PPI subnetwork	0.92
REACTOME_ABORTIVE_ELONGATION_OF_HIV:1_TRANSCRIPT_IN_THE_ABSENC	REACTOME_ABORTIVE_ELONGATION_OF_HIV:1_TRANSCRIPT_IN_THE_ABSENCE_O	0.92
GO:0051436	negative regulation of ubiquitin-protein ligase activity involved in mitotic cell cycl	0.92
GO:0030317	sperm motility	0.92
ENSG00000198824	CHAMP1 PPI subnetwork	0.92
GO:0048013	ephrin receptor signaling pathway	0.92
GO:0001706	endoderm formation	0.92
ENSG00000100241	SBF1 PPI subnetwork	0.92
GO:0048708	astrocyte differentiation	0.92
ENSG00000184432	COPB2 PPI subnetwork	0.92
GO:0016594	glycine binding	0.92
ENSG000000070182	SPTB PPI subnetwork	0.92
GO:0050657	nucleic acid transport	0.92
GO:0051236	establishment of RNA localization	0.92
GO:0050658	RNA transport	0.92
ENSG00000010818	HIVEP2 PPI subnetwork	0.92
GO:0071158	positive regulation of cell cycle arrest	0.92
ENSG00000122705	CLTA PPI subnetwork	0.92
ENSG00000105258	POLR2I PPI subnetwork	0.92
GO:0042588	zymogen granule	0.92
GO:0070665	positive regulation of leukocyte proliferation	0.92
GO:0005932	microtubule basal body	0.92
GO:0031594	neuromuscular junction	0.92
GO:0016862	intramolecular oxidoreductase activity, interconverting keto- and enol-group:	0.92
GO:0006370	mRNA capping	0.92
ENSG00000132639	SNAP25 PPI subnetwork	0.92
GO:0030900	forebrain development	0.92
GO:0070972	protein localization in endoplasmic reticulum	0.92
ENSG00000115128	ENSG00000115128 PPI subnetwork	0.92
GO:0060079	regulation of excitatory postsynaptic membrane potentia	0.92
GO:0070647	protein modification by small protein conjugation or remova	0.92
KEGG_VIBRIO_CHOLERAЕ_INFECTION	KEGG_VIBRIO_CHOLERAЕ_INFECTION	0.92
GO:0016676	oxidoreductase activity, acting on a heme group of donors, oxygen as accepto	0.92
GO:0015002	heme-copper terminal oxidase activity	0.92
GO:0004129	cytochrome-c oxidase activity	0.92
ENSG00000154710	RABGEF1 PPI subnetwork	0.92
GO:0044257	cellular protein catabolic process	0.92
GO:0016917	GABA receptor activity	0.92
ENSG00000048828	FAM120A PPI subnetwork	0.92
ENSG00000166226	CCT2 PPI subnetwork	0.92
GO:0009264	deoxyribonucleotide catabolic process	0.92
GO:0030313	cell envelope	0.92
GO:0044462	external encapsulating structure part	0.92
ENSG00000154723	ATP5J PPI subnetwork	0.92

Original gene set ID	Original gene set description	Nominal P value
ENSG00000137825	ITPKA PPI subnetwork	0.92
MP:0009838	abnormal sperm axoneme morphology	0.92
ENSG00000164402	SEPT8 PPI subnetwork	0.92
GO:0002637	regulation of immunoglobulin production	0.92
GO:0031334	positive regulation of protein complex assembly	0.92
REACTOME_ACTIVATION_OF_KAINATE_RECEPTORS_UPON_Glutamate_BINDING	REACTOME_ACTIVATION_OF_KAINATE_RECEPTORS_UPON_Glutamate_BINDING	0.92
GO:0001759	organ induction	0.92
ENSG00000109519	GRPEL1 PPI subnetwork	0.92
ENSG00000147099	HDAC8 PPI subnetwork	0.92
ENSG00000100410	PHF5A PPI subnetwork	0.92
ENSG00000160783	PMF1 PPI subnetwork	0.92
ENSG00000142856	ITGB3BP PPI subnetwork	0.92
GO:0072210	metanephric nephron development	0.92
GO:0050433	regulation of catecholamine secretion	0.92
ENSG00000065150	IPO5 PPI subnetwork	0.92
GO:0010959	regulation of metal ion transport	0.92
REACTOME_AMINE_COMPOUND_SLC_TRANSPORTERS	REACTOME_AMINE_COMPOUND_SLC_TRANSPORTERS	0.92
ENSG00000102109	PCSK1N PPI subnetwork	0.92
ENSG00000122952	ZWINT PPI subnetwork	0.92
GO:0043034	costamere	0.92
REACTOME_TRAFFICKING_OF_AMPA_RECEPTORS	REACTOME_TRAFFICKING_OF_AMPA_RECEPTORS	0.92
REACTOME_Glutamate_BINDING_ACTIVATION_OF_AMPA_RECEPTORS_AND_SYN	REACTOME_Glutamate_BINDING_ACTIVATION_OF_AMPA_RECEPTORS_AND_SYN	0.92
GO:0019395	fatty acid oxidation	0.92
GO:0042436	indole-containing compound catabolic process	0.92
GO:0046218	indolalkylamine catabolic process	0.92
GO:0006569	tryptophan catabolic process	0.92
ENSG00000188386	PPP3R2 PPI subnetwork	0.92
MP:0004615	cervical vertebral transformation	0.92
ENSG00000121621	KIF18A PPI subnetwork	0.92
ENSG00000119318	RAD23B PPI subnetwork	0.92
ENSG00000115254	ENSG00000115254 PPI subnetwork	0.92
ENSG00000167136	ENDOG PPI subnetwork	0.92
GO:0016197	endosomal transport	0.92
GO:0016469	proton-transporting two-sector ATPase complex	0.92
ENSG00000060558	GNA15 PPI subnetwork	0.92
MP:0001905	abnormal dopamine level	0.92
ENSG00000129473	BCL2L2 PPI subnetwork	0.92
ENSG00000168496	FEN1 PPI subnetwork	0.92
ENSG00000167083	GNGT2 PPI subnetwork	0.92
REACTOME_Glucagon:TYPE_Ligand_Receptors	REACTOME_Glucagon:TYPE_Ligand_Receptors	0.92
ENSG00000118680	MYL12B PPI subnetwork	0.92
GO:0046503	glycerolipid catabolic process	0.92
ENSG00000124610	HIST1H1A PPI subnetwork	0.92
REACTOME_INSULIN_RECEPTOR_RECYCLING	REACTOME_INSULIN_RECEPTOR_RECYCLING	0.92
GO:0006281	DNA repair	0.92
REACTOME_STRIATED_MUSCLE_CONTRACTION	REACTOME_STRIATED_MUSCLE_CONTRACTION	0.92
GO:0030148	sphingolipid biosynthetic process	0.92
GO:0016054	organic acid catabolic process	0.92
GO:0046395	carboxylic acid catabolic process	0.92

Original gene set ID	Original gene set description	Nominal P value
REACTOME_DARPP:32_EVENTS	REACTOME_DARPP:32_EVENTS	0.92
GO:0006521	regulation of cellular amino acid metabolic process	0.92
MP:0004101	abnormal brain interneuron morphology	0.93
ENSG00000129990	SYT5 PPI subnetwork	0.93
ENSG00000184702	SEPT5 PPI subnetwork	0.93
ENSG00000183474	GTF2H2C PPI subnetwork	0.93
ENSG00000124795	DEK PPI subnetwork	0.93
ENSG00000112290	WASF1 PPI subnetwork	0.93
GO:0009583	detection of light stimulus	0.93
GO:0072073	kidney epithelium development	0.93
GO:0016236	macroautophagy	0.93
MP:0003672	abnormal ureter development	0.93
ENSG00000159259	CHAF1B PPI subnetwork	0.93
ENSG00000143368	SF3B4 PPI subnetwork	0.93
GO:0006721	terpenoid metabolic process	0.93
REACTOME_IRON_UPTAKE_AND_TRANSPORT	REACTOME_IRON_UPTAKE_AND_TRANSPORT	0.93
ENSG00000153207	AHCTF1 PPI subnetwork	0.93
GO:0032446	protein modification by small protein conjugation	0.93
GO:0044447	axoneme part	0.93
GO:0007626	locomotory behavior	0.93
GO:0042033	chemokine biosynthetic process	0.93
GO:0005245	voltage-gated calcium channel activity	0.93
REACTOME_INHIBITION_OF_INSULIN_SECRETION_BY_ADRENALINENORADRENALIN	REACTOME_INHIBITION_OF_INSULIN_SECRETION_BY_ADRENALINENORADRENALIN	0.93
ENSG00000124172	ATP5E PPI subnetwork	0.93
ENSG00000025800	KPNA6 PPI subnetwork	0.93
REACTOME_TRYPTOPHAN_CATABOLISM	REACTOME_TRYPTOPHAN_CATABOLISM	0.93
ENSG00000184357	HIST1H1B PPI subnetwork	0.93
GO:0050905	neuromuscular process	0.93
ENSG00000138071	ACTR2 PPI subnetwork	0.93
REACTOME_ENERGY_DEPENDENT_REGULATION_OF_MTOR_BY_LKB1:AMPK	REACTOME_ENERGY_DEPENDENT_REGULATION_OF_MTOR_BY_LKB1:AMPK	0.93
MP:0001898	abnormal long term depression	0.93
KEGG_GLYOXYLATE_AND_DICARBOXYLATE_METABOLISM	KEGG_GLYOXYLATE_AND_DICARBOXYLATE_METABOLISM	0.93
GO:0006289	nucleotide-excision repair	0.93
ENSG00000163636	PSMD6 PPI subnetwork	0.93
ENSG00000168556	ING2 PPI subnetwork	0.93
GO:0030594	neurotransmitter receptor activity	0.93
GO:0000775	chromosome, centromeric region	0.93
ENSG00000166337	TAF10 PPI subnetwork	0.93
REACTOME_SYNTHESIS_AND_INTERCONVERSION_OF_NUCLEOTIDE_DI:_AND_T	REACTOME_SYNTHESIS_AND_INTERCONVERSION_OF_NUCLEOTIDE_DI:_AND_TRIP	0.93
GO:0007413	axonal fasciculation	0.93
ENSG00000143850	PLEKHA6 PPI subnetwork	0.93
REACTOME_INSULIN_SYNTHESIS_AND_PROCESSING	REACTOME_INSULIN_SYNTHESIS_AND_PROCESSING	0.93
GO:0032838	cell projection cytoplasm	0.93
ENSG00000106588	PSMA2 PPI subnetwork	0.93
MP:0000750	abnormal muscle regeneration	0.93
ENSG00000198947	DMD PPI subnetwork	0.93
GO:0034453	microtubule anchoring	0.93
GO:0042573	retinoic acid metabolic process	0.93
ENSG00000133059	DSTYK PPI subnetwork	0.93

Original gene set ID**Original gene set description****Nominal P value**

GO:0016829	lyase activity	0.93
GO:0009055	electron carrier activity	0.93
GO:0009620	response to fungus	0.93
MP:0002239	abnormal nasal septum morphology	0.93
GO:0004221	ubiquitin thiolesterase activity	0.93
GO:0010888	negative regulation of lipid storage	0.93
GO:0051287	NAD binding	0.93
MP:0004452	abnormal pterygoid process morphology	0.93
GO:0006120	mitochondrial electron transport, NADH to ubiquinone	0.93
ENSG00000088832	FKBP1A PPI subnetwork	0.93
GO:0051298	centrosome duplication	0.93
REACTOME_ACTIVATION_OF_CA:PERMEABLE_KAINATE_RECEPTOR	REACTOME_ACTIVATION_OF_CA:PERMEABLE_KAINATE_RECEPTOR	0.93
REACTOME_IONOTROPIC_ACTIVITY_OF_KAINATE_RECEPTORS	REACTOME_IONOTROPIC_ACTIVITY_OF_KAINATE_RECEPTORS	0.93
ENSG00000087263	OGFOD1 PPI subnetwork	0.93
ENSG00000100985	MMP9 PPI subnetwork	0.93
REACTOME_METABOLISM_OF_AMINO_ACIDS_AND_DERIVATIVES	REACTOME_METABOLISM_OF_AMINO_ACIDS_AND_DERIVATIVES	0.93
ENSG00000103423	DNAJA3 PPI subnetwork	0.93
ENSG00000172977	KAT5 PPI subnetwork	0.93
REACTOME_CELL_CYCLE_CHECKPOINTS	REACTOME_CELL_CYCLE_CHECKPOINTS	0.93
ENSG00000105726	ATP13A1 PPI subnetwork	0.93
ENSG00000089818	NECAP1 PPI subnetwork	0.93
GO:0006081	cellular aldehyde metabolic process	0.94
ENSG00000165868	HSPA12A PPI subnetwork	0.94
GO:0072283	metanephric renal vesicle morphogenesis	0.94
MP:0003054	spina bifida	0.94
ENSG00000105514	RAB3D PPI subnetwork	0.94
GO:0072170	metanephric tubule development	0.94
GO:0016706	oxidoreductase activity, acting on paired donors, with incorporation or reduction of	0.94
ENSG00000137575	SDCBP PPI subnetwork	0.94
ENSG00000185973	TMLHE PPI subnetwork	0.94
GO:0009063	cellular amino acid catabolic process	0.94
MP:0003137	abnormal impulse conducting system conduction	0.94
ENSG00000173366	ENSG00000173366 PPI subnetwork	0.94
GO:0030878	thyroid gland development	0.94
GO:0010043	response to zinc ion	0.94
GO:0006568	tryptophan metabolic process	0.94
GO:0016796	exonuclease activity, active with either ribo- or deoxyribonucleic acids and producin	0.94
GO:0007611	learning or memory	0.94
KEGG_RNA_DEGRADATION	KEGG_RNA_DEGRADATION	0.94
GO:0000783	nuclear telomere cap complex	0.94
GO:0000782	telomere cap complex	0.94
ENSG00000100167	SEPT3 PPI subnetwork	0.94
GO:0016574	histone ubiquitination	0.94
MP:0002090	abnormal vision	0.94
ENSG00000006740	ARHGAP44 PPI subnetwork	0.94
ENSG00000143106	PSMA5 PPI subnetwork	0.94
ENSG00000101654	RNMT PPI subnetwork	0.94
ENSG00000125814	NAPB PPI subnetwork	0.94
ENSG00000185104	FAF1 PPI subnetwork	0.94

Original gene set ID	Original gene set description	Nominal P value
GO:0031023	microtubule organizing center organization	0.94
GO:0030968	endoplasmic reticulum unfolded protein response	0.94
GO:0034620	cellular response to unfolded protein	0.94
ENSG00000120265	PCMT1 PPI subnetwork	0.94
ENSG00000169217	CD2BP2 PPI subnetwork	0.94
GO:0055093	response to hyperoxia	0.94
ENSG00000197299	BLM PPI subnetwork	0.94
REACTOME_METABOLISM_OF_PORPHYRINS	REACTOME_METABOLISM_OF_PORPHYRINS	0.94
GO:0001655	urogenital system development	0.94
ENSG00000107554	DNMBP PPI subnetwork	0.94
GO:0021954	central nervous system neuron development	0.94
ENSG00000125870	SNRBP2 PPI subnetwork	0.94
ENSG00000105509	HAS1 PPI subnetwork	0.94
REACTOME_HIV_INFECTION	REACTOME_HIV_INFECTION	0.94
REACTOME_REGULATION_OF_AMPK_ACTIVITY_VIA_LKB1	REACTOME_REGULATION_OF_AMPK_ACTIVITY_VIA_LKB1	0.94
REACTOME_ACTIVATION_OF_GENES_BY_ATF4	REACTOME_ACTIVATION_OF_GENES_BY_ATF4	0.94
MP:0000830	abnormal diencephalon morphology	0.94
ENSG00000181555	SETD2 PPI subnetwork	0.94
GO:0048168	regulation of neuronal synaptic plasticity	0.94
ENSG00000066248	NGEF PPI subnetwork	0.94
GO:0048557	embryonic digestive tract morphogenesis	0.94
ENSG00000172732	MUS81 PPI subnetwork	0.94
ENSG00000072864	NDE1 PPI subnetwork	0.94
GO:0031646	positive regulation of neurological system process	0.94
ENSG00000188486	H2AFX PPI subnetwork	0.94
GO:0009310	amine catabolic process	0.94
GO:0008066	glutamate receptor activity	0.94
GO:0001822	kidney development	0.94
ENSG00000065833	ME1 PPI subnetwork	0.94
ENSG00000164687	FABP5 PPI subnetwork	0.94
GO:0051297	centrosome organization	0.94
MP:0005533	increased body temperature	0.94
ENSG00000161057	PSMC2 PPI subnetwork	0.94
ENSG00000115808	STRN PPI subnetwork	0.94
GO:0060193	positive regulation of lipase activity	0.94
ENSG00000205726	ITSN1 PPI subnetwork	0.94
KEGG_NEUROACTIVE_LIGAND_RECEPTOR_INTERACTION	KEGG_NEUROACTIVE_LIGAND_RECEPTOR_INTERACTION	0.94
GO:0045295	gamma-catenin binding	0.94
ENSG00000115760	BIRC6 PPI subnetwork	0.94
MP:0003384	abnormal ventral body wall morphology	0.94
REACTOME_PACKAGING_OF_TELOMERE_ENDS	REACTOME_PACKAGING_OF_TELOMERE_ENDS	0.94
ENSG00000183091	NEB PPI subnetwork	0.94
GO:0072001	renal system development	0.94
ENSG00000107611	CUBN PPI subnetwork	0.94
MP:0008789	abnormal olfactory epithelium morphology	0.94
GO:0055072	iron ion homeostasis	0.94
MP:0001787	pericardial edema	0.94
MP:0001777	abnormal body temperature homeostasis	0.94
MP:0003063	increased coping response	0.94

Original gene set ID	Original gene set description	Nominal P value
ENSG00000189043	NDUFA4 PPI subnetwork	0.95
ENSG00000180817	PPA1 PPI subnetwork	0.95
GO:0003678	DNA helicase activity	0.95
GO:0006775	fat-soluble vitamin metabolic process	0.95
ENSG00000088320	REM1 PPI subnetwork	0.95
ENSG00000022355	GABRA1 PPI subnetwork	0.95
ENSG00000167491	GATAD2A PPI subnetwork	0.95
GO:0014075	response to amine stimulus	0.95
ENSG00000183765	CHEK2 PPI subnetwork	0.95
ENSG00000169189	NSMCE1 PPI subnetwork	0.95
MP:0004736	abnormal distortion product otoacoustic emission	0.95
GO:0010518	positive regulation of phospholipase activity	0.95
ENSG00000149136	SSRP1 PPI subnetwork	0.95
ENSG00000169925	BRD3 PPI subnetwork	0.95
GO:0072087	renal vesicle development	0.95
REACTOME_SYNTHESIS_SECRETION_AND_INACTIVATION_OF_GLU	REACTOME_SYNTHESIS_SECRETION_AND_INACTIVATION_OF_GLU	0.95
GO:0031234	extrinsic to internal side of plasma membrane	0.95
GO:0032982	myosin filament	0.95
GO:0060249	anatomical structure homeostasis	0.95
ENSG00000182473	EXOC7 PPI subnetwork	0.95
ENSG00000179091	CYC1 PPI subnetwork	0.95
GO:0031123	RNA 3'-end processing	0.95
GO:0021772	olfactory bulb development	0.95
GO:0021988	olfactory lobe development	0.95
GO:0006099	tricarboxylic acid cycle	0.95
ENSG00000173660	UQCRH PPI subnetwork	0.95
GO:0048024	regulation of nuclear mRNA splicing, via spliceosome	0.95
ENSG00000172757	CFL1 PPI subnetwork	0.95
GO:0050890	cognition	0.95
GO:0070997	neuron death	0.95
GO:0014013	regulation of gliogenesis	0.95
GO:0016411	acylglycerol O-acyltransferase activity	0.95
MP:0006007	abnormal basal ganglion morphology	0.95
ENSG00000090372	STRN4 PPI subnetwork	0.95
GO:0017137	Rab GTPase binding	0.95
REACTOME_POST:ELONGATION_PROCESSING_OF_INTRON:CONTAINING_PRE:M	REACTOME_POST:ELONGATION_PROCESSING_OF_INTRON:CONTAINING_PRE:MRN	0.95
REACTOME_MRNA_3:END_PROCESSING	REACTOME_MRNA_3:END_PROCESSING	0.95
GO:0072088	nephron epithelium morphogenesis	0.95
REACTOME_G_ALPHA_Z_SIGNALLING_EVENTS	REACTOME_G_ALPHA_Z_SIGNALLING_EVENTS	0.95
REACTOME_DUAL_INCISION_REACTION_IN_TC:NER	REACTOME_DUAL_INCISION_REACTION_IN_TC:NER	0.95
REACTOME_FORMATION_OF_TRANSCRIPTION:COUPLED_NER_TC:NER_REPAIR	REACTOME_FORMATION_OF_TRANSCRIPTION:COUPLED_NER_TC:NER_REPAIR_CO	0.95
ENSG00000087302	C14orf166 PPI subnetwork	0.95
GO:0001975	response to amphetamine	0.95
GO:0045454	cell redox homeostasis	0.95
GO:0072329	monocarboxylic acid catabolic process	0.95
ENSG00000130479	MAP1S PPI subnetwork	0.95
MP:0002938	white spotting	0.95
ENSG00000049245	VAMP3 PPI subnetwork	0.96
GO:0042168	heme metabolic process	0.96

Original gene set ID	Original gene set description	Nominal P value
REACTOME_TRANSFERRIN_ENDOCYTOSIS_AND_RECYCLING	REACTOME_TRANSFERRIN_ENDOCYTOSIS_AND_RECYCLING	0.96
MP:0004624	abnormal thoracic cage morphology	0.96
ENSG000000101182	PSMA7 PPI subnetwork	0.96
GO:0007270	neuron-neuron synaptic transmission	0.96
MP:0006054	spinal hemorrhage	0.96
GO:0051937	catecholamine transport	0.96
ENSG000000141543	EIF4A3 PPI subnetwork	0.96
ENSG000000134057	CCNB1 PPI subnetwork	0.96
GO:0019861	flagellum	0.96
REACTOME_RNA_POL_II_CTD_PHOSPHORYLATION_AND_INTERACTION_WITH_	REACTOME_RNA_POL_II_CTD_PHOSPHORYLATION_AND_INTERACTION_WITH_CE	0.96
GO:0030288	outer membrane-bounded periplasmic space	0.96
GO:0042597	periplasmic space	0.96
GO:0072077	renal vesicle morphogenesis	0.96
REACTOME_NEF_MEDIATED_DOWNREGULATION_OF_MHC_CLASS_I_COMPLEX	REACTOME_NEF_MEDIATED_DOWNREGULATION_OF_MHC_CLASS_I_COMPLEX_CE	0.96
ENSG000000163464	CXCR1 PPI subnetwork	0.96
GO:0042379	chemokine receptor binding	0.96
ENSG000000065057	NTHL1 PPI subnetwork	0.96
ENSG000000169021	UQCRFS1 PPI subnetwork	0.96
KEGG_VALINE_LEUCINE_AND_ISOLEUCINE_DEGRADATION	KEGG_VALINE_LEUCINE_AND_ISOLEUCINE_DEGRADATION	0.96
GO:0022900	electron transport chain	0.96
GO:0016358	dendrite development	0.96
GO:0072006	nephron development	0.96
ENSG000000166411	IDH3A PPI subnetwork	0.96
ENSG000000125356	NDUFA1 PPI subnetwork	0.96
GO:0072028	nephron morphogenesis	0.96
MP:0002804	abnormal motor learning	0.96
ENSG000000144848	ATG3 PPI subnetwork	0.96
ENSG000000125944	HNRNPR PPI subnetwork	0.96
KEGG_PARKINSONS_DISEASE	KEGG_PARKINSONS_DISEASE	0.96
GO:0014003	oligodendrocyte development	0.96
GO:0043269	regulation of ion transport	0.96
ENSG000000111445	RFC5 PPI subnetwork	0.96
GO:0031907	microbody lumen	0.96
GO:0005782	peroxisomal matrix	0.96
ENSG000000147133	TAF1 PPI subnetwork	0.96
GO:0031625	ubiquitin protein ligase binding	0.96
ENSG000000164683	HEY1 PPI subnetwork	0.96
GO:0042572	retinol metabolic process	0.96
ENSG000000145864	GABRB2 PPI subnetwork	0.96
ENSG000000170906	NDUFA3 PPI subnetwork	0.96
MP:0003964	abnormal noradrenaline level	0.96
GO:0048475	coated membrane	0.96
GO:0030117	membrane coat	0.96
MP:0000061	fragile skeleton	0.96
REACTOME_PROCESSING_OF_CAPPED_INTRONLESS_PRE:MRNA	REACTOME_PROCESSING_OF_CAPPED_INTRONLESS_PRE:MRNA	0.96
REACTOME_POST:ELONGATION_PROCESSING_OF_INTRONLESS_PRE:MRNA	REACTOME_POST:ELONGATION_PROCESSING_OF_INTRONLESS_PRE:MRNA	0.96
ENSG000000184270	HIST2H2AB PPI subnetwork	0.96
ENSG000000071564	TCF3 PPI subnetwork	0.96
GO:0045685	regulation of glial cell differentiation	0.96

Original gene set ID	Original gene set description	Nominal P value
GO:0008343	adult feeding behavior	0.96
GO:0051971	positive regulation of transmission of nerve impulse	0.96
GO:0022406	membrane docking	0.96
MP:0006090	abnormal utricle morphology	0.96
MP:0009453	enhanced contextual conditioning behavior	0.96
ENSG00000090266	NDUFB2 PPI subnetwork	0.96
ENSG00000115590	IL1R2 PPI subnetwork	0.96
GO:0090130	tissue migration	0.96
GO:0044450	microtubule organizing center part	0.96
GO:0034976	response to endoplasmic reticulum stress	0.96
ENSG00000112685	EXOC2 PPI subnetwork	0.96
GO:0048806	genitalia development	0.96
GO:0001756	somitogenesis	0.96
ENSG00000184445	KNTC1 PPI subnetwork	0.96
REACTOME_CITRIC_ACID_CYCLE_TCA_CYCLE	REACTOME_CITRIC_ACID_CYCLE_TCA_CYCLE	0.96
MP:0000285	abnormal heart valve morphology	0.96
GO:0007585	respiratory gaseous exchange	0.96
GO:0031124	mRNA 3'-end processing	0.96
MP:0001982	decreased chemically-elicited antinociception	0.96
GO:0033555	multicellular organismal response to stress	0.96
GO:0034599	cellular response to oxidative stress	0.96
GO:0006888	ER to Golgi vesicle-mediated transport	0.96
GO:0072075	metanephric mesenchyme development	0.96
GO:0010453	regulation of cell fate commitment	0.96
GO:0042775	mitochondrial ATP synthesis coupled electron transport	0.96
GO:0042773	ATP synthesis coupled electron transport	0.96
GO:0006733	oxidoreduction coenzyme metabolic process	0.96
ENSG00000107758	PPP3CB PPI subnetwork	0.96
GO:0031424	keratinization	0.96
GO:0004532	exoribonuclease activity	0.96
GO:0006936	muscle contraction	0.96
GO:0042162	telomeric DNA binding	0.96
GO:0072273	metanephric nephron morphogenesis	0.96
MP:0003425	abnormal optic vesicle formation	0.96
REACTOME_VIRAL_MESSENGER_RNA_SYNTHESIS	REACTOME_VIRAL_MESSENGER_RNA_SYNTHESIS	0.96
GO:0001657	ureteric bud development	0.96
GO:0003338	metanephros morphogenesis	0.96
GO:0009612	response to mechanical stimulus	0.96
ENSG00000169242	EFNA1 PPI subnetwork	0.96
GO:0030048	actin filament-based movement	0.96
ENSG00000103479	RBL2 PPI subnetwork	0.96
REACTOME_THE_CITRIC_ACID_TCA_CYCLE_AND_RESPIRATORY_ELECTRON_TRANSPORT	REACTOME_THE_CITRIC_ACID_TCA_CYCLE_AND_RESPIRATORY_ELECTRON_TRANSPORT	0.96
GO:0060688	regulation of morphogenesis of a branching structure	0.96
GO:0072524	pyridine-containing compound metabolic process	0.96
GO:0019362	pyridine nucleotide metabolic process	0.96
GO:0004970	ionotropic glutamate receptor activity	0.96
GO:0016646	oxidoreductase activity, acting on the CH-NH group of donors, NAD or NADP as acceptor	0.96
GO:0005859	muscle myosin complex	0.96
ENSG00000165288	BRWD3 PPI subnetwork	0.96

Original gene set ID	Original gene set description	Nominal P value
GO:0021984	adenohypophysis development	0.96
GO:0009713	catechol-containing compound biosynthetic process	0.97
GO:0042423	catecholamine biosynthetic process	0.97
GO:0034312	diol biosynthetic process	0.97
GO:0007202	activation of phospholipase C activity	0.97
GO:0010039	response to iron ion	0.97
ENSG00000036257	CUL3 PPI subnetwork	0.97
GO:0035967	cellular response to topologically incorrect proteir	0.97
MP:0001961	abnormal reflex	0.97
MP:0004859	abnormal synaptic plasticity	0.97
GO:0030261	chromosome condensation	0.97
ENSG00000063245	EPN1 PPI subnetwork	0.97
GO:0005227	calcium activated cation channel activity	0.97
MP:0000149	abnormal scapula morphology	0.97
GO:0009452	RNA capping	0.97
GO:0043928	exonucleolytic nuclear-transcribed mRNA catabolic process involved in deadenylatic	0.97
GO:0000291	nuclear-transcribed mRNA catabolic process, exonucleolytic	0.97
ENSG00000023228	NDUFS1 PPI subnetwork	0.97
ENSG00000009413	REV3L PPI subnetwork	0.97
GO:0006004	fucoase metabolic process	0.97
GO:0048169	regulation of long-term neuronal synaptic plasticity	0.97
MP:0001299	abnormal eye distance/ position	0.97
ENSG00000135940	COX5B PPI subnetwork	0.97
GO:0030219	megakaryocyte differentiation	0.97
ENSG00000151729	SLC25A4 PPI subnetwork	0.97
ENSG00000120656	TAF12 PPI subnetwork	0.97
MP:0002741	small olfactory bulb	0.97
GO:0045168	cell-cell signaling involved in cell fate commitment	0.97
ENSG00000124575	HIST1H1D PPI subnetwork	0.97
GO:0030145	manganese ion binding	0.97
GO:0030308	negative regulation of cell growth	0.97
GO:0005721	centromeric heterochromatin	0.97
GO:0007030	Golgi organization	0.97
REACTOME_PERK_REGULATED_GENE_EXPRESSION	REACTOME_PERK_REGULATED_GENE_EXPRESSION	0.97
MP:0004632	abnormal cochlear OHC efferent innervation pattern	0.97
GO:0051149	positive regulation of muscle cell differentiator	0.97
MP:0003031	acidosis	0.97
ENSG00000160075	SSU72 PPI subnetwork	0.97
MP:0000759	abnormal skeletal muscle morphology	0.97
MP:0000897	abnormal midbrain morphology	0.97
ENSG00000145216	FIP1L1 PPI subnetwork	0.97
GO:0035282	segmentation	0.97
ENSG00000175305	CCNE2 PPI subnetwork	0.97
ENSG00000163939	PBRM1 PPI subnetwork	0.97
GO:0048278	vesicle docking	0.97
MP:0001629	abnormal heart rate	0.97
ENSG00000120008	WDR11 PPI subnetwork	0.97
KEGG_HISTIDINE_METABOLISM	KEGG_HISTIDINE_METABOLISM	0.97
GO:0007379	segment specification	0.97

Original gene set ID	Original gene set description	Nominal P value
ENSG00000116903	EXOC8 PPI subnetwork	0.97
MP:0004180	failure of initiation of embryo turning	0.97
GO:0010863	positive regulation of phospholipase C activity	0.97
GO:0042375	quinone cofactor metabolic process	0.97
GO:0072074	kidney mesenchyme development	0.97
GO:0000132	establishment of mitotic spindle orientation	0.97
GO:0051294	establishment of spindle orientation	0.97
ENSG00000130288	ENSG00000130288 PPI subnetwork	0.97
GO:0033238	regulation of cellular amine metabolic process	0.97
KEGG_REGULATION_OF_AUTOPHAGY	KEGG_REGULATION_OF_AUTOPHAGY	0.97
ENSG00000197373	ENSG00000197373 PPI subnetwork	0.97
ENSG00000168255	POLR2J3 PPI subnetwork	0.97
GO:0060993	kidney morphogenesis	0.97
ENSG00000102977	ACD PPI subnetwork	0.97
ENSG00000139132	FGD4 PPI subnetwork	0.97
GO:0043270	positive regulation of ion transport	0.97
GO:0046496	nicotinamide nucleotide metabolic process	0.97
GO:0051925	regulation of calcium ion transport via voltage-gated calcium channel activity	0.97
ENSG00000100968	NFATC4 PPI subnetwork	0.97
GO:0031640	killing of cells of other organism	0.97
ENSG00000196628	TCF4 PPI subnetwork	0.97
GO:0042659	regulation of cell fate specification	0.97
ENSG00000145041	VPRBP PPI subnetwork	0.97
ENSG00000125968	ID1 PPI subnetwork	0.97
ENSG00000172288	CDY1 PPI subnetwork	0.97
ENSG00000172352	CDY1B PPI subnetwork	0.97
GO:0042417	dopamine metabolic process	0.97
GO:0070469	respiratory chain	0.97
GO:0007612	learning	0.97
GO:0010517	regulation of phospholipase activity	0.97
GO:0045778	positive regulation of ossification	0.97
GO:0005746	mitochondrial respiratory chain	0.97
GO:0000242	pericentriolar material	0.97
GO:0042745	circadian sleep/wake cycle	0.97
ENSG00000067829	IDH3G PPI subnetwork	0.97
GO:0006783	heme biosynthetic process	0.97
GO:0016896	exoribonuclease activity, producing 5'-phosphomonoesters	0.97
GO:0050832	defense response to fungus	0.98
ENSG00000119888	EPCAM PPI subnetwork	0.98
GO:0000940	condensed chromosome outer kinetochore	0.98
GO:0001656	metanephros development	0.98
REACTOME_MRNA_CAPPING	REACTOME_MRNA_CAPPING	0.98
ENSG00000206282	RGL2 PPI subnetwork	0.98
ENSG00000206210	ENSG00000206210 PPI subnetwork	0.98
ENSG00000164032	H2AFZ PPI subnetwork	0.98
GO:0009566	fertilization	0.98
GO:0031128	developmental induction	0.98
ENSG00000004779	NDUFAB1 PPI subnetwork	0.98
GO:0045471	response to ethanol	0.98

Original gene set ID	Original gene set description	Nominal P value
GO:0002825	regulation of T-helper 1 type immune response	0.98
MP:0002953	thick ventricular wall	0.98
ENSG00000204120	GIGYF2 PPI subnetwork	0.98
ENSG00000167792	NDUFV1 PPI subnetwork	0.98
REACTOME_DEPOSITION_OF_NEW_CENPA:CONTAINING_NUCLEOSOMES_AT_T	REACTOME_DEPOSITION_OF_NEW_CENPA:CONTAINING_NUCLEOSOMES_AT_THE_	0.98
REACTOME_NUCLEOSOME_ASSEMBLY	REACTOME_NUCLEOSOME_ASSEMBLY	0.98
ENSG00000164919	COX6C PPI subnetwork	0.98
GO:0040001	establishment of mitotic spindle localizati	0.98
GO:0003401	axis elongation	0.98
GO:0043524	negative regulation of neuron apoptotic process	0.98
GO:0043176	amine binding	0.98
GO:0009062	fatty acid catabolic process	0.98
ENSG00000136888	ATP6V1G1 PPI subnetwork	0.98
ENSG00000010244	ZNF207 PPI subnetwork	0.98
GO:0016835	carbon-oxygen lyase activity	0.98
KEGG_CARDIAC_MUSCLE_CONTRACTION	KEGG_CARDIAC_MUSCLE_CONTRACTION	0.98
ENSG00000140416	TPM1 PPI subnetwork	0.98
GO:0060572	morphogenesis of an epithelial bud	0.98
ENSG00000065534	MYLK PPI subnetwork	0.98
ENSG00000167306	MYO5B PPI subnetwork	0.98
GO:0031593	polyubiquitin binding	0.98
MP:0004725	decreased platelet serotonin level	0.98
GO:0072527	pyrimidine-containing compound metabolic process	0.98
MP:0006065	abnormal heart position or orientation	0.98
ENSG00000164258	NDUFS4 PPI subnetwork	0.98
MP:0009232	abnormal sperm nucleus morphology	0.98
GO:0010632	regulation of epithelial cell migration	0.98
GO:0051924	regulation of calcium ion transport	0.98
MP:0004215	abnormal myocardial fiber physiology	0.98
ENSG00000186230	ZNF749 PPI subnetwork	0.98
GO:0010824	regulation of centrosome duplication	0.98
ENSG00000187555	USP7 PPI subnetwork	0.98
ENSG00000215697	ENSG00000215697 PPI subnetwork	0.98
ENSG00000168397	ATG4B PPI subnetwork	0.98
GO:0071241	cellular response to inorganic substance	0.98
GO:0015939	pantothenate metabolic process	0.98
MP:0008412	increased cellular sensitivity to oxidative stress	0.98
ENSG00000173894	CBX2 PPI subnetwork	0.98
GO:0060675	ureteric bud morphogenesis	0.98
REACTOME_CLEAVAGE_OF_GROWING_TRANSCRIPT_IN_THE_TERMINATION_RI	REACTOME_CLEAVAGE_OF_GROWING_TRANSCRIPT_IN_THE_TERMINATION_REGIC	0.98
REACTOME_RNA_POLYMERASE_II_TRANSCRIPTION_TERMINATION	REACTOME_RNA_POLYMERASE_II_TRANSCRIPTION_TERMINATION	0.98
REACTOME_POST:ELONGATION_PROCESSING_OF_THE_TRANSCRIPT	REACTOME_POST:ELONGATION_PROCESSING_OF_THE_TRANSCRIPT	0.98
ENSG00000032514	ENSG00000032514 PPI subnetwork	0.98
ENSG00000119013	NDUFB3 PPI subnetwork	0.98
ENSG00000120251	GRIA2 PPI subnetwork	0.98
GO:0006119	oxidative phosphorylation	0.98
ENSG00000099246	RAB18 PPI subnetwork	0.98
GO:0061053	somite development	0.98
GO:0033275	actin-myosin filament sliding	0.98

Original gene set ID**Original gene set description****Nominal P value**

GO:0030049	muscle filament sliding	0.98
MP:0000433	microcephaly	0.98
ENSG000000167258	CDK12 PPI subnetwork	0.98
GO:0016634	oxidoreductase activity, acting on the CH-CH group of donors, oxygen as acceptor	0.98
GO:0021952	central nervous system projection neuron axonogenesis	0.98
ENSG000000124164	VAPB PPI subnetwork	0.98
GO:0009109	coenzyme catabolic process	0.98
MP:0004087	abnormal muscle fiber morphology	0.98
ENSG000000182117	NOP10 PPI subnetwork	0.98
GO:0051187	cofactor catabolic process	0.98
REACTOME_RESOLUTION_OF_AP_SITES_VIA_THE_MULTIPLE_NUCLEOTIDE_PATCH	REACTOME_RESOLUTION_OF_AP_SITES_VIA_THE_MULTIPLE_NUCLEOTIDE_PATCH	0.98
REACTOME_REMOVAL_OF_DNA_PATCH_CONTAINING_ABASIC_RESIDUE	REACTOME_REMOVAL_OF_DNA_PATCH_CONTAINING_ABASIC_RESIDUE	0.98
GO:0090183	regulation of kidney development	0.98
ENSG000000003096	KLHL13 PPI subnetwork	0.98
ENSG000000170515	PA2G4 PPI subnetwork	0.98
ENSG000000125447	GGA3 PPI subnetwork	0.98
ENSG000000077721	UBE2A PPI subnetwork	0.98
MP:0002674	abnormal sperm motility	0.98
MP:0001706	abnormal left-right axis patterning	0.98
MP:0004132	absent embryonic cilia	0.98
GO:0001658	branching involved in ureteric bud morphogenesis	0.98
GO:0008009	chemokine activity	0.98
GO:0060134	prepulse inhibition	0.98
ENSG000000163535	SGOL2 PPI subnetwork	0.98
GO:0006369	termination of RNA polymerase II transcription	0.98
GO:0009898	internal side of plasma membrane	0.98
ENSG000000105968	H2AFV PPI subnetwork	0.98
GO:0007098	centrosome cycle	0.98
ENSG000000092531	SNAP23 PPI subnetwork	0.98
GO:0006488	dolichol-linked oligosaccharide biosynthetic process	0.99
GO:0016101	diterpenoid metabolic process	0.99
ENSG000000171132	PRKCE PPI subnetwork	0.99
GO:0006513	protein monoubiquitination	0.99
GO:0042312	regulation of vasodilation	0.99
ENSG000000160194	NDUFV3 PPI subnetwork	0.99
GO:0009068	aspartate family amino acid catabolic process	0.99
GO:0006904	vesicle docking involved in exocytosis	0.99
ENSG000000010256	UQCRC1 PPI subnetwork	0.99
GO:0044236	multicellular organismal metabolic process	0.99
GO:0008045	motor axon guidance	0.99
REACTOME_TRAFFICKING_OF_GLUR2:CONTAINING_AMPA_RECEPTORS	REACTOME_TRAFFICKING_OF_GLUR2:CONTAINING_AMPA_RECEPTORS	0.99
ENSG000000139197	PEX5 PPI subnetwork	0.99
GO:0001523	retinoid metabolic process	0.99
MP:0002954	abnormal aerobic energy metabolism	0.99
MP:0011386	increased metanephric mesenchyme apoptosis	0.99
GO:0072163	mesonephric epithelium development	0.99
GO:0072164	mesonephric tubule development	0.99
ENSG000000180104	EXOC3 PPI subnetwork	0.99
ENSG000000212872	ENSG000000212872 PPI subnetwork	0.99

Original gene set ID	Original gene set description	Nominal P value
ENSG00000212871	ENSG00000212871 PPI subnetwork	0.99
ENSG00000198868	ENSG00000198868 PPI subnetwork	0.99
ENSG00000198840	MT-ND3 PPI subnetwork	0.99
GO:0042693	muscle cell fate commitment	0.99
ENSG00000100883	SRP54 PPI subnetwork	0.99
ENSG00000136521	NDUFB5 PPI subnetwork	0.99
ENSG00000164329	PAPD4 PPI subnetwork	0.99
GO:0006776	vitamin A metabolic process	0.99
ENSG00000132604	TERF2 PPI subnetwork	0.99
ENSG00000115286	NDUFS7 PPI subnetwork	0.99
ENSG00000104313	EYA1 PPI subnetwork	0.99
ENSG00000139112	GABARAPL1 PPI subnetwork	0.99
GO:0008527	taste receptor activity	0.99
MP:0008415	abnormal neurite morphology	0.99
ENSG00000105829	BET1 PPI subnetwork	0.99
GO:0043130	ubiquitin binding	0.99
ENSG00000197969	VPS13A PPI subnetwork	0.99
GO:0015844	monoamine transport	0.99
ENSG00000168653	NDUFS5 PPI subnetwork	0.99
GO:0005665	DNA-directed RNA polymerase II, core complex	0.99
GO:0045687	positive regulation of glial cell differentiation	0.99
ENSG00000106636	YKT6 PPI subnetwork	0.99
REACTOME_SYNTHESIS_OF_BILE_ACIDS_AND_BILE_SALTS	REACTOME_SYNTHESIS_OF_BILE_ACIDS_AND_BILE_SALTS	0.99
MP:0005399	increased susceptibility to fungal infection	0.99
ENSG00000198886	MT-ND4 PPI subnetwork	0.99
ENSG00000212869	ENSG00000212869 PPI subnetwork	0.99
ENSG00000198695	MT-ND6 PPI subnetwork	0.99
ENSG00000203811	HIST2H3C PPI subnetwork	0.99
ENSG00000183598	HIST2H3D PPI subnetwork	0.99
ENSG00000099795	NDUFB7 PPI subnetwork	0.99
ENSG00000159352	PSMD4 PPI subnetwork	0.99
ENSG00000204218	ENSG00000204218 PPI subnetwork	0.99
ENSG00000109911	ELP4 PPI subnetwork	0.99
ENSG00000180871	CXCR2 PPI subnetwork	0.99
GO:0004527	exonuclease activity	0.99
GO:0016645	oxidoreductase activity, acting on the CH-NH group of donors	0.99
GO:0050919	negative chemotaxis	0.99
GO:0001662	behavioral fear response	0.99
ENSG00000147601	TERF1 PPI subnetwork	0.99
GO:0030890	positive regulation of B cell proliferation	0.99
GO:0034311	diol metabolic process	0.99
GO:0006584	catecholamine metabolic process	0.99
GO:0009712	catechol-containing compound metabolic process	0.99
ENSG00000128513	POT1 PPI subnetwork	0.99
ENSG00000162129	CLPB PPI subnetwork	0.99
GO:0019783	small conjugating protein-specific protease activity	0.99
GO:0032182	small conjugating protein binding	0.99
ENSG00000006712	PAF1 PPI subnetwork	0.99
ENSG00000134014	ELP3 PPI subnetwork	0.99

Original gene set ID	Original gene set description	Nominal P value
GO:0042537	benzene-containing compound metabolic process	0.99
ENSG00000197579	TOPORS PPI subnetwork	0.99
ENSG00000054116	TRAPPC3 PPI subnetwork	0.99
GO:0071824	protein-DNA complex subunit organization	0.99
ENSG00000143614	GATAD2B PPI subnetwork	0.99
GO:0070252	actin-mediated cell contraction	0.99
GO:0021955	central nervous system neuron axonogenesis	0.99
GO:0046513	ceramide biosynthetic process	0.99
GO:0004843	ubiquitin-specific protease activity	0.99
ENSG00000213496	ENSG00000213496 PPI subnetwork	0.99
ENSG00000197265	GTF2E2 PPI subnetwork	0.99
GO:0005747	mitochondrial respiratory chain complex I	0.99
GO:0045271	respiratory chain complex I	0.99
GO:0030964	NADH dehydrogenase complex	0.99
GO:0045652	regulation of megakaryocyte differentiation	0.99
GO:0007099	centriole replication	0.99
MP:0001899	absent long term depression	0.99
ENSG00000197548	ATG7 PPI subnetwork	0.99
MP:0000819	abnormal olfactory bulb morphology	0.99
GO:0060174	limb bud formation	0.99
GO:0031055	chromatin remodeling at centromere	0.99
ENSG00000125798	FOXA2 PPI subnetwork	0.99
ENSG00000188459	ENSG00000188459 PPI subnetwork	0.99
ENSG00000197930	ERO1L PPI subnetwork	0.99
GO:0015872	dopamine transport	0.99
GO:0032963	collagen metabolic process	0.99
ENSG00000119048	UBE2B PPI subnetwork	0.99
ENSG00000168393	DTYMK PPI subnetwork	0.99
ENSG00000215694	ENSG00000215694 PPI subnetwork	0.99
GO:0043486	histone exchange	0.99
GO:0034502	protein localization to chromosome	0.99
GO:0005230	extracellular ligand-gated ion channel activity	0.99
ENSG00000147853	AK3 PPI subnetwork	0.99
GO:0009081	branched chain family amino acid metabolic process	0.99
GO:0007618	mating	0.99
GO:0030534	adult behavior	0.99
GO:0008137	NADH dehydrogenase (ubiquinone) activity	0.99
GO:0050136	NADH dehydrogenase (quinone) activity	0.99
GO:0003954	NADH dehydrogenase activity	0.99
ENSG00000163032	VSNL1 PPI subnetwork	0.99
GO:0004953	icosanoid receptor activity	0.99
GO:0004954	prostanoid receptor activity	0.99
GO:0033572	transferrin transport	0.99
GO:0015682	ferric iron transport	0.99
ENSG00000130176	CNN1 PPI subnetwork	0.99
ENSG00000183648	NDUFB1 PPI subnetwork	0.99
ENSG00000127184	COX7C PPI subnetwork	0.99
GO:0001964	startle response	0.99
REACTOME_MITOCHONDRIAL_FATTY_ACID_BETA:OXIDATION	REACTOME_MITOCHONDRIAL_FATTY_ACID_BETA:OXIDATION	0.99

Original gene set ID	Original gene set description	Nominal P value
GO:0007494	midgut development	0.99
ENSG00000124702	KLHDC3 PPI subnetwork	0.99
ENSG00000178127	NDUFB2 PPI subnetwork	0.99
ENSG00000212870	ENSG00000212870 PPI subnetwork	0.99
ENSG00000198786	MT-ND5 PPI subnetwork	0.99
GO:0042596	fear response	0.99
MP:0002243	abnormal vomeronasal organ morphology	0.99
GO:0072529	pyrimidine-containing compound catabolic process	0.99
ENSG00000147123	NDUFB11 PPI subnetwork	0.99
MP:0000747	muscle weakness	0.99
GO:0071103	DNA conformation change	0.99
ENSG00000185513	L3MBTL1 PPI subnetwork	0.99
GO:0050684	regulation of mRNA processing	1
GO:0006739	NADP metabolic process	1
GO:0044259	multicellular organismal macromolecule metabolic process	1
ENSG00000138029	HADHB PPI subnetwork	1
GO:0006740	NADPH regeneration	1
ENSG00000108587	GOSR1 PPI subnetwork	1
ENSG00000109390	NDUFC1 PPI subnetwork	1
ENSG00000172301	C17orf79 PPI subnetwork	1
GO:0002209	behavioral defense response	1
KEGG_PROTEIN_EXPORT	KEGG_PROTEIN_EXPORT	1
GO:0046520	sphingoid biosynthetic process	1
GO:0016655	oxidoreductase activity, acting on NADH or NADPH, quinone or similar compound as	1
ENSG00000112357	PEX7 PPI subnetwork	1
ENSG00000111875	ASF1A PPI subnetwork	1
ENSG00000185214	ENSG00000185214 PPI subnetwork	1
GO:0009262	deoxyribonucleotide metabolic process	1
ENSG00000155511	GRIA1 PPI subnetwork	1
GO:0065004	protein-DNA complex assembly	1
GO:0051952	regulation of amine transport	1
GO:0003924	GTPase activity	1
ENSG00000151366	NDUFC2 PPI subnetwork	1
ENSG00000147416	ATP6V1B2 PPI subnetwork	1
GO:0004869	cysteine-type endopeptidase inhibitor activity	1
MP:0010454	abnormal truncus arteriosus septation	1
GO:0034728	nucleosome organization	1
ENSG00000166963	MAP1A PPI subnetwork	1
ENSG00000115738	ID2 PPI subnetwork	1
ENSG00000187837	HIST1H1C PPI subnetwork	1
GO:0034080	CenH3-containing nucleosome assembly at centromere	1
GO:0006336	DNA replication-independent nucleosome assembly	1
GO:0034724	DNA replication-independent nucleosome organization	1
ENSG00000185621	LMLN PPI subnetwork	1
GO:0003995	acyl-CoA dehydrogenase activity	1
MP:0008531	increased chemical nociceptive threshold	1
ENSG00000121390	PSPC1 PPI subnetwork	1
GO:0021871	forebrain regionalization	1
ENSG00000206440	NFKBIL1 PPI subnetwork	1

Original gene set ID	Original gene set description	Nominal P value
ENSG00000168593	ENSG00000168593 PPI subnetwork	1
MP:0005480	increased circulating triiodothyronine leve	1
GO:0006098	pentose-phosphate shunt	1
GO:0042401	cellular biogenic amine biosynthetic process	1
GO:0000178	exosome (RNase complex)	1
ENSG00000198888	MT-ND1 PPI subnetwork	1
GO:0042136	neurotransmitter biosynthetic process	1
ENSG00000131747	TOP2A PPI subnetwork	1
ENSG00000131495	NDUFA2 PPI subnetwork	1
REACTOME_MRNA_DECAY_BY_3_TO_5_EXORIBONUCLEASE	REACTOME_MRNA_DECAY_BY_3_TO_5_EXORIBONUCLEASE	1
ENSG00000165264	NDUFB6 PPI subnetwork	1
MP:0002007	increased cellular sensitivity to gamma-irradiation	1
ENSG00000092330	TINF2 PPI subnetwork	1
ENSG00000212876	ENSG00000212876 PPI subnetwork	1
ENSG00000198763	MT-ND2 PPI subnetwork	1
GO:0006333	chromatin assembly or disassembly	1
GO:0031497	chromatin assembly	1
GO:0007628	adult walking behavior	1
GO:0016780	phosphotransferase activity, for other substituted phosphate group:	1
GO:0033540	fatty acid beta-oxidation using acyl-CoA oxidase	1
ENSG00000083896	YTHDC1 PPI subnetwork	1
GO:0032204	regulation of telomere maintenance	1
ENSG00000108671	PSMD11 PPI subnetwork	1
GO:0001504	neurotransmitter uptake	1
ENSG00000108468	CBX1 PPI subnetwork	1
ENSG00000079462	PFAFH1B3 PPI subnetwork	1
GO:0015992	proton transport	1
GO:0009378	four-way junction helicase activity	1
ENSG00000116288	PARK7 PPI subnetwork	1
REACTOME_RESPIRATORY_ELECTRON_TRANSPORT	REACTOME_RESPIRATORY_ELECTRON_TRANSPORT	1
GO:0021536	diencephalon development	1
REACTOME_RESPIRATORY_ELECTRON_TRANSPORT_ATP_SYNTHESIS_BY_CHEM	REACTOME_RESPIRATORY_ELECTRON_TRANSPORT_ATP_SYNTHESIS_BY_CHEMIOSM	1
ENSG00000013275	PSMC4 PPI subnetwork	1
GO:0006818	hydrogen transport	1
ENSG00000167774	NDUFA7 PPI subnetwork	1
GO:0006282	regulation of DNA repair	1
GO:0006323	DNA packaging	1
GO:0050922	negative regulation of chemotaxis	1
GO:0015991	ATP hydrolysis coupled proton transport	1
GO:0015988	energy coupled proton transport, against electrochemical gradien	1
GO:0015078	hydrogen ion transmembrane transporter activity	1
ENSG00000111880	RNGTT PPI subnetwork	1
KEGG_OXIDATIVE_PHOSPHORYLATION	KEGG_OXIDATIVE_PHOSPHORYLATION	1
GO:0008344	adult locomotory behavior	1
GO:0031290	retinal ganglion cell axon guidance	1
ENSG00000140990	NDUFB10 PPI subnetwork	1
ENSG00000153140	CETN3 PPI subnetwork	1
ENSG00000120696	KBTBD7 PPI subnetwork	1
GO:0006334	nucleosome assembly	1

Original gene set ID	Original gene set description	Nominal P value
GO:0006586	indolalkylamine metabolic process	1
GO:0042430	indole-containing compound metabolic process	1
GO:0018958	phenol-containing compound metabolic process	1
GO:0000381	regulation of alternative nuclear mRNA splicing, via spliceosome	1
ENSG00000108433	GOSR2 PPI subnetwork	1
GO:0001963	synaptic transmission, dopaminergic	1
REACTOME_E2F:ENABLED_INHIBITION_OF_PRE:REPLICATION_COMPLEX_FORM	REACTOME_E2F:ENABLED_INHIBITION_OF_PRE:REPLICATION_COMPLEX_FORMATI	1
GO:0006635	fatty acid beta-oxidation	1
ENSG00000203813	HIST1H3H PPI subnetwork	1
ENSG00000203852	HIST2H3A PPI subnetwork	1
ENSG00000131143	COX4I1 PPI subnetwork	1
ENSG00000166848	TERF2IP PPI subnetwork	1
MP:0000761	thin diaphragm muscle	1
GO:0021983	pituitary gland development	1
ENSG00000115677	HDLBP PPI subnetwork	1
ENSG00000113327	GABRG2 PPI subnetwork	1
GO:0006879	cellular iron ion homeostasis	1
GO:0021756	striatum development	1
GO:2001020	regulation of response to DNA damage stimulus	1
GO:0043044	ATP-dependent chromatin remodeling	1
GO:0006576	cellular biogenic amine metabolic process	1
GO:0009636	response to toxin	1
GO:0032200	telomere organization	1
GO:0009083	branched chain family amino acid catabolic process	1
REACTOME_BRANCHED:CHAIN_AMINO_ACID_CATABOLISM	REACTOME_BRANCHED:CHAIN_AMINO_ACID_CATABOLISM	1
REACTOME_PEROXISOMAL_LIPID_METABOLISM	REACTOME_PEROXISOMAL_LIPID_METABOLISM	1
ENSG00000179841	AKAP5 PPI subnetwork	1
GO:0000723	telomere maintenance	1
ENSG00000196532	HIST1H3C PPI subnetwork	1
ENSG00000198366	HIST1H3A PPI subnetwork	1
ENSG00000197153	HIST1H3J PPI subnetwork	1
ENSG00000197409	HIST1H3D PPI subnetwork	1
ENSG00000178458	ENSG00000178458 PPI subnetwork	1
ENSG00000112727	ENSG00000112727 PPI subnetwork	1
ENSG00000124693	HIST1H3B PPI subnetwork	1
ENSG00000196966	HIST1H3E PPI subnetwork	1
ENSG00000182572	HIST1H3I PPI subnetwork	1
ENSG00000180198	RCC1 PPI subnetwork	1
KEGG_ALZHEIMERS_DISEASE	KEGG_ALZHEIMERS_DISEASE	1
GO:0000380	alternative nuclear mRNA splicing, via spliceosome	1
GO:0017156	calcium ion-dependent exocytosis	1

SUPPLEMENTAL MATERIAL

Jones et al.: Meta-analysis of genome-wide association studies for abdominal aortic aneurysm identifies four new disease specific risk loci

ONLINE METHODS AND DATA*

	Page
Discovery and validation cohort descriptions	2
Meta-analysis	9
SNP lookup in GWAS for traits associated with AAA	30
Search for other associated traits and diseases using GWAS databases	32
PheWAS analysis	37
Annotation of AAA associated SNPs using the UCSC Genome Browser	38
Pupasuite analysis	41
GWAS3D analysis	44
DEPICT analysis	49
Functional effects of SNPs at AAA loci	60
Validation of GWAS3D results using mRNA expression data	67
Look-up for transcription factor binding sites	70
Network analysis	72
Consortia contributing data	76
References	79

*for clarity and ease of use each section contains methods, results, figures and tables relevant to that section.

INDIVIDUAL GWAS STUDIES

All known studies with AAA genome-wide genotyping data were invited to join the International Aneurysm Consortium effort. All studies agreed to participate in the meta-GWAS, with cohort case control descriptions and inclusion/exclusion criteria having been previously reported¹⁻³ (**Online Table I**). All AAA cases shared a common definition of infra-renal aortic diameter ≥ 30 mm. Patients with connective tissue disease associated AAAs (e.g. Marfan, Ehlers-Danlos, Loeys-Dietz) were excluded from the study. Each GWAS was based on a case-control analysis of AAA modelled as a discrete trait. The statistical analysis of the Aneurysm Consortium and New Zealand GWAS datasets was repeated specifically for this study and therefore was harmonized using identical imputation and analysis methods. Data from the remaining cohorts consisted of summary data obtained from previously performed analyses.

The use of the samples in each study cohort was approved by the local Ethics Committees or Institutional Review Boards.

DISCOVERY AND VALIDATION COHORT DESCRIPTIONS (Online Tables I and II)

a) Discovery Cohorts

Aneurysm Consortium (AC) AAA GWAS dataset: The Aneurysm Consortium recruited cases of AAA from centres across the United Kingdom and Western Australia. Cases were defined as an infra-renal aortic diameter ≥ 30 mm proven on ultrasound or computerized tomography (CT) scan. Controls were taken from the WTCCC2 common control group^{1,4} and were therefore unscreened for AAA.

Data were from 1,866 cases with AAA and 5,435 unscreened controls from the Wellcome Trust Case Control Consortium 2 (WTCCC2) study consisting of samples from the 1958 British Birth Cohort and from the UK National Blood Service. DNA samples were processed at the Wellcome Trust Sanger Institute (WTSI). Genomic DNA was quantified by PicoGreen assay, and quality control (QC) assured by both agarose gel electrophoresis and Sequenom iPLEX genotyping of 29 SNPs and 4 sex-specific markers. Genotyping for the discovery study was performed using Illumina 1.2M (controls) or 670K (AAA) BeadChips. Raw intensity data were normalized using BeadStudio and genotypes were called concurrently from the combined case-control data set using the Illuminus algorithm⁵.

As part of the original Aneurysm Consortium GWAS individual sample QC had been performed as follows. QC was first performed by exclusion of SNPs with call rates < 0.98 and those that demonstrated significant deviation from Hardy-Weinberg equilibrium in the control group ($P < 5 \times 10^{-4}$). Duplicate samples and those that failed genotyping (sample call rates < 0.98) were also excluded from further analysis. Genotyping cluster plots for all SNPs with $P < 1 \times 10^{-4}$ were visually inspected to exclude from further analysis positive associations generated by erroneous genotyping or calling. Checks for population stratification were performed by PLINK⁶ identical by state clustering and extreme outliers were removed from the analysis.

Imputation was performed using IMPUTE 2.2 run on the BCISNPmax database platform (version 3.5, BCI Platforms, Espoo, Finland). The reference haplotypes were based on the 1000 Genomes June 2011 release. Imputed calls were filtered by quality score (excluding those < 0.9) to restrict to higher quality imputed SNPs.

Following imputation further QC filtering was performed, excluding SNPs with call rates < 0.98 and those that demonstrated significant deviation from Hardy-Weinberg equilibrium in the control group ($P < 5 \times 10^{-4}$). Duplicate samples and those that failed genotyping (sample call rate < 0.98) were also excluded from further analysis. Association testing was carried out in PLINK⁶.

New Zealand (NZ) Vascular Genetics Study AAA GWAS dataset: The Vascular Research Consortium of New Zealand recruited New Zealand men and women with a proven history of AAA (infra-renal aortic diameter \geq 30 mm proven on ultrasound or CT scan). Approximately 80% had undergone surgical AAA repair (typically AAA's > 50-55 mm in diameter). The vast majority of cases (>97%) were of Anglo-European ancestry. The control group underwent an abdominal ultrasound scan to exclude (>25 mm) concurrent AAA and Anglo-European ancestry was required for inclusion. Controls were also screened for peripheral artery disease (PAD; using ankle brachial index), carotid artery disease (ultrasound) and other cardiovascular risk factors.

Two separate GWAS were performed using New Zealand samples. NZ GWAS 1 consisted of 608 AAA patients (474 male) and 612 elderly controls (450 male), genotyped using the Affymetrix SNP 6 GeneChip array. All samples had call rates >0.95 (mean 0.992). NZ GWAS 2 consisted of 397 AAA patients (332 male) and 384 elderly controls (308 male), genotyped using the Illumina Infinium Omni2.5 BeadChip array. All samples had call rates >0.95 (mean 0.990). All NZ genomic DNA samples exceeded manufacturer's quality and quantity requirements having undergone pre-assessment by Nanophotometer (Implen GmbH, München, Germany) and agarose gel electrophoresis.

Imputation was conducted separately on NZ GWAS 1 and 2 data sets using the same methods as used for the Aneurysm Consortium datasets. IMPUTE 2.2 was run on the BCISNPmax database platform (version 3.5, BCI Platforms, Espoo, Finland). The reference haplotypes were based on the 1000 Genomes June 2011 release. Imputed calls were filtered by quality score (excluding those <0.9) to restrict to higher quality imputed SNPs. The genomic inflation factors (λ) were 1.07 and 1.05, respectively (MAF >0.05).

Both NZ GWAS 1 and 2 data sets underwent QC filtering, excluding SNPs with call rates < 0.98 and those that demonstrated significant deviation from Hardy-Weinberg equilibrium in the control group ($P < 5 \times 10^{-4}$). Duplicate samples and those that failed genotyping (sample call rate <0.98) were also excluded from further analysis. Association testing was carried out in PLINK⁶.

US (PA) GWAS dataset: AAA patients were enrolled through the Department of Vascular Surgery at Geisinger Medical Center, Danville, Pennsylvania, USA as previously reported^{2,7}. To identify cases and controls from the electronic medical records, an ePhenotyping algorithm was developed⁸. Briefly, Structured Query Language (SQL) was used to script the algorithm utilizing "Current Procedural Terminology" (CPT) and "International Classification of Diseases" (ICD-9) codes as well as demographic and encounter data to classify individuals as case, control, or excluded. AAA cases were defined as having an AAA repair procedure (case Type 1), or at least one appropriate specialty encounter (vascular clinic) with a ruptured AAA (case Type 2), or at least two specialty encounters with an unruptured AAA (case Type 3). Controls were neither cases nor those excluded, had an encounter within the past 5 years, and had never been assigned an ICD9 code of 441.*, where * is a 1 or 2 digit code. Individuals were excluded if 1) they had a thoracic aortic aneurysm or a rare heritable disease with aortic manifestation; 2) they were younger than 40 or older than 89 years, 3) they had a single encounter with a code without mention of rupture (441.4), or 4) they had not had an encounter within the past 5 years. Rare heritable diseases were excluded because the goal of the current study was to identify non-syndromic AAA. Controls under 40 years might yet manifest an AAA, while cases under 40 years of age and without rare syndromic forms of aortic aneurysms are likely due to trauma. The AAA algorithm can be downloaded from www.PheKb.org. The algorithm was validated on a subset of individuals by manual chart review, and implemented at eMERGE network sites. The algorithm was implemented as a workflow in the Konstanz Information Miner (KNIME) (<http://www.knime.org/>).

AAA cases had infrarenal aortic diameter ≥ 30 mm as revealed by abdominal imaging. Approximately 20% of individuals with AAA had a family history of AAA. A control group was obtained through the Geisinger MyCode[®] Project, a cohort of Geisinger Clinic patients recruited for genomic studies. The MyCode[®] controls were matched for age distribution and sex to the Geisinger Vascular Clinic AAA cases. Based on electronic medical records, controls had no ICD-9 codes for AAA in their records, but they were not screened by ultrasonography for AAA. Both cases and controls from the Geisinger Clinic were of European descent.

The Geisinger cohort used for this study was a subset of a larger cohort comprising 3,264 samples from 3,149 individuals with three phenotypes: 922 putative AAA cases, 981 obesity cases and 1,246 controls. Samples were genotyped on the Illumina HumanOmniExpress-12v1.0 genotyping platform at the University of Pittsburgh Genomics and Proteomics Core Laboratories. Genotypes were called using the Illumina GenomeStudio v2010.3 software. QC consisted of a number of steps: identification of cross-contamination and removal of specimens, call rate of samples (> 0.98 SNPs called), sex consistency between annotated sex and genotyped sex, SNP discordance between replicate sample pairs, SNP call rate (> 0.95 calls in all specimens), SNP minor allele frequency (> 0.01), SNP Hardy-Weinberg equilibrium ($P > 1 \times 10^{-4}$), and selection of replicates to retain based on sex-specific Mahalanobis distance (< 4.1) and Illumina P10.GC (> 0.71). Cross-contamination of samples was detected by excess heterozygosity and excess relatedness (related to more than half of other samples at $P_i\text{-hat} > 0.0625$); four samples were removed prior to other QC steps. After the QC steps above, related individuals (pairwise $P_i\text{-hat} > 0.15$) were removed, retaining the individual and specimen with the highest call rate. A second round of QC was applied using the above SNP and sample criteria to ensure consistency after removal of SNPs and individuals. In addition, the SNP criteria were analyzed per chromosome to ensure that there were no systematic differences (no differences detected). Lastly, principle component analysis (PCA) was used to determine if there were any batch effects during genotyping (no evidence for batch effects). Of the 3,264 samples, 153 were removed for one or more of the QC reasons above. Of the 731,306 SNPs, 95,369 were removed; 2,012 were discordant, 13,107 had a low call rate, 78,086 had a MAF < 0.01 , and 14,056 had a HWE $P < 1 \times 10^{-4}$ (9,047 SNPs were removed for more than one reason).

The final meta-analysis cohort comprised only those individuals who were identified as definitive AAA cases or controls using the rigorous ePhenotyping algorithm described above.

Imputation was performed as previously described⁹. Briefly: SNPs were re-mapped to the Genome Reference Consortium Human build 37 (GRCh37) and the program liftOver run to ensure mapping consistency. Subsequently all SNPs were mapped from the Illumina TOP notation to the plus (+) strand. Strand was checked using SHAPEIT2 (version r2.644)¹⁰. Next the data were phased using SHAPEIT2. Imputation was performed using IMPUTE2 (version 2.3.0)¹¹. Chromosomes were divided into 6 MB segments with 250 kbp overlap between segments. A total of 5,719,283 SNPs with an info score of ≥ 0.9 were used for analysis.

Association analysis without adjustment was performed using PLINK (v1.09)⁶ and the imputed SNPs.

The eMERGE Network Imputed GWAS for 41 Phenotypes (the dbGaP eMERGE Phase 1 and 2 Merged data Submission) accession number is: phs000888.v1.p1 which includes the Geisinger AAA data.

Iceland, deCODE Genetics AAA GWAS dataset: Icelandic individuals with AAA (defined as infra-renal aortic diameter ≥ 30 mm) were recruited from a registry of individuals who were admitted at Landspítali University Hospital, in Reykjavik, Iceland, 1980 – 2006. AAA patients were either followed up or treated by intervention for emergency repair of symptomatic or ruptured AAA or for an elective repair by surgery or endovascular intervention. In total, whole genome data from 557 subjects with AAA, enrolled as part of the cardiovascular disease (CVD) genetics program at deCODE,

were included in the metaGWAS. The Icelandic controls used (n=89,235) were selected from individuals who have participated in various GWA studies and who were recruited as part of genetic programs at deCODE. Individuals with known CVD were excluded as controls² but controls were unscreened for AAA.

The Icelandic case and control samples were assayed with the Illumina HumanHap300, HumanHapCNV370 or HumanHap610 bead chips (Illumina, SanDiego, CA, USA). Only SNPs present on all chips were included in the analysis and SNPs were excluded if they had (a) call rates < 95% in cases or controls, (b) MAF<0.01 in the controls, or (c) showed significant deviation from HWE in the controls ($P < 1 \times 10^{-4}$). These criteria were applied separately to genotype data from each of the chip types used and SNPs that showed significant deviation ($P < 0.0001$ in an ANOVA test) in frequency between the chips were excluded from the analysis. Any samples with a call rate < 0.98 were excluded from the analysis. The final analysis included 293,677 SNPs present on all three chips.

For case-control association analysis, we used a standard likelihood ratio statistic, implemented in the NEMO software¹², to calculate two-sided P values and ORs for each individual allele, assuming a multiplicative model for risk¹³.

Familial imputation: For the Icelandic data set, we extended the classical case-control association analysis to include *in silico* genotypes of affected individuals who were not genotyped but who had genotyped relatives¹⁴ among the 40,000 Icelanders (about 13% of all living Icelanders) genotyped with the Illumina SNP chips at deCODE Genetics. For every ungenotyped affected individual, we calculated the probability distribution of the genotypes of his or her relatives, given his or her four possible phased genotypes. In practice, we included only genotypes of the affected individual's parents, children, siblings, half-siblings (and the half-sibling's parents), grandparents, grandchildren (and the grandchildren's parents) and spouses. The contribution of the ungenotyped affected individuals through this familial imputation to the effective sample size of the affected individuals, $n_{a,eff}$, was estimated using the Fisher information.

Genomic control: Some of the individuals in the Icelandic case-control groups are related to each other, causing the χ^2 test statistic to have a mean >1 and median >0.455. We estimated the genome-wide inflation factor λ_g as the average of the 293,677 χ^2 statistics to adjust for both relatedness and potential population stratification¹⁴.

The Netherlands AAA GWAS dataset: The AAA sample set from Utrecht was recruited in 2007-2009 from 8 centres in The Netherlands², mainly when individuals visited their vascular surgeon in the clinic or, in rare cases, during hospital admission for elective or emergency AAA surgery. An AAA was defined as an infrarenal aorta ≥ 30 mm. The sample set comprised 89.9% males, with a mean AAA diameter of 58.4 mm, 61.7% had been operated on, of which 8.1 % were after rupture. The Dutch controls used in the AAA GWAS were recruited as part of the Nijmegen Biomedical Study and the Nijmegen Bladder Cancer Study (see <http://dceg.cancer.gov/icbc/membership.html>).

Genotyping was performed on Illumina HumanHap610 chips.² As controls, we included 2,791 Dutch subjects who were recruited as part of the Nijmegen Biomedical Study (n=1,832) and the Nijmegen Bladder Cancer Study (n=1,278)^{15, 16} These controls were genotyped on Illumina CNV370 Duo BeadChips.

QC: We performed QC using PLINK version 1.07⁶. After removal of SNPs with A/T or C/G alleles and SNPs that were not called in any individual, we performed sample QC and SNP QC.

Sample QC was performed after merging cases and controls, using a subset of common, high-quality SNPs (as defined by SNPs without deviation from HWE ($P > 0.001$), with high MA) (>0.2) and with low rate of missing genotypes (<0.01)). Linkage disequilibrium (LD) pruning ($r^2 > 0.5$) was performed. Subjects were removed based on the following three criteria: missing genotypes (subjects with call

rates < 0.95 were removed), heterozygosity (subjects were excluded if the inbreeding coefficient deviated more than 3 standard deviations from the mean) and cryptic relatedness (by calculating identity-by-descent (IBD) for each pair of individuals). In each pair with an IBD proportion of >20%, a subject was excluded, if it exhibited distant relatedness with more than one individual. For case-control pairs, we removed the control subject. In the case-case or control-control pairs, the subject with the lowest call rate was excluded.

Using these common, high-quality SNPs, we performed PCA using EIGENSTRAT on the remaining study subjects and HapMap-CEU subjects. We excluded SNPs from three regions with known long-distance LD: the major histocompatibility (MHC) region (chr6: 25.8-36 Mbp), the chromosome 8 inversion (chr8: 6-16 Mbp) and a chromosome 17 region (chr17: 40-45 Mbp). We created PC plots with the first four PCs, using R version 2.11.¹⁷ Based on visual inspection of these plots, we excluded subjects that appeared to be outliers with respect to the CEU or the study population. After outlier removal, we recomputed PCs for them to be included as covariates in the logistic regression models.

After sample QC, we excluded SNPs with more than 2% missing genotypes, MAF < 0.01, missing genotype rate higher than MAF, and HWE deviation ($P < 0.001$). Because cases and controls had been genotyped separately, we performed these QC steps in each study cohort separately and again after merging cases and controls. We also removed SNPs with a differential degree of missing genotypes between cases and controls ($P < 1 \times 10^{-5}$; chi-squared test).

Imputation: We performed genotype imputation using the pre-phasing/imputation stepwise approach implemented in IMPUTE2 and SHAPEIT (chunk size of 3 Mb and default parameters)^{10, 18}. The imputation reference set consisted of 2,184 phased haplotypes from the full 1000 Genomes Project data set (February 2012; 40,318,253 variants). All genomic locations are given in NCBI Build 37/UCSC hg19 coordinates. After imputation, SNPs with an imputation accuracy score < 0.6 or MAF < 0.005 were excluded.

Association testing: Association testing was carried out in PLINK⁶ using imputed SNP dosages. We included as covariates the first four PCs. We calculated genomic inflation factors (λ_{GC}), defined as the ratio of the median of the empirically observed distribution of the test statistic to the expected median¹⁹.

b) Validation Cohorts

Aneurysm Consortium (AC) validation cohort: The same inclusion/exclusion criteria and recruitment sites were used as for the Aneurysm Consortium AAA GWAS. The lead SNPs (or their high LD proxies), identified in the discovery analysis, were genotyped at The Wellcome Trust Sanger Institute, Cambridge, UK using Sequenom iPLEX platform. Allele frequency summary results (odds ratio and 95% confidence interval) were generated using Chi-squared tests as implemented in the SHEsis web-based software package²⁰ (available: <http://analysis.bio-x.cn/SHEsisMain.htm>). Deviation from HWE was estimated and results are shown in **Online Table VI**.

New Zealand (NZ) Validation cohort: NZ validation cohort participants were recruited from the same sites as those in the GWAS. Case and control inclusion/exclusion criteria were identical to that of the NZ AAA GWAS, with all controls having been screened by ultrasound.

The lead SNPs (or their high LD proxies), identified in the discovery analysis, were genotyped at the Vascular Research Group, University of Otago using the TaqMan (LifeTechnologies) platform. Allele frequency summary results (odds ratio and 95% confidence interval) were generated using Chi-squared tests as implemented in the SHEsis web-based software package²⁰. Deviation from HWE was estimated and results are shown in **Online Table VI**.

Belgium and Canada validation cohorts: These sample-sets, in which all individuals were of European descent, included individuals with AAA who were admitted either for emergency repair of ruptured AAA or for an elective surgery to the University Hospital of Liege (Liege, Belgium) and to Dalhousie University Hospital (Halifax, Canada). AAA was defined as an infrarenal aortic diameter \geq 30 mm. Details of these case-control sets have been reported previously^{21, 22}. Approximately 40% of individuals with AAA had a family history of AAA. Control samples (51% males) were obtained from spouses of individuals with AAA or from individuals admitted to the same hospitals for reasons other than AAA. Controls had no known AAA, but they were not screened by ultrasonography for AAA.

The lead SNPs (or their high LD proxies), identified in the discovery analysis, were genotyped in the Tromp-Kuivaniemi Laboratory at Geisinger Health System using TaqMan (LifeTechnologies) platform. Allele frequency summary results (odds ratio and 95% confidence interval) were generated using Chi-squared tests as implemented in the SHESis web-based software package²⁰. Deviation from HWE was estimated and results are shown in **Online Table VI**.

eMERGE phase II (US) validation cohort: This cohort consisted of 338 AAA cases and 1,696 controls with GWAS data⁹ available from Mayo Clinic, Marshfield Clinic, Mount Sinai School of Medicine, Vanderbilt University, Northwestern University and Group Health Research Institute. The cases and controls were ascertained from the electronic medical records²³ using an ePhenotyping algorithm⁸ as described above. The samples had been genotyped in various GWAS and then imputed (see above). Allele frequency summary results (odds ratio and 95% confidence interval) were generated using Chi-squared tests as implemented in the SHESis web-based software package²⁰. Deviation from HWE was estimated and results are shown in **Online Table VI**. The eMERGE Network Imputed GWAS for 41 Phenotypes (the dbGaP eMERGE Phase 1 and 2 Merged data Submission) accession number is: phs000888.v1.p1 which includes these data.

US Validation 2 cohort: A second US case/control validation cohort was derived from the Mayo Vascular Disease Biorepository²⁴ (Mayo VDB; <http://www.mayo.edu/research/labs/cardiovascular-biomarkers/vascular-diseases-biorepository>), the Presbyterian University Hospital in Pittsburgh²⁵, Vanderbilt University (BioVU[®])²⁶, Marshfield Clinic (Personalized Medicine Research Project[®])²⁷, Mount Sinai School of Medicine (BioMe[®])²⁸, and Northwestern University (NUgene[®])²⁹. The cases and controls at Mayo Clinic, Vanderbilt University, Marshfield Clinic, Mount Sinai School of Medicine, and Northwestern University were phenotypically ascertained using the same ePhenotyping algorithm⁸ described above, whereas the AAA cases from the Presbyterian University Hospital in Pittsburgh were patients who had undergone elective or emergency surgery for AAA²⁵.

The lead SNPs (or their high LD proxies), identified in the discovery analysis, were genotyped in the Tromp-Kuivaniemi Laboratory at Geisinger Health System using TaqMan (LifeTechnologies) platform. Allele frequency summary results (odds ratio and 95% confidence interval) were generated using Chi-squared tests as implemented in the SHESis web-based software package²⁰. Deviation from HWE was estimated and results are shown in **Online Table VI**.

Italy validation cohort: This group consisted of 761 AAA cases and 520 controls. AAA cases were individuals referred to the Vascular Surgery Unit of the University of Florence. Familial and inflammatory AAAs were excluded from the study. All control subjects (n=520) had a negative personal and family history of AAA and were of comparable age and sex distribution to that of the AAA patients. A more detailed description of the study populations has been previously published³⁰.

The lead SNPs (or their high LD proxies), identified in the discovery analysis, were genotyped in the Giusti Laboratory at University of Florence using TaqMan (LifeTechnologies) platform. Allele frequency summary results (odds ratio and 95% confidence interval) were generated using Chi-squared tests as implemented in the SHEsis web-based software package²⁰. Deviation from HWE was estimated and results are shown in **Online Table VI**.

Poland validation cohort: This group consisted of 481 AAA cases scheduled for surgery at the Department of General and Vascular Surgery of the Poznan University of Medical Sciences in the years 1999–2011. The control group, consisting of 487 subjects matched for age (± 5 years) and sex to the AAA patients, was selected during the same time from the Poznan district³¹. The collection of samples was approved by the Bioethics Committee of the Poznan University of Medical Sciences. The diagnosis of AAA was evaluated by computed tomography angiography or magnetic resonance angiography. Based on physical examination supplemented with ultrasound duplex color scanning, the coexistence of PAD was recognized in 60.3% of the AAA patients. All patients were treated pharmacologically with statins, antiplatelet drugs and other drugs (antihypertensive or antidiabetic), depending on their clinical condition. The exclusion criteria for the controls included known aneurysms and PAD.

The lead SNPs (or their high LD proxies), identified in the discovery analysis, were genotyped in the Tromp-Kuivaniemi Laboratory at Geisinger Health System using TaqMan (LifeTechnologies) platform. Allele frequency summary results (odds ratio and 95% confidence interval) were generated using Chi-squared tests as implemented in the SHEsis web-based software package²⁰. Deviation from HWE was estimated and results are shown in **Online Table VI**.

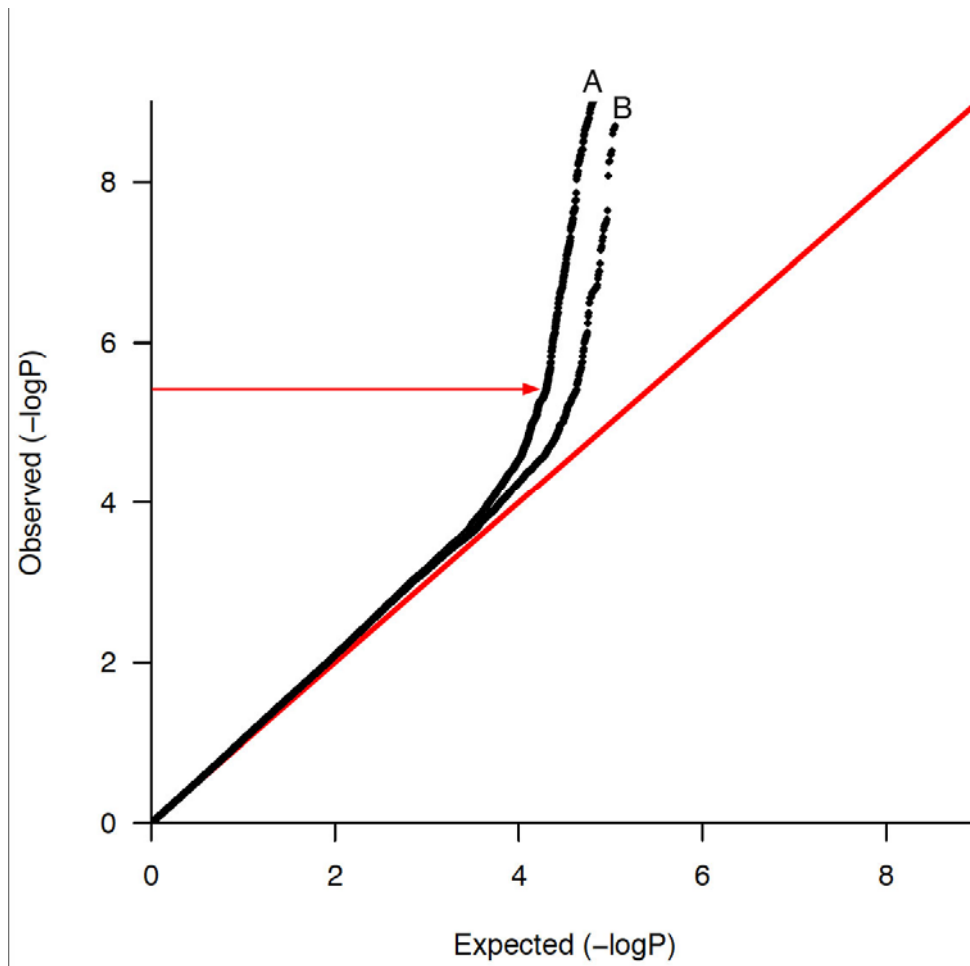
META-ANALYSIS of GWAS datasets

The discovery analysis consisted of the six cohorts with GWAS data detailed above, comprising 4,972 AAA cases and 99,858 controls, that were genotyped with a variety of genome-wide SNP arrays (**Online Table I**). All cohorts underwent QC filtering using the manufacturers' array-specific guidelines but with consistently applied inclusion criteria of SNP or sample call rates >95% and HWE $P > 5 \times 10^{-5}$ in controls^{1-3,7}. Each cohort then underwent imputation (⁹see above). Following imputation SNPs were quality controlled by quality score ($Q > 0.9$) and $MAF > 0.05$ in controls filtering, resulting in a common set of 5,363,770 SNPs across all discovery phase participants.

To obtain data for combination in the meta-analysis each case-control cohort was first analysed individually. Logistic regression models were used with AAA as a binary outcome in each cohort. Summary data [sample size, P-value, effect size (or log odds ratio), and the effect allele], unadjusted for covariates, for each SNP were combined in the meta-analysis.

The metaGWAS analysis was conducted using the METAL software package³² on the BCISNPmax database platform (version 3.5, BCI Platforms, Espoo, Finland). METAL was implemented using the sample size scheme with weighting based on the effective sample size [$N_{\text{eff}} = 4 / (1/N_{\text{cases}} + 1/N_{\text{controls}})$]. This approach was preferred over an inverse-variance weighted meta-analysis due to the disproportionate number of controls in some of the contributing cohorts and the fact that effect standard errors were not available in the data provided from Iceland and the United States (Geisinger) (**Online Table I**). The GWAS datasets from Iceland and the Netherlands were adjusted for genomic inflation prior to inclusion in the meta-analysis. The overall meta-GWAS analysis was adjusted for genomic inflation (λ) in each cohort (**Online Table I; Online Figure I**). An initial (λ -adjusted) discovery threshold of $P < 5 \times 10^{-6}$ was used to identify SNPs for subsequent validation genotyping.

The lead SNPs (or their high LD proxies), identified in the discovery analysis, were then genotyped in a further 8 independent cohorts (**Online Table II**). Each cohort's allele frequency summary results (odds ratio and 95% confidence interval) were generated using Chi-squared tests as implemented in the SHEsis web-based software package. Combined (discovery+validation) fixed effect meta-analysis was performed using a Maentel–Haenzel method with the genome-wide P -value significance threshold being set at 5×10^{-8} . The Maentel-Haenzel method was chosen since SNPs from the discovery and validation studies that were being combined demonstrated effects in the same direction and with low/medium heterogeneity. A sensitivity analyses of the combined (discovery+validation) study data were also performed using a random-effects model³³. The results from the discovery phase are presented in **Table 1; Online Tables III and IV; Figures 1 and 2; and Online Figures I and II**. The validation results are presented in **Table 1 and Online Tables V and VI**. Results from the combined analyses are presented in **Table 1 and Online Table VII**. Results from the sensitivity analysis are shown in **Online Table VIII**.



Online Figure I. Q-Q plot for the AAA meta-GWAS, showing (A) all 5.3 M SNPs with MAF>0.05 and (B) excluding the six previously identified loci (all SNPs within 100 kb of the peak variant associated with *SORT1*, *IL6R*, *CDKN2BAS1*, *DAB2IP*, *LDLR*, *LRP1*), generated from a comparison of 4,972 cases and 99,858 controls from 6 separate GWAS. The red arrow indicates the (λ -adjusted) $P < 5 \times 10^{-6}$ discovery threshold (362 SNPs in plot A).

Online Table I. Genome-wide association study (GWAS) cohort details. Individual level data were not available to calculate overall median age.

GWAS cohorts	Cases			Controls			GWAS Case weight (%)	Total* Case weight (%)	N _{effective}	Genotyping platform	Genomic inflation (λ) factor	Prior Adjustments
	Nn	%Male	Median Age (years)	N	% Male	Median Age (years)						
NZ 1	608	78	75	612	74	69	12.2	6.0	1,220	Affymetrix SNP6	1.07	None
NZ 2	397	84	77	384	80	67	8.0	3.9	781	Illumina Omni2.5	1.05	None
Aneurysm Consortium	1,846	98	72	5,605	49	52	37.1	18.1	5,555	Illumina 670	1.15	None
Netherlands	840	90	68	2,791	60	51	16.9	8.2	2,583	Illumina 300/370/610	1.11	Lambda
US (PA)	724	99	77	1,231	68	68	14.6	7.1	1,824	Illumina OmniExpress	1.06	None
Iceland deCODE	557	77	72	89,235	44	60	11.2	5.5	2,214	Illumina 300/370/610	0.70	Lambda
Total	4,972		N/A	99,858		N/A		48.7%	14,176			

Online Table II. Independent validation cohort details

Validation cohorts	Cases			Controls			Validation Case weight (%)	Total* Case weight (%)	N _{effective}	Genotyping platform
	N	% Male	Median Age (years)	N	% Male	Median Age (years)				
Aneurysm Consortium validation (AC)	1,236	84	72	2,196	93	68	23.6	12.1	3,163	Sequenom
NZ validation	753	81	77	1,237	67	68	14.4	7.4	1,872	Taqman
Italy validation	761	79	73	520	78	72	14.5	7.5	1,236	Taqman
Poland validation	481	86	69	487	72	59	9.2	4.7	968	Taqman
eMERGE US validation 1	338	80	82	1696	80	82	6.5	3.3	1127	Imputed data from various GWAS platforms
US validation 2	1,176	82	73	1,371	64	68	22.5	11.5	2,532	Taqman
Belgium validation	339	91	N/A	265	68	N/A	6.5	3.3	595	Taqman
Canada validation	148	75	N/A	136	79	N/A	2.8	1.5	283	Taqman
Total	5,232		N/A	7,908		N/A		51.3%		

*Combined (GWAS + Validation) analysis consisted of 10,204 AAA cases and 107,766 controls.

Online Table III: Summary of results for the lead SNPs at 19 putative AAA associated loci ($P < 5 \times 10^{-6}$) in the meta-analysis of 6 primary AAA GWAS datasets with a total of 4,972 AAA cases and 99,858 controls (see **Online Table I** for details on these cohorts). The results were based on an $N_{\text{effective}}$ weighted METAL analysis. The order of cohorts in the direction column is the same as that in **Online Table I** [NZ 1, NZ 2, Aneurysm Consortium, Netherlands, US (PA), Iceland (deCODE)]. See **Online Table IV** for MAF values for cases and controls separately.

Chr	SNP	Position	Gene	Risk allele	Other allele	Direction	$N_{\text{effective}}$ weighted analysis		
							P	Phet	I^2
1	rs602633	109821511	Near <i>PSRC1 CELSR2 SORT1</i>	T	G	-----	1.72×10^{-07}	0.097	46.3
1	rs12133641	154428283	<i>IL6R</i>	A	G	+++++	1.67×10^{-10}	0.903	0.0
1	<i>rs4129267 proxySNP</i>	154426264	<i>IL6R</i>	T	C	-----	9.26×10^{-10}	0.886	0.0
1	rs1795061	214409280	near <i>SMYD2</i>	T	C	+++++	1.80×10^{-07}	0.069	51.2
2	rs13382862	20882449	near <i>C2orf43</i> and <i>GDF7</i>	A	G	-----	3.03×10^{-08}	0.878	0.0
4	rs10029392	5616048	<i>EVC2</i>	T	G	+++++	4.60×10^{-06}	0.147	38.8
5	rs12659791	74757758	<i>COL4A3BP</i>	T	C	-----+	2.28×10^{-06}	0.105	45.1
6	rs3176334	36648364	<i>CDKN1A</i>	C	T	-----	1.45×10^{-06}	0.627	0.0
6	<i>rs733590 proxySNP</i>	36645203	<i>CDKN1A</i>	T	C	-----	8.74×10^{-06}	0.584	0.0
8	rs3110425	107649626	<i>OXR1</i>	T	C	-----	3.25×10^{-06}	0.895	0.0
9	rs10757274	22096055	<i>CDKN2BAS1/ANRIL</i>	A	G	-----	2.32×10^{-13}	0.520	0.0
9	rs10985349	124425243	<i>DAB2IP</i>	T	C	+++++	8.98×10^{-07}	0.181	34.0
12	rs1385526	57532749	<i>LRP1</i>	C	G	-----	1.31×10^{-09}	0.597	0.0
13	rs9316871	22861921	<i>LINC00540</i>	A	G	+++++	5.95×10^{-06}	0.143	39.4
15	rs17189674	89040591	<i>DET1</i>	A	G	+++++	1.05×10^{-06}	0.663	0.0
19	rs6511720	11202306	<i>LDLR</i>	T	G	-----	5.71×10^{-12}	0.679	0.0
19	rs12980543	56096197	<i>ZNF579</i>	A	G	+++++	2.30×10^{-06}	0.301	17.4
19	<i>rs11084402 proxySNP</i>	56093365	<i>ZNF579</i>	T	C	+++++	4.33×10^{-06}	0.218	29.0
20	rs6516091	6050622	near <i>FERMT1</i>	A	G	+++++	3.82×10^{-09}	0.027	60.5
20	rs58749629	44571317	near <i>PCIF1 ZNF335 MMP9</i>	A	G	+++++	7.97×10^{-10}	0.473	0.0
20	<i>rs3827066 proxySNP</i>	44586023	near <i>PCIF1 ZNF335 MMP9</i>	T	C	+++++	9.18×10^{-10}	0.729	0.0
21	rs2836411	39819830	<i>ERG</i>	T	C	+++++	1.53×10^{-07}	0.103	45.5
X	rs5954362	140673423	<i>SPANXA1</i>	G	C	---	2.73×10^{-07}	0.271	23.2

Online Table IV: Individual cohort data from the 6 primary AAA GWAS studies, combined using the Maentel–Haenzel fixed effect method, for the lead SNPs at the 19 putative AAA loci identified in the meta-analysis of GWAS. See **Online Table I** for details on these cohorts. This table spans this and the following 6 pages.

CHR	SNP	POSITION	Region	Cohort	OR (95% CI)	P	Case/ Control	MAF _{AAA}	MAF _{Control}	
1	rs602633	109821511	Near <i>PSRC1 CELSR2 SORT1</i>	NZ GWAS 1	0.653 (0.535 - 0.797)	2.59E-05	608/ 612	0.1743	0.2442	
				NZ GWAS 2	0.874 (0.680 - 1.125)	0.2952	397/ 384	0.1870	0.2083	
				Aneurysm Consortium GWAS	0.864 (0.785 - 0.950)	0.002639	1846/ 5605	0.1942	0.2181	
				Netherlands GWAS	0.899 (0.778 - 1.038)	0.1458	840/ 2791	0.2151	0.2336	
				US (PA) GWAS	0.793 (0.680 - 0.925)	0.003166	724/ 1231	0.1843	0.2217	
				Iceland deCODE GWAS	0.916 (0.783 - 1.073)	0.2768	557/ 89235	0.1944	0.2085	
									OR (95% CI)	Z-score
Combined					0.845 (0.796 - 0.897)	-5.534	3.1E-08	5	29.4	0.215
1	rs12133641 rs4129267 proxy	154428283 154426264	<i>IL6R</i>	NZ GWAS 1	0.841 (0.715 - 0.989)	0.03596	608/ 612	0.3881	0.43	
				NZ GWAS 2	0.838 (0.683 - 1.027)	0.08904	397/ 384	0.3687	0.4108	
				Aneurysm Consortium GWAS	0.878 (0.813 - 0.948)	8.50E-04	1846/ 5605	0.3762	0.4072	
				Netherlands GWAS	0.818 (0.723 - 0.924)	0.001291	840/ 2791	0.3475	0.3936	
				US (PA) GWAS	0.817 (0.720 - 0.927)	0.001744	724/ 1231	0.3455	0.3925	
				Iceland deCODE GWAS	0.879 (0.775 - 0.997)	0.04487	557/ 89235	0.3857	0.4169	
									OR (95% CI)	Z-score
Combined					0.854 (0.813 - 0.896)	-6.382	1.7E-10	5	0	0.945
1	rs1795061	214409280	near <i>SMYD2</i>	NZ GWAS 1	1.033 (0.868 - 1.229)	0.716	608/ 612	0.3224	0.3153	
				NZ GWAS 2	1.364 (1.087 - 1.713)	0.007383	397/ 384	0.3456	0.2791	
				Aneurysm Consortium GWAS	1.135 (1.048 - 1.229)	0.001908	1846/ 5605	0.3342	0.3067	
				Netherlands GWAS	1.075 (0.943 - 1.225)	0.2806	840/ 2791	0.2952	0.2784	
				US (PA) GWAS	1.324 (1.163 - 1.507)	2.16E-05	724/ 1231	0.3517	0.2907	
				Iceland deCODE GWAS	1.133 (0.997 - 1.287)	0.0559	557/ 89235	0.4247	0.3954	
									OR (95% CI)	Z-score
Combined					1.154(1.097 - 1.214)	5.527	3.3E-07	5	47.9	0.087

CHR	SNP	POSITION	Region	Cohort	OR (95% CI)	P	Case/ Control	MAF _{AAA}	MAF _{Control}
2	rs13382862	20882449	<i>C2orf43</i> and <i>GDF7</i>	NZ GWAS 1	0.886 (0.742 - 1.057)	0.1787	608/ 612	0.3424	0.3701
				NZ GWAS 2	0.766 (0.618 - 0.948)	0.01432	397/ 384	0.3307	0.3922
				Aneurysm Consortium GWAS	0.865 (0.799 - 0.937)	3.78E-04	1846/ 5605	0.3359	0.3689
				Netherlands GWAS	0.862 (0.763 - 0.974)	0.0176	840/ 2791	0.3430	0.3761
				US (PA) GWAS	0.855 (0.750 - 0.974)	0.01851	724/ 1231	0.3255	0.3609
				Iceland deCODE GWAS	0.892 (0.782 - 1.016)	0.08629	557/ 89235	0.3420	0.3683
				OR (95% CI)	Z-score	P-value	df (Q)	HetI²	HetPval
Combined	0.863 (0.820 - 0.907)	-5.75	8.8E-09	5	0	0.942			
4	rs10029392	5616048	<i>EVC2</i>	NZ GWAS 1	2.071 (1.444 - 2.968)	5.47E-05	608/ 612	0.0801	0.0404
				NZ GWAS 2	1.199 (0.733 - 1.961)	0.4692	397/ 384	0.0467	0.0393
				Aneurysm Consortium GWAS	1.306 (1.081 - 1.578)	0.005588	1846/ 5605	0.0436	0.0338
				Netherlands GWAS	1.180 (0.869 - 1.601)	0.2894	840/ 2791	0.0396	0.0358
				US (PA) GWAS	1.166 (0.882 - 1.542)	0.28	724/ 1231	0.0517	0.0447
				Iceland deCODE GWAS	1.402 (1.033 - 1.904)	0.03019	557/ 89235	0.0587	0.0445
				OR (95% CI)	Z-score	P-value	df (Q)	HetI²	HetPval
Combined	1.331 (1.1851 - 1.495)	4.825	1.4E-06	5	32.1	0.195			
5	rs12659791	74757758	<i>COL4A3BP</i>	NZ GWAS 1	1.284 (0.837 - 1.970)	0.2512	608/ 612	0.1763	0.1429
				NZ GWAS 2	1.067 (0.808 - 1.409)	0.6466	397/ 384	0.1549	0.1466
				Aneurysm Consortium GWAS	1.304 (1.181 - 1.440)	1.59E-07	1846/ 5605	0.1785	0.1428
				Netherlands GWAS	1.216 (1.040 - 1.421)	0.01392	840/ 2791	0.1710	0.1480
				US (PA) GWAS	1.077 (0.909 - 1.278)	0.3911	724/ 1231	0.1510	0.1417
				Iceland deCODE GWAS	0.986 (0.819 - 1.188)	0.8844	557/ 89235	0.1264	0.1279
				OR (95% CI)	Z-score	P-value	df (Q)	HetI²	HetPval
Combined	1.192 (1.115 - 1.274)	5.151	2.6E-07	5	45.5	0.102			

CHR	SNP	POSITION	Region	Cohort	OR (95% CI)	P	Case/ Control	MAF _{AAA}	MAF _{Control}
6	rs733590 proxy	36648364	CDKN1A	NZ GWAS 1	1.027 (0.870 - 1.213)	0.7498	608/ 612	0.3550	0.3489
				NZ GWAS 2	1.108 (0.896 - 1.371)	0.3434	397/ 384	0.3405	0.3178
				Aneurysm Consortium GWAS	1.128 (1.040 - 1.224)	0.003699	1846/ 5605	0.3612	0.3339
				Netherlands GWAS	1.228 (1.085 - 1.391)	0.001181	840/ 2791	0.4027	0.3552
				US (PA) GWAS	1.160 (1.024 - 1.315)	0.01962	724/ 1231	0.4052	0.3699
				Iceland deCODE GWAS	1.056 (0.925 - 1.206)	0.42	557/ 89235	0.3449	0.3329
				Combined	OR (95% CI)	Z-score	P-value	df (Q)	HetI²
	1.127 (1.072 - 1.186)	4.665	3.1E-06	5	0	0.546			
8	rs3110425	107649626	OXR1	NZ GWAS 1	0.909 (0.769 - 1.075)	0.2639	608/ 612	0.3460	0.3679
				NZ GWAS 2	0.852 (0.692 - 1.048)	0.1284	397/ 384	0.3469	0.3842
				Aneurysm Consortium GWAS	0.883 (0.816 - 0.955)	0.001861	1846/ 5605	0.3310	0.3613
				Netherlands GWAS	0.865 (0.764 - 0.980)	0.02225	840/ 2791	0.3340	0.3680
				US (PA) GWAS	0.954 (0.840 - 1.085)	4.68E-01	724/ 1231	0.3650	0.3760
				Iceland deCODE GWAS	0.849 (0.752 - 0.959)	0.012	557/ 89235	0.3480	0.3870
				Combined	OR (95% CI)	Z-score	P-value	df (Q)	HetI²
	0.885 (0.843 - 0.93)	-4.873	1.1E-06	5	0	0.784			
9	rs10757274	22096055	ANRIL/ CDKN2B-AS1	NZ GWAS 1	0.814 (0.694 - 0.955)	0.01152	608/ 612	0.4553	0.5066
				NZ GWAS 2	0.922 (0.755 - 1.125)	0.4232	397/ 384	0.4484	0.4686
				Aneurysm Consortium GWAS	0.842 (0.781 - 0.908)	7.91E-06	1846/ 5605	0.4707	0.5137
				Netherlands GWAS	0.742 (0.660 - 0.834)	6.31E-07	840/ 2791	0.4746	0.5465
				US (PA) GWAS	0.883 (0.782 - 0.997)	0.04425	724/ 1231	0.4793	0.5104
				Iceland deCODE GWAS	0.838 (0.739 - 0.949)	0.005418	557/ 89235	0.5111	0.555
				Combined	OR (95% CI)	Z-score	P-value	df (Q)	HetI²
	0.832 (0.793 - 0.872)	-7.612	2.7E-14	5	9.9	0.352			

CHR	SNP	POSITION	Region	Cohort	OR (95% CI)	P	Case/ Control	MAF _{AAA}	MAF _{Control}
9	rs10985349	124425243	DAB2IP	NZ GWAS 1	1.326 (1.078 - 1.630)	0.007382	608/ 612	0.2053	0.1631
				NZ GWAS 2	1.443 (1.112 - 1.872)	0.005649	397/ 384	0.2091	0.1549
				Aneurysm Consortium GWAS	1.159 (1.038 - 1.294)	0.008684	1846/ 5605	0.1666	0.1471
				Netherlands GWAS	1.036 (0.890 - 1.206)	0.6491	840/ 2791	0.2192	0.2110
				US (PA) GWAS	1.223 (1.050 - 1.425)	0.009782	724/ 1231	0.2055	0.1746
				Iceland deCODE GWAS	1.212 (1.027 - 1.429)	0.02253	557/ 89235	0.2427	0.2130
				Combined	OR (95% CI)	Z-score	P-value	df (Q)	HetI²
	1.185 (1.112 - 1.264)	5.198	2.0E-07	5	18.1	0.296			
12	rs1385526	57532749	LRP1	NZ GWAS 1	0.863 (0.728 - 1.024)	0.09069	608/ 612	0.3165	0.3491
				NZ GWAS 2	0.820 (0.659 - 1.021)	0.07616	397/ 384	0.3043	0.3478
				Aneurysm Consortium GWAS	0.798 (0.737 - 0.865)	3.19E-08	1846/ 5605	0.3125	0.3629
				Netherlands GWAS	0.893 (0.788 - 1.011)	0.07384	840/ 2791	0.3182	0.3452
				US (PA) GWAS	0.902 (0.790 - 1.030)	0.1277	724/ 1231	0.3047	0.3269
				Iceland deCODE GWAS	0.904 (0.796 - 1.028)	0.1233	557/ 89235	0.3945	0.4186
				Combined	OR (95% CI)	Z-score	P-value	df (Q)	HetI²
	0.851 (0.809 - 0.895)	-6.295	3.1E-10	5	0	0.613			
13	rs9316871	22861921	LINC00540	NZ GWAS 1	0.979 (0.804 - 1.190)	0.8279	608/ 612	0.2048	0.2083
				NZ GWAS 2	0.678 (0.530 - 0.869)	0.002047	397/ 384	0.1755	0.2388
				Aneurysm Consortium GWAS	0.823 (0.750 - 0.903)	3.92E-05	1846/ 5605	0.1923	0.2244
				Netherlands GWAS	0.891 (0.770 - 1.030)	0.1191	840/ 2791	0.1931	0.2104
				US (PA) GWAS	0.880 (0.760 - 1.020)	0.08905	724/ 1231	0.2103	0.2324
				Iceland deCODE GWAS	0.969 (0.821 - 1.143)	0.7052	557/ 89235	0.1763	0.1809
				Combined	OR (95% CI)	Z-score	P-value	df (Q)	HetI²
	0.864 (0.815 - 0.917)	-4.850	1.23E-06	5	33.2	0.187			

CHR	SNP	POSITION	Region	Cohort	OR (95% CI)	P	Case/ Control	MAF _{AAA}	MAF _{Control}
15	rs17189674	89040591	DET1	NZ GWAS 1	1.227 (0.966 - 1.559)	0.09398	608/ 612	0.1410	0.1180
				NZ GWAS 2	1.595 (1.140 - 2.230)	0.006056	397/ 384	0.1273	0.0838
				Aneurysm Consortium GWAS	1.241 (1.096 - 1.406)	6.51E-04	1846/ 5605	0.1123	0.0925
				Netherlands GWAS	1.194 (0.991 - 1.438)	0.06165	840/ 2791	0.1314	0.1148
				US (PA) GWAS	1.109 (0.916 - 1.344)	0.2889	724/ 1231	0.1167	0.1064
				Iceland deCODE GWAS	1.181 (0.983 - 1.418)	0.07515	557/ 89235	0.1645	0.1448
				OR (95% CI)	Z-score	P-value	df (Q)	HetI²	HetPval
Combined	1.216 (1.128 - 1.311)	5.091	3.6E-07	5	0	0.742			
19	rs6511720	11202306	LDLR	NZ GWAS 1	0.611 (0.403 - 0.927)	0.01942	608/ 612	0.04043	0.06452
				NZ GWAS 2	0.717 (0.514 - 1.001)	0.05007	397/ 384	0.08564	0.11550
				Aneurysm Consortium GWAS	0.764 (0.676 - 0.863)	1.48E-05	1846/ 5605	0.09778	0.12430
				Netherlands GWAS	0.650 (0.529 - 0.797)	3.74E-05	840/ 2791	0.08240	0.12150
				US (PA) GWAS	0.742 (0.608 - 0.905)	0.003207	724/ 1231	0.09655	0.12590
				Iceland deCODE GWAS	0.855 (0.684 - 1.068)	0.1668	557/ 89235	0.07480	0.08720
				OR (95% CI)	Z-score	P-value	df (Q)	HetI²	HetPval
Combined	0.743 (0.685 - 0.806)	-7.151	8.6E-13	5	0	0.829			
19	rs12980543 rs11084402 proxy	56096197 56093365	ZNF579	NZ GWAS 1	1.011 (0.832 - 1.227)	0.9147	608/ 612	0.2170	0.2152
				NZ GWAS 2	1.280 (1.006 - 1.628)	0.04423	397/ 384	0.2418	0.1995
				Aneurysm Consortium GWAS	1.077 (0.984 - 1.180)	0.1091	1846/ 5605	0.2153	0.2030
				Netherlands GWAS	1.217 (1.051 - 1.409)	0.00854	840/ 2791	0.2159	0.1824
				US (PA) GWAS	1.273 (1.094 - 1.481)	0.001733	724/ 1231	0.2131	0.1754
				Iceland deCODE GWAS	1.281 (1.059 - 1.549)	0.01071	557/ 89235	0.1734	0.1430
				OR (95% CI)	Z-score	P-value	df (Q)	HetI²	HetPval
Combined	1.152 (1.086 - 1.223)	4.669	3.0E-06	5	33.2	0.187			

CHR	SNP	POSITION	Region	Cohort	OR (95% CI)	P	Case/ Control	MAF _{AAA}	MAF _{Control}	
20	rs6516091	6050622	near <i>FERMT1</i>	NZ GWAS 1	1.263 (0.991 - 1.609)	0.05848	608/ 612	0.1381	0.1126	
				NZ GWAS 2	1.271 (0.931 - 1.734)	0.13	397/ 384	0.1297	0.1050	
				Aneurysm Consortium GWAS	1.399 (1.261 - 1.551)	1.73E-10	1846/ 5605	0.1655	0.1242	
				Netherlands GWAS	1.187 (0.994 - 1.416)	0.05749	840/ 2791	0.1298	0.1150	
				US (PA) GWAS	1.186 (0.987 - 1.426)	0.06916	724/ 1231	0.1290	0.1110	
				Iceland deCODE GWAS	0.968 (0.783 - 1.197)	0.7619	557/ 89235	0.0938	0.0966	
									OR (95% CI)	Z-score
Combined					1.262 (1.177 - 1.354)	6.525	6.8E-11	5	56.2	0.044
20	rs58749629 rs3827066 proxy	44571317 44586023	Near <i>MMP9/ZNF335</i>	NZ GWAS 1	1.062 (0.846 - 1.333)	0.6044	608/ 612	0.1503	0.1427	
				NZ GWAS 2	1.101 (0.847 - 1.430)	0.4723	397/ 384	0.1827	0.1688	
				Aneurysm Consortium GWAS	1.237 (1.119 - 1.368)	2.97E-05	1846/ 5605	0.1743	0.1457	
				Netherlands GWAS	1.287 (1.099 - 1.506)	0.001752	840/ 2791	0.1761	0.1414	
				US (PA) GWAS	1.246 (1.067 - 1.456)	0.005513	724/ 1231	0.1972	0.1647	
				Iceland deCODE GWAS	1.325 (1.094 - 1.606)	0.003994	557/ 89235	0.1492	0.1193	
									OR (95% CI)	Z-score
Combined					1.233 (1.156 - 1.314)	6.371	1.9E-10	5	0	0.444
21	rs2836411	39819830	<i>ERG</i>	NZ GWAS 1	1.313 (1.113 - 1.548)	0.001228	608/ 612	0.3980	0.3350	
				NZ GWAS 2	1.076 (0.876 - 1.321)	0.4862	397/ 384	0.3823	0.3652	
				Aneurysm Consortium GWAS	1.132 (1.048 - 1.223)	0.00155	1846/ 5605	0.3814	0.3525	
				Netherlands GWAS	1.204 (1.065 - 1.361)	0.002983	840/ 2791	0.4016	0.3611	
				US (PA) GWAS	1.232 (1.086 - 1.397)	0.001164	724/ 1231	0.3821	0.3342	
				Iceland deCODE GWAS	1.000 (0.878 - 1.139)	0.9964	557/ 89235	0.3330	0.3331	
									OR (95% CI)	Z-score
Combined					1.149 (1.095 - 1.207)	5.573	2.5E-08	5	30.1	0.209

CHR	SNP	POSITION	Region	Cohort	OR (95% CI)	P	Case/ Control	MAF _{AAA}	MAF _{Control}	
X	RS5954362	140673423	SPANXA1	NZ GWAS 1	0.750 (0.556 - 1.007)	0.05496	474/ 450	0.2372	0.2930	
				NZ GWAS 2	0.862 (0.586 - 1.269)	0.4522	332/ 308	0.2310	0.2584	
				Aneurysm Consortium GWAS	0.584 (0.499 - 0.685)	1.81E-11	1815/ 2736	0.1894	0.2856	
					OR (95% CI)	Z-score	P-value	df (Q)	HetI ²	HetPval
Combined					0.642 (0.563 - 0.732)	-6.105	1.0E-09	2	3.91	0.142

Online Table V: Summary of results for the combined (using the Maentel–Haenzel fixed effect method) validation study cohorts for the lead SNPs at putative AAA associated loci. The SNPs with $P < 5 \times 10^{-6}$ in the meta-analysis of 6 primary AAA GWAS datasets were genotyped in 8 different validation cohorts for a total of 5,232 AAA cases and 7,908 controls (see **Online Table II** for details on these cohorts). Results including MAFs for cases and controls in each individual cohort are shown in **Online Table VI**. Where a proxy SNP was typed the original lead SNP from the discovery study is shown above the proxy SNP typed in the validation study.

Chr	SNP	Position	Gene	Risk allele	Other allele	P	Direction	Phet	i^2
1	rs602633	109821511	Near <i>PSRC1 CELSR2 SORT1</i>	T	G	0.01	----+--	0.027	55.8
1	rs12133641	154428283	<i>IL6R</i>	A	G				
	<i>rs4129267 proxySNP</i>	154426264	<i>IL6R</i>	T	C	1.81×10^{-4}	+-----	0.294	17.2
1	rs1795061	214409280	near <i>SMYD2</i>	T	C	3.49×10^{-4}	+++++++	0	70.3
2	rs13382862	20882449	near <i>C2orf43</i> and <i>GDF7</i>	A	G	0.360	-----+	0.278	19.2
4	rs10029392	5616048	<i>EVC2</i>	T	G	0.267	++---++	0.195	29.2
5	rs12659791	74757758	<i>COL4A3BP</i>	T	C	0.966	-+-----	0.749	0.0
6	rs3176334	36648364	<i>CDKN1A</i>	C	T				
	<i>rs733590 proxySNP</i>	36645203	<i>CDKN1A</i>	T	C	0.789	+++++--	0.754	0.0
8	rs3110425	107649626	<i>OXR1</i>	T	C	0.261	+-----+	0.268	20.4
9	rs10757274	22096055	<i>CDKN2BAS1/ANRIL</i>	A	G	1.02×10^{-21}	-----	0.001	64.2
9	rs10985349	124425243	<i>DAB2IP</i>	T	C	2.30×10^{-5}	+++++++	0.4	3.9
12	rs1385526	57532749	<i>LRP1</i>	C	G	0.622	+++++++	0.33	12.8
13	rs9316871	22861921	<i>LINC00540</i>	A	G	8.28×10^{-5}	-----+	0.795	0.0
15	rs17189674	89040591	<i>DET1</i>	A	G	0.744	--++++-	0.102	41.5
19	rs6511720	11202306	<i>LDLR</i>	T	G	6.02×10^{-4}	-----++	0.003	68.2
19	rs12980543	56096197	<i>ZNF579</i>	A	G				
	<i>rs11084402 proxySNP</i>	56093365	<i>ZNF579</i>	T	C	0.364	+-----+	0.12	38.9
20	rs6516091	6050622	near <i>FERMT1</i>	A	G	0.867	+-----+	0.104	41.1
20	rs58749629	44571317	near <i>PCIF1 ZNF335 MMP9</i>	A	G				
	<i>rs3827066 proxySNP</i>	44586023	near <i>PCIF1 ZNF335 MMP9</i>	T	C	2.00×10^{-8}	+++++++	0.3	16.5
21	rs2836411	39819830	<i>ERG</i>	T	C	0.011	+++++++	0.203	28.3
X	rs5954362	140673423	<i>SPANXA1</i>	G	C	0.172	-+--+	0.005	73.2

Online Table VI: Results of validation for the lead SNPs (combined using the Maentel–Haenzel fixed effect method) at putative AAA loci identified in the meta-analysis of GWAS. The SNPs with $P < 5 \times 10^{-6}$ in the meta-analysis of 6 primary AAA GWAS datasets were genotyped in 8 different validation cohorts for a total of up to 5,232 AAA cases and 7,908 controls (see **Online Table II** for details on these cohorts). This table spans this and the following 5 pages. Where a proxy SNP is indicated the results are for that proxy SNP.

Chromosome	SNP	POSITION	Region	Cohort	OR (95% CI)	Case/control	MAFAAA	MAFControl	HWEControl	HWEAAA				
1	rs602633	109821511	Near PSRC1 CELSR2 SORT1	AC	0.885 (0.781-1.002)	1236/2196	0.191	0.211	0.079	0.799				
				US2	0.864 (0.757-0.987)	1157/1374	0.211	0.236	0.724	0.248				
				NZ	0.933 (0.794-1.095)	753/1237	0.201	0.213	0.473	0.183				
				Italy	1.201 (0.995-1.449)	718/636	0.220	0.190	0.200	0.210				
				Poland	1.133 (0.904-1.421)	443/474	0.218	0.197	0.652	0.995				
				eMERGE	0.784 (0.639-0.963)	330/1648	0.203	0.245	0.005	0.248				
				Belgium	0.8 (0.591-1.082)	302/216	0.192	0.229	0.198	0.959				
				Canada	0.803 (0.533-1.211)	126/118	0.230	0.271	0.881	0.870				
									OR (95% CI)	Z-score	P-value	df (Q)	HetPVal	I-squared
				Combined:					0.92 (0.863-0.98)	-2.582	0.010	7	0.027	55.770
1	rs12133641 rs4129267 proxy	154428283 154426264	IL6R	AC	1.001 (0.904-1.108)	1236/2196	0.386	0.386	0.706	0.293				
				US2	0.879 (0.783-0.986)	1137/1324	0.369	0.400	0.798	0.689				
				NZ	0.835 (0.732-0.954)	753/1237	0.377	0.420	0.155	0.022				
				Italy	0.897 (0.765-1.052)	714/585	0.364	0.390	0.286	0.179				
				Poland	0.925 (0.768-1.114)	480/481	0.353	0.371	0.731	0.000				
				eMERGE	0.927 (0.781-1.099)	345/1724	0.354	0.371	0.137	0.840				
				Belgium	0.767 (0.606-0.971)	334/256	0.361	0.424	0.440	0.410				
				Canada	0.761 (0.541-1.072)	139/133	0.381	0.447	0.025	0.427				
									OR (95% CI)	Z-score	P-value	df (Q)	HetPVal	I-squared
				Combined:					0.904 (0.857-0.953)	-3.743	1.81E-04	7	0.294	17.200
1	rs1795061	214409280	Near SMYD2	AC	1.171 (1.053-1.302)	1236/2196	0.332	0.298	0.869	0.360				
				US2	0.91 (0.808-1.024)	1172/1386	0.301	0.321	0.469	0.892				
				NZ	1.077 (0.939-1.236)	753/1237	0.336	0.319	0.060	0.026				
				Italy	1.434 (1.21-1.698)	761/558	0.340	0.264	0.226	0.071				
				Poland	1.025 (0.848-1.239)	470/487	0.332	0.326	0.823	0.025				
				eMERGE	1.088 (0.915-1.294)	340/1679	0.347	0.328	0.216	0.991				
				Belgium	1.28 (0.996-1.646)	335/260	0.327	0.275	0.605	0.583				
				Canada	1.32 (0.916-1.905)	132/132	0.352	0.292	0.075	0.364				
									OR (95% CI)	Z-score	P-value	df (Q)	HetPVal	I-squared
				Combined:					1.105 (1.046-1.168)	3.576	3.49E-04	7	0.000	70.300

Chromosome	SNP	POSITION	Region	Cohort	OR (95% CI)	Case/control	MAFAAA	MAFControl	HWEControl	HWEAAA				
2	rs13382862	20882449	near C2orf43 and GDF7	AC	0.942 (0.85-1.045)	1236/2196	0.358	0.372	0.224	0.156				
				US2	0.94 (0.836-1.057)	1109/1386	0.346	0.360	0.103	0.291				
				NZ	0.87 (0.759-0.997)	753/1237	0.335	0.366	0.140	0.741				
				Italy	1.109 (0.931-1.321)	727/558	0.287	0.266	0.158	0.345				
				Poland	1.099 (0.906-1.332)	450/452	0.366	0.344	0.465	0.098				
				eMERGE	1.083 (0.913-1.285)	335/1645	0.388	0.369	0.970	0.918				
				Belgium	1.024 (0.794-1.319)	310/256	0.310	0.305	0.821	0.209				
				Canada	0.998 (0.705-1.413)	142/131	0.370	0.370	0.720	0.021				
									OR (95% CI)	Z-score	P-value	df (Q)	HetPVal	I-squared
				Combined:					0.975 (0.923-1.029)	-0.915	0.360	7	0.278	19.156
4	rs10029392	5616048	EVC2	AC	1.014 (0.814-1.263)	1698/2209	0.044	0.043	0.655	0.110				
				US2*	0.876 (0.678-1.132)	1169/1387	0.046	0.052	0.217	0.088				
				NZ*	1.233 (0.92-1.651)	753/1237	0.057	0.047	0.809	0.106				
				Italy	0.767 (0.588-0.999)	678/556	0.088	0.112	0.423	0.709				
				Poland*	0.809 (0.6-1.092)	472/481	0.091	0.110	0.074	0.963				
				eMERGE	0.921 (0.642-1.321)	343/1707	0.054	0.058	0.998	0.006				
				Belgium*	1.09 (0.545-2.18)	335/225	0.030	0.027	0.652	0.573				
				Canada*	2.2 (0.754-6.422)	133/130	0.041	0.019	0.823	0.091				
									OR (95% CI)	Z-score	P-value	df (Q)	HetPVal	I-squared
				Combined:					0.94 (0.843-1.049)	-1.111	0.267	7	0.195	29.200
5	rs12659791	74757758	COL4A3BP	AC	0.963 (0.839-1.105)	1236/2196	0.149	0.154	0.071	0.307				
				US2	1.063 (0.91-1.242)	1151/1371	0.153	0.145	0.398	0.663				
				NZ	0.959 (0.802-1.148)	753/1237	0.152	0.158	0.149	0.581				
				Italy	1.051 (0.83-1.332)	732/439	0.151	0.145	0.484	0.177				
				Poland	0.976 (0.771-1.236)	486/488	0.169	0.172	0.002	0.553				
				eMERGE	0.979 (0.773-1.241)	345/1723	0.138	0.140	0.818	0.807				
				Belgium	0.91 (0.669-1.237)	339/266	0.156	0.169	0.298	0.126				
				Canada	1.62 (0.898-2.921)	105/91	0.167	0.110	0.239	0.953				
									OR (95% CI)	Z-score	P-value	df (Q)	HetPVal	I-squared
				Combined:					0.998 (0.929-1.073)	-0.043	0.966	7	0.749	0.000

Chromosome	SNP	POSITION	Region	Cohort	OR (95% CI)	Case/control	MAFAAA	MAFControl	HWEControl	HWEAAA				
6	rs3176334 rs733590 proxy	36648364 36645203	CDKN1A	AC	1.042 (0.94-1.156)	1236/2196	0.356	0.347	0.523	0.412				
				US2	1.006 (0.897-1.127)	1157/1374	0.379	0.378	0.871	0.072				
				NZ	1.026 (0.894-1.178)	753/1237	0.333	0.327	0.268	0.428				
				Italy	0.978 (0.831-1.149)	733/546	0.371	0.376	0.163	0.992				
				Poland	1.021 (0.846-1.232)	455/453	0.398	0.393	0.702	0.557				
				eMERGE	0.893 (0.748-1.066)	318/1599	0.357	0.383	0.525	0.391				
				Belgium	1.127 (0.888-1.43)	331/254	0.394	0.366	0.776	0.917				
				Canada	0.84 (0.585-1.205)	142/132	0.296	0.333	0.361	0.150				
									OR (95% CI)	Z-score	P-value	df (Q)	HetPVal	I-squared
				Combined:					1.007 (0.955-1.063)	0.2678	0.789	7	0.754	0.000
8	rs3110425	107649626	OXR1	AC	1.079 (0.974-1.196)	1225/2167	0.374	0.356	0.111	0.315				
				US2	0.933 (0.826-1.053)	987/1323	0.355	0.371	0.568	0.248				
				NZ	1.088 (0.949-1.247)	704/1174	0.382	0.361	0.107	0.279				
				Italy	1.058 (0.878-1.275)	532/445	0.359	0.346	0.883	0.226				
				Poland	1.214 (0.999-1.475)	449/457	0.363	0.319	0.770	0.164				
				eMERGE	0.942 (0.794-1.118)	342/1711	0.360	0.373	0.971	0.448				
				Belgium	0.910 (0.713-1.163)	313/246	0.356	0.378	0.558	0.672				
				Canada	1.036 (0.725-1.481)	126/118	0.230	0.271	0.881	0.870				
									OR (95% CI)	Z-score	P-value	df (Q)	HetPVal	I-squared
				Combined:					1.032 (0.977-1.090)	1.124	0.261	7	0.268	20.420
9	rs10757274	22096055	ANRIL CDKN2BAS1/	AC	0.831 (0.752-0.917)	1236/2196	0.456	0.502	0.273	0.163				
				US	0.748 (0.67-0.836)	1162/1382	0.451	0.523	0.099	0.622				
				NZ	0.885 (0.777-1.007)	753/1237	0.466	0.497	0.561	0.038				
				Italy	0.63 (0.527-0.753)	540/464	0.371	0.484	0.236	0.052				
				Poland	0.679 (0.565-0.816)	451/468	0.463	0.560	0.616	0.551				
				eMERGE	0.68 (0.576-0.804)	336/1696	0.435	0.530	0.333	0.922				
				Belgium	0.959 (0.757-1.214)	313/248	0.455	0.466	0.333	0.977				
				Canada	0.674 (0.468-0.97)	117/117	0.427	0.526	0.535	0.320				
									OR (95% CI)	Z-score	P-value	df (Q)	HetPVal	I-squared
				Combined:					0.774 (0.735-0.816)	-9.575	1.02E-21	7	0.001	64.200

Chromosome	SNP	POSITION	Region	Cohort	OR (95% CI)	Case/control	MAFAAA	MAFControl	HWEControl	HWEAAA				
9	rs10985349	124425243	DAB2IP	AC	0.998 (0.876-1.135)	1236/2196	0.179	0.179	0.878	0.696				
				US2	1.208 (1.051-1.387)	1171/1385	0.211	0.181	0.625	0.165				
				NZ	1.266 (1.072-1.495)	753/1237	0.199	0.164	0.865	0.720				
				Italy	1.227 (0.975-1.544)	729/620	0.138	0.115	0.061	0.327				
				Poland	1.182 (0.947-1.476)	485/488	0.215	0.189	0.322	0.228				
				eMERGE	1.215 (0.969-1.523)	299/1544	0.189	0.161	0.346	0.381				
				Belgium	1.139 (0.848-1.53)	338/266	0.192	0.173	0.682	0.220				
				Canada	1.304 (0.861-1.975)	149/134	0.221	0.179	0.177	0.116				
									OR (95% CI)	Z-score	P-value	df (Q)	HetPVal	I-squared
				Combined:					1.155 (1.081-1.235)	4.233	2.30E-05	7	0.400	3.900
12	rs1385526	57532749	LRP1	AC	0.983 (0.886-1.092)	1236/2196	0.339	0.343	0.293	0.297				
				US2	0.905 (0.804-1.019)	1161/1382	0.306	0.328	0.668	0.221				
				NZ	0.918 (0.801-1.052)	753/1237	0.333	0.352	0.160	0.840				
				Italy	1.135 (0.942-1.366)	509/493	0.351	0.323	0.072	0.392				
				Poland	1.058 (0.875-1.28)	453/480	0.359	0.346	0.083	0.580				
				eMERGE	1.124 (0.944-1.339)	342/1695	0.336	0.311	0.695	0.170				
				Belgium	0.966 (0.749-1.244)	324/246	0.306	0.313	0.744	0.647				
				Canada	1.031 (0.706-1.506)	132/120	0.311	0.304	0.181	0.607				
									OR (95% CI)	Z-score	P-value	df (Q)	HetPVal	I-squared
				Combined:					0.986 (0.933-1.042)	-0.493	0.622	7	0.330	12.800
13	rs9316871	22861921	LINC00540	AC	0.905 (0.801-1.023)	1236/2196	0.199	0.216	0.094	0.193				
				US2	0.845 (0.738-0.966)	1176/1384	0.202	0.231	0.624	0.052				
				NZ	0.834 (0.711-0.978)	753/1237	0.195	0.225	0.210	0.727				
				Italy	0.925 (0.776-1.102)	621/646	0.262	0.278	0.178	0.107				
				Poland	0.884 (0.721-1.085)	469/483	0.251	0.274	0.222	0.038				
				eMERGE	1.008 (0.828-1.226)	345/1724	0.223	0.222	0.049	0.954				
				Belgium	0.79 (0.592-1.053)	330/251	0.185	0.223	0.854	0.920				
				Canada	0.798 (0.515-1.235)	133/125	0.177	0.212	0.004	0.271				
									OR (95% CI)	Z-score	P-value	df (Q)	HetPVal	I-squared
				Combined:					0.883 (0.83-0.94)	-3.936	8.28E-05	7	0.795	0.000

Chromosome	SNP	POSITION	Region	Cohort	OR (95% CI)	Case/control	MAFAAA	MAFControl	HWEControl	HWEAAA				
15	rs17189674	89040591	DET1	AC	0.889 (0.763-1.036)	1236/2196	0.115	0.128	0.264	0.949				
				US2	0.934 (0.781-1.116)	1170/1381	0.104	0.110	0.000	0.846				
				NZ	1.301 (1.065-1.588)	753/1237	0.130	0.103	0.499	0.429				
				Italy	1.115 (0.862-1.441)	616/872	0.127	0.116	0.113	0.276				
				Poland	0.912 (0.686-1.212)	488/489	0.105	0.113	0.559	0.260				
				eMERGE	1.072 (0.815-1.411)	320/1649	0.108	0.101	0.553	0.114				
				Belgium	1.214 (0.849-1.737)	340/266	0.125	0.105	0.973	0.403				
				Canada	0.927 (0.557-1.542)	201/137	0.113	0.120	0.105	0.944				
									OR (95% CI)	Z-score	P-value	df (Q)	HetPVal	I-squared
				Combined:					1.014 (0.935-1.099)	0.327	0.744	7	0.102	41.500
19	rs6511720	11202306	LDLR	AC	0.969 (0.826-1.136)	1236/2196	0.107	0.110	0.144	0.384				
				US2	0.93 (0.792-1.092)	1166/1383	0.132	0.141	0.000	0.000				
				NZ	0.849 (0.69-1.045)	753/1237	0.103	0.119	0.737	0.454				
				Italy	0.566 (0.436-0.736)	667/567	0.079	0.132	0.736	0.242				
				Poland	0.607 (0.454-0.812)	477/479	0.087	0.136	0.944	0.132				
				eMERGE	0.933 (0.709-1.227)	320/1639	0.108	0.101	0.553	0.114				
				Belgium	1.162 (0.817-1.653)	336/260	0.129	0.113	0.102	0.079				
				Canada	1.025 (0.63-1.67)	141/133	0.138	0.135	0.676	0.231				
									OR (95% CI)	Z-score	P-value	df (Q)	HetPVal	I-squared
				Combined:					0.868 (0.801-0.941)	-3.431	6.02E-04	7	0.003	68.200
19	rs12980543 rs11084402 proxy	56096197 56093365	near ZNF579 near ZNF579	AC	1.033 (0.913-1.169)	1217/2169	0.205	0.199	0.239	0.604				
				US2	0.889 (0.771-1.025)	1164/1386	0.176	0.193	0.216	0.988				
				NZ	1.113 (0.953-1.3)	737/1217	0.230	0.212	0.665	0.832				
				Italy	1.075 (0.871-1.326)	648/503	0.196	0.185	0.124	0.203				
				Poland	1.014 (0.802-1.281)	474/485	0.177	0.176	0.737	0.780				
				eMERGE	1.145 (0.935-1.402)	344/1723	0.209	0.188	0.967	0.200				
				Belgium	1.293 (0.97-1.722)	337/262	0.223	0.181	0.068	0.140				
				Canada	0.73 (0.486-1.096)	135/125	0.207	0.264	0.130	0.142				
									OR (95% CI)	Z-score	P-value	df (Q)	HetPVal	I-squared
				Combined:					1.03 (0.966-1.099)	0.908	0.364	7.000	0.120	38.900

Chromosome	SNP	POSITION	Region	Cohort	OR (95% CI)	Case/control	MAFAAA	MAFControl	HWEControl	HWEAAA				
20	rs6516091	6050622	near FERMT1	AC	1.112 (0.961-1.287)	1236/2196	0.136	0.124	0.911	0.431				
				US2	0.901 (0.768-1.057)	1173/1384	0.132	0.144	0.625	0.149				
				NZ	1.094 (0.9-1.33)	753/1237	0.131	0.121	0.682	0.424				
				Italy	0.834 (0.667-1.043)	715/589	0.137	0.160	0.357	0.152				
				Poland	0.824 (0.619-1.096)	485/488	0.100	0.119	0.363	0.002				
				eMERGE	0.94 (0.741-1.192)	343/1716	0.137	0.145	0.047	0.511				
				Belgium	1.355 (0.947-1.939)	339/266	0.133	0.102	0.065	0.153				
				Canada	1.089 (0.671-1.768)	149/137	0.138	0.128	0.857	0.415				
									OR (95% CI)	Z-score	P-value	df (Q)	HetPVal	I-squared
				Combined:					0.994 (0.921-1.072)	-0.167	0.867	7	0.104	41.100
20	rs58749629 rs3827066 proxy	44571317 44586023	near PCIF1 ZNF335 MMP9 near PCIF1 ZNF335 MMP9	AC	1.076 (0.94-1.233)	1236/2196	0.160	0.151	0.688	0.617				
				US2	1.197 (1.035-1.385)	1171/1384	0.185	0.160	0.510	0.814				
				NZ	1.372 (1.153-1.632)	753/1237	0.185	0.142	0.132	0.899				
				Italy	1.263 (1.05-1.518)	709/579	0.256	0.214	0.380	0.275				
				Poland	1.373 (1.092-1.728)	487/486	0.210	0.163	0.958	0.907				
				eMERGE	1.077 (0.86-1.348)	345/1713	0.159	0.150	0.160	0.926				
				Belgium	1.291 (0.956-1.743)	340/265	0.196	0.158	0.280	0.733				
				Canada	1.469 (0.983-2.197)	146/132	0.260	0.193	0.023	0.028				
									OR (95% CI)	Z-score	P-value	df (Q)	HetPVal	I-squared
				Combined:					1.213 (1.134-1.298)	5.616	2.00E-08	7	0.300	16.500
21	rs2836411	39819830	ERG	AC	1.05 (0.947-1.164)	1236/2196	0.367	0.355	0.409	0.483				
				US2	1.085 (0.966-1.218)	1171/1382	0.350	0.331	0.073	0.877				
				NZ	1.171 (1.023-1.339)	753/1237	0.387	0.351	0.733	0.258				
				Italy	0.898 (0.757-1.065)	706/625	0.263	0.285	0.088	0.332				
				Poland	1.125 (0.935-1.354)	482/484	0.380	0.352	0.990	0.769				
				eMERGE	1.045 (0.88-1.241)	345/1724	0.349	0.339	0.485	0.797				
				Belgium	1.01 (0.797-1.281)	339/264	0.358	0.356	0.224	0.715				
				Canada	1.457 (1.04-2.041)	150/137	0.440	0.350	0.422	0.314				
									OR (95% CI)	Z-score	P-value	df (Q)	HetPVal	I-squared
				Combined:					1.072 (1.016-1.131)	2.533	0.011	7	0.203	28.300
X	rs5954362	140673423	SPANXA1	Males only										
				NZ	0.816 (0.636-1.047)	585/762	0.248	0.288						
				Belgium	1.301 (0.972-1.741)	319/183	0.310	0.257						
				Canada	0.536 (0.294-0.978)	155/32	0.272	0.411						
				eMERGE	1.189 (1.044-1.353)	1145/1134	0.311	0.276						
				Poland	0.948 (0.759-1.186)	426/355	0.286	0.297						
					OR (95% CI)	Z-score	P-value	df (Q)	HetPVal	I-squared				
Combined:					1.069 (0.972-1.175)	1.366	0.172	4	0.005	73.200				

Online Table VII: Combined results from GWAS meta-analysis and validation studies. Shaded rows indicate validated AAA risk loci that are also shown in Table 1 in the main text. A fixed effect meta-analysis was performed using a Maentel–Haenzel method with the genome-wide *P*-value significance threshold being set at 5×10^{-8} .

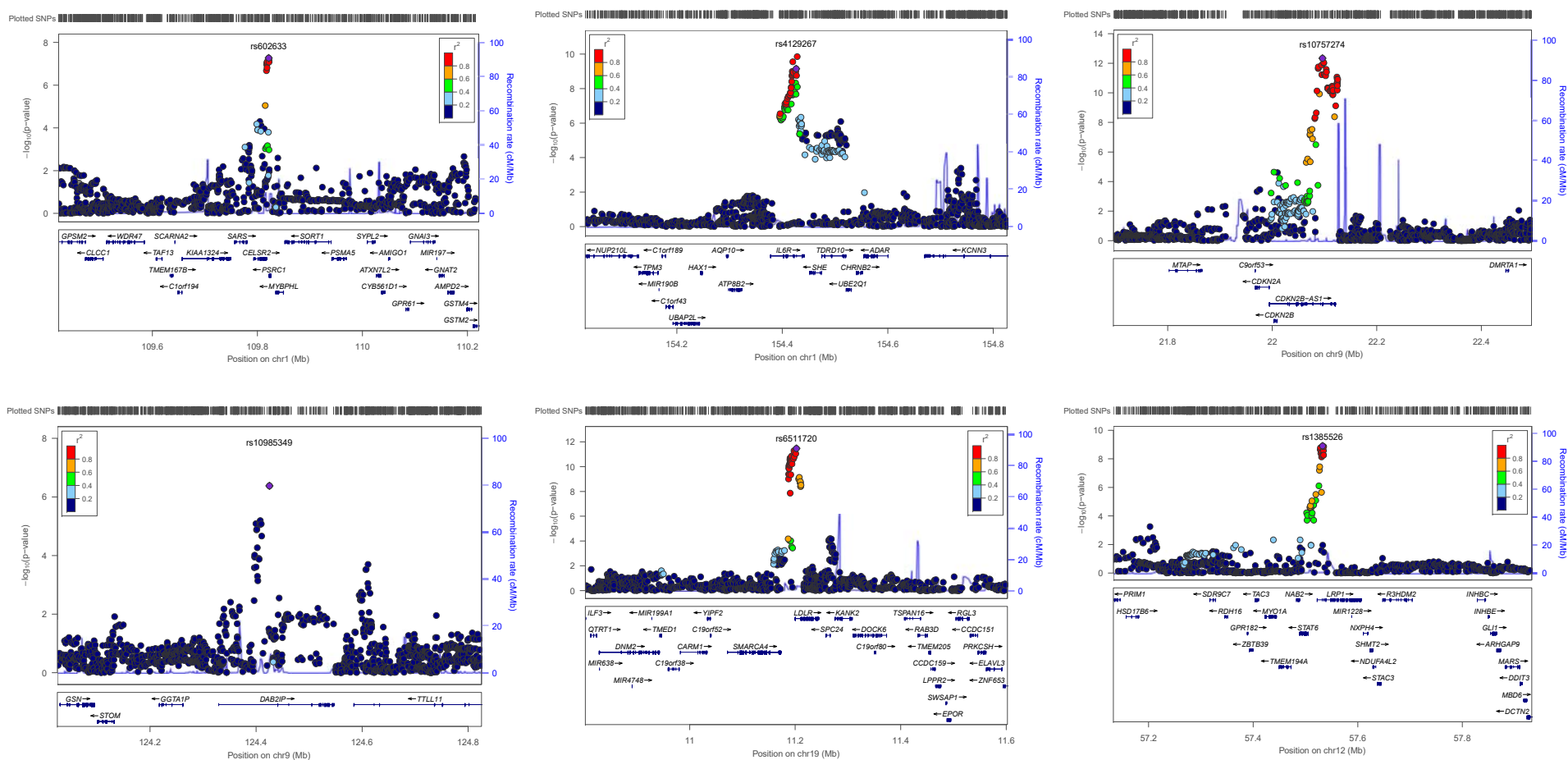
Chr	SNP	Position	Gene	Minor allele	Other allele	Meta-GWAS (lambda adjusted)				Combined validation studies					Combined meta-analysis and validation							
						MAF	P-value	Direction	HetPVal	OR	L95	U95	Z-score	P-value	OR	L95	U95	Z-score	P-value	df	HetPVal	
1*	rs602633	109821511	Near <i>PSRC1</i> <i>CELSR2</i> <i>SORT1</i>	T	G	0.199	1.72×10^{-07}	-----	0.097	0.920	0.863	0.980	-2.582	9.83×10^{-03}	0.879	0.842	0.918	-5.801	6.58×10^{-09}	13	7.60×10^{-03}	
1*	rs12133641	154428283	<i>IL6R</i>	A	G		1.67×10^{-10}	+++++	0.903													
1	rs4129267 (proxy)	154426264	<i>IL6R</i>	T	C	0.370	9.26×10^{-10}	-----	0.886	0.904	0.857	0.953	-3.743	1.81×10^{-04}	0.876	0.846	0.908	-7.232	4.76×10^{-13}	13	0.478	
1	rs1795061	214409280	near <i>SMYD2</i>	T	C	0.336	1.79×10^{-07}	+++++	0.069	1.105	1.046	1.168	3.576	3.49×10^{-04}	1.131	1.090	1.174	6.486	8.80×10^{-11}	13	1.14×10^{-03}	
2	rs13382862	20882449	near <i>C2orf43</i> and <i>GDF7</i>	A	G	0.341	3.03×10^{-08}	-----	0.878	0.975	0.923	1.029	-0.915	3.60×10^{-01}	0.913	0.880	0.947	-4.845	1.3×10^{-06}	13	8.01×10^{-02}	
4	rs10029392	5616048	<i>EVC2</i>	T	G	0.052	4.60×10^{-06}	+++++	0.147	0.940	0.843	1.049	-1.111	2.67×10^{-01}	1.107	1.022	1.198	2.496	1.25×10^{-02}	13	6.51×10^{-04}	
5	rs12659791	74757758	<i>COL4A3BP</i>	T	C	0.159	2.28×10^{-06}	--+--	0.105	0.998	0.929	1.073	-0.043	9.66×10^{-01}	1.098	1.046	1.153	3.752	1.8×10^{-04}	13	1.69×10^{-02}	
6	rs3176334	36648364	<i>CDKN1A</i>	T	C		1.50×10^{-06}	-----	0.627													
6	rs733590 (proxy)	36645203	<i>CDKN1A</i>	T	C	0.367	8.74×10^{-06}	-----	0.584	1.007	0.955	1.063	0.2678	7.89×10^{-01}	1.070	1.031	1.110	3.588	3.33×10^{-04}	13	0.183	
9*	rs10757274	22096055	<i>CDKN2BAS1/ANRIL</i>	A	G	0.351	2.32×10^{-13}	-----	0.520	0.774	0.735	0.816	-9.575	1.02×10^{-21}	0.806	0.778	0.834	-12.069	1.54×10^{-33}	13	5.94×10^{-03}	
9*	rs10985349	124425243	<i>DAB2IP</i>	T	C	0.462	8.98×10^{-07}	+++++	0.181	1.155	1.081	1.235	4.233	2.30×10^{-05}	1.171	1.118	1.226	6.682	2.4×10^{-11}	13	3.52×10^{-01}	
12*	rs1385526	57532749	<i>LRP1</i>	C	G	0.195	1.31×10^{-09}	-----	0.597	0.986	0.933	1.042	-0.493	6.22×10^{-01}	0.910	0.877	0.944	-4.980	6.4×10^{-07}	13	9.38×10^{-03}	
13	rs9316871	22861921	<i>LINC00540</i>	A	G	0.328	5.95×10^{-06}	+++++	0.143	0.883	0.830	0.940	-3.936	8.28×10^{-05}	0.873	0.837	0.911	-6.227	4.8×10^{-10}	13	0.488	
15	rs17189674	89040591	<i>DET1</i>	A	G	0.201	1.05×10^{-06}	+++++	0.663	1.014	0.935	1.099	0.327	7.44×10^{-01}	1.118	1.058	1.181	3.957	7.59×10^{-05}	13	1.71×10^{-02}	
19*	rs6511720	11202306	<i>LDLR</i>	T	G	0.122	5.71×10^{-12}	-----	0.679	0.868	0.801	0.941	-3.431	6.02×10^{-04}	0.804	0.759	0.851	-7.472	7.9×10^{-14}	13	1.53×10^{-03}	
19	rs12980543	56096197	near <i>ZNF579</i>	A	G		2.30×10^{-06}	+++++	0.301													
19	rs11084402 proxy	56093365	near <i>ZNF579</i>	T	C	0.206	4.33×10^{-06}	+++++	0.218	1.030	0.966	1.099	0.908	3.64×10^{-01}	1.095	1.048	1.144	4.050	5.1×10^{-05}	13	0.019	
20	rs6516091	6050622	near <i>FERMT1</i>	A	G	0.135	3.82×10^{-09}	+++++	0.027	0.994	0.921	1.072	-0.167	8.67×10^{-01}	1.131	1.074	1.190	4.680	2.9×10^{-06}	13	4.01×10^{-05}	
20	rs58749629	44571317	near <i>PCIF1</i> <i>ZNF335</i> <i>MMP9</i>	A	G		7.97×10^{-10}	+++++	0.760													
20	rs3827066 proxy	44586023	near <i>PCIF1</i> <i>ZNF335</i> <i>MMP9</i>	T	C	0.179	9.18×10^{-10}	+++++	0.729	1.213	1.134	1.298	5.616	2.00×10^{-08}	1.223	1.168	1.281	8.486	2.1×10^{-17}	13	0.552	
21	rs2836411	39819830	<i>ERG</i>	T	C	0.369	1.53×10^{-07}	+++++	0.103	1.072	1.016	1.131	2.533	1.13×10^{-02}	1.113	1.074	1.154	5.823	5.8×10^{-09}	13	4.83×10^{-02}	
X	rs5954362	140673423	<i>SPANXA1</i>	C	G	0.241	1.0310^{-09}	---	0.142	1.069	0.972	1.175	1.366	1.72×10^{-01}	0.896	0.829	0.967	-2.807	5.0×10^{-03}	7	4.18×10^{-10}	

*Loci previously identified as associated with AAA.

Online Table VIII: Sensitivity analysis comparing results from the combined GWAS meta-analysis and validation studies using a fixed effects model with a random-effects model. Results for loci surpassing the threshold for genome-wide significance are shown in bold. *Loci previously identified as associated with AAA

Chr	SNP	Position	Gene	Minor allele	Other allele	MAF	df	HetPVal	I ²	Fixed effects model		Random effects model	
										OR (95% CI)	P-value	OR (95% CI)	P-value
1*	rs602633	109821511	Near <i>PSRC1 CELSR2 SORT1</i>	T	G	0.199	13	7.60x10 ⁻⁰³	54.5	0.879 (0.842 - 0.918)	6.58x10⁻⁰⁹	0.881 (0.822 - 0.943)	3.18x10⁻⁹
1*	rs12133641	154428283	<i>IL6R</i>	A	G								
1	rs4129267 (proxy)	154426264	<i>IL6R</i>	T	C	0.370	13	0.478	0.0	0.876 (0.846 - 0.908)	4.76x10⁻¹³	0.876 (0.846 - 0.908)	1.03x10⁻¹²
1	rs1795061	214409280	near <i>SMYD2</i>	T	C	0.336	13	1.14x10 ⁻⁰³	61.9	1.131 (1.090 - 1.174)	8.80x10⁻¹¹	1.142 (1.07 - 1.218)	3.47x10⁻¹²
2	rs13382862	20882449	near <i>C2orf43</i> and <i>GDF7</i>	A	G	0.341	13	8.01x10 ⁻⁰²	37.1	0.913 (0.880 - 0.947)	1.3x10 ⁻⁰⁶	0.921 (0.877 - 0.968)	2.05x10 ⁻⁶
4	rs10029392	5616048	<i>EVC2</i>	T	G	0.052	13	6.51x10 ⁻⁰⁴	63.6	1.107 (1.022 - 1.198)	1.25x10 ⁻⁰²	1.120 (0.973 - 1.289)	1.88x10 ⁻⁴
5	rs12659791	74757758	<i>COL4A3BP</i>	T	C	0.159	13	1.69x10 ⁻⁰²	50.1	1.098 (1.046 - 1.153)	1.8x10 ⁻⁰⁴	1.071 (0.993 - 1.156)	8.18x10 ⁻⁶
6	rs3176334	36648364	<i>CDKN1A</i>	T	C								
6	rs733590 (proxy)	36645203	<i>CDKN1A</i>	T	C	0.367	13	0.183	25.2	1.070 (1.031 - 1.11)	3.33x10 ⁻⁰⁴	1.064 (1.017 - 1.112)	5.06x10 ⁻⁴
9*	rs10757274	22096055	<i>CDKN2BAS1/ANRIL</i>	A	G	0.351	13	5.94x10 ⁻⁰³	55.6	0.806 (0.778 - 0.834)	1.54x10⁻³³	0.797 (0.753 - 0.843)	1.21x10⁻³³
9*	rs10985349	124425243	<i>DAB2IP</i>	T	C	0.462	13	3.52x10 ⁻⁰¹	9.2	1.171 (1.118 - 1.226)	2.4x10⁻¹¹	1.174 (1.117 - 1.233)	4.47x10⁻¹¹
12*	rs1385526	57532749	<i>LRP1</i>	C	G	0.195	13	9.38x10 ⁻⁰³	53.4	0.910 (0.877 - 0.944)	6.4x10 ⁻⁰⁷	0.930 (0.877 - 0.986)	6.541x10 ⁻⁸
13	rs9316871	22861921	<i>LINC00540</i>	A	G	0.328	13	0.488	0.0	0.873 (0.837 - 0.911)	4.8x10⁻¹⁰	0.873 (0.837 - 0.911)	9.98x10⁻¹⁰
15	rs17189674	89040591	<i>DET1</i>	A	G	0.201	13	1.71x10 ⁻⁰²	50.0	1.118 (1.058 - 1.181)	7.59x10 ⁻⁰⁵	1.120 (1.031 - 1.217)	1.26x10 ⁻⁵
19*	rs6511720	11202306	<i>LDLR</i>	T	G	0.122	13	1.53x10 ⁻⁰³	61.0	0.804 (0.759 - 0.851)	7.9x10⁻¹⁴	0.795 (0.72 - 0.878)	7.19x10⁻¹⁵
19	rs12980543	56096197	near <i>ZNF579</i>	A	G								
19	rs11084402 (proxy)	56093365	near <i>ZNF579</i>	T	C	0.206	13	0.019	49.4	1.095 (1.048 - 1.144)	5.1x10 ⁻⁰⁵	1.101 (1.031 - 1.176)	2.51x10 ⁻⁵
20	rs6516091	6050622	near <i>FERMT1</i>	A	G	0.135	13	4.01x10 ⁻⁰⁵	70.0	1.131 (1.074 - 1.19)	2.9x10 ⁻⁰⁶	1.088 (0.983 - 1.203)	6.58x10⁻¹⁰
20	rs58749629	44571317	near <i>PCIF1 ZNF335 MMP9</i>	A	G								
20	rs3827066 (proxy)	44586023	near <i>PCIF1 ZNF335 MMP9</i>	T	C	0.179	13	0.552	0.0	1.223 (1.168 - 1.281)	2.1x10⁻¹⁷	1.223 (1.168 - 1.281)	6.12x10⁻¹⁷
21	rs2836411	39819830	<i>ERG</i>	T	C	0.369	13	4.83x10 ⁻⁰²	42.2	1.113 (1.074 - 1.154)	5.8x10⁻⁰⁹	1.112 (1.057 - 1.17)	7.07x10⁻⁹
X	rs5954362	140673423	<i>SPANXA1</i>	C	G	0.241	7	4.18x10 ⁻¹⁰	87.9	0.896 (0.829 - 0.967)	5.0x10 ⁻⁰³	0.857 (0.672 - 1.092)	3.08x10⁻¹¹

Online Figure II: Regional association plots for previously reported AAA risk loci.



Five of the 6 previously identified AAA loci at 1p13.3 (*SORT1*), 1q21.3 (*IL6R*), 9p21 (*CDKN2BAS1/ANRIL*), 9q33 (*DAB2IP*) and 19p13.2 (*LDLR*) were replicated in this meta-GWAS and validation analysis. Although the previously reported¹ 12q13 (*LRP1*) locus (lower right panel) reached the discovery threshold ($P=1.1 \times 10^{-9}$), it fell below the genome-wide threshold when combined with the validation cohorts (combined $P=6.4 \times 10^{-7}$).

SNP LOOKUP IN GWAS FOR OTHER TRAITS ASSOCIATED WITH AAA

Data for AAA associated SNPs (those passing the genome-wide association threshold after combination of the results of the meta-analysis and validation studies) were obtained from GWAS datasets for other traits associated with AAA to determine if the associations were unique to AAA or related to generalized CVD (**Online Table IX and Figure 3**). All results were from meta-analyses of multiple primary GWAS datasets for each trait. Summary results for each AAA associated SNP (P-value and effect size) were extracted. Results for type 2 diabetes³⁴ were obtained from the DIAGRAM consortium (<http://www.diagram-consortium.org/index.html>), CAD data from the CARDIoGRAM consortium³⁵ (www.CARDIOGRAMPLUSC4D.ORG), lipid trait data from the Global Lipids Genetics Consortium³⁶ (<http://csg.sph.umich.edu/abecasis/public/lipids2013>) and blood pressure data from the International Consortium for Blood Pressure³⁷ (http://www.ncbi.nlm.nih.gov/projects/gap/cgi-bin/study.cgi?study_id=phs000585.v1.p1).

Online Table IX: Results of lookup of AAA associated SNPs in GWAS of other cardiovascular traits (See also below). CAD: Coronary Artery Disease; HDL: High-density Lipoprotein; LDL: Low-density Lipoprotein; TG: Triglyceride; DBP: Diastolic Blood Pressure; SBP: Systolic Blood Pressure.

	Chr	Position	SNP	Locus	Gene(s)	AAA risk allele	OR (95%CI)			P					
							n cases	n controls							
Type 2 Diabetes	1	109821511	rs602633	1p13.3	CELSR2/ <i>SORT1</i>	T	1.05 (1.01 - 1.1)	9580	53810	0.025					
	1	154426264	rs4129267	1q21.3	<i>IL6R</i>	T	0.96 (0.93 - 1.00)	12171	56862	0.037					
	9	22096055	rs10757274	9p21	<i>ANRIL</i>	A	0.96 (0.94 - 1.00)	12171	56862	0.041					
	9	124425243	rs10985349	9q33.2	<i>DAB2IP</i>	T	1.03 (0.98 - 1.07)	12171	56862	0.210					
	19	11202306	rs6511720	19p13.2	<i>LDLR</i>	T	1.02 (0.96 - 1.10)	8558	52735	0.480					
CAD	1	109821511	rs602633	1p13.3	CELSR2/ <i>SORT1</i>	T	0.90 (0.87 - 0.93)	20375	61324	2.16x10 ⁻⁹					
	1	154426264	rs4129267	1q21.3	<i>IL6R</i>	T	0.95 (0.93 - 0.98)	20784	58718	0.001					
	9	22096055	rs10757274	9p21	<i>ANRIL</i>	A	0.78 (0.74 - 0.82)	21932	62260	1.44x10 ⁻²²					
	9	124425243	rs10985349	9q33.2	<i>DAB2IP</i>	T	1.04 (1.00 - 1.09)	14133	36016	0.036					
	19	11202306	rs6511720	19p13.2	<i>LDLR</i>	T	0.88 (0.83 - 0.94)	8948	47471	1.61x10 ⁻⁰⁴					
Lipid traits	1	109821511	rs602633	1p13.3	CELSR2/ <i>SORT1</i>	T	HDL beta (SE)	n	P	LDL beta (SE)	n	P	TG beta (SE)	n	P
	1	154426264	rs4129267	1q21.3	<i>IL6R</i>	T	0.0073 (0.0051)	94311	0.077	-0.0066 (0.0057)	89888	0.230	-0.0129 (0.005)	91013	0.032
	9	22096055	rs10757274	9p21	<i>ANRIL</i>	A	0.0328 (0.0041)	185599	3.50x10 ⁻¹⁴	-0.1591 (0.0044)	171593	1.50x10 ⁻²⁶¹	-0.0121 (0.004)	176361	0.003
	9	124425243	rs10985349	9q33.2	<i>DAB2IP</i>	T	-0.0047 (0.0048)	92706	0.371	0.0036 (0.0051)	83064	0.524	0.0012 (0.0047)	86702	0.907
	19	11202306	rs6511720	19p13.2	<i>LDLR</i>	T	-0.006 (0.0068)	86409	0.435	0.0067 (0.0075)	82099	0.557	-0.0039 (0.0066)	83111	0.944
Blood Pressure	1	109821511	rs602633	1p13.3	CELSR2/ <i>SORT1</i>	T	DBP beta (SE)	n	P	SBP beta (SE)	n	P			
	1	154426264	rs4129267	1q21.3	<i>IL6R</i>	T	0.0704 (0.0665)	66347	0.289	-0.0568 (0.1044)	66352	0.586			
	9	22096055	rs10757274	9p21	<i>ANRIL</i>	A	0.0257 (0.0748)	66774	0.731	0.0100 (0.1180)	66781	0.932			
	9	124425243	rs10985349	9q33.2	<i>DAB2IP</i>	T	NA	NA	NA	NA	NA				
	19	11202306	rs6511720	19p13.2	<i>LDLR</i>	T	-0.0020 (0.0807)	58126	0.980	0.1229 (0.1283)	58171	0.338			
Type 2 Diabetes	1	214409280	rs1795061	1q32.3	near <i>SMYD2</i>	T	OR (95%CI)	n cases	n controls	P					
	13	22861921	rs9316871	13q12.11	<i>LINC00540</i>	G	1.04 (1.00 - 1.08)	9580	53810	0.044					
	20	44586023	rs3827066	20q13.12	Near <i>MMP9/ZNF335</i>	T	1 (0.96 - 1.04)	11902	53152	0.940					
	21	39819830	rs2836411	21q22.2	<i>ERG</i>	T	1.00 (0.95 - 1.06)	9580	53810	0.890					
	21	39819830	rs2836411	21q22.2	<i>ERG</i>	T	1.01 (0.97 - 1.04)	12171	56862	0.720					
CAD	1	214409280	rs1795061	1q32.3	near <i>SMYD2</i>	T	OR	n cases	n controls	P					
	13	22861921	rs9316871	13q12.11	<i>LINC00540</i>	G	0.99 (0.96 - 1.02)	20441	61399	0.533					
	20	44586023	rs3827066	20q13.12	Near <i>MMP9/ZNF335</i>	T	1.00 (0.97 - 1.03)	21588	59365	0.974					
	21	39819830	rs2836411	21q22.2	<i>ERG</i>	T	1.07 (1.03 - 1.12)	19108	59177	5.48x10 ⁻⁰⁴					
	21	39819830	rs2836411	21q22.2	<i>ERG</i>	T	1.02 (0.99 - 1.05)	21424	59122	0.205					
Lipid traits	1	214409280	rs1795061	1q32.3	near <i>SMYD2</i>	T	HDL beta (SE)	n	P	LDL beta (SE)	n	P	TG beta (SE)	n	P
	13	22861921	rs9316871	13q12.11	<i>LINC00540</i>	G	0.0075 (0.0054)	94311	0.119	0.0023 (0.0059)	89888	0.572	-0.0047 (0.0052)	91013	0.501
	20	44586023	rs3827066	20q13.12	Near <i>MMP9/ZNF335</i>	T	-0.0013 (0.0058)	90317	0.883	0.006 (0.0063)	85936	0.417	0.0018 (0.0058)	86976	0.563
	21	39819830	rs2836411	21q22.2	<i>ERG</i>	T	0.0208 (0.0048)	185539	2.96x10 ⁻⁰⁵	-0.0092 (0.0052)	171507	0.103	-0.0156 (0.0047)	176203	0.003
	21	39819830	rs2836411	21q22.2	<i>ERG</i>	T	-0.0047 (0.005)	92801	0.402	-0.0082 (0.0055)	88414	0.269	0.0054 (0.0049)	89466	0.566
Blood pressure	1	214409280	rs1795061	1q32.3	near <i>SMYD2</i>	T	DBP beta (SE)	n	P	SBP beta (SE)	n	P			
	13	22861921	rs9316871	13q12.11	<i>LINC00540</i>	G	0.0320 (0.0691)	63232	0.643	0.0047 (0.1084)	63243	0.965			
	20	44586023	rs3827066	20q13.12	Near <i>MMP9/ZNF335</i>	T	0.0429 (0.0734)	69617	0.559	-0.0201 (0.1163)	69623	0.863			
	21	39819830	rs2836411	21q22.2	<i>ERG</i>	T	-0.0397 (0.0878)	59823	0.651	-0.0276 (0.1380)	59806	0.842			
	21	39819830	rs2836411	21q22.2	<i>ERG</i>	T	0.1536 (0.0650)	67634	0.018	0.0487 (0.1024)	67631	0.635			

SEARCH FOR OTHER ASSOCIATED TRAITS AND DISEASES USING GWAS DATABASES

The Phenotype-Genotype Integrator³⁸ (<http://www.ncbi.nlm.nih.gov/gap/phegeni#GenomeView>) and the GWAS catalog (<http://www.gwascentral.org/index>) were searched for diseases and traits associated with the lead SNPs at the AAA loci. In addition, we searched NHLBI GRASP catalog (GRASP v2.0; <http://grasp.nhlbi.nih.gov/Overview.aspx>)^{39, 40} to find any further associations. The results obtained using the Phenotype-Genotype Integrator are shown in **Online Table X**, the search results from the GWAS catalog are presented in **Online Table XI**, and those using GRASP in **Online Table XII**.

PheGenI includes results from the NHGRI/EBI catalog. GRASP (Genome-Wide Repository of Associations Between SNPs and Phenotypes) is the largest GWAS results database in terms of coverage. It includes all available genetic association results from papers, their supplements and web-based content meeting the following guidelines:

- All associations with $P < 0.05$ from GWAS defined as $\geq 25,000$ markers tested for 1 or more traits.
- Study exclusion criteria: CNV-only studies, replication/follow-up studies testing $< 25K$ markers, non-human only studies, article not in English, gene-environment or gene-gene GWAS where single SNP main effects are not given, linkage only studies, aCGH/LOH only studies, heterozygosity/homozygosity (genome-wide or long run) studies, studies only presenting gene-based or pathway-based results, simulation-only studies, studies which we judge as redundant with prior studies since they do not provide significant inclusion of new samples or exposure of new results (e.g., many methodological papers on the WTCCC and FHS GWAS).

Online Table X: Results from the GWAS database search using the tool called Phenotype-Genotype Integrator (<http://www.ncbi.nlm.nih.gov/gap/phegeni#GenomeView>). All lead SNPs at the AAA loci were used for the search, but only two of the SNPs (rs4129267 and rs6511720) had hits.

Chr	Location	SNP	Gene	Trait	Location in gene	P-Value	Source	PubMed ID
1	154426264	rs4129267	IL6R	Receptors, Interleukin-6	intron	2.00×10^{-57}	NHGRI	18464913
				C-Reactive Protein	intron	2.00×10^{-48}	NHGRI	21300955
				Asthma	intron	2.00×10^{-08}	NHGRI	21907864
				Maximal Midexpiratory Flow Rate	intron	7.00×10^{-06}	NHGRI	17903307
19	11202306	rs6511720	LDLR	Cholesterol, LDL	intron	4.00×10^{-117}	NHGRI	20686565
				Cholesterol	intron	7.00×10^{-97}	NHGRI	20686565
				Cholesterol, LDL	intron	2.00×10^{-51}	NHGRI	18193044
				Cholesterol, LDL	intron	2.00×10^{-26}	NHGRI	19060906
				Cholesterol, LDL	intron	4.00×10^{-26}	NHGRI	18193043
				1-Alkyl-2-acetylglycerophosphocholine Esterase	intron	3.00×10^{-11}	NHGRI	22003152
				Cholesterol, LDL	intron	5.00×10^{-11}	NHGRI	21943158
Atherosclerosis	intron	1.00×10^{-07}	NHGRI	21909108				

Online Table XI: Results of the dbGAP SNP lookup using the GWAS Catalog available at <http://www.gwascentral.org/index>. The total number of results in the GWAS Catalog (“n results in dbGAP”) and the number of associations with $P < 1 \times 10^{-3}$ (column labelled “n $P < 1 \times 10^{-3}$ ”) are shown. Details on the associations with $P < 1 \times 10^{-3}$ for each SNP are described.

SNP	Chromosome	Position	Gene(s)	n results in dbGAP	n $P < 1 \times 10^{-3}$	P-value	Phenotype	Study
rs602633	1	109821511	PSRC1-CELSR2-SORT1	16	3	4.80×10^{-14}	LDL cholesterol levels	Meta-analysis of plasma lipid concentrations (HGVST214)
						5.70×10^{-14}	Serum LDL cholesterol levels	GWAS of LDL-cholesterol concentrations (HGVST227)
						0.0001862	Height	GWAS of height (HGVST634)
rs4129267	1	154426264	IL6R	77	6	2.00×10^{-37}	Protein quantitative trait loci	GWAS of protein quantitative trait loci (HGVST264)
						2.00×10^{-48}	C-reactive protein level	GWAS of C-reactive protein levels (HGVST728)
						2.00×10^{-68}	Asthma	Unspecified analysis (HGVRS1753)
						7.39×10^{-66}	Percent predicted forced expiratory flow	GWAS of pulmonary function phenotypes in the Framingham Heart Study (HGVST212)
						1.92×10^{-65}	Asthma; Total asthma sample fixed effects (HGVRS1509)	GWAS of asthma (HGVST631)
						0.00014411	Asthma; Total asthma sample random effects (HGVRS1257)	GWAS of asthma (HGVST631)
rs1795061	1	214409280	SMYD2	19	0			
rs10757274	9	22096055	ANRIL	6	2	8.00×10^{-45}	Coronary heart disease	GWAS of Coronary heart disease (HGVST1380)
						3.70×10^{-56}	Coronary heart disease	GWAS of Coronary heart disease (HGVST57)
rs10985349	9	124425243	DAB2IP	19	0			
rs9316871	13	22861921	LINCO0540	101	2	0.0007248	Schizophrenia	GWAS of schizophrenia (HGVST903)
						0.00084	Crohn's disease	GWAS of Crohn's disease (HGVST680)
rs6511720	19	11202306	LDLR	57	14	2×10^{-51}	LDL cholesterol	Meta-analysis of lipid concentrations (HGVST203)
						4.2×10^{-26}	LDL cholesterol levels	Meta-analysis of plasma lipid concentrations (HGVST214)
						2×10^{-25}	LDL cholesterol	GWAS of HDL cholesterol, triglycerides and LDL cholesterol (HGVST235)
						0.00026672	Serum cholesterol	GWAS of serum cholesterol levels in a British population (HGVST312)
						0.0005127	Height	GWAS of height (HGVST634)
						0.0000001	Carotid intima media thickness, plaque	GWAS of carotid intima media thickness (HGVST923)
						3×10^{-11}	Lipoprotein-associated phospholipase A2 activity and mass (Activity concentrations)	GWAS of lipoprotein-associated phospholipase A2 activity and mass (HGVST931)
						5×10^{-11}	Cardiovascular disease risk factors (LDL)	GWAS of cardiovascular disease risk factors (HGVST956)
						0.000000004	Metabolite levels	GWAS of Metabolite levels (HGVST1409)
						2×10^{-31}	Lipid metabolism phenotypes (LDL-C.assay, whole)	GWAS of Lipid metabolism phenotypes (HGVST1667)
3×10^{-18}	Lipid metabolism phenotypes (APOB.assay, fasting)	GWAS of Lipid metabolism phenotypes (HGVST1667)						
1×10^{-25}	Lipid metabolism phenotypes (LDL-C.assay, fasting)	GWAS of Lipid metabolism phenotypes (HGVST1667)						
						5×10^{-25}	Lipid metabolism phenotypes (APOB.assay, whole)	GWAS of Lipid metabolism phenotypes (HGVST1667)
rs3827066	20	44586023	PCIF1-ZNF335-MMP9	15	0			
rs2836411	21	39819830	ERG	94	1	0.0009289	Height	GWAS of height (HGVST634)

Online Table XII: Previously reported associations of the lead SNPs from AAA loci identified from an analysis of GRASP v2.0 (<http://grasp.nhlbi.nih.gov/Overview.aspx>). The Phenotypes, P values and sample sizes are those reported in the original publication that is referenced under 'Phenotype' in the table. The SNP, chromosome, position and genes are those from this analysis that were entered into GRASP v2.0 as a query. This table spans 3 pages.

SNP	CHR	Position	Gene	Phenotype	P value	Ancestry	Total	Total Replication	Total				
rs602633	1	109821511	<i>PSRC1-CELSR2-SORT1</i>	LDL cholesterol ⁴¹	4.80x10 ⁻¹⁴	European	8656	11399	20055				
				LDL cholesterol in serum ⁴²	5.70x10 ⁻¹⁴	European	11685	5036	16721				
				LDL cholesterol ⁴³	7.60x10 ⁻⁴¹	European	19840	20623	40463				
				LDL cholesterol ⁴⁴	3.10x10 ⁻⁰⁸	European	5059	0	5059				
				APOB (apolipoprotein B) ⁴⁴	2.20x10 ⁻⁰⁷	European	5059	0	5059				
				Coronary artery disease (CAD) ⁴⁵	9.00x10 ⁻⁰⁸	Unspecified	8319	10707	19026				
				LDL cholesterol change with statins ⁴⁶	8.40x10 ⁻⁰⁸	European	3928	0	3928				
				LDL cholesterol ⁴⁶	8.40x10 ⁻⁰⁸	European	3928	0	3928				
				Total cholesterol change with statins ⁴⁶	5.50x10 ⁻⁰⁶	European	3928	0	3928				
				Total cholesterol ⁴⁶	5.50x10 ⁻⁰⁶	European	3928	0	3928				
				LDL cholesterol ⁴⁷	4.90x10 ⁻¹⁶	Mixed	100184	39875	140059				
				Total cholesterol ⁴⁷	3.90x10 ⁻¹⁷	Mixed	100184	39875	140059				
				HDL cholesterol ⁴⁷	5.20x10 ⁻⁰⁷	Mixed	100184	39875	140059				
				Height ⁴⁸	1.90x10 ⁻⁰⁴	European	133653	50074	183727				
				LDL cholesterol ⁴⁹	2.90x10 ⁻⁰⁶	African	8090	8849	16939				
				LDL cholesterol ⁵⁰	1.20x10 ⁻²²	European	11683	0	11683				
				LDL cholesterol (baseline) ⁵¹	5.00x10 ⁻⁰⁸	European	5244	0	5244				
				Lp-PLA2 activity ⁵²	1.40x10 ⁻¹⁶	European	13664	0	13664				
				Total cholesterol ⁵³	5.90x10 ⁻⁶⁵	European	66240	25282	91522				
				LDL cholesterol ⁵³	6.90x10 ⁻⁶⁵	European	66240	25282	91522				
				HDL cholesterol ⁵³	1.30x10 ⁻⁰⁷	European	66240	25282	91522				
				Coronary artery disease (CAD) ⁵⁴	4.70x10 ⁻²⁶	Mixed	194427	15613	210040				
				Coronary artery disease (CAD) age <=50 ⁵⁴	2.80x10 ⁻²⁰	Mixed	194427	15613	210040				
				Coronary artery disease (CAD) (males) ⁵⁴	1.30x10 ⁻¹⁸	Mixed	194427	15613	210040				
				Coronary artery disease (CAD) with myocardial infarction (MI) ⁵⁴	2.20x10 ⁻¹⁶	Mixed	194427	15613	210040				
				Coronary artery disease (CAD) age >50 ⁵⁴	5.00x10 ⁻⁰⁸	Mixed	194427	15613	210040				
				Coronary artery disease (CAD) (females) ⁵⁴	3.40x10 ⁻⁰⁵	Mixed	194427	15613	210040				
				rs4129267	1	154426264	<i>IL6R</i>	Lung function, predicted forced expiratory flow (FEF) ⁵⁵	7.40x10 ⁻⁰⁶	European	1222	0	1222
								Plasma C-reactive protein (female) ⁵⁶	2.00x10 ⁻⁰⁸	European	6345	0	6345
								Soluble IL6R (sIL6R) ⁵⁷	2.50x10 ⁻⁷⁶	European	1200	0	1200
C-reactive protein [log (mg/l)] ⁵⁸	4.40x10 ⁻⁰⁴	European	4763					0	4763				
Plasma fibrinogen (females) ⁵⁹	1.80x10 ⁻¹¹	European	17686					0	17686				
Asthma ⁶⁰	1.90x10 ⁻⁰⁵	European	26475					0	26475				
Fibrinogen ⁶¹	8.40x10 ⁻⁰⁷	Mixed	30291					0	30291				
C-reactive protein (CRP) ⁶²	2.10x10 ⁻⁴⁸	European	66185					16540	82725				
Asthma ⁶⁰	2.40x10 ⁻⁰⁸	European	7197					57800	64997				
Interleukin-6 (IL-6) levels ⁶³	2.40x10 ⁻⁰⁸	European	4694					1392	6086				
C-reactive protein (CRP) ⁶⁴	1.80x10 ⁻⁰⁵	Mixed	11828					11991	23819				
Coronary artery disease (CAD) ⁵⁴	1.70x10 ⁻⁰⁸	Mixed	194427					15613	210040				
Interleukin-6 (IL-6) levels ⁶⁵	1.60x10 ⁻²¹	European	8356					0	8356				
C-reactive protein (CRP) ⁶⁵	8.80x10 ⁻¹²	European	8356					0	8356				
rs1795061	1	214409280	<i>SMYD2</i>					None					
rs10757274	9	22096055	<i>ANRIL</i>	Coronary heart disease (CHD) ⁶⁶	3.70x10 ⁻⁰⁶	Mixed	634	28047	28681				
				Coronary artery disease (CAD) ⁴⁵	7.00x10 ⁻¹¹	Unspecified	8319	10707	19026				
				Coronary artery disease (CAD) ⁶⁷	7.60x10 ⁻⁴⁵	Asian	6534	26932	33466				
				Coronary artery calcification (CAC) ⁶⁸	8.00x10 ⁻¹⁰	European	4518	0	4518				

SNP	CHR	Position	Gene	Phenotype	P value	Ancestry	Total	Total Replication	Total
				Coronary artery calcification (CAC) ⁶⁹	6.80x10 ⁻⁸⁸	Mixed	1509	3344	4853
rs10985349	9	124425243	DAB2IP	None					
rs9316871	13	22861921	LINC00540	Body mass index (BMI) ⁷⁰	6.90x10 ⁻⁰⁴	European	5217	0	5217
				Schizophrenia ⁷¹	9.40x10 ⁻⁰⁵	European	16161	31375	47536
				HDL cholesterol change with statins ⁴⁶	7.70x10 ⁻⁰⁴	European	3928	0	3928
rs6511720	19	11202306	LDLR	LDL cholesterol ⁴¹	4.20x10 ⁻²⁶	European	8656	11399	20055
				LDL cholesterol ⁷²	2.00x10 ⁻⁵¹	Mixed	2758	22803	25561
				LDL cholesterol ⁴³	5.20x10 ⁻³⁰	European	19840	20623	40463
				LDL cholesterol exam 1 values ⁴³	3.00x10 ⁻⁰⁴	European	19840	20623	40463
				Total cholesterol (exam 1) ⁴³	3.40x10 ⁻⁰⁴	European	19840	20623	40463
				LDL cholesterol (mmol/l) ³⁸	1.50x10 ⁻⁰⁹	European	4763	0	4763
				Total cholesterol ⁷³	6.80x10 ⁻¹⁸	European	22562	0	22562
				APOB (apolipoprotein B) ⁷⁴	7.00x10 ⁻¹⁸	European	6382	970	7352
				LDL cholesterol ⁷⁴	5.20x10 ⁻¹⁵	European	6382	970	7352
				LDL cholesterol ⁴⁴	7.30x10 ⁻²⁴	European	5059	0	5059
				APOB (apolipoprotein B) ⁴⁴	6.80x10 ⁻¹⁵	European	5059	0	5059
				LDL cholesterol lipoprotein fraction concentration ⁷⁵	2.30x10 ⁻³¹	European/Unspecified	17296	9472	26768
				LDL cholesterol lipoprotein fraction concentration in fasting sample ⁷⁵	1.50x10 ⁻²⁵	European/Unspecified	17296	9472	26768
				APOB assay lipoprotein fraction concentration ⁷⁵	4.80x10 ⁻²⁵	European/Unspecified	17296	9472	26768
				APOB assay lipoprotein fraction concentration in fasting sample ⁷⁵	2.80x10 ⁻¹⁸	European/Unspecified	17296	9472	26768
				LDL cholesterol large lipoprotein fraction concentration ⁷⁵	4.30x10 ⁻¹⁵	European/Unspecified	17296	9472	26768
				LDL cholesterol total lipoprotein fraction concentration ⁷⁵	1.90x10 ⁻¹³	European/Unspecified	17296	9472	26768
				LDL cholesterol large lipoprotein fraction concentration in fasting sample ⁷⁵	3.00x10 ⁻¹²	European/Unspecified	17296	9472	26768
				VLDL cholesterol small lipoprotein fraction concentration ⁷⁵	1.60x10 ⁻¹⁰	European/Unspecified	17296	9472	26768
				LDL cholesterol total lipoprotein fraction concentration in fasting sample ⁷⁵	2.10x10 ⁻⁰⁹	European/Unspecified	17296	9472	26768
				VLDL cholesterol small lipoprotein fraction concentration in fasting sample ⁷⁵	1.90x10 ⁻⁰⁸	European/Unspecified	17296	9472	26768
				LDL cholesterol change with statins ⁴⁶	2.80x10 ⁻⁰⁵	European	3928	0	3928
				LDL cholesterol ⁴⁶	2.80x10 ⁻⁰⁵	European	3928	0	3928
				LDL cholesterol ⁴⁷	8.60x10 ⁻¹²	Mixed	100184	39875	140059
				Total cholesterol ⁴⁷	1.70x10 ⁻¹⁰	Mixed	100184	39875	140059
				Coronary artery disease (CAD) ⁴⁷	5.00x10 ⁻⁰⁹	Mixed	100184	39875	140059
				Height ⁴⁸	5.10x10 ⁻⁰⁴	European	133653	50074	183727
				LDL cholesterol ⁴⁹	2.00x10 ⁻⁵¹	African	8090	8849	16939
				Presence of carotid artery plaque ⁷⁶	8.20x10 ⁻⁰⁸	European	31211	11273	42484
				Carotid artery plaque ⁷⁶	1.00x10 ⁻⁰⁷	European	31211	11273	42484
				Coronary artery disease (CAD) ⁷⁶	2.00x10 ⁻⁰⁴	European	31211	11273	42484
				LDL cholesterol ⁵⁰	5.00x10 ⁻¹¹	European	11683	0	11683
				Coronary artery disease (CAD) ⁷⁷	1.10x10 ⁻⁰⁸	Mixed	50587	57594	108181
				LDL cholesterol (baseline) ⁵¹	5.20x10 ⁻¹⁵	European	5244	0	5244
				Lp-PLA2 activity ⁵²	2.60x10 ⁻¹¹	European	13664	0	13664
				Lp-PLA2 mass ⁵²	5.50x10 ⁻⁰⁵	European	13664	0	13664
				Metabolic syndrome domains (Atherogenic Dyslipidemia - PC1) ⁷⁸	5.20x10 ⁻³⁰	Mixed	25755	0	25755
				Metabolic syndrome domains (Multivariate analysis) ⁷⁸	8.30x10 ⁻²⁸	Mixed	25755	0	25755
				LDL cholesterol ⁷⁹	1.40x10 ⁻⁴⁹	Mixed	44957	0	44957
				LDL cholesterol (female) ⁷⁹	7.50x10 ⁻²⁹	Mixed	44957	0	44957
				LDL cholesterol (male) ⁷⁹	3.10x10 ⁻²⁵	Mixed	44957	0	44957
				LDL cholesterol ⁵³	1.30x10 ⁻⁷⁹	European	66240	25282	91522
				Total cholesterol ⁵³	1.70x10 ⁻⁷¹	European	66240	25282	91522
				APOB (apolipoprotein B) ⁸⁰	4.10x10 ⁻²⁷	European	3895	14810	18705
				LDL cholesterol ⁸⁰	3.80x10 ⁻²⁵	European	3895	14810	18705
				APOB (apolipoprotein B) response after 40mg daily simvastatin treatment ⁸⁰	1.40x10 ⁻⁰⁷	European	3895	14810	18705
				LDL cholesterol response after 40mg daily simvastatin treatment ⁸⁰	4.30x10 ⁻⁰⁷	European	3895	14810	18705
				LDL cholesterol ⁸¹	2.60x10 ⁻¹⁷	Mixed	9813	7000	16813
				Total cholesterol ⁸¹	1.80x10 ⁻¹⁶	Mixed	9813	7000	16813

SNP	CHR	Position	Gene	Phenotype	P value	Ancestry	Total	Total Replication	Total
				Total cholesterol ⁵²	4.40x10 ⁻⁵⁴	Hispanic	2240	2121	4361
rs3827066	20	44586023	<i>PCIF1-ZNF335-MMP9</i>	Coronary artery disease (CAD) ⁵⁴	1.40x10 ⁻⁰⁵	Mixed	194427	15613	210040
rs2836411	21	39819830	<i>ERG</i>	None					

PheWAS ANALYSIS

We performed a phenome-wide association study (PheWAS)^{83, 84} exploring the association between the 9 AAA-associated SNPs and an extensive group of diagnoses to identify novel associations and uncover potential pleiotropy. For the PheWAS we used data from the electronic Medical Records and Genomics (eMERGE) Network²³ derived from 7 adult sites with a total of 27,077 unrelated patients of European ancestry above 19 years of age. We divided these samples into two datasets by proportional sampling based on eMERGE site, sex, and genotyping platform (13,559 and 13,518 individuals in sets 1 and 2, respectively). We calculated associations between the 9 AAA-associated SNPs and case or control status based on the extensive set of ICD-9 diagnoses, where for a specific diagnosis, individuals with the diagnosis are considered cases. Associations were adjusted for sex, site, genotyping platform and the first 3 principal components to account for global ancestry. We considered the identification of previously known associations, such as rs602633 associated with hyperglyceridemia and rs10757274 associated with CAD, to be indications that the PheWAS approach was robust. The PheWAS results are presented in **Online Table XIII**.

Online Table XIII: PheWAS Results

Chr	Position	SNP	Locus	Gene(s)	PheWAS associations	ICD-9 Description	PheWAS dataset 1			PheWAS dataset 2		
							n cases/controls	Beta(SE)	P	n cases/controls	Beta(SE)	P
1	214409280	rs1795061	1q32.3	near <i>SMYD2</i>	None							
1	154426264	rs4129267	1q21.3	<i>IL6R</i>	None							
1	109821511	rs602633	1p13.3	<i>CELSR2/SORT1</i>	6	Other and unspecified hyperlipidemia	5467/5722	-0.187 (0.035)	7.86171x10 ⁻⁰⁸	5539/5645	-0.151 (0.035)	1.54x10 ⁻⁰⁵
						Other and unspecified hyperlipidemia	5467/5722	-0.187 (0.0345)	7.86171x10 ⁻⁰⁸	2506/8687	-0.114 (0.042)	0.006402
						Pure hypercholesterolemia	2436/8780	-0.116 (0.042)	0.0055185	5539/5645	-0.151 (0.035)	1.54x10 ⁻⁰⁵
						Pure hypercholesterolemia	2436/8780	-0.116 (0.042)	0.0055185	2506/8687	-0.114 (0.042)	0.006402
						Mixed hyperlipidemia	1310/11032	-0.141 (0.054)	0.0083104	5539/5645	-0.151 (0.035)	1.54x10 ⁻⁰⁵
						Mixed hyperlipidemia	1310/11032	-0.141 (0.054)	0.0083104	2506/8687	-0.114 (0.042)	0.006402
9	22096055	rs10757274	9p21	<i>ANRIL</i>	2	Coronary atherosclerosis of native coronary artery	2332/9886	0.210 (0.034)	3.70081x10 ⁻¹⁰	2141/9972	0.158 (0.035)	6.9x10 ⁻⁰⁶
						Coronary atherosclerosis of unspecified type of vessel, native or graft	2167/10004	0.202 (0.035)	4.61186x10 ⁻⁰⁹	2141/9972	0.158 (0.035)	6.9x10 ⁻⁰⁶
9	124425243	rs10985349	9q33.2	<i>DAB2IP</i>	None							
13	22861921	rs9316871	13q12.11	<i>LINC00540</i>	None							
19	11202306	rs6511720	19p13.2	<i>LDLR</i>	4	Other and unspecified hyperlipidemia	5638/5878	-0.201 (0.046)	1.05931x10 ⁻⁰⁵	2583/8928	-0.218 (0.055)	4.95x10 ⁻⁰⁵
						Other and unspecified hyperlipidemia	5638/5878	-0.201 (0.046)	1.05931x10 ⁻⁰⁵	5697/5803	-0.173 (0.045)	9.53x10 ⁻⁰⁵
						Pure hypercholesterolemia	2502/9017	-0.183 (0.056)	0.000948352	2583/8928	-0.218 (0.055)	4.95x10 ⁻⁰⁵
						Pure hypercholesterolemia	2502/9017	-0.183 (0.056)	0.000948352	5697/5803	-0.173 (0.045)	9.53x10 ⁻⁰⁵
20	44586023	rs3827066	20q13.12	Near <i>PCIF1/MMP9/ZNF335</i>	None							
21	39819830	rs2836411	21q22.2	<i>ERG</i>	None							

ANNOTATION OF AAA ASSOCIATED SNPs USING THE UCSC GENOME BROWSER

The 9 AAA-associated loci were manually annotated using the UCSC Genome Browser (<http://genome.ucsc.edu/cgi-bin/hgGateway>) on the hg19 human genome assembly. To annotate a gene, the SNP identification number (rs ID) was typed into the browser, and the genomic region centered on the SNP was examined. We noted genomic elements within 10 kbp of the SNP and on either side of the SNP. Within the browser, there were eleven main tracks that were used to annotate the SNP, which displayed gene locations, related literature, full-length public transcriptome data (mRNAs and ESTs), regulation, conservation, and repetitive elements. The results of this annotation are presented in **Online Table XIV**.

Gene Location

We used several UCSC Genome Browser tracks to determine whether a locus was exonic, intronic, or intergenic, as well as the identity and classification of the gene, if any, at the locus. One of the tracks used was the UCSC Known Genes track. This track displays information on genes and their location, including both protein-coding and non-coding RNA genes⁸⁵. Within this track, NCBI Reference Sequence (RefSeq) genes and GenBank genes were aligned to the genome (by the UCSC Genome Bioinformatics team) using the BLAST-like alignment tool (BLAT)⁸⁶⁻⁸⁸. In order to be included, genes needed a 98% alignment. The track also included gene models from the Consensus CDS (CCDS) project. Predicted genes from tRNA and mouse genes from Rfam with synteny to the human genome are also included in the track^{89, 90}. The track also reports whether the gene is coding or non-coding. In addition to using the NCBI RefSeq to search proteins, UniProt proteins are also reported⁹¹.

Another UCSC track that describes the location of coding and non-coding genes is the NCBI RefSeq track. This displays genes that were aligned to genome with at least a 96% match⁸⁸. We also used ENCODE Consortium's Gencode human gene catalog (v19)⁹². The track combines automatic annotations with manual and experimentally validated entries. Another track used to examine gene location is the Broad Institute lincRNA track. The long intergenic non-coding RNA (lincRNA) data were collected by RNA sequencing (RNA-seq)⁹³. In addition to lincRNAs, the track also displays transcripts of uncertain coding potential (TUCP). For each of these gene types, expression was displayed across 22 different cell and tissue types⁹⁴.

Related Literature

The loci were also annotated according to their relationship to other SNPs. The National Human Genome Research Institute (NHGRI) has a UCSC track of manually curated loci from published Genome-Wide Association Studies (GWAS)⁹⁵ with $P < 1.0 \times 10^{-5}$. This track was used to check independent previously reported disease or phenotype association of each SNP, and to see if the locus of interest fell within a "SNP cloud", which is an area with several SNPs all significantly associated with complementary or biologically similar quantitative traits.

mRNAs and ESTs

In addition to looking at genes, mRNAs and expressed sequence tags (ESTs) were examined. One track used was the human mRNA track. This is comprised of human mRNAs from GenBank aligned to the genome using BLAT^{86, 87}. The Human ESTs track was compiled in the same manner, and included both spliced and un-spliced ESTs. Both of these tracks contain raw full-length public transcriptome data

captured through transcript-to-genome alignments and were used to confirm the presence of genes, to interrogate gene expression profiles, to derive comprehensive information on gene structures (promoters, splice junctions, 3'ends), and novel transcriptional units absent from gene databases.

Regulation

There were also several UCSC Browser tracks used to examine epigenetic and post-transcriptional regulation in the vicinity of a SNP. One track is the TS miRNA track. This shows 3' untranslated region (UTR) microRNA (miRNA) binding sites predicted using TargetScanHuman version 5.1. First, the UTRs were scanned for miRNA sites⁹⁶. After all the matches were found, they were ranked⁹⁷. Another track that displayed regulatory information was the ENCODE Regulation supertrack, which consists of 7 sub-tracks. All of the tracks were used in annotating the locus. The first of these sub-tracks is the transcription track, which displays ENCODE RNA-seq results from cells representing 9 different tissues⁹⁸.

Three of the sub-tracks show information on histone modifications. This was collected by ENCODE using chromatin immunoprecipitation sequencing (ChIP-seq) on cells representing seven different tissues⁹⁹. One histone modification is the monomethylation of lysine 4 in the histone 3 protein, referred to as H3K4Me1. Another modification is the acetylation of lysine 27 in the same histone protein, referred to as H3K27Ac. The presence of either modification suggests an activating regulatory element, and the co-occurrence of the two modifications indicates a putative enhancer region. The third histone modification examined is a trimethylation of lysine 4 in the same histone protein, referred to as H3K4Me3. This signal indicates the presence of a promoter.

Another sub-track we used is the DNase hypersensitivity track version 3, which shows areas of open chromosome accessibility in 125 different cell lines¹⁰⁰. The final two sub-tracks display transcription factor binding sites (TFBSs). Both were created using ChIP-Seq and have information for 161 different transcription factors in 91 different cell types¹⁰¹. The differentiating factor between the two tracks is that one includes information from Factorbook, which displays consensus motifs in binding sites¹⁰².

Conservation

To examine the evolutionary conservation of a locus, the PhyloP Conservation track is used. This displays conservation across 100 different species in a human-centric multispecies alignment¹⁰³.

Repetitive Elements

The final track used is RepeatMaster, which searches the genome for 10 different forms of repeating elements, including long interspersed nuclear elements (LINE), short interspersed nuclear element (SINE), and retrotransposons. This track uses information from the Genetic Information Research Institute's (GIRI) Repbase Update library¹⁰⁴ and makes it possible to determine whether a SNP resides within a genomic repetitive element.

Online Table XIV. Annotation of AAA-Associated SNPs using the UCSC Genome Browser
(<http://genome.ucsc.edu/cgi-bin/hgGateway>)

SNP rs#	Information Available in UCSC Genome Browser
rs1795061	Intron of one mRNA (AY343912), but no ESTs ~550 bp downstream of CEBP beta binding site with consensus motif
rs4129267	In a LINE repeat NHGRI: associated with CAD, asthma, C-protein levels, and protein quantitative traits. Intron of <i>IL6R</i> (involved in immune responses), H3K4Me1 expression In a DNase hypersensitivity cluster (83/125) and 7 TFBSs, including one with a consensus site (MYC). Low expression level. Two ESTs are near the hypersensitivity site, but are not related to any gene/mRNAs.
rs602633	NHGRI: associated with stroke 850 bp downstream of 3' end of <i>PSRC1</i> (involved in mitosis) 900 bp downstream of large H3K4Me1 peak; high transcription levels Associated with a DNase site (9/125) and 3 TFBSs, including a consensus site in <i>EGR1</i> . Approximately 1 kb upstream of a DNase hypersensitivity region (125/125, 100% of cell types) with a large H3K4Me1 peak and mild H3K27Ac levels. There are 36 TFBSs, 6 with consensus motifs. 3 kb downstream of <i>CELSR2</i> (brain expressed cadherin like protein). This region also has high H3K4Me1 expression and moderate H3K27Ac levels, indicating an enhancer region. There are also high transcription levels. There is a DNase hypersensitivity region (62/125) that correlates with 50 TFBSs, 18 with consensus motifs. 5 kbp downstream of another DNase hypersensitivity site (20/125) with 6 TFBSs, 4 of which have consensus motifs. SNP cloud with 9 other SNPs, which have been associated with cholesterol and lipid levels, as well as stroke, and CAD
rs10757274	NHGRI: associated with CAD In a LINE and intron of <i>ANRIL</i> 1.6 kb upstream from high H3K4Me1 and moderate H3K27Ac DNase hypersensitivity site (61) and 15 TFBSs (2 consensus motifs) 7 kbp upstream from a putative enhancer region (high H3K4Me1 and H3K27Ac), associated with DNase hypersensitivity (88) and over 50 TFBSs
rs10985349	Intron of <i>DAB2IP</i> In a DNase hypersensitivity cluster (22) and H3K4Me1 peak
rs9316871	Intergenic
rs6511720	NHGRI: associated with CAD and aneurysm, as well as with lipid and cholesterol levels Intronic to <i>LDLR</i> Moderate transcription levels High levels of H3K4Me1, H3K4Me3, and H3K27Ac (indicating an enhancer/promoter region) In a DNase hypersensitivity cluster of 105/125 with approximately 40 TFBSs (9 consensus motifs)
rs3827066	Intron of <i>ZNF335</i> Moderate transcription levels
rs2836411	Intron of <i>ERG</i> High H3K4Me1 levels, mild H3K27Ac levels Inside a DNase hypersensitivity cluster (11)

PUPASUITE ANALYSIS

The lead SNPs at the 4 novel AAA risk loci (**Table 1**) were identified in the 1000 Genomes phase 3 CEU panel. SNPs in LD ($r^2 > 0.5$) and the lead SNPs were extracted from the 1000 Genomes data and entered into Pupasuite v3.1¹⁰⁵ (**Online Table XV**). No non-synonymous, transcript structure, transcript processing, transcription factor (TF) binding site (Transfac/Jaspar/Oreganno), miRNA sequence, miRNA target, splice site or other functional results were identified.

Online Table XV: Pupasuite 3.1 output for SNPs in LD ($r^2 > 0.5$) with lead SNPs at novel AAA loci.

*Transcript IDs are shown without the full Ensembl Transcript ID (ENST number) for display purposes.

This table spans 2 pages.

Lead SNP	Chr	Position	Nearest gene(s)	LD SNPs	r^2	Location relative to transcript	Gene	Transcript(s)*
rs1795061	1	214409280	SMYD2	rs1795065	1	INTERGENIC		
				rs1660364	1	INTERGENIC		
				rs1660365	1	INTERGENIC		
				rs1795064	1	INTERGENIC		
				rs1795063	1	INTERGENIC		
				rs1795062	1	INTERGENIC		
				rs1660368	1	INTERGENIC		
				rs199679227	1	INTERGENIC		
				rs1660371	1	INTERGENIC		
				rs1795060	1	INTERGENIC		
				rs201675223	0.978	INTERGENIC		
				rs1147673	0.912	INTERGENIC		
				rs12745411	0.724	INTERGENIC		
				rs11585945	0.724	INTERGENIC		
				rs61819142	0.724	INTERGENIC		
				rs12754343	0.724	INTERGENIC		
rs17784245	0.628	INTERGENIC						
rs1021639	0.609	INTERGENIC						
rs9316871	13	22861921	LINC00540	rs9506822	0.85	INTERGENIC		
				rs9510086	0.763	INTERGENIC		
				rs12863716	0.763	INTERGENIC		
				rs7336555	0.763	INTERGENIC		
				rs12857403	0.763	INTERGENIC		
				rs12866004	0.763	INTERGENIC		
				rs11618858	0.763	INTERGENIC		
				rs7994761	0.763	INTERGENIC		
				rs9506820	0.696	INTERGENIC		
				rs3827066	20	44586023	PCIF1-ZNF335-MMP9	rs73128528
		INTRONIC	ZNF335					322927
		INTRONIC	ZNF335					426788
rs17448653	0.629	DOWNSTREAM	ZNF335					494955
		INTRONIC	ZNF335					243961
		INTRONIC	ZNF335					322927
		INTRONIC	ZNF335					426788
		UPSTREAM	ZNF335					475002
		WITHIN_NON_CODING_GENE	ZNF335					476822
rs2836411	21	39819830	ERG					rs2836399
						WITHIN_NON_CODING_GENE	ERG	468474, 473107, 481609, 492833
				rs2298336	0.53	INTRONIC	ERG	288319, 357391, 398897, 398899, 398905, 398907, 398910, 398911, 398916, 398919, 415743, 417133, 429727, 442448, 451178, 453032
						WITHIN_NON_CODING_GENE	ERG	468474, 473107, 481609, 492833
				rs2836402	0.53	INTRONIC	ERG	288319, 357391, 398897,

					398899, 398905, 398907, 398910, 398911, 398916, 398919, 415743, 417133, 429727, 442448, 451178, 453032
				WITHIN_NON_CODING_GENE	ERG 468474, 473107, 481609, 492833
rs2836400	0.519	INTRONIC		ERG	288319, 357391, 398897, 398899, 398905, 398907, 398910, 398911, 398916, 398919, 415743, 417133, 429727, 442448, 451178, 453032
				WITHIN_NON_CODING_GENE	ERG 468474, 473107, 481609, 492833
rs2836407	0.519	INTRONIC		ERG	288319, 357391, 398897, 398899, 398905, 398907, 398910, 398911, 398916, 398919, 415743, 417133, 429727, 442448, 451178, 453032
				UPSTREAM	ERG 492833
				WITHIN_NON_CODING_GENE	ERG 468474, 473107, 481609
rs2836409	0.519	INTRONIC		ERG	288319, 398897, 398899, 398905, 398907, 398910, 398911, 398916, 398919, 417133, 442448, 451178, 453032
				UPSTREAM	ERG 357391, 415743, 429727, 492833
				WITHIN_NON_CODING_GENE	ERG 468474, 473107, 481609

GWAS3D ANALYSIS

The 9 AAA GWAS SNPs (LeadSNP) were entered into the GWAS3D¹⁰⁶ web-portal (<http://jjwanglab.org/gwas3d>), using the following settings: 1. SNP dataset: 1000 Genomes pilot 1, 2. Population: EUR, 3. LD threshold: $R^2 > 0.8$, 4. Cell type: All; and 5. all ENCODE TF Family Motifs (binding site P-value 0.02).

The predicted lead functional SNP (Fn_SNPID) associations for the 9 AAA SNPs are shown in **Figure 4 and Online Table XVI**. For example, the AAA GWAS SNP rs602633 is in high LD with rs599839, which has previously been associated with AAA³. GWAS3D predicted the rs599839 variant to alter STAT, Ets, p300 and RFX5 binding affinities.

The extended list of potential functional variant associations within each locus is shown in **Online Table XVII**. All AAA SNPs were predicted to be associated with transcription factor binding site affinity variants and eight map to interactions with distal regions.

Online Table XVI: Lead functional associations for each of the 9 replicated AAA SNPs.

Fn_SNPID	Chr:Position	Locus	Combined P	LeadSNP	GWAS P	R ²	Status
rs4977575	9:22124744	9p21.3	1.70x10 ⁻³⁵	rs10757274	1.5x10 ⁻³³	0.87	█
rs73128528	20:44582187	ZNF335	3.72x10 ⁻¹⁹	rs3827066	2.1x10 ⁻¹⁷	0.83	█
rs73015013	19:11190873	19p13.2	2.58x10 ⁻¹⁶	rs6511720	7.9x10 ⁻¹⁴	0.94	█
rs4845620	1:154406656	IL6R	9.92x10 ⁻¹⁵	rs4129267	4.8x10 ⁻¹³	0.87	█
rs1660368	1:214407335	1q32.3	4.64x10 ⁻¹⁴	rs1795061	8.8x10 ⁻¹¹	0.97	█
rs599839	1:109822166	1p13.3	3.07x10 ⁻¹³	rs602633	6.6x10 ⁻⁰⁹	0.92	█
rs9510086	13:22862440	13q12.11	8.33x10 ⁻¹²	rs9316871	4.8x10 ⁻¹⁰	0.82	█
rs10985349	9:124425243	DAB2IP	7.46x10 ⁻¹¹	rs10985349	2.4x10 ⁻¹¹	1	█
rs2836411	21:39819830	ERG	4.72x10 ⁻⁰⁹	rs2836411	5.8x10 ⁻⁰⁹	1	█

█	Leading variant		
█	Significant TFBS		
█	Mapping on distal interaction		
█	Mapping on putative enhancer region		
█	Mapping on GERP++ conservation element		

Online Table XVII: Significant regulatory variants detected by the GWAS3D algorithm. Status: distal interaction (td), transcription factor binding affinity (bda), chromatin modification state (chromhmm), sites under evolutionary constraint (gerp). This table spans 4 pages.

SNPID	CHRPOS	GENOTYPE	LOCUS	FINALP	LeadSNP	LEADSNP_P	RSQUARE	STATUS
rs4977575	9:22124744	C G	9p21.3	1.70x10 ⁻³⁵	rs10757274	1.54x10 ⁻³³	0.87	td,bda,enhancer,gerp
rs1333049	9:22125503	G C	9p21.3	3.13x10 ⁻³⁵	rs10757274	1.54x10 ⁻³³	0.88	td,bda,enhancer
rs1333046	9:22124123	T A	9p21.3	6.47x10 ⁻³⁵	rs10757274	1.54x10 ⁻³³	0.93	td,bda,enhancer
rs10738610	9:22123766	A C	9p21.3	4.51x10 ⁻³⁴	rs10757274	1.54x10 ⁻³³	0.93	td,bda,enhancer
rs7857118	9:22124140	A T	9p21.3	4.85x10 ⁻³⁴	rs10757274	1.54x10 ⁻³³	0.92	td,bda,enhancer
rs7859362	9:22105927	T C	ANRIL	7.83x10 ⁻³⁴	rs10757274	1.54x10 ⁻³³	0.93	td,bda,enhancer
rs10217586	9:22121349	A T	9p21.3	9.21x10 ⁻³⁴	rs10757274	1.54x10 ⁻³³	0.81	td,bda,enhancer
rs7859727	9:22102165	C T	ANRIL	1.12x10 ⁻³³	rs10757274	1.54x10 ⁻³³	0.97	td,bda,enhancer
rs10811656	9:22124472	C T	9p21.3	1.19x10 ⁻³³	rs10757274	1.54x10 ⁻³³	0.85	td,bda,enhancer
rs1333043	9:22106731	T A	ANRIL	2.16x10 ⁻³³	rs10757274	1.54x10 ⁻³³	0.93	td,bda,enhancer
rs2891168	9:22098619	A G	ANRIL	2.44x10 ⁻³³	rs10757274	1.54x10 ⁻³³	0.99	td,bda,enhancer
rs10738608	9:22094796	A C	ANRIL	2.72x10 ⁻³³	rs10757274	1.54x10 ⁻³³	0.95	td,bda,enhancer
rs10738607	9:22088094	A G	ANRIL	2.72x10 ⁻³³	rs10757274	1.54x10 ⁻³³	0.95	td,bda,enhancer
rs6475609	9:22106271	A G	ANRIL	4.57x10 ⁻³³	rs10757274	1.54x10 ⁻³³	0.93	td,bda,enhancer
rs2383207	9:22115959	A G	ANRIL	4.60x10 ⁻³³	rs10757274	1.54x10 ⁻³³	0.90	td,bda,enhancer
rs1537370	9:22084310	C T	ANRIL	1.19x10 ⁻³²	rs10757274	1.54x10 ⁻³³	0.84	td,bda,enhancer
rs10511701	9:22112599	T C	ANRIL	1.39x10 ⁻³²	rs10757274	1.54x10 ⁻³³	0.90	td,bda,enhancer
rs1333047	9:22124504	A T	9p21.3	1.53x10 ⁻³²	rs10757274	1.54x10 ⁻³³	0.87	td,bda,enhancer
rs10757275	9:22106225	G A	ANRIL	1.67x10 ⁻³²	rs10757274	1.54x10 ⁻³³	0.94	td,bda,enhancer
rs1333048	9:22125347	A C	9p21.3	1.67x10 ⁻³²	rs10757274	1.54x10 ⁻³³	0.94	td,bda,enhancer
rs4977574	9:22098574	A G	ANRIL	2.01x10 ⁻³²	rs10757274	1.54x10 ⁻³³	0.99	td,bda,enhancer
rs10757278	9:22124477	A G	9p21.3	2.25x10 ⁻³²	rs10757274	1.54x10 ⁻³³	0.88	td,bda,enhancer
rs1537374	9:22116046	A G	ANRIL	2.27x10 ⁻³²	rs10757274	1.54x10 ⁻³³	0.90	td,bda,enhancer
rs1537375	9:22116071	T C	ANRIL	2.66x10 ⁻³²	rs10757274	1.54x10 ⁻³³	0.91	td,bda,enhancer
rs7341791	9:22112427	A G	ANRIL	2.69x10 ⁻³²	rs10757274	1.54x10 ⁻³³	0.89	td,bda,enhancer
rs10757279	9:22124630	A G	9p21.3	3.05x10 ⁻³²	rs10757274	1.54x10 ⁻³³	0.88	td,bda,enhancer
rs2383206	9:22115026	A G	ANRIL	3.05x10 ⁻³²	rs10757274	1.54x10 ⁻³³	0.90	td,bda,enhancer
rs7341786	9:22112241	A C	ANRIL	3.35x10 ⁻³²	rs10757274	1.54x10 ⁻³³	0.89	td,bda,enhancer
rs10757272	9:22088260	C T	ANRIL	3.38x10 ⁻³²	rs10757274	1.54x10 ⁻³³	0.96	td,bda,enhancer
rs1537376	9:22116220	T C	ANRIL	3.95x10 ⁻³²	rs10757274	1.54x10 ⁻³³	0.90	td,bda,enhancer
rs1537373	9:22103341	T G	ANRIL	5.37x10 ⁻³²	rs10757274	1.54x10 ⁻³³	0.96	td,bda,enhancer
rs10757274	9:22096055	A G	ANRIL	6.09x10 ⁻³²	rs10757274	1.54x10 ⁻³³	1.00	td,bda,enhancer,self
rs2210538	9:22092257	G A	ANRIL	6.51x10 ⁻³²	rs10757274	1.54x10 ⁻³³	0.85	td,bda,enhancer
rs1537371	9:22099568	C A	ANRIL	6.84x10 ⁻³²	rs10757274	1.54x10 ⁻³³	0.96	td,bda,enhancer
rs10757277	9:22124450	A G	9p21.3	6.93x10 ⁻³²	rs10757274	1.54x10 ⁻³³	0.88	td,bda,enhancer
rs10733376	9:22114469	G C	ANRIL	7.49x10 ⁻³²	rs10757274	1.54x10 ⁻³³	0.90	td,bda,enhancer

SNPID	CHRPOS	GENOTYPE	LOCUS	FINALP	LeadSNP	LEADSNP_P	RSQUARE	STATUS
rs10738606	9:22088090	A T	ANRIL	9.11x10 ⁻³²	rs10757274	1.54x10 ⁻³³	0.95	td,bda,enhancer
rs4977757	9:22094330	A G	ANRIL	9.23x10 ⁻³²	rs10757274	1.54x10 ⁻³³	0.91	td,bda,enhancer
rs1004638	9:22115589	A T	ANRIL	9.85x10 ⁻³²	rs10757274	1.54x10 ⁻³³	0.90	td,bda,enhancer
rs10738609	9:22114495	A C,G,T	ANRIL	1.05x10 ⁻³¹	rs10757274	1.54x10 ⁻³³	0.91	td,bda,enhancer
rs9644860	9:22090603	C T	ANRIL	1.08x10 ⁻³¹	rs10757274	1.54x10 ⁻³³	0.81	td,bda,enhancer
rs944797	9:22115286	T C	ANRIL	1.14x10 ⁻³¹	rs10757274	1.54x10 ⁻³³	0.90	td,bda,enhancer
rs1556516	9:22100176	G C	ANRIL	1.37x10 ⁻³¹	rs10757274	1.54x10 ⁻³³	0.96	td,bda,enhancer
rs10116277	9:22081397	G T	ANRIL	1.58x10 ⁻³¹	rs10757274	1.54x10 ⁻³³	0.85	td,bda,enhancer
rs1412834	9:22110131	T C	ANRIL	1.59x10 ⁻³¹	rs10757274	1.54x10 ⁻³³	0.91	td,bda,enhancer
rs1333042	9:22103813	A G	ANRIL	1.84x10 ⁻³¹	rs10757274	1.54x10 ⁻³³	0.95	td,bda,enhancer
rs6475606	9:22081850	C T	ANRIL	2.11x10 ⁻³¹	rs10757274	1.54x10 ⁻³³	0.85	td,bda,enhancer
rs1970112	9:22085598	T C	ANRIL	2.49x10 ⁻³¹	rs10757274	1.54x10 ⁻³³	0.86	td,bda,enhancer
rs73128528	20:44582187	A T	ZNF335	3.72x10 ⁻¹⁹	rs3827066	2.10x10 ⁻¹⁷	0.83	bda,enhancer
rs7267295	20:44570683	C T	PCIF1	4.78x10 ⁻¹⁸	rs3827066	2.10x10 ⁻¹⁷	0.84	td,bda,enhancer
rs58749629	20:44571317	G A	PCIF1	1.84x10 ⁻¹⁶	rs3827066	2.10x10 ⁻¹⁷	0.91	td,bda,enhancer
rs73015013	19:11190873	C T	19p13.2	2.58x10 ⁻¹⁶	rs6511720	7.90x10 ⁻¹⁴	0.94	td,bda,enhancer
rs8124182	20:44608901	G A	20q13.12	2.86x10 ⁻¹⁶	rs3827066	2.10x10 ⁻¹⁷	0.84	td,bda,enhancer
rs7270354	20:44607661	G A	20q13.12	4.86x10 ⁻¹⁶	rs3827066	2.10x10 ⁻¹⁷	0.91	td,bda,enhancer
chr19:11190074	19:11190074	G A	19p13.2	1.41x10 ⁻¹⁵	rs6511720	7.90x10 ⁻¹⁴	0.96	td,bda,enhancer
chr19:11189272	19:11189272	T C	19p13.2	1.65x10 ⁻¹⁵	rs6511720	7.90x10 ⁻¹⁴	0.94	td,bda,enhancer
chr19:11189937	19:11189937	T A	19p13.2	1.81x10 ⁻¹⁵	rs6511720	7.90x10 ⁻¹⁴	0.96	td,bda,enhancer
rs6511720	19:11202306	G T	LDLR	2.06x10 ⁻¹⁵	rs6511720	7.90x10 ⁻¹⁴	1	bda,enhancer,chromhmm,self
rs56289821	19:11188247	G A	19p13.2	3.84x10 ⁻¹⁵	rs6511720	7.90x10 ⁻¹⁴	0.92	td,bda,enhancer
rs8106503	19:11196886	T C	19p13.2	6.27x10 ⁻¹⁵	rs6511720	7.90x10 ⁻¹⁴	0.94	td,bda,enhancer,chromhmm
rs4845620	1:154406656	A G	IL6R	9.92x10 ⁻¹⁵	rs4129267	4.76x10 ⁻¹³	0.87	td,bda,enhancer
rs17248720	19:11198187	C T	LDLR	1.87x10 ⁻¹⁴	rs6511720	7.90x10 ⁻¹⁴	0.91	td,bda,enhancer,chromhmm
rs1660368	1:214407335	C T	1q32.3	4.64x10 ⁻¹⁴	rs1795061	8.80x10 ⁻¹¹	0.97	td,bda,enhancer,gerp
rs4537545	1:154418879	C T	IL6R	4.72x10 ⁻¹⁴	rs4129267	4.76x10 ⁻¹³	0.87	td,bda,enhancer
chr19:11187358	19:11187358	T G	19p13.2	5.55x10 ⁻¹⁴	rs6511720	7.90x10 ⁻¹⁴	0.92	td,bda,enhancer
rs56383622	1:154405024	A G	IL6R	5.67x10 ⁻¹⁴	rs4129267	4.76x10 ⁻¹³	0.87	td,bda,enhancer
chr19:11191197	19:11191197	G A	19p13.2	7.26x10 ⁻¹⁴	rs6511720	7.90x10 ⁻¹⁴	0.94	td,bda,enhancer
rs57217136	19:11201124	T C	LDLR	8.82x10 ⁻¹⁴	rs6511720	7.90x10 ⁻¹⁴	1	bda,enhancer,chromhmm
rs4129267	1:154426264	C T	IL6R	9.12x10 ⁻¹⁴	rs4129267	4.76x10 ⁻¹³	1	bda,enhancer,self
rs12151108	19:11197261	G A	19p13.2	1.10x10 ⁻¹³	rs6511720	7.90x10 ⁻¹⁴	0.93	td,bda,enhancer
rs17248727	19:11198502	T C	LDLR	1.31x10 ⁻¹³	rs6511720	7.90x10 ⁻¹⁴	0.92	td,bda,enhancer,chromhmm
rs2228145	1:154426970	A C,T	IL6R	1.39x10 ⁻¹³	rs4129267	4.76x10 ⁻¹³	0.99	bda,enhancer
chr19:11189205	19:11189205	C G	19p13.2	1.54x10 ⁻¹³	rs6511720	7.90x10 ⁻¹⁴	0.94	td,bda,enhancer
chr19:11189980	19:11189980	C A	19p13.2	1.73x10 ⁻¹³	rs6511720	7.90x10 ⁻¹⁴	0.96	td,bda,enhancer
chr19:11188899	19:11188899	C T	19p13.2	1.74x10 ⁻¹³	rs6511720	7.90x10 ⁻¹⁴	0.94	td,bda,enhancer
rs73015021	19:11192915	A G	19p13.2	1.91x10 ⁻¹³	rs6511720	7.90x10 ⁻¹⁴	0.96	td,bda,enhancer

SNPID	CHRPOS	GENOTYPE	LOCUS	FINALP	LeadSNP	LEADSNP_P	RSQUARE	STATUS
chr19:11190544	19:11190544	C T	19p13.2	2.15x10 ⁻¹³	rs6511720	7.90x10 ⁻¹⁴	0.88	td,bda,enhancer
rs6684439	1:154395839	C T	<i>IL6R</i>	2.51x10 ⁻¹³	rs4129267	4.76x10 ⁻¹³	0.83	td,bda,enhancer
chr19:11191729	19:11191729	C T	19p13.2	2.95x10 ⁻¹³	rs6511720	7.90x10 ⁻¹⁴	0.94	td,bda,enhancer
rs599839	1:109822166	G A	1p13.3	3.07x10 ⁻¹³	rs602633	6.58x10 ⁻⁰⁹	0.92	td,bda,enhancer,gerp
chr19:11190481	19:11190481	G T	19p13.2	3.15x10 ⁻¹³	rs6511720	7.90x10 ⁻¹⁴	0.96	td,bda,enhancer
rs10412048	19:11193949	A G	19p13.2	3.58x10 ⁻¹³	rs6511720	7.90x10 ⁻¹⁴	0.93	td,bda,enhancer
rs73015011	19:11189764	T C	19p13.2	3.78x10 ⁻¹³	rs6511720	7.90x10 ⁻¹⁴	0.94	td,bda,enhancer
rs4845373	1:154417829	C T	<i>IL6R</i>	4.52x10 ⁻¹³	rs4129267	4.76x10 ⁻¹³	0.87	td,bda,enhancer
rs55997232	19:11188117	C T	19p13.2	4.98x10 ⁻¹³	rs6511720	7.90x10 ⁻¹⁴	0.94	td,bda,enhancer
rs56125973	19:11188164	T C	19p13.2	5.03x10 ⁻¹³	rs6511720	7.90x10 ⁻¹⁴	0.91	td,bda,enhancer
chr19:11188850	19:11188850	T C	19p13.2	6.17x10 ⁻¹³	rs6511720	7.90x10 ⁻¹⁴	0.93	td,bda,enhancer
rs12126142	1:154425456	G A	<i>IL6R</i>	6.17x10 ⁻¹³	rs4129267	4.76x10 ⁻¹³	1	bda,enhancer
chr19:11187422	19:11187422	T C	19p13.2	6.25x10 ⁻¹³	rs6511720	7.90x10 ⁻¹⁴	0.93	td,bda,enhancer
chr19:11190556	19:11190556	T C	19p13.2	6.99x10 ⁻¹³	rs6511720	7.90x10 ⁻¹⁴	0.93	td,bda,enhancer
rs10402112	19:11191677	T A	19p13.2	7.26x10 ⁻¹³	rs6511720	7.90x10 ⁻¹⁴	0.94	td,bda,enhancer
rs11265613	1:154418415	T C	<i>IL6R</i>	7.93x10 ⁻¹³	rs4129267	4.76x10 ⁻¹³	0.88	td,bda,enhancer
chr19:11187324	19:11187324	C G	19p13.2	8.25x10 ⁻¹³	rs6511720	7.90x10 ⁻¹⁴	0.93	td,bda,enhancer
rs55791371	19:11188153	A C	19p13.2	8.67x10 ⁻¹³	rs6511720	7.90x10 ⁻¹⁴	0.93	td,bda,enhancer
rs1147673	1:214402313	A G	1q32.3	9.07x10 ⁻¹³	rs1795061	8.80x10 ⁻¹¹	0.93	td,bda,enhancer
rs61194703	19:11192193	A T	19p13.2	9.20x10 ⁻¹³	rs6511720	7.90x10 ⁻¹⁴	0.94	td,bda,enhancer
chr19:11190292	19:11190292	T C	19p13.2	1.03x10 ⁻¹²	rs6511720	7.90x10 ⁻¹⁴	0.94	td,bda,enhancer
rs4845622	1:154411419	A C	<i>IL6R</i>	1.13x10 ⁻¹²	rs4129267	4.76x10 ⁻¹³	0.87	td,bda,enhancer
rs73015024	19:11197598	G T	19p13.2	1.13x10 ⁻¹²	rs6511720	7.90x10 ⁻¹⁴	0.94	td,bda,enhancer
rs12133641	1:154428283	A G	<i>IL6R</i>	1.32x10 ⁻¹²	rs4129267	4.76x10 ⁻¹³	0.97	bda,enhancer
chr19:11190534	19:11190534	G A	19p13.2	1.36x10 ⁻¹²	rs6511720	7.90x10 ⁻¹⁴	0.93	td,bda,enhancer
chr19:11190110	19:11190110	A G	19p13.2	1.44x10 ⁻¹²	rs6511720	7.90x10 ⁻¹⁴	0.96	td,bda,enhancer
chr19:11190549	19:11190549	G A	19p13.2	1.50x10 ⁻¹²	rs6511720	7.90x10 ⁻¹⁴	0.93	td,bda,enhancer
rs73015016	19:11191300	G A	19p13.2	1.56x10 ⁻¹²	rs6511720	7.90x10 ⁻¹⁴	0.94	td,bda,enhancer
rs12730935	1:154419892	G A	<i>IL6R</i>	1.60x10 ⁻¹²	rs4129267	4.76x10 ⁻¹³	0.86	td,bda
chr19:11192831	19:11192831	A G	19p13.2	1.88x10 ⁻¹²	rs6511720	7.90x10 ⁻¹⁴	0.94	td,bda,enhancer
rs73015020	19:11192550	G A	19p13.2	1.98x10 ⁻¹²	rs6511720	7.90x10 ⁻¹⁴	0.93	td,bda,enhancer
rs4576655	1:154418749	C T	<i>IL6R</i>	2.56x10 ⁻¹²	rs4129267	4.76x10 ⁻¹³	0.88	td,bda,enhancer
rs4845621	1:154409730	G A	<i>IL6R</i>	2.95x10 ⁻¹²	rs4129267	4.76x10 ⁻¹³	0.87	td,bda
rs4393147	1:154414037	C T	<i>IL6R</i>	3.16x10 ⁻¹²	rs4129267	4.76x10 ⁻¹³	0.87	td,bda,enhancer
rs12753254	1:154416935	G A	<i>IL6R</i>	3.49x10 ⁻¹²	rs4129267	4.76x10 ⁻¹³	0.87	td,bda,enhancer
rs4845372	1:154415396	C A	<i>IL6R</i>	4.58x10 ⁻¹²	rs4129267	4.76x10 ⁻¹³	0.83	td,bda,enhancer
rs6664201	1:154414296	C T	<i>IL6R</i>	5.08x10 ⁻¹²	rs4129267	4.76x10 ⁻¹³	0.87	td,bda,enhancer
rs4845623	1:154415777	A G	<i>IL6R</i>	5.10x10 ⁻¹²	rs4129267	4.76x10 ⁻¹³	0.83	td,bda,enhancer
rs7521458	1:154407713	T C	<i>IL6R</i>	5.55x10 ⁻¹²	rs4129267	4.76x10 ⁻¹³	0.87	td,bda
rs12730036	1:154416969	C T	<i>IL6R</i>	6.86x10 ⁻¹²	rs4129267	4.76x10 ⁻¹³	0.87	td,bda,enhancer

SNPID	CHRPOS	GENOTYPE	LOCUS	FINALP	LeadSNP	LEADSNP_P	RSQUARE	STATUS
rs9510086	13:22862440	G C	13q12.11	8.33x10 ⁻¹²	rs9316871	4.80x10 ⁻¹⁰	0.81	td,bda,enhancer
rs7518199	1:154407419	A C	<i>IL6R</i>	8.49x10 ⁻¹²	rs4129267	4.76x10 ⁻¹³	0.87	td,bda,enhancer
rs4453032	1:154414086	A G	<i>IL6R</i>	8.54x10 ⁻¹²	rs4129267	4.76x10 ⁻¹³	0.87	td,bda,enhancer
rs1795065	1:214405194	G A	1q32.3	1.75x10 ⁻¹¹	rs1795061	8.80x10 ⁻¹¹	0.97	td,bda,enhancer
rs1795060	1:214410021	C T	1q32.3	1.90x10 ⁻¹¹	rs1795061	8.80x10 ⁻¹¹	1	bda,enhancer
rs12740374	1:109817590	G T	<i>CELSR2</i>	2.07x10 ⁻¹¹	rs602633	6.58x10 ⁻⁰⁹	0.90	td,bda,enhancer,chromhmm,gerp
rs904320	1:214408457	A T	1q32.3	4.93x10 ⁻¹¹	rs1795061	8.80x10 ⁻¹¹	0.98	td,bda,enhancer
rs1795061	1:214409280	T C	1q32.3	5.62x10 ⁻¹¹	rs1795061	8.80x10 ⁻¹¹	1	td,bda,enhancer,self
rs629301	1:109818306	G T	<i>CELSR2</i>	7.32x10 ⁻¹¹	rs602633	6.58x10 ⁻⁰⁹	0.90	td,bda,enhancer,chromhmm,gerp
rs10985349	9:124425243	C T	<i>DAB2IP</i>	7.46x10 ⁻¹¹	rs10985349	2.40x10 ⁻¹¹	1	td,bda,enhancer,self
rs10985350	9:124429196	A C	<i>DAB2IP</i>	1.67x10 ⁻¹⁰	rs10985349	2.40x10 ⁻¹¹	0.81	td,bda,enhancer
rs660240	1:109817838	T C	<i>CELSR2</i>	1.88x10 ⁻¹⁰	rs602633	6.58x10 ⁻⁰⁹	0.96	td,bda,enhancer,chromhmm,gerp
rs7528419	1:109817192	A G	<i>CELSR2</i>	4.03x10 ⁻¹⁰	rs602633	6.58x10 ⁻⁰⁹	0.90	td,bda,enhancer,chromhmm,gerp
rs1795064	1:214406272	C T	1q32.3	5.07x10 ⁻¹⁰	rs1795061	8.80x10 ⁻¹¹	0.97	td,bda,enhancer
rs1795062	1:214406721	T C	1q32.3	5.73x10 ⁻¹⁰	rs1795061	8.80x10 ⁻¹¹	0.97	td,bda,enhancer
rs1660371	1:214409248	T A	1q32.3	9.29x10 ⁻¹⁰	rs1795061	8.80x10 ⁻¹¹	0.97	td,bda,enhancer
rs1795063	1:214406508	G A	1q32.3	9.72x10 ⁻¹⁰	rs1795061	8.80x10 ⁻¹¹	0.97	td,bda,enhancer
rs9316871	13:22861921	A G	13q12.11	1.26x10 ⁻⁰⁹	rs9316871	4.80x10 ⁻¹⁰	1	td,bda,enhancer,self
rs9506822	13:22862220	A G	13q12.11	1.89x10 ⁻⁰⁹	rs9316871	4.80x10 ⁻¹⁰	0.87	td,bda,enhancer
rs2836411	21:39819830	C T	<i>ERG</i>	4.72x10 ⁻⁰⁹	rs2836411	5.80x10 ⁻⁰⁹	1	bda,enhancer,self

107

BIOINFORMATIC IDENTIFICATION OF CANDIDATE AAA GENES AND PATHWAYS USING DEPICT

An integrated gene function analysis was performed using the DEPICT version 1.1 tool¹⁰⁸. DEPICT was installed, tested and run using meta-GWAS summary statistics following the recommended procedure outlined at <https://github.com/perslab/depict>. Two separate runs were performed using either all independent SNPs with discovery metaGWAS $P < 5 \times 10^{-6}$ or just those 10 SNPs which reached $P < 1 \times 10^{-6}$ in the combined analysis. Results are shown in **Online Table XVIII** and the full dataset is available in the online data supplement.

Online Table XVIII, DEPICT gene enrichment sets (nominal $P < 0.05$) based on the top 10 validated loci.

There is a notable presence of descriptions associated with transforming growth factor beta regulation, lipoprotein metabolism, inflammation induced extracellular matrix remodelling (eg. RFX1), vascular smooth muscle cell function, vascular injury (including haemorrhage), immune cell function (particularly T & B cells), acute phase response (including IL6 secretion), apoptosis, hyperglycemia and the PIK3K, JNK and MAPK cascades. In addition, there are several descriptions associated with long bone size, an observation which may be consistent with previous reports linking height with cardiovascular disease risk. All gene sets had a false discovery rate > 0.2 with the exception of the most significant gene set, MP:0006396 (decreased long bone epiphyseal plate size), where the FDR was < 0.2 . This table spans 11 pages.

Original gene set ID	Original gene set description	DEPICT Nominal P-value
MP:0006396	decreased long bone epiphyseal plate size	1.14×10^{-9}
GO:0034381	plasma lipoprotein particle clearance	5.22×10^{-7}
ENSG00000205250	E2F4 PPI subnetwork	1.27×10^{-6}
ENSG00000132005	RFX1 PPI subnetwork	2.28×10^{-6}
MP:0000708	thymus hyperplasia	6.32×10^{-6}
ENSG00000167553	TUBA1C PPI subnetwork	3.18×10^{-5}
ENSG00000170421	KRT8 PPI subnetwork	9.59×10^{-5}
MP:0003645	increased pancreatic beta cell number	1.12×10^{-4}
ENSG00000166866	MYO1A PPI subnetwork	2.32×10^{-4}
REACTOME	REACTOME_apoptotic_execution__phase	2.92×10^{-4}
MP:0008182	decreased marginal zone B cell number	3.06×10^{-4}
GO:0008375	acetylglucosaminyltransferase activity	3.62×10^{-4}
ENSG00000131941	RHPN2 PPI subnetwork	3.75×10^{-4}
ENSG00000169710	FASN PPI subnetwork	4.55×10^{-4}
REACTOME	Reactome_apoptotic_cleavage_of_cellular_proteins	5.46×10^{-4}
ENSG0000013297	CLDN11 PPI subnetwork	6.28×10^{-4}
ENSG00000070159	PTPN3 PPI subnetwork	6.56×10^{-4}
ENSG00000091409	ITGA6 PPI subnetwork	7.26×10^{-4}
ENSG00000178209	PLEC PPI subnetwork	8.57×10^{-4}
REACTOME	Reactome_p75_ntr_receptor:mediated_signalling	1.07×10^{-3}
GO:0001890	placenta development	1.08×10^{-3}
ENSG00000164344	KLKB1 PPI subnetwork	1.09×10^{-3}
MP:0002136	abnormal kidney physiology	1.17×10^{-3}
MP:0002655	abnormal keratinocyte morphology	1.45×10^{-3}

Original gene set ID	Original gene set description	DEPICT Nominal P-value
ENSG00000143375	CGN PPI subnetwork	1.48x10 ⁻³
MP:0005595	abnormal vascular smooth muscle physiology	1.55x10 ⁻³
ENSG00000122641	INHBA PPI subnetwork	1.79x10 ⁻³
MP:0002764	short tibia	1.79x10 ⁻³
MP:0003662	abnormal long bone epiphyseal plate proliferative zone	2.01x10 ⁻³
ENSG00000169047	IRS1 PPI subnetwork	2.21x10 ⁻³
ENSG00000125503	PPP1R12C PPI subnetwork	2.23x10 ⁻³
MP:0001179	thick pulmonary interalveolar septum	2.30x10 ⁻³
GO:0043256	laminin complex	2.33x10 ⁻³
ENSG00000116809	ZBTB17 PPI subnetwork	2.46x10 ⁻³
GO:0050431	transforming growth factor beta binding	2.47x10 ⁻³
ENSG00000039560	RAI14 PPI subnetwork	2.60x10 ⁻³
ENSG00000164733	CTSB PPI subnetwork	2.64x10 ⁻³
ENSG00000139567	ACVRL1 PPI subnetwork	2.75x10 ⁻³
MP:0005590	increased vasodilation	3.45x10 ⁻³
GO:0071813	lipoprotein particle binding	3.51x10 ⁻³
GO:0071814	protein-lipid complex binding	3.51x10 ⁻³
MP:0002082	postnatal lethality	3.53x10 ⁻³
GO:0071902	positive regulation of protein serine/threonine kinase activity	3.87x10 ⁻³
ENSG00000130147	SH3BP4 PPI subnetwork	3.91x10 ⁻³
GO:0005178	integrin binding	4.08x10 ⁻³
ENSG00000133056	PIK3C2B PPI subnetwork	4.40x10 ⁻³
ENSG00000172725	CORO1B PPI subnetwork	4.45x10 ⁻³
ENSG00000136286	MYO1G PPI subnetwork	4.65x10 ⁻³
ENSG00000078142	PIK3C3 PPI subnetwork	4.72x10 ⁻³
MP:0005095	decreased T cell proliferation	4.84x10 ⁻³
ENSG00000145715	RASA1 PPI subnetwork	4.96x10 ⁻³
ENSG00000104725	ENSG00000104725 PPI subnetwork	5.08x10 ⁻³
KEGG_PATHWAYS	KEGG_PATHWAYS_IN_CANCER	5.17x10 ⁻³
GO:0008194	UDP-glycosyltransferase activity	5.46x10 ⁻³
ENSG00000078747	ITCH PPI subnetwork	5.48x10 ⁻³
ENSG00000149257	SERPINH1 PPI subnetwork	5.79x10 ⁻³
ENSG00000114062	UBE3A PPI subnetwork	5.85x10 ⁻³
ENSG00000139144	PIK3C2G PPI subnetwork	5.85x10 ⁻³
ENSG00000143393	PI4KB PPI subnetwork	5.87x10 ⁻³
ENSG00000148498	PARD3 PPI subnetwork	6.00x10 ⁻³
ENSG00000196455	PIK3R4 PPI subnetwork	6.19x10 ⁻³
ENSG00000148660	CAMK2G PPI subnetwork	6.48x10 ⁻³
ENSG00000034152	MAP2K3 PPI subnetwork	6.58x10 ⁻³
ENSG00000123124	WWP1 PPI subnetwork	6.95x10 ⁻³
MP:0008813	decreased common myeloid progenitor cell number	7.37x10 ⁻³
ENSG00000204175	GPRIN2 PPI subnetwork	7.39x10 ⁻³
GO:0001772	immunological synapse	7.40x10 ⁻³
REACTOME	Reactome_caspase:mediated_cleavage_of_cytoskeletal_proteins	7.46x10 ⁻³
ENSG00000017427	IGF1 PPI subnetwork	7.51x10 ⁻³
MP:0001954	respiratory distress	7.56x10 ⁻³
GO:0016051	carbohydrate biosynthetic process	7.65x10 ⁻³

Original gene set ID	Original gene set description	DEPICT Nominal P-value
GO:0043406	positive regulation of MAP kinase activity	7.65x10 ⁻³
REACTOME	Reactome_cell_death_signalling_via_nrage_nrif_and_nade	7.67x10 ⁻³
MP:0000180	abnormal circulating cholesterol level	7.71x10 ⁻³
ENSG00000170759	KIF5B PPI subnetwork	7.79x10 ⁻³
ENSG00000180530	NRIP1 PPI subnetwork	7.86x10 ⁻³
ENSG00000138771	SHROOM3 PPI subnetwork	7.89x10 ⁻³
ENSG00000065882	TBC1D1 PPI subnetwork	7.97x10 ⁻³
ENSG00000138592	USP8 PPI subnetwork	7.99x10 ⁻³
MP:0001915	intracranial hemorrhage	8.00x10 ⁻³
ENSG00000131746	TNS4 PPI subnetwork	8.01x10 ⁻³
MP:0004883	abnormal vascular wound healing	8.15x10 ⁻³
ENSG00000091073	ENSG00000091073 PPI subnetwork	8.22x10 ⁻³
ENSG00000081189	MEF2C PPI subnetwork	8.24x10 ⁻³
ENSG00000154415	PPP1R3A PPI subnetwork	8.33x10 ⁻³
ENSG00000188313	PLSCR1 PPI subnetwork	8.55x10 ⁻³
MP:0004933	abnormal epididymis epithelium morphology	8.61x10 ⁻³
ENSG00000147065	MSN PPI subnetwork	8.64x10 ⁻³
ENSG00000165409	TSHR PPI subnetwork	8.64x10 ⁻³
ENSG00000106992	AK1 PPI subnetwork	8.69x10 ⁻³
GO:0007292	female gamete generation	8.93x10 ⁻³
ENSG00000144061	NPHP1 PPI subnetwork	8.95x10 ⁻³
MP:0003419	delayed endochondral bone ossification	8.98x10 ⁻³
ENSG00000110880	CORO1C PPI subnetwork	9.04x10 ⁻³
ENSG00000197879	MYO1C PPI subnetwork	9.22x10 ⁻³
ENSG00000176476	CCDC101 PPI subnetwork	9.31x10 ⁻³
ENSG00000176108	CHMP6 PPI subnetwork	9.44x10 ⁻³
REACTOME	Reactome_integrin_cell_surface_interactions	9.47x10 ⁻³
GO:0016758	transferase activity, transferring hexosyl groups	9.49x10 ⁻³
ENSG00000103197	TSC2 PPI subnetwork	9.49x10 ⁻³
MP:0003909	increased eating behavior	9.57x10 ⁻³
MP:0000716	abnormal immune system cell morphology	9.63x10 ⁻³
MP:0008803	abnormal placental labyrinth vasculature morphology	9.67x10 ⁻³
ENSG00000137801	THBS1 PPI subnetwork	9.71x10 ⁻³
ENSG00000130522	JUND PPI subnetwork	9.72x10 ⁻³
GO:0005088	Ras guanyl-nucleotide exchange factor activity	9.78x10 ⁻³
ENSG00000170581	STAT2 PPI subnetwork	9.79x10 ⁻³
ENSG00000173757	STAT5B PPI subnetwork	9.84x10 ⁻³
GO:0043277	apoptotic cell clearance	9.98x10 ⁻³
GO:0006917	induction of apoptosis	0.01
MP:0001828	abnormal T cell activation	0.01
ENSG00000171241	SHCBP1 PPI subnetwork	0.01
REACTOME	REACTOME_apoptosis	0.01
MP:0011106	partial embryonic lethality before somite formation	0.01
GO:0030169	low-density lipoprotein particle binding	0.01
MP:0003731	abnormal retinal outer nuclear layer morphology	0.01
MP:0009400	decreased skeletal muscle fiber size	0.01
ENSG00000137693	YAP1 PPI subnetwork	0.01

Original gene set ID	Original gene set description	DEPICT Nominal P-value
REACTOME	Reactome_nrage_signals_death_through_jnk	0.01
ENSG00000145794	MEGF10 PPI subnetwork	0.01
MP:0008478	increased spleen white pulp amount	0.01
MP:0005079	defective cytotoxic T cell cytolysis	0.01
ENSG00000141506	PIK3R5 PPI subnetwork	0.01
GO:0000989	transcription factor binding transcription factor activity	0.01
MP:0002161	abnormal fertility/fecundity	0.01
GO:0040029	regulation of gene expression, epigenetic	0.01
ENSG00000115963	RND3 PPI subnetwork	0.01
GO:0043236	laminin binding	0.01
ENSG00000211660	ENSG00000211660 PPI subnetwork	0.01
ENSG00000211653	ENSG00000211653 PPI subnetwork	0.01
ENSG00000160310	PRMT2 PPI subnetwork	0.01
ENSG00000127688	GAN PPI subnetwork	0.01
ENSG00000167711	SERPINF2 PPI subnetwork	0.01
GO:0043491	protein kinase B signaling cascade	0.01
ENSG00000136068	FLNB PPI subnetwork	0.01
GO:0002020	protease binding	0.01
ENSG00000198053	SIRPA PPI subnetwork	0.01
ENSG00000182319	SGK223 PPI subnetwork	0.01
ENSG00000174292	TNK1 PPI subnetwork	0.01
ENSG00000132825	PPP1R3D PPI subnetwork	0.01
GO:0051015	actin filament binding	0.01
ENSG00000140443	IGF1R PPI subnetwork	0.01
MP:0000281	abnormal interventricular septum morphology	0.01
ENSG000000067560	RHOA PPI subnetwork	0.01
MP:0006094	increased fat cell size	0.01
ENSG00000197555	SIPA1L1 PPI subnetwork	0.01
ENSG00000183386	FHL3 PPI subnetwork	0.01
MP:0003229	abnormal vitelline vasculature morphology	0.01
MP:0001231	abnormal epidermis stratum basale morphology	0.01
MP:0000511	abnormal intestinal mucosa morphology	0.01
KEGG	KEGG_ACUTE_MYELOID_LEUKEMIA	0.01
GO:0007254	JNK cascade	0.01
GO:0008624	induction of apoptosis by extracellular signals	0.01
GO:0000988	protein binding transcription factor activity	0.02
MP:0002452	abnormal antigen presenting cell physiology	0.02
ENSG00000185950	IRS2 PPI subnetwork	0.02
KEGG	KEGG_leukocyte_transendothelial_migration	0.02
GO:0051568	histone H3-K4 methylation	0.02
ENSG00000165516	KLHDC2 PPI subnetwork	0.02
REACTOME	Reactome_cell_surface_interactions_at_the_vascular_wall	0.02
ENSG00000198838	RYR3 PPI subnetwork	0.02
MP:0001711	abnormal placenta morphology	0.02
GO:0014910	regulation of smooth muscle cell migration	0.02
ENSG00000104960	PTOV1 PPI subnetwork	0.02
GO:0001968	fibronectin binding	0.02

Original gene set ID	Original gene set description	DEPICT Nominal P-value
GO:0012502	induction of programmed cell death	0.02
ENSG00000100364	KIAA0930 PPI subnetwork	0.02
ENSG00000165410	CFL2 PPI subnetwork	0.02
MP:0004994	abnormal brain wave pattern	0.02
MP:0001552	increased circulating triglyceride level	0.02
ENSG00000116141	MARK1 PPI subnetwork	0.02
GO:0032403	protein complex binding	0.02
ENSG00000179364	PACS2 PPI subnetwork	0.02
MP:0001559	hyperglycemia	0.02
ENSG00000105851	PIK3CG PPI subnetwork	0.02
MP:0004031	insulinitis	0.02
MP:0010124	decreased bone mineral content	0.02
ENSG00000165197	FIGF PPI subnetwork	0.02
ENSG00000126561	STAT5A PPI subnetwork	0.02
ENSG00000136156	ITM2B PPI subnetwork	0.02
ENSG00000164327	RICTOR PPI subnetwork	0.02
ENSG00000159166	LAD1 PPI subnetwork	0.02
MP:0001716	abnormal placenta labyrinth morphology	0.02
MP:0002427	disproportionate dwarf	0.02
ENSG00000105371	ICAM4 PPI subnetwork	0.02
ENSG00000165476	REEP3 PPI subnetwork	0.02
GO:0046625	sphingolipid binding	0.02
MP:0000585	kinked tail	0.02
MP:0000889	abnormal cerebellar molecular layer	0.02
ENSG00000105699	LSR PPI subnetwork	0.02
GO:0005545	1-phosphatidylinositol binding	0.02
MP:0001134	absent corpus luteum	0.02
ENSG00000100097	LGALS1 PPI subnetwork	0.02
MP:0002079	increased circulating insulin level	0.02
ENSG00000150093	ITGB1 PPI subnetwork	0.02
GO:0001871	pattern binding	0.02
GO:0030247	polysaccharide binding	0.02
ENSG00000126934	MAP2K2 PPI subnetwork	0.02
ENSG00000110395	CBL PPI subnetwork	0.02
ENSG00000179151	EDC3 PPI subnetwork	0.02
ENSG00000154162	CDH12 PPI subnetwork	0.02
ENSG00000184363	PKP3 PPI subnetwork	0.02
ENSG00000020577	SAMD4A PPI subnetwork	0.02
MP:0004139	abnormal gastric parietal cell morphology	0.02
ENSG00000168476	REEP4 PPI subnetwork	0.02
ENSG00000110651	CD81 PPI subnetwork	0.02
ENSG00000134184	GSTM1 PPI subnetwork	0.02
ENSG00000105376	ICAM5 PPI subnetwork	0.02
ENSG00000196954	CASP4 PPI subnetwork	0.02
MP:0003704	abnormal hair follicle development	0.02
ENSG00000050820	BCAR1 PPI subnetwork	0.02
ENSG00000151748	SAV1 PPI subnetwork	0.02

Original gene set ID	Original gene set description	DEPICT Nominal P-value
GO:0003714	transcription corepressor activity	0.02
ENSG00000115904	SOS1 PPI subnetwork	0.02
ENSG00000175793	SFN PPI subnetwork	0.02
ENSG00000100345	MYH9 PPI subnetwork	0.02
GO:0035091	phosphatidylinositol binding	0.02
ENSG00000149930	TAOK2 PPI subnetwork	0.02
GO:0042054	histone methyltransferase activity	0.02
MP:0000689	abnormal spleen morphology	0.02
GO:0001892	embryonic placenta development	0.02
ENSG00000130294	KIF1A PPI subnetwork	0.02
ENSG00000148965	SAA4 PPI subnetwork	0.02
GO:0034774	secretory granule lumen	0.02
ENSG00000166483	WEE1 PPI subnetwork	0.02
ENSG00000110237	ARHGEF17 PPI subnetwork	0.02
GO:0032608	interferon-beta production	0.02
ENSG00000152518	ZFP36L2 PPI subnetwork	0.02
MP:0010792	abnormal stomach mucosa morphology	0.02
ENSG00000189319	FAM53B PPI subnetwork	0.02
ENSG00000117461	PIK3R3 PPI subnetwork	0.02
GO:0034362	low-density lipoprotein particle	0.02
ENSG00000134072	CAMK1 PPI subnetwork	0.02
ENSG00000163362	C1orf106 PPI subnetwork	0.02
MP:0002816	colitis	0.02
GO:0050900	leukocyte migration	0.03
GO:0044304	main axon	0.03
ENSG00000071909	MYO3B PPI subnetwork	0.03
ENSG00000100714	MTHFD1 PPI subnetwork	0.03
ENSG00000198836	OPA1 PPI subnetwork	0.03
ENSG00000197442	MAP3K5 PPI subnetwork	0.03
ENSG00000206306	HLA-DRB1 PPI subnetwork	0.03
ENSG00000206240	HLA-DRB1 PPI subnetwork	0.03
GO:0031983	vesicle lumen	0.03
KEGG	KEGG_regulation_of_actin_cytoskeleton	0.03
GO:0004713	protein tyrosine kinase activity	0.03
GO:0006953	acute-phase response	0.03
GO:0003712	transcription cofactor activity	0.03
MP:0000295	trabecula carnea hypoplasia	0.03
ENSG00000105647	PIK3R2 PPI subnetwork	0.03
GO:0060205	cytoplasmic membrane-bounded vesicle lumen	0.03
ENSG00000107566	ERLIN1 PPI subnetwork	0.03
ENSG00000114270	COL7A1 PPI subnetwork	0.03
ENSG00000135930	EIF4E2 PPI subnetwork	0.03
MP:0006413	increased T cell apoptosis	0.03
ENSG00000211949	ENSG00000211949 PPI subnetwork	0.03
ENSG00000125731	SH2D3A PPI subnetwork	0.03
MP:0000414	alopecia	0.03
ENSG00000160691	SHC1 PPI subnetwork	0.03

Original gene set ID	Original gene set description	DEPICT Nominal P-value
MP:0001282	short vibrissae	0.03
MP:0003996	clonic seizures	0.03
ENSG00000019991	HGF PPI subnetwork	0.03
MP:0010025	decreased total body fat amount	0.03
GO:0007568	aging	0.03
GO:0042809	vitamin D receptor binding	0.03
MP:0005331	insulin resistance	0.03
GO:0045682	regulation of epidermis development	0.03
MP:0001923	reduced female fertility	0.03
MP:0001219	thick epidermis	0.03
ENSG00000068615	REEP1 PPI subnetwork	0.03
ENSG00000171219	CDC42BPG PPI subnetwork	0.03
MP:0009583	increased keratinocyte proliferation	0.03
ENSG00000105810	CDK6 PPI subnetwork	0.03
ENSG00000105662	CRTC1 PPI subnetwork	0.03
MP:0003957	abnormal nitric oxide homeostasis	0.03
KEGG	KEGG_small_cell_lung_cancer	0.03
GO:0030669	clathrin-coated endocytic vesicle membrane	0.03
ENSG00000100030	MAPK1 PPI subnetwork	0.03
GO:0046328	regulation of JNK cascade	0.03
GO:0014070	response to organic cyclic compound	0.03
GO:0033500	carbohydrate homeostasis	0.03
GO:0042593	glucose homeostasis	0.03
REACTOME	Reactome_ptm_gamma_carboxylation_hypusine_formation_and_arylsulfatase_activation	0.03
REACTOME	Reactome_regulation_of_signaling_by_cbl	0.03
MP:0002418	increased susceptibility to viral infection	0.03
MP:0003721	increased tumor growth/size	0.03
GO:0071845	cellular component disassembly at cellular level	0.03
GO:0030518	intracellular steroid hormone receptor signaling pathway	0.03
ENSG00000116824	CD2 PPI subnetwork	0.03
MP:0003566	abnormal cell adhesion	0.03
GO:0034061	DNA polymerase activity	0.03
ENSG00000141968	VAV1 PPI subnetwork	0.03
GO:0001701	in utero embryonic development	0.03
MP:0000166	abnormal chondrocyte morphology	0.03
MP:0003400	kinked neural tube	0.03
GO:0000790	nuclear chromatin	0.03
ENSG00000197102	DYNC1H1 PPI subnetwork	0.03
GO:0043566	structure-specific DNA binding	0.03
ENSG00000075413	MARK3 PPI subnetwork	0.03
GO:0000271	polysaccharide biosynthetic process	0.03
REACTOME	Reactome_cell:cell_communication	0.03
MP:0000410	waved hair	0.03
ENSG00000154556	SORBS2 PPI subnetwork	0.03
ENSG00000104368	PLAT PPI subnetwork	0.03
GO:0043123	positive regulation of I-kappaB kinase/NF-kappaB cascade	0.03
ENSG00000156127	BATF PPI subnetwork	0.03

Original gene set ID	Original gene set description	DEPICT Nominal P-value
ENSG00000132470	ITGB4 PPI subnetwork	0.03
GO:0038024	cargo receptor activity	0.03
ENSG00000100014	SPECC1L PPI subnetwork	0.03
ENSG00000163083	INHBB PPI subnetwork	0.03
ENSG00000110931	CAMKK2 PPI subnetwork	0.03
MP:0002088	abnormal embryonic growth/weight/body size	0.03
GO:0016571	histone methylation	0.03
GO:0033559	unsaturated fatty acid metabolic process	0.03
MP:0005350	increased susceptibility to autoimmune disorder	0.03
ENSG00000136111	TBC1D4 PPI subnetwork	0.03
REACTOME	Reactome_nephrin_interactions	0.03
ENSG00000182195	LDOC1 PPI subnetwork	0.03
ENSG00000123685	BATF3 PPI subnetwork	0.03
ENSG00000215699	ENSG00000215699 PPI subnetwork	0.03
GO:0005720	nuclear heterochromatin	0.03
ENSG00000092969	TGFB2 PPI subnetwork	0.03
KEGG	KEGG_ECM_receptor_interaction	0.03
MP:0001201	translucent skin	0.03
GO:0016278	lysine N-methyltransferase activity	0.03
GO:0016279	protein-lysine N-methyltransferase activity	0.03
ENSG00000196586	MYO6 PPI subnetwork	0.03
GO:0004702	receptor signaling protein serine/threonine kinase activity	0.03
ENSG00000072518	MARK2 PPI subnetwork	0.03
ENSG00000165025	SYK PPI subnetwork	0.03
MP:0002109	abnormal limb morphology	0.03
ENSG00000157764	BRAF PPI subnetwork	0.03
ENSG00000152256	PDK1 PPI subnetwork	0.03
ENSG00000065618	COL17A1 PPI subnetwork	0.04
ENSG00000169220	RGS14 PPI subnetwork	0.04
ENSG00000100311	PDGFB PPI subnetwork	0.04
ENSG00000134202	GSTM3 PPI subnetwork	0.04
ENSG00000142515	KLK3 PPI subnetwork	0.04
MP:0002619	abnormal lymphocyte morphology	0.04
ENSG00000161395	PGAP3 PPI subnetwork	0.04
ENSG00000145431	PDGFC PPI subnetwork	0.04
ENSG00000170962	PDGFD PPI subnetwork	0.04
ENSG00000153879	CEBPG PPI subnetwork	0.04
ENSG00000077380	DYNC1I2 PPI subnetwork	0.04
ENSG00000197122	SRC PPI subnetwork	0.04
MP:0004399	abnormal cochlear outer hair cell morphology	0.04
ENSG00000174996	KLC2 PPI subnetwork	0.04
MP:0002376	abnormal dendritic cell physiology	0.04
MP:0000709	enlarged thymus	0.04
MP:0008706	decreased interleukin-6 secretion	0.04
MP:0004686	decreased length of long bones	0.04
GO:0050810	regulation of steroid biosynthetic process	0.04
ENSG00000138396	ENSG00000138396 PPI subnetwork	0.04

Original gene set ID	Original gene set description	DEPICT Nominal P-value
ENSG00000148400	NOTCH1 PPI subnetwork	0.04
ENSG00000137171	KLC4 PPI subnetwork	0.04
ENSG00000196396	PTPN1 PPI subnetwork	0.04
ENSG00000148672	GLUD1 PPI subnetwork	0.04
GO:0000975	regulatory region DNA binding	0.04
GO:0001067	regulatory region nucleic acid binding	0.04
GO:0022411	cellular component disassembly	0.04
ENSG00000026025	VIM PPI subnetwork	0.04
ENSG00000061273	HDAC7 PPI subnetwork	0.04
ENSG00000104067	TJP1 PPI subnetwork	0.04
MP:0004813	absent linear vestibular evoked potential	0.04
ENSG00000091136	LAMB1 PPI subnetwork	0.04
KEGG	KEGG_renal_cell_carcinoma	0.04
KEGG	KEGG_focal_adhesion	0.04
GO:0031581	hemidesmosome assembly	0.04
ENSG00000141068	KSR1 PPI subnetwork	0.04
MP:0004214	abnormal long bone diaphysis morphology	0.04
ENSG00000123836	PFKFB2 PPI subnetwork	0.04
ENSG00000168090	COPS6 PPI subnetwork	0.04
ENSG00000132356	PRKAA1 PPI subnetwork	0.04
GO:0031093	platelet alpha granule lumen	0.04
GO:0048545	response to steroid hormone stimulus	0.04
MP:0003109	short femur	0.04
ENSG00000113758	DBN1 PPI subnetwork	0.04
GO:0008276	protein methyltransferase activity	0.04
MP:0003383	abnormal gluconeogenesis	0.04
ENSG00000162614	NEXN PPI subnetwork	0.04
ENSG00000162614	NEXN PPI subnetwork	0.04
ENSG00000169641	LUZP1 PPI subnetwork	0.04
MP:0002152	abnormal brain morphology	0.04
ENSG00000204257	HLA-DMA PPI subnetwork	0.04
ENSG00000206229	ENSG00000206229 PPI subnetwork	0.04
ENSG00000206293	ENSG00000206293 PPI subnetwork	0.04
ENSG00000138439	FAM117B PPI subnetwork	0.04
GO:0006636	unsaturated fatty acid biosynthetic process	0.04
ENSG00000176444	CLK2 PPI subnetwork	0.04
MP:0000703	abnormal thymus morphology	0.04
REACTOME	Reactome_zinc_transporters	0.04
ENSG00000125952	MAX PPI subnetwork	0.04
GO:0046456	icosanoid biosynthetic process	0.04
ENSG00000132964	CDK8 PPI subnetwork	0.04
MP:0008688	decreased interleukin-2 secretion	0.04
ENSG00000196218	RYR1 PPI subnetwork	0.04
MP:0004770	abnormal synaptic vesicle recycling	0.04
ENSG00000121879	PIK3CA PPI subnetwork	0.04
ENSG00000196735	HLA-DQA1 PPI subnetwork	0.04
MP:0009355	increased liver triglyceride level	0.04

Original gene set ID	Original gene set description	DEPICT Nominal P-value
MP:0009399	increased skeletal muscle fiber size	0.04
ENSG00000160678	S100A1 PPI subnetwork	0.04
ENSG00000064999	ANKS1A PPI subnetwork	0.04
ENSG00000173327	MAP3K11 PPI subnetwork	0.04
GO:0051183	vitamin transporter activity	0.04
GO:0006690	icosanoid metabolic process	0.04
ENSG00000134363	FST PPI subnetwork	0.04
GO:0060053	neurofilament cytoskeleton	0.04
ENSG00000151914	DST PPI subnetwork	0.04
ENSG00000189079	ARID2 PPI subnetwork	0.04
ENSG00000065559	MAP2K4 PPI subnetwork	0.05
ENSG00000120709	FAM53C PPI subnetwork	0.05
MP:0002110	abnormal digit morphology	0.05
GO:0005976	polysaccharide metabolic process	0.05
ENSG00000054523	KIF1B PPI subnetwork	0.05
ENSG00000100906	NFKBIA PPI subnetwork	0.05
ENSG00000136518	ACTL6A PPI subnetwork	0.05
GO:0004709	MAP kinase kinase kinase activity	0.05
GO:0060711	labyrinthine layer development	0.05
KEGG_	KEGG_circadian_rhythm_mammal	0.05
REACTOME	Reactome_classical_antibody:mediated_complement_activation	0.05
ENSG00000211979	ENSG00000211979 PPI subnetwork	0.05
ENSG00000211973	ENSG00000211973 PPI subnetwork	0.05
ENSG00000172534	HCFC1 PPI subnetwork	0.05
ENSG00000136270	TBRG4 PPI subnetwork	0.05
GO:0032648	regulation of interferon-beta production	0.05
GO:0034375	high-density lipoprotein particle remodeling	0.05
ENSG00000185811	IKZF1 PPI subnetwork	0.05
ENSG00000198802	ENSG00000198802 PPI subnetwork	0.05
MP:0006262	testis tumor	0.05
ENSG00000171992	SYNPO PPI subnetwork	0.05
ENSG00000213341	CHUK PPI subnetwork	0.05
ENSG00000175197	DDIT3 PPI subnetwork	0.05
MP:0005150	cachexia	0.05
GO:0043122	regulation of I-kappaB kinase/NF-kappaB cascade	0.05
GO:0097006	regulation of plasma lipoprotein particle levels	0.05
ENSG00000162772	ATF3 PPI subnetwork	0.05
GO:0000122	negative regulation of transcription from RNA polymerase II promoter	0.05
GO:0005858	axonemal dynein complex	0.05
ENSG00000051382	PIK3CB PPI subnetwork	0.05
GO:0043405	regulation of MAP kinase activity	0.05
MP:0008722	abnormal chemokine secretion	0.05
KEGG	KEGG_chronic_myeloid_leukemia	0.05
REACTOME	Reactome_regulated_PROTEOLYSIS_OF_P75NTR	0.05
GO:0043588	skin development	0.05
GO:0010627	regulation of intracellular protein kinase cascade	0.05
GO:0044212	transcription regulatory region DNA binding	0.05

Original gene set ID	Original gene set description	DEPICT Nominal P-value
GO:0030027	lamellipodium	0.05
ENSG00000105976	MET PPI subnetwork	0.05
MP:0002792	abnormal retinal vasculature morphology	0.05
MP:0000069	kyphoscoliosis	0.05
GO:0034339	regulation of transcription from RNA polymerase II promoter by nuclear hormone receptor	0.05
ENSG00000141551	CSNK1D PPI subnetwork	0.05
MP:0005108	abnormal ulna morphology	0.05
MP:0002419	abnormal innate immunity	0.05
GO:0016757	transferase activity, transferring glycosyl groups	0.05
ENSG00000161800	RACGAP1 PPI subnetwork	0.05
MP:0006387	abnormal T cell number	0.05
GO:0005089	Rho guanyl-nucleotide exchange factor activity	0.05
ENSG00000117984	CTSD PPI subnetwork	0.05
ENSG00000105971	CAV2 PPI subnetwork	0.05
ENSG00000115085	ZAP70 PPI subnetwork	0.05
MP:0004609	vertebral fusion	0.05
ENSG00000135862	LAMC1 PPI subnetwork	0.05
MP:0003449	abnormal intestinal goblet cell morphology	0.05
MP:0002687	oligozoospermia	0.05
MP:0000714	increased thymocyte number	0.05
ENSG00000133030	MPRIIP PPI subnetwork	0.05
ENSG00000079841	RIMS1 PPI subnetwork	0.05
ENSG00000130638	ATXN10 PPI subnetwork	0.05
MP:0002656	abnormal keratinocyte differentiation	0.05
ENSG00000129691	ASH2L PPI subnetwork	0.05
MP:0002650	abnormal ameloblast morphology	0.05
ENSG00000135503	ACVR1B PPI subnetwork	0.05
GO:0004715	non-membrane spanning protein tyrosine kinase activity	0.05
ENSG00000001497	LAS1L PPI subnetwork	0.05
GO:0018024	histone-lysine N-methyltransferase activity	0.05
GO:0000792	heterochromatin	0.05
ENSG00000111961	SASH1 PPI subnetwork	0.05
MP:0008840	abnormal spike wave discharge	0.05
ENSG00000139514	SLC7A1 PPI subnetwork	0.05
GO:0007249	I-kappaB kinase/NF-kappaB cascade	0.05

Functional effects of SNPs at AAA loci

1: Expression SNP database lookup (Online Table XIX)

Evidence for functional effects of AAA associated SNPs/loci was sought in two eQTL datasets curated by Andrew Johnson at the NIH National Heart Lung and Blood Institute, Framingham, USA. Firstly, index and proxy SNPs were queried in a collected database of expression SNP (eSNP) results. The collected eSNP results met criteria for statistical thresholds for association with gene transcript levels as described in the original papers. A general overview of a subset of >50 eQTL studies has been published¹⁰⁹, with specific citations for >100 studies included in the current query following here:

Blood cell related eQTL studies included fresh lymphocytes¹¹⁰, fresh leukocytes¹¹¹, leukocyte samples in individuals with Celiac disease¹¹², whole blood samples¹¹³⁻¹²⁶, lymphoblastoid cell lines (LCL) derived from asthmatic children^{127, 128}, HapMap LCL from 3 populations¹²⁹, a separate study on HapMap CEU LCL¹³⁰, additional LCL population samples¹³¹⁻¹³⁶, CD19⁺ B cells¹³⁷, primary PHA-stimulated T cells^{133, 135}, CD4⁺ T cells¹³⁸, peripheral blood monocytes^{137, 139, 140} and CD14⁺ monocytes before and after stimulation with LPS or interferon-gamma¹⁴¹, CD11⁺ dendritic cells before and after *Mycobacterium tuberculosis* infection¹⁴² and a separate study of dendritic cells before or after stimulation with LPS, influenza or interferon-beta¹⁴³. Micro-RNA QTLs¹⁴⁴ and DNase-I QTLs¹⁴⁵ were also queried for LCL.

Non-blood cell tissue eQTLs searched included omental and subcutaneous adipose^{115, 134, 146, 147}, stomach¹⁴⁷, endometrial carcinomas¹⁴⁸, ER+ and ER- breast cancer tumor cells¹⁴⁹, liver^{147, 150-153}, osteoblasts¹⁵⁴, intestine¹⁵⁵ and normal and cancerous colon¹⁵⁶, skeletal muscle¹⁵⁷, breast tissue (normal and cancer)^{158, 159}, lung^{146, 160, 161}, skin^{134, 146, 162}, primary fibroblasts^{133, 135, 163}, sputum¹⁶⁴, pancreatic islet cells¹⁶⁵ and heart tissue from left ventricles^{146, 166} and left and right atria¹⁶⁷. Micro-RNA QTLs were also queried for gluteal and abdominal adipose¹⁶⁸ and liver¹⁶⁹. Further mRNA and micro-RNA QTLs were queried from ER+ invasive breast cancer samples, colon-, kidney renal clear-, lung- and prostate-adenocarcinoma samples¹⁷⁰.

Brain eQTL studies included brain cortex^{139, 171, 172}, cerebellar cortex¹⁷³, cerebellum^{172, 174-177}, frontal cortex^{173, 175, 176}, gliomas¹⁷⁸, hippocampus^{173, 176}, inferior olivary nucleus (from medulla)¹⁷³, intralobular white matter¹⁷³, occipital cortex¹⁷³, parietal lobe¹⁷⁴, pons¹⁷⁵, pre-frontal cortex^{176, 177, 179, 180}, putamen (at the level of anterior commissure)¹⁷³, substantia nigra¹⁷³, temporal cortex^{172, 173, 175, 176}, thalamus¹⁷⁶ and visual cortex¹⁷⁷.

Secondly, additional eQTL data were integrated from online sources including ScanDB, the Broad Institute GTex browser, and the Pritchard Lab (eqtl.uchicago.edu). Cerebellum, parietal lobe and liver eQTL data was downloaded from ScanDB and cis-eQTLs were limited to those with $P < 1.0 \times 10^{-6}$ and trans-eQTLs with $P < 5.0 \times 10^{-8}$. The top 1000 eQTL results were downloaded from the GTex Browser at the Broad Institute for 9 tissues on 11/26/2013: thyroid, leg skin (sun exposed), tibial nerve, tibial artery, skeletal muscle, lung, heart (left ventricle), whole blood, and subcutaneous adipose¹⁴⁶. All GTex results had associations with $P < 8.4 \times 10^{-7}$.

2: eQTL lookup in the Advanced Study of Aortic Pathology (Online Table XX and Online Figure III)

eQTL data were obtained from the Advanced Study of Aortic Pathology (ASAP) dataset which has previously been described¹⁸¹. Tissue samples were selected from individuals undergoing aortic valve surgery. Five tissue types were collected from each patient: mammary artery, liver, aorta intima-media, aorta adventitia, and heart. RNA was extracted from tissues and hybridised to Affymetrix ST 1.0 exon arrays (Santa Clara, CA, USA) and data were robust multiarray average normalised before log₂ transformation. DNA extracted from whole blood was genotyped on the Illumina 610w-Quad

bead array (San Diego, CA, USA) platform. SNPs with >95% call rate were used for imputation, and imputed SNPs with quality scores of MACH <0.3 were excluded from analysis. An additive model for associations between SNPs and gene expression was assumed. Genotypes for 5 of the 10 lead SNPs at AAA risk loci were directly genotyped on Illumina 610wQuad arrays.

3: RNA-seq (Online Table XXI)

RNA-seq data were obtained from the Stockholm-Tartu Atherosclerosis Reverse Network Engineering Task (STARNET) database¹⁸² (<http://www.mountsinai.org/profiles/johan-bjorkegren>). These consist of RNA-seq data from 9 cardiovascular tissues from up to 600 CAD patients obtained during coronary artery by-pass grafting surgery. Gene expression was measured with a standard RNA-seq protocol, followed by normalization of raw read counts to adjust for library size and batch effects. Adjusted read counts were subsequently log₂-transformed, and the association between genotype and expression was tested using a linear model. Permutation was used to assess the statistical significance. Significant results for the lead SNPs at each AAA risk locus are shown in **Online Table XX**.

4: Peripheral blood monocyte eQTL analysis (Online Table XXII)

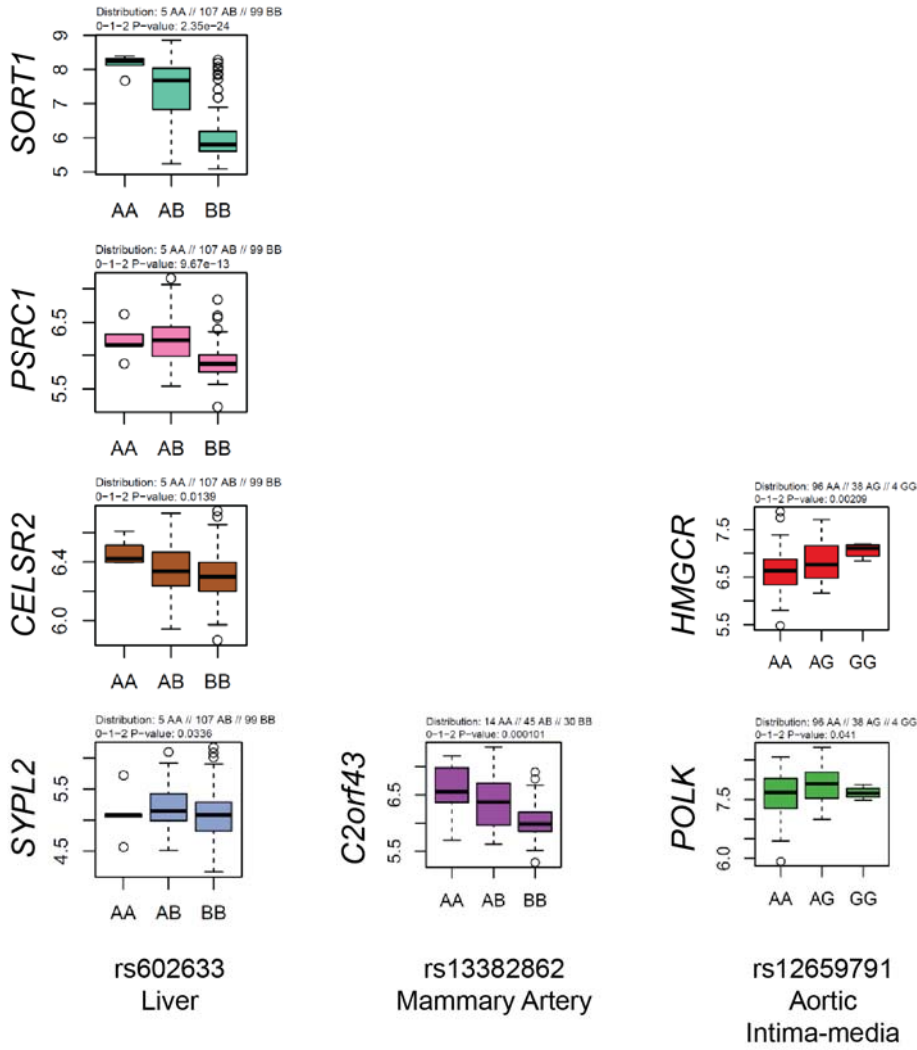
Data from an eQTL analysis of peripheral blood monocytes was obtained from the Cardiogenics Consortium^{183, 184}. The description of the cohort sample collection and processing and the eQTL analysis have previously been described in detail. Briefly, genome-wide expression and genotype data were obtained from peripheral blood monocytes from 363 patients with CAD or myocardial infarction and 395 healthy individuals. Expression profiling was performed using the Illumina HumanRef-8 v3 beadchip array (Illumina Inc., San Diego, CA) containing 24,516 probes corresponding to 18,311 distinct genes and 21,793 Ref Seq annotated transcripts. Genome-wide genotyping was carried out using two Illumina arrays, the Sentrix Human Custom 1.2M array and the Human 610 Quad Custom array. SNP analysis was restricted to autosomal SNPs with MAF >0.01, call rate >0.95 and HWE testing $P > 1 \times 10^{-5}$. After quality control, 522,603 SNPs were used for association analyses with expression. All replicated AAA associated SNPs were tested for association with regional gene expression. Significant results are shown in **Online Table XXII**.

Online Table XIX: eQTL data (1). This table spans 2 pages.

Locus	Lead AAA SNP	Gene	Tissue	Transcript	Proxy SNP looked up in eQTL database			Peak regional SNP in eQTL database					
					Proxy SNP	r2 to AAA SNP	eQTL P-Value for lead AAA SNP or proxy	Peak SNP	r2 (Peak SNP to AAA SNP)	eQTL P-Value for peak SNP			
1q21.3	rs4129267	IL6R	Average in 10 brain regions [PMID 25174004]	INTS3	rs4576655	1	5.59x10 ⁻⁰⁶	rs12068901	NA	3.32x10 ⁻⁴²			
			Average in 10 brain regions [PMID 25174004]	SLC39A1	rs4845372	0.965	4.75x10 ⁻⁰⁶	rs4845372	0.965	4.75x10 ⁻⁰⁶			
			Average in 10 brain regions [PMID 25174004]	PYGO2	rs6684439	0.839	2.96x10 ⁻⁰⁶	rs6684439	0.839	2.96x10 ⁻⁰⁶			
			CD14+ monocytes (untreated) [PMID 24604202]	IL6R			6.64x10 ⁻⁰⁴	rs7518199	0.965	5.27x10 ⁻⁰⁴			
			Intestine (normal ileum) [PMID 23474282]	IL6R			8.81x10 ⁻⁰⁶	rs7553796	0.49	8.20x10 ⁻¹¹			
			Lymph [PMID 17873875]	IL6R	rs4537545	1	2.63x10 ⁻⁰³	rs4845623	0.965	1.88x10 ⁻⁰³			
			Prefrontal cortex (all samples) [PMID 23622250]	MUC1	rs8192284	0.982	6.33x10 ⁻⁰⁵	rs8192284	0.982	6.33x10 ⁻⁰⁵			
			Whole blood (Battle) [PMID 24092820]	IL6R	rs4537545	1	2.62x10 ⁻²⁰	rs4537545	1	2.62x10 ⁻²⁰			
			Whole blood (CHARGE) [PMID 24013639]	IL6R			3.15x10 ⁻²⁷	rs4537545	1	2.02x10 ⁻²⁹			
			Whole blood (CHARGE) [PMID 24013639]	UBE2Q1			9.75x10 ⁻⁰⁸	rs6660775	0.058	3.93x10 ⁻²¹			
			1p13.3	rs602633	CELSR2/SORT1	CD14+ monocytes (24h LPS stimulated) [PMID 24604202]	PSRC1	rs599839	1	9.50x10 ⁻⁰⁵	rs646776	0.895	3.53x10 ⁻⁰⁵
						CD14+ monocytes (IFNg stimulated) [PMID 24604202]	PSRC1	rs599839	1	4.25x10 ⁻¹³	rs646776	0.895	7.40x10 ⁻¹⁴
						CD14+ monocytes (untreated) [PMID 24604202]	PSRC1	rs599839	1	7.31x10 ⁻⁴⁴	rs599839	1	7.31x10 ⁻⁴⁴
						Cerebellum (all samples) [PMID 23622250]	PSRC1			9.12x10 ⁻⁰⁶	rs602633	Same SNP	9.12x10 ⁻⁰⁶
Cerebellum (Huntington's) [PMID 23622250]	PSRC1	rs646776				0.895	5.19x10 ⁻⁰⁵	rs646776	0.895	5.19x10 ⁻⁰⁵			
Liver (ScanDB)	SORT1	rs646776				0.895	3.18x10 ⁻⁴³	rs646776	0.895	3.18x10 ⁻⁴³			
Liver (ScanDB)	PSRC1	rs646776				0.895	2.92x10 ⁻³⁷	rs646776	0.895	2.92x10 ⁻³⁷			
Liver (ScanDB)	CELSR2	rs646776				0.895	4.48x10 ⁻²⁴	rs646776	0.895	4.48x10 ⁻²⁴			
Liver (Greenawalt) [PMID 21602305]	SORT1	rs646776				0.895	5.20x10 ⁻⁸⁸	rs646776	0.895	5.20x10 ⁻⁸⁸			
Liver (Greenawalt) [PMID 21602305]	PSRC1	rs646776				0.895	3.05x10 ⁻⁸⁶	rs646776	0.895	3.05x10 ⁻⁸⁶			
Liver (Greenawalt) [PMID 21602305]	CELSR2	rs646776				0.895	6.27x10 ⁻⁶⁸	rs646776	0.895	6.27x10 ⁻⁶⁸			
Liver (Schroder) [PMID 22006096]	SORT1	rs646776				0.895	2.14x10 ⁻²⁷	rs646776	0.895	2.14x10 ⁻²⁷			
Liver (Schroder) [PMID 22006096]	CELSR2	rs646776				0.895	3.66x10 ⁻²²	rs646776	0.895	3.66x10 ⁻²²			
Liver (Schroder) [PMID 22006096]	PSRC1	rs646776				0.895	8.72x10 ⁻¹⁷	rs646776	0.895	8.72x10 ⁻¹⁷			
Liver (UChicago) [PMID 21637794]	CELSR2	rs12740374				0.895	<1x10 ⁻¹⁶	rs12740374	0.895	<1e ⁻¹⁶			
Liver (UChicago) [PMID 21637794]	SORT1	rs12740374				0.895	<1x10 ⁻¹⁶	rs12740374	0.895	<1e ⁻¹⁶			
Liver (UWash) [PMID 21637794]	SORT1	rs12740374				0.895	2.86x10 ⁻²²	rs12740374	0.895	2.86x10 ⁻²²			
Liver (UWash) [PMID 21637794]	CELSR2	rs12740374				0.895	5.31x10 ⁻¹¹	rs12740374	0.895	5.31x10 ⁻¹¹			
Lymph [PMID 17873875]	PSRC1	rs646776				0.895	2.10x10 ⁻⁰⁸	rs646776	0.895	2.10x10 ⁻⁰⁸			
Monocytes (CD14+) [PMID 22446964]	PSRC1	rs599839				1	6.65x10 ⁻¹⁸	rs599839	1	6.65x10 ⁻¹⁸			
Monocytes [PMID 20502693]	PSRC1	rs599839				1	5.30x10 ⁻⁵⁵	rs629301	0.895	2.34x10 ⁻⁵⁶			
Muscle_Skeletal [PMID 23715323]	CELSR2	rs12740374				0.895	1.40x10 ⁻⁰⁸	rs12740374	0.895	1.40x10 ⁻⁰⁸			
Prefrontal cortex (all samples) [PMID 23622250]	CELSR2	rs646776				0.895	4.10x10 ⁻¹⁰	rs646776	0.895	4.10x10 ⁻¹⁰			
Prefrontal cortex (all samples) [PMID 23622250]	PSRC1	rs646776				0.895	1.67x10 ⁻⁰⁹	rs646776	0.895	1.67x10 ⁻⁰⁹			
Prefrontal cortex (Alzheimer's) [PMID 23622250]	PSRC1	rs646776				0.895	7.93x10 ⁻⁰⁸	rs646776	0.895	7.93x10 ⁻⁰⁸			
Prefrontal cortex (Alzheimer's) [PMID 23622250]	CELSR2	rs646776				0.895	3.24x10 ⁻⁰⁵	rs646776	0.895	3.24x10 ⁻⁰⁵			
Prefrontal cortex (Huntington's) [PMID 23622250]	CELSR2						1.52x10 ⁻⁰⁶	rs602633	Same SNP	1.52x10 ⁻⁰⁶			
PrefrontalCortex [PMID 20351726]	PSRC1	rs599839				1	2.62x10 ⁻⁰⁶	rs599839	1	2.62x10 ⁻⁰⁶			
SchadtLiver [PMID 18462017]	SORT1	rs599839				1	1.52x10 ⁻⁵⁶	rs599839	1	1.52x10 ⁻⁵⁶			
SchadtLiver [PMID 18462017]	CELSR2	rs646776				0.895	3.09x10 ⁻²⁴	rs646776	0.895	3.09x10 ⁻²⁴			
SubCutAdipose (Greenawalt) [PMID 21602305]	CELSR2			2.93x10 ⁻⁰⁸	rs602633	Same SNP	2.93x10 ⁻⁰⁸						

			Visual cortex (all samples) [PMID 23622250]	<i>PSRC1</i>	rs646776	0.895	7.66x10 ⁻¹¹	rs646776	0.895	7.66x10 ⁻¹¹
			Visual cortex (Alzheimer's) [PMID 23622250]	<i>PSRC1</i>	rs646776	0.895	1.44x10 ⁻⁰⁹	rs646776	0.895	1.44x10 ⁻⁰⁹
			Whole blood (Battle) [PMID 24092820]	<i>PSRC1</i>	rs599839	1	4.93x10 ⁻⁸⁷	rs599839	1	4.93x10 ⁻⁸⁷
			Whole blood (Schramm et al.) [PMID 24740359]	<i>PSRC1</i>	rs599839	1	1.23x10 ⁻²⁴	rs599839	1	1.23x10 ⁻²⁴
			Whole blood (Wright, n=4,647) [PMID 24728292]	<i>CELSR2</i>	rs629301	0.895	6.73x10 ⁻¹⁸	rs629301	0.895	6.73x10 ⁻¹⁸
9p21	rs10757274	<i>ANRIL</i>	SubCutAdipose(Greenawalt) [PMID 21602305]	<i>CDKN2B</i>	rs1537370	0.901	1.48x10 ⁻⁰⁴	rs1537370	Same SNP	1.48x10 ⁻⁰⁴
			Omental adipose [PMID 21602305]	<i>CDKN2B</i>	rs2383207	0.846	3.10x10 ⁻⁰⁷	rs2383207	Same SNP	3.10x10 ⁻⁰⁷
9q33.2	rs10985349	<i>DAB2IP</i>	CD14+ monocytes (2h LPS stimulated) [PMID 24604202]	<i>GGTA1</i>			6.64x10 ⁻⁰⁴	rs10985349	Same SNP	6.64x10 ⁻⁰⁴
20q13.12	rs3827066	Near <i>PCIF1/MMP9/ZNF335</i>	Bcells (CD19+) [PMID 22446964]	<i>PLTP</i>			2.98x10 ⁻⁰⁹	rs394643	0.229	9.89x10 ⁻⁴⁰
			CD14+ monocytes (24h LPS stimulated) [PMID 24604202]	<i>PLTP</i>			2.46x10 ⁻¹¹	rs3827066	Same SNP	2.46x10 ⁻¹¹
			CD14+ monocytes (24h LPS stimulated) [PMID 24604202]	<i>DNTTIP1</i>			8.41x10 ⁻⁰⁹	rs2664529	0.108	1.02x10 ⁻⁶³
			CD14+ monocytes (2h LPS stimulated) [PMID 24604202]	<i>PLTP</i>			3.89x10 ⁻¹¹	rs3843763	0.506	2.46x10 ⁻¹³
			CD14+ monocytes (2h LPS stimulated) [PMID 24604202]	<i>DNTTIP1</i>			9.56x10 ⁻¹⁰	rs2664529	0.108	1.60x10 ⁻⁶³
			CD14+ monocytes (IFNg stimulated) [PMID 24604202]	<i>PLTP</i>			2.20x10 ⁻⁴³	rs3827066	Same SNP	2.20x10 ⁻⁴³
			CD14+ monocytes (IFNg stimulated) [PMID 24604202]	<i>DNTTIP1</i>			2.68x10 ⁻¹⁰	rs6032531	0.148	8.85x10 ⁻⁷⁶
			CD14+ monocytes (IFNg stimulated) [PMID 24604202]	<i>PLTP</i>			8.25x10 ⁻⁰⁷	rs3827066	Same SNP	2.20x10 ⁻⁴³
			CD14+ monocytes (untreated) [PMID 24604202]	<i>DNTTIP1</i>			3.69x10 ⁻⁰⁹	rs6032531	0.148	1.11x10 ⁻⁴⁹
			CD14+ monocytes (untreated) [PMID 24604202]	<i>CD40</i>			4.03x10 ⁻⁰⁴	rs745307	0.086	4.24x10 ⁻⁸⁸
			LCL (MuTHER) [PMID 22941192]	<i>PLTP</i>			1.20x10 ⁻⁰⁶	rs441346	0.214	1.64x10 ⁻³⁷
			Liver(UChicago) [PMID 21637794]	<i>NEURL2</i>			2.29x10 ⁻⁰⁶	rs3827066	Same SNP	2.29x10 ⁻⁰⁶
			Liver(UChicago) [PMID 21637794]	<i>C20orf165</i>	rs7270354	1	1.22x10 ⁻⁰³	rs7270354	1	1.22x10 ⁻⁰³
			Liver(UWash) [PMID 21637794]	<i>NEURL2</i>			1.02x10 ⁻⁰³	rs3827066	Same SNP	1.02x10 ⁻⁰³
			Peripheral artery plaque [PMID 24973796]	<i>NEURL2</i>	rs7270354	1	2.51x10 ⁻⁰⁸	rs7270354	1	2.51x10 ⁻⁰⁸
			Skin (MuTHER) [PMID 22941192]	<i>WFDC3</i>			2.60x10 ⁻¹²	rs2664529	0.108	5.47x10 ⁻⁷⁴
			Subc adipose (MuTHER) [PMID 22941192]	<i>PLTP</i>			6.67x10 ⁻¹¹	rs6104410	0.486	2.62x10 ⁻¹¹
			Subc adipose (MuTHER) [PMID 22941192]	<i>NEURL2</i>			9.51x10 ⁻⁰⁹	rs3827066	Same SNP	9.51x10 ⁻⁰⁹
			Subc adipose (MuTHER) [PMID 22941192]	<i>WFDC3</i>			1.26x10 ⁻⁰⁵	rs6032544	0.11	5.99x10 ⁻³⁶
			Whole blood (CHARGE) [PMID 24013639]	<i>TNNC2</i>			3.98x10 ⁻¹⁹	rs6104350	0.11	3.33x10 ⁻⁶³
			Whole blood (CHARGE) [PMID 24013639]	<i>DNTTIP1</i>			2.52x10 ⁻¹⁴	rs6104350	0.11	7.89x10 ⁻⁷¹

Online Figure III: Significant eQTL plots for data from ASAP study. Each column of plots represents data for the SNP and tissue stated at the bottom of each column. The gene for which expression has been assessed in each plot is shown to the left of each plot.



Online Table XXI: eQTL results based on RNA seq data

Chr	Position	SNP	Locus	Gene(s)	Tissue	gene for RNA-Seq	index SNP	index SNP beta	index SNP P	Lead SNP in region	Lead SNP beta	Lead SNP P	index SNP effect independent
1	109821511	rs602633	1p13.3	CELSR2/ <i>SORT1</i>	Blood	<i>PSRC1</i>	rs602633	0.640465606	4.49x10 ⁻¹⁷	rs629301	0.61412198	1.03x10 ⁻¹⁵	Yes
					LIV	<i>PSRC1</i>	rs602633	-1.292449889	9.43x10 ⁻¹⁰	rs7528419	1.26797503	4.33x10 ⁻¹⁰³	Yes
					LIV	<i>SARS</i>	rs602633	0.495537791	2.37x10 ⁻¹²	rs1277930	0.49333558	2.97x10 ⁻¹²	Yes
					LIV	<i>SORT1</i>	rs602633	-1.365654087	2.98x10 ⁻¹³	rs7528419	1.33525433	1.79x10 ⁻¹²²	Yes
					LIV	<i>CELSR2</i>	rs602633	1.298741331	1.79x10 ⁻¹⁰	rs629301	1.27447629	8.75x10 ⁻¹⁰⁵	Yes
1	154426264	rs4129267	1q21.3	<i>IL6R</i>	MAM	<i>IL6R</i>	rs4129267	0.652344491	1.97x10 ⁻²⁶	rs7518199	0.63498045	3.78x10 ⁻²⁴	Yes
13	22861921	rs9316871	13q12.11	<i>LINC00540</i>	MAM	<i>FGF9</i>	rs9316871	-0.699526462	1.76x10 ⁻²³	rs9506822	-0.7027035	2.44x10 ⁻²³	Yes
20	44586023	rs3827066	20q13.12	Near <i>PCIF1/MMP9/ZNF335</i>	AOR	<i>PLTP</i>	rs3827066	-0.756619944	1.65x10 ⁻²¹	rs7267295	-0.7193854	5.40x10 ⁻¹⁸	Yes
					SF	<i>PLTP</i>	rs3827066	-0.905646216	4.93x10 ⁻²⁹	rs7270354	-0.8474133	2.10x10 ⁻²⁶	Yes
					SKLM	<i>PLTP</i>	rs3827066	-0.484882963	2.76x10 ⁻²⁹	rs7267295	-0.4860579	1.40x10 ⁻⁰⁸	Yes
					VAF	<i>PLTP</i>	rs3827066	-0.610415837	1.39x10 ⁻¹²	rs8124182	-0.5513566	1.48x10 ⁻¹⁰	Yes
					MAM	<i>ERG</i>	rs386574671	0.271607451	1.88x10 ⁻⁰⁵	rs386574671	0.27160745	1.88x10 ⁻⁰⁵	Yes

Online Table XXII: Peripheral blood monocyte eQTLs

Chr	Position	SNP	Locus	Gene(s)	Probe_ID	ILMN_Gene	beta	beta_se	P	FDR	Cell type					
1	109821511	rs602633	1p13.3	CELSR2/ <i>SORT1</i>	ILMN_1671843	<i>PSRC1</i>	-0.2202	0.0195	7.91x10 ⁻²⁷	1.08x10 ⁻²³	Macrophage					
					ILMN_2315964	<i>PSRC1</i>	-0.0763	0.0168	6.32x10 ⁻⁰⁶	8.65x10 ⁻⁰⁴	Macrophage					
					ILMN_1671843	<i>PSRC1</i>	-0.1512	0.0121	1.96x10 ⁻³²	2.33x10 ⁻²⁹	Monocyte					
					ILMN_2315964	<i>PSRC1</i>	-0.1261	0.0158	4.72x10 ⁻¹⁵	1.83x10 ⁻¹²	Monocyte					
					ILMN_1711208	<i>CELSR2</i>	-0.0696	0.0139	7.41x10 ⁻⁰⁷	1.23x10 ⁻⁰⁴	Macrophage					
					ILMN_1707077	<i>SORT1</i>	-0.0752	0.0183	4.38x10 ⁻⁰⁵	4.95x10 ⁻⁰³	Macrophage					
					ILMN_1671843	<i>PSRC1</i>	-0.2202	0.0195	7.91x10 ⁻²⁷	1.08x10 ⁻²³	Macrophage					
					ILMN_1711208	<i>CELSR2</i>	-0.0696	0.0139	7.41x10 ⁻⁰⁷	1.23x10 ⁻⁰⁴	Macrophage					
					ILMN_2315964	<i>PSRC1</i>	-0.0763	0.0168	6.32x10 ⁻⁰⁶	8.65x10 ⁻⁰⁴	Macrophage					
					ILMN_1707077	<i>SORT1</i>	-0.0752	0.0183	4.38x10 ⁻⁰⁵	4.95x10 ⁻⁰³	Macrophage					
					ILMN_1671843	<i>PSRC1</i>	-0.1512	0.0121	1.96x10 ⁻³²	2.33x10 ⁻²⁹	Monocyte					
					ILMN_2315964	<i>PSRC1</i>	-0.1261	0.0158	4.72x10 ⁻¹⁵	1.83x10 ⁻¹²	Monocyte					
					20	44586023	rs3827066	20q13.12	Near <i>PCIF1/MMP9/ZNF335</i>	ILMN_1777113	<i>NEURL2</i>	-0.1058	0.0255	3.86x10 ⁻⁰⁵	3.11x10 ⁻⁰³	Macrophage
										ILMN_1773389	<i>PLTP</i>	-0.3127	0.0796	9.57x10 ⁻⁰⁵	6.86x10 ⁻⁰³	Macrophage
ILMN_1711748	<i>PLTP</i>	-0.2266	0.0587	1.27x10 ⁻⁰⁴						8.82x10 ⁻⁰³	Macrophage					
ILMN_2367818	<i>CD40</i>	0.0828	0.0245	7.75x10 ⁻⁰⁴						4.08x10 ⁻⁰²	Macrophage					
ILMN_1691117	<i>DNTTIP1</i>	0.0741	0.0109	1.95x10 ⁻¹¹						3.13x10 ⁻⁰⁹	Monocyte					
ILMN_2367818	<i>CD40</i>	0.0752	0.0176	2.20x10 ⁻⁰⁵						1.45x10 ⁻⁰³	Monocyte					
ILMN_1779257	<i>CD40</i>	0.1136	0.0317	3.63x10 ⁻⁰⁴						1.74x10 ⁻⁰²	Monocyte					
21	39819830	rs2836411	21q22.2	<i>ERG</i>	ILMN_1757074	<i>GNG10</i>	-0.0626	0.0138	6.84x10 ⁻⁰⁶	5.28x10 ⁻⁰¹	Monocyte					

VALIDATION OF GWAS3D RESULTS USING mRNA EXPRESSION DATA FOR AAA AND CONTROL AORTA

To determine the potential utility of the GWAS3D chromatin state analysis to identify trans interactions, a validation analysis was performed comparing mRNA expression of putative genes in abdominal aortic tissue. Relative mRNA expression profiles of candidate genes, indicated by either SNP proximity (cis-acting regulatory variant) or GWAS3D predicted distal interaction, was derived using the Biros *et al* 2015 (GSE57691) dataset (**Online Table XXIII**). The composition and analysis of this dataset has been previously described¹⁰⁷. All genes at AAA loci (Table 1) were included in this analysis. Case (49 AAA, including 29 large and 20 small) and control (10 organ donor) abdominal aortic samples were compared using data generated from the Illumina HumanHT-12 V4.0 expression beadchip (GPL10558).

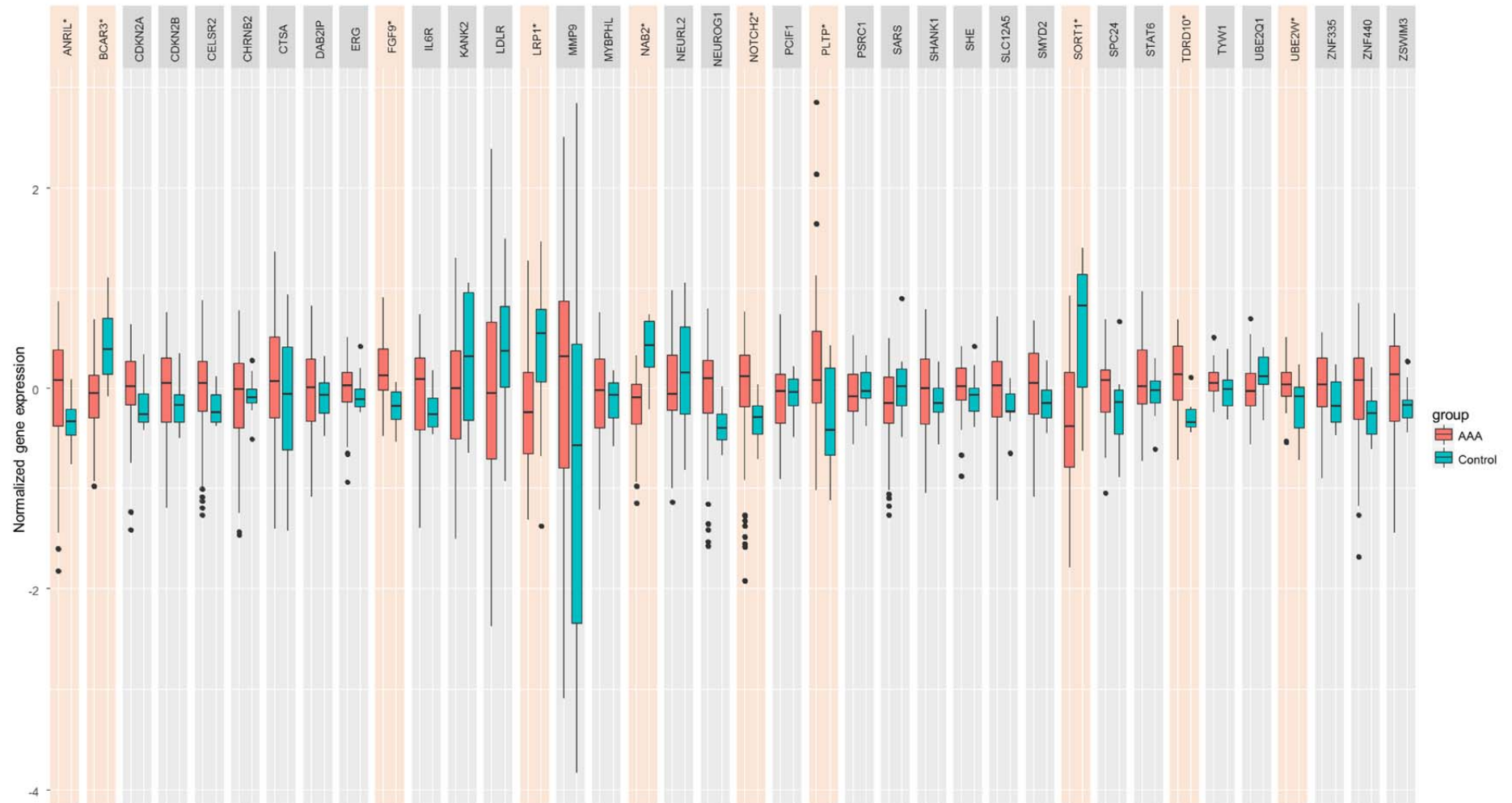
Several of the GWAS3D predicted distal gene interactions appeared to have differential case/ control gene expression (**Online Table XXIII and Online Figure IV**). For example, not only was the mRNA expression of *SORT1* (which is within the locus suggested by rs602633) significantly different between cases and controls, but predicted distal interactions in *BCAR3* and *NOTCH2* also had altered expression. The predicted distal interaction between rs4129267 (*IL6R* locus) and *TDRD10* also appeared concordant with an observed differential gene expression profile. The intergenic SNP rs9316871 (closest gene *LINC0540*) had a predicted interaction with *FGF9* which also had increased expression in AAA versus control aortic tissue.

It should be noted that absence of differential gene expression in this analysis does not specifically preclude a role in AAA pathogenesis. Many genes will have temporal expression and may, for example, only be differentially expressed in specific phases of the pathology. In addition, other genes may have significantly altered expression in other tissues (such as the liver, kidney or circulating leukocytes) the results of which may have indirect effects on the aortic wall. Nevertheless, these results appear to, at least in part, validate the potential utility of chromatin state-based analysis to identify functional mechanisms underlying SNP associations.

Online Table XXIII: AAA tissue mRNA expression for genes in close proximity to validated SNPs or having predicted distal gene interactions based on GWAS3D analysis.

Gene selection criteria	Gene	Locus	Entrez Gene ID	mRNA p-value	AAA mRNA expression
metaGWAS SNP proximity	ANRIL	9p21.3	1030	0.0025	increased
GWAS3D predicted distal interaction (SORT1)	BCAR3	1p22.1	8412	1.8x10⁻⁴	decreased
metaGWAS SNP proximity	CDKN2A	9p21.3	1029	0.217	
metaGWAS SNP proximity	CDKN2BAS1	9p21.3	100048912	0.266	
metaGWAS SNP proximity	CELSR2	1p13.3	1952	0.479	
metaGWAS SNP proximity	CHRN2	1q21.3	1141	0.829	
metaGWAS SNP proximity	CTSA	20q13.12	5476	0.174	
metaGWAS SNP proximity	DAB2IP	9q33.1	153090	0.213	
metaGWAS SNP proximity	ERG	21q21.3	2078	0.095	
GWAS3D predicted distal interaction (LINC00540)	FGF9	13q11	2254	0.002	increased
metaGWAS SNP proximity	IL6R	1q21	3570	0.087	
metaGWAS SNP proximity	KANK2	19p13.2	25959	0.132	
metaGWAS SNP proximity	LDLR	19p13.2	3949	0.197	
metaGWAS SNP proximity	LRP1	12q13.3	4035	0.0084	decreased
metaGWAS SNP proximity	MMP9	20q13.12	4318	0.132	
metaGWAS SNP proximity	MYBPHL	1p13.3	343263	0.897	
metaGWAS SNP proximity	NAB2	12q13.3	4665	1.1x10⁻⁵	decreased
metaGWAS SNP proximity	NEURL2	20q13.12	140825	0.576	
GWAS3D predicted distal interaction (LDLR)	NEUROG1	5q23	4762	0.138	
GWAS3D predicted distal interaction (SORT1)	NOTCH2	1p12	4853	4.6x10⁻⁷	increased
metaGWAS SNP proximity	PCIF1	20q13.12	63935	0.968	
metaGWAS SNP proximity	PLTP	20q13.12	5360	0.011	increased
metaGWAS SNP proximity	PSRC1	1p13.3	84722	0.440	
metaGWAS SNP proximity	SARS	1p13.3	6301	0.095	
GWAS3D predicted distal interaction (LDLR)	SHANK1	19p13.3	50944	0.567	
metaGWAS SNP proximity	SHE	1q21.3	126669	0.396	
metaGWAS SNP proximity	SLC12A5	20q13.12	57468	0.329	
metaGWAS SNP proximity	SMYD2	1q41	56950	0.317	
metaGWAS SNP proximity	SORT1	1p13.3	6272	1.1x10⁻⁴	decreased
metaGWAS SNP proximity	SPC24	19p13.2	147841	0.211	
metaGWAS SNP proximity	STAT6	12q13.3	6778	0.423	
GWAS3D predicted distal interaction (IL6R)	TDRD10	1q21.3	126668	0.006	increased
GWAS3D predicted distal interaction (IL6R)	TYW1	7q11.21	55253	0.320	
metaGWAS SNP proximity	UBE2Q1	1q21.3	55585	0.157	
GWAS3D predicted distal interaction (CDKN2B-AS1)	UBE2W	8q21.11	55284	0.0292	increased
metaGWAS SNP proximity	ZNF335	20q13.12	63925	0.205	
GWAS3D predicted distal interaction (LDLR)	ZNF440	19p13.2	126070	0.406	
metaGWAS SNP proximity	ZSWIM3	20q13.12	140831	0.235	

Online Figure IV: Box and whiskers plots of gene expression in AAA tissue and control tissue for genes in close proximity to validated SNPs or having predicted distal gene interactions based on GWAS3D analysis. Significant differences between AAA and controls are highlighted. Gene expression is log base 2, normalized to the 75th percentile.



LOOK-UP FOR TRANSCRIPTION FACTOR BINDING SITES IN GENES HARBORING AAA-ASSOCIATED VARIANTS

We previously performed a chromatin-immunoprecipitation (ChIP) study using AAA and control aorta tissue for the TFs ELF1, ETS2, RUNX1 and STAT5¹⁸⁵. These TFs were chosen because they were enriched in genes differentially expressed between AAA and control aorta; ELF1, ETS2, and RUNX1 were identified as relevant to most upregulated genes¹⁸⁶ and STAT5 was a driver for genes in the complement cascade¹⁸⁷.

The TF binding data were obtained from tables published in a paper by Pahl et al.¹⁸⁵, which describes ChIP-chip for TFs ELF1, ETS2, RUNX1 and STAT5 using human aortic tissue (AAA and control aorta). We performed a lookup in these data for evidence supporting that the genes near the SNPs identified by the meta-GWAS are relevant to AAA pathobiology. Lack of evidence in these data does not preclude involvement in AAA, but presence of evidence is a useful indicator that the gene is likely involved. This is especially useful for genes with little or no annotation in the major databases such as *SMYD2* and *ERG*. The results are summarized in **Online Table XXIV**. Chromatin enriched regions (cher) with binding sites for the TF ETS2 were found in *SMYD2* and *SORT1*. TF STAT5 had binding sites with chers in *CDKN2B-AS1ANRIL*, *ERG* and *DAB2IP*, and TF ELF1 had multiple binding sites in *ERG*. None of the TF binding sites in these genes contained the lead SNPs identified at the AAA risk loci.

Online Table XXIV: ChIP-chip data on human aortic tissue for the genes harbouring AAA-associated SNPs. Genome-wide ChIP-chip data were available on 4 transcription factors: ETS2, ELF1, STAT5 and RUNX1. For details, see Pahl et al. 2015¹⁸⁵. AAA, aortic tissue from abdominal aortic aneurysm; cher, chromatin enriched region; CTL, control abdominal aorta; TFBS, transcription factor binding site as defined by Transfac®.

SNP	Chr	Position	Gene(s)	Gene Symbol	Cher for TF (tissue source)	TFBS in cher
rs602633	1	109821511	PSRC1-CELSR2-SORT1	<i>CELSR2</i>	None	
				<i>SORT1</i>	ETS2 (CTL)	ETS2 (1 site)
				<i>PSRC</i>	None	
rs4129267	1	154426264	IL6R	<i>IL6R</i>	None	
rs1795061	1	214409280	SMYD2	<i>SMYD2</i>	ETS2 (AAA)	ETS2 (4 sites)
rs10757274	9	22096055	ANRIL	<i>ANRIL</i>	STAT5 (CTL)	STAT5 (1 site)
rs10985349	9	124425243	DAB2IP	<i>DAB2IP</i>	STAT5 (CTL)	STAT5 (1 site)
rs9316871	13	22861921	LINC00540	<i>LINC00540</i>	None	
rs6511720	19	11202306	LDLR	<i>LDLR</i>	None	
rs3827066	20	44586023	PCIF1-ZNF335-MMP9	<i>PCIF1</i>	None	
				<i>MMP9</i>	None	
				<i>ZNF335</i>	None	
rs2836411	21	39819830	ERG	<i>ERG</i>	STAT5 (AAA)	STAT5 (1 site)
					ELF1 (AAA)	ELF1 (4 sites)
					ELF1 (CTL)	

NETWORK ANALYSIS

We investigated whether most of the loci could be connected into a single network through intermediate nodes and interactions. A network integrating most of the loci would suggest mechanisms by which the loci could act in concert, whether synergistically or antagonistically, to affect the phenotype. The network(s) would also provide hypotheses for future investigation. Potential interactions between molecules encoded by genes harboring AAA-associated SNPs were analyzed using two independent analysis tools: Ingenuity Pathway Analysis® (IPA) tool version 9.0 (Qiagen's Ingenuity Systems, Redwood City, CA, USA; www.ingenuity.com) and ConsensusPathDB (<http://cpdb.molgen.mpg.de/CPDB>)¹⁸⁸⁻¹⁹¹. The analyzed gene set had 14 genes: 2 loci identified by the 9 AAA-associated SNPs included clusters of 3 genes (see **Online Table XIV** for SNP annotations), we also included TNF since recent literature indicated that SMYD2 suppresses IL6 and TNF production^{192, 193} and this had been published since the latest database update for each pathway analysis tool used. The gene symbols included in the network analyses were: *CDKN2BAS1*, *CELSR2*, *DAB2IP*, *ERG*, *IL6R*, *LDLR*, *LINC00540*, *MMP9*, *PCIF1*, *PSRC1*, *SMYD2*, *SORT1*, *ZNF335*, and *TNF*.

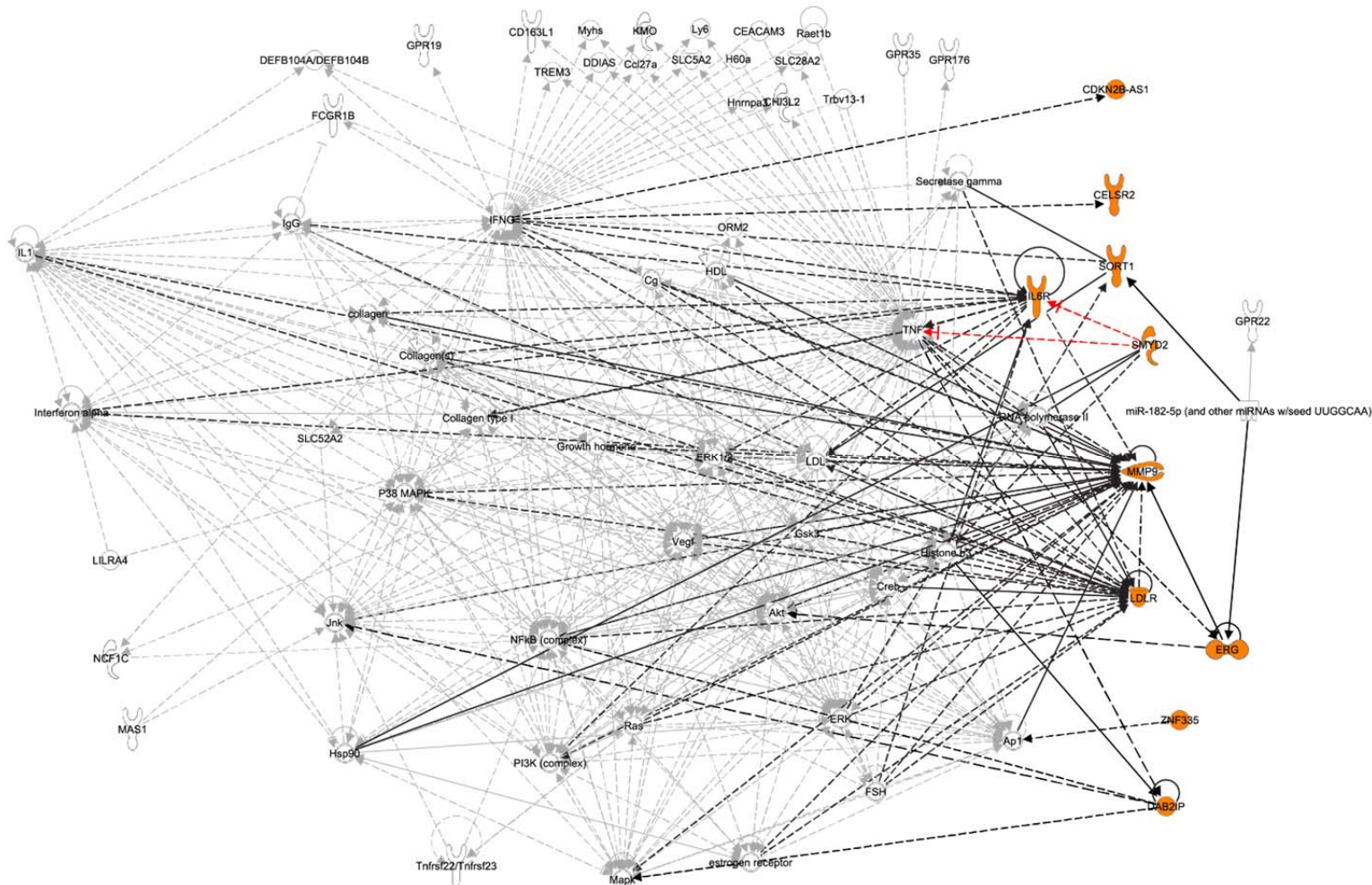
The parameters for the IPA were: 1. the Ingenuity Knowledge Base was used as a reference set; 2. both direct and indirect relationships were considered; and 3. only relationships that were either experimentally observed or had predictions with high confidence were considered. The relationships displayed as direct interactions mean that the two molecules make physical contact with each other such as binding or phosphorylation, and those displayed as indirect interactions do not require physical contact between the two molecules, such as signaling events. The IPA network generation algorithm has been described previously¹⁹⁴. The IPA's Core Analysis generated 2 networks, (1) "cardiovascular disease, cellular movement, developmental disorders" ($P=1 \times 10^{-21}$; 8/12 molecules), and (2) "cell signalling, nucleic acid metabolism, small molecular biochemistry" ($P=1 \times 10^{-7}$; 3/12 molecules). We merged the two networks into an interaction figure (**Online Figure V**). This identified that *ERG*, *IL6R* and *LDLR* were predicted modifiers of *MMP9*, with a direct interaction between *ERG* and *MMP9*. *SORT* and *LDLR* appear coupled via *ERK* and *LDL*. *IL6R* affects *DAB2IP* which in turn regulates *NFKB*. Several gene products, such as *ANRIL*, *CELSR2*, *ZNF335* and *SMYD2* have poorly defined functions at present, and *LINC00540*, a long non-coding RNA expressed in the hippocampus and lacking annotation information, did not belong to either of the 2 networks. The long non-coding RNA *ANRIL*, our strongest hit in the genome (**Figure 1**), has been reported in numerous studies as a GWAS hotspot and a candidate gene for CAD, intracranial aneurysms, and diverse cardiometabolic disorders¹⁹⁵.

The same gene list was submitted to the ConsensusPathDB web-based tool for generating an inferred network. ConsensusPathDB-human integrates interaction networks in *Homo sapiens* including binary and complex protein-protein, genetic, metabolic, signaling, gene regulatory and drug-target interactions, as well as biochemical pathways. Data currently originate from 32 public resources for interactions and interactions that have been curated from the literature. The interaction data are integrated in a manner to avoid redundancies, resulting in an interaction network containing different types of interactions. When the analysis was carried out, the database contained the following annotations: 158,523 unique physical entities; 458,570 unique interactions (17,098 gene regulation, 261,085 protein interaction, 443 genetic, 21,070 biochemical reactions, and 158,874 drug-target interactions), and 4,593 pathways. ConsensusPathDB infers a network to include proteins or metabolites that are not in the user-supplied input list, but associate two or more nodes (gene/protein/metabolite) on the input list with each other. These nodes are termed intermediate nodes and are ranked according to the significance of association with the input nodes given their overall connectivity in the background network. This is quantified by a z-score calculated for each intermediate node with the binomial

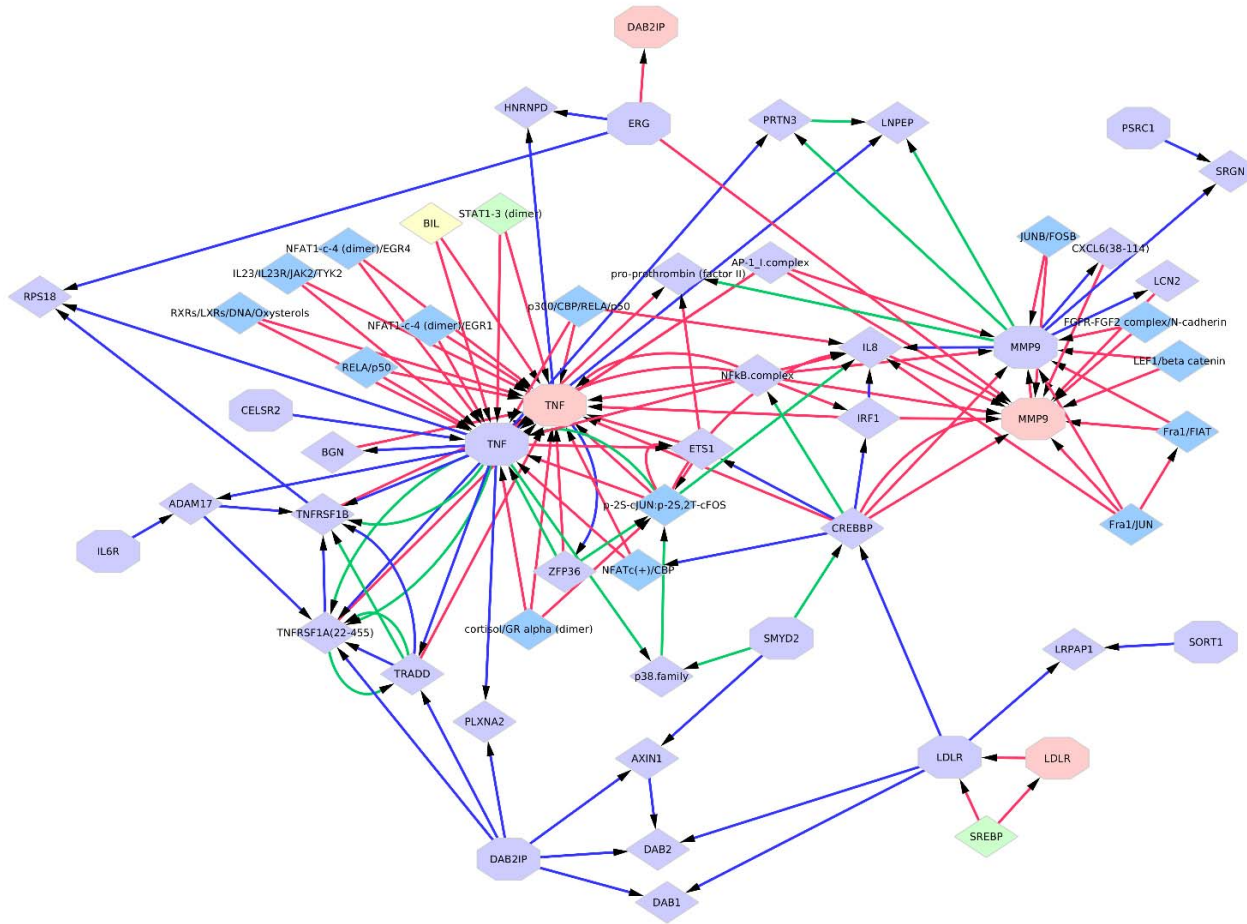
proportions test. The default z-score was used. The network was visualized using Cytoscape (version 3.4.0).

Four genes from the input list did not map to known entities in ConsensusPathDB: ANRIL and LINC00540 are long non-coding RNAs and not represented; similarly PCIF1 and ZNF335 are poorly annotated and not currently represented in source databases (**Online Figure VI**). The inferred network generated by ConsensusPathDB is largely similar to that produced by IPA, although it lacks the interaction between SMYD2 and IL6R, and SMYD2 and TNF. The absence of these interactions could be due to the recent elucidation as well as the unknown mechanism by which the SMYD2 suppression of TNF and IL6 occurs. The number of interactions of a node is a function of the true number of interactions as well as how well studied the protein or gene is. In the network (**Online Figure VI**) MMP9 and TNF have a large number of interactions. Interestingly LDLR and SMYD2 both have indirect interactions with MMP9 and TNF through CREBP, and could have synergistic effects on the AAA phenotype. Additionally CREBP has an interaction with NFKB complex and ETS1. Inhibition of NFKB and ETS1 was shown to reduce AAA in a rat model¹⁹⁶ and their promoter binding sites were enriched in the promoters of genes upregulated in human AAA¹⁹⁷.

Online Figure V. Potential interactions between gene products of AAA related genes. This figure shows IPA networks 1 and 2 merged together. Molecules are represented as nodes, and the biological relationship between two nodes as a line. Solid lines represent direct and dashed lines indirect interactions. All lines are supported by at least one literature citation or are from canonical information stored in the Ingenuity Pathways Knowledge Base (Qiagen's Ingenuity Systems). Nodes are displayed using various shapes that represent the functional class of the gene product. Molecules in orange are encoded by genes harboring AAA-associated variants. Red dashed lines indicate new information on SMYD2, IL6 and TNF found in recent literature^{192, 193}



Online Figure VI: Induced network generated by ConsensusPathDB from 14 input genes. The network comprises, genes, gene products (proteins), protein complexes, and metabolites, represented as nodes of different colors: pink, protein; light-blue, gene; medium blue, protein complexes; yellow, metabolite; and light green, unknown complex. Node shape indicates whether the node was on the input list: octagons, input list; rhomboids, induced nodes. Interactions are represented as edges, with color indicating interaction type: blue, protein interaction; red, gene regulatory interaction; and green, biochemical interaction.



CONSORTIA CONTRIBUTING DATA

List of members of the Cardiogenics consortium

Tony Attwood¹, Stephanie Belz², Peter Braund³, Jessy Brocheton⁴, François Cambien⁴, Jason Cooper⁵, Abi Crisp-Hihn¹, Patrick Diemert (formerly Linsel-Nitschke)², Panos Deloukas⁶, Jeanette Eardman², Nicola Foad¹, Tiphaine Godefroy⁴, Alison H Goodall^{3,11}, Jay Gracey³, Emma Gray⁶, Rhian Gwilliams⁶, Susanne Heimerl⁷, Christian Hengstenberg⁷, Jennifer Jolley¹, Unni Krishnan³, Heather Lloyd-Jones¹, Ulrika Liljedahl⁸, Ingrid Lugauer⁷, Per Lundmark⁸, Seraya Maouche^{2,4}, Jasbir S Moore³, Gilles Montalescot⁴, David Muir¹, Elizabeth Murray¹, Chris P Nelson³, Jessica Neudert⁹, David Niblett⁶, Karen O'Leary¹, Willem H Ouweland^{1,6}, Helen Pollard³, Carole Proust⁴, Angela Rankin¹, Augusto Rendon¹², Catherine M Rice⁶, Hendrik B Sager², Nilesh J Samani^{3,11}, Jennifer Sambrook¹, Gerd Schmitz¹⁰, Michael Scholz⁹, Laura Schroeder², Heribert Schunkert², Jonathan Stephens¹, Ann-Christine Syvannen⁸, Stefanie Tennstedt (formerly Gulde)², Chris Wallace⁵.

¹Department of Haematology, University of Cambridge, Long Road, Cambridge, CB2 2PT, UK and National Health Service Blood and Transplant, Cambridge Centre, Long Road, Cambridge, CB2 2PT, UK;

²Medizinische Klinik 2, Universität zu Lübeck, Lübeck Germany

³Department of Cardiovascular Sciences, University of Leicester, Glenfield Hospital, Groby Road, Leicester, LE3 9QP, UK

⁴INSERM UMRS 937, Pierre and Marie Curie University (UPMC, Paris 6) and Medical School, 91 Bd de l'Hôpital 75013, Paris, France

⁵Juvenile Diabetes Research Foundation/Wellcome Trust Diabetes and Inflammation Laboratory, Department of Medical Genetics, Cambridge Institute for Medical Research, University of Cambridge, Wellcome Trust/MRC Building, Cambridge, CB2 0XY, UK

⁶The Wellcome Trust Sanger Institute, Wellcome Trust Genome Campus, Hinxton, Cambridge CB10 1SA, UK

⁷Klinik und Poliklinik für Innere Medizin II, Universität Regensburg, Germany

⁸Molecular Medicine, Department of Medical Sciences, Uppsala University, Uppsala, Sweden

⁹Trium, Analysis Online GmbH, Hohenlindenerstr. 1, 81677, München, Germany

¹⁰Institut für Klinische Chemie und Laboratoriumsmedizin, Universität, Regensburg, D-93053 Regensburg, Germany

¹¹Leicester NIHR Biomedical Research Unit in Cardiovascular Disease, Glenfield Hospital, Leicester, LE3 9QP, UK

¹²European Bioinformatics Institute, Wellcome Trust Genome Campus, Hinxton, Cambridge, CB10 1SD, UK

List of members of ICBP: The International Consortium for Blood Pressure Genome-Wide Association Studies¹⁹⁸

Georg B. Ehret, Patricia B. Munroe, Kenneth M. Rice, Murielle Bochud, Andrew D. Johnson, Daniel I. Chasman, Albert V. Smith, Martin D. Tobin, Germaine C. Verwoert, Shih-Jen Hwang, Vasyl Pihur, Peter Vollenweider, Paul F. O'Reilly, Najaf Amin, Jennifer L. Bragg-Gresham, Alexander Teumer, Nicole L. Glazer, Lenore Launer, Jing Hua Zhao, Yurii Aulchenko, Simon Heath, Siim Söber, Afshin Parsa, Jian'an Luan, Pankaj Arora, Abbas Dehghan, Feng Zhang, Gavin Lucas, Andrew A. Hicks, Anne U. Jackson, John F Peden, Toshiko Tanaka, Sarah H. Wild, Igor Rudan, Wilmar Igl, Yuri Milaneschi, Alex N. Parker, Cristiano Fava, John C. Chambers, Ervin R. Fox, Meena Kumari, Min Jin Go, Pim van der Harst, Wen Hong Linda Kao, Marketa Sjögren, D. G. Vinay, Myriam Alexander, Yasuharu Tabara, Sue Shaw-Hawkins, Peter H. Whincup, Yongmei Liu, Gang Shi, Johanna Kuusisto, Bamidele Tayo, Mark Seielstad, Xueling Sim, Khanh-Dung Hoang Nguyen, Terho Lehtimäki, Giuseppe Matullo, Ying Wu, Tom R. Gaunt, N. Charlotte Onland-

Moret, Matthew N. Cooper, Carl G. P. Platou, Elin Org, Rebecca Hardy, Santosh Dahgam, Jutta Palmen, Veronique Vitart, Peter S. Braund, Tatiana Kuznetsova, Cuno S. P. M. Uiterwaal, Adebowale Adeyemo, Walter Palmas, Harry Campbell, Barbara Ludwig, Maciej Tomaszewski, Ioanna Tzoulaki, Nicholette D. Palmer, CARDIoGRAM consortium, CKDGen Consortium, KidneyGen Consortium, EchoGen consortium, CHARGE-HF consortium, Thor Aspelund, Melissa Garcia, Yen-Pei C. Chang, Jeffrey R. O'Connell, Nanette I. Steinle, Diederick E. Grobbee, Dan E. Arking, Sharon L. Kardia, Alanna C. Morrison, Dena Hernandez, Samer Najjar, Wendy L. McArdle, David Hadley, Morris J. Brown, John M. Connell, Aroon D. Hingorani, Ian N.M. Day, Debbie A. Lawlor, John P. Beilby, Robert W. Lawrence, Robert Clarke, Jemma C. Hopewell, Halit Ongen, Albert W. Dreisbach, Yali Li, J. Hunter Young, Joshua C. Bis, Mika Kähönen, Jorma Viikari, Linda S. Adair, Nanette R. Lee, Ming-Huei Chen, Matthias Olden, Cristian Pattaro, Judith A. Hoffman Bolton, Anna Köttgen, Sven Bergmann, Vincent Mooser, Nish Chaturvedi, Timothy M. Frayling, Muhammad Islam, Tazeen H. Jafar, Jeanette Erdmann, Smita R. Kulkarni, Stefan R. Bornstein, Jürgen Grässler, Leif Groop, Benjamin F. Voight, Johannes Kettunen, Philip Howard, Andrew Taylor, Simonetta Guarrera, Fulvio Ricceri, Valur Emilsson, Andrew Plump, Inês Barroso, Kay-Tee Khaw, Alan B. Weder, Steven C. Hunt, Yan V. Sun, Richard N. Bergman, Francis S. Collins, Lori L. Bonnycastle, Laura J. Scott, Heather M. Stringham, Leena Peltonen, Markus Perola, Erkki Vartiainen, Stefan-Martin Brand, Jan A. Staessen, Thomas J. Wang, Paul R. Burton, Maria Soler Artigas, Yanbin Dong, Harold Snieder, Xiaoling Wang, Haidong Zhu, Kurt K. Lohman, Megan E. Rudock, Susan R. Heckbert, Nicholas L. Smith, Kerri L. Wiggins, Ayo Doumatey, Daniel Shriener, Gudrun Veldre, Margus Viigimaa, Sanjay Kinra, Dorairaj Prabhakaran, Vikal Tripathy, Carl D. Langefeld, Annika Rosengren, Dag S. Thelle, Anna Maria Corsi, Andrew Singleton, Terrence Forrester, Gina Hilton, Colin A. McKenzie, Tunde Salako, Naoharu Iwai, Yoshikuni Kita, Toshio Ogihara, Takayoshi Ohkubo, Tomonori Okamura, Hirotsugu Ueshima, Satoshi Umemura, Susana Eyheramendy, Thomas Meitinger, H.-Erich Wichmann, Yoon Shin Cho, Hyung-Lae Kim, Jong-Young Lee, James Scott, Joban S. Sehmi, Weihua Zhang, Bo Hedblad, Peter Nilsson, George Davey Smith, Andrew Wong, Narisu Narisu, Alena Stančáková, Leslie J. Raffel, Jie Yao, Sekar Kathiresan, Christopher J. O'Donnell, Stephen M. Schwartz, M. Arfan Ikram, W. T. Longstreth Jr, Thomas H. Mosley, Sudha Seshadri, Nick R.G. Shrine, Louise V. Wain, Mario A. Morken, Amy J. Swift, Jaana Laitinen, Inga Prokopenko, Paavo Zitting, Jackie A. Cooper, Steve E. Humphries, John Danesh, Asif Rasheed, Anuj Goel, Anders Hamsten, Hugh Watkins, Stephan J. L. Bakker, Wiek H. van Gilst, Charles S. Janipalli, K. Radha Mani, Chittaranjan S. Yajnik, Albert Hofman, Francesco U. S. Mattace-Raso, Ben A. Oostra, Ayse Demirkan, Aaron Isaacs, Fernando Rivadeneira, Edward G. Lakatta, Marco Orzu, Angelo Scuteri, Mika Ala-Korpela, Antti J. Kangas, Leo-Pekka Lytykäinen, Pasi Soininen, Taru Tukiainen, Peter Würtz, Rick Twee-Hee Ong, Marcus Dörr, Heyo K. Kroemer, Uwe Völker, Henry Völzke, Pilar Galan, Serge Herberg, Mark Lathrop, Diana Zelenika, Panos Deloukas, Massimo Mangino, Tim D. Spector, Guangju Zhai, James F. Meschia, Michael A. Nalls, Pankaj Sharma, Janos Terzic, M. V. Kranthi Kumar, Matthew Denniff, Ewa Zukowska-Szczechowska, Lynne E. Wagenknecht, F. Gerald R. Fowkes, Fadi J. Charchar, Peter E. H. Schwarz, Caroline Hayward, Xiuqing Guo, Charles Rotimi, Michiel L. Bots, Eva Brand, Nilesh J. Samani, Ozren Polasek, Philippa J. Talmud, Fredrik Nyberg, Diana Kuh, Maris Laan, Kristian Hveem, Lyle J. Palmer, Yvonne T. van der Schouw, Juan P. Casas, Karen L. Mohlke, Paolo Vineis, Olli Raitakari, Santhi K. Ganesh, Tien Y. Wong, E Shyong Tai, Richard S. Cooper, Markku Laakso, Dabeeru C. Rao, Tamara B. Harris, Richard W. Morris, Anna F. Dominiczak, Mika Kivimaki, Michael G. Marmot, Tetsuro Miki, Danish Saleheen, Giriraj R. Chandak, Josef Coresh, Gerjan Navis, Veikko Salomaa, Bok-Ghee Han, Xiaofeng Zhu, Jaspal S. Kooner, Olle Melander, Paul M Ridker, Stefania Bandinelli, Ulf B. Gyllensten, Alan F. Wright, James F. Wilson, Luigi Ferrucci, Martin Farrall, Jaakko Tuomilehto, Peter P. Pramstaller, Roberto Elosua, Nicole Soranzo, Eric J. G. Sijbrands, David Altshuler, Ruth J. F. Loos, Alan R. Shuldiner, Christian Gieger, Pierre Meneton, Andre G. Uitterlinden, Nicholas J. Wareham, Vilmundur Gudnason, Jerome I. Rotter, Rainer Rettig, Manuela Uda, David P. Strachan, Jacqueline C. M. Witteman, Anna-Liisa Hartikainen, Jacques S. Beckmann, Eric Boerwinkle, Ramachandran S. Vasan, Michael Boehnke, Martin G. Larson,

Marjo-Riitta Järvelin, Bruce M. Psaty, Gonçalo R. Abecasis, Aravinda Chakravarti, Paul Elliott, Cornelia M. van Duijn, Christopher Newton-Cheh, Daniel Levy, Mark J. Caulfield & Toby Johnson.

REFERENCES

1. Bown MJ, Jones GT, Harrison SC, et al. Abdominal aortic aneurysm is associated with a variant in low-density lipoprotein receptor-related protein 1. *Am J Hum Genet.* 2011;89:619-627
2. Gretarsdottir S, Baas AF, Thorleifsson G, et al. Genome-wide association study identifies a sequence variant within the *dab2ip* gene conferring susceptibility to abdominal aortic aneurysm. *Nature Genet.* 2010;42:692-U671
3. Jones GT, Bown MJ, Gretarsdottir S, et al. A sequence variant associated with sortilin-1 (*sort1*) on 1p13.3 is independently associated with abdominal aortic aneurysm. *Hum Mol Genet.* 2013
4. Harrison SC, Zabaneh D, Asselbergs FW, et al. A gene-centric study of common carotid artery remodelling. *Atherosclerosis.* 2013;226:440-446
5. Teo YY. Genotype calling for the illumina platform. *Methods Mol Biol.* 2012;850:525-538
6. Purcell S, Neale B, Todd-Brown K, Thomas L, Ferreira MA, Bender D, Maller J, Sklar P, de Bakker PI, Daly MJ, Sham PC. Plink: A tool set for whole-genome association and population-based linkage analyses. *Am J Hum Genet.* 2007;81:559-575
7. Elmore JR, Obmann MA, Kuivaniemi H, Tromp G, Gerhard GS, Franklin DP, Boddy AM, Carey DJ. Identification of a genetic variant associated with abdominal aortic aneurysms on chromosome 3p12.3 by genome wide association. *J Vasc Surg.* 2009;49:1525-1531
8. Borthwick KM, Smelser DT, Bock JA, et al. Ephenotyping for abdominal aortic aneurysm in the electronic medical records and genomics (emerge) network: Algorithm development and konstanz information miner workflow. *Int J Biomed Data Mining.* 2015;4
9. Verma SS, de Andrade M, Tromp G, et al. Imputation and quality control steps for combining multiple genome-wide datasets. *Front Genet.* 2014;5:370
10. Delaneau O, Marchini J, Zagury JF. A linear complexity phasing method for thousands of genomes. *Nat Methods.* 2012;9:179-181
11. Howie B, Fuchsberger C, Stephens M, Marchini J, Abecasis GR. Fast and accurate genotype imputation in genome-wide association studies through pre-phasing. *Nat Genet.* 2012;44:955-959
12. Gretarsdottir S, Thorleifsson G, Reynisdottir ST, et al. The gene encoding phosphodiesterase 4d confers risk of ischemic stroke. *Nat Genet.* 2003;35:131-138
13. Rice JA. Generalized likelihood ratio tests. In: Rice ja, editor. *Mathematical statistics and data analysis.* Vol. 1. International thomson publishing; 1995. P. 308–310.
14. Rafnar T, Sulem P, Stacey SN, et al. Sequence variants at the *tert-clptm1l* locus associate with many cancer types. *Nat Genet.* 2009;41:221-227
15. Kiemeny LA, Thorlacius S, Sulem P, et al. Sequence variant on 8q24 confers susceptibility to urinary bladder cancer. *Nat Genet.* 2008;40:1307-1312
16. Wetzels JF, Kiemeny LA, Swinkels DW, Willems HL, den Heijer M. Age- and gender-specific reference values of estimated gfr in caucasians: The nijmegen biomedical study. *Kidney Int.* 2007;72:632-637

17. Bown MJ, Braund PS, Thompson J, London NJ, Samani NJ, Sayers RD. Association between the coronary artery disease risk locus on chromosome 9p21.3 and abdominal aortic aneurysm. *Circ Cardiovasc Genet*. 2008;1:39-42
18. Howie B, Marchini J, Stephens M. Genotype imputation with thousands of genomes. *G3 (Bethesda)*. 2011;1:457-470
19. Devlin B, Roeder K. Genomic control for association studies. *Biometrics*. 1999;55:997-1004
20. Shi YY, He L. Shesis, a powerful software platform for analyses of linkage disequilibrium, haplotype construction, and genetic association at polymorphism loci. *Cell Res*. 2005;15:97-98
21. Helgadóttir A, Thorleifsson G, Magnusson KP, et al. The same sequence variant on 9p21 associates with myocardial infarction, abdominal aortic aneurysm and intracranial aneurysm. *Nat Genet*. 2008;40:217-224
22. Ogata T, Shibamura H, Tromp G, Sinha M, Goddard KA, Sakalihan N, Limet R, MacKean GL, Arthur C, Sueda T, Land S, Kuivaniemi H. Genetic analysis of polymorphisms in biologically relevant candidate genes in patients with abdominal aortic aneurysms. *J Vasc Surg*. 2005;41:1036-1042
23. Gottesman O, Kuivaniemi H, Tromp G, et al. The electronic medical records and genomics (emerge) network: Past, present, and future. *Genet Med*. 2013;15:761-771
24. Ye Z, Kalloo FS, Dalenberg AK, Kullo IJ. An electronic medical record-linked biorepository to identify novel biomarkers for atherosclerotic cardiovascular disease. *Glob Cardiol Sci Pract*. 2013;2013:82-90
25. St Jean PL, Zhang XC, Hart BK, Lamlum H, Webster MW, Steed DL, Henney AM, Ferrell RE. Characterization of a dinucleotide repeat in the 92 kda type iv collagenase gene (clg4b), localization of clg4b to chromosome 20 and the role of clg4b in aortic aneurysmal disease. *Ann Hum Genet*. 1995;59:17-24
26. Pulley J, Clayton E, Bernard GR, Roden DM, Masys DR. Principles of human subjects protections applied in an opt-out, de-identified biobank. *Clin Transl Sci*. 2010;3:42-48
27. McCarty CA, Wilke RA, Giampietro PF, Wesbrook SD, Caldwell MD. Marshfield clinic personalized medicine research project (pmrp): Design, methods and recruitment for a large population-based biobank. *Personalized Medicine*. 2005;2:49-79
28. Tayo BO, Teil M, Tong L, Qin H, Khitrov G, Zhang W, Song Q, Gottesman O, Zhu X, Pereira AC, Cooper RS, Bottinger EP. Genetic background of patients from a university medical center in manhattan: Implications for personalized medicine. *PLoS One*. 2011;6:e19166
29. Kho AN, Hayes MG, Rasmussen-Torvik L, et al. Use of diverse electronic medical record systems to identify genetic risk for type 2 diabetes within a genome-wide association study. *J Am Med Inform Assoc*. 2012;19:212-218
30. Galora S, Saracini C, Pratesi G, Sticchi E, Pulli R, Pratesi C, Abbate R, Giusti B. Association of rs1466535 lrp1 but not rs3019885 slc30a8 and rs6674171 tdrd10 gene polymorphisms with abdominal aortic aneurysm in italian patients. *J Vasc Surg*. 2014
31. Strauss E, Waliszewski K, Oszkinis G, Staniszewski R. Polymorphisms of genes involved in the hypoxia signaling pathway and the development of abdominal aortic aneurysms or large-artery atherosclerosis. *J Vasc Surg*. 2015;61:1105-1113.e1103

32. Willer CJ, Li Y, Abecasis GR. Metal: Fast and efficient meta-analysis of genomewide association scans. *Bioinformatics*. 2010;26:2190-2191
33. Han B, Eskin E. Random-effects model aimed at discovering associations in meta-analysis of genome-wide association studies. *Am J Hum Genet*. 2011;88:586-598
34. Morris AP, Voight BF, Teslovich TM, et al. Large-scale association analysis provides insights into the genetic architecture and pathophysiology of type 2 diabetes. *Nat Genet*. 2012;44:981-990
35. Schunkert H, König IR, Kathiresan S, et al. Large-scale association analysis identifies 13 new susceptibility loci for coronary artery disease. *Nat Genet*. 2011;43:333-338
36. Willer CJ, Schmidt EM, Sengupta S, et al. Discovery and refinement of loci associated with lipid levels. *Nat Genet*. 2013;45:1274-1283
37. Wain LV, Verwoert GC, O'Reilly PF, et al. Genome-wide association study identifies six new loci influencing pulse pressure and mean arterial pressure. *Nat Genet*. 2011;43:1005-1011
38. Ramos EM, Hoffman D, Junkins HA, Maglott D, Phan L, Sherry ST, Feolo M, Hindorff LA. Phenotype-genotype integrator (phegeni): Synthesizing genome-wide association study (gwas) data with existing genomic resources. *Eur J Hum Genet*. 2014;22:144-147
39. Eicher JD, Landowski C, Stackhouse B, Sloan A, Chen W, Jensen N, Lien JP, Leslie R, Johnson AD. Grasp v2.0: An update on the genome-wide repository of associations between snps and phenotypes. *Nucleic Acids Res*. 2015;43:D799-804
40. Leslie R, O'Donnell CJ, Johnson AD. Grasp: Analysis of genotype-phenotype results from 1390 genome-wide association studies and corresponding open access database. *Bioinformatics*. 2014;30:i185-194
41. Willer CJ, Sanna S, Jackson AU, et al. Newly identified loci that influence lipid concentrations and risk of coronary artery disease. *Nat Genet*. 2008;40:161-169
42. Sandhu MS, Waterworth DM, Debenham SL, et al. Ldl-cholesterol concentrations: A genome-wide association study. *Lancet*. 2008;371:483-491
43. Kathiresan S, Willer CJ, Peloso GM, et al. Common variants at 30 loci contribute to polygenic dyslipidemia. *Nat Genet*. 2009;41:56-65
44. Talmud PJ, Drenos F, Shah S, et al. Gene-centric association signals for lipids and apolipoproteins identified via the human cvd beadchip. *Am J Hum Genet*. 2009;85:628-642
45. Clarke R, Peden JF, Hopewell JC, et al. Genetic variants associated with lp(a) lipoprotein level and coronary disease. *N Engl J Med*. 2009;361:2518-2528
46. Barber MJ, Mangravite LM, Hyde CL, et al. Genome-wide association of lipid-lowering response to statins in combined study populations. *PLoS One*. 2010;5:e9763
47. Teslovich TM, Musunuru K, Smith AV, et al. Biological, clinical and population relevance of 95 loci for blood lipids. *Nature*. 2010;466:707-713
48. Lango Allen H, Estrada K, Lettre G, et al. Hundreds of variants clustered in genomic loci and biological pathways affect human height. *Nature*. 2010;467:832-838
49. Lettre G, Palmer CD, Young T, et al. Genome-wide association study of coronary heart disease and its risk factors in 8,090 african americans: The nhlbi care project. *PLoS Genet*. 2011;7:e1001300

50. Middelberg RP, Ferreira MA, Henders AK, Heath AC, Madden PA, Montgomery GW, Martin NG, Whitfield JB. Genetic variants in *lpl*, *oasl* and *tomm40/apoe-c1-c2-c4* genes are associated with multiple cardiovascular-related traits. *BMC Med Genet.* 2011;12:123
51. Trompet S, de Craen AJ, Postmus I, Ford I, Sattar N, Caslake M, Stott DJ, Buckley BM, Sacks F, Devlin JJ, Slagboom PE, Westendorp RG, Jukema JW. Replication of *ldl* gwas hits in *prosper/phase* as validation for future (pharmaco)genetic analyses. *BMC Med Genet.* 2011;12:131
52. Grallert H, Dupuis J, Bis JC, et al. Eight genetic loci associated with variation in lipoprotein-associated phospholipase a2 mass and activity and coronary heart disease: Meta-analysis of genome-wide association studies from five community-based studies. *Eur Heart J.* 2012;33:238-251
53. Asselbergs FW, Guo Y, van Iperen EP, et al. Large-scale gene-centric meta-analysis across 32 studies identifies multiple lipid loci. *Am J Hum Genet.* 2012;91:823-838
54. Deloukas P, Kanoni S, Willenborg C, et al. Large-scale association analysis identifies new risk loci for coronary artery disease. *Nat Genet.* 2013;45:25-33
55. Wilk JB, Walter RE, Laramie JM, Gottlieb DJ, O'Connor GT. Framingham heart study genome-wide association: Results for pulmonary function measures. *BMC Med Genet.* 2007;8 Suppl 1:S8
56. Ridker PM, Pare G, Parker A, Zee RY, Danik JS, Buring JE, Kwiatkowski D, Cook NR, Miletich JP, Chasman DI. Loci related to metabolic-syndrome pathways including *lepr*, *hnf1a*, *il6r*, and *gckr* associate with plasma c-reactive protein: The women's genome health study. *Am J Hum Genet.* 2008;82:1185-1192
57. Melzer D, Perry JR, Hernandez D, et al. A genome-wide association study identifies protein quantitative trait loci (pqtls). *PLoS Genet.* 2008;4:e1000072
58. Sabatti C, Service SK, Hartikainen AL, et al. Genome-wide association analysis of metabolic traits in a birth cohort from a founder population. *Nat Genet.* 2009;41:35-46
59. Danik JS, Pare G, Chasman DI, Zee RY, Kwiatkowski DJ, Parker A, Miletich JP, Ridker PM. Novel loci, including those related to crohn disease, psoriasis, and inflammation, identified in a genome-wide association study of fibrinogen in 17 686 women: The women's genome health study. *Circ Cardiovasc Genet.* 2009;2:134-141
60. Ferreira MA, Matheson MC, Duffy DL, et al. Identification of *il6r* and chromosome 11q13.5 as risk loci for asthma. *Lancet.* 2011;378:1006-1014
61. Wassel CL, Lange LA, Keating BJ, et al. Association of genomic loci from a cardiovascular gene snp array with fibrinogen levels in european americans and african-americans from six cohort studies: The candidate gene association resource (care). *Blood.* 2011;117:268-275
62. Dehghan A, Dupuis J, Barbalic M, et al. Meta-analysis of genome-wide association studies in >80 000 subjects identifies multiple loci for c-reactive protein levels. *Circulation.* 2011;123:731-738
63. Naitza S, Porcu E, Steri M, et al. A genome-wide association scan on the levels of markers of inflammation in sardinians reveals associations that underpin its complex regulation. *PLoS Genet.* 2012;8:e1002480

64. Reiner AP, Beleza S, Franceschini N, Auer PL, Robinson JG, Kooperberg C, Peters U, Tang H. Genome-wide association and population genetic analysis of c-reactive protein in african american and hispanic american women. *Am J Hum Genet.* 2012;91:502-512
65. Shah T, Zabaneh D, Gaunt T, et al. Gene-centric analysis identifies variants associated with interleukin-6 levels and shared pathways with other inflammation markers. *Circ Cardiovasc Genet.* 2013;6:163-170
66. McPherson R, Pertsemlidis A, Kavaslar N, Stewart A, Roberts R, Cox DR, Hinds DA, Pennacchio LA, Tybjaerg-Hansen A, Folsom AR, Boerwinkle E, Hobbs HH, Cohen JC. A common allele on chromosome 9 associated with coronary heart disease. *Science.* 2007;316:1488-1491
67. Lu X, Wang L, Chen S, et al. Genome-wide association study in han chinese identifies four new susceptibility loci for coronary artery disease. *Nat Genet.* 2012;44:890-894
68. Pechlivanis S, Muhleisen TW, Mohlenkamp S, Schadendorf D, Erbel R, Jockel KH, Hoffmann P, Nothen MM, Scherag A, Moebus S. Risk loci for coronary artery calcification replicated at 9p21 and 6q24 in the heinz nixdorf recall study. *BMC Med Genet.* 2013;14:23
69. Ferguson JF, Matthews GJ, Townsend RR, et al. Candidate gene association study of coronary artery calcification in chronic kidney disease: Findings from the cric study (chronic renal insufficiency cohort). *J Am Coll Cardiol.* 2013;62:789-798
70. Saxena R, Voight BF, Lyssenko V, et al. Genome-wide association analysis identifies loci for type 2 diabetes and triglyceride levels. *Science.* 2007;316:1331-1336
71. Stefansson H, Ophoff RA, Steinberg S, et al. Common variants conferring risk of schizophrenia. *Nature.* 2009;460:744-747
72. Kathiresan S, Melander O, Guiducci C, et al. Six new loci associated with blood low-density lipoprotein cholesterol, high-density lipoprotein cholesterol or triglycerides in humans. *Nat Genet.* 2008;40:189-197
73. Aulchenko YS, Ripatti S, Lindqvist I, et al. Loci influencing lipid levels and coronary heart disease risk in 16 european population cohorts. *Nat Genet.* 2009;41:47-55
74. Chasman DI, Pare G, Zee RY, et al. Genetic loci associated with plasma concentration of low-density lipoprotein cholesterol, high-density lipoprotein cholesterol, triglycerides, apolipoprotein a1, and apolipoprotein b among 6382 white women in genome-wide analysis with replication. *Circ Cardiovasc Genet.* 2008;1:21-30
75. Chasman DI, Pare G, Mora S, et al. Forty-three loci associated with plasma lipoprotein size, concentration, and cholesterol content in genome-wide analysis. *PLoS Genet.* 2009;5:e1000730
76. Bis JC, Kavousi M, Franceschini N, et al. Meta-analysis of genome-wide association studies from the charge consortium identifies common variants associated with carotid intima media thickness and plaque. *Nat Genet.* 2011;43:940-947
77. Large-scale gene-centric analysis identifies novel variants for coronary artery disease. *PLoS Genet.* 2011;7:e1002260
78. Avery CL, He Q, North KE, et al. A phenomics-based strategy identifies loci on apoc1, brap, and plcg1 associated with metabolic syndrome phenotype domains. *PLoS Genet.* 2011;7:e1002322

79. Musunuru K, Romaine SP, Lettre G, et al. Multi-ethnic analysis of lipid-associated loci: The nhlbi care project. *PLoS One*. 2012;7:e36473
80. Hopewell JC, Parish S, Offer A, Link E, Clarke R, Lathrop M, Armitage J, Collins R. Impact of common genetic variation on response to simvastatin therapy among 18 705 participants in the heart protection study. *Eur Heart J*. 2013;34:982-992
81. Elbers CC, Guo Y, Tragante V, et al. Gene-centric meta-analysis of lipid traits in african, east asian and hispanic populations. *PLoS One*. 2012;7:e50198
82. Weissglas-Volkov D, Aguilar-Salinas CA, Nikkola E, et al. Genomic study in mexicans identifies a new locus for triglycerides and refines european lipid loci. *J Med Genet*. 2013;50:298-308
83. Denny JC, Ritchie MD, Basford MA, Pulley JM, Bastarache L, Brown-Gentry K, Wang D, Masys DR, Roden DM, Crawford DC. Phewas: Demonstrating the feasibility of a phenome-wide scan to discover gene-disease associations. *Bioinformatics*. 2010;26:1205-1210
84. Pendergrass SA, Brown-Gentry K, Dudek S, et al. Phenome-wide association study (phewas) for detection of pleiotropy within the population architecture using genomics and epidemiology (page) network. *PLoS Genet*. 2013;9:e1003087
85. Hsu F, Kent WJ, Clawson H, Kuhn RM, Diekhans M, Haussler D. The ucsc known genes. *Bioinformatics*. 2006;22:1036-1046
86. Benson DA, Karsch-Mizrachi I, Lipman DJ, Ostell J, Wheeler DL. Genbank: Update. *Nucleic Acids Res*. 2004;32:D23-26
87. Kent WJ. Blat--the blast-like alignment tool. *Genome Res*. 2002;12:656-664
88. Pruitt KD, Tatusova T, Maglott DR. Ncbi reference sequence (refseq): A curated non-redundant sequence database of genomes, transcripts and proteins. *Nucleic Acids Res*. 2005;33:D501-504
89. Gardner PP, Daub J, Tate J, Moore BL, Osuch IH, Griffiths-Jones S, Finn RD, Nawrocki EP, Kolbe DL, Eddy SR, Bateman A. Rfam: Wikipedia, clans and the "decimal" release. *Nucleic Acids Res*. 2011;39:D141-145
90. Lowe TM, Eddy SR. Trnascan-se: A program for improved detection of transfer rna genes in genomic sequence. *Nucleic Acids Res*. 1997;25:955-964
91. Reorganizing the protein space at the universal protein resource (uniprot). *Nucleic Acids Res*. 2012;40:D71-75
92. Harrow J, Frankish A, Gonzalez JM, et al. Gencode: The reference human genome annotation for the encode project. *Genome Res*. 2012;22:1760-1774
93. Cabili MN, Trapnell C, Goff L, Koziol M, Tazon-Vega B, Regev A, Rinn JL. Integrative annotation of human large intergenic noncoding rnas reveals global properties and specific subclasses. *Genes Dev*. 2011;25:1915-1927
94. Trapnell C, Williams BA, Pertea G, Mortazavi A, Kwan G, van Baren MJ, Salzberg SL, Wold BJ, Pachter L. Transcript assembly and quantification by rna-seq reveals unannotated transcripts and isoform switching during cell differentiation. *Nat Biotechnol*. 2010;28:511-515
95. Kent WJ, Sugnet CW, Furey TS, Roskin KM, Pringle TH, Zahler AM, Haussler D. The human genome browser at ucsc. *Genome Res*. 2002;12:996-1006

96. Friedman RC, Farh KK, Burge CB, Bartel DP. Most mammalian mRNAs are conserved targets of miRNAs. *Genome Res.* 2009;19:92-105
97. Grimson A, Farh KK, Johnston WK, Garrett-Engele P, Lim LP, Bartel DP. MicroRNA targeting specificity in mammals: Determinants beyond seed pairing. *Mol Cell.* 2007;27:91-105
98. Mortazavi A, Williams BA, McCue K, Schaeffer L, Wold B. Mapping and quantifying mammalian transcriptomes by RNA-seq. *Nat Methods.* 2008;5:621-628
99. Ernst J, Kheradpour P, Mikkelson TS, Shores N, Ward LD, Epstein CB, Zhang X, Wang L, Issner R, Coyne M, Ku M, Durham T, Kellis M, Bernstein BE. Mapping and analysis of chromatin state dynamics in nine human cell types. *Nature.* 2011;473:43-49
100. An integrated encyclopedia of DNA elements in the human genome. *Nature.* 2012;489:57-74
101. Wang J, Zhuang J, Iyer S, et al. Sequence features and chromatin structure around the genomic regions bound by 119 human transcription factors. *Genome Res.* 2012;22:1798-1812
102. Wang J, Zhuang J, Iyer S, Lin XY, Greven MC, Kim BH, Moore J, Pierce BG, Dong X, Virgil D, Birney E, Hung JH, Weng Z. Factorbook.org: A wiki-based database for transcription factor-binding data generated by the ENCODE Consortium. *Nucleic Acids Res.* 2013;41:D171-176
103. Hubisz MJ, Pollard KS, Siepel A. Phast and rPhast: Phylogenetic analysis with space/time models. *Brief Bioinform.* 2011;12:41-51
104. Jurka J. Repbase update: A database and an electronic journal of repetitive elements. *Trends Genet.* 2000;16:418-420
105. Reumers J, Conde L, Medina I, Maurer-Stroh S, Van Durme J, Dopazo J, Rousseau F, Schymkowitz J. Joint annotation of coding and non-coding single nucleotide polymorphisms and mutations in the SNPeff and PupaSuite databases. *Nucleic Acids Res.* 2008;36:D825-829
106. Li MJ, Wang LY, Xia Z, Sham PC, Wang J. Gwas3d: Detecting human regulatory variants by integrative analysis of genome-wide associations, chromosome interactions and histone modifications. *Nucleic Acids Res.* 2013;41:W150-158
107. Biros E, Gabel G, Moran CS, Schreurs C, Lindeman JH, Walker PJ, Nataatmadja M, West M, Holdt LM, Hinterseher I, Pilarsky C, Golledge J. Differential gene expression in human abdominal aortic aneurysm and aortic occlusive disease. *Oncotarget.* 2015;6:12984-12996
108. Pers TH, Karjalainen JM, Chan Y, et al. Biological interpretation of genome-wide association studies using predicted gene functions. *Nat Commun.* 2015;6:5890
109. Zhang X, Gierman HJ, Levy D, Plump A, Dobrin R, Goring HH, Curran JE, Johnson MP, Blangero J, Kim SK, O'Donnell CJ, Emilsson V, Johnson AD. Synthesis of 53 tissue and cell line expression QTL datasets reveals master eQTLs. *BMC Genomics.* 2014;15:532
110. Goring HH, Curran JE, Johnson MP, et al. Discovery of expression QTLs using large-scale transcriptional profiling in human lymphocytes. *Nat Genet.* 2007;39:1208-1216
111. Idaghdour Y, Czika W, Shianna KV, Lee SH, Visscher PM, Martin HC, Miclaus K, Jadallah SJ, Goldstein DB, Wolfinger RD, Gibson G. Geographical genomics of human leukocyte gene expression variation in southern Morocco. *Nat Genet.* 2010;42:62-67

112. Heap GA, Trynka G, Jansen RC, Bruinenberg M, Swertz MA, Dinesen LC, Hunt KA, Wijmenga C, Vanheel DA, Franke L. Complex nature of snp genotype effects on gene expression in primary human leucocytes. *BMC Med Genomics*. 2009;2:1
113. Battle A, Mostafavi S, Zhu X, Potash JB, Weissman MM, McCormick C, Haudenschild CD, Beckman KB, Shi J, Mei R, Urban AE, Montgomery SB, Levinson DF, Koller D. Characterizing the genetic basis of transcriptome diversity through rna-sequencing of 922 individuals. *Genome Res*. 2014;24:14-24
114. Benton MC, Lea RA, Macartney-Coxson D, Carless MA, Goring HH, Bellis C, Hanna M, Eccles D, Chambers GK, Curran JE, Harper JL, Blangero J, Griffiths LR. Mapping eqtls in the norfolk island genetic isolate identifies candidate genes for cvd risk traits. *Am J Hum Genet*. 2013;93:1087-1099
115. Emilsson V, Thorleifsson G, Zhang B, et al. Genetics of gene expression and its effect on disease. *Nature*. 2008;452:423-428
116. Fehrmann RS, Jansen RC, Veldink JH, et al. Trans-eqtls reveal that independent genetic variants associated with a complex phenotype converge on intermediate genes, with a major role for the hla. *PLoS Genet*. 2011;7:e1002197
117. Landmark-Hoyvik H, Dumeaux V, Nebdal D, Lund E, Tost J, Kamatani Y, Renault V, Borresen-Dale AL, Kristensen V, Edvardsen H. Genome-wide association study in breast cancer survivors reveals snps associated with gene expression of genes belonging to mhc class i and ii. *Genomics*. 2013;102:278-287
118. Mehta D, Heim K, Herder C, Carstensen M, Eckstein G, Schurmann C, Homuth G, Nauck M, Volker U, Roden M, Illig T, Gieger C, Meitinger T, Prokisch H. Impact of common regulatory single-nucleotide variants on gene expression profiles in whole blood. *Eur J Hum Genet*. 2013;21:48-54
119. Narahara M, Higasa K, Nakamura S, Tabara Y, Kawaguchi T, Ishii M, Matsubara K, Matsuda F, Yamada R. Large-scale east-asian eqtl mapping reveals novel candidate genes for ld mapping and the genomic landscape of transcriptional effects of sequence variants. *PLoS One*. 2014;9:e100924
120. Quinlan J, Idaghdour Y, Goulet JP, Gbeha E, de Malliard T, Bruat V, Grenier JC, Gomez S, Sanni A, Rahimy MC, Awadalla P. Genomic architecture of sickle cell disease in west african children. *Front Genet*. 2014;5:26
121. Sasayama D, Hori H, Nakamura S, Miyata R, Teraishi T, Hattori K, Ota M, Yamamoto N, Higuchi T, Amano N, Kunugi H. Identification of single nucleotide polymorphisms regulating peripheral blood mrna expression with genome-wide significance: An eqtl study in the japanese population. *PLoS One*. 2013;8:e54967
122. Schramm K, Marzi C, Schurmann C, et al. Mapping the genetic architecture of gene regulation in whole blood. *PLoS One*. 2014;9:e93844
123. van Eijk KR, de Jong S, Boks MP, Langeveld T, Colas F, Veldink JH, de Kovel CG, Janson E, Strengman E, Langfelder P, Kahn RS, van den Berg LH, Horvath S, Ophoff RA. Genetic analysis of DNA methylation and gene expression levels in whole blood of healthy human subjects. *BMC Genomics*. 2012;13:636
124. Westra HJ, Peters MJ, Esko T, et al. Systematic identification of trans eqtls as putative drivers of known disease associations. *Nat Genet*. 2013;45:1238-1243

125. Wright FA, Sullivan PF. Heritability and genomics of gene expression in peripheral blood. *2014*;46:430-437
126. Zhernakova DV, de Klerk E, Westra HJ, et al. Deepsage reveals genetic variants associated with alternative polyadenylation and expression of coding and non-coding transcripts. *PLoS Genet.* 2013;9:e1003594
127. Dixon AL, Liang L, Moffatt MF, Chen W, Heath S, Wong KC, Taylor J, Burnett E, Gut I, Farrall M, Lathrop GM, Abecasis GR, Cookson WO. A genome-wide association study of global gene expression. *Nat Genet.* 2007;39:1202-1207
128. Liang L, Morar N, Dixon AL, Lathrop GM, Abecasis GR, Moffatt MF, Cookson WO. A cross-platform analysis of 14,177 expression quantitative trait loci derived from lymphoblastoid cell lines. *Genome Res.* 2013;23:716-726
129. Stranger BE, Nica AC, Forrest MS, Dimas A, Bird CP, Beazley C, Ingle CE, Dunning M, Flicek P, Koller D, Montgomery S, Tavare S, Deloukas P, Dermitzakis ET. Population genomics of human gene expression. *Nat Genet.* 2007;39:1217-1224
130. Kwan T, Benovoy D, Dias C, Gurd S, Provencher C, Beaulieu P, Hudson TJ, Sladek R, Majewski J. Genome-wide analysis of transcript isoform variation in humans. *Nat Genet.* 2008;40:225-231
131. Bryois J, Buil A, Evans DM, Kemp JP, Montgomery SB, Conrad DF, Ho KM, Ring S, Hurles M, Deloukas P, Davey Smith G, Dermitzakis ET. Cis and trans effects of human genomic variants on gene expression. *PLoS Genet.* 2014;10:e1004461
132. Cusanovich DA, Billstrand C, Zhou X, Chavarria C, De Leon S, Michelini K, Pai AA, Ober C, Gilad Y. The combination of a genome-wide association study of lymphocyte count and analysis of gene expression data reveals novel asthma candidate genes. *Hum Mol Genet.* 2012;21:2111-2123
133. Dimas AS, Deutsch S, Stranger BE, et al. Common regulatory variation impacts gene expression in a cell type-dependent manner. *Science.* 2009;325:1246-1250
134. Grundberg E, Small KS, Hedman AK, et al. Mapping cis- and trans-regulatory effects across multiple tissues in twins. *Nat Genet.* 2012;44:1084-1089
135. Gutierrez-Arcelus M, Lappalainen T, Montgomery SB, et al. Passive and active DNA methylation and the interplay with genetic variation in gene regulation. *Elife.* 2013;2:e00523
136. Mangravite LM, Engelhardt BE, Medina MW, et al. A statin-dependent qtl for gatm expression is associated with statin-induced myopathy. *Nature.* 2013;502:377-380
137. Fairfax BP, Makino S, Radhakrishnan J, Plant K, Leslie S, Dilthey A, Ellis P, Langford C, Vannberg FO, Knight JC. Genetics of gene expression in primary immune cells identifies cell type-specific master regulators and roles of hla alleles. *Nat Genet.* 2012;44:502-510
138. Murphy A, Chu JH, Xu M, et al. Mapping of numerous disease-associated expression polymorphisms in primary peripheral blood cd4+ lymphocytes. *Hum Mol Genet.* 2010;19:4745-4757
139. Heinzen EL, Ge D, Cronin KD, Maia JM, Shianna KV, Gabriel WN, Welsh-Bohmer KA, Hulet CM, Denny TN, Goldstein DB. Tissue-specific genetic control of splicing: Implications for the study of complex traits. *PLoS Biol.* 2008;6:e1
140. Zeller T, Wild P, Szymczak S, et al. Genetics and beyond--the transcriptome of human monocytes and disease susceptibility. *PLoS One.* 2010;5:e10693

141. Fairfax BP, Humburg P, Makino S, Naranbhai V, Wong D, Lau E, Jostins L, Plant K, Andrews R, McGee C, Knight JC. Innate immune activity conditions the effect of regulatory variants upon monocyte gene expression. *Science*. 2014;343:1246949
142. Barreiro LB, Tailleux L, Pai AA, Gicquel B, Marioni JC, Gilad Y. Deciphering the genetic architecture of variation in the immune response to mycobacterium tuberculosis infection. *Proc Natl Acad Sci U S A*. 2012;109:1204-1209
143. Lee MN, Ye C, Villani AC, et al. Common genetic variants modulate pathogen-sensing responses in human dendritic cells. *Science*. 2014;343:1246980
144. Huang RS, Gamazon ER, Ziliak D, Wen Y, Im HK, Zhang W, Wing C, Duan S, Bleibel WK, Cox NJ, Dolan ME. Population differences in microRNA expression and biological implications. *RNA Biol*. 2011;8:692-701
145. Degner JF, Pai AA, Pique-Regi R, Veyrieras JB, Gaffney DJ, Pickrell JK, De Leon S, Michelini K, Lewellen N, Crawford GE, Stephens M, Gilad Y, Pritchard JK. DNase I sensitivity QTLs are a major determinant of human expression variation. *Nature*. 2012;482:390-394
146. The genotype-tissue expression (GTEx) project. *Nat Genet*. 2013;45:580-585
147. Greenawald DM, Dobrin R, Chudin E, et al. A survey of the genetics of stomach, liver, and adipose gene expression from a morbidly obese cohort. *Genome Res*. 2011;21:1008-1016
148. Kompass KS, Witte JS. Co-regulatory expression quantitative trait loci mapping: Method and application to endometrial cancer. *BMC Med Genomics*. 2011;4:6
149. Li Q, Seo JH, Stranger B, McKenna A, Pe'er I, Laframboise T, Brown M, Tyekuceva S, Freedman ML. Integrative eQTL-based analyses reveal the biology of breast cancer risk loci. *Cell*. 2013;152:633-641
150. Chen TH, D'Ambrosio D, Gallins P, et al. Mapping of hepatic expression quantitative trait loci (eQTLs) in a Han Chinese population. *Nat Genet*. 2014;51:319-326
151. Innocenti F, Cooper GM, Stanaway IB, et al. Identification, replication, and functional fine-mapping of expression quantitative trait loci in primary human liver tissue. *PLoS Genet*. 2011;7:e1002078
152. Schadt EE, Molony C, Chudin E, et al. Mapping the genetic architecture of gene expression in human liver. *PLoS Biol*. 2008;6:e107
153. Schroder A, Klein K, Winter S, Schwab M, Bonin M, Zell A, Zanger UM. Genomics of adverse gene expression: Mapping expression quantitative trait loci relevant for absorption, distribution, metabolism and excretion of drugs in human liver. *Pharmacogenomics J*. 2013;13:12-20
154. Grundberg E, Kwan T, Ge B, et al. Population genomics in a disease targeted primary cell model. *Genome Res*. 2009;19:1942-1952
155. Kabakchiev B, Silverberg MS. Expression quantitative trait loci analysis identifies associations between genotype and gene expression in human intestine. *Gastroenterology*. 2013;144:1488-1496, 1496.e1481-1483
156. Ongen H, Andersen CL, Bramsen JB, et al. Putative cis-regulatory drivers in colorectal cancer. *Nature*. 2014;512:87-90
157. Keildson S, Fadista J, Ladenvall C, et al. Expression of phosphofructokinase in skeletal muscle is influenced by genetic variation and associated with insulin sensitivity. *Diabetes*. 2014;63:1154-1165

158. Curtis C, Shah SP, Chin SF, et al. The genomic and transcriptomic architecture of 2,000 breast tumours reveals novel subgroups. *Nature*. 2012;486:346-352
159. Quigley DA, Fiorito E, Nord S, et al. The 5p12 breast cancer susceptibility locus affects mrps30 expression in estrogen-receptor positive tumors. *Mol Oncol*. 2014;8:273-284
160. Gao C, Tignor NL, Salit J, Strulovici-Barel Y, Hackett NR, Crystal RG, Mezey JG. Heft: Eqtl analysis of many thousands of expressed genes while simultaneously controlling for hidden factors. *Bioinformatics*. 2014;30:369-376
161. Hao K, Bosse Y, Nickle DC, et al. Lung eqtls to help reveal the molecular underpinnings of asthma. *PLoS Genet*. 2012;8:e1003029
162. Ding J, Gudjonsson JE, Liang L, Stuart PE, Li Y, Chen W, Weichenthal M, Ellinghaus E, Franke A, Cookson W, Nair RP, Elder JT, Abecasis GR. Gene expression in skin and lymphoblastoid cells: Refined statistical method reveals extensive overlap in cis-eqtl signals. *Am J Hum Genet*. 2010;87:779-789
163. Wagner JR, Busche S, Ge B, Kwan T, Pastinen T, Blanchette M. The relationship between DNA methylation, genetic and expression inter-individual variation in untransformed human fibroblasts. *Genome Biol*. 2014;15:R37
164. Qiu W, Cho MH, Riley JH, et al. Genetics of sputum gene expression in chronic obstructive pulmonary disease. *PLoS One*. 2011;6:e24395
165. Fadista J, Vikman P, Laakso EO, et al. Global genomic and transcriptomic analysis of human pancreatic islets reveals novel genes influencing glucose metabolism. *Proc Natl Acad Sci U S A*. 2014;111:13924-13929
166. Koopmann TT, Adriaens ME, Moerland PD, et al. Genome-wide identification of expression quantitative trait loci (eqtls) in human heart. *PLoS One*. 2014;9:e97380
167. Lin H, Dolmatova EV, Morley MP, Lunetta KL, McManus DD, Magnani JW, Margulies KB, Hakonarson H, del Monte F, Benjamin EJ, Cappola TP, Ellinor PT. Gene expression and genetic variation in human atria. *Heart Rhythm*. 2014;11:266-271
168. Rantalainen M, Herrera BM, Nicholson G, et al. MicroRNA expression in abdominal and gluteal adipose tissue is associated with mrna expression levels and partly genetically driven. *PLoS One*. 2011;6:e27338
169. Gamazon ER, Innocenti F, Wei R, Wang L, Zhang M, Mirkov S, Ramirez J, Huang RS, Cox NJ, Ratain MJ, Liu W. A genome-wide integrative study of micrnas in human liver. *BMC Genomics*. 2013;14:395
170. Li Q, Stram A, Chen C, Kar S, Gayther S, Pharoah P, Haiman C, Stranger B, Kraft P, Freedman ML. Expression qtl-based analyses reveal candidate causal genes and loci across five tumor types. *Hum Mol Genet*. 2014;23:5294-5302
171. Webster JA, Gibbs JR, Clarke J, et al. Genetic control of human brain transcript expression in alzheimer disease. *Am J Hum Genet*. 2009;84:445-458
172. Zou F, Chai HS, Younkin CS, et al. Brain expression genome-wide association study (egwas) identifies human disease-associated variants. *PLoS Genet*. 2012;8:e1002707
173. Ramasamy A, Trabzuni D, Guelfi S, Varghese V, Smith C, Walker R, De T, Coin L, de Silva R, Cookson MR, Singleton AB, Hardy J, Ryten M, Weale ME. Genetic variability in the regulation of gene expression in ten regions of the human brain. *Nat Neurosci*. 2014;17:1418-1428

174. Gamazon ER, Badner JA, Cheng L, et al. Enrichment of cis-regulatory gene expression snps and methylation quantitative trait loci among bipolar disorder susceptibility variants. *Mol Psychiatry*. 2013;18:340-346
175. Gibbs JR, van der Brug MP, Hernandez DG, et al. Abundant quantitative trait loci exist for DNA methylation and gene expression in human brain. *PLoS Genet*. 2010;6:e1000952
176. Kim S, Cho H, Lee D, Webster MJ. Association between snps and gene expression in multiple regions of the human brain. *Transl Psychiatry*. 2012;2:e113
177. Zhang B, Gaiteri C, Bodea LG, et al. Integrated systems approach identifies genetic nodes and networks in late-onset alzheimer's disease. *Cell*. 2013;153:707-720
178. Shpak M, Hall AW, Goldberg MM, Derryberry DZ, Ni Y, Iyer VR, Cowperthwaite MC. An eqtl analysis of the human glioblastoma multiforme genome. *Genomics*. 2014;103:252-263
179. Colantuoni C, Lipska BK, Ye T, Hyde TM, Tao R, Leek JT, Colantuoni EA, Elkahloun AG, Herman MM, Weinberger DR, Kleinman JE. Temporal dynamics and genetic control of transcription in the human prefrontal cortex. *Nature*. 2011;478:519-523
180. Liu C, Cheng L, Badner JA, Zhang D, Craig DW, Redman M, Gershon ES. Whole-genome association mapping of gene expression in the human prefrontal cortex. *Mol Psychiatry*. 2010;15:779-784
181. Folkersen L, van't Hooft F, Chernogubova E, Agardh HE, Hansson GK, Hedin U, Liska J, Syvanen AC, Paulsson-Berne G, Franco-Cereceda A, Hamsten A, Gabrielsen A, Eriksson P. Association of genetic risk variants with expression of proximal genes identifies novel susceptibility genes for cardiovascular disease. *Circ Cardiovasc Genet*. 2010;3:365-373
182. Björkegren JLM, Kovacic JC, Dudley JT, Schadt EE. Genome-wide significant loci: How important are they?: Systems genetics to understand heritability of coronary artery disease and other common complex disorders. *J Am Coll Cardiol*. 2015;65:830-845
183. Garnier S, Truong V, Brocheton J, et al. Genome-wide haplotype analysis of cis expression quantitative trait loci in monocytes. *PLoS Genet*. 2013;9:e1003240
184. Heinig M, Petretto E, Wallace C, et al. A trans-acting locus regulates an anti-viral expression network and type 1 diabetes risk. *Nature*. 2010;467:460-464
185. Pahl MC, Erdman R, Kuivaniemi H, Lillvis JH, Elmore JR, Tromp G. Transcriptional (chip-chip) analysis of elf1, ets2, runx1 and stat5 in human abdominal aortic aneurysm. *Int J Mol Sci*. 2015;16:11229-11258
186. Lenk GM, Tromp G, Weinsheimer S, Gatalica Z, Berguer R, Kuivaniemi H. Whole genome expression profiling reveals a significant role for immune function in human abdominal aortic aneurysms. *BMC Genomics*. 2007;8:237
187. Hinterseher I, Erdman R, Donoso LA, et al. Role of complement cascade in abdominal aortic aneurysms. *ATVB*. 2011;31:1653-1660
188. Kamburov A, Pentchev K, Galicka H, Wierling C, Lehrach H, Herwig R. Consensuspathdb: Toward a more complete picture of cell biology. *Nucleic Acids Res*. 2011;39:D712-717
189. Kamburov A, Stelzl U, Lehrach H, Herwig R. The consensuspathdb interaction database: 2013 update. *Nucleic Acids Res*. 2013;41:D793-800

190. Kamburov A, Wierling C, Lehrach H, Herwig R. Consensuspathdb--a database for integrating human functional interaction networks. *Nucleic Acids Res.* 2009;37:D623-628
191. Pentchev K, Ono K, Herwig R, Ideker T, Kamburov A. Evidence mining and novelty assessment of protein-protein interactions with the consensuspathdb plugin for cytoscape. *Bioinformatics.* 2010;26:2796-2797
192. Nguyen H, Allali-Hassani A, Antonysamy S, et al. Lly-507, a cell-active, potent, and selective inhibitor of protein-lysine methyltransferase smyd2. *J Biol Chem.* 2015;290:13641-13653
193. Xu G, Liu G, Xiong S, Liu H, Chen X, Zheng B. The histone methyltransferase smyd2 is a negative regulator of macrophage activation by suppressing interleukin 6 (il-6) and tumor necrosis factor alpha (tnf-alpha) production. *J Biol Chem.* 2015;290:5414-5423
194. Calvano SE, Xiao W, Richards DR, et al. A network-based analysis of systemic inflammation in humans. *Nature.* 2005;437:1032-1037
195. Hannou SA, Wouters K, Paumelle R, Staels B. Functional genomics of the cdkn2a/b locus in cardiovascular and metabolic disease: What have we learned from gwass? *Trends Endocrinol Metab.* 2015;26:176-184
196. Nakashima H, Aoki M, Miyake T, Kawasaki T, Iwai M, Jo N, Oishi M, Kataoka K, Ohgi S, Ogihara T, Kaneda Y, Morishita R. Inhibition of experimental abdominal aortic aneurysm in the rat by use of decoy oligodeoxynucleotides suppressing activity of nuclear factor kappaB and ets transcription factors. *Circulation.* 2004;109:132-138
197. Nischan J, Gatalica Z, Curtis M, Lenk GM, Tromp G, Kuivaniemi H. Binding sites for ets family of transcription factors dominate the promoter regions of differentially expressed genes in abdominal aortic aneurysms. *Circ Cardiovasc Genet.* 2009;2:565-572
198. Genetic variants in novel pathways influence blood pressure and cardiovascular disease risk. *Nature.* 2011;478:103-109